THE UNIVERSITY
of EDINBURGH

THE DEVELOPMENT OF ANTIBODIES AGAINST THE CANINE CSF-1R

Breno Castello Branco Beirão

Thesis submitted for the degree of Doctor of Philosophy (PhD)

The University of Edinburgh

2015

Declaration

I declare that I have composed this thesis and that the work presented here is my own, except where acknowledgement has been made in the text. This work has not been submitted for any other degree or professional qualification.

Breno Castello Branco Beirão

Acknowledgements

Many thanks to my supervisor, David Argyle, for accepting me for the project, and for the support throughout. I am also thankful for his trust in my work and for allowing me to make mistakes. The experience I have had at the University of Edinburgh was invaluable, and I am forever grateful for the opportunity. I am also grateful to my second supervisor, David Hume, for the help and insights, which helped to build a stronger result. Thanks to Adriana Mercadante for the guidance during the whole process.

Thanks also to all the members of our laboratory for the help provided and the great time spent together: Craig, Carola, Emma, Alex, Tina, Seungmee, Fox, Julie, Ylenia, Erika, Adam, Karen, Lorna, the summer students and the vets. Special thanks to Lisa, for proof-reading so many texts, to Rhona, without whom there wouldn't be a lab (that star was well deserved!) and to Teresa, for the great help in many occasions and for having the patience to learn good Portuguese.

To the members of the Hume lab, especially Debbie Gow, Lindsey Waddell and Anna Raper, for the great assistance in project planning and troubleshooting.

To Ted Hupp and Saurabh Jain for the discussions about the project, the assistance with arranging the immunizations and for teaching me the technique of phage display.

To Borek Vojtěšek and the team at the Czech Republic, for receiving me so warmly and for making the antibodies. Thanks also to Margaret Chambers for the help during the immunizations.

Thanks to the many friends I made here during these years, which I dare not name, with the fear of making the fatal mistake of forgetting; you know who you are. Apparently Edinburgh has the property of attracting some of the best people from all around the world, and I had the luck to be here to meet them.

The friends in Brazil have been a great support, as always. I hope you'll still be there when I come back! Thanks for the guys at Imunova for letting me do this.

My family went in this journey with me. They made my dream theirs also, and then made it happen. There wouldn't be any of this without Pai, Mãe, Gustavo and Carla, who gladly brought us Glauco and Bentinho. I can only hope not to have fallen far from the tree.

To my love, Carolina. This work is as much mine as it is yours. Thanks for coming here in the first place. How do I even repay everything you did for me?

To Olívia, for giving the best reason in the world for me to finish this thing quickly.

Lay summary

Cancer occurs because some cells within the body deviate from their usual, controlled behaviour. In breast cancer, for instance, a group of cells within the breast multiplies abnormally, more rapidly than the normal breast cells, creating tumours. The body has mechanisms for combating these uncontrolled cells, such as the immune system. In many circumstances, the immune system kills the abnormal cells, suppressing cancer. However, in other situations, the immune system actually collaborates with cancer growth. The macrophages are part of the immune system, and have been implicated in promoting cancer, instead of suppressing it. The tumour evades and even hijacks the immune response by changing how macrophages react. Instead of killing cancer cells, macrophages start contributing to provide blood supply to the tumour, to reduce the anti-cancer responses of the rest of the immune system and to assist in cancer invasion of unaffected organs (metastasis). This research had the aim of creating drugs (called monoclonal antibodies) to eliminate macrophages and, in this manner, reduce cancer burden. The drugs developed here targeted CSF-1R, which is important for macrophage survival and proliferation. Several drug candidates were created and tested in a variety of assays. Some candidates could kill macrophages and cancer cells that also depended on CSF-1R. However, these initial drugs did not possess the necessary potency. They also were not very selective for the CSF-1R target, indicating that they could show side-effects in patients. Therefore, to increase potency and selectivity, one of the initial drug candidates was modified. This modification generated several new possible drug candidates, which were once more tested against CSF-1R and macrophages. Some of the latest drugs showed better properties and could kill macrophages more effectively and with higher selectivity. Some further steps are now necessary to assess the qualities of the latest drugs and their utility for use in cancer patients.

Abstract

The colony-stimulating factor-1 receptor (CSF-1R) is expressed by the mononuclear phagocytic lineage, and is important for the development of these cells from their progenitors and also for promoting their survival and activation after maturation. The receptor has two ligands, CSF-1 and IL-34, which induce the formation of a stable dimer between two receptor monomers. This leads to intracellular autophosphorylation of tyrosine residues and subsequent signalling cascades, leading to rapid protein expression, cytoskeleton remodelling and cellular motility. Although CSF-1R signalling is crucial for normal embryogenic development and other physiological functions mediated by the phagocytic lineage, it has also been found to promote the pathogenic progression of cancer. Tumour-associated macrophages (TAMs) can comprise a large proportion of the cellular population in several solid tumours. These cells promote several hallmarks of cancer malignancy, such as increased neovascularization, tissue invasion, induction of metastases and immunosuppression. In this work, it was confirmed that CSF-1 had a prominent role in inducing cancer-promoting cellular phenotypes. Both canine cancer cells and macrophages respond to this cytokine, respectively increasing cancer cell proliferation and reducing inflammatory activation. Given the importance of CSF-1R signalling in the tumour microenvironment, antibodies were generated with the objective of blocking receptor function. Mice were immunized with either the extracellular region or the dimerization domain of the CSF-1R. Hybridomas were produced using the primed splenocytes, and monoclonal antibody (mAb) candidates were selected based on their performance in immunostaining and on their capacity to inhibit CSF-1R^{+} cells. The best antibodies were subjected to speciation. Chimeric antibodies maintained the ability of the parental mAbs to inhibit macrophage proliferation following CSF-1R stimulation. However, the mAbs possessed moderate affinity and specificity for their target, failing to stain monocytes and presenting a degree of cross-reactivity. The binding properties of one of such mAbs were altered by PCR-induced mutations, generating semi-synthetic antibody libraries. These were screened by phage display, yielding novel clones that show reduced cross-reactivity with unrelated proteins and retain the property of inhibiting macrophage survival. These results are a step in the development of therapeutic monoclonal antibodies for cancer treatment in dogs.

Table of Contents

List of Figures

Chapter 1 - Introduction

Chapter 3 - CSF-1 is an important mediator in the interaction between cancer cells and macrophages

Chapter 4 - Characterization of murine monoclonal antibodies against canine CSF-1R

Chapter 5 - Production of chimeric and caninised antibodies

Chapter 6 - Phage display screening of a semi-synthetic antibody library based on mAb 3.1

List of Tables

List of Abbreviations

7-AAD	7-aminoactinomycin D
A/N	author’s note
ADCC	antibody-dependent cell cytotoxicity
Ang1/2	angiopoietin 1/2
ANOVA	analysis of variance
ATP	adenosine triphosphate
BCG	Bacillus Calmette-Guérin
BMDM	bone marrow-derived macrophages
bp	base pairs
BSA	bovine serum albumin
C1P	ceramide-1-phosphate
CAM	chorioallantoic membrane
Cbl	casitas B-lineage lymphoma
CCL	chemokine (C-C motif) ligand
CCR	chemokine (C-C motif) ligand receptor
CCR2i	RS102895
CD	cluster of differentiation
CDC	complement-dependent cytotoxicity
CDC42	cell division control protein 42
cDNA	complementary DNA
CDR	complementarity-determining region
cKit	mast/stem cell growth factor receptor
CM	conditioned medium
COX	cyclooxygenase
CSCs	cancer stem cells
CSF-1	colony-stimulating factor
CSF-1R	colony stimulating factor 1 receptor
CTLA-4	cytotoxic T-lymphocyte antigen 4
CX3CR1	CX3C chemokine receptor 1
DAB	3,3'-diaminobenzidine
DAPI	4',6-diamidino-2-phenylindole
dATP	deoxyadenosine triphosphate
DC	dendritic cell

DMEM	Dulbecco's modified Eagle's medium
DMSO	dimethyl sulfoxide
DNA	deoxyribonucleic acid
dNTP	deoxynucleotide triphosphate
DTT	dithiothreitol
EC	extracellular
ECL	enhanced chemiluminescence
EDTA	ethylenediamine tetraacetic acid
EGF(R)	epidermal growth factor (receptor)
ELISA	enzyme-linked immunosorbent assay
EMT	epithelial-mesenchymal transition
EpCAM	epithelial cell adhesion molecule
ERK	extracellular signal-regulated kinase
FasL	Fas ligand
FBS	fetal bovine serum
Fc(R)	fragment crystallisable (receptor)
FcRn	Fc receptor neonatal
FDA	Food and Drug Administration
FGF	fibroblast growth factor
FIMP	Fms-interacting protein
FIRE	Fms-intronic regulatory element
FOXP3	forkhead box P3
FITC	fluorescein
FR	framework region
FSC	forward scatter
FWD	forward primer
Gab2	GRB2-associated-binding protein 2
GAG	glycosaminoglycan
GAPDH	glyceraldehyde 3-phosphate dehydrogenase
G-CSF	granulocyte colony stimulating factor
GM-CSF(R)	granulocyte macrophage colony-stimulating factor (receptor)
Grb2	growth factor receptor-bound protein 2
GST	glutathione S-transferase
GTP	guanosine-5'-triphosphate
HAT	hypoxanthine-aminopterin-thymidine

HEPES	N-2-hydroxyethylpiperazine-N′-2-ethanesulfonic acid
HGF	hepatocyte growth factor
HGPRT	hypoxanthine-guanine phosphoribosyltransferase
HIF	hypoxia-inducible factor
His	histidine
HPRT	hypoxanthine guanine phosphoribosyl transferase
HR	hypervariable region
HRP	horseradish peroxidase
HuR	human antigen R
IDO	indoleamine 2,3-dioxygenase
IFN	interferon
Ig	immunoglobulin
IL	interleukin
IPTG	isopropyl β-D-1-thiogalactopyranoside
IRF	interferon regulatory factor
IRS	insulin receptor substrate
JNK	c-Jun N-terminal protein kinase
LB	Luria-Bertani
LOX	lipoxygenase
LPS	lipopolysaccharide
mAb	monoclonal antibody
MAPK	mitogen activated protein kinase
mCSF-1	membrane-bound CSF-1
MDF	myocardial depressant factor
MDSC	myeloid-derived suppressor cells
MEK	mitogen-activated protein kinase kinase
MHC	major histocompatibility complex
MIC1	macrophage inhibitory cytokine 1
miRNA	microRNA
MMP	matrix metalloproteinase
mRNA	messenger RNA
Ms	mouse
MWCO	molecular weight cut-off
МΦ	macrophage
N/A	not applicable

NF	nuclear factor
Ni-NTA	nickel-nitrilotriacetic acid
NO	nitric oxide
NOS_2	nitric oxide synthase 2
ns	not significant
OD	optical density
p__	phosphorylated
PAGE	polyacrylamide gel electrophoresis
PBMC	peripheral blood mononuclear cells
PBS	phosphate buffered saline
PCR	polymerase chain reaction
PDGF(R)	platelet-derived growth factor (receptor)
PE	phycoerythrin
PFA	paraformaldehyde
PGE	prostaglandin E
PI3K	phosphoinositide 3-kinase
PIR	paired immunoglobulin-like receptor
PK	protein kinase
PKare	PKA-related gene
PLC	phospholipase C
PlGF	placenta-derived growth factor
PPAR	peroxisome proliferator-activated receptor
PTP-ζ	receptor-type protein tyrosine phosphatase-ζ
RACE	rapid amplification of cDNA ends
RANKL	receptor activator of nuclear factor κ-B ligand
rc	recombinant canine
rh	recombinant human
RNA	ribonucleic acid
Rpm	rotations per minute
RPMI	Roswell Park Memorial Institute
RT	room temperature
RTK(i)	receptor tyrosine kinase (inhibitor)
RVS	reverse primer
scFv	single-chain variable fragment
SD	standard deviation

SDF-1	stromal-derived factor-1
SDS	sodium dodecyl sulphate
SFK	Src family kinase
siRNA	small interfering RNA
SOC	super optimal broth
SOCS	suppressor of cytokine signalling
Sos	Son of Sevenless
SSC	side scatter
STAT	signal transducer and activator of transcription
TAE	Tris-acetate-EDTA
TAM	tumour-associated macrophage;
TdT	terminal deoxynucleotidyl transferase
TGF	transforming growth factor
TIMP	tissue inhibitor of metalloproteinase
TLR	Toll-like receptor
TM	transmembrane
TMB	3,3′,5,5′-tetramethylbenzidine
TNF	tumour necrosis factor
Treg	T regulatory
U	units
uPA	urinary plasminogen activator
UTR	untranslated region
VC	vehicle control
VEGF	vascular endothelial growth factor
Vh	variable heavy
VL	variable light
WASP	Wiskott-Aldrich Syndrome protein
WAVE	WASP-family verprolin homologous

Chapter 1

Introduction

Highlights

- Constituents of the mononuclear phagocytic system include the monocytes, macrophages, dendritic cells and their myeloid progenitors.
- CSF-1R is expressed by most of the mononuclear phagocytes, being crucial for their development and function in physiological conditions and in disease.
- Tumour-associated macrophages and CSF-1R are correlated to cancer progression through several mechanisms. Possible therapeutic approaches include targeting the CSF-1R with a monoclonal antibody.

1.1 The mononuclear phagocytic system

The mononuclear phagocytic system is comprised of a variety of cells that, starting with the discovery of macrophages, were found to engulf particles by phagocytosis and were derived from the same monoblast progenitor. Mononuclear phagocytes represent *circa* 10 – 15 % of the total of cells in many organs. This family of cells also includes the monocytes, the microglia in the brain, dendritic antigen presenting cells and the osteoclasts, responsible for osseous resorption (Geissmann et al., 2010; Hume, 2006; Sunderkötter et al., 2004). In contrast to the adaptive immune system – comprised of lymphocytes – macrophages or simpler phagocytes are present in all animal species, demonstrating the importance of these cells (Seljelid and Eskeland, 1993).

The term "mononuclear phagocytic system" stands to highlight the distinction between its components and the polymorphonuclear phagocytes (neutrophils), the lymphoid cells and the endothelial cells, although some of the divisions between these cells have been blurred by recent findings (Gordon, 2007; Hume, 2008; Hume, 2006; Seljelid and Eskeland, 1993).

The mononuclear phagocytes are present in a wide variety of activation states. The morphology, gene expression and functions of cells within the mononuclear phagocytic

system are very heterogeneous, and depend on the site in which they are found. These cells differ from each other in relation to maturation levels but they can also vary within a spectrum of effector functions and markers (Hume, 2008; Serbina et al., 2008). These are presented below.

1.1.1 Bone marrow progenitors

The bone marrow precursors of the mononuclear phagocytes arise from a common myeloid progenitor which also gives rise to the neutrophils. These multipotent myeloid progenitors generate macrophage/dendritic cell-restricted progenitors that express the fractalkine receptor (CX3CR1) and c-Kit (cluster of differentiation 117, CD117). Bone marrow monocyte intermediates ($CD11b^{+}Gr\text{-}1^{+}$) are then formed from the committed progenitors, later maturing into monocytes and entering the circulation (Fogg et al., 2006; Serbina et al., 2008; Strauss-Ayali et al., 2007). The most commonly accepted pathway of development of cells within the mononuclear phagocytic system is represented in Figure 1.1.

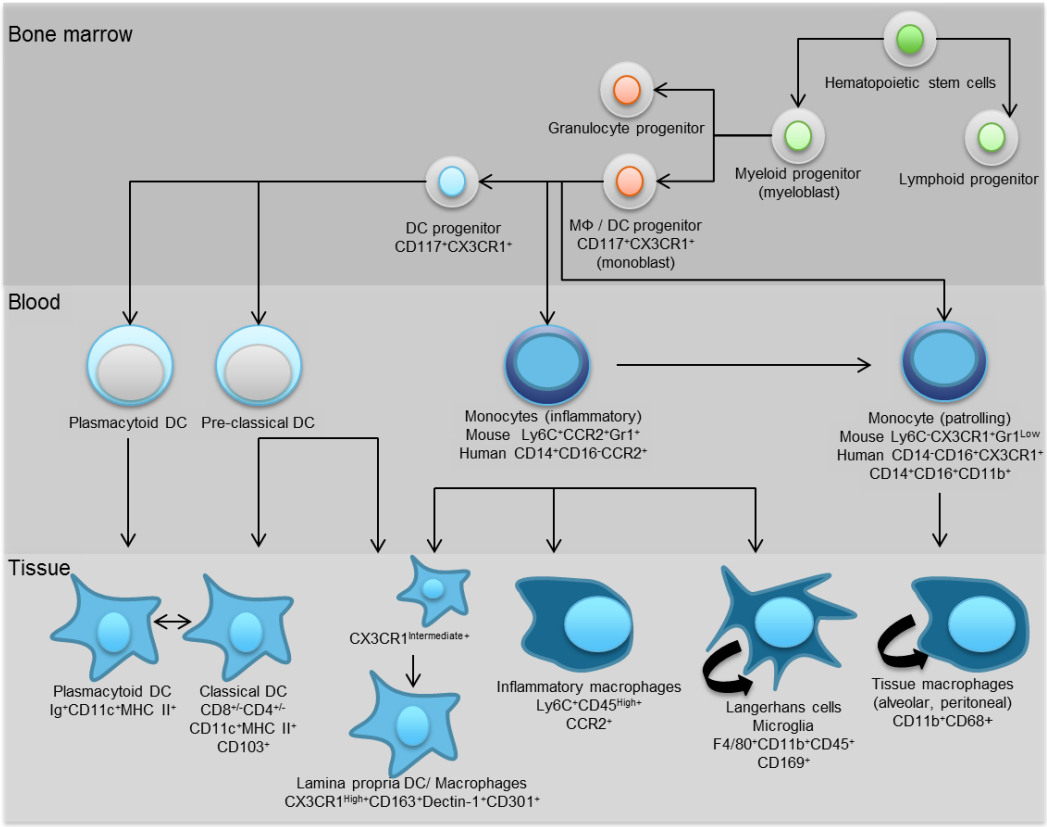

Figure 1.1 – Overview of the mononuclear phagocytic system and markers associated with each cell. The arrows indicate the course of cellular maturation. The larger semi-circular arrows indicate self-renewal of that cellular population. The cell markers that characterize blood and tissue mononuclear phagocytes and the pathways that originate macrophages are highly variable and are shown here as some of the possible combinations, although many others are described in the literature. Cellular maturation and marker expression depend on the tissue considered, presence of inflammation, experimental conditions, definition of the terms used, among other factors. References: (Bain et al., 2013; Davies et al., 2013; Fogg et al., 2006; Geissmann et al., 2010; Jay et al., 2015; Strauss-Ayali et al., 2007; Thomas et al., 2015; Wong et al., 2011).

Interestingly, it has been found that lineage differentiation generated by various progenitors in the bone marrow is less marked than commonly believed. Although generated by a different committed myeloid progenitor, the polymorphonuclear cells are very similar to the mononuclear phagocytes at the transcriptional level; neutrophils can be reprogrammed into macrophages by the addition of granulocyte macrophage-colony-stimulating factor (GM-CSF), tumour necrosis factor-α (TNF-α), interferon-γ (IFN-γ), interleukin-4 (IL-4), followed by colony-stimulating factor-1 (CSF-1) (Araki et al., 2004; Hume, 2006; Sasmono

et al., 2007). Even B-lymphocytes, which do not share the myeloid progenitor with mononuclear phagocytes, can be transformed into macrophages by altering the transcription factor network (Xie et al., 2004). Indeed, the fetal liver can produce mixed colonies of macrophages and B-lymphocytes (Hume, 2008). Mononuclear phagocytes can also display properties that are similar to those of cells of the vasculature, and monocytes and macrophages can be found lining blood vessels, for instance; this characteristic is represented in the term "reticuloendothelial system", which was used until recently to encompass the mononuclear phagocytes (Hume, 2008; Jabs et al., 2005; Saba, 1970).

1.1.2 Monocytes

Monocytes are the least differentiated cells of the mononuclear phagocytes outside the bone marrow. Nonetheless, these cells are capable of effector functions, such as phagocytosis and cytokine production (Geissmann et al., 2010). In humans, the monocytes are commonly divided into subsets based on the expression of CD14 and CD16. $CD14^+$ are called classical monocytes due to their larger presence in the human blood (90 % of monocytes), and $CD16^+$ are termed nonclassical, responding to the remaining 10 % of cells. These cells also vary in the expression of other surface receptors. $CD14^+$ cells express high levels of chemokine (C-C) motif receptor 1 (CCR1), CCR2 and CXC chemokine receptor 2 (CXCR2). $CD16^+$ monocytes express high levels of CX3CR1, MHC II and CD32, produce higher levels of the inflammatory cytokines tumour necrosis factor-α (TNF-α) and IL-1β, have lower phagocytic ability and increased antigen-presenting abilities (Chitu and Stanley, 2006; Serbina et al., 2008; Wong et al., 2011).

The function of each monocyte subset is still largely debated. Generally, $CD14^+CD16^-CCR2^+$ (classical) monocytes migrate rapidly to sites of injury and infection and differentiate into inflammatory macrophages. The nonclassical $CD16^+$ monocytes are responsible for luminal patrolling and clearing within blood vessels. These cells are rapidly increased in response to free nucleic acids and viruses. The $CD14^+CD16^+CCR2^-$ cells, which are a minor intermediate subpopulation in the steady-state, may be able to induce phagocytosis in response to antibody complexes and present antigen through highly expressed MHC II. Nevertheless, the intermediate and nonclassical subsets are similar at the transcriptional level (Thomas et al., 2015; Wong et al., 2011).

Murine monocytes are usually subdivided by the differential expression of Ly6C, CX3CR1 and CCR2. $Ly6C^{High+}$ monocytes are also $CCR2^+$. These cells are large, granular and respond to inflammatory stimuli, and are the murine equivalent of the classical

monocytes. $CX3CR1^{+}Ly6C^{Low}$ monocytes migrate to tissues to form the resident subset of macrophages and have the scavenging functions of the human nonclassical cells. Each of the Ly6C subsets is present in equal proportions in the murine blood. It has been suggested that the gradient in LyC6 expression may represent stages of cellular maturation, and that $LyC6^{+}$ cells develop into $LyC6^{-}CX3CR1^{+}$ monocytes in response to GM-CSF (Hume, 2006; Serbina et al., 2008).

It must be noted however that the human and murine classical and nonclassical monocyte subsets are not entirely parallel and the differences can often make difficult the comparison of results between these species. The proportion between the classical and nonclassical monocyte subsets is different in each species, for instance (Hume, 2006; Louis et al., 2015; Serbina et al., 2008). The human and murine subsets also express different levels of CSF-1R, a receptor which will be further discussed below (Louis et al., 2015; Wong et al., 2011).

Variations in the definitions of monocyte subpopulations are significant between humans and mice, but the monocytes of other animals have not been so thoroughly examined in relation to the function and the relative expression of each marker. Canine monocytes are known to express CD14, CD16, CCR2, CX3CR1 and other receptors also used for characterizing human cells, but these have only been studied within restricted experimental contexts (Fogle, 2015; Reis et al., 2006).

1.1.3 Macrophages

Under inflammatory conditions, the circulating monocytes ($LyC6^{High}$, in the mouse or $CD14^{+}$, in humans) are recruited into the peripheral tissues, where they mature into macrophages and dendritic cells. The circulating monocytes are also the precursors for many resident tissue macrophage populations, such as those of the gut. Resident macrophages in the spleen, peritoneal cavity and other tissues can be derived and replenished directly from the bone marrow macrophage/dendritic cell progenitors ($CX3CR1^{+}CD117^{+}$). Among the resident macrophages are the Langerhans cells of the skin, the microglia in the brain, alveolar macrophages, peritoneal macrophages and the Kupffer cells in the liver. Microglia and Langerhans cells can self-renew *in situ*, without the need for bone marrow precursors. These cells are occasionally also classified as dendritic cells (Davies et al., 2013; Geissmann et al., 2010). Other tissue macrophages may also be independent from circulating precursors, such as those cells under the influence of IL-4 (Jenkins et al., 2013, 2011).

1.1.4 Dendritic cells

Dendritic cells are capable of high levels of phagocytosis and antigen presentation. They are defined by the expression of CD11c and the ability to activate T-lymphocytes. The origin of these cells is varied, depending on the subset being considered, but they can derive from a bone marrow precursor or from monocytes (Geissmann et al., 2010; Savina and Amigorena, 2007). Myeloid dendritic cells, also named classical dendritic cells, are short-lived, circulatory (in humans) and are replaced by precursors present in the blood. They can express CD4, CD8, CD103 and several other markers. Marker expression varies within different tissues and following activation of a specific immune response. Plamacytoid dendritic cells are long-lived and express immunoglobulin rearrangements. Both dendritic cell types are derived from a common dendritic precursor in the bone marrow. The plasmacytoid dendritic cells directly originate from the common dendritic precursor, while the classical dendritic cells originate from a second intermediary cell (Geissmann et al., 2010). However, it has been suggested that plasmacytoid and classical myeloid dendritic cells are interchangeable, depending on the presence of certain stimuli (MacDonald et al., 2005).

1.1.5 Multinucleated phagocytes

Some functionally distinct cells are derived from the fusion of several macrophages. Osteoclasts are multinucleated cells derived from $CD16^-$ monocytes or macrophages under the influence of receptor activator of nuclear factor κ-B ligand (RANKL) and CSF-1. These cells are responsible for bone resorption (Komano et al., 2006; Udagawa et al., 1990). Langhans cells are multinucleated giant cells generated by the fusion of granuloma macrophages in response to infection with *Mycobacterium* spp. Virulent *M. tuberculosis* are able to induce Langhans cells that lose their phagocytic capacity, while still presenting antigens (Lay et al., 2007).

Many more different cellular subsets and marker-defined activation states have been described within the mononuclear phagocytic system, especially within the dendritic cell classification (Guilliams et al., 2014). Those were not explored here for clarity and brevity. Furthermore, it has been argued that the extenuating classification of subtypes of mononuclear phagocytes is artificial and does not reflect the natural process of cellular development and activation, which is gradual and interchangeable. For example, it has been

proposed that myeloid dendritic cells and macrophages are simply differently activated phenotypes of a same cell (Hume, 2006), and that resident and pro-inflammatory macrophages in the intestine are context variants of cells derived from the same monocyte precursor (Bain et al., 2013).

The several receptors and cytokines produced and recognized by the mononuclear phagocytic system are constantly self-regulating, fluidly altering the phenotype of the cells. The expression of cell markers changes according to the microenvironment in which the cells are inserted and the presence of other stimulants. Some of the possible relationships between factors and receptors are shown in Table 1.1 to illustrate the complex interactions that guide the mononuclear phagocytic system. Some of these interactions will be further discussed in the text.

Table 1.1 – Co-regulation of several factors in the mononuclear phagocytic system. The arrows indicate how the factors on the vertical line influence the expression of factors on the horizontal line. Changes in expression can refer to protein or mRNA levels. A square with arrows in opposing directions indicates divergent results in different conditions or in various references. No references were found for the empty squares. References: (Bailey et al., 2008; Barve et al., 2013; Caux et al., 1992; Ciccia et al., 2013; Eda et al., 2011; Foucher et al., 2013; Lauener et al., 1990; Liu et al., 2001; MacDonald et al., 2005; Mantovani and Allavena, 2015; Matsumura et al., 2000; Muzio et al., 2000; Park et al., 2004; Rey-Giraud et al., 2012; Ross et al., 2008; Shibata et al., 2001a; Sierra-Filardi et al., 2014; Sozzani et al., 1997; Sweet et al., 2002; Temeles et al., 1993; Vellenga et al., 1988; Voloshin et al., 2013; Wei et al., 2010; Wong et al., 1991; Xu et al., 2015; Yeung and Stanley, 2003).

	CSF-1R	TLR2	TLR4	CCR2	CSF-1	IL-34	CD14	CD16
CSF-1	↑(monocyte) ↓(MΦ)	↓	→	↓	↑	→	↑(+IL10) ↓(+IL4)	↑
IL-34	↓ (MΦ)	↓	→	↓	↑		↑ ↓(+LPS)	↑
GM-CSF	↓	↑	↑	↑	↑		↓ ↑(+LPS) →	↑
LPS	↓	↑	↑	↓	↑	↑	↑(+CSF-1)	↑(+CSF-1)
CCL2			↑	↓				↑
IL-6	↑	↑	→				→	
TNF-α	↓	↑	→		↑	↑	→	↑ ↓

1.2 A common marker: the CSF-1R

The extensive functional differences between the cells of the mononuclear phagocytic system are reflected by the fact that only rare markers, if any, are common to all members of this cellular group. Many surface markers such as CD14, CD16, CD11, CD163, F4/80 and LyC6 (in mice) and chemokine receptors such as CCR1, CCR2 and CX3CR1 are expressed in separate presumptive functional subgroups (Gordon and Taylor, 2005; Sasmono et al., 2003). Probably the most widespread marker expressed by the mononuclear phagocytes is CSF-1R, the receptor for the macrophage colony-stimulating factor, or colony stimulating factor-1 (CSF-1). Signalling through the CSF-1R controls proliferation, differentiation, adaptation and survival of a large proportion of the cells of the mononuclear phagocytic system (Hume, 2006; Louis et al., 2015; MacDonald et al., 2005).

CSF-1R is expressed by the majority cells of the mononuclear phagocytic lineage, from the macrophage/dendritic cell progenitors (monoblasts), promonocytes and monocytes to the macrophages, dendritic cells and osteoclasts. This illustrates the importance of CSF-1R during the maturation and function of the mononuclear phagocytic lineage (Pixley and Stanley, 2004; Stanley and Chitu, 2014; Wiktor-Jedrzejczak et al., 1982).

The components of the CSF-1R signalling axis are discussed below.

1.2.1 The CSF-1R

The CSF-1 receptor tyrosine kinase (CSF-1R, CD115 or Fms) is encoded by the c-*fms* (*Csf1r*/*CSF1R*) proto-oncogene (Chihara et al., 2010; Pixley and Stanley, 2004; Sherr et al., 1985). It is located in the human chromosome 5, in the mouse chromosome 18 and in the canine chromosome 4 (Ensembl). There are two different promoters driving CSF-1R expression: the T/OC promoter controls expression in trophoblasts and osteoclasts; the M promoter, which is more proximal, controls CSF-1R production in macrophages. In the mouse, trophoblast transcripts are started 500 – 300 bp upstream of the start codon in exon 2; macrophage transcripts are initiated within 300 bp of the initiation codon. Strong expression requires a conserved enhancer element in intron 2, called Fms-intronic regulatory element (FIRE) (Stanley and Chitu, 2014).

CSF-1R is a type III receptor tyrosine kinase, member of the platelet derived growth factor receptor (PDGFR) family (Yeung and Stanley, 2003). It possesses structural similarities to the PDGFR and c-Kit (Qiu et al., 1988). The c-*fms* was firstly identified as the human homologue of a feline sarcoma viral gene (v-*fms*) which is capable of cellular

transformation and oncogenesis through constitutive activation of the receptor kinase in the absence of the ligand (Heisterkamp et al., 1983; Mcdonough et al., 1971; Sherr et al., 1985). The feline c-*fms* and the v-*fms* differ in a carboxy-terminal truncation and two mutations in the dimerization region of the receptor (the feline amino acids L301S and A374S) (Stanley and Chitu, 2014).

The structure of CSF-1R is as follows (Yeung and Stanley, 2003) (Figure 1.2):

- Extracellular region – five immunoglobulin-like domains, highly glycosylated. Binding to the ligands occurs on the second and third extracellular domains, with prominence to the second domain. Receptor signalling following ligand contact is dependent on homo-dimerization of domain 4 (Stanley and Chitu, 2014);
- Transmembrane region – amino acids 512-534 (murine), composing a hydrophobic region;
- Intracellular region – a tyrosine kinase domain interrupted by an interkinase domain. ATP binding occurs within the N-terminal lobe and the hinge region. Substrate binding and catalysis occurs at the C-terminal lobe.

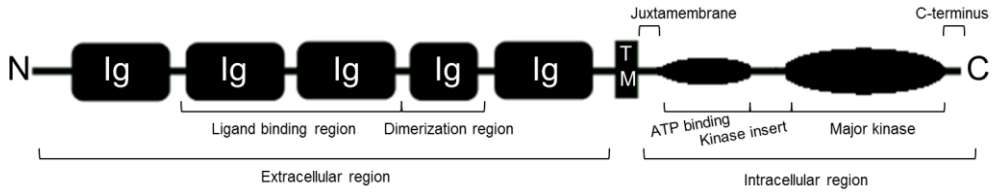

Figure 1.2 – Structure of the CSF-1R. "Ig" indicates the immunoglobulin regions. "TM" indicates the transmembrane region. The N- and C- termini are indicated. Adapted from Yeung and Stanley, 2003.

The receptor is expressed as an immature 130 kD glycoprotein which is transformed on its way to the cellular membrane by the addition of *N*-linked oligosaccharide chains; this increases the molecular weight of the receptor to 150 kD (Rettenmier et al., 1987). The CSF-1R expression pattern within the mononuclear phagocytic system is shown in Figure 1.3. Other cell types outside the mononuclear phagocytic system are also CSF-1R^{+}: oocytes, preimplantation embryos, decidual and trophoblastic cells, neural progenitor cells, renal proximal tubule epithelial cells and colonic epithelial cells (Stanley and Chitu, 2014).

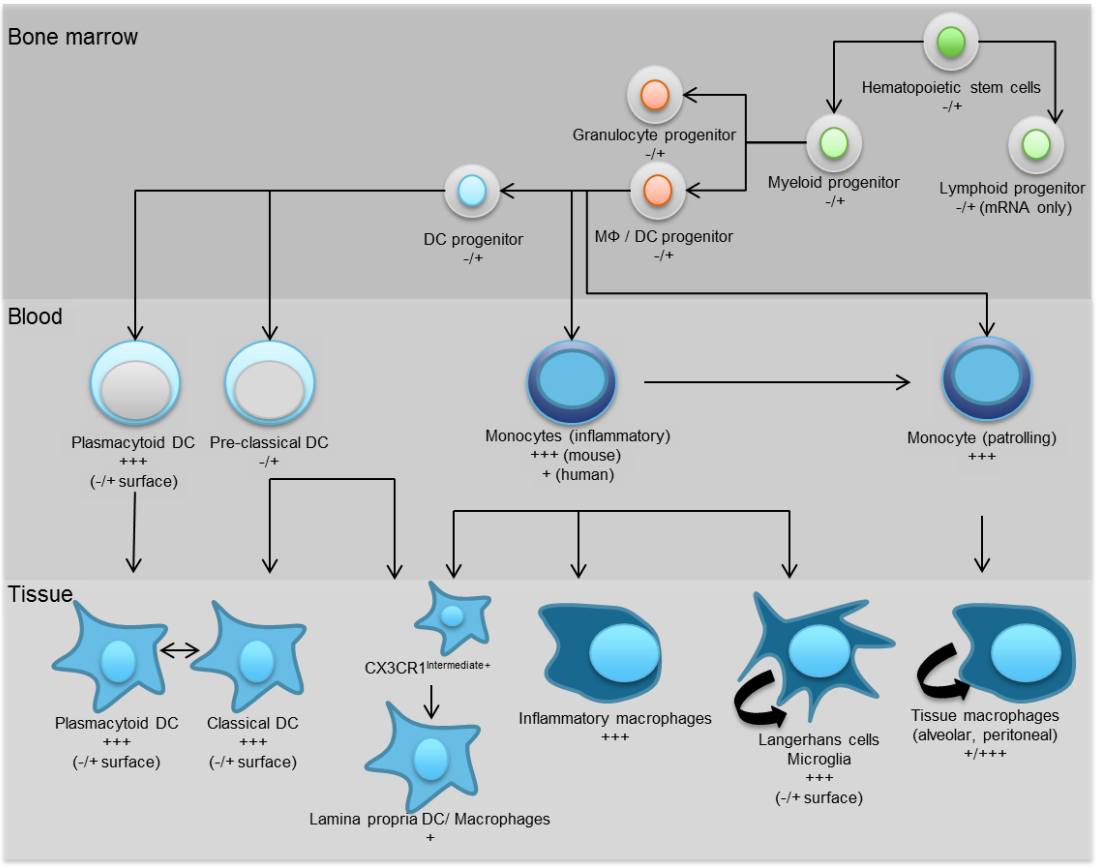

Figure 1.3 – CSF-1R expression by the cells of the mononuclear phagocytic system. The arrows indicate the course of cellular maturation. The larger semi-circular arrows indicate self-renewal of that cellular population. The number of crosses under each cell indicates the relative CSF-1R expression, from low (-/+) to high (+++). References: (MacDonald et al., 2005, 2010; Sasmono et al., 2003; Stanley and Chitu, 2014; Wong et al., 2011).

Prior to contact with the ligands, CSF-1R is constantly undergoing rapid changes between monomer/dimer forms (Yeung and Stanley, 2003). The result of CSF-1R binding to its ligands is the stabilization of the dimer form (through non-covalent bonds) and subsequent rapid phosphorylation of CSF-1R and coupled intracellular proteins, which leads to the actual signalling process. Subsequently, the receptor undergoes endocytosis and lysosomal degradation (Figure 1.4). Consequently, lower surface expression of the CSF-1R is seen in cells that have been activated by the presence of the ligands (Sester et al., 1999; Yeung and Stanley, 2003). The coupled endocytosis and elimination of CSF-1R along with its ligand is a self-regulatory mechanism: a reduction in the concentration of either ligands or receptor increases the concentration of the other (Bartocci et al., 1987). It is not known if a

similar internalization of the receptors occur after binding of CSF-1R with the membrane isoform of CSF-1 (mCSF-1), which will be discussed below (Dai et al., 2004).

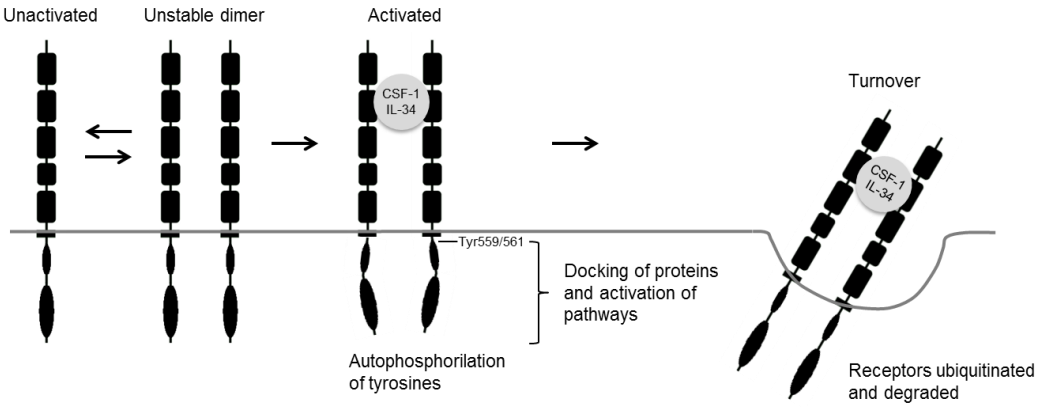

Figure 1.4 – Schematic representation of the activation and degradation process for CSF-1R. The grey line represents the cellular membrane. The immunoglobulin domains of the CSF-1R extracellular region are represented by the rectangles. Ligand binding occurs in EC domains 2-3 and promotes receptor dimerization. This leads to Tyr559 phosphorylation in the intracellular region, receptor signalling and subsequent degradation of the complex. Adapted from Douglass et al., 2008.

1.2.2 Intracellular signalling of CSF-1R

Three stages are present during CSF-1 signalling: the first is the active signalling stage that occurs through auto-phosphorylation of the receptor and activation of coupled-protein pathways after ligand binding; the second stage prepares the CSF-1/CSF-1R complex for endocytosis; the internalization of the receptor/ligand complex occurs in the third stage (Sester et al., 1999; Yeung and Stanley, 2003).

In the inactive state, before ligand binding, the ATP-binding cleft of the tyrosine kinase domain is blocked due to the folding conformation of an activation loop, which, in its turn, is caused by the positioning of the juxtamembrane region. The amino acid Asp-796, necessary for magnesium coordination of ATP, is also in an "out" conformation. After ligand binding, the first residue to be phosphorylated is Tyr-561 in humans or Tyr-559 in mouse (Figures 1.4, above and Figure 1.5). From this point, the CSF-1R undergoes two waves of phosphorylation. In the first wave, the receptor forms complexes with Grb2/Sos and with SFK, Cbl, the regulatory subunit of PI-3 kinase (PI3K) (p85), Grb2, among others. Grb2/Sos dissociates and the second wave follows, which also leads to Cbl-dependent CSF-1R

ubiquitination. The receptor is internalized and is transported via endosomes to the lysosomal system, where CSF-1R and the ligand are degraded. Within the endosomes, the CSF-1R can still mediate signalling. The initial response following CSF-1R activation is cytoskeletal remodelling, followed by increased motility, chemotaxis and protein synthesis (Stanley and Chitu, 2014).

The signalling pathways following CSF-1R activation and their biological consequences are represented in Figure 1.5. Downstream signalling pathways from CSF-1R are presented in Table 1.2.

Table 1.2 – Downstream signalling pathways from CSF-1R involved with different cellular functions. References: (Caescu et al., 2015; Lee and States, 2006; Stanley and Chitu, 2014).

Macrophage survival	Cell proliferation	Cell differentiation	Chemotaxis
PI3K/Akt pathway, activated by phosphorylation of Tyr 721 or indirectly by ceramide-1-phosphate (C1P) or the Gab2/PI3K pathway. Effect in cell glycolysis. PI3K, $ERK_{1/2}$ and NF-κB p65 induce microRNA-21 (miRNA-21) and suppress miRNA-155. miRNA-21 provides a negative feedback on the activation of $ERK_{1/2}$ and PI3K	MEK, PI3K, SFK and C1P-induced production of PI3K/Akt, JNK, and $ERK_{1/2}$	MEK/$ERK_{1/2}$ phosphorylation, independent of Grb2/Sos assembly or PI3K activity. Adaptor proteins Mona and Gab3 increase $ERK_{1/2}$ phosphorylation, but are not essential	First wave of actin polymerization through GTPases, Cdc42, Rac, and Rho and their downstream effectors, Wiskott-Aldrich syndrome protein (WASP) and WASP-family verprolin homologous 2 (WAVE 2) actin nucleators. SFK activation of WASP is necessary for chemotaxis to CSF-1
Phospholipase C (PLC) and Fms-interacting protein (FIMP)	DAP12-mediated activation of Syk, which activates the Pyk2 tyrosine kinase that phosphorylates β-catenin	PKC-δ leading to increased expression of PKA-related protein kinase (Pkare)	Rac1/IRS p53 activation of the WAVE2/Abi complex in a second wave of actin polymerization
		p46/52 Shc	
		PLC-γ2	

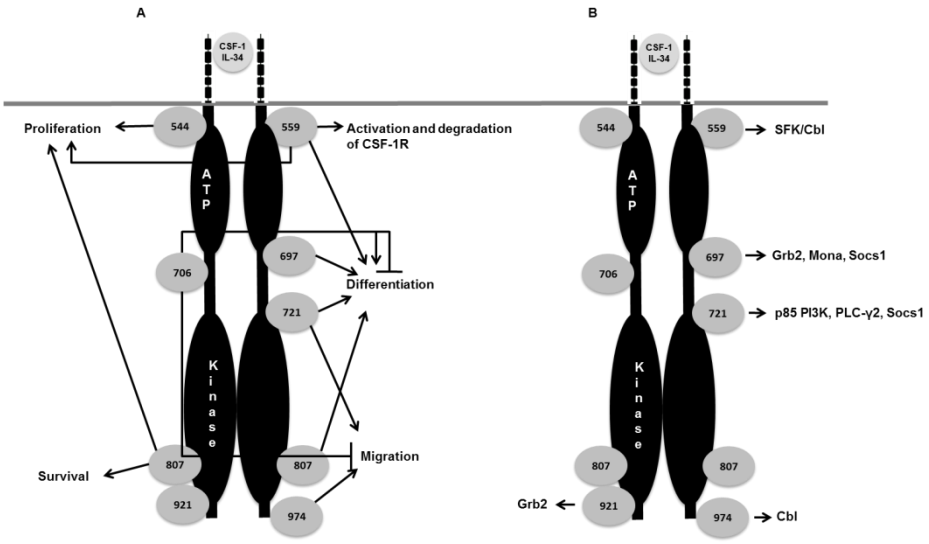

Figure 1.5 – Sites of tyrosine phosphorylation in the CSF-1R. **(A)** The biological consequences of phosphorylation of each tyrosine residue. **(B)** Pathway mediators at each tyrosine residue after phosphorylation. The intracellular region of CSF-1R is depicted under the horizontal grey line. The numbers inside the grey spheres indicate the sites of tyrosine phosphorylation in the mouse. Arrows indicate activation; T-shaped lines indicate inhibition. "ATP" indicates the ATP-binding site. "Kinase" indicates the major kinase domain. Reference: Stanley and Chitu, 2014.

1.2.3 The CSF-1R ligands: CSF-1 and IL-34

CSF-1R has two ligands, CSF-1 and IL-34, which are conserved across vertebrates (Chihara et al., 2010; Garceau et al., 2010). CSF-1 can be expressed as three different isoforms: either as a secreted 80 – 100 kD glycoprotein or a 130 – 160 kD proteoglycan, both found in the circulation, or as a 68 – 86 kD cell surface glycoprotein (csCSF-1 or mCSF-1). The secreted isoforms are disulphide-linked homodimers. Differential proteolysis from the full-length precursors in secretory vesicles yields the secreted isoforms: the glycoprotein by N-terminal cleavage and the proteoglycan by C-terminal cleavage. The latter form possesses a longer polypeptide chain and chondroitin sulphate glycosaminoglycan (GAG) attached (Droin and Solary, 2010; Stanley, 2000). All three isoforms are glycosylated with *N*- and *O*- linked carbohydrates. The biologically active portion is comprised of the first 150 amino acids of the N-terminus of the protein (Dai et al., 2004; Stanley, 2000).

Different isoforms of CSF-1 have differences in action, even though these are overlapping, and are regulated differentially within tissues. Expression of the membrane-

bound isoform alone is not enough to perform all roles of CSF-1, and developmental defects arise if it is the sole form present. Not all of the roles of mCSF-1 are known, neither are its dynamics after activation of cells (Dai et al., 2004; Nandi et al., 2006). The secreted isoforms of CSF-1 rescue the effects of CSF-1 knockout more efficiently than mCSF-1 does, and of the two secreted forms, the proteoglycan is more effective at restoring normal functions. Therefore, it seems that the chondroitin sulphate chain which is present on the proteoglycan isoform is important for CSF-1 localization and/or signalling (Nandi et al., 2006).

Interleukin-34 (IL-34) is a homodimeric secreted glycoprotein. IL-34 has no obvious sequence homologies to CSF-1, although there are structural similarities. Both ligands have four cytokine folds and form self-dimers (Droin and Solary, 2010). Unlike CSF-1, IL-34 is capable of binding to another receptor, receptor-type protein tyrosine phosphatase-ζ (PTP-ζ). This receptor is expressed by neural progenitors and glial cells. IL-34 binding to this receptor induces tyrosine phosphorylation of downstream effectors, leading to inhibition of cellular proliferation and motility (Nandi et al., 2013).

CSF-1 and IL-34 have different spatiotemporal expression patterns. CSF-1 mRNA is produced by the uterus during pregnancy between the murine embryonic days 8.5 and 11.5. IL-34 is not increased during this stage. Mouse embryos have high mRNA levels of CSF-1 during development days 11.5 and 13.5, while IL-34 levels are increased between 8.5 and 17.5 days. Within the embryo, IL-34 mRNA is most apparent in the telencephalon of E11.5 embryos. CSF-1 appears at day 13.5 in several other areas of the embryo. In adult brain and ear, IL-34 mRNA is more present than CSF-1. Keratinocytes and neurons are the main sources of IL-34, but the cytokine is also highly produced by proximal renal tubule cells and seminiferous tubule germ cells (Y. Wang et al., 2012; Wei et al., 2010). Another group stated that IL-34 mRNA is mainly present in the spleen (Lin et al., 2008). Osteoblasts and the adult heart preferentially produce CSF-1 over IL-34; other mesenchymal cells that also produce CSF-1 include fibroblasts, bone marrow stromal cells, keratinocytes, astrocytes, liver parenchymal cells, among others. Secreted isoforms of CSF-1 are thought to be produced by endothelial cells (Nandi et al., 2006; Pixley and Stanley, 2004; Stanley, 2000; Wei et al., 2010).

In mice, a natural mutation of the *Csf1* gene, designated osteopetrotic mutation (*op/op*), or a knockout of the *Csf1r* gene (*Csf1r*$^{-}$*/Csf1r*$^{-}$) can both cause a substantial reduction in the number of mononuclear phagocytes in most tissues (Dai, 2002; Wiktor-Jedrzejczak et al., 1982). Removal of CSF-1 in the *op/op* mouse can be partially compensated by IL-34. This is illustrated by the fact that the *Csf1r*$^{-}$*/Csf1r*$^{-}$ animal has a stronger phenotype than the *op/op* knockout (Droin and Solary, 2010). However, IL-34

mRNA is not increased to compensate the absence of CSF-1 in the *op/op* mouse (Wei et al., 2010).

1.2.4 Consequences of CSF-1R signalling in the mononuclear phagocytes

CSF-1 and IL-34 have multiple functions. These cytokines have a major role in the stimulation of the survival, proliferation and differentiation from the myeloid precursor of the mononuclear phagocytes (Hume, 2008; Pixley and Stanley, 2004).

IL-34 and CSF-1 share the same receptor, but the signalling activated and their biological activities are not identical. Even though they are both capable of supporting cell growth in culture systems, they do not elicit the same responses. IL-34 induces a stronger but transient tyrosine phosphorylation of CSF-1R, and rapidly down regulates the presence of the receptor on the cell surface (Ma et al., 2012). Both ligands stimulate the transcription of a similar set of genes, but IL-34 drives an attenuated transcription pattern of some genes. Both ligands repress *CCR2* transcription, for instance, but IL-34 does so more mildly (Barve et al., 2013).

Although both ligands bind to the extracellular domains 2 and 3 of the CSF-1R, conformation adaptations occur on the receptor when binding either ligand, explaining the capacity of the receptor of interacting with both. The receptor contact points also differ between the two ligands. Nevertheless, after binding to the receptor, both ligands drive receptor dimerization (Ma et al., 2012). Confirming this difference in binding sites, a monoclonal antibody (mAb) was identified that is able to block the binding of both CSF-1 and IL-34 to CSF-1R, but a second mAb was able to block only the CSF-1/CSF-1R interaction, but not that of IL-34 with the receptor (Chihara et al., 2010).

The roles of CSF-1R signalling throughout the mononuclear phagocytic system are detailed below, separated by each of its cellular components.

Myeloid precursors: These cells respond to CSF-1 signalling (MacDonald et al., 2005). CSF-1 does not seem to be exclusively required for monopoiesis, since blocking the growth factor or its receptor does not reduce total monocyte counts. CSF-1 is important for the maintenance of steady-state mature ($Ly6C^-$) monocytes, but can be substituted by GM-CSF for earlier cell precursors (that is, from the myeloid precursors to the $Ly6C^+$ cells) (Louis et al., 2015).

Monocytes: Signalling through CSF-1 is required for the proliferation and differentiation of monocytes only after the $Ly6C^-$ stage of development is reached. This is

confirmed by the CSF-1 and CSF-1R-deficient mice, which have only partial reduction in monocyte counts (Louis et al., 2015). After maturation, even prolonged CSF-1R blockade has only moderate effects over the monocytes, depleting exclusively the $Ly6C^-$ monocytes (Sauter et al., 2014). $CD16^+$ cells, which are the human nonclassical monocyte counterparts of the murine $Ly6C^-$, express more CSF-1R than $CD16^-$. Together with CSF-1R, $CD16^+$ monocytes transcribe a macrophage/dendritic cell set of genes (Ancuta et al., 2009).

Although monocytopoiesis and classical monocyte survival is not dependent on CSF-1R, administration of CSF-1 increases blood monocytes (Stanley, 2000). CSF-1 is also important in determining the fate of monocytes. Monocytes that are cultured with CSF-1 and interleukin-4 (IL-4) differentiate into macrophages ($CD14^+$), while cells kept with GM-CSF and IL-4 turn into dendritic cells ($CD1a^+$) (Witmer-Pack et al., 1993).

Macrophages: The dependence of macrophages on CSF-1R for maturation is variable across diverse tissues. Resident macrophages in the steady-state can be divided with regard to their CSF-1 dependence during development and after maturity (Table 1.3) (Stanley, 2000). Therefore, blocking CSF-1R does not reduce macrophage numbers within some tissues. In the blood and bone marrow, for instance, only the more mature $LyC6^-$ macrophages are affected by blocking the CSF-1R, as already discussed, whereas liver macrophages are readily depleted (Louis et al., 2015; MacDonald et al., 2010).

Kupffer cells, the liver resident mononuclear phagocytes, are among the most CSF-1-dependent cells (Wiktor-Jedrzejczak et al., 1994). Osteopetrotic mice respond with increasing numbers of Kupffer cells after a single injection of CSF-1, and normal levels are almost restored when CSF-1 is given on a daily basis (Yamamoto et al., 2008). Kupffer cells are also completely removed by prolonged CSF-1R blockade even after maturity (Sauter et al., 2014).

Langerhans cells and microglia are absent from CSF-1R- but not from CSF-1-deficient mice; IL-34 produced by keratinocytes and neurons directs the differentiation of the resident dendritic cells of the skin and central nervous system (Wang et al., 2012). In the microglia, CSF-1 is considered a key regulator of inflammatory responses, increasing brain injury due to neurotoxicity, but also improving clearance of abnormal protein aggregates since phagocytic activity is enhanced. Apparently in the glia CSF-1 signalling has an autocrine pathway (Chitu and Stanley, 2006).

Administration of CSF-1 increases tissue macrophage numbers, but some tissue populations do not require circulating CSF-1, such as peritoneal and alveolar macrophages (Stanley, 2000). Nevertheless, these populations are depleted if the CSF-1R is blocked (Louis et al., 2015), indicating that they may rely on IL-34 production (Wang et al., 2012).

IL-34 is less active than CSF-1 in inducing macrophage proliferation. Either ligand is sufficient, however, to sustain tissue macrophage numbers (Wei et al., 2010).

Other cytokines such as IL-4 and GM-CSF can replace or complement the CSF-1 signal for stimulating resident tissue macrophages. IL-4 is capable of inducing tissue resident macrophage proliferation independently from CSF-1, but this cytokine is not able to recruit peripheral macrophages, a function which requires CSF-1R signalling (Jenkins et al., 2013). Alveolar macrophages are present at reduced levels in young *op/op* mice, but were found to be normal in the adult mice. This correction after maturity is thought to occur due to increased production of IL-3 (Shibata et al., 2001b).

Table 1.3 – CSF-1R dependence of macrophage populations in the steady-state during development and after maturity. Adapted from Stanley, 2000. Other references: (Louis et al., 2015; MacDonald et al., 2010; Sauter et al., 2014; Y. Wang et al., 2012). [a]Depending on which tissue population is considered. [b]Depending on the methodology used to assess.

Tissue	Development	Maturity
Dermis	Complete	Complete/none[b]
Kidney	Complete	Complete
Lymph node subcap. sinus CD11b$^+$	Complete	
Muscle	Complete	Complete
Periosteum	Complete	Partial/none[a]
Peritoneal cavity	Complete	Complete
Pleural cavity	Complete	Complete
Retina	Complete	Complete
Spleen metallophils	Complete	Complete
Synovium	Complete	None
Tendon	Complete	None
Testis	Complete	Complete
Adrenals	Partial	None
Bladder	Partial	Partial/none[a]
Bone marrow macrophage	Partial	Partial
Gut	Partial	Partial/none[a]
Liver	Partial	Complete
Lung alveolar macrophage	Partial	
Osteoclast	Partial	Complete
Salivary gland	Partial	Partial
Spleen	Partial	Complete
Stomach	Partial	Partial/none[a]
Uterus	Partial	None
Bone marrow `monocyte'	Independent	None
Langerhans/microglia	Independent	None
Lymph node	Independent	None
Thymus	Independent	None

GM-CSF and CSF-1 are usually seen as opposing cytokines in the development of the mononuclear phagocytic system. CSF-1-conditioned macrophages in the steady-state show less inflammatory characteristics, decreasing lymphocyte activation, performing angiogenesis and tissue repair. GM-CSF macrophages, in contrast, are pro-inflammatory,

with increased CD80, CD86 and MHC II when compared to CSF-1 macrophages. GM-CSF-derived macrophages are also more stellate and have more organelles than the CSF-1-cultured counterparts. GM-CSF can also overrule the CSF-1R signal to drive the formation of inflammatory macrophages. The maintenance of cells with GM-CSF induces a reduction in the expression of CSF-1R mRNA (Droin and Solary, 2010; Gliniak and Rohrschneider, 1990; Rey-Giraud et al., 2012; Sester et al., 1999; Willman et al., 1989; Yeung and Stanley, 2003).

Hence, in many circumstances, CSF-1R signalling leads to reduced inflammatory responses *in vivo;* CSF-1R signalling leads to persistence of HIV infection in the brain by driving an anti-inflammatory phenotype (Gerngross and Fischer, 2014; Gerngross et al., 2015), and CSF-1 has also been shown to reduce LPS responses in macrophages through modulation of Activin A (Sierra-Filardi et al., 2014, 2011). While CSF-1 can increase macrophage activation and the innate response, it is immunosuppressive for antigen-specific responses, and CSF-1 expression is inducible in T cells upon activation, which may serve as a negative feedback (Sweet and Hume, 2003).

CSF-1R can also be a promoter of inflammation. Some cell-surface molecules, such as CD16 and CD14, are expressed preferentially after LPS stimulation in CSF-1-conditioned macrophages when compared to GM-CSF (Droin and Solary, 2010). Cells that are maintained in CSF-1 medium express higher levels of IL-1α, an inflammatory cytokine (Witsell, 1991). CSF-1 enhances cytotoxicity, superoxide production, phagocytosis, chemotaxis and cytokine production in monocytes and macrophages. This factor has pronounced effects on macrophage motility. It enhances phagocytic and microbial action against several pathogens *in vivo* (Sweet and Hume, 2003). CSF-1 is important for the accumulation of inflammatory macrophages, but is not needed for their local proliferation. Blocking CSF-1R with an antibody reduces the number of recruited macrophages in peritonitis and lung inflammation models (Louis et al., 2015). However, this effect may be antibody-dependent, since another blocking mAb which also reduced resident macrophage populations had no effect in inflammatory macrophage recruitment, including in peritoneum, lung, in wound healing and in graft-versus-host disease (MacDonald et al., 2010).

The molecular interactions in inflammation are complex. Signalling through CSF-1R induces loss of macrophage surface expression of Toll-like receptor 1 (TLR1), TLR2, TLR6 and TLR9, has no effect on TLR4 but increases expression of CD14, one of the subunits of TLR4. TLR signalling also has the same effect on CSF-1 receptor, that is, it down-regulates membrane expression of CSF-1R (Chitu and Stanley, 2006; Sweet et al., 2002). Therefore, CSF-1R reduces the response to CpG DNA, which is dependent on TLR9 (Chitu and

Stanley, 2006; Sweet et al., 2002). Although it does not affect the expression of TLR4, CSF-1R enhances LPS responses possibly by inducing autocrine stimulation of macrophages through GM-CSF (Conway et al., 2005). Some of the interactions in inflammation between CSF-1R and GM-CSFR signals are illustrated in Figure 1.6.

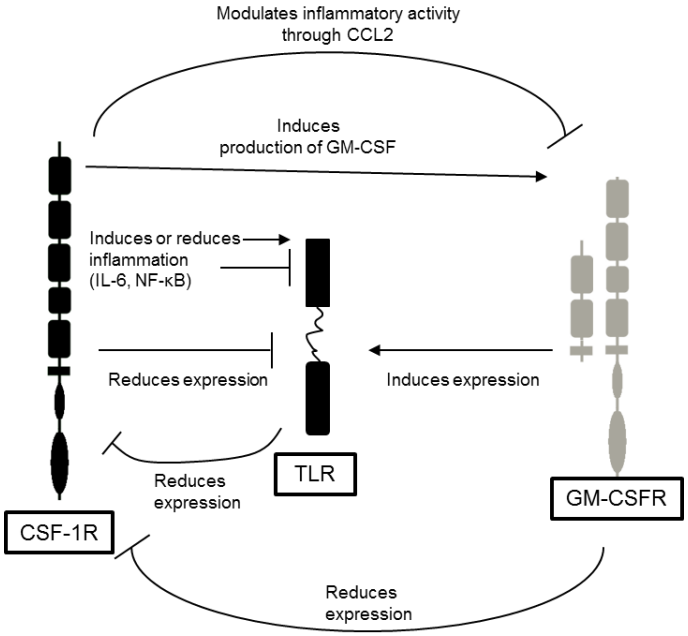

Figure 1.6 – The interactions between CSF-1R and GM-CSFR signals in relation to inflammation (represented by the TLR receptor). Arrows indicate stimulation and T-shaped lines indicate repression of a pathway (not necessarily of the receptor). The mechanisms of interaction are cited with each line. References: (Droin and Solary, 2010; Saccani et al., 2006; Sierra-Filardi et al., 2014; Sweet and Hume, 2003; Yasukawa et al., 2003).

Osteoclasts: Either CSF-1 or IL-34 is required to induce osteoclast formation, in association with RANKL (Wei et al., 2010). These cells are dependent on CSF-1R signalling even after maturity, since receptor blockade depletes these cells (Sauter et al., 2014). The osteopetrotic (*op/op*) mutation leads to a depletion of functional osteoclasts, which are the primary cells involved in bone reabsorption, giving the mutation its name; since the number of bone resorbing cells is diminished in this mutation, bones present reduced marrow cavities. Tooth eruption is also impaired in *op/op* animals once this event requires resorption of alveolar bone during embryogenesis and soon after birth (Marks and Lane, 1976; Yoshino et al., 2003).

Dendritic cells: The effect of CSF-1R signalling on dendritic cell development and function is still debated. Apparently not all dendritic cells express CSF-1R, such as $CD4^+$ dendritic cells (that could either be immature/precursor cells or dendritic cells of lymphoid origin) and other precursor populations that occur in the peripheral blood (Hume et al., 2002; MacDonald et al., 2005). Nevertheless, CSF-1-deficient mice have reductions of 50 – 70 % of all dendritic cells (MacDonald et al., 2005).

Until the late cellular maturation state, it is possible that some macrophages and dendritic cell subtypes are interconvertible depending on the cytokine microenvironment (Palucka et al., 1998). Therefore, dendritic cell numbers are also dependent on macrophages. Monocyte stimulation with GM-CSF alone is believed to induce dendritic cell phenotypes, while co-stimulation with GM-CSF and CSF-1 leads to a macrophage-like population (Droin and Solary, 2010). It has also been highlighted that monocyte stimulation with GM-CSF alone produces inflammatory macrophages and that IL-4 is necessary to produce monocyte-derived dendritic cells (Holla et al., 2014). In the absence of GM-CSF, CSF-1 and IL-4 can drive the differentiation of mature tolerogenic dendritic cells, and CSF-1 can suppress antigen presentation by dendritic cells through increased MHC II turnover (Chitu and Stanley, 2006). After dendritic cell activation, loss of CSF-1R expression is seen as a marker of commitment of the dendritic cells to the antigen-presenting phenotype (Sester et al., 1999). Only $CSF\text{-}1R^+$ dendritic cells are capable of taking up antigens, indicating a less mature phenotype (Chitu and Stanley, 2006).

After full maturation, it seems that GM-CSF is the essential factor for dendritic cell viability and function (Witmer-Pack et al., 1993), and this cytokine is usually held as the classical dendritic cell stimulus (van de Laar et al., 2012). Among the dendritic cell phenotypes, monocyte-derived dendritic cells appear to be the most sensitive to GM-CSF stimulation (Louis et al., 2015).

1.2.5 Pleiotropic effects of CSF-1R signalling

Even though the *Csf1 op/op* and the *Csf1r*$^-$*/Csf1r*$^-$ mice are viable, the importance of the CSF-1-dependent macrophages is indicated by the incapacity of the mutants to develop. Apart from having a crucial role in the immune system, macrophages are important for normal embryonic development and homeostasis (Hume, 2008; Hume et al., 2002). Deficiencies in CSF-1R signalling are evident in the development of the central nervous system (aberrant development of the sex-steroid-hormone feedback response), pancreas (delayed and aberrant morphogenesis), mammary glands (impaired branching

morphogenesis), in weight gain and in the reproductive functions of both sexes. Severe lymphopenia is also seen, as well as an expected monocytopenia, reduced counts of microglia, with a ten-fold decrease in the number of marrow cells (Hume et al., 2002; Kondo et al., 2007; Marks and Lane, 1976; Pollard, 2004; Wiktor-Jedrzejczak et al., 1982). It is noteworthy that CSF-1 also exerts profound effects on pluripotent cell recruitment and differentiation in many tissues (Levine et al., 1998).

In the reproductive system, CSF-1 is an important paracrine factor for normal development. Its receptor may be important for steroid-regulated epithelial maturation (Ide et al., 2002). CSF-1 regulates cells of the trophoblast and other cells in the female reproductive tract via interaction with macrophages. Macrophages in the ovary are needed for correct ovulation rates due to effects in gonadotropin responsiveness and steroidogenesis (Stanley, 2000).

CSF-1R is essential for embryonic implantation in the endometrial epithelium (Stanley, 2000). CSF-1R mRNA is generally increased in the uterus, embryo and placenta between the murine embryonic days 8.5 and 17.5, while CSF-1 mRNA is highly present in the uterus on days 11.5 to 17.5, as explained above (Wei et al., 2010). In the pregnant uterus, CSF-1 is even further upregulated, up to 1000-fold. It is suspected that CSF-1 may contribute to maternal tolerance to the fetus through its capacity of controlling T-cell activation (Sweet and Hume, 2003).

Levels of CSF-1 are also highly upregulated in lactating epithelial cells, and its receptor, which is not expressed in the nonlactating human breast, begins to be expressed by the last trimester of pregnancy. CSF-1 and its receptor can have their expression increased by several times through stimulation with steroid hormones. CSF-1R may contribute to ductal and alveolar development, milk production and remodelling of breast tissue during pregnancy and lactation (Sapi, 2004; Yeung and Stanley, 2003).

Adipocytes also express CSF-1 and are in close contact with macrophages in the adipose tissue. CSF-1 is upregulated in rapidly growing adipose tissues when it is associated with inflammation or even if it is a consequence of overfeeding. The presence of CSF-1 in adipose tissues is down-regulated by the tumour necrosis factor-α (TNF-α). These relationships may be responsible for the weight gain deficiency seen in CSF-1R/CSF-1 knockouts (Levine et al., 1998; Nandi et al., 2006). It has been reported that macrophages can produce insulin-like growth factor (IGF)-1 in response to CSF-1 stimulation, being the major extra-hepatic source of this growth factor and also probably regulating its production by the liver. IGF-1 is regulated by the growth hormone (GH), and negatively feedbacks the

production of GH. It is believed that CSF-1 might interact with the IGF-1/GH axis, and so contribute to the control of postnatal growth and organ maturation (Gow et al., 2010).

Macrophage deficit within the pancreas during maturation is correlated to reduced insulin production throughout development and maturation, coupled with abnormal β-cell islet morphogenesis. This is probably due to the reduced clearance of apoptotic cells in the absence of macrophages and also with the contribution from macrophages in tissue remodelling and adaptation (Banaei-Bouchareb et al., 2004).

In the small intestine, local production of the membrane form of CSF-1 is important for the regulation of Paneth cells. These cells are components of the innate immune system and are CSF-1R^{+}. Although CSF-1R is not expressed by cells of the intestinal crypts, the Paneth cells are physically close to the crypt, and CSF-1-defective animals have reduced crypt proliferation and villi sizes in consequence. The Paneth cells are important for the intestinal stem cell niche, and in their absence the cellular renovation in the intestine is affected (Akcora et al., 2013; Huynh et al., 2009).

Most of the phenotypic defects seen in the *Csf1 op/op* mice, including the reproductive deficiencies and the disturbances in the development of organs, are seen with more intensity in the *Csf1r*$^{-}$*/Csf1r*$^{-}$ mouse (Conway et al., 2008; Dai, 2002; Wiktor-Jedrzejczak et al., 1982). Because of the severe pleiotropic effects of the mutations over the *Csf1* and *Csf1r* genes on the normal development, the mutant animals cannot clarify about the physiologic role of signalling through the CSF-1R in the adult animal (Dai, 2002), and this has to be studied by blocking the receptor with antibodies (Sauter et al., 2014).

Inhibition of the CSF-1R with mAbs demonstrates that the effects of the receptor in many tissues, including in the reproductive tract, are more important over the developmental period than after maturity. CSF-1 and CSF-1R-knockouts have severe defects in the reproductive system due to extensive removal of tissue macrophages. These resident macrophages are in intimate association with Leydig cells in the testes, for instance, and may have a role in steroidogenesis. Accordingly, the knockouts have reduced testosterone levels and low sperm counts. Equally, in the ovary macrophages assist in the regulation of the reproductive cycle (Stanley, 2000). However, prolonged treatment with an anti-CSF-1R in adult animals does not remove macrophages from the uterus, for instance, and although it depletes interstitial macrophages of the testes, it does not affect testosterone and LH production. In the intestine, although mAb treatment removes Paneth cells, it is not correlated with reduced growth of the villi, as occurs with CSF-1/CSF-1R knockouts. Overall, no toxicity arises from blocking CSF-1R in adult animals in the steady-state (Sauter et al., 2014).

Normal microglia require a functional CSF-1R to provide full cerebral development during embryogenesis, at birth and beyond weaning. The loss of CSF-1R causes cerebral architectural perturbations, leading to a defect in the olfactory sense, for instance, and slow response to external stimuli (Erblich et al., 2011). Dominant inactivating mutations in the CSF-1R leads to adult-onset leukoencephalopathy with axonal spheroids and pigmented glia (Stanley and Chitu, 2014). CSF-1R and its ligands are expressed as early as day 11.5 in the brain of murine embryos, as cited before (Wei et al., 2010).

However, CSF-1R is also expressed in a small variety of cells outside the mononuclear phagocytic system, and can modulate these cells directly, even after maturity. Some neurons in the hippocampus and cortex express CSF-1R in the steady-state condition, but the receptor is also upregulated in the neurons after injury. The receptor is believed to be relevant in the protection of neurons against injury and neurodegeneration (Luo et al., 2013). The prostate is another such example of the direct effects of CSF-1R without intermediation by the mononuclear phagocytes. In the prostate epithelium, CSF-1R is expressed during the prepubertal androgen-driven expansion of the gland, declining in older animals (Ide et al., 2002). However, the expression of CSF-1R by neurons or other cells outside the mononuclear phagocytic system and the trophoblast is contested (Sauter et al., 2014).

The relative importance of CSF-1R signalling in tissue development and in maturity is summarized in Table 1.4.

Table 1.4 – The importance of CSF-1R signalling during development and after maturity for the function or phenotype of tissues outside the mononuclear phagocytic system. The relative importance of the signalling axis is shown by the "+", "+/-" or "-" signs. N/A, not applicable. References: (MacDonald et al., 2010; Sauter et al., 2014; Stanley, 2000).

Tissue	Development	Maturity
Prostate	+	-
Testes	+	-
Gut	+	+/-
Liver	+	+/-
Kidney	+	-
Ovary	+	-
Muscle		-
Uterus		-
Placenta	-	N/A
Mammary glands	+	
Brain	+	- (+ inflammation)
Pancreas	+	-
Auditory/visual	+	
Tooth eruption	+	N/A
Weight gain	+	-

1.3 CSF-1R in inflammatory diseases and cancer

Excessive CSF-1R signalling can lead to several diseases, in many of which the disease occurs as a consequence of prolonged activation of mononuclear phagocytes. This can be illustrated by the fact that local autocrine production of CSF-1 in CSF-1R-bearing cells, driven by a transgene, leads to an aggressive inflammatory phenotype with osteoporosis followed by an increase in tissue macrophages (Wei et al., 2006). Several diseases are correlated with such a pathogenic mechanism following CSF-1R activation.

Paget's disease is associated with variants of *CSF1* which increase the expression of that cytokine, lead to bone remodelling, pain and osteoarthritis through excessive osteoclast function (Albagha et al., 2010). CSF-1 and CSF-1R are also correlated to inflammation-dependent diseases, such as atherosclerosis, for instance, in which macrophages play an important role (Murayama et al., 1999), autoimmune diseases (e.g. lupus) and rheumatoid arthritis (Chitu and Stanley, 2006). Presence of macrophages has also been connected to adipose tissue hyperplasia and obesity; adipocytes are CSF-1 producers (Levine et al., 1998; Weisberg et al., 2003).

The retroviral oncogene v-*fms*, present in the McDonough strain of feline sarcoma virus, induces fibrosarcoma growth in domestic cats (Mcdonough et al., 1971). This gene was found to share extensive similarities with c-*fms*, which codes the CSF-1R. The viral and cellular genes differ by 11 amino acids in the C-terminus, and these mutations in the v-*fms* drive constitutive activation, without the need for the receptor ligand (Coussens et al., 1986; Sherr et al., 1985; Wheeler et al., 1986). The finding that the v-*fms* product could drive oncogenesis motivated research on the potential of CSF-1R to also promote cancer formation (Roussel et al., 1987). Even though several differences exist between the cellular and the oncogenic forms of *fms*, overexpression of normal c-*fms* is sufficient to induce a transformed phenotype. Transfection of mammary carcinoma cells with wild-type *CSF1R* confers invasive and tumorigenic potential and *CSF1* enhances ovarian cancer tumourigenesis and metastasis (Kluger et al., 2004; Sapi, 2004; Toy et al., 2009).

Some tumours show increased CSF-1 or CSF-1R expression due to mutations of the respective genes or their regulatory elements. A few haematological conditions are derived from these mechanisms. Chromosomal translocation combining the N-terminus of RNA-binding motif-6 and the C-terminus of CSF-1R can drive megakaryoblastic leukemia, which is characterized by growth of clonal hematopoietic progenitor cells (Gu et al., 2007). Mutations in proteins related to CSF-1R transcription factors lead to overexpression of the receptor, and are important in maintaining stem cells that generate and sustain acute myeloid

leukemia (Aikawa et al., 2010). B-cell-derived Hodgkin's lymphoma and anaplastic large cell lymphoma aberrantly express the CSF-1R due to loss of expression of a repressor, CBFA2T3 (Lamprecht et al., 2010).

However, a number of cancers outside the haematological system are also associated with CSF-1R or CSF-1 expression. CSF-1 is suggested to be a valuable biomarker for a great number of cancers, including pancreatic, colorectal, breast and ovarian cancers, and generally predicts prognosis more effectively than other commonly used biomarkers. Higher expression of CSF-1 or of its receptor is associated with worse outcomes, but in many cases it is not yet certain if high levels of this factor are the cause or the effect of neoplasia (Douglass et al., 2008; Khatami, 2007). The role of CSF-1 in cancer progression is best demonstrated by the fact that *op*/*op* mice have a 60 % reduction in malignant transformation when compared to normal mice, having much reduced mitotic index in carcinomas (Nowicki et al., 1996).

In some tumours, high CSF-1 or CSF-1R expression is due to increased cancer cell production of these proteins. CSF-1R and CSF-1 can be associated with tumour growth via autocrine or paracrine pathways, therefore not requiring mutations in the receptor to elicit continuous signalling (Kluger, 2004; Lin et al., 2001; Patsialou et al., 2009). In mammary cells and in mammary cancers, CSF-1R and CSF-1 expression can be driven by lactogenic hormones, such as insulin, prolactin and glucocorticoids. Prolactin and glucocorticoids are linked to mammary tumours, presenting a possible explanation for the frequent increase of CSF-1R and CSF-1 in those cancers. In the lactating human breast, interestingly, the levels of CSF-1 and of its receptor are comparable with the levels observed in carcinomas (Chambers, 2009; Sapi, 2004).

Examples of other tumour types in which the cancer cells express CSF-1R include prostatic, ovarian, lung, endometrial and trophoblastic cancers. In these cases, there is no or little expression of CSF-1R/CSF-1 in normal tissues, and these proteins are upregulated in malignancies. In prostatic cancers the overexpression of CSF-1 is such that there is a propensity to produce bone metastases with extensive bone resorption, likely due to osteoclast activation. In this type of cancer, CSF-1R is important for the survival of tumour-initiating cells (Bauknecht et al., 1993; Chambers, 2009; Ide et al., 2002).

The mechanisms driving CSF-1R/CSF-1 expression in non-haematological tumours are likely to be variable. A small cellular subpopulation within tenosynovial giant cell tumours (TGCT) and also within pigmented villonodular synovitis (PVNS) have a translocation resulting in fusion of *COL6A3* and *CSF1* genes, generating high levels of CSF-1. The remaining cells of the tumour do not produce CSF-1, but do express its receptor,

stimulating the growth of the tumour mass (Cassier et al., 2014; Cupp et al., 2007; West et al., 2006). In renal clear cell carcinomas there are increased copies of the chromosomal *CSF1R*, offering an explanation for the increase of CSF-1R in that malignancy (Soares, 2007). Gene regulation of CSF-1 and CSF-1R production in cancers is also likely to occur post-transcriptionally, where microRNAs (miRNAs) are known to play a role. In chemotherapy-resistant ovary cancer cells, several miRNA are downregulated, and in the case of miR-130a, this leads to increased production of CSF-1 (Chambers, 2009; Sorrentino et al., 2008). In ovarian cancer *CSF1* transcripts also have prolonged stability with an extended half-life (Chambers and Kacinski, 1994). The increased levels of *CSF1* transcripts in ovarian cancer lead to higher CSF-1 protein expression (Ramakrishnan et al., 1989). GAPDH is a RNA-binding protein that is upregulated in several ovarian cancer specimens. It has been shown to stabilize the mRNA of CSF-1 (Chambers, 2009). HuR, also an RNA-binding protein, increases the expression of CSF-1R in breast cancer cells. HuR is necessary for glucocorticoid-induced CSF-1R overexpression by these cells (Woo et al., 2009). Accordingly, HuR expression is linked with metastasis and reduced survival (Chambers, 2009).

The phosphorylation pattern following CSF-1R activation varies in epithelial cells when compared to macrophages, indicating that the signal may be different between these cells (Kacinski, 1997; Welsch and Nagasawa, 1977). In breast carcinoma, the phosphorylation of Tyr809 in the CSF-1R kinase domain is associated with local invasiveness, while phosphorylation of Tyr723 leads to metastatic potential in both breast and ovary carcinomas (Toy et al., 2001). Following receptor phosphorylation, $ERK_{1/2}$ is activated in breast cancer cells, leading to cell proliferation (Morandi et al., 2011). In these cells, CSF-1R can also be located in the nucleus, where it binds to the promoters of the proliferation-related genes *CCND1*, *c-JUN*, *c-MYC* and also to the promoter of *CSF1*, inducing its overexpression (Barbetti et al., 2014).

Despite the roles that CSF-1R signalling has in inducing tumour growth by direct activation of receptors on the cancer cells, CSF-1R also has another important role in promoting cancer. Clinical data and experimental studies have determined the pro-tumorigenic and metastatic potential of tumour-associated macrophages (TAMs), for which CSF-1R signalling is evidently essential (Lewis and Pollard, 2006).

1.4 Tumour-associated macrophages (TAMs)

Cancer malignancy is determined by a progressive acquisition of characteristics that enable continuous tumour growth. Some of the traits that lead to such a phenotype are self-sufficiency from external stimuli, resistance to apoptosis and to obstructive signals, evasion from immunity, neoangiogenesis to support growth, the capacity to invade surrounding tissues and to metastasize (Laoui et al., 2014). Monocyte and macrophage infiltration occurs throughout the development of a tumour, from early stage nodules to late-stage metastatic cancers. Thus, solid tumours contain a significant population of infiltrating myeloid cells. Migration of leucocytes into tumours was first interpreted as evidence of an immunological response of the host against the tumour. However, most cancers have been found to be non-immunogenic, and even further, tumours incite macrophages to participate in every process implicated with cancer progression (Lewis and Pollard, 2006; Ohno et al., 2004).

1.4.1 Entry of TAMs and their initial steps – neovascularization

The production of inflammatory factors (cytokines, prostaglandins, among others) associated with tumour growth creates a microenvironment that is responsible for recruiting and activating leukocytes, particularly the cells of the myelomonocytic lineage. The angiogenic vascular endothelial growth factor (VEGF), produced by cancer cells, is also responsible for increased chemo-attraction of monocytes, both towards primary tumours and metastatic foci. However, macrophage infiltration can be independent of the local presence of neoangiogenesis. Foreign macrophages are derived from blood monocytes and can be recruited to the tumour site by the 'CC' chemokines CCL2, CCL3-5, CCL8, by VEGF, by stromal-derived factor-1 (SDF-1) and by CSF-1 (Sica et al., 2006; Wang et al., 2012). CSF-1-deficient mice have impaired tumour vascularization, denoting the importance of this cytokine in this context (Nowicki et al., 1996).

TAMs are correlated with high vascular grades in many tumour types, and macrophage infiltration precedes vigorous angiogenesis (Lin et al., 2006). Macrophages induce the production of angiogenic factors as an adaptation response to the hypoxia in the tumour environment. Hypoxic areas of the tumours appear when the cell mass outgrows neoangiogenesis. Rapid tumour growth leads to areas of low vascular supply and attraction of TAMs due to the necrotic debris emanating from these areas; TAMs are debris-scavengers. Therefore, spots of low pH and higher lactate concentrations stimulate proangiogenic gene expression in TAMs. Hypoxia induces the expression of hypoxia-

inducible factors (HIF-1 and HIF-2) in TAMs, which in their turn drive upregulation of genes encoding angiogenic proteins (Doedens et al., 2010; Lewis and Murdoch, 2005; Ramanathan et al., 2007).

These newly arrived leukocytes promote, therefore, further angiogenesis. Blood vessels produced in the absence of macrophages are fragile and not fully formed. Macrophages stabilize and physically participate in the endothelial lining of new vessels. Monocytes and macrophages can show endothelial and myofibroblast phenotypes and allow the formation of vessels that withstand higher shear forces (Ito and Khmelevski, 2003; Jabs et al., 2005; Okazaki et al., 2005; Pujol et al., 2000; Saba, 1970; Schmeisser et al., 2001). The production of new blood vessels by macrophages can rely on or be independent of VEGF. In women with endometriosis, macrophages are capable of eliciting further endothelial cell proliferation through VEGF. Macrophages can be sensitive to oestrogen and progesterone signalling to enhance the production of VEGF in these patients (McLaren et al., 1996). Other pro-angiogenic factors produced by macrophages include angiopoietins (Ang1 and Ang2), CCL2, thymidine phosphorylase, CXCL8 and COX-2. Interestingly, TAMs that express the angiopoietin receptor Tie2 are more aggressive modulators of tumour behaviour than $Tie2^-$ TAMs (Sica et al., 2012). The expression of MMP may also support angiogenesis by stimulating endothelial cell proliferation and migration (Lewis and Pollard, 2006; Polverini and Leibovich, 1984). siRNA targeted to CSF-1 or CSF-1R reduces human mammary cancer xenografts in mice through a reduction of recruitment of macrophages to tumours and down-regulation of MMP-2 and MMP-12. In this siRNA model, CSF-1R-mediated reduction of MMP in the tumour is one explanation for slower progression of the cancer, since it contributes to tissue remodelling and angiogenic activity (Aharinejad et al., 2004). Because of the capacity of macrophages to induce blood vessel formation through a wide set of signals, after treatment of tumours with inhibitors of VEGF signalling there follows a period of renewed vascular formation (Priceman et al., 2010).

Macrophages are capable of not only neoangiogenesis at the tumoural site, but also of lymphangiogenesis, offering another route for cancer metastasis. $CD11b^+$ macrophages are capable of forming tubular structures that express several markers of lymphatic endothelium. Lymphangiogenesis may normally be induced by VEGF and IL-1β, whose production is stimulated by CSF-1 (Maruyama et al., 2005).

The formation of a high-density vessel network is associated with the cancer progression to malignancy, and infiltrating macrophages in primary mammary tumours regulate both vessel formation and subsequent malignancy traits, such as loss of tissue architecture. Very importantly, the size of a tumour is not a determinant of the formation of

new vessels and malignancy, whereas the presence of macrophages is (Lin et al., 2006; Mantovani et al., 2008; Priceman et al., 2010).

There is still some debate on the mechanics that drive macrophage-induced angiogenesis. While the consensus is that hypoxia attracts TAMs, as presented above, another group suggested that hypoxia reduces the expression of CSF-1, and that macrophages tend to localize in the invasive zones of the tumour, where oxygen concentration is higher. Murine macrophages also show reduced ability to migrate under hypoxic conditions, which corroborates the hypothesis that TAM function would be more pronounced in the oxygenated tumour margins (Green et al., 2009). It is known that the localization within a tumour affects the response of macrophages. Just as low pH and necrosis attract TAMs, these, and other factors, influence TAMs to collaborate further with tumour growth.

1.4.2 Not all TAMs are made the same – the M1 and M2 phenotypes

TAMs can have varying localizations within a tumour and possess different characteristics in each. TAMs along the invasive tumour margin or near necrotic foci, in hypoxic areas, produce angiogenic factors which lead to poor prognosis, as described above. In contrast, TAMs in strict contact with cancer cells may produce cytotoxic mediators leading to cancer cell death (Ohno et al., 2004). In endometrial cancer, TAMs are preferentially positioned along the invasive margins, in necrotic foci and in the tumour stroma, but can also be found within the tumour nest (embedded between cancer cells). While presence of TAMs in the nest reduces tumour relapse, being thus correlated with good prognosis, TAMs in the hot-spots (the necrotic foci) are associated with tumour aggressiveness and relapse, and TAMs in the margin are linked to immunosuppression. Therefore, localization of the macrophages inside a tumour is relevant for determining their roles (Lewis and Pollard, 2006; Ohno et al., 2005, 2004; Sica et al., 2006).

Even the sites of CSF-1 production within the tumour have been associated with different outcomes (Chambers et al., 1997). Curiously, macrophages appear to possess cytotoxic effects against tumours which have the membrane isoform of CSF-1 (mCSF-1), but not the secreted isoform (Jadus et al., 1996). The cytotoxic activity of macrophages against mCSF-1^{+} tumour cells might corroborate the finding that TAMs in close contact with cancer cells are able to eliminate them, instead of contributing to tumour growth (Jadus et al., 1996; Lewis and Pollard, 2006). Also, the balance of the CSF-1 isoforms by the tumour could affect the response created against the malignancy (Chitu and Stanley, 2006).

Therefore, it is clear that in the appropriate environment macrophages can show anti-tumour activity (Baldwin et al., 1993). However, to achieve anti-tumour effects, macrophages must be stimulated into what is called the M1 classical phenotype, which is activated by microbial products and IL-12, TNF, GM-CSF or interferon-γ, most of which are not found in the tumour hot-spots (Chitu and Stanley, 2006).

The cellular phenotype of tumour-associated macrophages is commonly denominated as "M2". The M2 phenotype is stimulated by signals coming from regulatory T cells or from the tumour cells, which secrete CSF-1 with other cytokines that lead to inhibition of the cytotoxicity of TAMs. Some of the cytokines involved in M2 cell formation, besides CSF-1, are IL-10, IL-4, IL-6, MDF, TGF-β1 and prostaglandin E_2 (PGE_2) (Hagemann et al., 2009; Lewis and Pollard, 2006; Sica et al., 2006). CSF-1R signalling itself is capable of inducing higher sensitivity to IL-4, an M2 driver (Caescu et al., 2015). Whereas M1-activated macrophages would lead to cancer cell killing, the M2-type of activation leads to angiogenesis, tissue remodelling and an immune suppressing phenotype (Sica et al., 2006).

More specifically, M2 macrophages can be subdivided into M2a cells, differentiated under the influence of IL-4/IL-13, especially in parasitic diseases; M2b, formed with immune complexes; and M2c cells, an anergic state, prompted by IL-10; this cytokine induces a process of apoptosis of macrophages before they can ever be activated and cytotoxic. It is evident that in the tumour site these cytokines that drive M2 subtypes are not found in isolation and, indeed, their interactions are important for many biological effects. Thus, macrophages grown in the presence of tumour-secreted factors express M2 characteristics which interpolate between the three M2 subsets: TAMs are stimulated by IL-4 and produce IL-10, with the capacity of carrying out Fc-dependent antitumour functions. Because of this varied phenotype, a new name for the TAM activation state has also been proposed, M2d, although it is not commonly used (Duluc et al., 2009). Because the formation of M1 and M2 characteristics in uneven throughout the tumour, some macrophages are also likely to receive conflicting signals, displaying pro- and anti-tumoural characteristics in rapid succession (Grugan et al., 2012; Jenkins et al., 2013; Joimel et al., 2010; Kataki et al., 2002). The M1-M2 cellular characteristics are illustrated in Figure 3.1, Chapter 3.

Therefore, inside tumours and in the presence of M2-inducing characteristics, such as CSF-1 signalling, TAMs can have immunosuppressive roles which are otherwise physiologically important for wound repair and injury resolution. Interleukin-4, IL-10, IL-13, glucocorticoids and transforming growth factor (TGF)–β upregulate the expression of a set of molecules in macrophages that enables them to take part in the resolution of inflammatory reaction, tolerance induction and "organ formation", such as during placentation (Biswas and Mantovani, 2010; Bronte et al., 2001). Indeed, many of the mechanisms used by TAMs in assisting tumour progression are reflected by "repair macrophages", such as the production of VEGF, nitric oxide (NO) and TNF (Park and Barbul, 2004). However, although beneficial in other contexts, these mechanisms have a role in tumour development (Erreni et al., 2011). The characteristics are presented in Figure 1.7.

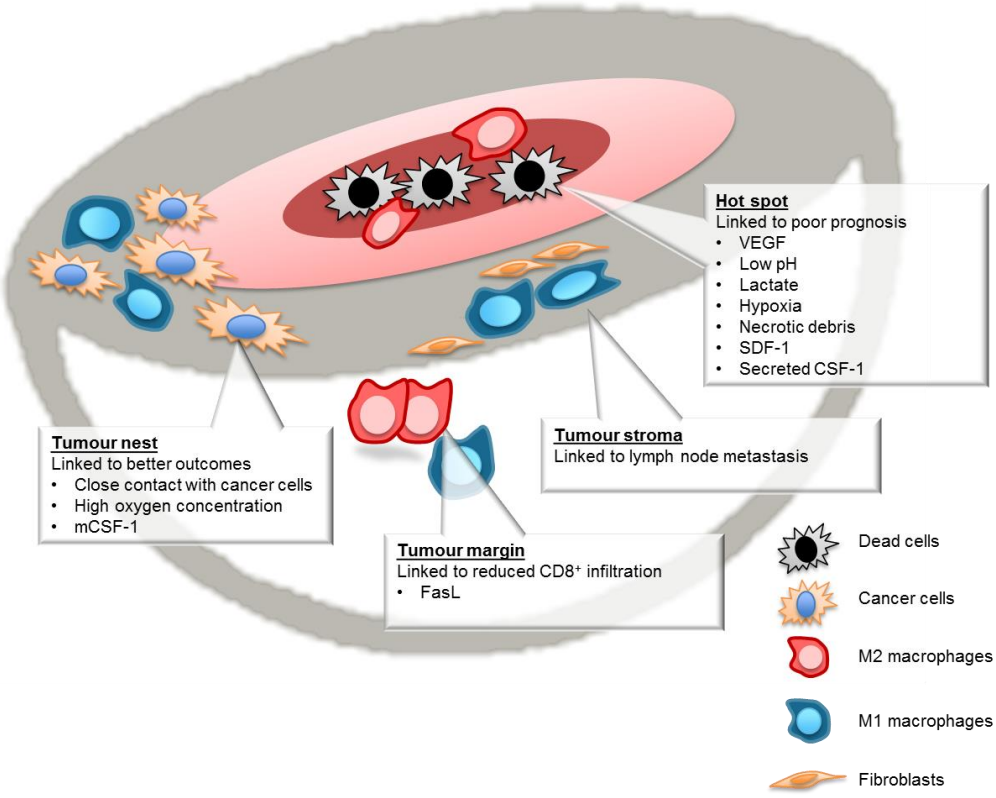

Figure 1.7 – Effects of TAM distribution inside tumours. The tumour compartments are named in bold caption. The effect of TAMs in each compartment and the tumoural factors modulating TAMs are cited inside the boxes. References: (Chambers et al., 1997; Ohno et al., 2005, 2004; Wang et al., 2012).

1.4.3 TAMs and cancer growth

Once inside the tumour and under its influence, TAMs can contribute to cancer cell proliferation and the creation of new hypoxic areas, perpetuating of a circle of formation of more M2 TAMs and further cancer growth. Cancer cell mitotic genes are promoted through the macrophage-induced production of several factors, among which EGF, platelet-derived growth factor (PDGF), TGF-β1, hepatocyte growth factor and basic fibroblast growth factor (bFGF) (Lewis and Pollard, 2006). Another important factor for direct cancer proliferation is CSF-1R, as discussed in section 1.3. In breast cancers, CSF-1R expression is associated with larger tumour size and decreased patient survival (Kluger, 2004). Placenta-derived growth factor (PlGF), produced in breast cancers, can promote the survival of TAM, which will, in their turn, induce more CSF-1R production by cancer cells (Król et al., 2012; Sica et al., 2006).

1.4.4 TAMs and metastases

Metastasis has been demonstrated to require autocrine and paracrine signalling through CSF-1R, and requires macrophages for optimal invasion. A paracrine loop occurs between macrophages and cancer cells. Macrophages secrete epidermal growth factor (EGF), which acts on the EGF receptor (EGFR), expressed by carcinoma cells. The cancer cell, in its turn, secretes CSF-1, which acts both on CSF-1R on its own surface as well as on receptors on the macrophages. This signalling then drives tissue invasion through increased carcinoma mobility. Eighty percent of cancer cell movements occur near macrophages, reflecting the biological significance of the paracrine interaction between these cells (Patsialou et al., 2009; Wyckoff et al., 2007).

Intravasation (movement of cancer cells into blood vessels) occurs preferentially in sites where macrophages are found. Many macrophages are found in association with tumour blood vessels and decreasingly throughout the stroma. The invading macrophages are associated with a vessel either as isolated motile cells or in clusters of around 3 macrophages. Cancer cells migrate towards perivascular macrophages, which contribute with intravasation of cancer cells (Wyckoff et al., 2007). Targeting neoangiogenesis may be in itself an interesting approach to cancer therapy, as the expression of angiogenic factors has been associated with prognosis in several tumours (Bamias and Dimopoulos, 2003). However, the number of tumour perivascular macrophages is more important for intravasation than the number of vessels (Wyckoff et al., 2007). The physical interaction

between carcinoma cells, macrophages and endothelial cells predicts the development of systemic haematogenous metastases in breast cancer (Robinson et al., 2009).

Naturally occurring breast cancers confirm the experimental data linking macrophages to metastases. The presence of CSF-1 and infiltration of macrophages into the primary tumour accelerates the malignant transformation to the late carcinoma stages. The absence of CSF-1, on the other hand, delays the development of invasive, metastatic carcinomas (Lin et al., 2001). As is common in the literature involving CSF-1, its responsibility in metastasis is also not unanimous. It has been seen that *in vivo* administration of CSF-1 to mice with metastatic murine melanoma increased the number of macrophages and that metastatic lesions were reduced (Hume et al., 1989).

Macrophages contribute to cancer spread not only through circulatory dissemination. Normal tissue invasion may also be facilitated by presence of TAMs and stimulation through CSF-1R. Activation of this receptor in macrophages and the subsequent IL-1β production induces high expression of MMP-2 and MMP-9 as well as of urinary plasminogen activator (uPA), which in brief terms generates plasmin; MMPs and plasmin are extracellular proteases (Lewis and Pollard, 2006; Michel and Quertermous, 1989). These proteases break the basement membrane of the tumour, thereby prompting their escape into the surrounding tissue and promoting deregulated growth. In cervical cancer, CSF-1R is linked with invasiveness and severity, alongside VEGF and COX-2 (Hammes et al., 2008). CSF-1 is capable of inducing more protease activity and tumour invasiveness of surrounding tissue than GM-CSF or G-CSF (Lewis and Pollard, 2006; Pei et al., 1999).

TAMs can also induce cancer cells to directly produce proteases. TGF-β1 produced by the TAMs stimulates the production of MMP-9 by glioma cells with stem-cell properties, which then can promote tissue invasion (Ye et al., 2012). TGF-β1 is a known regulator of cancer epithelial-mesenchymal transition (EMT). The interaction between CSF-1R and TGF-β1 controls a switch between proliferation and invasion in some breast cancer cells. Through EMT, epithelial cells de-differentiate, acquiring stem cell-like characteristics and motility. These de-differentiated cancer cells have better abilities to metastasize and to invade (Katsuno et al., 2013; Patsialou et al., 2015). Thus, through the production of TGF-β1, TAMs simultaneously assist in breaking tumour barriers and in the formation of an invasive cancer phenotype.

1.4.5 TAMs and immunosuppression – effects over lymphocytes

Contrarily to TAMs, tumour-infiltrating lymphocytes are usually linked to better immune responses against the cancer and, therefore, to improved prognosis. As an example, a low lymphocyte to macrophage ratio is linked with poorer prognosis in Hodgkin's lymphoma (Koh et al., 2012). In their "wound-repair" M2 mode, macrophages limit lymphocyte survival and function within the tumour (Park and Barbul, 2004). Some of the mechanisms used by TAMs to limit lymphocyte action are listed here.

Suppressor macrophages found on tumour-bearing hosts are down-regulated for MHC II molecules. The increase in immature MHC II^- macrophages results in reduced antigen-presenting capacity, which favours tumour progression through decreased lymphocyte activation. More than that, MHC II^- macrophages exert a direct cytotoxic and suppressor activity against T lymphocytes, as a result of increased secretion of PGE_2, NO, H_2O_2, reactive oxygen intermediates, arginase-1 and TNFα (Bak et al., 2008; Bronte et al., 2001).

Upon contact with activated lymphocytes, but not when in contact with inactivated cells, TAMs induce T cell death through the production of NO. IFNγ and TNF produced by the activated T-lymphocytes cooperate to induce macrophage killing of T cells (Saio et al., 2001). The production of IFNγ and TNF by lymphocytes is, in fact, a stimulus to create M1 macrophages (Duluc et al., 2009). For some reason, within the tumour these cytokines activate the inflammatory potential against the lymphocytes themselves. The outcome of NF-κB activation in macrophages (which controls IFNγ responses, for instance) can be quite different depending on the context in which it is being activated. NF-κB stimulation during the onset of inflammation is associated with the expression of inflammatory genes (e.g. NOS_2), while NF-κB activation during the resolution phase of inflammation results in the expression of anti-inflammatory genes (e.g. TGF-β1) and a M2 activation state. The vast variety of signals (from necrotic cell debris to hypoxia) derived from tumours may act on regulating macrophages through NF-κB to eliminate lymphocytes (Hagemann et al., 2009).

NF-κB activity is reduced in TAMs due to defective nuclear translocation of its subunits; this transcription factor is important for the production of inflammatory signals, for instance. Following an inflammatory stimulus, M2 cells favour the signal transducer and activator of transcription 1 (STAT1) transcription factor, leading to the preferential expression of immunosuppressing cytokines. In the same situation, M1 macrophages produce inflammatory cytokines through NF-κB (Biswas et al., 2006; Saccani et al., 2006). In follicular lymphoma, it is suggested that the expression of the STAT1 is involved in the

inhibition of T cell function; indeed, the expression of STAT1 was shown to reduce the survival rate (Álvaro et al., 2006).

Myeloid-derived suppressor cells (MDSC) are immature myeloid precursors that also affect host immunity during cancer. These cells are M2-differentiated and accumulate in lymphoid tissues, instead of the tumour itself. Their roles and the mechanisms they use for reducing immune responses against the tumour are very similar to those of TAMs. In these cells, mouse paired immunoglobulin-like receptors (PIRs) have been found to be important for STAT and NF-κB signalling pathways. Myeloid cells ablated for PIR-B tend to develop into M1 cells, leading to reduction of T-regulatory lymphocytes (Treg), reduced tumour growth and metastases (Ma et al., 2011). In PIR-B-deficient animals, the growth of Lewis lung carcinoma is diminished, implying an important role for this molecule in cancer immunosuppression (Sica et al., 2012).

Prostaglandins are highly produced in TAMs as a consequence of the abnormal metabolism of arachidonic acid. TAMs have high activity of 15-lipoxygenase-2 (15-LOX2), involved in the arachidonic acid pathway. Interestingly, production of IL-10 by TAMs is dependent on the activity of 15-LOX2. IL-10, which is anti-inflammatory, is also responsible for suppression of adaptive immunity and antitumor responses. In this way, TAMs stimulate the creation of Treg, inducing the T-regulatory cell transcription factor forkhead box P3 (FOXP3) and the co-inhibitory cytotoxic T-lymphocyte antigen 4 (CTLA-4) (Daurkin et al., 2011). In turn, Tregs are capable of feedback reinforcement of the transformation of macrophages into the M2 phenotype, therefore creating more immunosuppressive TAMs (Biswas and Mantovani, 2010).

CSF-1 plays a direct role in immunosuppression. As cited before, this cytokine is seen as the counterbalance to GM-CSF (Sierra-Filardi et al., 2014). CSF-1-conditioned monocytes inhibit mitogen- and antigen-stimulated T cell proliferation through a mechanism involving T cell starvation of tryptophan caused by the enzyme indoleamine 2,3-dioxygenase (IDO) (Biswas et al., 2006; Bronte et al., 2001; Sica et al., 2006; Sweet and Hume, 2003). Although CSF-1R can increase immune responses against pathogens by stimulation of macrophages, it can also reduce antigen-specific and mitogen-induced T lymphocyte proliferation or macrophage stimulation of T lymphocytes (Sakurai et al., 1996; Sester et al., 1999). Unfortunately, CSF-1R blockade also upregulates T cell inhibitory molecules such as CTLA-4, reducing beneficial effects of this form of therapy. Therefore, there is a synergistic effect in blocking both CSF-1R and CTLA-4 (Zhu et al., 2014).

1.4.6 TAMs and immunosuppression – effects over dendritic cells

Most dendritic cells in tumours are not in a fully differentiated state, which occurs after M1 activation (Sica et al., 2006). Mature dendritic cells seem to be limited to peritumoral areas in breast carcinomas, while immature dendritic cells are found infiltrating breast carcinoma tissue (Bell et al., 1999). Immature dendritic cells prime $CD4^+$ or $CD8^+$ lymphocytes to produce IL-10, which is a driver of M2 phenotypes (Bronte et al., 2001). Imiquimod, a TLR7 agonist, is currently being tested for cancer treatment by selective stimulation of the innate immune response, which enhances the maturation of dendritic cells (Sternberg et al., 2011).

1.4.7 TAMs and resistance to therapy

Macrophages have been shown to increase cancer resistance to several treatment modalities. In prostate cancer models, inhibition of CSF-1R enhances the response to radiation therapy. Irradiation recruits the DNA damage-induced kinase ABL1; it binds to the *Csf1* promoter and induces protein expression, which then counteracts the treatment by increasing cancer growth through the mechanisms discussed above in the presence of TAMs (Laoui et al., 2014; Xu et al., 2013). A similar effect has been seen also following chemotherapy treatment (DeNardo et al., 2011). Chemotherapy resistance in prostate cancer can be predicted by high circulating levels of IL-4, IL-6 and macrophage inhibitory cytokine 1 (MIC1), which recruit and alter the phenotype of TAMs into M2 characteristics (Mahon et al., 2015). Inhibiting CSF-1R and CCR2 improves chemotherapy results in prostate cancer not only by the direct effect of decreasing TAMs, but also by inhibiting the effects of TAMs on the survival of stem-like tumour-initiating cells through STAT3 activation (Mitchem et al., 2013). Macrophage-derived STAT3 and IL-6 have also been incriminated in pancreatic ductal adenocarcinoma, promoting the survival of stem cells following chemotherapy (Jinushi et al., 2011; Ruffell and Coussens, 2015).

Following chemotherapy treatment of breast cancer, there is macrophage infiltration and cathepsin protease production by the TAMs. Cathepsin increases cancer cell resistance to several chemotherapeutics (Shree et al., 2011). Cathepsins are produced by TAMs in response to IL-4 stimulation in several tumour types, such as pancreatic islet cancers, mammary tumours, and lung metastases (Gocheva et al., 2010). Chemotherapy-driven cathepsin release stimulates IL-1β production by macrophages and the consequent generation of a regulatory immune response through T lymphocyte-derived IL-17 (Bruchard

et al., 2013). Because IL-17 and IL-1β also drive IL-6 production in several cancer cell lines, cathepsin could also be associated with STAT-3 activation (Ruffell and Coussens, 2015). Cathepsin also regulates the trafficking of vesicles containing TNF-α. Production of TNF-α by TAMs can occur from NF-κB or STAT3 activation. TNF-α has been correlated with cancer resistance to MAPK pathway inhibitors (Ruffell and Coussens, 2015; Smith et al., 2014).

Other general effects of TAMs which may promote treatment resistance include extracellular matrix deposition and remodelling, and cell-cell interactions (Ruffell and Coussens, 2015).

A positive factor of the presence of TAMs is the improvement of outcomes following antibody treatment. While IL-10 suppresses the expression of MHC II on the surface of macrophages, it also stimulates the presence of CD16. An increase in CD16 is also caused by CSF-1. The expression of CSF-1 is highly increased in the recovery phase of bone marrow hypoplasia induced by chemotherapy (Kimura et al., 1992). Accordingly, human patients recovering from myelosuppressive chemotherapy show also an increase in the expression of CD16, with a reduced expression of CD14 (MacEwen and Kurzman, 1996). The role of CD16 is to send survival signals to macrophages when coupled to IgG. In this way, IL-10 suppresses macrophages in healthy tissues, but favours accumulation and activation of macrophages when in the presence of antibodies (Wang et al., 2001). This may justify why after combined treatment with rituximab (an anti-CD20 mAb) and chemotherapy, high TAM content was linked with better prognosis, while TAM content predicted poor prognosis in untreated patients (Taskinen et al., 2007). Other works have confirmed the capacity of M2 TAMs to induce antibody-dependent cell cytotoxicity against cancer cells (Grugan et al., 2012).

An overview of the effects of TAMs on the cancer hallmarks of malignancy is shown in Figure 1.8.

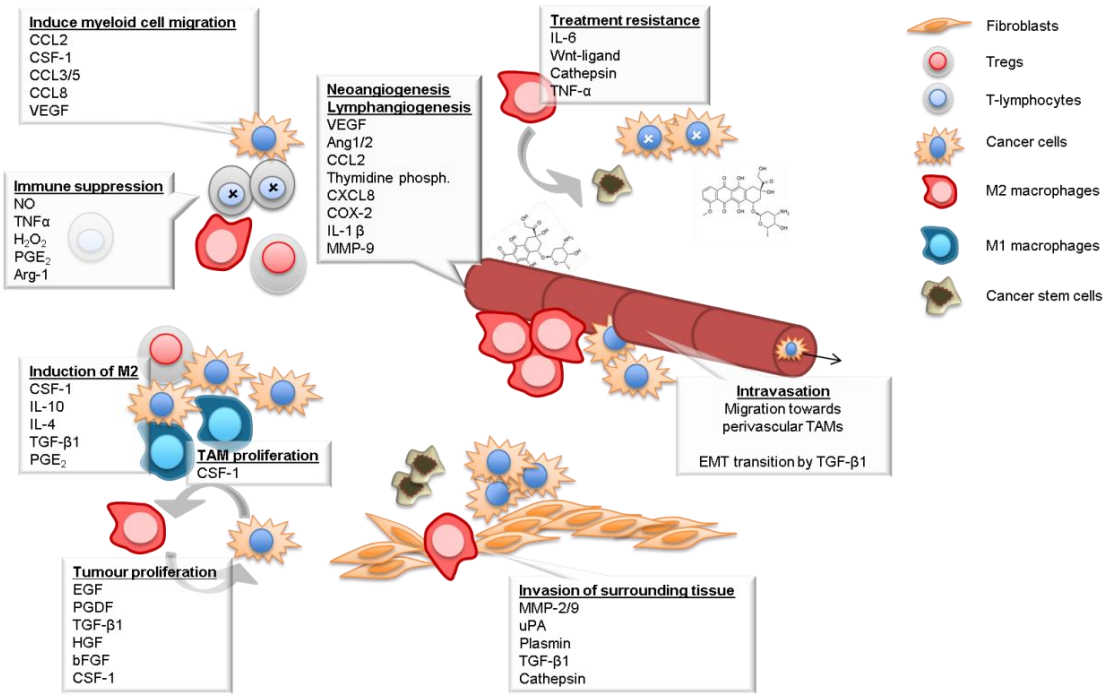

Figure 1.8 – Tumour-promoting effects of TAMs. The cancer hallmarks of malignancy influenced by TAMs are denoted in bold caption. The factors mediating the effect of TAMs in each hallmark is shown inside the boxes. References: (Allavena et al., 2008; Bonde et al., 2012; Gocheva et al., 2010; Grugan et al., 2012; Lewis and Pollard, 2006; Mitchem et al., 2013; Shree et al., 2011; Sica et al., 2006; Wyckoff et al., 2007). Chemotherapy is represented by the molecular structure of doxorubicin ("Doxorubicin2DCSD" by Fuse809 (talk)). Licensed under Public Domain.

1.5 CSF-1R as a target

The abundant evidences that macrophages are required for tumour growth in cancer patients and in experimental models suggests that depleting this cellular population could generate clinical benefit. Because of the crucial roles of CSF-1R in the survival and function development of cells of the mononuclear phagocytic system and of cancer cells themselves, this receptor is a candidate target for a new anti-tumour drug (Hume and MacDonald, 2012). Below, strategies for CSF-1R inhibition are discussed.

1.5.1 CSF-1R as a target – receptor tyrosine kinase inhibitors

Small-molecule inhibitors of receptor tyrosine kinases (RTKi) are currently one of the most pursued anticancer therapeutics (J. G. Moffat et al., 2014). RTK are related to carcinogenesis and cancer progression in three different ways: firstly, many kinases can become directly involved in cancer transformation. Through the occurrence of mutation or translocation, kinases develop into an oncogenic form, essential for tumour survival and/or proliferation, such as is seen in feline fibrosarcomas induced by the v-*fms* form of mutated CSF-1R (Wheeler et al., 1986); secondly, kinases can be located in signalling pathways downstream of oncogenes or be activated by other oncogenes, and even though not in themselves oncogenic, they become necessary for cancer survival. This is seen in acute myeloid leukaemia due to deregulation of CSF-1R transcription factors (Aikawa et al., 2010); thirdly, the kinase can be expressed in tissues that are peripheral to the tumour, and may be required for tumour formation or maintenance in the host. For the latter, examples would be receptors important for the development of blood supply to the tumour, such as VEGFR or again CSF-1R (Zhang et al., 2009).

Toceranib phosphate (Palladia, Pfizer), one of such RTK inhibitors, has been used in veterinary medicine with some success in treating several tumour types (London et al., 2009). Toceranib is a non-specific inhibitor of vascular endothelial growth factor receptor, platelet derived growth factor receptor (PDGFR), c-Kit and other kinases. In clinical trials, toceranib phosphate has shown clinical relevance mainly in dogs with mast cell tumours which contain a driving mutation in the c-Kit receptor (London et al., 2009; Yancey et al., 2010). In this case, toceranib falls into the category of acting on kinases directly involved in cancer through oncogenic mutations. However, the inhibitor still seems to possess activity against tumours which are negative for the c-Kit mutations. Clinical response can also be observed in several other tumours, such as thyroid carcinoma and osteosarcoma, especially when in combination with other treatment modalities (Carlsten et al., 2012; Chon et al., 2011; London et al., 2012, 2009, 2003).

Mast cells and monocytes are derived from the same early precursor cells (Kirshenbaum et al., 1999), and c-Kit is also a RTK of known similarities to CSF-1R, especially in the tyrosine kinase region; PDGFR is, as has already been described in this text, from the same family of receptors as CSF-1R (Qiu et al., 1988; Yeung and Stanley, 2003). Therefore, at least part of the response of toceranib is derived from inhibiting kinases that help to support the tumour growth, such as CSF-1R. Other inhibitors of c-Kit are also known to inhibit CSF-1R (Mashkani et al., 2010).

Several other RTKi are being currently developed or tested for oncologic treatment. Masitinib mesytilate, for instance, has also been used in veterinary medicine, with relative success in oncologic therapy, both in dogs and cats, also in various cancer types. Special interest in using this drug is also given for mast cell tumours, or in investigations of VEGF inhibition (Conway et al., 2008; Marech et al., 2014).

The inhibitor effects of 3-amido-4-anilinoquinolines, of 3-amido-4-anilinocinnolines and of bisamides, among others, have just recently been identified, all with highly selective activity against CSF-1R. The anilinoquinoline inhibitor has had success in reducing TAM in a breast cancer xenograft model (El-Gamal et al., 2010; Scott et al., 2009, 2011; Wall et al., 2008).

GW2580 is one of the most specific kinase inhibitors for CSF-1R. It can inhibit CSF-1-induced expression of IL-6 by monocytes and macrophages (Conway et al., 2005; Kitagawa et al., 2012). By affecting TAMs, GW2580 could reduce tumour evasion of chemotherapy, avoid metastasis and immunosuppression (Mitchem et al., 2013; Priceman et al., 2010).

Advantages of kinase inhibition of CSF-1R include the fact that it does not interfere with the clearance of CSF-1, since the uptake of the ligand and receptor internalization does not require the kinase function. Most antibodies blocking CSF-1R interfere with this process (see more below); increased circulating CSF-1 causes a rebound effect when inhibitory antibody treatment is discontinued. Also, kinases are more likely to block autocrine signalling through CSF-1R, which are less accessible to antibodies (Hume and MacDonald, 2012).

However, a disadvantage of RTKi is the occurrence of adverse effects. These can derive from cross reactivity between kinases, since inhibitors can have variable selectivity to a specific kinase. Most inhibitors block the ATP-binding sites on the kinases, and since these sites are well conserved among several receptors, even inhibitors with considerate selectivity can block various kinases at the same time. Some of the reported side-effects are neutropenia, proteinuria, increase in serum creatinine concentration, myocardial degeneration, and with the greatest number of reports, gastrointestinal disorders (Aguirre et al., 2010; Daly et al., 2011; London et al., 2009). Curiously, it has been found that inhibition of c-Kit with small-molecules in human gastric sarcomas induces M2 macrophage polarization (Cavnar et al., 2013). Therefore, if using a RTKi against CSF-1R that cross-reacts with c-Kit, this adverse effect can be generated.

1.5.2 CSF-1R as a target – TLR agonists

The down-regulation of CSF-1R on the cell membrane after contact with LPS or other TLR agonists could be an alternative to impede macrophages from exerting the immunosuppressive effects of CSF-1R signalling (Sester et al., 1999). TAMs are mostly incapable of producing IL-12, a pro-inflammatory cytokine, even after LPS activation. Instead, the cytokines produced by tumour macrophages tend to create T regulatory cells (Treg) which suppress effector T cells and monocytes (Porta et al., 2009; Ruffell and Coussens, 2015). It is reported that defective activation of NF-κB in TAMs correlate with the impaired expression of M1 cytokines, and so restoration of the NF-κB would therefore impact on the cellular profile that is activated (Biswas et al., 2006; Sica et al., 2006). A combination of an IL-10R blocking antibody and of TLR9 agonists (which are NF-κB activators) switches infiltrating macrophages from M2 to an M1 phenotype, and the innate response triggered is capable of debulking large tumours within 16 hours (Kawai and Akira, 2007; Sica et al., 2006). TLR4 and TLR7 agonists have also been tested as anti-cancer agents, inducing higher IL-12 production from macrophages and demonstrating usefulness in combination with chemotherapy. It is believed that LPS increases the cytotoxicity of macrophages in close contact with cancer cells (in the tumour "nest") (Hirota et al., 2010; Sawachi et al., 2010; Sternberg et al., 2011).

Even though LPS or other TLR agonists reduce CSF-1R expression, they are able to maintain cell viability probably by activation of $ERK_{1/2}$, while obviously impeding cell signalling through CSF-1R. TLR agonists are reported to increase the time macrophages remain in secondary lymphoid organs, raising the probability of a macrophage activating circulating T cells. In summary, the presence of pathogen-associated molecular patterns such as LPS and other TLR agonists may contribute towards more efficient antigen-presenting cells (an M1 activation state), instead of the immunosuppressive macrophages that result from CSF-1 signalling (an M2 activation state). These M1 activated cells are potent effector cells, capable of killing tumours (Sester et al., 1999). Confirming this prediction, LPS is capable of inducing the maturation of dendritic cells, which are potent antigen presenters (Palucka et al., 1998).

The interaction between CSF-1R and TLR agonists is not simple, however. Cells pre-stimulated with CSF-1 produce more IL-6, IL-12 and TNF-α (mostly M1 markers) when in contact with LPS, a TLR4 agonist, but suppressed the same response to CpG DNA, a TLR9 agonist. As stated before, CSF-1 suppresses the expression of various TLRs, except for TLR4 (Sweet and Hume, 2003). Also, IL-6 produced by CSF-1 can have pro- or anti-

inflammatory effects, depending on the activity of suppressor of cytokine signalling 3 (SOCS3) (Yasukawa et al., 2003), adding more levels of control over the final phenotype after TLR regulation. Therefore, using TLR agonists can have conflicting effects over macrophage activation in several different situations, depending on other factors. Indeed, the use of a TLR agonist in bladder cancer can have various outcomes, being subject to the tumour microenvironment. BCG, a TLR agonist, has long been used as an adjuvant in the therapy of bladder cancer. However, instead of BCG modulating the phenotype of the TAMs, an extensive infiltrate of M2 macrophages seems to limit the therapeutic potential of BCG (Suriano et al., 2013).

1.5.3 CSF-1R as a target – antibodies

Several antibodies have been tested against CSF-1R and its ligands. The use of antibodies against the receptor is especially relevant because of the existence of two ligands for CSF-1R (Chihara et al., 2010). Targeting the receptor instead of its ligand also has the advantage of avoiding the issue of the short half-life of the ligands (10 min for CSF-1). When blocking CSF-1, constant high levels of blocking antibody need to be maintained in the circulation to suppress its functions (Wei et al., 2005). However, anti-CSF-1R antibodies have been found that are able to inhibit only CSF-1 or IL-34 binding to the receptor, due to variations in the contact residues on the surface of CSF-1R between the ligands (Chihara et al., 2010).

Despite the disadvantages of blocking the ligands, an anti-CSF-1 monoclonal antibody (mAb) is capable of retarding tumour growth by 40 %. In combination with CMF chemotherapy (cyclophosphamide, methotrexate, 5-fluorouracil), the growth of a breast cancer xenograft was retarded by 56 %. Angiogenesis, MMP expression and macrophage recruitment are all down-regulated by this treatment (Paulus et al., 2006).

The evaluation of mice treated with anti-CSF-1R antibodies reinforces the idea of the functional heterogeneity of the monocytes/macrophages and provides a unique treatment option in which tissue populations of macrophages can be selectively depleted. Animals that received anti-CSF-1R antibodies are healthy throughout the experiments, and circulating monocytes are mostly kept at stable levels during the period. Some anti-CSF-1R antibodies are capable of depleting resident subsets of macrophages without affecting inflammation, while still preventing lesions that were derived from the selective accumulation of macrophages, including tumours. Thus, at least in the state of developmental maturity of an individual, there is markedly little impact on the use of antibodies over the animal, and this

may represent an optimal approach to modulate macrophage responses within tumours *in vivo* (Haegel et al., 2013; MacDonald et al., 2010; Murayama et al., 1999; Sauter et al., 2014).

Side effects of CSF-1R signalling inhibition with antibodies are usually seen only during the embryonic period or soon after birth. When an antibody against CSF-1 was administered to mice in the immediate post-natal period, osteopetrosis was induced, as well as depletion of macrophages, reduced growth rate, among other signs that indicate blocking of the CSF-1 function, similarly to what is seen in the knockout animals. Osteoclast suppression was not maintained as animals grew older, possibly because of the action of IL-34 (Wei et al., 2010, 2005). In *op*/*op* mice, tooth eruption is completely annulled due to the absence of osteoclasts, which reabsorb alveolar bones around developing teeth. To produce the same effect by injection of antibodies specific to CSF-1R, the drug has to be administered from embryonic day 15.5 until postnatal day 12.5 (Yoshino et al., 2003).

In adult animals, it has also been reported that immunity against a *Listeria monocytogenes* infection could be annulled when an antibody against CSF-1R was administered (Gregory et al., 1992). However, blockade of CSF-1R signalling does not necessarily block macrophage tissue function because tissue resident cells are able to proliferate in the presence of IL-4, independently from CSF-1R (Jenkins et al., 2013). Also, some predecessor dendritic cell populations do not express CSF-1R and are able to replenish all dendritic cell subsets subsequently (Araki et al., 2004; MacDonald et al., 2005; Palucka et al., 1998).

A possible setback of antibody blockade of CSF-1R is the accumulation of circulating ligands, since their clearance occurs after binding to the receptor. With the receptor competitively bound by the antibody, CSF-1 accumulates in the circulation, and when antibody concentration decreases, a rebound effect might occur (Hume and MacDonald, 2012). To circumvent this, an antibody has been identified that is capable of blocking CSF-1R while still allowing the internalization of the receptor and removal of the ligand from the circulation (Haegel et al., 2013).

The main characteristics of the CSF-1R-modulating therapies cited here are shown in Figure 1.9.

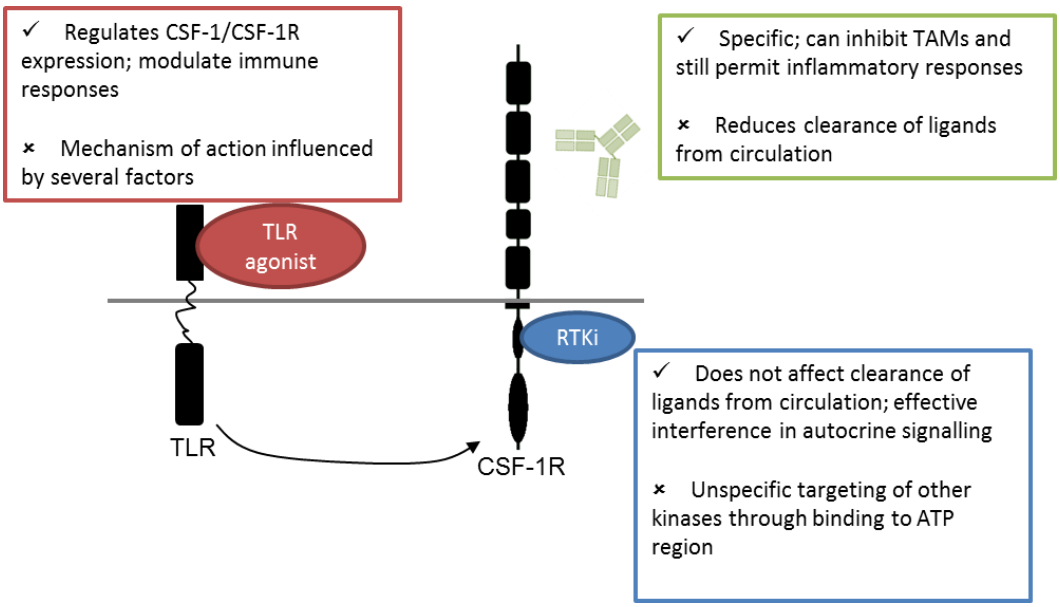

Figure 1.9 – Advantages (✓) and disadvantages (×) of CSF-1R-modulating therapies. The modulators shown are TLR agonists, receptor tyrosine kinase inhibitors (RTKi) and antibodies. References: (Haegel et al., 2013; Hume and MacDonald, 2012; Jenkins et al., 2013; Sester et al., 1999; Sica et al., 2006; Yasukawa et al., 2003).

1.6 The dog as a model to study cancer

Not only in human malignancies have macrophages been associated with poor prognosis. Malignant canine mammary tumours have more macrophages than benign masses. When considering only canine malignant tumours, macrophages also associate with more aggressive phenotypes. Presence of TAMs correlates with skin ulceration and histological types, for example (Król et al., 2011; Raposo et al., 2012).

Research on cancers of veterinary interest does not only regard the better care of animal patients, but also serves as a model for human diseases (Reichert and Dhimolea, 2012). Despite the large investments for the development of new therapeutic monoclonal antibodies, few have been produced for use in the treatment of cancer in dogs. The first ever monoclonal antibody against cancer was targeted against canine lymphoma, in 1996, but was withdrawn from the market a few years later for lack of efficacy (Jeglum, 2009). More recently, anti-CD20, anti-EGFR and anti-CD52 monoclonals have been produced against canine targets (Acharya et al., 2015), but this is only a small fraction of the work being conducted against human cancer targets (Killick et al., 2015).

There are many characteristics in canine cancer that make it amenable for use as a model in the study of human cancer. Dogs possess the closest telomere biology compared to humans: they have similar telomere size and telomerase activity (Nasir et al., 2001); spontaneously arising canine cancer shows many genetic similarities to human cancers; the cancer-associated genes in dogs show great similarities to those of humans; there are greater similarities between canine and human proteins than between murine and human; cancer develops in canine patients with a functional immune system, as in humans and in opposition to many mouse models; there is great genetic diversity between animals and breeds, which can be useful in translational medicine, as drugs act differently in different genetic backgrounds; dogs and humans share the same environment and also some of carcinogens in these spaces, such as cigarette smoke; dogs are kept until old age and frequently treated with a high level of medical care (Rowell et al., 2011). Indeed, clinical studies in dogs have shown that they serve as good predictors of both clinical toxicity and response to therapy (London et al., 2009; Paoloni and Khanna, 2008).

It is consequently expected that dogs will become increasingly important as models in the study of human cancer, hopefully decreasing the costs, the attrition rates and the disappointing results when drugs reach human trials (Paoloni and Khanna, 2007; Riccardo et al., 2014). Also, the increasing restrictions in the use of laboratory animals (RCUK, 2015) may turn the attention of researchers towards naturally-occurring disease models – such as dogs – for pre-clinical trials.

1.7 Aim

CSF-1R is important for the dissemination and progression of cancer. Blocking this receptor impedes macrophage tumoural invasion and phenotypic alteration into M2 cells. It is also likely to affect the CSF-1R autocrine-mediated malignant transformation of cancer cells. Therefore, the aim of this project was to generate antibodies that blocked signalling of the canine CSF-1R with the purpose of treating cancer.

The specific objectives of this project were:

1) To analyse the interaction of cancer cells and macrophages *in vitro* and to characterize the importance of CSF-1R signalling for the cross-talk between these cells in the context of canine cancer.
2) To generate monoclonal antibodies against the canine CSF-1R by immunization of mice with recombinant proteins. It was intended that several IgG clones

against CSF-1R would be created by hybridoma fusions to ensure that blocking antibodies could be identified.

3) To test the capacity of the monoclonal antibodies in affecting CSF-1R signalling, as well as to test other parameters of antibody binding. The antibodies were expected to block CSF-1R-dependent cell survival with high specificity and affinity.
4) To produce speciated antibodies that could potentially be used for clinical testing in dogs. These speciated mAbs should maintain antibody blocking properties when compared to the mouse antibodies while preventing immunogenic reactions by increasing the level of caninisation of the molecule.

These objectives are explored in the following chapters.

Chapter 2

Materials and Methods

2.1 Reagents

Reagents specific for a method are detailed in the method section of each chapter. Names of kits, equipment and other supplies are registered trademarks of the respective companies. Details of manufacturers are shown below.

Agilent, Santa Clara, US; Amersham, a GE Healthcare company; Becton Dickinson (BD), Franklin Lakes, US; Biochrom, Cambridge, UK; Bioline, London, UK; Cole-Parmer, Vernon Hills, US; Corning Life Sciences, Acton, US; Dako, Fort Collins, US; eBioscience, San Diego, US; Eppendorf, Hamburg, Germany; Fisher, Hampton, US; Fluka, a Sigma-Aldrich company; Gibco, a ThermoFisher Scientific company; Grant, Cambridge, UK; GraphPad Software, San Diego, US; Greiner, Kremsmünster, Austria; Invitrogen, a ThermoFisher Scientific company; Life Technologies, Paisley, UK; Miltenyi Biotec, Cologne, Germany; New Brunswick, an Eppendorf company; New England Biolabs, Beverly, US; Peprotech, Rocky Hill, US; Pfizer Animal Health, New York, US; Progen Biotchnik GmbH, Heidelberg, Germany; R&D Systems, Minneapolis, US; Roche, Basel, Switzerland; Sigma-Aldrich, St. Louis, US; SLS, Hessle, UK; Sorvall, a Thermo Scientific company; Southern Biotech, Birmingham, US; Starlab, Milton Keynes, UK; Stemcell, Vancouver, Canada; Sterilin, a ThermoFisher Scientific company; ThermoFisher Scientific, Waltham, US; TreeStar, Ashland, US; Vector Laboratories, Burlingame, US.

Unless stated otherwise, 15 and 50 ml plastic tubes were from Greiner. Small (0.5 and 1.5 ml) tubes were from Eppendorf. Pipette tips were from Starlab. In most instances, centrifugations of 0.5 and 1.5 ml tubes were done using the centrifuge 5415R (Eppendorf); 15 ml and 50 ml tubes were centrifuged using 5810R (Eppendorf). Larger (250 ml) flasks were centrifuged using RC6 floor centrifuge (Sorvall). Reagents were weighed using L2200S+ or BP210D (Sartorius) balances.

Throughout the thesis, basic chemicals used were: NaCl, KCl, Na_2CO_3, H_2SO_4, SDS, ethanol, methanol, isopropanol, xylene, glycerol, urea, glacial acetic acid, Tris base,

NaH_2PO_4, glucose (Fisher); Hepes, BSA, H_2O_2, $Na_2S_2O_3$, Na_3PO_4, $NaHCO_3$, NH_4Cl, EDTA, KH2PO4, acetone, formaldehyde, paraformaldehyde, glycine, skimmed milk powder, DTT, NP-40, DOC, PMSF, Tris-HCl, $MgCl_2$ (Sigma); Tween 20 (SIS); Tryptone, yeast extract, peptone, sucrose (Fluka); PEG6000 (Millipore); BactoAgar (BD); Triton X-100 (Thermo Scientific); $AgNO_3$ (VWR).

2.2 General use solutions

All solutions were made with distilled water. The potential hydrogen (pH) of solutions was measured using a 7-easy pH meter (Mettler Toledo). The pH meter was calibrated using three solutions of standard pH (10, 7 and 4).

PBS: NaCl (137 mM), KCl (2.7 mM), Na_2HPO_4 (10 mM), KH_2PO_4 (1.8 mM), pH 7.2. This was prepared by the Central Service Unit at the Roslin Institute.

PBST: PBS containing Tween 20 (0.05 %).

2.3 Microbiological techniques

All techniques were carried out using sterile plastic consumables under aseptic conditions. Bacterial plates, plastic universal tubes by Sterilin. Plate spreaders and inoculation loops by VWR. Bacterial shakers were usually Innova 4330 or Innova 4000 (New Brunswick). Autoclaving was performed by the Central Service Unit at the Roslin Institute.

2.3.1 Bacterial media

Luria-Bertani (LB): tryptone (1 %), NaCl (1 %), yeast extract (0.5 %). For agar plates, agar was added at 1.5 %. The mixture was sterilized by autoclaving. This was prepared by the Central Service Unit at the Roslin Institute.

2xTY: peptone (1.6 %), yeast extract (1 %), NaCl (5 %). For agar plates, agar was added at 1.5 %. The mixture was sterilized by autoclaving.

SOC medium: tryptone (2 %), yeast extract (0.5 %), NaCl (10 mM), KCl (2.5 mM), The mixture was sterilized by autoclaving. Sterile glucose (at 20 mM final concentration) and $MgCl_2$ (at 10 mM) were added aseptically to the autoclaved solution. This was prepared by the Central Service Unit at the Roslin Institute.

Top agar: 2xTY medium containing 7.5 g of agar/litre.

Antibiotics (Sigma) for bacterial selection were ampicillin (used at 100 µg/ml), carbenicillin (75 µg/ml), tetracycline (12 µg/ml) and kanamycin (25 µg/ml). Stocks at 1000 × the working concentration were made by diluting the powder in 50 % glycerol and filter-sterilizing (0.22 µm) the solution. Stocks were kept at – 20°C and were added to media which were at less than 60°C.

2.3.2 Transformation of bacterial chemically competent cells

Two microliters of plasmid (either ligation or cloning product) were added to the bottom of a 15 ml plastic tube (Greiner). Chemically competent cells *E. coli* Bronze Efficiency (Bioline), Top10 (Invitrogen), JM109 or BL21 (DE3) (Agilent) were thawed on ice from – 80°C and 100 µl were added to the tube on top of the plasmid drop. The contents were gently mixed by agitation and kept on ice for 45 min. The tube was heat-shocked at 42°C in a water bath for 45 sec and placed back on ice for 2 min. SOC medium (900 µl) at room temperature was added to the bacterial cells. The mixture was placed in an orbital incubator at 37°C, agitating at 200 rpm, for 1 h. One hundred microliters were plated with disposable plastic spreaders onto agar plates containing the appropriate antibiotics for selection. The remaining 900 µl were spun at 1000 × *g* for 5 min. The supernatant was discarded and the bacterial pellet was plated in a second agar plate with 100 µl of media. The plates were incubated overnight at 37°C.

2.3.3 Bacterial glycerol stocks

Overnight bacterial cultures containing plasmids of interest were diluted 1:1 in LB medium containing 20 % sterile glycerol. The stock was maintained at – 80°C. When needed, the stock was stabbed with a sterile microbial loop, which was streaked on an agar plate containing the necessary antibiotic. The plate was then incubated overnight at 37°C and individual colonies were picked for liquid growth.

2.3.4 Bacterial liquid cultures

Single bacterial colonies were grown overnight at 37°C with shaking at 225 rpm in a 25 ml plastic tube containing 5 ml of the necessary medium with antibiotic. High copy plasmids were grown in LB medium and low copy plasmids were grown in 2xTY medium.

For larger culture volumes, the initial culture was diluted 1:50 to the larger volume of media. Flasks had at least 4 times the volume of the liquid contents to permit aeration of the culture.

2.3.5 Measuring optical density

Optical density of bacterial cultures was measured by adding 1 ml of the culture into transparent disposable cuvettes. A blank control was made by adding 1 ml of sterile culture media into another cuvette. These were inserted in the spectrophotometer (WPA Biowave, Biochrom) and the light transmittance was measured at 600 nm.

2.3.6 Electrocompetent XL-1blue

Protocol from (Martineau, 2010). XL-1blue was picked from a commercial stock (Agilent) and grown overnight on LB agar containing tetracycline at 37^{o}C. A single colony was picked and grown overnight in 10 ml of 2xTY with tetracycline. The contents of this initial inoculum were poured into a 5 l flask containing 1 l of 2xTY and tetracycline. The culture was grown shaking at 200 rpm until OD_{600nm} = 0.7. The culture was poured into 4 × 250 ml centrifuge flasks and cooled down on ice for 30 min, regularly mixing the bottles. These were centrifuged at 5000 × *g* for 5 min at 2^{o}C. The supernatant was discarded. A cold and sterile magnetic bar was added to each bottle. The bottles were filled with 250 ml of cold de-ionized water with Hepes (1 mM). The pellet was resuspended using the magnetic stirrer. After all pellets were broken, the tubes were centrifuged as above for 10 min. The supernatant was discarded and water with Hepes was added again, repeating the steps above. The pellet was then resuspended 25 ml in cold glycerol (0.1 %) with Hepes (1 mM). The contents of the 4 bottles were collected into a new bottle without the magnetic stirrer. This was centrifuged as above for 15 min and the supernatant was discarded. The pellet was resuspended in 1 ml of cold glycerol with Hepes using a 10 ml pipette. If not used, the bacteria were aliquoted, snap frozen in dry ice and stored at – 80^{o}C until used.

2.3.7 Sonication

Bacterial cultures were sonicated either in 15 ml or 50 ml plastic tubes using a microtip ultrasonic processor (Misonix). Amplitude of sonication was regulated to allow the formation of visible cavitation bubbles while avoiding foaming. The microtip did not touch

the sides of the tubes. The bursts of sonication were followed by maintaining the samples for at least 10 sec on ice.

2.4 Molecular biology techniques

Thermal cycling was performed using G-Storm (Labtech). Electrophoresis of proteins or genetic material was performed using equipment from Bio-Rad.

2.4.1 Plasmid preparations

For plasmid minipreparations, 5 ml (10 ml for low copy plasmids) of bacterial liquid cultures containing the desired plasmid were centrifuged at 3000 × *g* for 5 min. The supernatant was discarded. The plasmid was then purified using QIAprep Spin Miniprep Kit (Qiagen). Briefly, the protocol consists of 1) alkaline lysis of bacterial cells; 2) lysate clearing by rapidly neutralizing the alkaline buffer and centrifugation of precipitates; 3) adsorption of plasmid DNA on a silica membrane with high salt concentrations; 3) washing with ethanol to remove non-specifically bound DNA; 4) eluting plasmid from membrane with Tris-Cl (10 mM), pH 8.0.

For larger scale plasmid maxipreparations, 150 ml cultures were grown overnight and the plasmids were purified using the HiSpeed Plasmid Kit (Qiagen).

Plasmid concentration in the elution fraction was quantified using a Nanodrop spectrophotometer (Thermo Scientific). Plasmids were stored at – 20^{o}C.

2.4.2 mRNA extraction and reverse transcription (RT)

Messenger RNA (mRNA) from cultured cells was extracted from the cells using QIAshredder columns (Qiagen), spinning 10^7 cells at full speed for 2 min in the RLT lysis buffer from RNeasy Mini Kit (Qiagen). Animal tissues were stored in RNAlater (Life Technologies) at room temperature for 6 h and then at – 20^{o}C. For RNA extaction, the tissues were placed in RLT buffer and disrupted with the Lysis Matrix plastic beads (MPBio) in a FastPrep FP120 machine (Thermo Scientific). The protocol of RNA extraction from this kit consists of: 1) lysis of the samples in a highly denaturing buffer, as described above; 2) addition of ethanol to increase binding to the silica membrane; 3) binding to the silica membrane after spinning the samples through the column; 4) on-column digestion of contaminant DNA (using the DNase Free Set, Qiagen); 5) removal of contaminants by

washing; 6) elution of mRNA with 30 µl of RNase-free water. mRNA concentration was measured using a NanoDrop spectrophotometer (Thermo Scientific). RNA was stored at –80^{o}C.

Reverse transcription was performed using either Omniscript RT Kit (Qiagen) or M-MLV RT Kit (Promega). Omniscript RT was carried out by mixing the following reagents: 10 x Buffer RT; dNTP (to 0.5 mM of each dNTP, Promega); Specific primers (to 0.5 µM)/Random nonamers (to 10 µM, Sigma); RNase inhibitor (10 units, Promega); Omniscript reverse transcriptase (4 units); template RNA (1 µg); water to 20 µl. Unless stated otherwise, the reaction was incubated for 60 min at 37^{o}C.

2.4.3 Polymerase chain reaction (PCR)

PCR primers are mentioned in each chapter separately. In primer design, it was attempted to maintain the Tm temperature among the pair and to avoid primer hairpins, self-dimers and heterodimers that involved the 3'-end of the sequence. When not obtained from the literature, primers were designed manually and the parameters mentioned were quantified using the IDT OligoAnalyzer online program (https://www.idtdna.com/calc/analyzer). Primers were produced by Eurofins Genomics.

2.4.4 Agarose gels

Gel concentration varied according to the size of the product to be resolved. Products up to 300 bp were resolved in 2 % agarose. From 300 bp to 1500 bp gel concentration was 1.5 %. Bigger products were resolved in 1 % agarose. Gels were made by dissolving the agarose powder (UltraPure Agarose, Invitrogen) at the stated concentrations in TAE buffer (40 mM Tris, 20 mM acetic acid, and 1 mM EDTA). The mixture was heated in a microwave until gel was completely dissolved. Gel Red (Biotium) was added from 10000 × stock. Gel was then poured into mould and left to set. Samples were prepared by mixing with 6 × Loading Dye (to 1 ×, Promega). Ladders with bands of known size were 100 bp DNA ladder or 1.5 Kb DNA ladder (Promega). Five microliters of the DNA ladders were mixed with loading dye. Ladder and samples were loaded into the gel and ran at 80 V until the samples were satisfactorily resolved.

2.4.5 Gel extraction and PCR clean-up

Gel extractions were carried out using QIAquick Gel Extraction Kit (Qiagen). Bands were visualized in the gel using a Safe Imager Transilluminator (Invitrogen). Bands were cut using disposable scalpel blades. Weight was reduced to 0.4 g/purification. Followed manufacturer's protocol for gel extraction of the DNA. PCR clean-ups were carried out using Wizard SV Gel and PCR Clean-Up System (Promega).

2.4.6 Sequencing

Product was diluted to 600 ng of plasmid in 30 µl of nuclease-free water or between 20 – 2000 ng of PCR product in 30 µl of water, depending on the product size. Primer was diluted to 3.2 µM. Samples and primers were sent to Dundee DNA Sequencing and Services, University of Dundee, Dundee, Scotland.

2.4.7 DNA digest and ligations

Digests are described individually in each chapter. After digests of PCR products destined for ligations, samples were cleaned-up to remove the unwanted digested fragments. Plasmids were gel purified for the same purpose. Clean-up was performed as described elsewhere in this chapter. Ligation concentrations were calculated with the formula below. Vector mass was usually 50 ng.

$$\boldsymbol{Insert\ mass\ (ng) = 3 \times \frac{insert\ length\ (bp)}{vector\ length\ (bp)} \times vector\ mass\ (ng)}$$

Ligation reaction was: Vector (50 ng), insert (as calculated above), ligase buffer (to 1 ×), T4 DNA ligase (1 U), nuclease-free water (to 10 µl). Reagents from Promega.

2.5 Tissue culture techniques

2.5.1 Cell lines

The cell lines used throughout the work are described in Table 2.1.

Table 2.1 – Cell lines used throughout the thesis.

Cell name	Description
Ba/F3	Murine bone marrow pro-B cell
CHO-K1	Chinese hamster ovary
CHO-K1-S	Suspension adaptation of CHO-K1
DH82	Canine histiocytic sarcoma
HEK293T	Human embryonic kidney
Lilly	Canine inflammatory mammary carcinoma
MCF-7	Human mammary carcinoma
NIH/3T3	Mouse fibroblast
RAW264.7	Mouse macrophage
REM134	Canine mammary carcinoma

2.5.2 Maintenance of cell lines

Cells were maintained in an incubator (HERA cell 150i, Thermo Scientific) at 37^{o}C and 5 % CO_2 in a humidified atmosphere. Unless stated otherwise, cells were grown in tissue culture treated disposable plates (Thermo Scientific). Disposable plastic pipettes were used for cell culture (Corning). Cell culture manipulations were performed within a BioMat 2 Class 2 Biological Safety cabinet (CAS). Media were stored at 4^{o}C and were warmed to 37^{o}C before use in JB Aqua18 Plus waterbath (Grant).

All cell media were supplemented with 10 % fetal bovine serum (FBS, Gibco), penicillin/streptomycin (100 U/ml, Gibco) and L-glutamine (2 mM, Gibco) unless stated otherwise. REM134 (Else et al., 1982), MCF-7 (European Collection of Cell Cultures, 86012803), Lilly (a gift from Dr R. de Maria, University of Turin, Italy), RAW264.7, Human embryonic kidney (HEK) 293T, Chinese Hamster Ovary (CHO)-K1 (American Type Culture Collection) were maintained in Dulbecco's Modified Eagle's Medium (DMEM) media (Gibco). DMEM contained 4 mM l-glutamine, 4.5 g/L glucose, 1.0 mM sodium pyruvate.

Bone marrow-derived macrophages (BMDMs), osteoclasts and Ba/F3 cells were maintained in Roswell Park Memorial Institute medium (RPMI). RPMI contained 2 mM l-glutamine, 4.5 g/l glucose, 10 mM HEPES [N-2-hydroxyethylpiperazine-N′-2-ethanesulfonic acid], 1.0 mM sodium pyruvate. Culture supplements were as above with the addition of amphotericin B (2.05 µg/ml, Fungizone, Invitrogen).

Cell subculture of adherent cells was made by trypsinization, with the exception of the BMDMs. At 80 – 90 % confluence, the culture supernatant was removed by aspiration. Cells were then washed by PBS, added slowly to the culture. This was removed by aspiration and Trypsin-EDTA (0.25 %, Gibco) was added to the cells (around 1 ml was added to 75 cm^2 plates. Volume was adjusted accordingly to other culture sizes). Cells were placed in the

incubator for 2 min (10 min for RAW264.7 cells). Adherent cells and clumps were broken by repetitive pipetting with 5 ml of media. Cells were plated at the desired densities and media was added to the required volume.

BMDM were resuspended by repeated vigorous jets of media using a 10 ml syringe and a 20 gauge needle (Becton Dickinson).

RAW264.7 cells used for flow cytometry were resuspended by scraping the plate with a disposable plastic cell scraper (Becton Dickinson). The scraper was gently moved along the plate until all cells were detached.

Suspension CHO-K1-S cells were passaged by transferring the desired amount of cells into fresh media. When media needed to be replaced (assessed by colour and cell survival), the necessary volume of culture was spun at 100 × g for 10 min and the supernatant was replaced for fresh media.

2.5.3 Determination of cell viability

Detached or suspension cells were diluted 1:1 with Trypan blue dye (Gibco). The mixture was visualized in a Neubauer counting chamber (SLS). The live cells (not stained by the Trypan dye) in the central 5 × 5 square were counted. Cell number was calculated by the following formula:

$$\boldsymbol{Cells/_{ml} = Cells\ in\ central\ square\ \times 2\ (dilution\ factor) \times 10^4}$$

2.5.4 Freezing and thawing cells

Cells were frozen by resuspending 2 x 10^6 cells in 500 µl of ice-cold FBS (Gibco). A solution of FBS + DMSO (20 %) was then added dropwise to the cells, to a final volume of 1 ml. Cells were placed in cryovials (Corning) and placed on ice. The vials were frozen overnight in a – 80^{o}C freezer, inside a Mr. Frosty Freezing Container containing isopropanol (Thermo Scientific). The following day the cells were transferred to a – 150^{o}C freezer for prolonged stock.

To revive frozen cells, the vials were placed in a water bath at 37^{o}C until most of the contents were defrosted. The cells were transferred to a 15 ml tube and warm media was added dropwise (to 10 ml). This was centrifuged at 300 × g for 5 min, the supernatant was removed and cells were plated in a 20 cm^2 bottle with 5 ml of media.

2.5.5 Lipofection

Lipofection was performed with Lipofectamine 2000 (Invitrogen). For this, cells were grown overnight in antibiotic-free medium with 10 % FBS (Gibco). For transfection of a single well from a 24-well plate, cells were grown in 500 µl of media to 90 % confluence. OptiMEM (Gibco) was used for diluting the lipofection complexes. Lipofectamine 2000 (1.75 µl) was added to 25 µl of OptiMEM. The plasmid DNA (0.5 µg) was added to another tube with 25 µl of OptiMEM. These were kept at room temperature for 5 min, after which both volumes were mixed and incubated for 20 min. The Lipofectamine/plasmid mixture was gently pipetted into the cell culture media. Unless stated otherwise, the cells were maintained with the lipofection complex until cells or medium were used.

2.5.6 Bone marrow derived macrophages (BMDM)/osteoclasts

Canine or feline bone marrows were isolated from animals euthanized at the Royal (Dick) School Small Animal Veterinary Hospital. Samples were collected from animals from the Edinburgh Dog and Cat home euthanized for humane reasons. Femur was collected and kept on ice. In a tissue culture hood, the epiphyses of the bone were removed by sawing and the marrow was flushed several times using 20 ml of RPMI medium + EDTA (5 mM). This was centrifuged for 400 × *g* for 10 min, the supernatant was removed and red blood cell lysis buffer was added ($KHCO_3$ (10 mM), NH_4Cl (155 mM), EDTA (0.1 M), filter sterilized). This was left for 5 min on ice, then 45 ml of PBS were added and the tube was centrifuged. Twenty-four millilitres of RPMI were added to the cell pellet. Cells were grown in culture with the addition of rhCSF1 (20 ng/ml, Invitrogen) in three bacterial 100 mm plates/bone marrow (non-culture treated) (Sterilin). For the formation of osteoclasts, cells were cultured in normal tissue culture plates with rhCSF-1 (10 ng/ml, R&D Systems) and rhRANKL (30 ng/ml, R&D Systems). Macrophages were expected to survive on non-bacterial plastic (Sasmono et al., 2003). After two days, the culture media from the initial 3 plates was passaged on to new plates to allow space for floating cells to adhere. All plates were cultured until the macrophage phenotype had developed (around 10 days).

2.5.7 Endpoint cellular proliferation

Cell viability was assessed using CellTiter-Glo kit (Promega) following the manufacturer's recommendations. Briefly, the cell culture plate and the kit reagents were

allowed to stabilize to room temperature for 1 h. The two kit reagents were mixed and 100 µl were added to each well. The plate was inserted into the Victor3 plate reader (Perkin Elmer). The plate was shaken for 10 min, and the luminescence was allowed to stabilize for 2 min. The luminescence was read at 1 sec/well.

2.6 Protein methods

2.6.1 Nickel affinity purification

Ni-NTA affinity was performed by adding the resin (Qiagen) to plastic 12 ml Poly-Prep columns (Bio-Rad). The storage buffer was allowed to drain and the resin was washed with Binding buffer (Hepes (100 mM), imidazole (10 mM), NaCl (500 mM), pH 7.75). The solution containing the His-tagged protein was then mixed with the resin and incubated at 4^{o}C for 1 h. The solution was allowed to drain through the column containing proteins that did not bind to the resin. The unbound fraction was collected for analysis. Non-specific binders were removed by washing the column thrice with 20 × the column volume of washing buffer (Hepes (100 mM), imidazole (50 mM), NaCl (500 mM), pH 7.75). The desired protein was then eluted from the column in four fractions of 1 × column volume of elution buffer (Hepes (100 mM), imidazole (500 mM), pH 7.75).

2.6.2 Protein quantification

For protein quantification using the Bradford assay, 200 µl of the ready-made reagent (QuickStart Bradford reagent, Bio-Rad) were added to 18 wells of a transparent 96-well plate for the standard curve + the necessary amount of wells for the samples (done in triplicates). BSA was added as the standard protein in increasing concentrations, in triplicates: 0, 0.42, 0.85, 1.27, 1.7 and 2.12 mg/ml. The wells containing the BSA were mixed to allow the development of the blue colour. The sample proteins were added and mixed im their respective wells in concentrations that were within the standard range. The plate was then read in a Victor3 plate reader (Perkin Elmer) at 595 nm.

2.6.3 Western blots and gel stains

Gels were made using the recipes in (Gallagher, 2001). Briefly, the protocol was as follows: 30 % acrylamide/0.8 % bisacrylamide solution (National Diagnostics) (at 8 – 15 %

final acrylamide concentration); 1.5 M Tris-Cl with 0.4 % SDS, pH 8.8 (3.75 ml); distilled water to 15 ml; 10 % ammonium persulfate (50 µl, Bio-Rad); TEMED (10 µl, Bio-Rad). These were mixed and poured to 2/3 of the height of Mini-Protean glass plates of either 1 – 1.5 mm, depending on the sample volumes (Bio-Rad). The gel was covered with distilled water and allowed to set. After setting, the water was removed and the stacking gel was added to the plates (30 % acrylamide/0.8 % bisacrylamide solution (0.65 ml), 0.5 M Tris-HCl with 0.4 % SDS, pH 6.8 (1.25 ml), distilled water (3.05 ml), 10 % ammonium persulfate (25 µl), TEMED (5 µl)). The plastic comb was added into the poured stacking gel to shape the wells. The gel was allowed to set.

Bis-Tris 4 – 12 % acrylamide gels (Invitrogen) were used to separate the peptide of the His-tagged dimerization region of CSF-1R.

The samples were prepared by the addition of 6 × sample buffer (Tris-Cl/SDS, pH 6.8 as above (7 ml), glycerol (3.8 g or ~ 3 ml), SDS (1 g), DTT (0.93 g), bromphenol blue (1.2 mg), water (to 10 ml if needed)). DTT was omitted from the sample buffer in non-reducing conditions. Unless stated otherwise, samples were heated at 95^{o}C for 5 min after the addition of the sample buffer. The samples were pipetted into the wells of the gel. The size standard used was Precision Plus Protein Dual Colour (5 µl, Bio-Rad). The gel was run at 17 mA/gel until the samples reached the running gel, when current was increased to 23 mA/gel.

For Coomassie staining of the gel, it was removed from the glass and immersed in the staining solution (methanol (50 %), Coomassie brilliant blue R-250 (0.05 %), acetic acid (10 %), water (40 %)). Coomassie brilliant blue R was dissolved in methanol before adding acetic acid and water. When the gel was thoroughly blue, it was washed with the destaining buffer in 5 min incubation steps: methanol (5 %); acetic acid (7 %); distilled water (88 %). Washing was repeated until the bands were clearly visible.

For silver staining, the gel was incubated in the following solutions: Fixing solution (methanol (50 %), acetic acid (10 %)) for 30 min; methanol (5 %) for 15 min; 3 washes of 5 min with deionized water; $Na_2S_2O_3.5H_2O$ (0.02 %) for 2 min; 3 washes of 30 sec with water; $AgNO_3$ (0.2 %) for 25 min; 3 washes of 1 min with water; up to 10 min developing in developing solution (Na_2CO_3 (3 %), formaldehyde (0.018 %), $Na_2S_2O_3.5H_2O$ (0.0004 %)). The development reaction was stopped with EDTA (1.4 %) for 10 min.

For western blots, when running was complete, gel was removed from glass plates and the stacking gel was cut off. The gel was used for transfer of proteins to a nitrocellulose membrane. The transfer cassette (Bio-Rad) was assembled in the following order, from the anode (white) to the cathode (black) side: sponge, filter paper, nitrocellulose membrane (GE Healthcare), gel, filter paper, sponge. The cassette was placed in a transfer apparatus with

transfer buffer (Tris base (18.2 g), glycine (86.5 g), methanol (1200 ml), distilled water (to 6 l)). Transfer was performed at either 100 V for 1 h or 25 V overnight, both at 4^{o}C.

If necessary, the membrane was stained using Ponceau red (Ponceau S (Sigma), 0.5 g dissolved in 1 ml glacial acetic acid. Water was added to 100 ml). The staining solution was placed on the nitrocellulose membrane and incubated for 30 sec mixing. The stain was returned to the container for reuse. The membrane was washed with distilled water until the bands were visible.

The membrane was blocked with PBST + skimmed milk (5 %) for 3 h at room temperature or overnight at 4^{o}C. The primary and secondary antibodies, diluted in blocking buffer, were added sequentially, with 3 washing steps with PBST after each antibody.

2.6.4 Dot blots

Dot blots were performed by pipetting 1 µl of the samples onto nitrocellulose membranes (GE Healthcare). The samples dotted on the membrane were allowed to dry (2 – 5 min). Membrane blocking and antibody incubations were as for western blots.

2.6.5 Chemoluminescent detection

Western and dot blots were developed by a luminescence reaction with the HRP conjugated with the secondary antibodies. The enhanced chemoluminescence reagents (GE Healthcare) were mixed 1:1 (total of 1 ml for an average western blot membrane) and added onto the membranes after washing the secondary antibody. The reagent was kept for 1 min on the membrane, after which it was drained. The membrane was covered in plastic film (Saran) and exposed to radiograph films (GE Healthcare) in a dark room. Exposure times varied from 15 sec to 4 min depending on signal strength. The film was developed by immersion in developer solution, water, fixer solution and water, in this order. The molecular weight markers were drawn on the radiographic films by superposing it on the membrane.

2.7 Imaging

2.7.1 Immunofluorescence

Methods for staining are described separately in each chapter. Normal goat serum (Gibco) was commonly used for blocking binding sites (10 % in PBS). A secondary antibody

control was commonly used. The control samples received only blocking buffer in substitution for the primary antibody, and received the same concentration of secondary antibodies as the test samples. Images were obtained using a Leica DM LB fluorescence microscope. When necessary colour channels were joined using the ImageJ 1.46 software (open source).

2.7.2 Flow cytometry

FACSCalibur or FACSAria flow cytometers were used. Specific protocols and antibodies are detailed in each chapter. Cells were gated by adjusting the size (forward scatter/FSC) and granularity or complexity (side scatter/SSC) of the cells to the middle of a FSC × SSC graph. The fluorescent antibodies were excited by a blue argon-ion laser. Green fluorescence emission (FITC or Alexa 488 fluorochromes) was captured in FL1, yellow fluorescence emission (PE) was captured in the FL2 channel and red fluorescence emission (7-AAD) was captured in the FL3 channel. A secondary antibody control was added, when pertinent, as a negative control. Isotype controls were added when mentioned. Dual-colour cytometry was performed by using single-stained controls to set the fluorescence intensity of each channel. Results were analysed after setting the gate on the cellular population, eliminating debris. The percentage of positive cells was determined by comparison to the negative (secondary antibody or isotype) control level, which was set to 1 %.

Chapter 3

CSF-1 is an important mediator in the interaction between cancer cells and macrophages

Highlights

- Canine mammary carcinoma cells reduced the activation of macrophages in response to LPS.
- The effect of cancer cells on macrophages was partially dependent on CSF-1R signalling.
- CSF-1 had a dual effect on macrophages, inducing cellular activation but reducing inflammatory responses.
- Macrophages had a counter-effect on cancer cells, inducing CSF-1R expression and glucose uptake.

Abstract

Tumour-associated macrophages (TAMs) can constitute a large proportion of the cellular mass of solid tumours. Within tumours, macrophages can be in an alternative state of activation that acts in favour of carcinogenesis, instead of counteracting it. Consequently, TAMs can lead to poorer clinical prognosis, as they assist in cancer progression such as local tissue invasion and immunosuppression. In this chapter, it is demonstrated that canine mammary carcinoma cells reduced macrophage responses to LPS stimulation. CSF-1 is an important factor for macrophage survival and is highly expressed in several cancers. Blocking CSF-1 reduced the effect of cancer cells on macrophages, indicating that this is an important factor in the interaction between these cells. Independently, this cytokine induced macrophage activation, but it reduced LPS-induced activation. Macrophages also exerted an effect on cancer cells, inducing canine mammary carcinoma cells to up-regulate CSF-1R and glucose uptake. Canine mammary cancer cells showed increased proliferation in the presence of CSF-1 and were sensitive to a CSF-1R tyrosine kinase inhibitor. Overall, these

data support the significance of the collaboration between macrophages and canine cancer cells, evidencing the role of CSF-1R signalling in this interaction.

3.1 Introduction

The macrophage content of solid tumours is variable, but these cells have been found to compose up to 30 % of the cellular mass of naturally occurring human cancers and up to 83 % of syngeneic tumours of mice of both epithelial and mesenchymal origins (Gauci and Alexander, 1975; Milas et al., 1987).

For many years, it was believed that the presence of macrophages within tumours indicated that the immune system was developing a response against the neoplasms (Lauder et al., 1977; Morantz et al., 1979). However, over time the paradigm of the role of macrophages within tumours shifted, and macrophages are currently linked with a myriad of events that lead to malignant transformation (Mantovani et al., 2002; Milas et al., 1987). The shift in our understanding of the significance of macrophages within cancer changed due to consistent findings that the presence of these cells within tumours correlated with poorer clinical outcomes (Lewis and Pollard, 2006; Richardsen et al., 2015).

The term "tumour-associated macrophages" is consequently now widely used to report the negative effects of macrophage function within tumours. From 1960 to 1980, only one paper could be found in the PubMed database that contained the words "TAM", "macrophage" and "cancer". In the following twenty years, 88 papers associated with those three terms were indexed in that database. From 2000 to the time of writing, 506 articles were added to that list (http://www.ncbi.nlm.nih.gov/pubmed). The expansion of the literature on TAMs is a reflection of the protagonist role now being attributed to macrophages in cancer malignancy. For this reason, much attention is being given to therapeutic modalities that may target TAMs (Aharinejad et al., 2004; Hume and MacDonald, 2012; Paulus et al., 2006).

The "new" role of macrophages within cancer is justified by the concept that there are, in fact, differently polarized macrophage phenotypes – named M1 and M2 – which are anti- or pro-tumoural, respectively (Sica et al., 2006). The current understanding of TAMs is evolving into a more complex picture whereby the tumour microenvironment alters how macrophages react to the cancer cells. The idea of extremely polarized TAMs, either killing or assisting cancer cells, is being replaced by a more nuanced concept where several factors influence the activity of macrophages, such as the tumour sites where they are inserted (Grugan et al., 2012; Lewis and Pollard, 2006; Quatromoni and Eruslanov, 2012).

3.1.1 M1 and M2

The M1 and M2 classification was first generated to explain the different macrophage activation pathways following anti-microbial and anti-parasitic responses. The M2 was then further subdivided into three categories to denote other alternative activation routes: M2a (generated by parasitic responses, dependent on IL-4 and IL-13); M2b (induced by Fc receptors and immune-complexes); M2c (anergic state, promoted by IL-10) (Martinez and Gordon, 2014). The factors inducing the different macrophage activation pathways and the corresponding cellular markers are depicted in Figure 3.1.

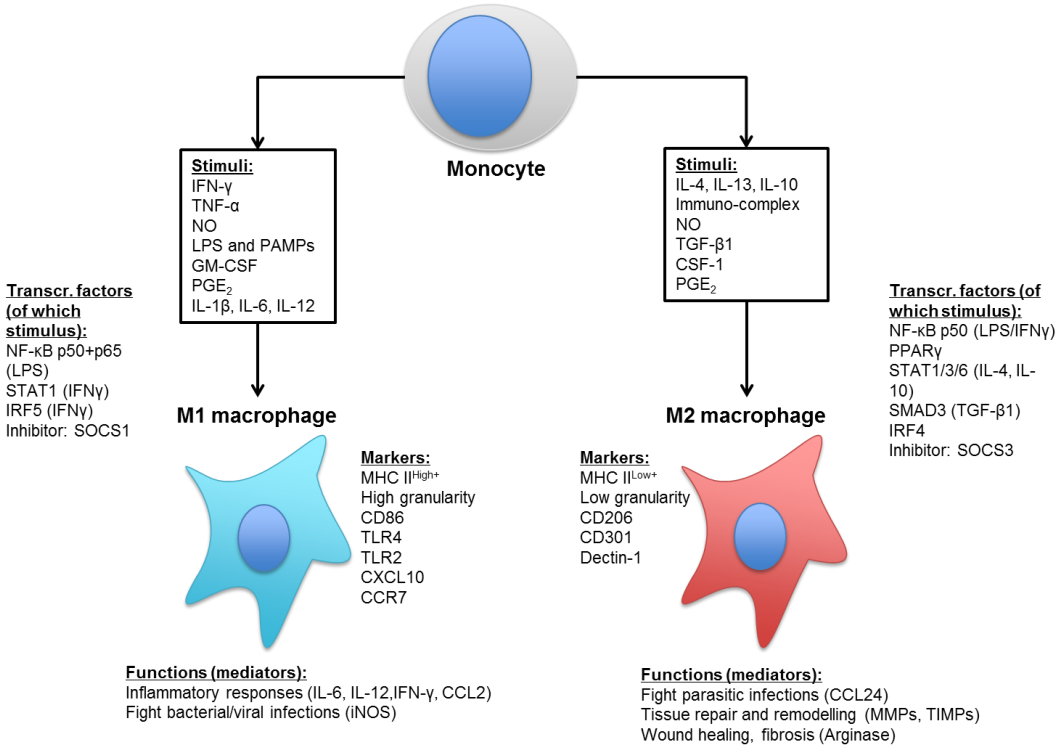

Figure 3.1 – The stimuli and markers of M1/M2 macrophage activation. The stimuli, promoters, markers and functions cited are examples and are not exhaustive of the whole literature. References: (Bouhlel et al., 2007; Lawrence and Natoli, 2011; Mantovani et al., 2002; Martinez and Gordon, 2014; Saccani et al., 2006; Van Ginderachter et al., 2006; Wilson, 2014).

3.1.2 Tumour sites

The tumour sites in which macrophages are embedded seem crucial in determining the fate of these cells. Areas of varying oxygen levels form within tumours due to the growth patterns of the neoplasms. Hypoxic regions form within tumours due to the rapid expansion of the cancerous tissue, overloading the capacity of new blood vessel formation. As the distance between the provisioning capillaries and the cancer cells increase, the intra-tumoural oxygen levels decrease. Also, emboli and the high pressure from the tumour mass on the capillaries can inhibit perfusion. Hypoxic sites therefore lead to apoptosis of the cancer cells, accumulating cellular debris and stimulating the tumoural production of chemokines such as the vascular endothelial growth factor (VEGF) in response to the low oxygen concentration (Jögi, 2015; Lewis and Pollard, 2006).

TAM density is higher in hypoxic and necrotic foci within tumours, areas that are denominated as "hot-spots". The cellular debris and chemokines may be important to lead macrophages into the necrotic sites within the tumour mass. Hypoxic tumoural tissue also produces anti-inflammatory factors, such as IL-10 and prostaglandin E_2 (PGE_2); these may reduce the reactivity of macrophages against the cancer cells, reducing MHC II expression, for instance (Wiemer et al., 2011).

In those tumoural areas, macrophages assume an "organ building" function, scavenging the necrotic foci (Murdoch et al., 2004) and increasing oxygenation by promoting blood vessel formation. The low oxygen concentration and reactive oxygen species within the tumour induce macrophages to express hypoxia-inducible transcription factors (HIFs) and NF-κB (Jögi, 2015). Abnormal expression of the p50 portion of NF-κB leads macrophages to become insensitive to inflammatory signals, a characteristic of TAMs (Saccani et al., 2006). In the tumour environment, macrophage HIFs act through NF-κB to express the pro-angiogenic factor VEGF (Eubank et al., 2011). The rapid neovascularization that follows is associated with malignant transformation of the tumour and further macrophage recruitment (Lewis and Pollard, 2006).

As an endorsement of the great variability of macrophage functions, if these cells are under pro-inflammatory signals, they can be either pro- or anti-angiogenic, depending on which agonist or culture condition is used (Eubank et al., 2011; Ramanathan et al., 2007).

The presence of macrophages in different tumour sites is therefore correlated to different biologic effects. Macrophage numbers in the hypoxic foci are more relevant for determining poor prognosis than TAMs in other tumour sites (Murdoch et al., 2004). TAMs away from the hot-spots but in the tumour stroma are linked to greater lymph node

metastasis. In contrast, TAMs in close contact with cancer cells are more likely to show anti-tumour properties, leading to better clinical outcomes (Ohno et al., 2004, 2002).

3.1.3 Effects of TAMs

Pro-tumoural and other non-inflammatory macrophages share several features, such as nuclear accumulation of the inhibitory p50 NF-κB homodimer (Mantovani and Sica, 2010). Indeed, many of the characteristics of TAMs occur due to an upregulation of genes which occur in non-inflammatory macrophages associated with physiological tissue development. Wnt-signalling is one of such organ development pathways that have increased activity in cancer macrophages, driving MMP and TNF-α overexpression. The same Wnt signals have a role in the vasculogenesis of the developing eye, for instance (Ojalvo et al., 2010; Pukrop et al., 2006). These anti-inflammatory and tissue-remodelling characteristics of TAMs lead to several of the pro-tumoural effects of these macrophages, such as invasion of surrounding tissues, immunosuppression, intravasation and neovascularization (Van Ginderachter et al., 2006).

As discussed above, TAMs are important drivers of neovascularization through the expression of VEGF. These cells also circumvent anti-VEGF therapies by increasing blood vessel formation through other signals when VEGF is blocked. Matrix metalloproteinase-9 (MMP-9), secreted by macrophages in response to CSF-1, is one of the factors that contribute to enhancement of neovascularization (Lewis and Pollard, 2006; Priceman et al., 2010). MMP-9 modifies the extracellular matrix and attracts endothelial cells, organizing newly formed blood vessels (Vu et al., 1998). The blood supply provided by the macrophages allows the expansion of the tumour by removing waste products and increasing the oxygen concentration. It also provides cancer cells access to the circulation for metastasis (Jögi, 2015). Along with an increase in vascularization, perivascular macrophages assist cancer cells to infiltrate into the blood vessels, leading to haematogenous metastasis (Wyckoff et al., 2007). Transforming growth factor-β1 (TGF-β1) produced by the TAMs influences epithelial cancer cells to acquire motility through the process of epithelial-mesenchymal transition (EMT), another step towards metastasis formation (Jögi, 2015; Ye et al., 2012).

Another cancer hallmark which can be stimulated by TAMs is the invasion of surrounding tissues. Stimulation of cancer cells with EGF produced by macrophages is required by some breast carcinoma cells to demonstrate invasive properties, moving into surrounding tissues in the presence of this factor (Goswami et al., 2005). Surrounding tissue

invasion also depends on MMP expression by the macrophages in response to TNF-α (Pukrop et al., 2006). TAMs secrete TGF-β1 that can also increase cancer invasion through cancer cell production of MMP-9 (Ye et al., 2012).

The immunosuppressive characteristics of TAMs are enhanced by the tumour environment. Low oxygen concentration induces macrophages to express HIF-1α; hypoxia and HIF-1α production are sufficient to induce macrophages to suppress T-lymphocytes (Doedens et al., 2010). Tumour-derived anti-inflammatory cytokines (such as IL-10 and PGE_2) also lead TAMs to express IL-10, for instance (Sica et al., 2000), and mediate lysis of $CD8^+$ T-cells (Mitchem et al., 2013). Another cytokine which is produced by several tumour types is CSF-1 (Sapi, 2004). CSF-1-conditioned macrophages have increased activity of STAT1, a transcription regulator. In its turn, STAT1 promotes NO and arginase expression, which are necessary to induce apoptosis of T-lymphocytes by TAMs (Kusmartsev and Gabrilovich, 2005). Much is still not understood about the biology of immune evasion of tumours. Some regulators, such as STAT1, have even been implied in both M1 and M2 formation (Mantovani and Sica, 2010). This regulator is connected with macrophage killing of lymphocytes but is also important for IFN-γ expression, a cytokine capable of inhibiting cancer growth (Dunn et al., 2002).

Despite the extensive incrimination of TAMs in assisting cancer progression, macrophages are in some circumstances capable of exerting anti-tumoural effects. TAMs showing pro-tumoural characteristics – such as promoting tumour cell invasion – are still capable of performing antibody-mediated cancer cell lysis, for instance (Grugan et al., 2012). This has been confirmed in a clinical trial with rituximab (anti-CD20), where high TAM counts were correlated to better treatment responses (Taskinen et al., 2007). As mentioned previously, depending on the localization within a tumour, some macrophages are also capable of phagocytic activity against the cancer cells (Ohno et al., 2004).

3.1.4 CSF-1R signalling

As discussed above, the presence of TAMs does not necessarily correlate with malignancy, since these cells can perform different functions depending on the tumoural site where they are embedded. It has also been shown that altering the phenotype displayed by the "hot-spot" macrophages can be sufficient to impede pro-tumorigenic action. CSF-1 secretion by the cancer cells attracts blood monocytes to the tumoural bed. The monocytes mature into TAMs inside the tumour and again CSF-1 seems important in directing macrophages towards tumour-promoting characteristics (Grugan et al., 2012). However,

depending on the inhibitor used, blocking CSF-1R does not reduce TAM counts. Although the number of macrophages may remain stable after blocking this receptor, improvements in the clinical outcome can still derive. This occurs because inhibiting CSF-1R can alter the phenotype of certain macrophage subsets. Thus, macrophages can be turned away from the tumour-promoting phenotype without affecting macrophage survival. In the event of CSF-1R blockade, the number of TAMs is maintained by other cytokines, such as GM-CSF and interferon-γ (Haegel et al., 2013; Louis et al., 2015; Pyonteck et al., 2013).

Transgenic mice with altered expression of CSF-1 or CSF-1R demonstrate the importance of this signalling pathway for tumour progression. The CSF-1 knockout (*op/op*) has unchanged incidence and growth rate of primary tumours, but exhibits delayed metastasis formation when compared to the wild-type (Lin et al., 2001). Overexpression of CSF-1 and its receptor leads to mammary hyperplasia and tumour formation, with increased cellular proliferation markers and macrophage infiltration (Kirma et al., 2004). On the other hand, the GM-CSF + IFN-γ knockout – both are cytokines associated with inflammatory macrophages – has the opposite effect, leading to spontaneous formation of a variety of tumours (Smyth et al., 2006).

CSF-1 is believed to be an important mediator in the paracrine signalling between cancer cells and macrophages. There is a loop of activation between these cells where CSF-1 produced by cancer cells recruits macrophages and leads them to express epidermal growth factor (EGF), which in its turn has proliferative action on the cancer cells (Escamilla et al., 2015; Wyckoff et al., 2004). For cancer cells that express the CSF-1R, production of CSF-1 also drives an autocrine activation pathway that is important for tumoural tissue invasion (Patsialou et al., 2009).

Because of the subtleties of macrophage functions within tumours, it is important to understand the mechanisms which drive each of these roles (Martinez and Gordon, 2014). In this chapter, co-cultures and cell-conditioned media were used to model the cancer cell and macrophage interaction. A canine mammary cancer cell line, REM134, had the effect of impeding LPS-induced activation of a murine macrophage cell line, RAW264.7. Activation was measured by MHC II and TLR 2 expression and cellular granularity. CSF-1 was an important mediator of the TAM/cancer cell interaction. Blocking this cytokine abrogated the effect of the cancer cells on the macrophages. Although CSF-1 was capable of inducing macrophage activation, it prevented LPS stimulation of these cells. Cancer cells were also sensitive to CSF-1, and macrophages increased CSF-1R expression on cancer cells. These data illustrate the importance of TAMs and of CSF-1R signalling to cancer progression.

3.2 Materials and Methods

Basic methodological descriptions and brands not stated here are presented in Chapter 2.

3.2.1 Effect of cancer cells on macrophage activation by LPS

RAW264.7 macrophages and REM134 canine mammary carcinoma cells were grown in co-cultures or in the presence of conditioned medium in 6-well tissue culture plates. Cells were kept in subconfluent conditions for the experiments.

REM134-conditioned medium (CM) was collected after culturing these cells from 60 % confluence for 72 h. Supernatant was removed from the culture, was centrifuged in 50 ml tubes for 400 × *g* and was filtered through a 0.45 μm syringe filter (Cole-Parmer). The conditioned medium was stored at 4^{o}C until used.

For co-culture experimentation, RAW264.7 macrophages were stained with CFSE (eBioscience) in order to separate macrophages from cancer cells in flow cytometry. For this, cells were suspended in FBS-free DMEM medium (Gibco). CFSE was added to the cells at 10 μM for 15 min at room temperature, protected from light. Cells were then washed twice with complete medium. This was performed for the first experiment only, since it was found that REM134 and RAW264.7 cells could easily be discriminated based on the forward scatter by flow cytometry.

When in co-culture, cells were grown at a ratio of 2:1 of REM:RAW. Co-cultures and RAW264.7 cells with REM-conditioned medium were grown for 3 days, when *Escherichia coli* O111:B4 LPS (1 μg/ml, Sigma) was added (when stated in the text) and incubated with cells for 48 h. Cells were removed from the plate by scraping and were assessed by flow cytometry.

3.2.2 Effect of CSF-1 on REM134 and RAW264.7 proliferation

For cell proliferation assays, 7×10^3 cells were grown in black opaque 96-well plates (Corning). Cells were treated with the indicated concentrations of rhCSF-1 (Invitrogen) for 48 h starting at the time of plating. Cell proliferation was analysed with CellTiter-Glo (Promega).

3.2.3 Blocking CSF-1 by competitive inhibition

Cancer cells and macrophages were co-cultured for 3 days in the presence or absence of recombinant canine CSF-1R extracellular region (1 µg/ml). RAW264.7 cells in isolation also received the CSF-1R as a control. The recombinant receptor was cloned, expressed and purified as is detailed in Chapter 7. rhCSF-1 (50 ng/ml, Invitrogen) was used when stated during the same period. LPS (1 µg/ml, Sigma) was then added for 48 h. Cells were scraped and analysed by flow cytometry.

3.2.4 Effect of CSF-1 on MHC II expression by RAW cells

Macrophages in 6-well plates at 60 % confluence were incubated with increasing concentrations of rhCSF-1 (Invitrogen) for 48 h. When stated, LPS (1 µg/ml, Sigma) was added and cells were incubated for another 48 h. Cells were harvested by scraping and MHC II expression was analysed by flow cytometry.

3.2.5 Flow cytometry of RAW264.7 cells

One million cells were used for each analysis. Cells were scraped from culture plates. To differentiate RAW264.7 and REM134 cells by flow cytometry in co-culture experiments, RAW cells were stained with CFSE, as described in 3.2.1, above.

Macrophages in 100 µl of complete DMEM medium were stained with the primary antibody for 20 min at 4^{o}C: anti-mouse MHC II I-A/I-E, PE-conjugated (0.125 µg/test, eBiosciences), anti-mouse TLR2, FITC-conjugated (0.5 µg/test, eBiosciences). Cells were then washed with PBS thrice at 4^{o}C and centrifuged between washes at 400 × *g* for 5 min to remove the supernatant. Unstained cells and RAW264.7 macrophages unstimulated with LPS were used in flow cytometry as controls.

Samples were analysed using a FACScalibur flow cytometer (Becton Dickinson). Cells in the macrophage gate were assessed. Results were analysed using the Summit 4.1 software (Dako), assessing the percentage of positive cells and the mean fluorescence intensity within the macrophage gate.

3.2.6 Immunofluorescent staining of cancer cells

Lilly cells (2.5×10^4) were grown on tissue culture treated chamber slides (Nunc Lab-Tek II Chamber Slide System, Thermo Scientific) overnight in the presence or absence of conditioned medium from macrophages (conditioned medium was added to 20 % of total culture volume). RAW264.7 macrophage-conditioned medium was collected after culturing these cells from 60 % confluence for 48 h. Lilly cells were fixed with ice cold acetone for 20 min at – 20°C and blocked with PBS + goat serum (10 %) for 1 h at room temperature. Rabbit anti-human C-terminal CSF-1R (1:100, Abcam) was diluted in blocking buffer. Slides were incubated overnight at 4°C. After 3 washes in PBS for 5 min, secondary goat anti-rabbit Alexa 488 (1:200, Invitrogen) in blocking buffer was used for 1 h at room temperature. The secondary antibody was washed with PBS as before. DAPI (4',6-diamidino-2-phenylindole) nuclear staining was included in the mounting medium (Vectashield Mounting Media with DAPI, Vector Labs). A coverslip (Thermo Scientific) was placed on top of the section with a drop of mounting medium. The section was isolated using nail polish.

3.2.7 Sequencing of CSF-1R from a canine cancer cell line

mRNA was extracted from the Lilly inflammatory canine mammary carcinoma cell line using RNeasy Mini Kit (Qiagen). cDNA was synthesized using random nonamers (Sigma) and the Omniscript RT Kit (Qiagen). The receptor was amplified using the primers shown on Table 3.1 using Phusion High-fidelity polymerase (Thermo Scientific) and the protocol in Chapter 7 for the cloning of the full CSF-1R receptor. The product was cloned into the pCR4-TOPO vector (Invitrogen) following the same protocol as in Chapter 7. The plasmid was sequenced using the T3 and T7 primers (provided by the sequencing service), and also the primers shown in Table 3.1, which are specific for the canine CSF-1R. Sequencing was performed by DNA Sequencing and Services, Dundee, Scotland.

Table 3.1 – Primers used to sequence the CSF-1R from Lilly cells. Primers shown as 5` to 3`.

Canine full CSF-1R receptor	Forward: ATGGGCCTAGGGGCTCCACTG Reverse: GCAGAACTGGTAGTTGTTGGGCTGCAGCAG
Sequencing primers	CCGAGTACTGTTGCTATGGTGAC CTTCCACAAGGTGATCGTCCAC GATGATCTTCCAGCGCACCT T3 primer: Chapter 7 T7 primer: Chapter 7

3.2.8 Effect of RAW264.7-conditioned medium on cancer cell proliferation

The xCELLigence Real-Time Cell Analyzer (Roche) was standardized with 50 µl of DMEM medium before adding cells. REM134 cells (10^4 or 3×10^4 cells) were plated on a 16-well xCelligence plate (Roche). The plate was scanned to measure the initial numbers of cells in each well, and then treatment was added. RAW264.7 macrophage-conditioned medium was collected after culturing these cells from 60 % confluence for 48 h. This conditioned medium was added to the REM134 cells (20 % of final culture volume). Where stated, rhCSF-1 (Invitrogen) was also added (100 ng/ml). Cells were then maintained at the usual culture conditions for the duration of the experiment. The amount of cells attached to the bottom of each well was measured by the equipment through assessment of the interference with the electrical impedance of the sensor on the plate. Cell proliferation was assessed every 15 min for 21 h (3×10^4 cells) or for 90 h (10^4 cells).

3.2.9 PCR for the CSF-1R in REM134 cells

cDNA from REM134 cells was generated as presented above for the Lilly cells. PCR was performed to assess the expression of CSF-1R mRNA by REM cells. PCR conditions and primers were as for the His-tagged dimerization domain (Chapter 7). The positive control was cDNA from canine spleen, produced as shown in Chapter 7. A no-template reaction was added as a negative control.

3.2.10 Glucose uptake

REM134 cells were pre-incubated with RAW264.7 macrophage-conditioned medium for 72 h. Glucose uptake by cancer cells was assessed using 2NBDG fluorescent glucose (50 µM, Invitrogen). The reagent was added to the cells for 30 min at 37^{o}C or on ice

(as a negative metabolic control). Ethanol was used as a vehicle control (VC) for the glucose. After glucose uptake, the cells were resuspended by trypsinization, washed with 10 ml of cold PBS thrice (400 × *g* centrifugations) and were analysed by flow cytometry. Samples were analysed using a FACScalibur flow cytometer (Becton Dickinson). Cells in the REM134 cell gate were assessed. Results were analysed using the Summit 4.1 software (Dako), assessing the percentage of positive cells in comparison to cells that did not receive 2NBDG fluorescent glucose.

3.2.11 Effect of small molecule inhibitors

For cell proliferation assays, 7×10^3 cells were grown in black opaque 96-well plates (Corning). GW2580 (Cayman Chemical), toceranib phosphate (Palladia, Pfizer) or RS102895 hydrochloride (Sigma) were added at the stated concentrations. Concentrations of inhibitors differ between cells because they were increased from previous assays until an effect was seen or until the volume of vehicle became toxic to cells. All the inhibitors were dissolved in dimethyl sulfoxide (DMSO) Hybri-Max (Sigma) to create the stock solution. Toceranib phosphate was supplied as a tablet. It was crushed manually to create the stock solution. DMSO Hybri-Max (Sigma) was added at the same volumes as the inhibitors as a vehicle control. Cell proliferation was analysed with CellTiter-Glo (Promega).

3.2.12 Statistical analyses

Assumption tests were performed using Minitab 16 software (MiniTab Inc). Kruskal-Wallis, Student's t-test, ANOVA statistical analyses ($P < 0.05$, unless indicated) and graphs were made using GraphPad Prism 5 (GraphPad Inc).

3.3 Results

3.3.1 Effects of cancer cells on macrophages – reduced inflammatory activation

Activation of RAW264.7 macrophages in response to LPS was impeded by the presence of mammary cancer cells. Size, granularity and MHC II expression were increased in macrophages after LPS stimulation, indicating inflammatory activation of these cells. Co-culture with canine and human mammary cancer cells (REM134 and MCF7, respectively)

hindered macrophage activation as measured by these parameters. The presence of a control cell line (HEK293T) had a minor effect on LPS-induced macrophage activation (Figure 3.2). RAW264.7 do not normally express MHC II (Saxena et al., 2003), so LPS activation as measured by MHC II could be quantified as the percentage of positive cells and the mean fluorescence intensity, showing similar patterns by percentage and intensity.

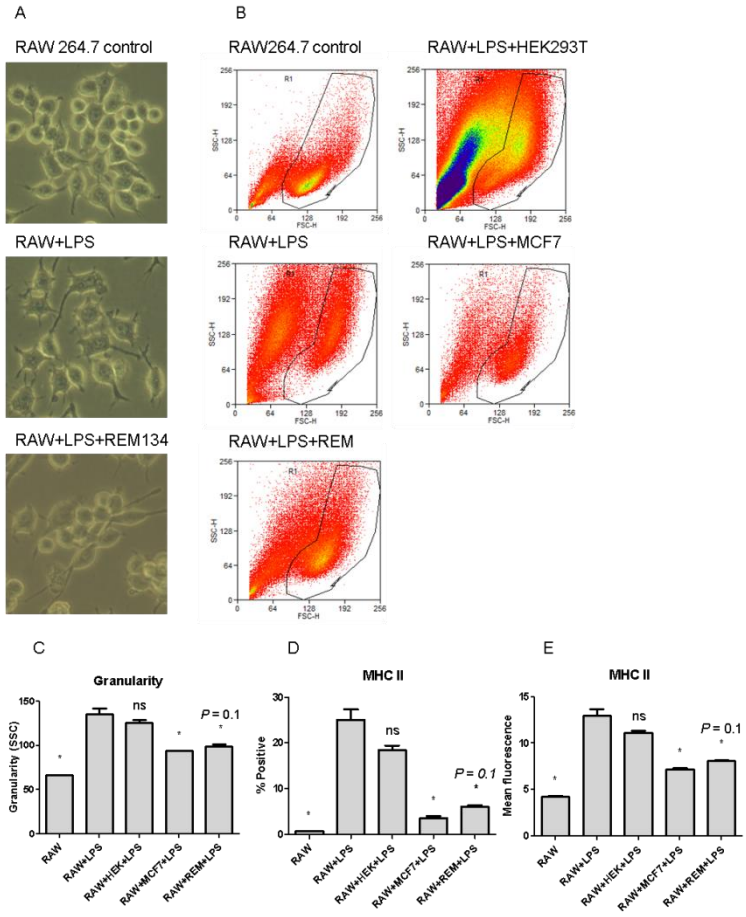

Figure 3.2 – Mammary cancer cells inhibited LPS-induced RAW 267.7 macrophage activation. Macrophages were cultured for 72 h in the presence or absence of two mammary cancer cell lines (REM134 and MCF-7) or a control cell line (HEK293T). *E.coli* O111:B4 LPS (1 µg/ml, Sigma) was added for 48 h. Notice how co-culture with cancer cells reduced macrophage activation by LPS. **(A)** Bright-field images of macrophages cultures. **(B)** Size (FSC) × granularity (SSC) flow cytometry plots of different treatments. Macrophages are marked inside the gate. **(C)** Quantification of macrophage granularity (SSC). **(D)** Macrophage MHC II, percentage of positive cells. Cells were stained with anti-mouse MHC II I-A/I-E PE (0.125 µg/test, eBiosciences). **(E)** Macrophage MHC II, mean fluorescence intensity quantification. Results represent the means of 4 replicates ± SD. Asterisks represent statistical difference by ANOVA from the "RAW+LPS" group. "ns", non-significant difference from the "RAW+LPS" group.

The effect of cancer cells on macrophages was not dependent on cell-cell interaction. The suppressive effects of REM134 cells over macrophages could be replicated by adding only conditioned medium (CM) from the cancer cells into the RAW264.7 macrophage culture. In the presence of conditioned medium, macrophages had reduced granularity and expression of MHC II after LPS exposure. TLR2, a second membrane cellular activation marker (Saccani et al., 2006), was also evaluated to confirm the analysis with MHC II. TLR2 presented a similar pattern to MHC II (Figure 3.3).

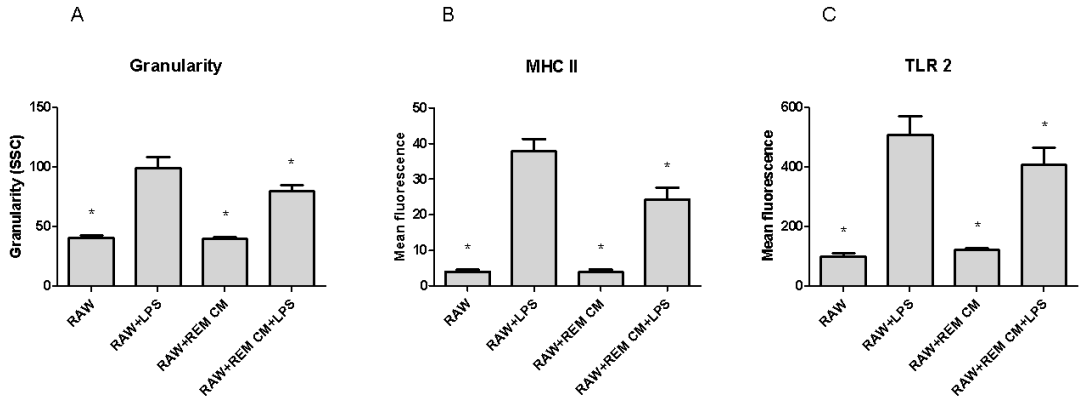

Figure 3.3 – The effects of cancer cells over macrophages were not dependent on cell-cell interactions. RAW264.7 macrophages cultured for 72 h in the presence or absence of conditioned medium (CM) from REM134 cells and then another 48 h with *E.coli* O111:B4 LPS (1 µg/ml). Cancer cell-conditioned medium reduced macrophage activation by LPS. **(A)** Macrophage granularity (SSC). **(B)** Macrophage MHC II, mean fluorescence intensity quantification. **(C)** Macrophage TLR2, mean fluorescence intensity quantification. Cells were stained with anti-mouse TLR2, FITC-conjugated (0.5 µg/test, eBiosciences). Results represent the means of 3 replicates ± SD. Asterisks represent statistical difference by ANOVA from the "RAW+LPS" group. "ns", non-significant difference from the "RAW+LPS" group.

3.3.2 CSF-1-induced proliferation

Since CSF-1 is known to be relevant for progression of several types of cancer (Lin et al., 2001), the effect of this cytokine was analysed on the REM134 canine mammary cancer cells and the RAW264.7 macrophages. Both cell types were analysed with regards to their proliferation capacity in response to recombinant human (rh) CSF-1. Cancer cells and macrophages proliferated in response to rhCSF-1. The proliferation of the cells was dose-dependent (Figure 3.4). The presence of CSF-1R in REM134 cells was confirmed by PCR

(not shown). The CSF-1R from another canine mammary cancer cell line (Lilly) was sequenced. It contained no differences from the known receptor sequence (Chapter 7).

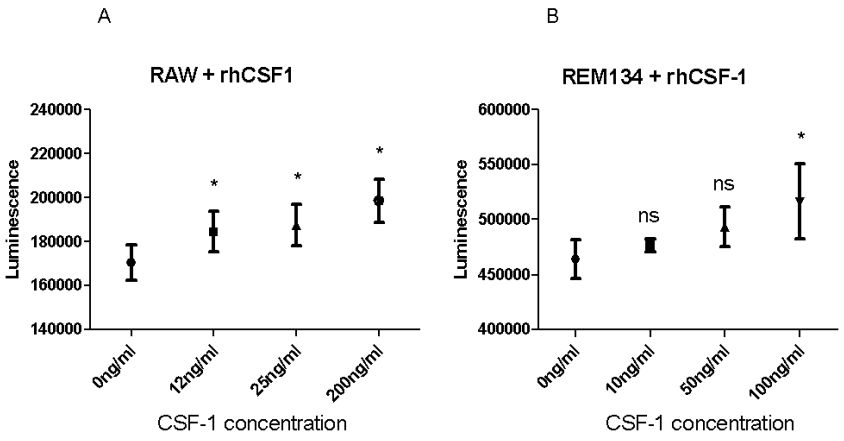

Figure 3.4 – Mammary cancer cells and macrophages proliferated in response to CSF-1. **(A)** Proliferative response of RAW264.7 macrophages 48 h after addition of rhCSF-1 (Invitrogen). **(B)** Proliferative responses of REM134 canine mammary cancer cells 48 h after addition of rhCSF-1. Proliferation results as measured by luciferase activity (CellTiter-Glo, Promega). Results represent the means of 6 replicates ± SD. Asterisks indicate statistically significant difference by ANOVA in relation to the control (0 ng/ml). "ns", non-significant difference from the control group.

3.3.3 CSF-1 as a mediator in the cancer cell/macrophage cross-talk

Work from other groups had suggested that CSF-1 signalling could not only promote cancer proliferation, as confirmed in Figure 3.4, but also induce the M2 phenotype of TAMs (Grugan et al., 2012). To assess if CSF-1 played such a role in the interaction between canine mammary cancer cells and macrophages, this growth factor was blocked by the addition of recombinant canine (rc) CSF-1R. The recombinant receptor is able to actively bind to CSF-1 (Chapter 7), thus competitively inhibiting its functions on cells within the cell culture system.

Macrophages were co-cultured with cancer cells with the addition of rcCSF-1R. LPS was added to induce macrophage inflammatory stimulation. As expected (based in Figure 3.2), the co-culture of macrophages with cancer cells impeded macrophage activation after LPS stimulation – as measured by cellular granularity and MHC II expression. However, the addition of rcCSF-1R allowed a marked stimulation of macrophages after LPS addition, apparently circumventing the effect that cancer cells had on macrophages. The receptor itself

had only a small effect on macrophages. Addition of CSF-1 to the co-culture marginally enhanced the suppression of macrophages. The marked stimulation of macrophages by LPS in the presence of cancer cells indicates that this growth factor is important in the cross-talk between these cells (Figure 3.5).

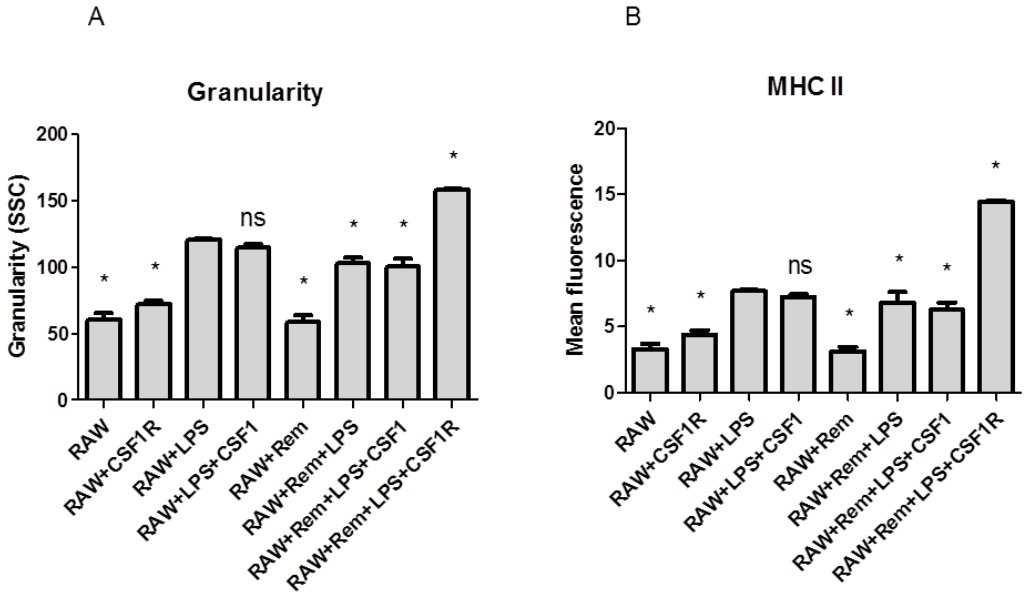

Figure 3.5 – Blockade of CSF-1 circumvented cancer inhibition of macrophages. RAW macrophages were grown for 72 h in co-culture with REM134 cancer cells with/out rhCSF-1 (50 ng/ml) or rcCSF-1R (1 µg/ml). *E.coli* O111:B4 LPS (1 µg/ml) was then added for 48 h. CSF-1R-treated cells were activated by LPS even in the presence of cancer cells. **(A)** Macrophage granularity (SSC). **(B)** Macrophage MHC II, mean fluorescence intensity quantification. Results represent the means of 3 replicates ± SD. Asterisks represent statistical difference by ANOVA from the "RAW+LPS" group. "ns", non-significant difference from the "RAW+LPS" group.

3.3.4 The role of CSF-1 in macrophage activation

To further evaluate the effects of CSF-1 on macrophages, these cells were cultured with increasing concentrations of rhCSF-1. In isolation, CSF-1 induced macrophage activation, as measured by MHC II expression. However, LPS-induced activation was reduced after cells were grown with CSF-1; this effect seemed to be dose-dependent, although statistically significant differences were only apparent between the control group and the highest dose of CSF-1. The differences are more evident when considering the percentage of MHC II^+ macrophages than when assessing the mean fluorescence intensity,

so both graphs are shown (Figure 3.6). These results indicate that CSF-1 has the potential to promote macrophage activation while impeding inflammatory stimulation.

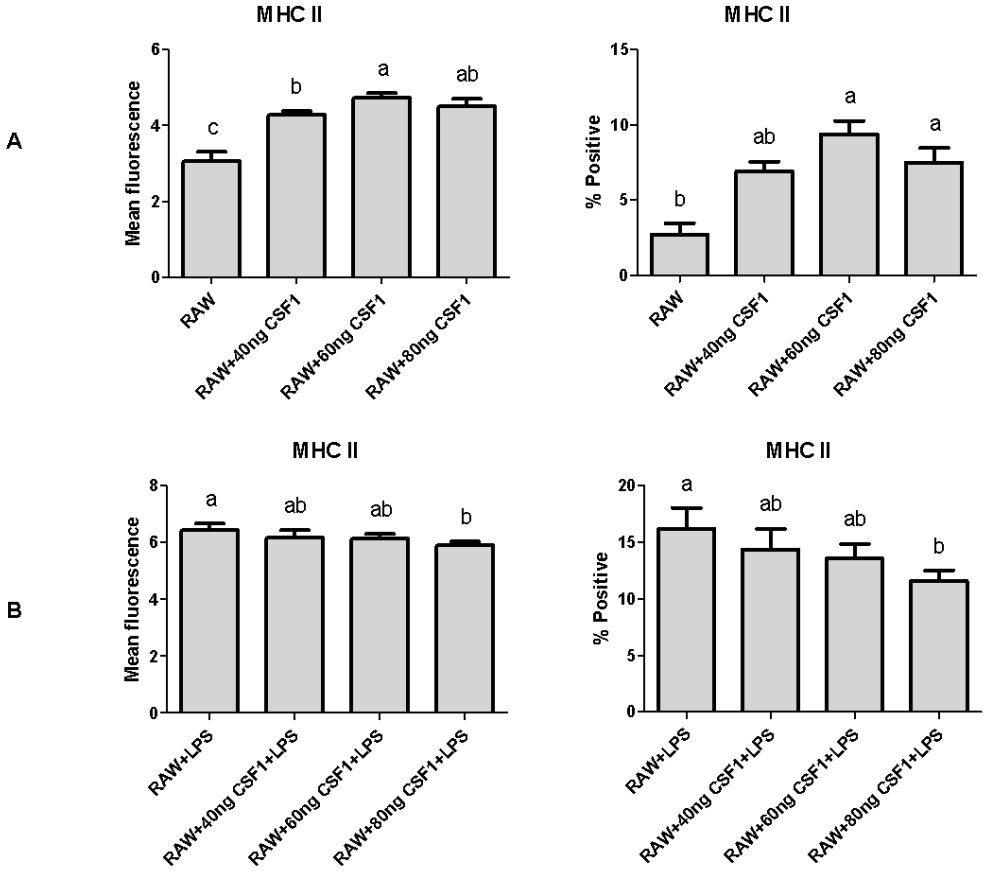

Figure 3.6 – CSF-1 prompted macrophage activation but impeded LPS-induced stimulation. **(A)** RAW264.7 macrophages were grown in the presence of increasing concentrations of rhCSF-1 for 48 h, and MHC II expression (measured as the percentage of positive cells and mean fluorescence intensity) was assessed after 48 h. Macrophages were activated with increasing concentrations of CSF-1. **(B)** RAW264.7 macrophages were grown with increasing concentrations of rhCSF-1 for 48 h. *E.coli* O111:B4 LPS (1 µg/ml) was added to the culture for another 48 h. MHC II expression was then evaluated. Macrophage activation was reduced in the presence of increasing concentrations of CSF-1. Results represent the means of 3 replicates ± SD. Different letters above the bars indicate statistically significant differences.

3.3.5 Effects of macrophages on cancer cells

After being stimulated into the TAM phenotype, macrophages provide feedback to the cancer cells and intensify malignant progression of the tumour (Wyckoff et al., 2004). The effect of RAW264.7 macrophages on canine mammary carcinoma cells was therefore analysed to assess the counter-effects of the macrophages over the cancer cells. Macrophage-conditioned medium increased the expression of CSF-1R in Lilly cells, a canine inflammatory mammary carcinoma cell line (Figure 3.7).

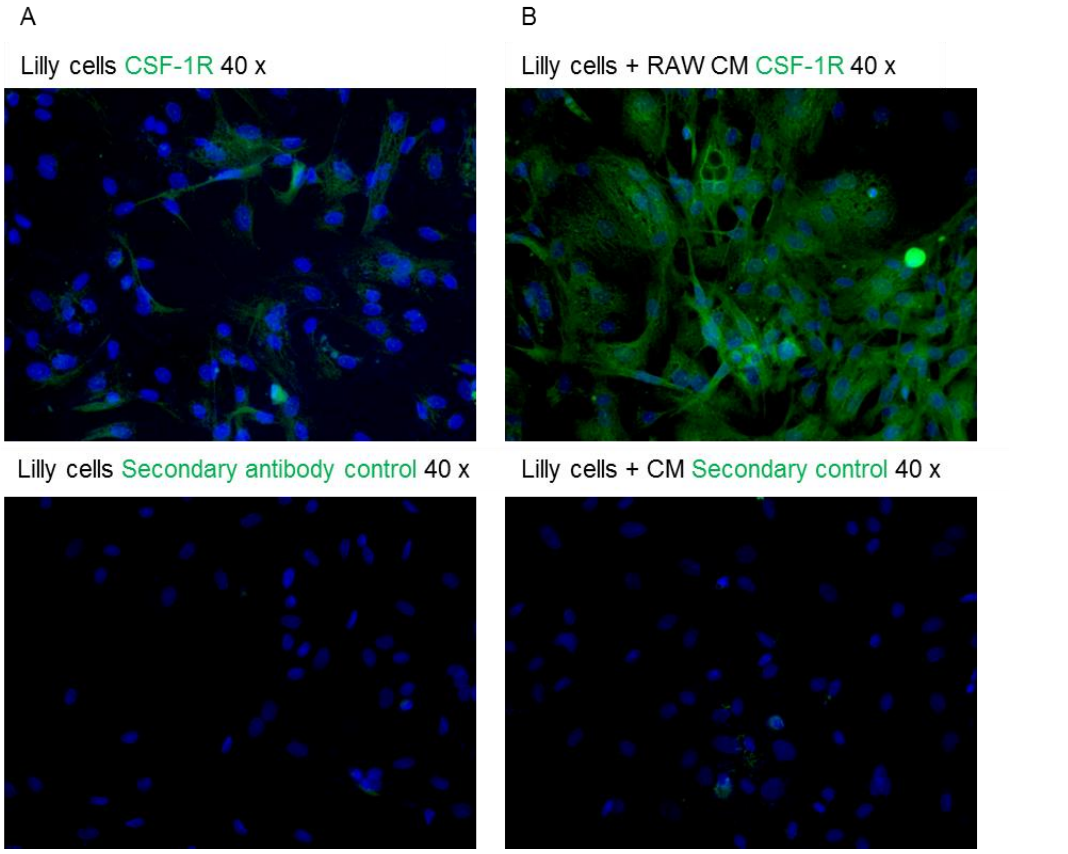

Figure 3.7 – Macrophage-conditioned medium induced CSF-1R expression in canine mammary inflammatory carcinoma cells. **(A)** Lilly cancer cells were grown in the absence of conditioned medium from macrophages. **(B)** Lilly cancer cells were incubated overnight with conditioned medium from RAW264.7 macrophages (CM was 20 % of culture volume). Notice higher CSF-1R expression. Cells were stained with rabbit anti-human CSF-1R C-terminus (1:100, Abcam). Secondary antibody was goat anti-rabbit, Alexa 488-conjugated (1:200, Invitrogen). The negative control was stained only with the secondary antibody. Nuclear stain is in blue (DAPI). "40 ×" indicates the magnification used to acquire the images.

The biological relevance of the macrophage conditioned medium over cancer cells was analysed next. Addition of RAW264.7-conditioned medium to REM134 cells increased the proliferation rate of the cancer cells, irrespective of the initial REM134 cell density (10^4 or 3×10^4 cells/well). Addition of rhCSF-1 did not increment the proliferative effect of the macrophage-conditioned medium over the cancer cells. (Figure 3.8 A, only higher cell concentration shown). Results were statistically significant (two-way ANOVA). Addition of macrophage-conditioned medium also increased glucose uptake by the cancer cells (Figure 3.8 B). These results indicate that macrophage-conditioned medium can increase the metabolic activity of the cancer cells.

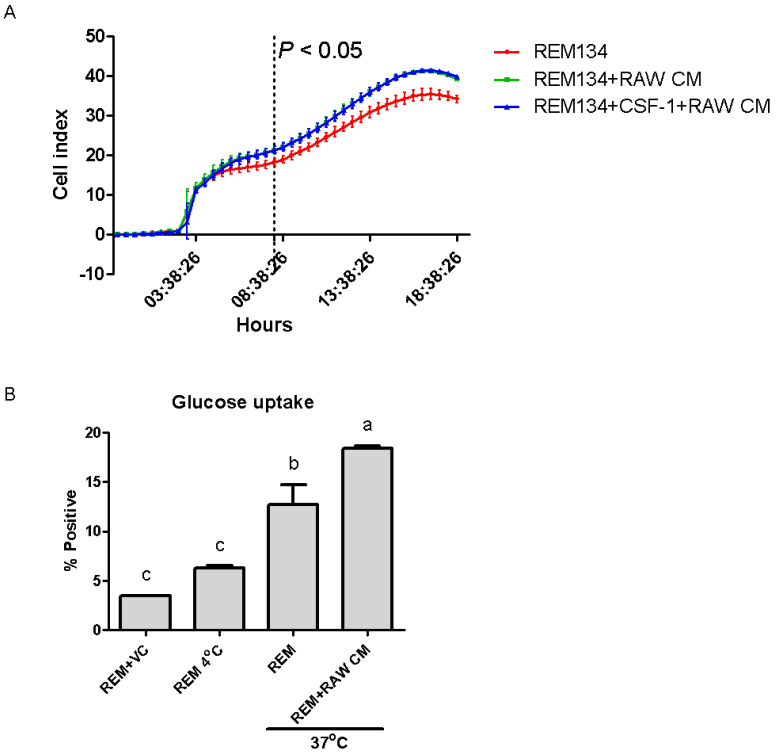

Figure 3.8 – RAW264.7 macrophage-conditioned medium increased REM134 cell proliferation and glucose uptake. **(A)** REM134 cells received conditioned medium (CM) from macrophages at 20 % of culture volume (and 100ng/ml rhCSF-1, where stated) at plating. Cell proliferation was measured every 15 min. Representative result showing an initial plating of 3×10^4 REM134 cells. Lower cell concentration not shown. Cell index (y-axis) is correlated to cell number. Each point represents the average of 4 wells ± SD. Statistical analysis by two-way ANOVA. Where $P < 0.05$ is indicated in the graph, the points containing CM or CM + CSF-1 were statistically superior to the control group containing only REM134 cells. **(B)** REM134 cells were cultured with/out macrophage-conditioned medium (20 % culture volume). Cells received 2NBDG fluorescent glucose (50 µM, Invitrogen). After washing out extracellular glucose, cells were analysed by flow cytometry. REM cells were kept at 4°C during glucose uptake as a negative control. "VC" is the vehicle control for the glucose, ethanol. Each point represents the average of 3 wells ± SD. Statistical analysis by one-way ANOVA.

3.3.6 Cancer cells and CSF-1R signalling

The CSF-1R dependence of two canine mammary carcinoma cell lines was tested. REM134 and Lilly cells were evaluated for their susceptibility to three small molecule inhibitors. CSF-1R was targeted by GW2580, CCR2 was affected by RS102895 (CCR2i). A multi-tyrosine kinase inhibitor was also used (toceranib). Among other kinases, it is known to target c-Kit (Conway et al., 2005; Liao et al., 2002; Tang and Tsai, 2012). Both cell lines were susceptible to GW2580, but the Lilly line was resistant to the other small molecule inhibitors tested. This indicates that dependence on CSF-1R may be a common occurrence in canine mammary carcinomas, in comparison to other receptors commonly implicated in malignancy (Cavnar et al., 2013; Mitchem et al., 2013) (Figure 3.9).

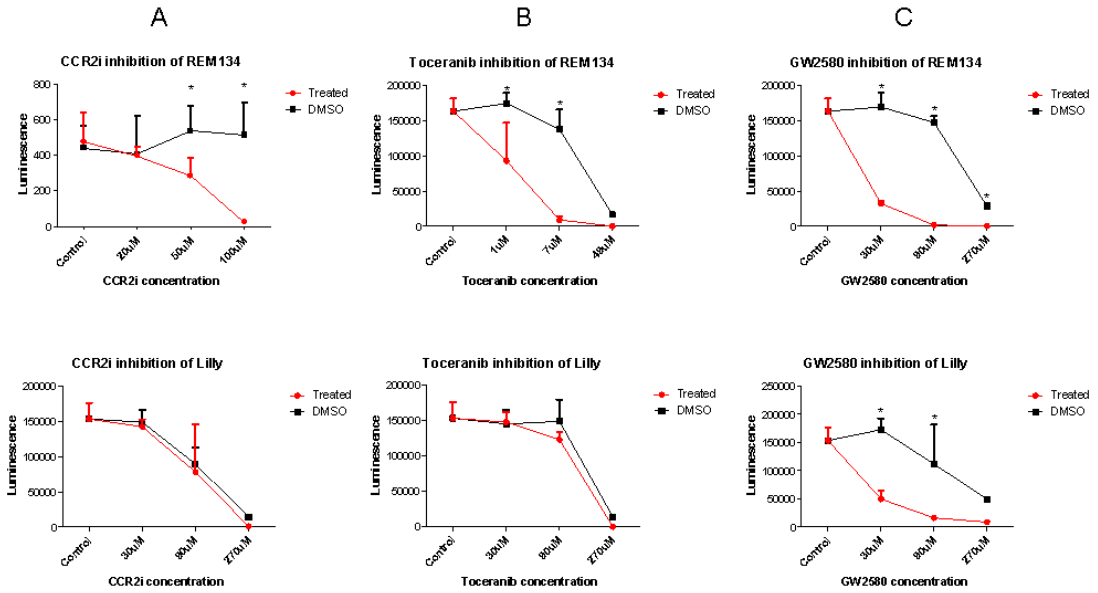

Figure 3.9 – CSF-1R dependence was a common feature in two canine mammary cancer cell lines. Lilly and REM134 mammary carcinoma cells were grown in 96-well plates and were cultured for 48 h with different concentrations of inhibitors: **(A)** RS102895 hydrochloride, a CCR2 small molecule inhibitor; **(B)** toceranib phosphate, a c-Kit tyrosine kinase inhibitor; **(C)** GW2580, a CSF-1R tyrosine kinase inhibitor. Notice the different response of both cell lines to the treatments in (A) and (B). Each point represents the average of 3 wells ± SD. Asterisks indicate statistically significant differences to the DMSO vehicle control group. Statistical analysis by two-way ANOVA.

3.4 Discussion

Infiltration of tumours by macrophages has been associated with metastasis and poor prognosis. Under the influence of the cancer cells and in the presence of low oxygen levels and necrosis, macrophages are differentially activated into a non-inflammatory state. This macrophage phenotype is denominated "M2", in contrast to the classically activated "M1" inflammatory cells stimulated by microbial pathogens. M2 macrophages are dependent on the localized tumoural production of CSF-1 and other factors, such as IL-10 and TGF-β1. These alternatively activated macrophages can be immunosuppressive and can drive tumour neoangiogenesis, tumour intravasation and assist cancers in invading surrounding tissues (Allavena et al., 2008; Biswas et al., 2013).

This chapter aimed to explore the mechanisms involved in the cross-talk between canine cancer cells and macrophages and the role played by CSF-1R signalling in this process.

The canine REM134 and the human MCF-7 mammary carcinoma cell lines inhibited lipopolysaccharide (LPS) activation of RAW264.7 macrophages. The addition of LPS is known to induce dendritic-like morphology and MHC II expression in RAW264.7 macrophages, which are otherwise MHC II^- (Saxena et al., 2003). MHC II expression and increased macrophage granularity indicate inflammatory (M1) cellular maturation (Michelsen et al., 2001; Saxena et al., 2003). Tumour associated macrophages (TAMs) are normally directed into an activation phenotype that shows low antigen-presenting capacities (Lewis and Murdoch, 2005), for which MHC II is essential (Lin et al., 1996).

As cited above, the influence of cancer cells over macrophages and the consequent transformation of these cells into M2 TAMs is due largely to the cytokine microenvironment. The expression of anti-inflammatory cytokines, such as prostaglandin E_2 (PGE_2), IL-10, transforming growth factor-β1 (TGF-β1) and IL-4 leads macrophages into a "wound-healing" and "tissue remodelling" phenotype, which characterizes M2 cells (Lewis and Pollard, 2006).

Within tumours, the localization of TAMs is also believed to be important for the phenotypic transformation of the macrophages. The low oxygen concentration and high necrotic content of tumour hot-spots can alter the gene expression of macrophages to a non-inflammatory phenotype, with increased characteristics of scavenger and "organ building" cells (De Villiers et al., 1994; Murdoch et al., 2004). Macrophages outside these necrotic "hot-spots" are believed to be more inflammatory and even capable of phagocytic activity against the cancer cells (Ohno et al., 2004). However, one of the characteristics of TAMs,

reduced inflammatory activation, could be induced in the present study in 2-dimensional co-cultures and even without cellular contact, exclusively through conditioned medium. This shows that positioning of the macrophages inside the tumours is not necessary for macrophage phenotype alteration. Cell culture was carried out at common oxygen levels, far from the 1 % oxygen level needed to induce hypoxia in culture (Jögi, 2015); this demonstrates that hypoxia is also not a necessary condition for at least partial alternative macrophage activation. The soluble factors produced by the cancer cells are sufficient for induction of at least part of the M2 characteristics. The results shown here confirmed the findings of another work studying canine macrophages which also used soluble factors from cancer cells to suppress macrophage activation and MHC II expression (Wasserman et al., 2012). Whether the RAW264.7 macrophages carried out phagocytosis of the cancer cells, as expected of TAMs outside the hot-spots, was not assessed (Ohno et al., 2004).

Another study analysing the effect of MCF-7 cells on RAW264.7 macrophages found that the co-culture induced the macrophages to form osteoclasts via a RANKL pathway. The authors suggested that osteoclast formation from TAMs is correlated with increased bone metastases and mineral resorption. As expected from osteoclasts, these cells were larger and more granular than the original RAW macrophages (Nicolin et al., 2008), a finding that is similar to the results presented in this chapter. Thirty percent of RAW macrophages present osteoclast phenotype within 48 h of co-culture with MCF-7 (Nicolin et al., 2008). Although osteoclast formation was not evaluated in the present study, the similar methodology and time course in relation to the cited work indicate that comparable findings may have occurred here.

LPS-non-responsive macrophages share characteristics with TAMs, such as nuclear accumulation of the inhibitory p50 NF-κB homodimer (Mantovani and Sica, 2010) and changes to STAT1 phosphorylation (Porta et al., 2009). Normally, p50 is translocated to the nucleus after LPS stimulation, where it dimerizes with p65 to regulate transcription activity. In TAMs, nuclear overexpression of p50 with inhibition of p65 prevents the production of IL-12, an inflammatory cytokine. After LPS or LPS/IFNγ [inflammatory] stimulation, cells overexpressing p50 produce IL-10 – which is anti-inflammatory –, in contrast to resting macrophages. IL-10, PGE_2 and TGF-β, which are known to be produced by cancer cells, are factors capable of inducing overexpression and nuclear translocation of the p50 homodimer. The excessive nuclear p50 also is correlated to a reduction of surface expression of TLR2 by the macrophages (Bellone et al., 1999; Saccani et al., 2006). This mechanism of p50 nuclear expression may explain the findings of the present work with relation to LPS stimulation of

the RAW264.7 macrophages and cell surface MHC II/TLR2 expression following exposure to cancer cells.

Another group showed that co-culture between canine cancer cells and macrophages reduced the transcription of TLR2 and TLR4 by macrophages (Król et al., 2012). LPS activation is dependent on the expression of its receptor, TLR4 (Hirschfeld et al., 2000). Therefore, LPS activation of the RAW264.7 cells after co-culture with REM134 cells or MCF-7 cells could have been impaired because of the absence of the receptor to recognize the ligand.

CSF-1 was identified as an important mediator of the cross-talk between the cancer cells and macrophages. Free recombinant CSF-1R was used to competitively inhibit CSF-1 present in the cell culture system. The same strategy of competitive inhibition by the free recombinant receptor is used in the drug VEGF-trap, in which the vascular endothelial growth factor binds to a decoy receptor, therefore having its action inhibited (Holash et al., 2002). Blocking CSF-1 signalling resulted in increased activation of RAW264.7 macrophages by LPS, as measured by cellular granularity and MHC II expression. The expression of MHC II molecules on macrophages has been shown to be regulated by colony stimulating factors. CSF-1 inhibits MHC II expression while IFNγ and the granulocyte-macrophage colony-stimulating factor (GM-CSF) stimulate it. CSF-1 is also able to overcome the effects of IFNγ and GM-CSF over MHC II (Rey-Giraud et al., 2012; Willman et al., 1989). Importantly, it has been suggested that the role of CSF-1 in generating M2 macrophages *in vitro* is reduced when cells are in serum-containing medium, due to unknown factors in the FBS (Rey-Giraud et al., 2012). Therefore, cultivation of macrophages in serum-free conditions could have enhanced the effects seen in the present study. However, CSF-1 must not have been responsible for all the effect of cancer cells over the macrophages. The human breast cancer MCF-7 cells do not express CSF-1, but were still able to reduce LPS activation of the macrophages (Lee et al., 1999).

CSF-1 can prime macrophage activation or suppress inflammatory responses, depending on what co-signals are present (Sweet and Hume, 2003). Other studies have indicated that pre-treatment with CSF-1 increased macrophage sensitivity to LPS while reducing stimulation through other bacterial molecular patterns, such as CpG DNA. CSF-1 can enhance LPS-induced IL-6, TNF-α and PGE_2 expression. It is believed that CSF-1 increases macrophage sensitivity to LPS by inducing autocrine stimulation by GM-CSF (Conway et al., 2005; Sweet and Hume, 2003). In RAW264.7 macrophages, LPS stimulates the expression of the GM-CSF receptor (Rosas et al., 2007).

This is in apparent disagreement with the findings of the present study, where CSF-1 stimulation of RAW264.7 macrophages reduced LPS-induced MHC II expression. Another group also found reduced LPS activation of CSF-1-conditioned macrophages, corroborating the results shown here. They demonstrated that CSF-1 reduced the expression of Activin A, an inflammatory differentiation factor. Through the reduction of Activin A, CSF-1-macrophages produced more IL-10 and less IL-6 following LPS stimulation. In their study, CSF-1 also emulated cancer-conditioned medium in reducing macrophage activation (Sierra-Filardi et al., 2014, 2011).

However, it is also possible that the results shown here after stimulation with CSF-1 are derived from reduced activation through non-LPS dependent pathways. CSF-1 down-regulates the expression of TLR2, but not TLR4 (Sweet et al., 2002). Purified LPS is exclusively able to signal in the extracellular compartment through TLR4, but contaminants in LPS preparations can activate cells through different pathways. The LPS used in this study, *E. coli* O111:B4, from Sigma, has been shown to contain contaminants – probably bacterial lipoproteins – that are able to signal through TLR2 (Hirschfeld et al., 2000; Rutledge et al., 2012). Therefore, down-regulation of TLR2 by CSF-1 may have prevented RAW264.7 macrophage stimulation by the LPS preparation with contaminants. Regardless of the molecular route affected, the results of the present study indicate that cancer cells and CSF-1 reduced inflammatory activation of macrophages.

CSF-1 could have reduced LPS activation through receptors other than TLR4/TLR2. LPS is known to be able to act in a TLR4-independent pathway. Intracellularly, LPS can activate caspase-11 independently of TLR4 and lead to inflammatory activation of macrophages. Another group used ultrapure O111:B4 *E. coli* LPS – O111:B4 LPS was also used in the present work – to elicit caspase-11 activation (Kayagaki et al., 2013). Aberrant intracellular LPS localization and signalling occur at very high concentrations of LPS, activating the caspase-11 pathway (Hagar et al., 2013). CSF-1 may have altered the STAT1 pathway, which is relevant for LPS reactivity of macrophages through caspase-11. Mice knocked out for STAT1 have reduced levels of caspase-11 (Ramana et al., 2000). LPS-irresponsive M2 macrophages show reduced activation of STAT1 (Porta et al., 2009). However, CSF-1 can increase STAT1 activation (Novak et al., 1995), and both TLR4 and caspase-11 are up/down-regulated in similar conditions, raising the possibility that if CSF-1 did not act through TLR4 it also would not reduce LPS activation through caspase-11 (Jung et al., 2005).

LPS can counter-regulate CSF-1 by modulating the expression of its receptor. LPS can induce the production of both CSF-1 and GM-CSF by macrophages. However, one of

the effects of LPS is the down-regulation of the CSF-1R. Therefore, CSF-1-conditioned macrophages have reduced proliferation when LPS is added (Sester et al., 1999; Yeung and Stanley, 2003).

Modulation of cellular activity occurs both ways in the TAM/cancer cell interaction. Canine mammary adenocarcinomas are known to express CSF-1R, and this is linked to malignancy and ability to metastasize (Król et al., 2011). Also, co-culture with macrophages increases transcription of the mRNA for CSF-1R in canine tumours (Król et al., 2012). Here, it is shown that macrophage-conditioned medium increased cancer cell proliferation and expression of CSF-1R. Since cancer cells could replicate in response to CSF-1, it is likely that the interaction with the macrophage-conditioned medium lead to higher cancer cell proliferation through increased CSF-1R signalling. Sequencing of the CSF-1R from the Lilly cell line showed that the receptor had no mutations, which could lead to constitutive activation of the receptor (Heisterkamp et al., 1983). Therefore, signalling through CSF-1R in the cancer cells must occur through binding of ligand to the receptor. Cancer cells are capable of autocrine stimulation with CSF-1 (Patsialou et al., 2009). A large number, if not the majority, of breast tumours express the CSF-1R, indicating that this is an important pathway for this cancer (Lee et al., 1999). CSF-1R signalling in epithelial cancer cells can induce radiotherapy resistance, for instance. *CSF1* is a target gene for p53, and CSF-1R signalling feeds back to p53 to decrease apoptosis. In cancer, radiotherapy resistance is induced by CSF-1R signalling in a p53-dependent manner (Azzam et al., 2013).

The importance of CSF-1R to canine mammary cancer cells was confirmed using small molecule inhibitors of three receptors. GW2580 is a tyrosine kinase inhibitor of CSF-1R (Conway et al., 2005). Toceranib phosphate is a pan-tyrosine kinase inhibitor that is currently licensed for treatment of cancer in dogs (Bernabe et al., 2013; Liao et al., 2002). RS102895 hydrochloride is an inhibitor of the CCR2 (CCR2i). These inhibitors were chosen for the significance of the respective targets in cancer development. Of these, only GW2580 was able to effectively target both canine mammary carcinoma cell lines tested, indicating that dependence on CSF-1R signalling is a common trait among canine mammary carcinomas. As stated before, not all mammary cancer cell lines/tumours rely on CSF-1R for survival or proliferation. CSF-1 leads to arrest of insulin or estradiol-induced proliferation of hormone-dependent cancer cells, such as MCF-7. This is mediated by upregulation of p21, which induces a G1 arrest in these cells (Lee et al., 1999). The REM134 cell line is not hormone-dependent (Else et al., 1982); that information is not available for the Lilly cell line.

The Lilly cell line was originated from a canine inflammatory mammary carcinoma (R. de Maria, University of Turin, Italy), an aggressive form of the disease with very poor prognosis (Alenza et al., 2001; Peña et al., 2003). The canine inflammatory mammary carcinoma shows several similarities to the human inflammatory breast cancer (Lerebours et al., 2008). Among the genes overexpressed in inflammatory breast cancers in relation to other forms of breast cancer, are those encoding CCL2 and CSF-1 (Lerebours et al., 2008). It was shown here that Lilly cells express the CSF-1R, and may therefore involve CSF-1 in an autocrine stimulation pathway. If these cells express CCL2, as do inflammatory breast cancers, this chemokine is probably connected with factors other than the autocrine stimulation of the cancer cells – such as recruitment of macrophages – since the Lilly cell line was not inhibited by the CCR2i. CCL2 function in breast cancers is believed to be mainly associated to cancer migration and metastasis, not direct proliferation (Soria and Ben-Baruch, 2008). Nevertheless, the REM134 cell line was successfully inhibited by the CCR2i. In experiments conducted by other members of the group, CCL2 demonstrated some capacity to induce REM134 proliferation (Teresa Raposo, Roslin Institute/Universidade de Trás-os-Montes e Alto D'Ouro, personal communication).

Toceranib was first licensed for use against mast cell tumours, but has been shown to be reactive against canine mammary cancers (Ranieri et al., 2013). However, as seen for the CCR2i, toceranib was only able to target REM134 cells, but not Lilly cells in the present study. The effectiveness of toceranib against different forms of canine mammary carcinomas has not yet been established (Chon et al., 2012).

Macrophages also influenced mammary cancer cells to increase glucose uptake. Tumoural consumption of glucose is a marker of cellular metabolism that is associated with cancer grade and prognosis. However, the association of higher glucose uptake and presence of TAMs is not certain in clinical samples (Bos et al., 2002; Brown et al., 1999). Increased CSF-1R expression due to macrophage conditioned medium and autocrine CSF-1 signalling may have increased proliferation and metabolism of the cancer cells.

The general interactions evidenced in this chapter and proposed mechanisms are illustrated in Figure 3.10.

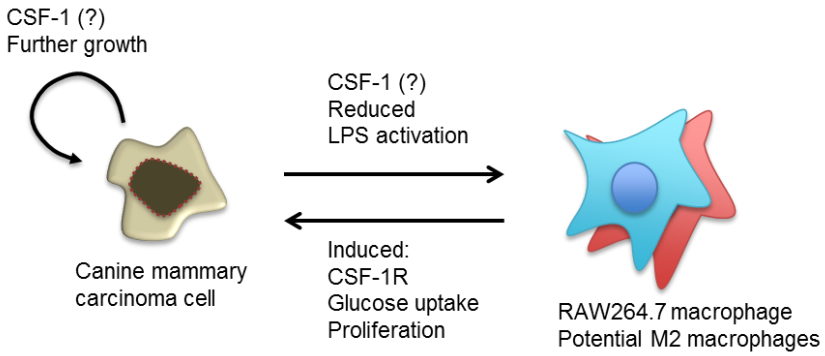

Figure 3.10 – Summary of the results and proposed mechanisms. Cancer cells affected LPS-induced increases in macrophage MHC II, TLR2 and granularity possibly due to the production of CSF-1. Mammary carcinoma cells also depended on CSF-1R signalling for proliferation and survival, suggesting that these cells may rely on autocrine CSF-1R stimulation. The expression of this receptor by cancer cells and also proliferation and glucose uptake was induced by macrophage-derived factors.

3.5 Conclusion

These results underline the importance of CSF-1R-inhibiting therapies in cancer, which would block TAMs and cancer cells expressing this receptor. The cancer cells seem to have reduced inflammatory responses of macrophages partially through CSF-1 mediation. The mechanism through which CSF-1 affects LPS stimulation is not fully clarified, but is likely to involve regulation of the receptors that recognize LPS. Both cancer cell lines studied in this chapter expressed the CSF-1R and at least one of the cancer lines proliferated in response to CSF-1. Although not studied directly here, evidence from the literature indicates that CSF-1R autocrine stimulation of cancer cells is a common event. Macrophages may enhance this event, since cultivation of cancer cells with macrophage-conditioned medium increased carcinoma CSF-1R expression and cellular metabolism, indicating that there is a loop of activation between cancer cells and macrophages.

Chapter 4

Characterization of murine monoclonal antibodies against canine CSF-1R

Highlights

- Several monoclonal antibody candidates were tested for the capacity to bind to CSF-1R and block macrophage proliferation.
- mAb 3.1, raised against the dimerization domain of CSF-1R, emerged as the most promising clone, effectively binding to macrophages in tissues and blocking cellular proliferation.
- However, mAb 3.1 seemed to have moderate specificity for CSF-1R, requiring improvements in its binding characteristics before it is translated into clinical use.

Abstract

In Chapter 3, it was shown that CSF-1R signalling is relevant in the context of tumour progression. The receptor induces tumour promoting phenotypes both in tumour-associated macrophages and in the cancer cells themselves. Therefore, blocking CSF-1R could be beneficial to cancer patients. With this purpose, monoclonal antibodies (mAbs) were raised against the canine CSF-1R using the hybridoma technology. This chapter describes the validation of the antibodies generated by hybridoma in Chapter 7. Several antibodies were produced, of which mAb 3.1 showed the greatest potential, having been used successfully in immunostaining assays and to block macrophage proliferation. However, the results also indicate that this mAb only binds to CSF-1R with moderate affinity and specificity. mAb 3.1 seemed to only stain cells with high CSF-1R expression, and, by ELISA, presented a degree of non-specific binding. Inhibition of macrophage proliferation was only achievable at high antibody concentrations. In conclusion, it was functionally validated that mAb 3.1 binds to its target, but improvements in its binding characteristics are required before it can be indicated for clinical uses.

4.1 Introduction

CSF-1R and tumour associated macrophages (TAMs) are known causes of poor prognosis in several cancer types (Chambers et al., 1997; Raposo et al., 2012). The presence of TAMs has been correlated with increased proteinase expression, which leads to tissue invasion (Paulus et al., 2006); TAMs assist cancer cells in penetrating blood vessels (Wyckoff et al., 2007); they are linked to tumoural immunosuppression; and are associated with reduced chemotherapeutic responses (Mitchem et al., 2013). Cancer cells recruit TAMs and establish a paracrine loop of stimulation where the tumour secretes CSF-1, which acts on the macrophages, and in response TAMs produce EGF, which induces cancer cell growth (Wyckoff et al., 2004). Furthermore, the cancer cells can be stimulated by CSF-1 in an autocrine manner, reinforcing the importance of this receptor for cancer progression (Patsialou et al., 2009). Because of its significance in the pathogenic progression of cancer, CSF-1R is an attractive target for drug development.

Several antibodies have been raised against human and murine CSF-1R (Haegel et al., 2013; MacDonald et al., 2010; Murayama et al., 1999) or against the CSF-1 (Paulus et al., 2006). Clinical trials for breast and prostatic human cancer are currently in progress with an inhibitory anti-CSF-1R (https://www.clinicaltrials.gov/ct2/show/study/NCT02265536). However, none of the previously described antibodies targets the canine receptor. Conversely, antibodies which were designed to identify canine macrophages through other receptors have been raised, although none have been assessed for their ability to block macrophage function or survival (Aguiar et al., 2004; Yamate et al., 2000).

As a clinical tool, antibodies that target the CSF-1R are more suitable than antibodies that target the ligands, since these have short circulation half-lives. Also, CSF-1R has two ligands, CSF-1 and IL-34, which are structurally unrelated, therefore requiring different antibodies to block both (Bartocci et al., 1987; Liu et al., 2012). Additionally, both of these cytokines have dissimilar spatiotemporal expression patterns, making the targeting of both difficult (Wei et al., 2010).

4.1.1 Approaches for targeting TAMs

Macrophage depletion within tumours has been explored using alternative methods to monoclonal antibody treatment, such as liposome clodronate therapy and small molecule inhibitors of CSF-1R (Guth et al., 2013; Mashkani et al., 2010; Zeisberger et al., 2006). Small molecule inhibitors of CSF-1R affect the tyrosine kinase function of this receptor.

However, a common disadvantage of this method is the off-target binding, whereby the drug indiscriminately affects other tyrosine kinase receptors, leading to a range of unanticipated side-effects (Zhang et al., 2009). Antibody therapy would have greater selectivity, limiting the off-target effects. Liposome clodronate therapy involves the employment of a bisphosphonate drug, clodronate, to inhibit osteoclast and macrophage survival. Bisphosphonates are commonly used in medical practice to inhibit osteoclast function in diseases such as osteoporosis (Coxon et al., 2006). Liposome is used as a delivery agent to improve the pharmacokinetic properties of the bisphosphonate. This form of therapy has shown promising results as an anti-cancer agent. One disadvantage of clodronate therapy is a complete depletion of macrophages. It has been shown, for instance, that following clodronate treatment there is rapid reduction of circulating monocytes, loss of inflammatory mediators and reduced inflammatory cell recruitment. This could potentially permit infections in patients which are already immunocompromised due to the cancer (Davies et al., 2013; Ono, 2008; Zeisberger et al., 2006). Targeted anti-CSF-1R therapy has the advantageous effect of limiting only certain subpopulations of macrophages such as TAMs, while allowing for the function of cells with inflammatory phenotypes (Haegel et al., 2013; MacDonald et al., 2010).

Among the unconjugated mAbs approved for clinical use, antibodies with capacity to block the function of the target are the most common. This characteristic improves the efficacy of the drug, even if other mechanisms of action are present, such as antibody-dependent cellular cytotoxicity (ADCC) (Adams and Weiner, 2005; Iannello and Ahmad, 2005). However, another possible antibody approach to depleting tumour macrophages could be to couple anti-CSF-1R antibodies to toxins or radioactive compounds. In this case, the mAb would not need to have receptor-blocking capacity and would overcome the difficulties in finding a suitable blocking antibody. Nevertheless, the technology of conjugated antibodies also presents some hurdles of its own, such as immunogenicity of the coupled drug/toxin; increased side effects due to non-specific targeting; and increased cost of production, which is very relevant in the veterinary practice (Teicher and Chari, 2011). Also, as stated above, CSF-1R-blocking mAbs have the advantage of sparing inflammatory macrophages, which are CSF-1R$^+$ but are being stimulated by other cytokines. A drug-conjugated antibody would completely remove CSF-1R$^+$ cells, irrespective of the cytokine stimulation background. Therefore, both TAMs and macrophage protective responses would be lost (MacDonald et al., 2010). Due to these considerations, the aim of the work presented here was to identify a CSF-1R-blocking mAb.

Two major strategies were identified for blocking CSF-1R using a mAb. The antibody could either inhibit ligand binding to the receptor or it could inhibit receptor dimerization. These effects could be performed by direct binding of the antibody to the receptor regions responsible for ligand recognition/dimerization or through stabilization of a folded conformation of the receptor (Bradbury et al., 2011). Stable dimerization is essential for CSF-1R signalling (Li and Stanley, 1991). Blocking dimerization would impede signalling through both IL-34 and CSF-1, and should fully stop CSF-1R signalling. Although both IL-34 and CSF-1 share a binding site on the surface of CSF-1R, there are differences on the receptor contact points for binding both ligands; these overlap, but are not identical (Liu et al., 2012; Ma et al., 2012). Indeed, while an antibody has been identified that can block the binding of CSF-1R to both ligands, another mAb was only capable of blocking the interaction of the receptor with CSF-1, but not IL-34 (Chihara et al., 2010).

Given the different possible mechanisms to block receptor function using antibodies, two strategies of antibody production were used in the present work. Antibodies were generated against either the full extracellular portion of the receptor (expressed in mammalian cells) or the dimerization domain only (produced in bacteria).

4.1.2 Published CSF-1R-blocking antibodies

There is a considerably extensive literature on CSF-1R blocking antibodies. The knowledge acquired with those mAbs presents important arguments regarding the usefulness of anti-CSF-1R therapies. Also, a comparison can be drawn between these published clones and the antibodies discussed in the present work. Therefore, the main findings in the literature on the anti-CSF-1R are presented here.

M279 is a mAb against the mouse CSF-1R. When administered *in vivo* for short periods (3 weeks), it causes mononuclear cell depletion of peritoneal macrophages (the antibody was injected in the peritoneal cavity) and of most tissue-resident macrophages and their monocyte precursors ($CSF\text{-}1R^{+}Gr\text{-}1^{-}$), but has little effect on bone marrow, blood, lymph node and spleen macrophages. Over long treatment protocols (6 weeks), osteoclasts, Kupffer cells, $Ly6C^{Low}$ monocytes in the bone marrow and testis macrophages are depleted. Importantly, this antibody does not affect the inflammatory monocyte subset ($CSF\text{-}1R^{+}Gr\text{-}1^{+}Ly6C^{+}$). This translates in no effect of M279 treatment on induced inflammation models of lung and peritoneum, and no effect on wound healing and graft-versus-host disease. This mAb is capable of reducing the burden of tumour-associated macrophages on a murine

model of mesothelioma, but not of macrophages present in the tumour growth front. The mAb does not reduce tumour growth, maybe because of the short test period (3 weeks) or the presence of surrounding macrophages which were not eliminated. Notably, not even with a long treatment protocol, which reduced several tissue macrophage subsets, did this antibody induce toxicity or side-effects (MacDonald et al., 2010; Sauter et al., 2014).

AFS98 is also a mAb against murine CSF-1R and, like M279, has little effect on bone marrow macrophages (Sudo et al., 1995). This antibody is capable, however, of depleting tumour-associated macrophages in murine tumour models. This is sufficient to delay tumour appearance, reduce its growth and increase survival and chemotherapy sensitivity (Fend et al., 2013). Although AFS98 does not reduce all macrophages within the bone marrow, it does deplete nonclassical ($Ly6C^-$) monocyte subsets from the bone marrow and circulation. AFS98 also reduces $Ly6C^-$ resident peritoneal, alveolar and splenic macrophages by reducing cellular viability, not by affecting proliferation. This antibody also strongly reduces inflammatory recruitment of macrophages in peritoneal inflammation models (Louis et al., 2015) and after muscular lesion; in the latter model, less macrophages resulted in reduced proliferation of muscular satellite cells and increased fibrosis (Segawa et al., 2008). Interestingly, the antibody not only depletes most $CSF\text{-}1R^+$ but also $CSF\text{-}1R^-$ cells in peritoneal inflammation models. The authors believed that the reduction of $CSF\text{-}1R^-$ cells in inflammation following mAb treatment was due to reduced governing signals from the depleted $CSF\text{-}1R^+$ cells. The effects of AFS98 on inflammation are in disagreement with other anti-CSF-1R mAbs, such as M279, described above, which do not seem to affect inflammatory function. It had been suggested that AFS98 only reduced inflammation because it acted though ADCC via its IgG_{2a} heavy chain to kill monocytes. It was later confirmed that AFS98 reduces inflammation due to neutralization of CSF-1R signalling, not through ADCC (Louis et al., 2015).

mAb 2-4A5 is an anti-murine CSF-1R. It inhibits bone marrow-derived macrophage and monocyte survival, without inducing internalization or degradation of the receptors (Haegel et al., 2013; Sherr et al., 1989).

RG7155 is a mAb against the human CSF-1R. It binds to the fourth extracellular region of the receptor, inhibiting macrophage survival by impeding receptor dimerization. The mAb depletes CSF-1 and tumour-conditioned macrophages, but not GM-CSF-conditioned macrophages. RG7155 only eliminates $CD14^+CD16^+$ monocytes from peripheral blood. Kupffer cells and colonic macrophages are depleted, but the effect is lesser against lung macrophages. CSF-1R inhibition by mAb 2G2, an anti-murine CSF-1R described together with RG7155, decreases TAM counts, which is followed by a concomitant increase

in neutrophil and lymphocyte infiltration of the tumour. When RG7155 was administered to human patients with diffuse-type Giant Cell tumours, clinical improvements could be seen, reducing tumour burden. In several other human tumour types, RG7155 reduced TAM counts (Ries et al., 2014). In human patients with tenosynovial giant cell tumours, which occur due to mutations leading to abnormal CSF-1 expression, mAb RG7155 decreased $CD14^{+}CD16^{+}$ monocytes and the presence of TAMs, which was correlated with rapid clinical improvement (Cassier et al., 2014).

H27K15 is a somewhat different monoclonal antibody in that it does not block CSF-1 binding to CSF-1R and their removal from the cell surface, unlike the previously described antibodies. It is an intermediate-affinity clone and its function is mainly dependent on Fc binding. It does not kill monocytes, but impedes their activation into the M2 state, suppressing CCL2 and IL-6 expression by these cells (Haegel et al., 2013).

4.1.3 Targeting TAMs in dogs

Targeting canine cancer offers the evident benefit of providing better care for these patients. However, targeting naturally occurring canine cancers in a clinical setting also generates information for the study of human diseases. There are many characteristics in canine cancer that make it amenable for use as a model in the study of human cancer, such as genetic similarities, shared environmental risk factors, similar responses to treatment and spontaneous occurrence of several cancer types (Rowell et al., 2011). Drug trials in dogs can be valuable in predicting the clinical value of new pharmaceuticals when these are tested in humans. A high rate of human clinical trials end in failure following encouraging results in mice (Gordon et al., 2009; Natanson, 2011). As an example, while mouse experiments indicated very positive outcomes after TAM depletion using clodronate therapy (Zeisberger et al., 2006), initial results in dogs showed little effect (Guth et al., 2013), reflecting the more conservative results seen in early human tests (Diel et al., 1998; Paterson et al., 1993; Saarto et al., 2001).

The goal of this work was to identify an antibody that could block the function of canine CSF-1R with the intent of treating cancer patients. This chapter describes the validation tests for several monoclonal antibodies raised against the canine CSF-1R. Although numerous clones were tested in some of the assays shown here, greater emphasis is given to mAb 3.1, which was analysed through a large array of tests. This antibody could bind to bone marrow macrophages and $CSF\text{-}1R^{+}$ canine mammary cancer cells. It also

presented staining patterns in canine tissues that were in accordance with the expected distribution of macrophages. However, this antibody also presented issues with specificity and affinity, as it could not bind to canine peripheral blood monocytes and cross-reacted with control proteins in ELISA.

4.2 Materials and Methods

Basic methodological descriptions and brands not stated here are presented in Chapter 2.

4.2.1 Immunofluorescence

For cellular stains, cells were grown on tissue culture-treated glass slides (between 10^3 – 5 × 10^3 cells per chamber) (Nunc Lab-Tek II Chamber Slide System, Thermo Scientific). Canine bone marrow-derived macrophages (BMDM) were allowed to adhere to the slide overnight and were fixed with ice cold acetone at – 20°C for 20 min, washed with PBS and blocked for 60 min with PBS + normal goat serum (10 %) at room temperature.

For histological stains, tissue samples were fixed in PBS + paraformaldehyde (4 %, agitated for 1 h at 60°C for solubilisation) for 3 h. The tissue was then immersed in 20 % and then 40 % sucrose, until sunk in each solution. The samples were embedded in OCT compound (Fisher) and snap-frozen by submersion in liquid nitrogen. Sections of 6 µm were obtained using an OTF5000 cryostat (Bright) and these were placed on SuperFrost glass slides (Thermo Scientific). The sections were stored at – 80°C until used. After removing from the freezer, the slides were washed with PBS and blocked as for the cellular stains. Sections were permeabilized by addition of PBS + Triton X-100 (0.2 %) for 10 min at room temperature. Slides were rinsed with PBS after permeabilization.

Cells or sections were incubated overnight at 4°C with hybridoma cell culture supernatants. Mouse anti-human CD163 AM3K (1:75, TransGenic Inc.), mouse anti-canine CD11b (1:10, AbD Serotec) and rabbit anti-human c-Kit (1:100, Dako) were also used for comparison where stated. Isotype control was mouse IgG_1 (20 µg/test, Abcam). Antibodies were diluted in blocking buffer.

For assessment of competitive inhibition of staining, DH82 cells were stained with the hybridoma supernatant of mAb 3.1 or anti-CD11b adding increasing concentrations of purified recombinant His-tagged dimerization domain of CSF-1R (produced as shown in Chapter 7).

Goat anti-mouse Alexa 488 or goat anti-rabbit Alexa 647 fluorescent secondary antibody (Invitrogen) was diluted 1:300 in blocking buffer and cell staining was performed at room temperature for 2 h. Slides were washed with PBS thrice for 5 min after the antibody incubation steps. DAPI (4',6-diamidino-2-phenylindole) nuclear stain was included in the mounting medium (Vectashield Mounting Media with DAPI, Vector Labs). A coverslip was placed on top of the section with a drop of mounting medium. The section was isolated using nail polish.

4.2.2 Dot blot

For determination of the concentration of mAb 3.1 in the hybridoma supernatant, it was compared to an isotype control by dot blot. Mouse IgG_1 isotype control (Abcam) at 20, 40, 80 and 160 µg/ml was diluted in PBS in 1:2 steps until 1:2048. This was compared to a similar dilution of the supernatant containing mAb 3.1. The dilutions were dotted on a nitrocellulose membrane (1 µl). The membrane was blocked with PBST + milk (5 %). Bound antibodies were detected with rabbit anti-mouse immunoglobulins, HRP-conjugated (1:1000, Dako) diluted in blocking buffer. HRP activity was detected using ECL reagent (GE Healthcare). The concentration of antibody in the supernatant was determined by visual comparison against the different concentrations of the isotype control. The isotype control used for staining canine duodenum (see 4.2.1, above) was adjusted according to the concentration of mAb 3.1.

4.2.3 Immunohistochemistry

Cancer samples were obtained from Teresa Raposo (Universidade de Trás-os-Montes e Alto Douro, Portugal and The Roslin Institute). Samples were collected from clinical cases with owner's consent. Paraffin wax-embedded mammary cancer samples were cut in 4 µm sections with a microtome (RM2235, Leica). The sections were placed on glass slides (Thermo Scientific) and rehydrated by dipping the slides successively in solutions with higher water content:

1. Xylene: 2 × 3 min;
2. Xylene 1:1 with 100 % ethanol: 3 min;
3. 100 % ethanol: 2 × 3 min;
4. 95 % ethanol: 3 min;
5. 70 % ethanol: 3 min;

6. 50 % ethanol: 3 min;
7. Running cold tap water to rinse.

Antigens were retrieved by Proteinase K treatment (Promega) for 20 min at 37°C. Sections were blocked with H_2O_2 (0.3 %) for endogenous peroxidase activity. Peroxide was removed by rinsing with PBS. Non-specific binding sites were blocked with PBS + goat serum (10 %). Mouse hybridoma supernatants were used to probe the slides. These were incubated overnight at 4°C. Goat anti-mouse Ig, HRP-conjugated secondary antibody (1:1000 in blocking buffer, Dako) detected the bound mAbs by incubation at room temperature for 1 h. Slides were washed with PBS thrice for 5 min after both antibody incubation steps.

HRP activity was detected using NovaRed substrate (Vector Labs). The reagents were mixed and placed on the sections. When colour had developed, slides were rinsed with water. Slides were counterstained with Mayer's haematoxylin solution (Sigma) for 30 s and washed twice in water for 5 min. The sections were dehydrated by following the rehydration protocol above in reverse. DPX mountant (Fluka) and the coverslips were placed covering the sections.

4.2.4 Flow cytometry

For all cell types, 10^6 cells were used for flow cytometry. For REM134 staining, cells were centrifuged at 400 × *g* and the supernatant was discarded. Cells were fixed with PBS + formaldehyde (0.01 %) for 10 min at room temperature and permeabilized with PBST for 15 min at room temperature (where stated). Cells were washed and stained with undiluted mAb supernatants containing Tween 20 (0.05 %), for 20 min at room temperature. After washing in PBST thrice, secondary antibody was added in blocking buffer + Tween 20 (0.05%).

Canine blood was collected from animals from the Edinburgh Dog and Cat Home, euthanized for humane reasons. Leucocytes were isolated from whole blood using ficoll density separation (Ficoll-Paque, density of 1.077, Sigma). Blood (3 ml) was diluted 1:1 with PBS at room temperature and layered slowly over the same volume of ficoll. Cells were separated by centrifugation (30 min, 400 × *g*, room temperature). The cloudy interface containing white cells was collected and washed with PBS (10 ml). The leucocytes were centrifuged again. This was followed by lysis of remaining red blood cells in the pellet for 5 min on ice (lysis buffer: NH_4Cl (150 mM), $NaHCO_3$ (10 mM), EDTA (0.1 mM), pH 7.2). PBMCs were blocked with cold PBS + FBS (10 %) for the first attempt and then PBS +

human Fc Blocking Reagent (20 µl, Miltenyi Biotec) or PBS + canine serum (10 %) for the following trials. PBMCs were stained with purified mAbs or hybridoma supernatants for 30 min, 2 h or overnight, at 4°C. For overnight stains, cells were fixed in PBS + paraformaldehyde (2 %). After washing thrice in cold PBS, secondary antibody was added. A mouse anti-swine CSF-1R mAb was used as positive control for the staining of PBMCs (produced by Lindsey Waddell, David Hume group, The Roslin Institute). For PBMCs, Sytox blue (Life Technologies) or 7-AAD (5 µl/sample, eBioscience) stains were added 5 min before the analysis for assessment of cell viability by flow cytometry.

To assess the differences in expression of CSF-1R in the presence or absence of CSF-1, BMDM were differentiated as explained in Chapter 2. Cells were FBS-starved overnight in the presence or absence of 100 ng/ml rhCSF-1 (Invitrogen). When stated, cells were fixed for 30 min at 4°C with PBS + paraformaldehyde (2 %). Cells were placed in round bottom 96-well plates (Greiner) and blocked with PBS + goat serum (10 %) for 30 min, at 4°C. IgG_1 isotype control (Abcam), anti-pig CSF-1R (Lindsey Waddell) (both at 25 µg/ml in blocking buffer) or mAb 3.1 (hybridoma supernatant or 10 µg) were used for cell staining. After 3 washes in PBS (centrifugations at 400 × *g*), secondary antibody was added. When stated, cell viability was assessed using 7-AAD (5 µl/sample, eBioscience). To confirm the identity of BMDM in a separate experiment, cells were stained with a mouse anti-canine CD11b antibody (1:10, AbD Serotec) in blocking buffer, followed by a secondary antibody.

For all cells, secondary antibody used was goat anti-mouse antibody, Alexa 488-conjugated (Invitrogen). It was added at 1:800 in 100 µl blocking buffer /10^6 cells for 30 min at 4°C. This was followed by three washes, as for the primary antibodies.

Cells were analysed on a FACScalibur flow cytometer (Becton Dickinson). Data were analysed using Summit 4.1 software (Dako), assessing the percentage of positive cells as determined in relation to the secondary antibody control. The first result showing the flow cytometry of PBMCs was analysed on a FACSAria flow cytometer (Becton Dickinson) and was analysed on FlowJo (TreeStar). Cells in the BMDM or the leukocyte gate were assessed, depending on the experiment.

4.2.5 Immunoprecipitation

mAbs (21 µg or supernatant from mAb 1C6) in sodium phosphate buffer (pH 7.0) were bound to 75 µl (dried volume) of Protein G beads (GE Healthcare) for 2 h at 4°C. Unbound mAbs were removed by centrifuging the beads at 1000 × *g* and washing once with

sodium phosphate buffer. HEK293T cells were transiently transfected to express the extracellular region of CSF-1R (Chapter 7). One millilitre of the supernatant was incubated overnight, at 4^{o}C, with the Protein G + mAbs. The resin was washed 5 × with sodium phosphate buffer. The resin was incubated with 30 µl PBS + reducing sample buffer (considered the volume of the resin to calculate the sample buffer volume). This was incubated at 95^{o}C for 5 min. Centrifuged to precipitate the resin. Loaded the supernatant into 10 % SDS-PAGE gel. Probed western blot nitrocellulose membrane with mouse anti-His tag, 1:500 (Invitrogen) and with goat anti-mouse, HRP-conjugated, 1:1000 (Dako).

4.2.6 Endpoint proliferation assays

Between 10^3 and 10^4 REM134 or RAW264.7 cells were plated in 100 µl of DMEM medium (Gibco) in individual wells of black opaque 96-well plates (Greiner). Hybridoma supernatants (where stated) and/or rhCSF-1 (100 ng/ml, Invitrogen) were added to the culture at the same time as the cells. After 48 h, viable cells were quantified using CellTiter-Glo, Promega.

4.2.7 Real time cell proliferation assay

The xCELLigence Real-Time Cell Analyzer (Roche) was standardized with 50 µl of DMEM medium (Gibco) before adding cells. Between 10^4 and 3×10^4 cells were used (either REM134 or canine bone marrow macrophages). Bone marrow macrophages and REM134 cells were grown in the presence of rhCSF-1 (50 ng/ml and 100 ng/ml, respectively, Invitrogen). Cells were placed on an xCelligence 16 or 96-well plate (Roche) in 100 µl of culture medium. The plate was scanned to measure the initial numbers of cells in each well, and then treatment was added. Between 5 – 20 µl of hybridoma supernatant or purified mouse antibodies were used for each assay. Controls received equivalent volumes of vehicle (medium or PBS) or the equivalent concentration of murine serum IgG (Sigma). Cells received rhCSF-1 and antibodies *circa* every 48 h during the experiment. Cells were then maintained at the usual culture conditions for the duration of the experiment. The amount of cells attached to the bottom of each well was measured by the equipment through assessment of the interference with the electrical impedance of the sensor on the plate. Cell proliferation was assessed every 15 min.

4.2.8 Chorioallantoic membrane (CAM) assay

The biological effect of blocking CSF-1R in REM134 cells was studied by the CAM assay. These cancer cells were grafted onto the chick embryo CAM and blood vessel formation was quantified in the presence or absence of mAbs. The protocol of Ribatti et al., 2006 was followed. The technique is illustrated in Figure 4.1. The use of chicken embryonated eggs is allowed by the Home Office until day 11 of incubation without the need for a licence. Briefly, chicken embryonated eggs (National Avian Research Facility, The Roslin Institute) were incubated rocking (Brinsea Octagon 40 OX incubator) at 37.5^{o}C until day 4 of development in a horizontal position. At this date, *circa* 2 ml of egg albumin was removed with a syringe and a 24 gauge needle (Becton Dickinson). A 1 cm × 1 cm window was opened on the shell with a scissor, having the egg in the horizontal position. The embryo received 150 µl of 10 × tissue culture-grade penicillin/streptomycin (Gibco), pipetted slowly. The window was closed with a plastic adhesive tape and the egg was incubated statically at 37.5^{o}C (RCOM Maru Digital Incubator) until day 7. The window was reopened by removing the tape and the cancer cells were grafted onto the CAM. Cells were stained with CFSE (eBiosciences). For this, cells were suspended in FBS-free DMEM medium. CFSE was added to the cells at 10 µM for 15 min at room temperature protected from light. Cells were then washed twice with complete medium. The stained cells were absorbed in a 5 × 5 × 5 mm gelatine sponge (Gelatamp, Roeko) (around 10^6 cells/sponge), either in the presence of mAb 3.1 hybridoma supernatant or in control medium. After placing the sponge on the CAM, eggs were returned to the static incubator. On day 10, eggs were moved to 4^{o}C for 30 min before imaging. Images acquired using Axio ZoomV16 coupled with AxioCAM HRM camera (Zeiss). Blood vessel formation around the sponge graft was assessed. Blood vessel density and blood vessel branching near the graft were scored according to Ribatti et al., 2006. Briefly, vessel density was given a score between 0 (no vessel convergence towards graft) and 5 (intense convergence of large vessels towards graft). Branching was given a score where distant branching from the implant was scored 2 points; near branches received 1 point; and unbranched vessels reaching the sponge at an angle of less than 45^{o} were scored 1 point. If doubtful about the score to be attributed for each picture, the lowest score was given to the control samples and the highest was given to the test samples.

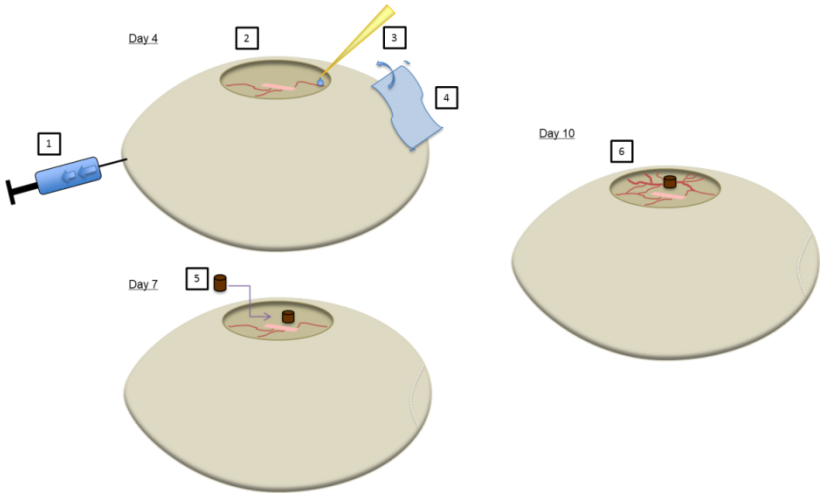

Figure 4.1 – The chicken chorioallantoic membrane assay. **(1)** On day 4 of egg incubation, 2 ml of egg white is removed with a syringe. **(2)** A 1 × 1 cm window is opened on the egg shell close to where the embryo is located. **(3)** Antibiotic is added. **(4)** The window is closed with an adhesive tape. **(5)** On day 7, cancer cells are absorbed in a gelatine sponge, in the presence or absence of treatment. The sponge is placed on the CAM without touching the embryo. **(6)** On day 10, the sponge and its surroundings are imaged for quantification of blood vessel formation and branching.

4.2.9 Inhibition of feline osteoclasts

Feline bone marrow cells were differentiated for 10 days in rhRANKL (30 ng/ml, R&D Systems) and rhCSF-1 (10 ng/ml, R&D Systems) in low adherence tissue culture plates (Corning). Anti-CSF-1R mAb 3.1 hybridoma supernatant or an anti-CCR2 hybridoma supernatant (produced by Teresa Raposo, Universidade de Trás-os-Montes e Alto Douro, Portugal and The Roslin Institute) was added to the cells at 1/6 of the total culture volume. One control well received no CSF-1 after the beginning of the experiment. The culture medium and supplements were renewed at 48 h. Cells were lysed on day 4 using 1 ml/well of Lysis buffer 15 (R&D Systems, Apoptosis array kit) for 30 min at 4^{o}C. Protein concentration was measured using a Bradford assay. The protein mixture was resolved on a 10 % SDS-PAGE (20 µg of protein/lane) and transferred to nitrocellulose. The membranes were probed with anti-pAkt (Ser 473), total Akt and pMAPK, (all at 1:1000, Cell Signalling) in PBST + skimmed milk powder (5 %) for 2 h at room temperature. Antibodies were used sequentially on the same membrane, after stripping the nitrocellulose membrane using

Restore PLUS Western Blot Stripping Buffer (ThermoFisher Scientific) and blocking the membrane. Secondary antibody used was swine anti-rabbit HRP-conjugated (1:1700, Dako), in the same buffer as the primary antibody.

4.2.10 ELISA assays

Competition ELISA for the CSF-1R binding region

An ELISA was used to test the ability of some mAbs to block the binding of CSF-1 to CSF-1R. This methodology has been used previously for testing the effect of mAbs on the CSF-1/CSF-1R interaction (Haegel et al., 2013). This assay is based on the capacity of the recombinant canine CSF-1R to bind to rhCSF-1 (Chapter 7), which is in turn detected by a commercial antibody. If the mAb being tested is able to block the binding of ligand/receptor, CSF-1 is washed away and the signal is reduced (Figure 4.2). A Nunc Maxisorp 96-well plate (Thermo Scientific) was coated overnight at 4^{o}C with 300 ng/well of canine recombinant CSF-1R extracellular region (Chapter 7) in 100 µl of carbonate buffer (Na_2CO_3 (15 mM), $NaHCO_3$ (35 mM), pH 9.6). The plate was rinsed with PBST and blocked with PBS + BSA (2 %) for 2 h at 37^{o}C. After rinsing with PBST, the culture supernatants containing mAbs were added to the wells for 1 h at room temperature. Wells were washed 6 × 2 min with PBST. rhCSF-1 (BioLegend) was added at 18 ng/well in blocking buffer and incubated for 2 h at room temperature. After washing the plate with PBST, the bound CSF-1 was detected using an anti-CSF-1 antibody (Peprotech) at 1:75 in blocking buffer, at 4^{o}C, overnight. Wells were washed and a goat anti-rabbit secondary, HRP-conjugated (1:10000, Life Technologies) in blocking buffer was added for 3 h at room temperature. After washing the plate, the reaction was developed using 100 µl of chemoluminescent substrate (GE Healthcare). Luminescence was read for 1 sec/well using Victor3 plate reader (Perkin Elmer).

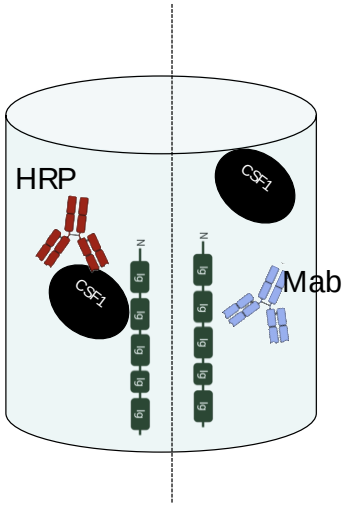

Figure 4.2 – Schematic representation of the ELISA to test the capacity of mAbs to block CSF-1/CSF-1R interaction. The cylinder represents a well in a 96-well plate. On the left half, CSF-1 is shown bound to the adsorbed rCSF-1R (represented by the vertical bar with five subunits). Bound CSF-1 is then quantified by a HRP system with commercial antibodies. On the right half, the anti-CSF-1R mAb is blocking the CSF-1/CSF-1R interaction, allowing CSF-1 to be washed away and reducing the HRP signal.

ELISA for determination of non-specific mAb binding

Maxisorp 96-well plates (Thermo Scientific) were coated with 400 ng/well of either canine recombinant CSF-1R extracellular region or BSA in 50 µl of PBS at 4°C, overnight. Plates were blocked with PBS + BSA (2 %) for 2 h at 37°C. Hybridoma supernatants containing mAb were added for 2 h at 37°C. Plate was washed with PBST for 6 × 2 min. Secondary rabbit anti-mouse HRP (1:2000, Dako) was added for 1 h at room temperature in blocking buffer. Reaction was developed with 50 µl TMB Ultra (Fisher) and was stopped with the same volume of H_2SO_4 (2 M). Absorbance at 450 nm was read using a Victor3 plate reader (Perkin Elmer).

4.2.11 Antibody purification by protein G chromatography

Purification was performed as detailed in Chapter 7.

4.2.12 Statistical analyses

Blood vessel remodelling in the CAM assay was analysed using a Mann-Whitney test. The endpoint proliferation assay was analysed using one-way ANOVA with a Bonferroni post-test. The real-time proliferation assays were assessed using repeated-measures two-way ANOVA with a Bonferroni post-test. For all tests, $P < 0.05$. Assumption tests were performed on Minitab 16 (Minitab Inc.). Statistical tests and graphs were made on GraphPad Prism 5 (GraphPad Inc.).

4.3 Results

Overall, four hybridoma fusions were performed for the production of anti-CSF-1R monoclonal antibodies, three using the extracellular fraction of CSF-1R as the immunogen and one using the dimerization domain of the receptor. Of the several antibodies selected in the initial phases of ELISA screenings (Chapter 7), two of the most promising clones were mAb 3.1 (using the dimerization antigen) and mAb 1C6 (using the extracellular region antigen), which are described in the results below. mAb 1C6 lost binding affinity over time, and for this reason work on it was discontinued.

4.3.1 Cellular immunofluorescence

REM134 (canine mammary cancer cells), Lilly (canine inflammatory mammary cancer cells), DH82 (canine histiocytic sarcoma), canine bone marrow-derived macrophages (BMDM) and RAW264.7 (mouse macrophages) were used for immunofluorescence assays with the mAbs (Figure 4.3). Several antibodies were tested as tissue culture supernatants in the immunofluorescences (not purified). mAb 3.1 showed the best results. These results show that mAb 3.1 stained cells that express the canine CSF-1R, but it did not stain a murine macrophage cell line, RAW264.7, that is also CSF-1R^{+} (Chang et al., 2013).

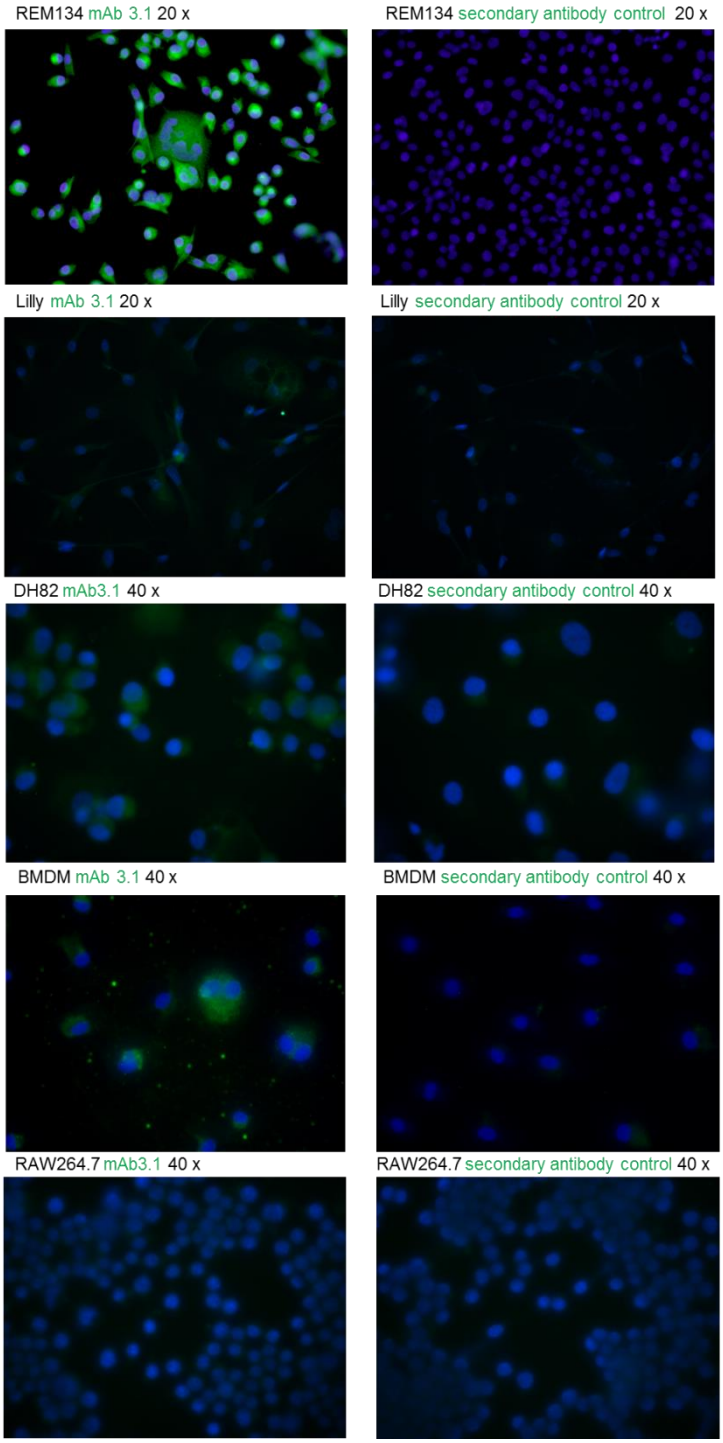

Figure 4.3 – mAb 3.1 stained canine but not murine CSF-1R-expressing cells. Canine mammary carcinoma cells REM134 and Lilly, canine histiocytic sarcoma DH82, canine BMDM and mouse macrophages RAW264.7 were stained with hybridoma culture supernatants containing mAb 3.1. Secondary antibody was goat anti-mouse Alexa 488 (1:300, Invitrogen). Negative controls were stained only with the secondary antibody. Nuclear stain is in blue (DAPI). "20 ×" or "40 ×" indicate the magnification used to acquire the images.

The specificity of mAb 3.1 was assessed by a “peptide competition” assay. DH82 cells were stained with mAb 3.1 in the presence or absence of recombinant canine CSF-1R protein (His-tagged dimerization domain). If mAb 3.1 stained DH82 cells strictly by binding to CSF-1R, adding the recombinant protein would have the effect of blocking the staining. If mAb 3.1cross-reacted with other antigens, adding the recombinant protein would have no effect or little effect on cellular staining. An antibody against canine CD11b was used as a control. Adding the recombinant CSF-1R should not block the binding of the anti-CD11b antibody.

As shown in Figure 4.4, the addition of increasing amounts of recombinant CSF-1R was able to block the staining of the cells by mAb 3.1, but not by the CD11b mAb (the same secondary antibody was used for both stains).

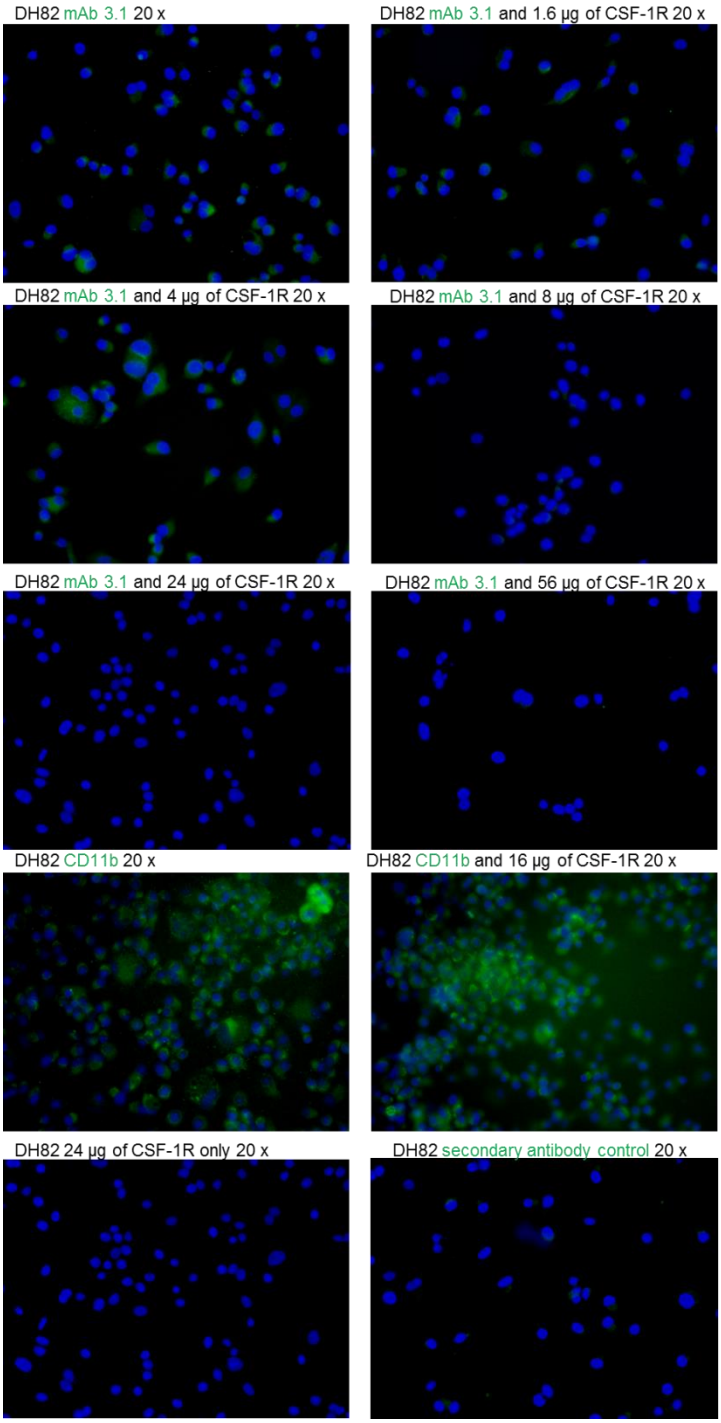

Figure 4.4 – Recombinant CSF-1R was able to competitively inhibit the binding of mAb 3.1 to DH82 cells. DH82 cells were stained with the hybridoma supernatant containing mAb 3.1 or with anti-CD11b (1:10, AbD Serotec), as a control. The primary antibody was competitively inhibited by adding increasing concentrations of His-tagged recombinant dimerization domain of CSF-1R. The addition of CSF-1R did not affect CD11b staining. The concentration of the dimerization domain is shown above each figure. Secondary antibody was goat anti-mouse Alexa 488 (1:300, Invitrogen). Negative controls were stained only with the secondary antibody. Nuclear stain is in blue (DAPI). "20 ×" indicates the magnification used for acquiring the images.

4.3.2 Tissue immunofluorescence

A range of canine tissues from healthy animals were stained with mAb 3.1 by immunofluorescence using the hybridoma supernatant. mAb 3.1 bound to cells in all tissues tested, duodenum, lymph node and spleen. Staining of these tissues with anti-CD163 and anti-CD11b antibodies showed patterns of staining similar to mAb 3.1. In the duodenum, mAb 3.1^+ cells were present around the duodenal glands and within the villus lamina propria, as were $CD163^+$ cells. Staining was stronger around the duodenal glands (Figure 4.5). In the spleen, mAb 3.1^+ cells surrounded the white pulp, as did $CD11b^+$ cells (Figure 4.6). In the lymph node, mAb 3.1^+ cells were mostly seen in the medullary cords and in the paracortical areas, but also close to the subcapsular space and the trabeculae (Figure 4.7).

Exclusively for the duodenal staining, the antibody concentration of the hybridoma supernatant was titrated in order to adjust the concentration of the isotype control used in immunofluorescence. To assess the concentration of mAb 3.1 in the hybridoma supernatant, a scale of isotype control was made by dot blotting several dilutions of the isotype. This allowed for the correct concentration of isotype to be used in the immunostaining. Using this assay, the concentration of mAb 3.1 in the hybridoma supernatant was estimated to be between 40 and 80 µg/ml (Figure 4.8).

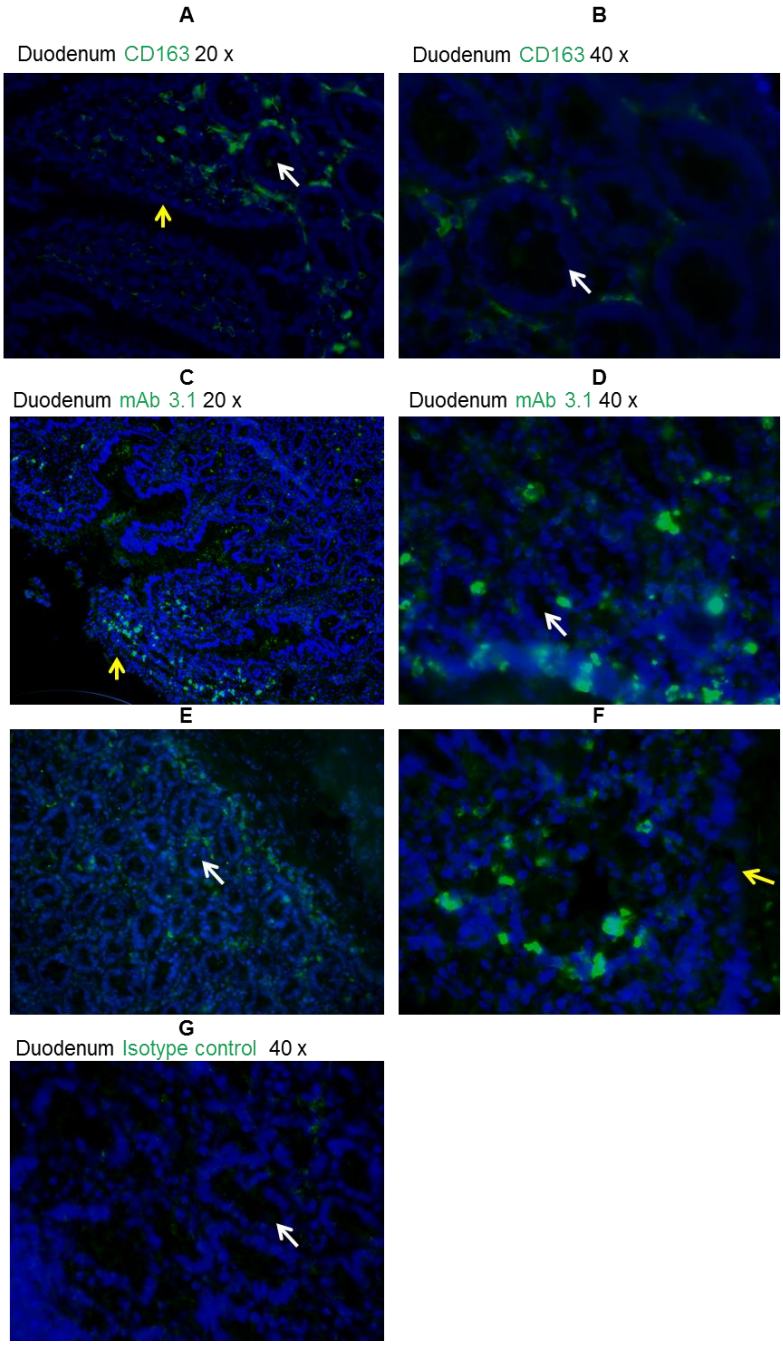

Figure 4.5 – mAb 3.1 stained cells around the duodenal glands and in villi of canine duodenum. **(A)** Duodenal villi and **(B)** glands stained with anti-CD163 (1:75, TransGenic Inc), used as a positive control. **(C)** Duodenum stained with hybridoma supernatant containing mAb 3.1 showing villi in profile. **(D)** and **(E)**, mAb 3.1 stain showing duodenal glands. **(F)** mAb 3.1 stain showing villus in cross section. **(G)** Mouse IgG_1 isotype control (80 µg/ml, Abcam), showing duodenal glands. Notice the similar distribution of cells stained with the control (A) and mAb 3.1 (C-F). Secondary antibody was goat anti-mouse Alexa 488 (1:300, Invitrogen). Nuclear stain is in blue (DAPI). The white arrows indicate duodenal glands; the yellow arrows indicate the edges of villi. "20 ×" and "40 ×" indicate the magnification used to acquire the images.

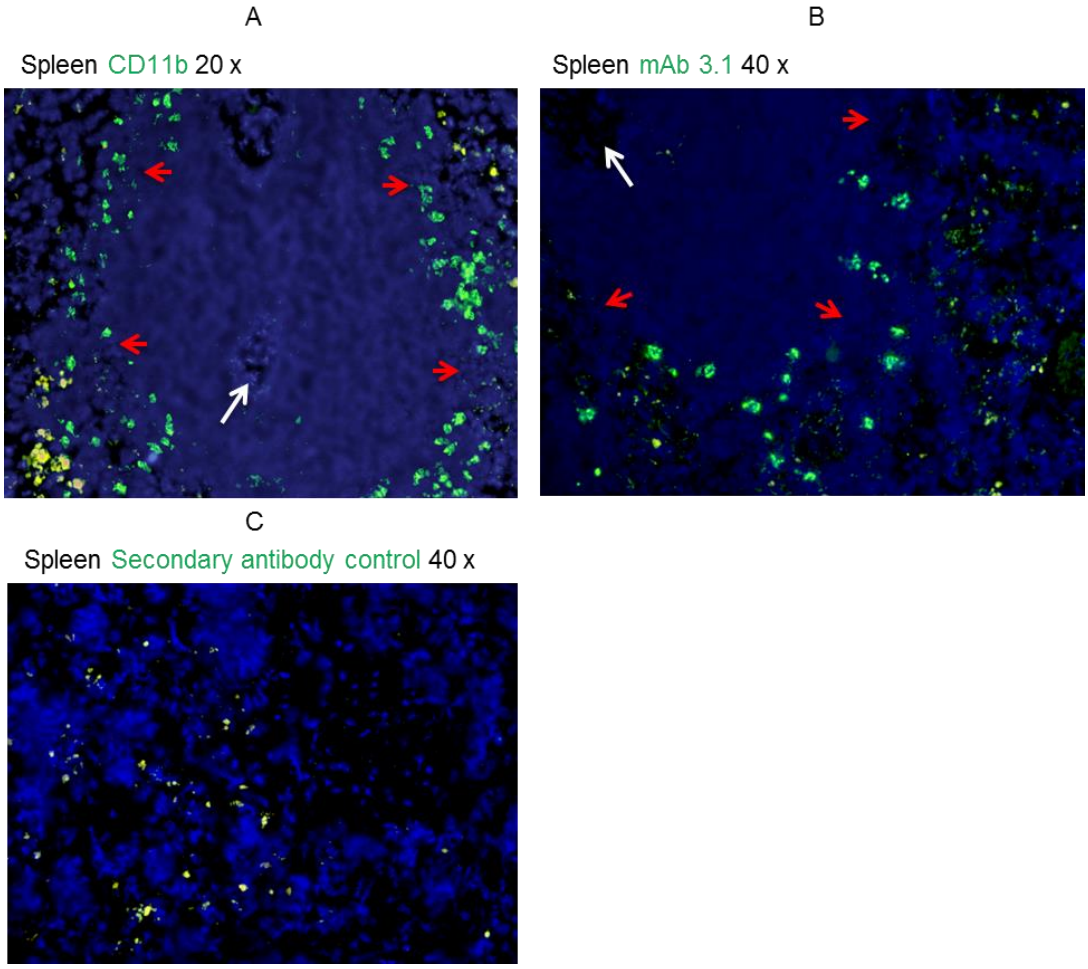

Figure 4.6 – mAb 3.1 stained cells surrounding the white pulp in canine spleen. **(A)** CD11b (1:10, AbD Serotec) stained spleen, used as a positive control. **(B)** Spleen stained with hybridoma supernatant containing mAb 3.1. **(C)** Negative control was stained only with the secondary antibody. Notice the similar distribution of cells stained with the control (A) and mAb 3.1 (B). Secondary antibody was goat anti-mouse Alexa 488 (1:300, Invitrogen). Nuclear stain is in blue (DAPI). The white arrows indicate the central arteriole. The red arrows indicate the limits of the white pulp. "20 ×" and "40 ×" indicate the magnification used to acquire the images.

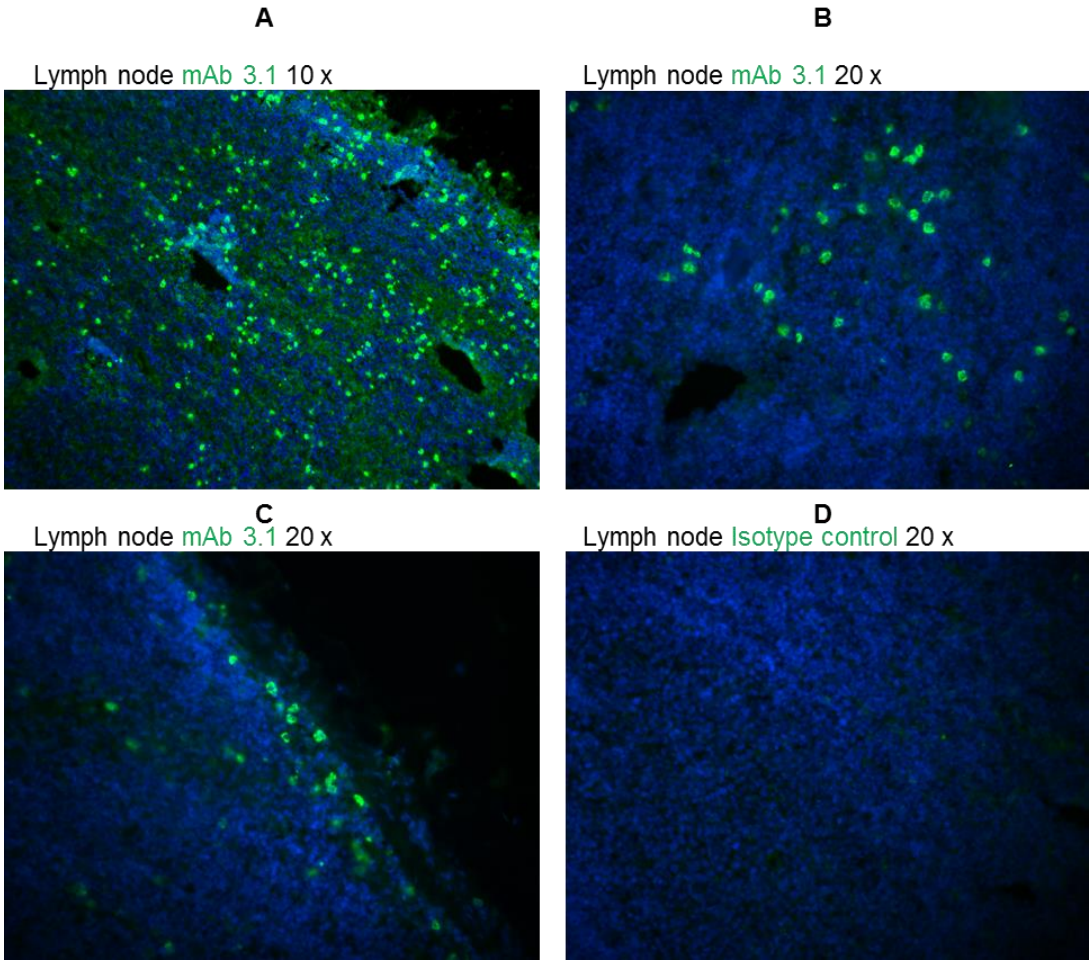

Figure 4.7 – mAb 3.1 stained cells throughout the canine lymph node. **(A)** Paracortical area showing staining with hybridoma supernatant containing mAb 3.1. **(B)** Medullary cords stained with mAb 3.1. **(C)** Subcapsular region stained with mAb 3.1. **(D)** Mouse IgG_1 isotype (20 µg/ml, Abcam) stain of the medullary cord. Secondary antibody was goat anti-mouse Alexa 488 (1:300, Invitrogen). Nuclear stain is in blue (DAPI). "10 ×" and "20 ×" indicate the magnification used to acquire the images.

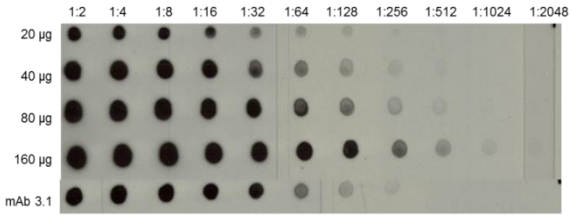

Figure 4.8 – Titration of mAb 3.1 in the hybridoma supernatant. Four concentrations of mouse IgG_1 isotype (Abcam) and the supernatant containing mAb 3.1 were sequentially diluted and dotted on a nitrocellulose membrane. After blocking, bound antibody was detected using rabbit anti-mouse Ig, HRP-conjugated (1:1000, Dako). The concentration of mAb 3.1 was estimated to be ~ 40 – 80 µg/ml by comparison with the isotype antibody scale.

To analyse the cross-reactivity of mAb 3.1 with c-Kit, a similar receptor to CSF-1R, normal canine thyroid tissue was double-stained with an anti-cKit and mAb 3.1. The C-cells of the thyroid stained positive for c-Kit, but no individual cell was double-stained with mAb 3.1 and anti-c-Kit (Figure 4.9). This indicates that mAb 3.1 did not cross-react with c-Kit.

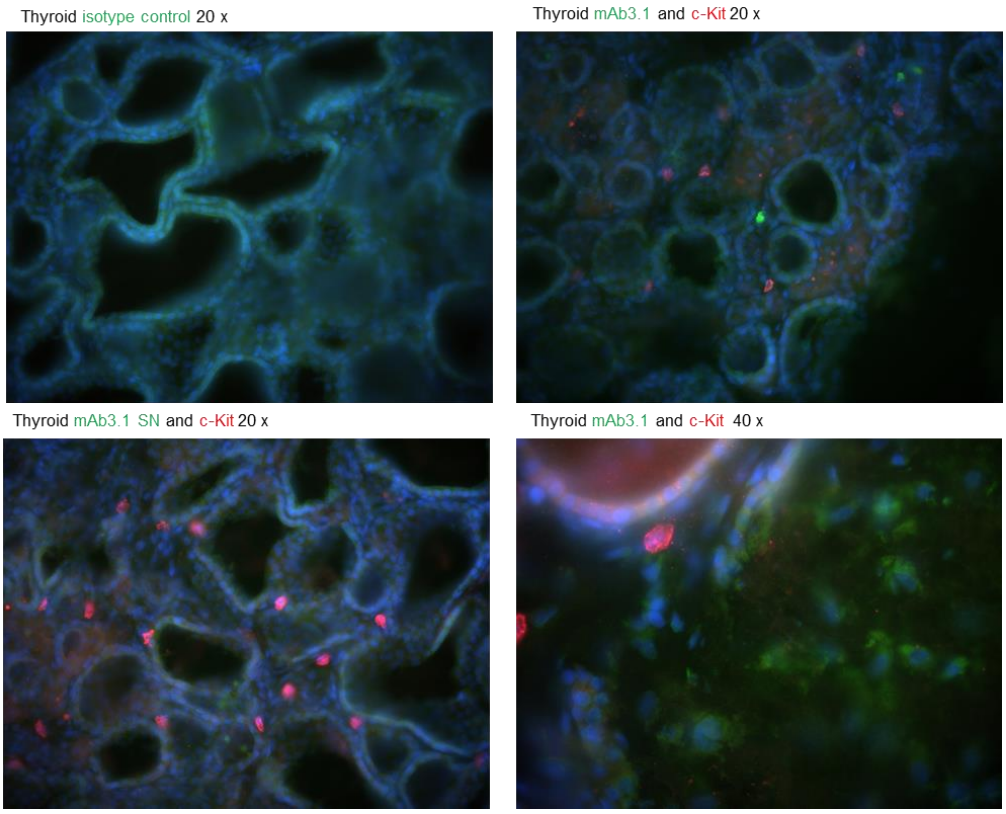

Figure 4.9 – mAb 3.1 did not cross-react with c-Kit. Canine thyroid tissue was double-stained with hybridoma supernatant containing mAb 3.1 and rabbit anti-human c-Kit (1:100, Dako). No cells were double-stained with anti-cKit and mAb 3.1. Secondary antibodies were goat anti-mouse Alexa 488 and goat anti-rabbit Alexa 647 (1:300, Invitrogen). Mouse IgG_1 isotype (20 µg/ml, Abcam) was used as a negative control. Nuclear stain is in blue (DAPI). "20 ×" and "40 ×" indicate the magnification used to acquire the images.

4.3.3 Immunohistochemistry

Canine mammary tumours were stained with mAb 3.1 to assess its binding in paraffin wax-embedded tissues. While mammary carcinoma epithelial cells stained with mAb 3.1, normal breast tissue showed only minimal background staining (Figure 4.10).

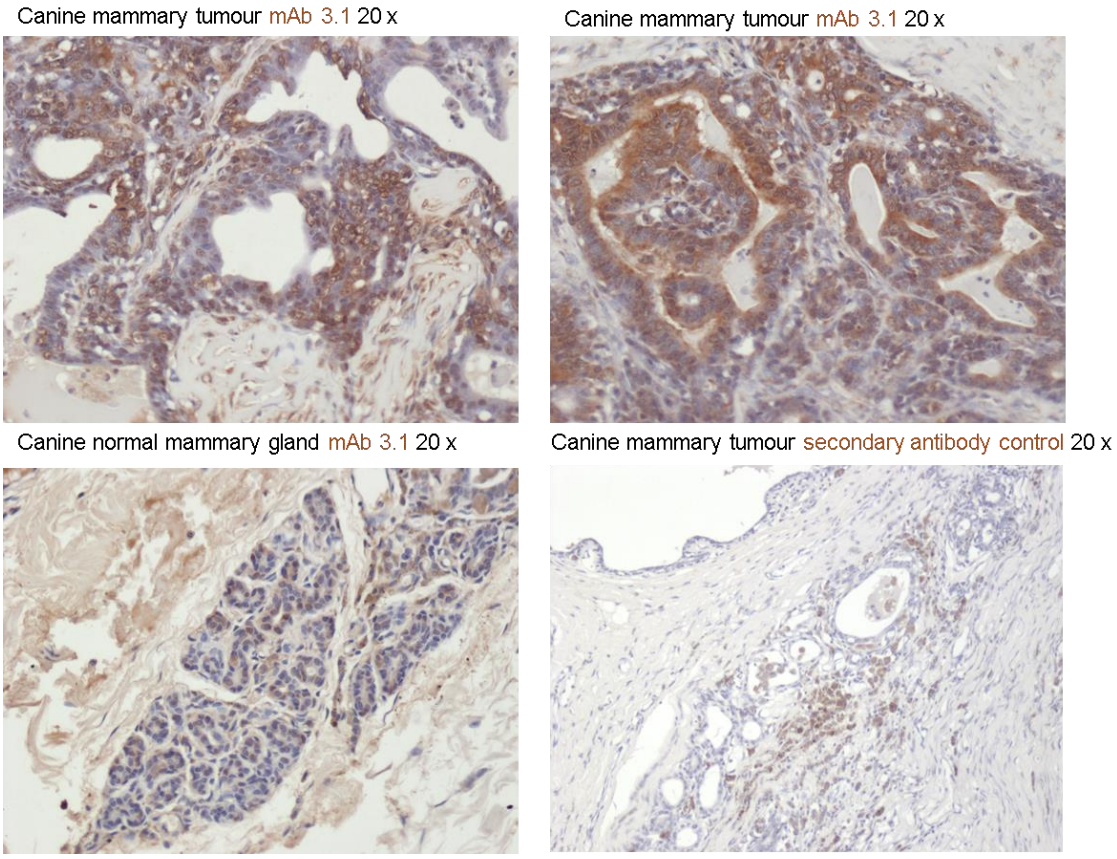

Figure 4.10 – mAb 3.1 stained canine epithelial mammary cancer cells but not cells of normal tissue. Formaldehyde-fixed paraffin wax-embedded samples of canine mammary tissue and carcinomas. Tissues were stained with hybridoma supernatants containing mAb 3.1. Negative control was stained only with the secondary antibody. Secondary antibody was rabbit anti-mouse, HRP-conjugated (1:1000, Dako). "20 ×" indicates the magnification used to acquire the images.

4.3.4 Flow cytometry

Three cell types were analysed by flow cytometry using the anti-CSF-1R antibodies: REM134 cells, bone marrow-derived macrophages (BMDM) and peripheral blood mononuclear cells (PBMCs).

Flow cytometry using REM134

To assess mAb 3.1 in flow cytometry, REM134 (canine mammary carcinomas) cells were evaluated using this technique. The first trial was performed on non-permeabilized,

non-fixed cells. This resulted on very low percentage of stained cells using mAbs against either the dimerization or the extracellular region (< 1 %). Subsequently the cells were fixed and then permeabilized using PBST before the antibody staining, showing increased positivity (Figure 4.11).

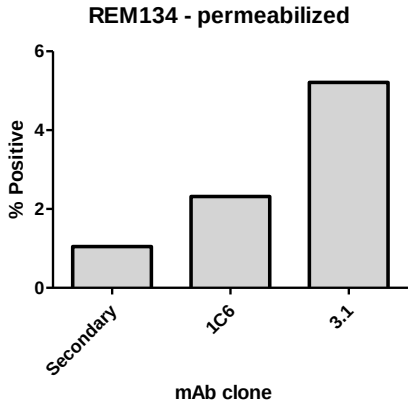

Figure 4.11 – Permeabilized REM134 carcinoma cells were stained with mAbs. REM134 cells permeabilized with Tween 20 stained with two IgG hybridoma supernatants containing mAbs against the extracellular (1C6) or dimerization domain (3.1) of CSF-1R (200 µl/10^6 cells). The y-axis shows the percentage of cells stained by each mAb. Negative control was stained only with the secondary antibody. Secondary antibody was goat anti-mouse Alexa 488 (1:800, Invitrogen).

Although permeabilization increased the number of REM134 cells stained with mAb 3.1, the percentage of positive cells was still reduced when compared to the number of positive cells seen in some of the replicates of immunofluorescence (Figure 4.3, above). Therefore, the assay was repeated using permeabilized REM134 cells. In this replicate of the assay (Figure 4.12), the percentage of cells stained by mAb 3.1 was greatly increased when compared to the previous attempt (Figure 4.11, above).

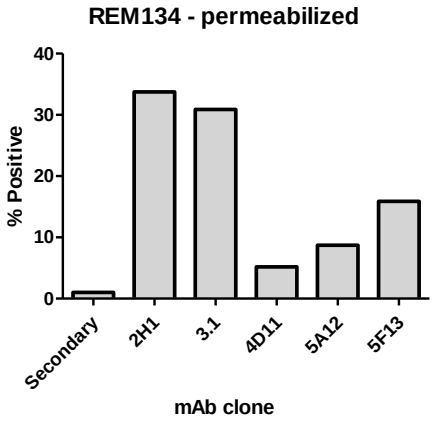

Figure 4.12 – The percentage of cells stained by mAbs was variable between replicates. REM134 cells permeabilized with Tween 20 stained with various hybridoma supernatants containing mAbs (200 µl/10^6 cells). The y-axis shows the percentage of cells stained by each mAb. Negative control was stained only with the secondary antibody. Secondary antibody was goat anti-mouse Alexa 488 (1:800, Invitrogen).

In accordance with the flow cytometry findings on the expression of CSF-1R by REM134 cells, which showed great variation, these cells responded differently to CSF-1 in several assay replicates. Depending on the culture conditions, REM134 cells increased, did not respond or even reduced replication in the presence of CSF-1. It was determined that sensitivity of REM134 cells was density-dependant. High cell density before they were used in the proliferation assay reduced the sensitivity of REM134 to CSF-1. Whereas cells grown in low densities proliferated in response to the addition of CSF-1 to the culture, cells in 100 % confluence before they were harvested for the assay did not respond or had reduced proliferation with the addition of the growth factor. Adding more or less cells to the assay (from either high or low density backgrounds) also affected the results (Figure 4.13).

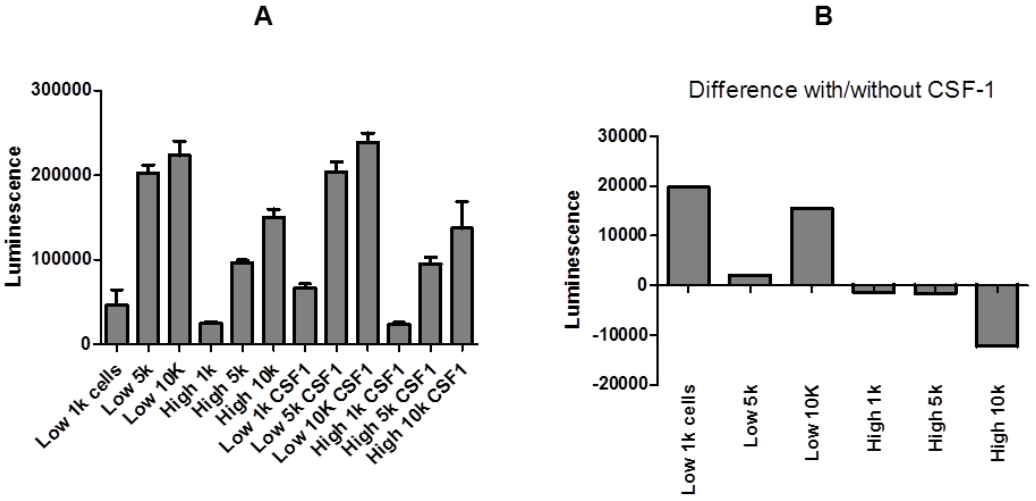

Figure 4.13 – High culture density reduced REM134 sensitivity to CSF-1. The assay measured the effect of culture density before and during proliferation assays on the sensitivity of REM134 cells to CSF-1. **(A)** Cells grown in either low or high densities were harvested and plated for the assay also in varying densities. On the graph, "Low" and "High" indicate the density of the cells in culture before they were harvested for the assay, and "1k", "5k" and "10k" indicate the number of cells plated for the actual proliferation assay. "CSF-1" indicates the addition of rhCSF-1 (100 ng/ml, Invitrogen). The y-axis indicates luminescence intensity, which is correlated to cell number. The results are the mean of at least 4 replicates ± SD. **(B)** Difference of proliferation with/without the addition of CSF-1. Cells from high-density plates showed reduced proliferation in the presence of CSF-1. The y-axis shows the difference between the results of cells coming from high or low densities. Cells were grown for 48 h after addition of treatment. Proliferation results as measured by luciferase activity (CellTiter-Glo, Promega).

REM134 cells grown at different densities were stained for CSF-1R using mAbs 1C6 and 3.1. The cells were then analysed by flow cytometry. When grown at high density, fewer cells were CSF-1R$^+$ (as per mAb 1C6 or 3.1 staining) in comparison to cells at lower densities. This result was consistent using both antibodies tested, although there was significant difference in the percentage of cells bound by each mAb (Figure 4.14). Therefore, culture conditions that reduced REM134 responsiveness to CSF-1 also reduced CSF-1R expression on these cells. This suggests a mechanism where a decrease in receptor expression lead to diminished responsiveness to the ligand.

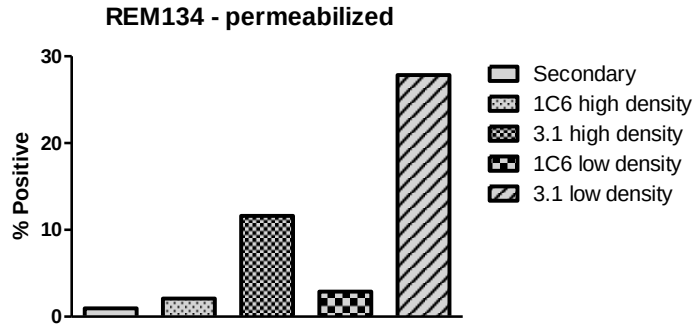

Figure 4.14 – High culture density decreased CSF-1R expression by REM134 cells. REM134 cells were permeabilized with Tween 20 and stained with hybridoma supernatants containing mAbs 1C6 and 3.1 (200 µl/10^6 cells). "Low density" and "high density" indicate the density of the cells in culture before they were harvested for the assay. The y-axis shows the percentage of cells stained by each mAb. Negative control was stained only with the secondary antibody. Secondary antibody was goat anti-mouse Alexa 488 (1:800, Invitrogen).

Flow cytometry using BMDM

Next, the capacity of mAbs to bind to BMDM in flow cytometry was assessed. This allowed for a direct comparison between the canine anti-CSF-1R described here and an anti-porcine CSF-1R positive control, produced elsewhere (this antibody did not stain cells in tissues).

mAb 3.1 and the anti-pig CSF-1R stained canine BMDM with similar patterns. CSF-1-conditioned BMDM showed a low percentage of cell surface CSF-1R. mAb 3.1 stained 8.7 % of cells in this condition, while the anti-swine CSF-1R stained 3.24 % of cells. (Figure 4.15 A). When BMDM were starved of CSF-1 overnight, there was no significant difference in the staining patterns with both mAb 3.1 and the anti-swine CSF-1R (not shown). Therefore, in a subsequent assay, cells were starved of FBS overnight, with or without CSF-1. Unexpectedly, serum starvation seemed to abolish the surface expression of CSF-1R on these cells, while 12 and 14 % of cells cultured without FBS but with rhCSF-1 were positive for the receptor using mAb 3.1 and the anti-swine mAb, respectively (Figure 4.15 B-D).

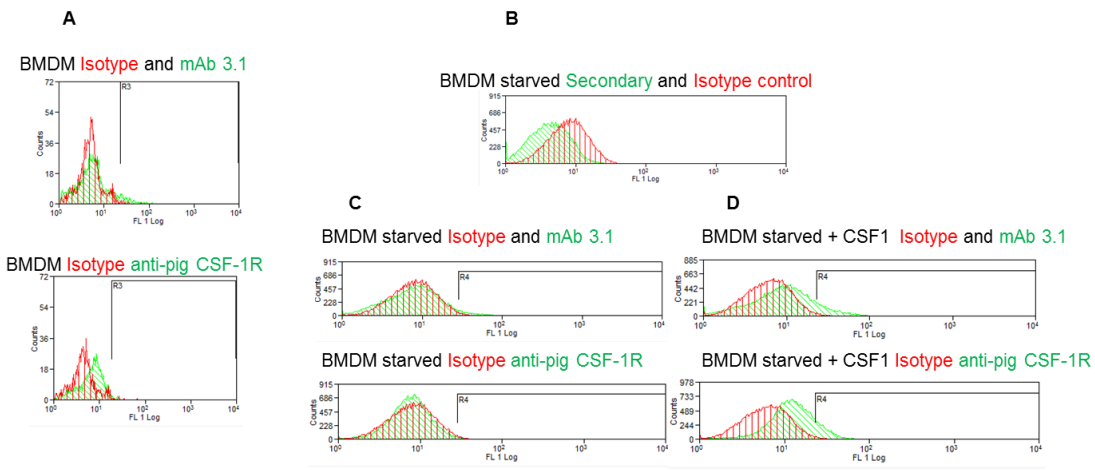

Figure 4.15 – mAb 3.1 and anti-swine CSF-1R showed similar flow cytometry staining patterns of BMDM. **(A)** BMDM in complete medium with rhCSF-1 (100 ng/ml, Invitrogen). Live cells stained with hybridoma supernatant containing mAb 3.1 (200 µl/10^6 cells) or pure mouse anti-swine CSF-1R (25 µg/ml, Lindsey Waddell). Cell viability was assessed for this assay only using 7-AAD (eBioscience). The line R3 indicates the positivity threshold determined in comparison with the mouse IgG_1 isotype control (25 µg/ml, Abcam). **(B)** A second assay was performed comparing BMDM starved of FBS overnight. Negative control was stained only with the secondary antibody or with isotype antibody. **(C)** Staining patterns of serum-starved BMDM using mAb 3.1 and anti-swine CSF-1R in the absence of rhCSF-1 or **(D)** presence of rhCSF-1. In serum-starved cells, CSF-1 increased the expression of the receptor. The line R4 indicates the positivity threshold. Cells in (B-D) were fixed in PFA (2 %) before staining. The y-axis shows the number of cells. The x-axis shows green fluorescence intensity. Secondary antibody was goat anti-mouse Alexa 488 (1:800, Invitrogen).

In an independent assay, the identity of the BMDMs was confirmed by staining cells with an antibody against canine CD11b. These cells were not serum starved. This assay indicated that nearly all cells from canine bone marrow cultivated in rhCSF-1 and in bacterial plates expressed CD11b (Figure 4.16).

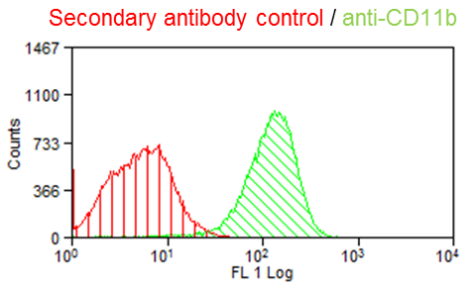

Figure 4.16 – Putative BMDM express CD11b. BMDM were grown in the presence of rhCSF-1 (100 ng/ml, Invitrogen) for 10 days in bacterial plastic and were used for flow cytometry. Cells were stained with CD11b (1:10, AbD Serotec) for characterization of the cells. All BMDM expressed CD11b. The y-axis shows the number of cells. The x-axis shows green fluorescence intensity. Negative control was stained only with the secondary antibody. Secondary antibody was goat anti-mouse Alexa 488 (1:800, Invitrogen).

Flow cytometry using PBMCs

When the monoclonal antibodies were used to stain peripheral blood mononuclear cells (PBMCs) from dogs, no specific binding to monocytes was obtained with any of the anti-canine CSF-1R mAbs, regardless of staining time (from 30 min to overnight) or whether purified antibodies or hybridoma supernatants were used. The positive control, anti-swine CSF-1R, bound almost exclusively to canine monocytes, showing little background staining of lymphocytes (Figure 4.17).

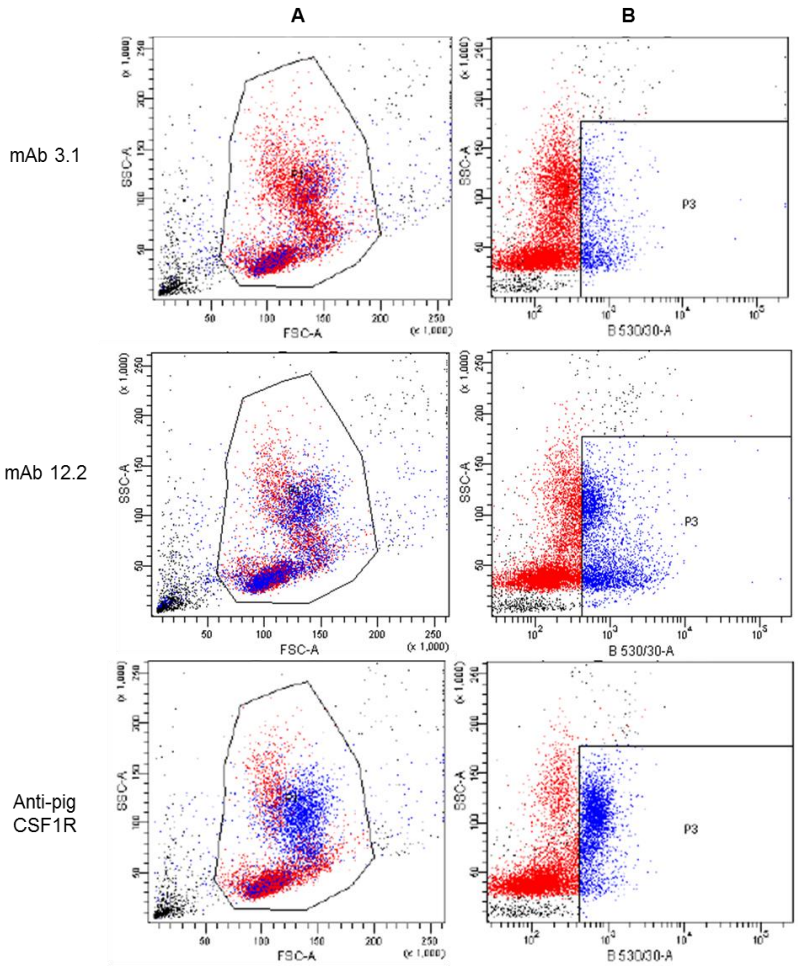

Figure 4.17 – mAb 3.1 did not stain canine PBMCs. **(A)** PBMCs discriminated by cell granularity (SSC) and size (FSC). The cells with granularity around 100 and 150 are monocytes. **(B)** Live cells stained with mAb 3.1 or 12.2 (10 µg/10^6 cells) or mouse anti-swine CSF-1R (25 µg/ml, Lindsey Waddell). Notice the absence of positive monocytes in the gate P3 of mAb 3.1-stained cells. Notice the unspecific staining of lymphocytes with mAb 12.2. Cell viability was assessed using Sytox blue (Invitrogen). Fluorescence intensity is shown on the x-axis and cell granularity on the y-axis. The cells shown in (B) are inside the gate drawn in (A). Positive cells, as determined by the P3 gate in (B), were set in relation to the isotype control (not shown). Positive cells are depicted in blue in both graphs. Secondary antibody was goat anti-mouse Alexa 488 (1:800, Invitrogen).

However, binding of the anti-swine CSF-1R antibody to the canine cells seems to have been at least partially mediated through Fc receptor activity. When these receptors were blocked using a high concentration of an Fc blocking reagent, binding of the anti-swine

antibody to the canine receptor was greatly reduced. Fc blocking had no effect on mAb 3.1, since it showed no staining of the monocytes (Figure 4.18).

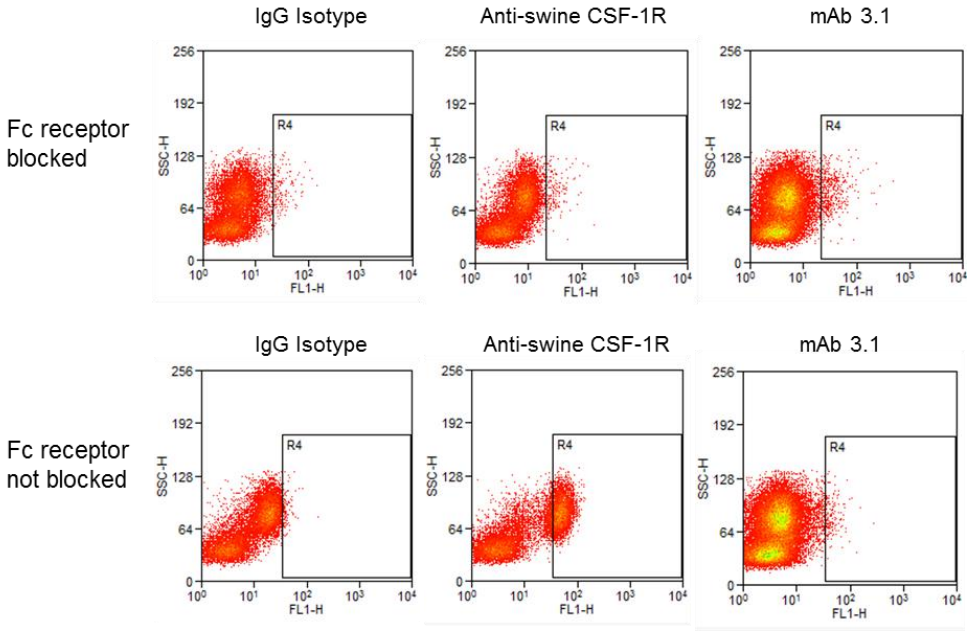

Figure 4.18 – Blocking the Fc receptor reduced anti-swine CSF-1R staining of canine PBMCs. Live cells stained with hybridoma supernatant containing mAb 3.1 (200 µl/10^6 cells) or pure mouse anti-swine CSF-1R (25 µg/ml, Lindsey Waddell). Fc receptor-block reduced the staining by the anti-swine antibody. Cell viability was assessed using 7-AAD (eBiosciences). The rectangle R4 indicates the positivity threshold determined in comparison with the mouse IgG_1 isotype control (25 µg/ml, Abcam). The x-axis shows fluorescence intensity and the y-axis shows cell granularity (SSC). The results on the top row are of cells that received the Fc blocking reagent (20 µl, Miltenyi Biotec). The results on the lower row show cells that were not Fc-blocked. Secondary antibody was goat anti-mouse Alexa 488 (1:800, Invitrogen).

4.3.5 Immunoprecipitation

The monoclonal antibodies were tested in an immunoprecipitation assay to further verify for specificity. Purified mAbs 3.1, 2H1 and 12.2 and the supernatant of mAb 1C6 were bound to protein G. These were then incubated with culture supernatant from HEK293T cells that transiently expressed the CSF-1R extracellular region. After removing unspecific binders by washing, the immunoprecipitated proteins were detected by western blot with an anti-His tag monoclonal (this tag is coupled to CSF-1R). mAbs 3.1 and 12.2 recovered proteins with the correct molecular weight of CSF-1R. mAb 3.1 seemed to only

bind to a narrow range of the glycoforms of CSF-1R, as seen by the tight band in the western blot assay. mAb 12.2 recognized a broader range of the glycoforms of CSF-1R. Since an anti-mouse HRP-conjugate was used to detect the anti-His antibody, the anti-CSF-1R mAbs also appeared on the western blot (Figure 4.19).

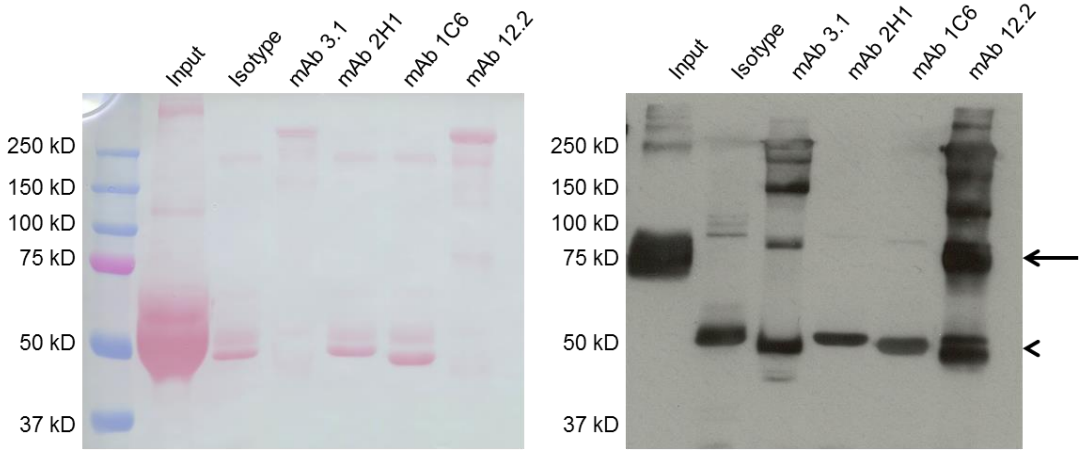

Figure 4.19 – Immunoprecipitation with anti-canine CSF-1R murine mAbs. Purified murine mAbs (21 µg) or hybridoma supernatant (mAb 1C6 only) were coupled to protein G beads (75µl, GE Healthcare). Unbound antibodies were removed by washing. Medium from transiently transfected HEK293T cells expressing CSF-1R extracellular region was added to the beads and incubated overnight at 4^{o}C. Unbound proteins were removed by washing. The resin was incubated with reducing sample buffer at 95^{o}C for 5 min. The mixture was centrifuged and the supernatant was resolved by SDS-PAGE. His-tagged proteins were identified by western blotting (anti-His at 1:500, Invitrogen). Secondary antibody was anti-mouse, HRP-conjugated (Dako, 1:1000). The arrow indicates the extracellular CSF-1R. Notice the positive results from mAbs 3.1 and 12.2. The arrowhead indicates the size of the antibody heavy chain.

4.3.6 mAbs blocked REM134 proliferation

REM134 cells express the CSF-1R receptor (Chapter 3) and are also capable of proliferating in response to CSF-1 (Figure 4.13, above, and Chapter 3). This cell model was therefore utilised to determine if inhibition of CSF-1R by the mAbs would decrease cancer cell proliferation. The anti-proliferative activity of mAbs generated in the first hybridoma against the extracellular CSF-1R was tested exclusively in this assay, with the exception of mAb 1C6, which was also tested by real time proliferation assay against REM134 cells.

The supernatant of 1C6 was capable of inhibiting REM134 proliferation, as tested in an endpoint proliferation assay (Figure 4.20). Several IgM clones were able to affect REM134 cell proliferation, such as mAbs 7G3 and 6C2 (not shown).

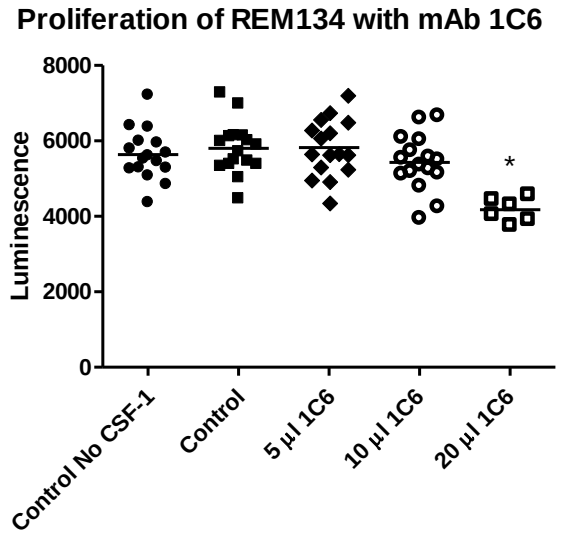

Figure 4.20 – mAb 1C6 inhibited REM134 proliferation. Hybridoma supernatant containing mAb 1C6 was used, with the addition of rhCSF-1 (100 ng/ml, Invitrogen) to the culture. The REM134 cells (in 100 µl medium) received between 5 – 20 µl of the supernatant. Cells were grown for 48 h after addition of treatment. There is a dose-dependent effect of mAb 1C6 on REM134 survival. Proliferation results as measured by luciferase activity (CellTiter-Glo, Promega). Results shown as mean of at least 6 replicates. The asterisk indicates statistically significant difference from the Control group by ANOVA.

To test if mAb 1C6 could inhibit proliferation of murine macrophages, this antibody was used in an assay with RAW264.7 cells (mouse macrophage cell line). Contrarily, mAb 1C6 increased RAW264.7 cell proliferation (Figure 4.21).

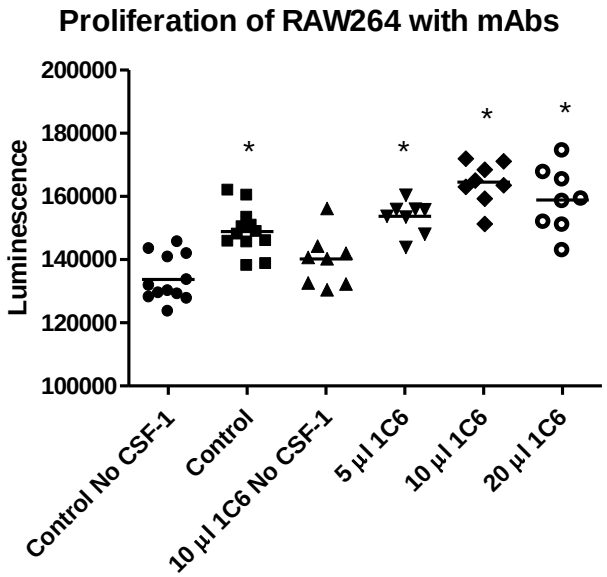

Figure 4.21 – mAb 1C6 did not reduce proliferation of RAW264.7. The murine macrophages (in 100 µl medium) were supplemented with rhCSF-1 (100 ng/ml, Invitrogen) and/or hybridoma supernatant containing mAb 1C6 (40 µl). Results shown as mean of at least 8 replicates. Asterisks indicate statistically significant difference from the "Control No CSF-1" group by ANOVA.

mAbs originated from the hybridoma fusion against the dimerization domain were tested only in real time proliferation assays, as shown below in relation to the proliferation of REM134 (mammary carcinoma cells). Cells were maintained in the presence of CSF-1 and received two different concentrations of antibodies. Several antibody clones against the dimerization domain of CSF-1R demonstrated the capacity to reduce REM134 proliferation. Some of the mAbs could not affect these cells, serving therefore as internal controls (Figure 4.22).

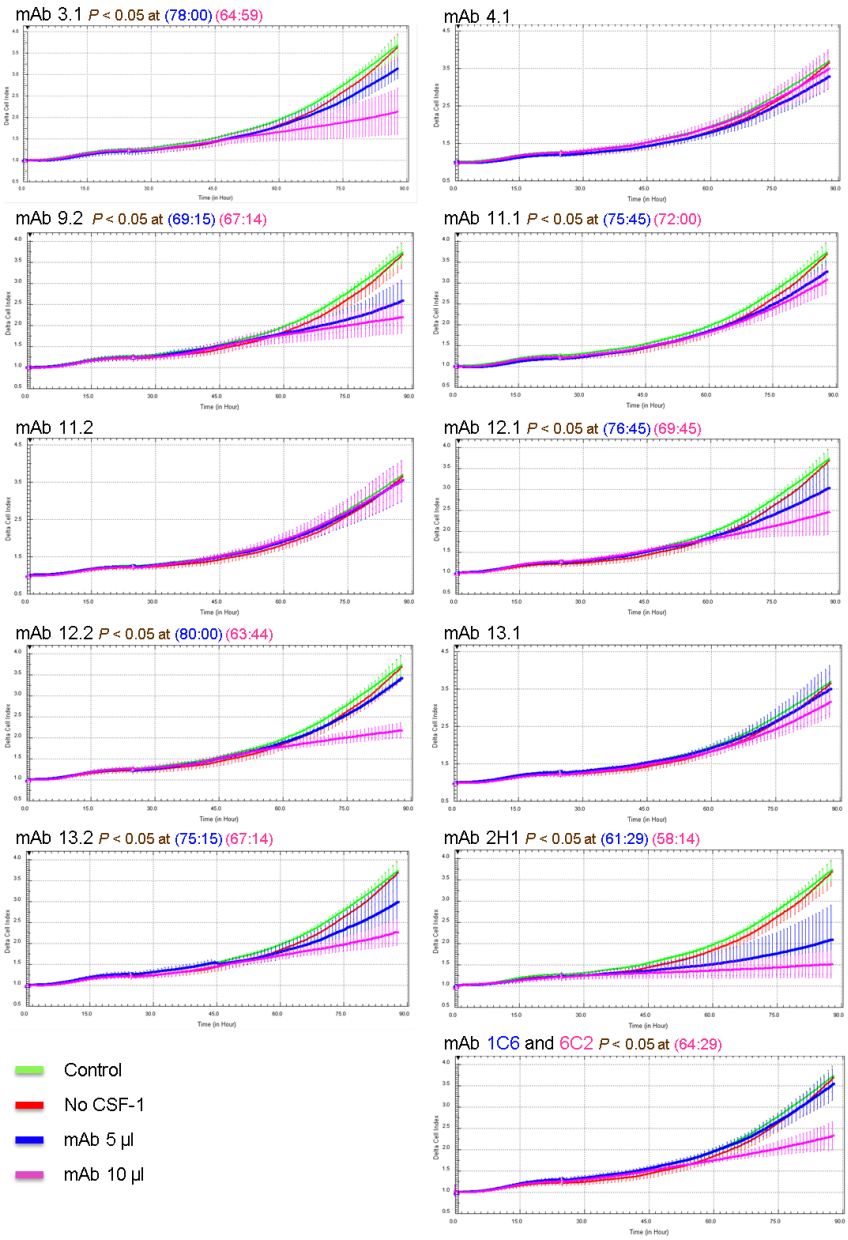

Figure 4.22 – Effect of mAb supernatants in the proliferation of canine REM134 mammary carcinoma cells. Cells (in 100 µl medium) were cultured with rhCSF-1 (100 ng/ml, Invitrogen) and treated with hybridoma culture supernatants containing the indicated antibodies (5 µl or 10 µl) or with 10 µl of DMEM (control). Notice that some mAbs reduced REM134 proliferation. A control without CSF-1 is shown. Data was collected every 15 min. The vertical line and arrowhead at around 1 h indicates when the treatments were added. The data was also normalized by subtraction (delta) from that point. Delta cell index (y-axis) is correlated to cell number. Results are shown as the mean of 4 wells ± SD for each time point. Results analysed by repeated measures two-way ANOVA with a Bonferroni post-test. The coloured values next to mAb names indicate the time in hours when treatments were different from Control.

4.3.7 mAb 3.1 reduced blood vessel remodelling in the CAM assay

To assess if the effect of antibody activity on cancer cells was sufficient to provide biologically relevant outcomes, mAb 3.1 was tested in a chorioallantoic membrane (CAM) assay, analysing blood vessel remodelling. A sponge containing REM134 cells was implanted onto the CAM of day-7 chick embryos. Four days after grafting the sponge, CAM blood vessels became strongly directed towards the graft. mAb 3.1 was able to reduce blood vessel growth towards the sponge containing REM134 cancer cells. Blood vessel remodelling towards the graft was quantified by two parameters, a score on blood vessel number and blood vessel branching counts.

The REM134 cells were largely confined to the sponge throughout the experiment, as can be seen by the presence of the green fluorescent cells (Figure 4.23 A). Treatment with mAb 3.1 significantly reduced blood vessel branching surrounding the sponge graft (Figures 4.23 B, C and D) and showed a trend in reducing blood vessel number (P = 0.086) (not shown).

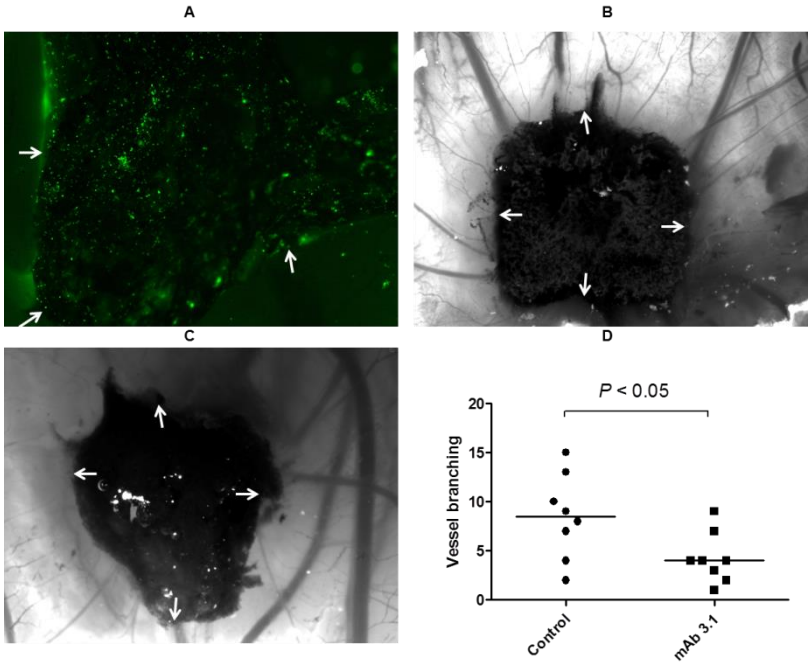

Figure 4.23 – mAb 3.1 reduced cancer cell-directed blood vessel remodelling in the chorioallantoic membrane (CAM) assay. **(A)** REM134 cells were stained with CFSE (green fluorescence), and cells were absorbed in a gelatine sponge (~ 10^6 cells), which was placed on the CAM at embryonic day 7, in the presence or absence of hybridoma culture supernatant containing mAb 3.1. The sponges and surrounding vessels were imaged at embryonic day 11. The limits of the sponge are shown by the white arrows. **(B)** Representative picture of blood vessel formation towards the sponge graft (dark square) in the absence of treatment. **(C)** Blood vessel formation in the presence of mAb 3.1. Notice the reduced vascular reorientation surrounding the sponge compared to (B). The limits of the sponge are shown by the white arrows. **(D)** Blood vessel branching counts in control or mAb 3.1 treated cells. Horizontal bar represents the median. Results analysed by Mann-Whitney test.

4.3.8 mAbs blocked macrophage proliferation

The capacity of the anti-CSF1-1R mAbs to block the proliferation of canine macrophages was analysed by real time proliferation assay. Bone marrow-derived macrophages were harvested and plated onto the real time analysis plates, where cells were then treated with monoclonal antibodies in the presence of CSF-1. Five of the ten antibodies tested were able to inhibit macrophage survival in a dose-dependent manner (Figure 4.24), all of which had also shown at least partial response against REM134 cells in the same assay (Figure 4.22, above). mAb 2H1 was the only antibody that had shown evident activity against REM134 cells but did not inhibit macrophage proliferation in this test.

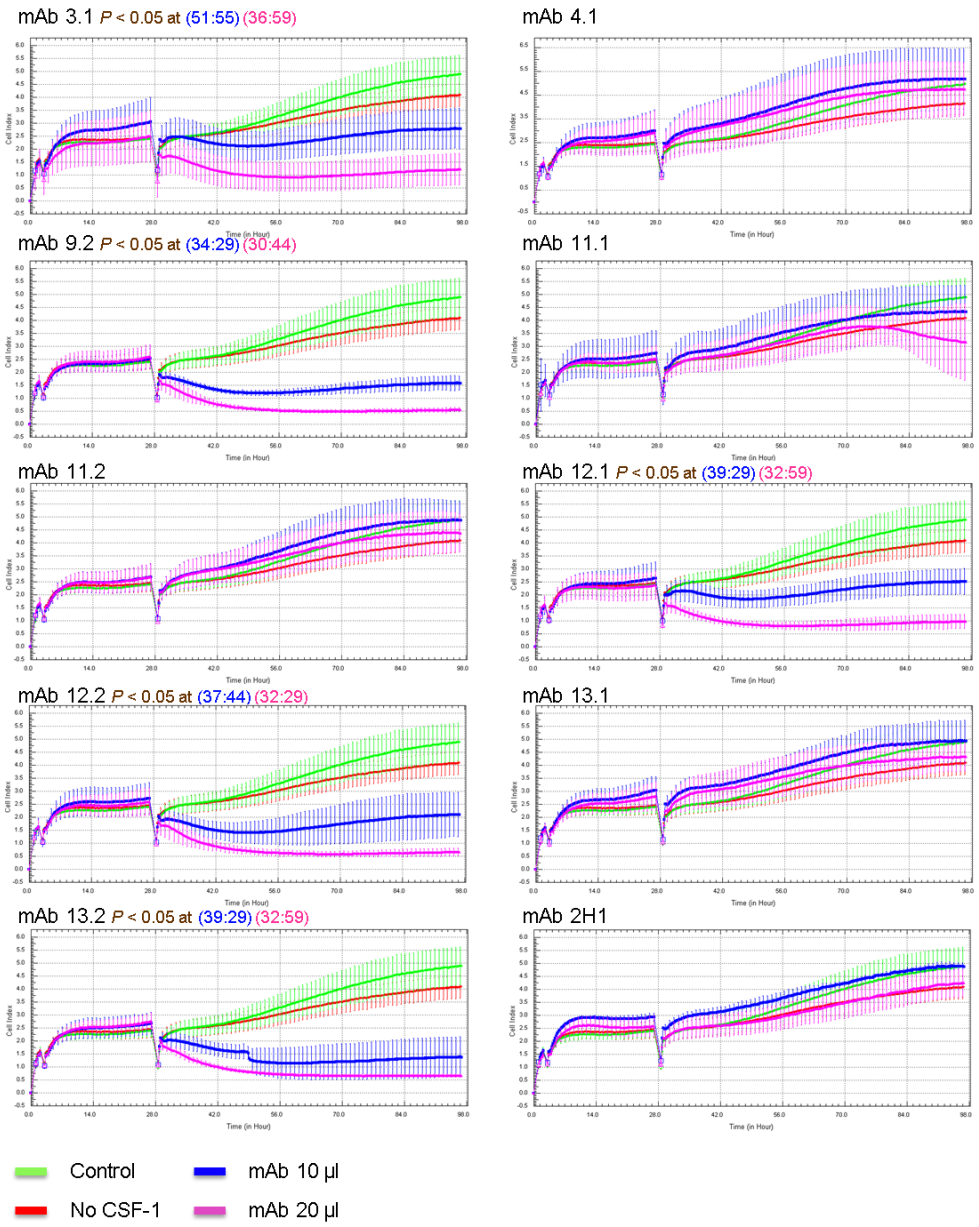

Figure 4.24 – Effect of mAb supernatants against CSF-1R in real time proliferation assay of canine BMDM. Cells (in 100 µl medium) were grown in rhCSF-1 (50 ng/ml, Invitrogen) and treated with hybridoma culture supernatants containing the indicated antibodies (10 µl or 20 µl) or with 20 µl of DMEM (control). Notice that some mAbs reduced BMDM proliferation. A control without CSF-1 is shown. Data was collected every 15 min. Antibodies were added in the first hour of the assay. The abrupt drops in the graphs indicate when the plate was removed from the xCelligence equipment for change of medium/treatment. Cell index (y-axis) is correlated to cell number. Results are shown as means of 4 wells ± SD for each time point. Results analysed by repeated measures two-way ANOVA with a Bonferroni post-test comparing all groups to the control. The coloured values next to mAb names indicate the time in hours when treatments were different from Control.

The proliferation assays shown previously used hybridoma supernatants as the source of antibodies. When purified antibodies were used for inhibition of BMDM proliferation, the lowest mAb concentration to exhibit significant biological activity in relation to the mouse antibody control was of 1.25 µg/well for mAbs 12.2 and 2H1. However, this was inconstant, and mAb 2H1 was not significantly different from the control antibody at higher concentrations. Also, mAb 12.2 was relatively more efficacious at the lowest dose, since statistically significant differences from the control occurred in earlier time points in the 1.25 µg/well dose compared to 3.75 and 7.5 µg/well. mAb 3.1 showed a trend of significant activity at 7.5 µg/well, when all mAbs yielded visibly lower cell proliferation than the control antibody. However, at that dose, only 2 wells were used as replicates for control and mAb-treated cells, and the differences seen with mAb 3.1 did not reach statistical significance (Figure 4.25). For clarity, antibody purification is shown in Chapter 7.

mAb 3.1 hybridoma supernatant (SN) was used as a control for the purified antibody response, as it had previously been shown to affect macrophage proliferation. It showed a similar effect to 3.75 µg/well of purified mAb 3.1, indicating that the concentration of antibody in the supernatant estimated from Figure 4.8, above, was correct. Based on that figure, mAb 3.1 hybridoma supernatant had up to 80 µg/ml of antibody (= 3.2 µg per 40 µl, the volume of supernatant used).

GW2580, a small-molecule inhibitor of CSF-1R, also showed dose-specific response and was able to reduce macrophage survival at 20 µM and 30 µM in relation to their DMSO vehicle controls. The curve trends were similar to the effect of the mAbs (Figure 4.25).

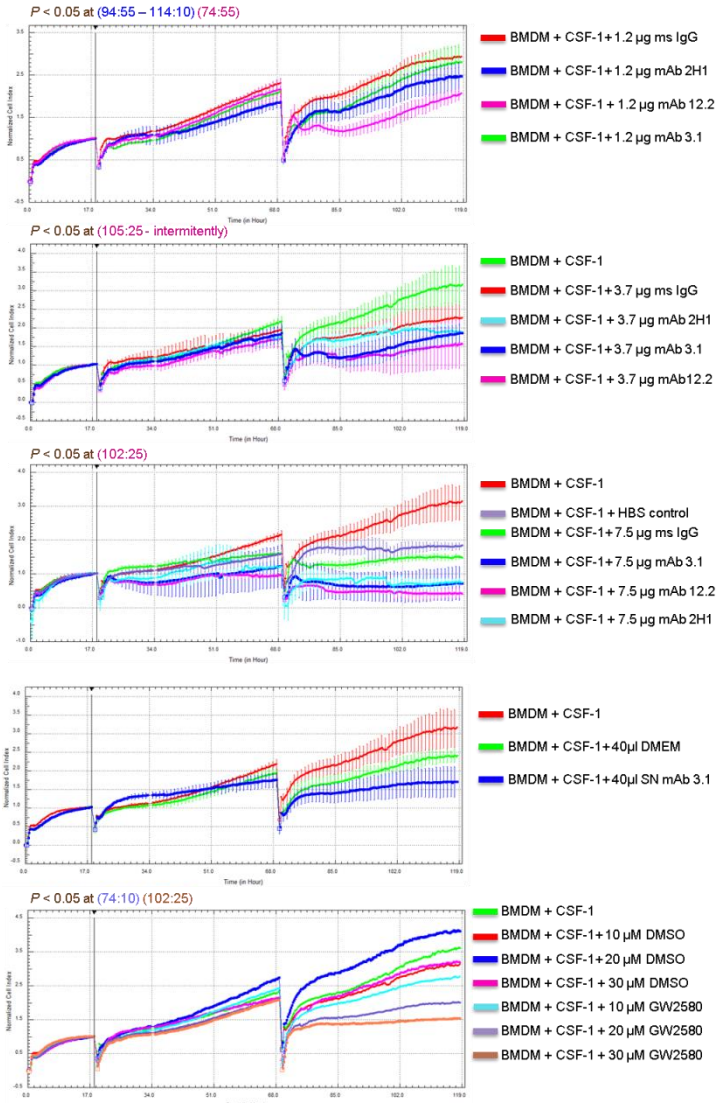

Figure 4.25 – Effect of purified mAbs in proliferation assay of canine BMDM. Cells (in 100 µl medium) were grown in rhCSF-1 (20 ng/ml, Invitrogen) and treated with one of three purified mAbs (at 1.2, 3.7 or 7.5 µg), the hybridoma supernatant of mAb 3.1 (40 µl) or GW2580 (10 – 30 µM), as indicated. Only mAb 12.2 consistently reduced BMDM proliferation. The controls received equivalent concentrations of mouse serum IgG antibody (Sigma), PBS (antibody vehicle control) or DMSO (GW2580 vehicle control). The untreated control is not shown on the first graph as its curve overlaps with that of the mouse IgG control. Data was collected every 15 min. The vertical line at around 17 h indicates when the treatments were added. Data were also normalized at that point. Normalized cell index (y-axis) is correlated to cell number. The abrupt drops in the graphs indicate when the plate was removed from the xCelligence equipment for change of medium/treatment. Results are shown as means of 4 wells (2 wells at 7.5 µg) ± SD for each time point. SD bars are not shown on the last graph for clarity. Results analysed by repeated measures two-way ANOVA with a Bonferroni post-test comparing all groups to the control. The coloured values next to mAb names indicate the time in hours when treatments were different from their respective controls (either ms IgG, DMEM or DMSO groups).

4.3.9 mAb 3.1 inhibited osteoclast survival

Osteoclasts have a distinct morphology, forming a tight "tiled" structure in culture. Because of this, apoptosis is easy to identify in the cell culture, as this tiled pattern is then broken (Lacey et al., 2000). Feline osteoclasts were differentiated from the bone marrow and kindly provided by Seungmee Lee (Gura Bergkvist group, Roslin Institute). The feline and the canine CSF-1R have 82 % homology when only the extracellular region is considered (Chapter 7) – this is the region targeted by mAb 3.1. When mAb 3.1 was used on feline osteoclasts, it induced phenotypical alterations that indicate cellular contraction and membrane blebbing. The use of a control antibody (anti-CCR2 mAb) or the removal of CSF-1 after the cells had differentiated had no effect on cellular morphology and in these cases the cells maintained a "tiled" pattern (Figure 4.26). Next, the CSF-1R signalling pathways were evaluated by western blotting. Osteoclasts were removed from the plates and were lysed for analysis by western blot. While total Akt was stable between treatments, pAkt was reduced in mAb 3.1 treated cells. The antibody treatment had no effect on pMAPK. This indicates that mAb 3.1 specifically induced apoptosis of feline osteoclasts, affecting survival pathways dependent on Akt phosphorylation (Figure 4.27).

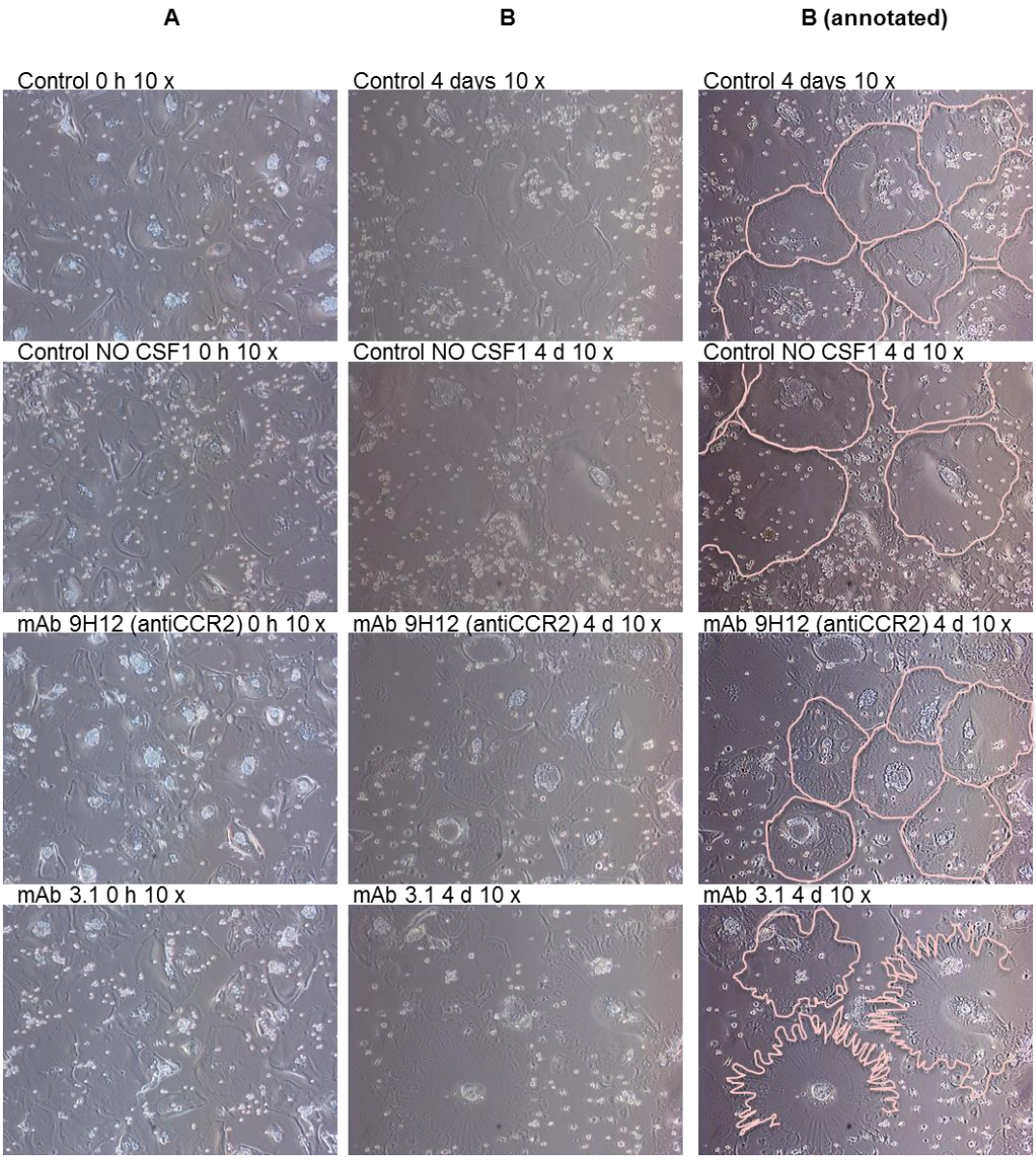

Figure 4.26 – mAb 3.1 induced apoptosis of feline osteoclasts. Bright field images of feline osteoclasts grown with rhCSF-1 (10 ng/ml, R&D Systems) and rhRANKL (30 ng/ml, R&D Systems) treated with hybridoma culture supernatant containing mAb 3.1 (1/6 of medium volume in osteoclast culture) for 4 days and comparisons with anti-CCR2 hybridoma culture supernatant (similar dose, Teresa Raposo), untreated and no CSF-1 controls. **(A)** Cells at 0 h (beginning of the assay). **(B)** and **(B (annotated))** Cells at 4 days of treatment. **(B (annotated))** display the same images as (B), but the images were consistently digitally altered and the cellular membranes were manually outlined to highlight the differences between the groups. Notice the membrane retraction in mAb 3.1-treated osteoclasts, typical of apoptosis. Pictures are representative of two wells for the negative controls and mAb 3.1 treated cells, and of a single well for the anti-CCR2 treated cells.

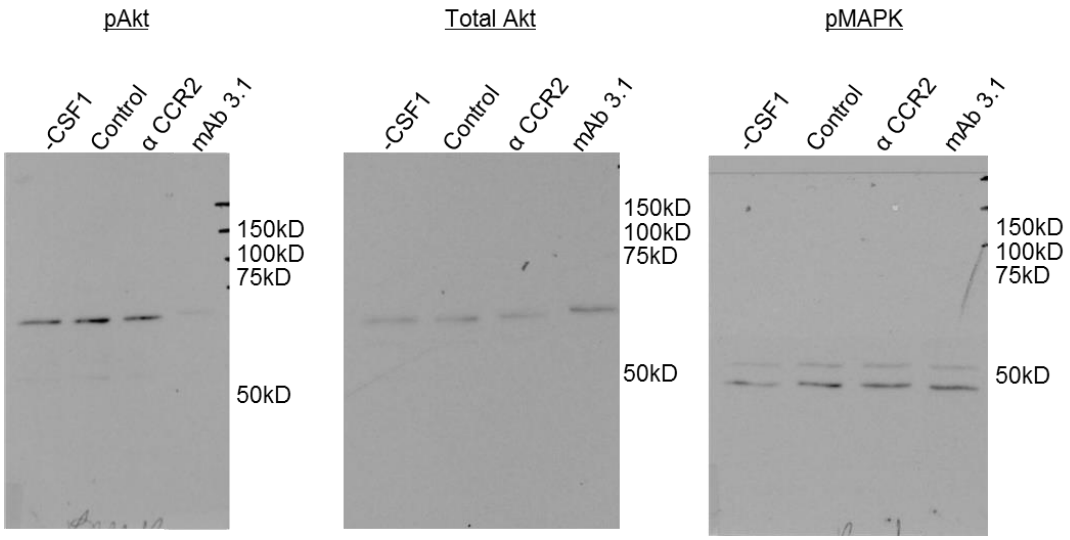

Figure 4.27 – mAb 3.1 reduced pAkt in feline osteoclasts. Feline osteoclasts were grown with rhCSF-1 (10 ng/ml, R&D Systems) and rhRANKL (30 ng/ml, R&D Systems) and were treated with hybridoma culture supernatant containing mAb 3.1 (1/6 of medium volume in osteoclast culture) for 4 days. Controls were: anti-CCR2 hybridoma culture supernatant (similar dose, Teresa Raposo), labelled as "α CCR2" in the figure, untreated cells ("Control") and no CSF-1 after cells had matured into osteoclasts ("-CSF-1"). Proteins from the lysed osteoclasts (20 µg/well) were resolved by SDS-PAGE and transferred onto a nitrocellulose membrane. The same membrane was probed with anti-pAkt, anti-total Akt and anti-pMAPK (all at 1:1000, Cell Signalling). Notice the reduced pAkt band in the mAb 3.1-treated lane. Secondary antibody was swine anti-rabbit Ig, HRP-conjugated (1:1700, Dako).

4.3.10 ELISA assays

CSF-1 binding inhibition assay

A selection of clones that showed promising results in the proliferation assays using the REM134 cells were analysed in their capacity to block CSF-1 binding to CSF-1R. This was tested by ELISA, where immobilized CSF-1R was used to capture CSF-1, which was detected with a commercial antibody. Anti-CSF-1R mAbs were tested for the ability to inhibit CSF-1R/CSF-1 binding. The IgG mAb 1C6 showed the best response, producing a signal lower than the control, indicating that less CSF-1 bound to the receptor (Figure 4.28). All other tested antibodies were IgM clones. However, in later assays, mAb 1C6 seemed to lose its capacity to bind to CSF-1R, as measured by ELISA. mAb 3.1 was not tested in this

assay since it was produced against the dimerization domain of the CSF-1R and was therefore not expected to interfere with CSF-1 binding.

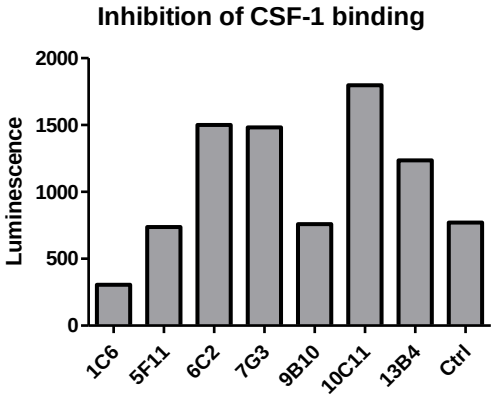

Figure 4.28 – mAb 1C6 reduced CSF-1/CSF-1R interaction. Competition ELISA for the CSF-1R ligand-binding region using hybridoma culture supernatants containing mAbs. Monoclonal antibodies were added to plates containing the immobilized canine CSF-1R (300 ng/well, Chapter 7). rhCSF-1 (18 ng/well, Biolegend) was added subsequently, and the amount of bound CSF-1 was detected using anti-CSF-1 (1:75, Peprotech). Only mAb 1C6 reduced CSF-1 binding when compared to the control. Secondary antibody was anti-rabbit Ig, HRP-conjugated (Life Technologies). The negative control was stained only with the secondary antibody. The y-axis indicates the relative amount of CSF-1 bound to CSF-1R. The result shown here is the difference in luminescence between the wells with mAb competing with CSF-1 and the wells with the mAb only. Results lower than the control suggest that the respective mAb supernatant reduced CSF-1 binding. The figure is representative of 4 wells in each of two independent assays.

Cross reactivity of mAb 3.1

All of the monoclonal antibodies were originally selected for the ability to bind CSF-1R in dot-blots or ELISA assays (Chapter 7). However, when the antibodies were tested against unrelated control proteins, it became evident that many clones showed non-specific binding. mAb 3.1 bound strongly to the antigen against which it was raised, the dimerization domain of CSF-1R, produced in bacteria. However, it bound weakly to the full CSF-1R receptor, which was produced in mammalian cells, and also to a control protein, bovine serum albumin (BSA) (Figure 4.29).

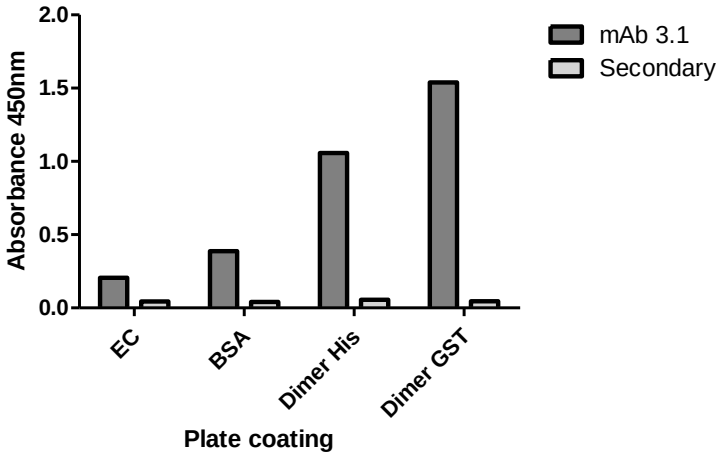

Figure 4.29 – mAb 3.1 showed cross-reactivity with other proteins in ELISA. Plates were coated with either the extracellular region (EC) of canine CSF-1R (400 ng/well), with similar concentrations of BSA or with the dimerization domain of the CSF-1R with the respective tags (Dimer His/Dimer GST). mAb 3.1 bound similarly to the EC region and to the control protein, BSA. Secondary antibody was rabbit anti-mouse Ig, HRP-conjugated (1:2000, Dako). The negative control was stained only with the secondary antibody.

4.4 Discussion

Several monoclonal antibodies exist for therapies against human cancer. Common targets, such as CD20, are overrepresented among the existing drugs as companies tend to follow the commercial success of preceding mAbs (Scott et al., 2012). The same is true for veterinary medicine, and CD20 is one of the two currently licensed (FDA) targets of mAbs for dogs (Acharya et al., 2015). To fully achieve the potential of mAbs in cancer therapy, there is a need to develop targeted treatments against a wider range of antigens (Zhao et al., 2014). The tumour microenvironment and the infiltrated immune cells are believed to be potential targets. The immune components of the tumour bulk are not only tolerant to the cancer cells, but can in fact promote cancer growth (Bonde et al., 2012; Marabelle et al., 2014).

This chapter shows the characterization of antibodies with potential to inhibit macrophage survival and proliferation by blocking the CSF-1R. These antibodies were created with the intent of affecting the population of tumour-associated macrophages (TAMs). The two best candidates were described here: mAb 1C6 was produced against the full extracellular fraction of the CSF-1R; mAb 3.1 was generated against the dimerization domain of CSF-1R. The hybridoma clone 1C6, however, seemed to lose binding to CSF-1R

over time and was therefore not studied using the full complement of assays described here. The second antibody, mAb 3.1, was thoroughly characterized.

Although not shown, none of the mAbs tested here reacted against the CSF-1R in western blots. Therefore, other assays were performed to determine mAb specificity, such as immunostaining of different cells and tissues.

4.4.1 Immunostaining assays

Bone marrow-derived macrophages express CSF-1R on the cell surface, as has been shown in cells from other species, such as pigs and chickens (Garcia-Morales et al., 2014; Moffat et al., 2014). mAb 3.1 was able to stain BMDM and a canine histiocytic sarcoma cell line (DH82) by immunofluorescence, although the staining was weak. BMDM were supplemented with rhCSF-1, which leads to receptor degradation (Garcia-Morales et al., 2014). Also, cells that co-express CSF-1 and its receptor have a reduced number of copies of the receptor on the cell surface, due to an increased rate of turnover (Rettenmier et al., 1987). BMDM cells in culture are capable of expressing CSF-1 after an initial exogenous CSF-1 stimulation (Temeles et al., 1993), and therefore low concentrations of the receptor were expected. However, because of the fixation method, intracellular receptor could be detected by immunofluorescence. For flow cytometry, BMDM were starved of CSF-1 in an attempt to increase CSF-1R expression on the cell surface, without effect, as measured using both the anti-swine CSF-1R (positive control antibody) and mAb 3.1 (not shown). This may be due to the long period of CSF-1 conditioning to which those cells had previously been subjected. In these conditions, as mentioned above, BMDM can produce CSF-1 (Temeles et al., 1993), rendering the CSF-1 starvation inefficacious. When cells were starved of FBS overnight, no CSF-1R expression could be detected with mAb 3.1 or the control antibody, probably due to forced cell cycle arrest (Rosner et al., 2013). If cells were supplemented with CSF-1 during serum starvation, CSF-1R could be detected in similar levels by both the control and 3.1 antibodies.

mAb 3.1 specifically bound to dog cells as no staining was detected in the murine macrophage cell line (RAW264.7). This is an important negative control, since staining cannot therefore be attributed to binding to the Fc receptors. The function of Fc receptors is illustrated in Figure 4.30. These receptors are present in several leukocytes and are responsible for binding to the Fc region of the antibodies (Fridman, 1991). RAW264.7 cells express Fc receptors (Rosa et al., 2007) and since mAb 3.1 is a murine antibody it would be possible for it bind to the receptors on the surface of RAW264.7 cells leading to non-specific

staining. However, it has been suggested elsewhere that Fc receptor binding during immunostaining is an unproven dogma and does not occur (Buchwalow et al., 2011).

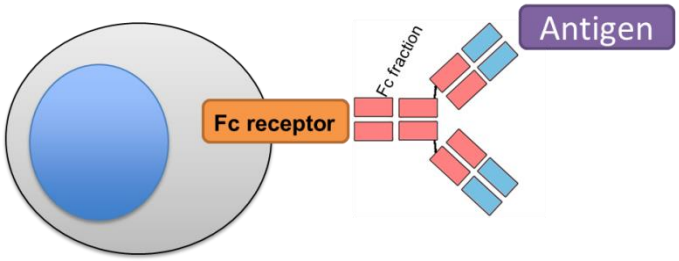

Figure 4.30 – Schematic representation of the role of Fc receptors. Cells expressing these receptors are activated upon binding to the Fc fraction of an antibody.

Fc receptors are expressed throughout several leucocytes lineages (Fridman, 1991). If mAb staining was dependent on Fc receptors, immune tissues stained with mAb 3.1 should demonstrate non-specific staining of several FcR^+ cells, such as granulocytes or lymphocytes in the lymph node or spleen. On the contrary, mAb 3.1 could identify cells within normal canine tissues – lymph node, spleen and duodenum – that are compatible with the spatial distribution of macrophages (Sasmono et al., 2003). In the MacGreen mouse, which expresses a CSF-1R-GFP transgene, it is possible to recognize a subpopulation of especially bright $CSF\text{-}1R^+$ cells surrounding the lymphoid follicles of the spleen (MacDonald et al., 2010) which could correspond to the cells stained by mAb 3.1. When the mAb was used to stain lymph nodes, the cells of the medullary cords were preferentially marked, with increased intensity compared to other areas of the organ. This subpopulation of cells is known to highly express the CSF-1R (Sasmono et al., 2003). Strong staining of cells throughout other regions of the lymph node only was obtained when cells were permeabilized, as shown in the Results, indicating that most receptors expressed by these cells were intracellular. These data indicate that mAb 3.1 binds to cells expressing high concentrations of CSF-1R. mAb 3.1 stained cells in the same tissue compartments as other markers such as CD163 and CD11b, which confirms that those cells are likely macrophages. CD163 is commonly expressed in macrophages in the intestine (Bain et al., 2013; Komohara et al., 2006). CD11b is a common myeloid cell marker, although it can be expressed by other leukocytes, such as neutrophils (Jämsä et al., 2015).

There does not seem to exist cross reactivity between the monoclonal antibody 3.1 and receptors of similar structure to CSF-1R. The CSF-1R is structurally similar to other tyrosine kinase receptors, such as c-Kit and the platelet-derived growth factor receptor (PDGFR), although the canine amino acid sequences share only 29.18 % and 23.12 % identity in the extracellular portions, respectively (NCBI) (Qiu et al., 1988). A thyroid section was co-stained with c-Kit antibody and mAb 3.1. No cells were double-stained by these antibodies. It is suggested that the c-Kit$^+$ cells within the thyroid are C cell precursors (Bosse et al., 1997). The distribution of c-Kit$^+$ staining in the current work is similar to what is expected for C cells (Islam, 2013). Few macrophages are present in the thyroid (Kimura et al., 2005), as was observed here with mAb 3.1. Antibody specificity was also confirmed by a competitive inhibition assay where increasing concentrations of recombinant CSF-1R was used to block the staining of DH82 cells by mAb 3.1. The same competition protocol could not reduce the staining by the control CD11b antibody.

mAb 3.1 also was able to stain cancer cells. Two canine mammary cancer cell lines (REM134 and Lilly) and also epithelial cells in paraffin wax-embedded tumours were positive using mAb 3.1. Canine mammary tumour epithelial cells have previously been shown to express the CSF-1R (Król et al., 2011), and the expression pattern was confirmed here. As is shown in Chapter 3, both cancer cell lines transcribe CSF-1R mRNA and can be repressed by a CSF-1R small-molecule inhibitor. The expression of CSF-1R (as stained by mAbs 1C6 and 3.1) and the reliance on this receptor for cancer cell proliferation was variable and dependent on cell density, probably due to contact inhibition and cell cycle arrest (Rosner et al., 2013). This could justify some of the large differences in cell positivity seen in the replicates of flow cytometry staining of REM134 cells.

mAb 3.1 could not stain peripheral blood monocytes from dogs, however. An anti-mouse CSF-1R inhibiting antibody, mAb 2-4A5, has been found not to be able to stain CSF-1R on the surface of a transfected cell line and the authors believed this was due to the proximity of the epitope to the cellular membrane (Haegel et al., 2013). The region used as the immunogen for mAb 3.1 spanned the amino acids 344 to 444 of the extracellular portion of the canine receptor. This is similar to the epitope of mAb 2-4A5, which is located between the amino acids 349 and 512 of the murine sequence (Sherr et al., 1989). Therefore, epitope unavailability of the soluble receptor could potentially inhibit the binding of mAb 3.1.

It is possible that some of the monocytes express low levels of CSF-1R and were not detected by mAb 3.1. Other antibodies also selectively target some of the CSF-1R$^+$ monocytes. M279, a blocking anti-CSF-1R, only depletes GR-1$^-$ and a small subpopulation of F4/80$^+$ CSF-1R$^+$ cells from the blood of mice (MacDonald et al., 2010), leaving some of

the CSF-1R^{+} monocytes unaffected. The number of CSF-1R copies on the cell surface is much smaller for blood monocytes than for tissue or activated macrophages (Byrne et al., 1981). Additionally, in humans, CSF-1R is only highly expressed in the nonclassical monocyte subset, which represents less than 10 % of the circulating total of monocytes (Thomas et al., 2015; Wong et al., 2011). These CSF-1R^{Low} cells could potentially evade staining by mAb 3.1. As was seen when staining tissues, mAb 3.1 may not detect cells expressing low concentrations of CSF-1R, as it preferentially seems to bind to CSF-1R^{High} populations such as medullary cord macrophages in the lymph nodes (Sasmono et al., 2003) and perifollicular macrophages in the spleen (MacDonald et al., 2010).

The positive control used for staining of canine monocytes was an anti-swine CSF-1R. It is interesting to note that some of its binding was dependent on the antibody Fc fraction. When a human Fc receptor block was used, binding of the control antibody to monocytes was greatly diminished. Human antibodies can bind to canine Fc receptors (Bergeron et al., 2014), and therefore the human Fc blocking reagent used – dependent on the presence of human antibodies to compete for Fc binding – was suitable for blocking dog cells. Mouse IgG_1 antibodies can bind to the canine FcγRIII. Binding to this receptor only occurs when there is an antigen-antibody complex. It is possible that the Fc receptor could have served to strengthen the binding of the anti-swine mAb to CSF-1R on the same cell (Figure 4.31) (Bergeron et al., 2014; van der Poel et al., 2011).

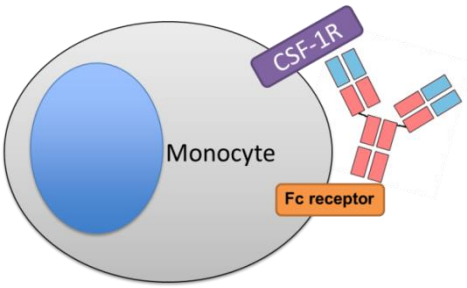

Figure 4.31 – Fc receptor binding can modulate the antibody contact with its antigen on the same cell (cis-interaction). This can alter the binding properties of the antibody to its target (Haegel et al., 2013).

Lack of antibody specificity or affinity could also justify why mAb 3.1 did not bind to blood monocytes. This is supported by the ELISA assay of specificity, where mAb 3.1 failed to bind to the extracellular fraction of CSF-1R. This antibody was raised against the dimerization domain of CSF-1R, a fraction which is contained within the extracellular region. However, while the extracellular region was produced in mammalian cells, therefore

being folded and glycosylated similarly to the wild-type protein, the dimerization domain was expressed in bacteria. Also, the recombinant antigen used for generating mAb 3.1 formed aggregates. The different protein conformation due to bacterial origin and aggregate formation could explain the binding of mAb 3.1 to fixed tissues but not to the native soluble protein expressed on monocytes. Immunization with a non-conformational peptide is known to reduce the formation of antibodies that recognize the conformational epitopes (Beil et al., 1973).

In immunoprecipitation, it could be verified that mAb 3.1 bound only to a narrow range of the glycoforms of CSF-1R, reinforcing the hypothesis that the bacterial origin of the antigen used for producing this antibody had an effect on its affinity. Surprisingly, mAb 12.2 immunoprecipitated a large range of glycoforms, although it was originated from the same immunization as mAb 3.1.

4.4.2 Proliferation assays

The capacity of an antibody to interfere with signalling from a receptor can be derived from several separate mechanisms. Possible means include blockade of ligand-receptor interaction, impediment of dimerization/aggregation of receptor units and alteration of receptor conformation (Bradbury et al., 2011).

mAb 1C6 was raised against the extracellular portion of this receptor, and seemed to reduce canine mammary cancer cell survival based on the competitive inhibition of CSF-1 binding, as shown by ELISA. Other antibodies could not affect CSF-1 binding to the receptor, and some seemed to increase this interaction possibly through cooperative binding (Lu et al., 2004) or allosteric control (Rizk et al., 2011). All other antibodies tested in the assay of CSF-1 binding inhibition were IgM, and could present some allosteric interaction with CSF-1, increasing its binding. However, over time the 1C6 hybridoma clone seemed to lose binding for the CSF-1R, as later assessed in confirmatory ELISAs.

To increase the likelihood of finding an inhibitory antibody against this receptor, monoclonal antibodies were raised using the dimerization domain of CSF-1R as an antigen. Stable dimerization of the receptor monomers after ligand binding is essential for signal transduction via the CSF-1R (Li and Stanley, 1991). Blocking receptor dimerization has been shown to be an effective means to impede receptor function (Adams et al., 2006). The monoclonal antibody (mAb) 3.1, originated from this hybridoma production strategy, was capable of reducing BMDM survival, and it is therefore likely that this effect was mediated

by blocking the CSF-1R. Blocking the function of CSF-1R abrogates the growth of bone marrow macrophages (Dewar et al., 2005).

It could be hypothesized that an effect on cell survival could also be derived from affecting the Fc receptors on the macrophage surface. The high affinity Fc receptor FcγRI is capable of binding free antibodies (not coupled to an antigen) and could have mediated some of the effects that the mAbs showed on the canine macrophages (van der Poel et al., 2011). However, murine IgG_1, such as mAb 3.1, is not able to bind to the canine FcγRI (Bergeron et al., 2014), indicating that contact with this receptor could not have affected the canine BMDM. mAb 12.2 was of the IgG_{2b} isotype, which also cannot interact with the canine FcγRI. This antibody showed a strong effect on macrophage proliferation in the dosing assays, but this effect was removed upon antibody chimerization (Chapter 5). This indicates that when Fc binding was added to mAb 12.2, its affinity towards CSF-1R was removed, perhaps as an effect of the obligatory cis-interaction between mAb and CSF-1R after chimerization (see Figure 4.31, above).

If there is an interaction of mAb 3.1 with Fc receptors, it is more likely that Fc binding modulates, rather than substitutes, the CSF-1R binding effects. This could happen through FcγRIII, which requires the formation of an antibody-antigen complex for binding to the Fc region and which can interact with murine IgG_1 (Bergeron et al., 2014; van der Poel et al., 2011). This interaction may have occurred with the anti-pig CSF-1R antibody, discussed above in the flow cytometry assays. Another anti-CSF-1R mAb has been described which depends largely on the Fc region for functional impairment of the CSF-1R signalling (Haegel et al., 2013). FcγRI and FcγRIII binding is believed to increase, rather than inhibit, macrophage proliferation (Luo et al., 2010). However, the stimulation through Fc receptors paradoxically can induce immunosuppression through the release of cytokines such as IL-10 (Gerber and Mosser, 2001). In this way, mAb 3.1 could bind to CSF-1R through the variable regions and to the FcγRIII through the Fc fraction, leading to reduced cellular survival (see Figure 4.31, above). Again, the activity of mAb 12.2 must have been Fc-independent since the murine IgG_{2b} does not bind to FcγRIII (Bergeron et al., 2014).

The binding to Fc receptors may, however, explain the large influence of the control IgG used in the dose-dependent proliferation assay. The commercial control antibodies used in that assay are purified from mouse serum and therefore are comprised of all antibody isotypes. As such, no direct comparison can be made between IgG_1 or IgG_{2b} clones, such as mAb 3.1 and mAb 12.2, and the control antibody, which contains IgG_{2a}, a strong binder of canine Fc receptors (Bergeron et al., 2014). Another group also found that the isotype control altered macrophage functionality. When mAb AFS98 (anti-murine CSF-1R) was used in a

tumour model, it was revealed that treatment of animals with rat isotype control could reduce CSF-1R$^+$ cells within the tumours, although the mAb displayed superior results. Nonetheless, improved clinical outcomes could only be seen when using mAb AFS98 (Fend et al., 2013).

Mammary cancer cells are not expected to express effector Fc receptors, and therefore this mechanism cannot be even considered to explain the cellular inhibition of these cells with the mAbs (Cianga et al., 1999; Dougherty et al., 1987; Kerbel and Dennis, 1980). As stated above, these cells express the CSF-1R. Our results (Chapter 3) and other works from the literature suggest that CSF-1R can be relevant for cancer cell metabolic activity (Patsialou et al., 2009). Even if exogenous CSF-1 has only a small effect in cancer cell proliferation, autocrine expression of the ligand can activate the receptor (Patsialou et al., 2009). The effect of mAb 3.1 in reducing cancer cell survival also was translated as reduced vascular remodelling in the CAM assay even in the absence of macrophages, indicating that the effect of the mAb solely on the cancer cells could be biologically relevant. However, it was verified by flow cytometry that CSF-1R expression and proliferation by REM134 carcinoma cells was very sensitive to contact inhibition, as discussed above. This could have affected the screening of the first hybridoma fusion against the extracellular region of CSF-1R (Chapter 7). The anti-proliferative activity of these first antibodies was tested mainly against REM134 cells; for those assays, cellular confluence was not observed and potential clones may have been discarded due to weak anti-proliferative responses in cells that were overconfluent at the time of testing.

The effects of mAb 3.1 on cellular proliferation were confirmed using feline osteoclasts. The inhibition assay with osteoclasts was performed because these cells have a distinct morphology, forming a tight "tiled" structure. When cells undergo apoptosis, they naturally retract. Detecting this occurrence on osteoclasts is simple because of the characteristic arrangement of the cells in culture (Lacey et al., 2000). Apoptosis was induced using mAb 3.1 but not a control anti-CCR2 monoclonal. When the molecular pathways were analysed, it could be seen that only mAb 3.1 induced a reduction in the phosphorylation of Akt, which is important for cell survival mediated through CSF-1R (Kelley et al., 1999).

However, FcγRIIb is capable of inhibiting macrophage activation also by affecting the Akt phosphorylation (Tridandapani et al., 2002). Although the human FcγRII can bind to murine IgG_1 and IgG_2 (Warmerdam et al., 1993), it is not known to which murine isotypes the feline version of the receptor can bind. Against this hypothesis is the fact that IL-4 can induce the expression of FcγRIIb, and would therefore increase the inhibition of macrophages in the presence of mAbs. However, this did not happen when chimeric mAbs were used in the presence of IL-4 (Chapter 5) (Tridandapani et al., 2002). Analysis of CSF-

1R phosphorylation would clarify the pathways involved in the osteoclast apoptosis, but there are no commercially available antibodies that detect this in feline or canine cells.

Although mAb 3.1 seemed consistent in being able to affect cellular proliferation, only high concentrations of the mAb was able to reduce macrophage replication; because only two replicates were used at the relevant antibody dose, no statistical difference from the murine antibody control was found. Because the unpurified supernatants were compared initially, it is not possible to know if the concentration of antibodies being secreted by the hybridomas was the cause of the variation of the inhibitory ability of different mAbs in those assays. When the purified mAbs were compared, only doses of 7.5 µg/well (75 µg/ml) were able to (visually) reduce macrophage proliferation in comparison to the control antibody. mAb 12.2 had higher efficacy, and inhibited proliferation at 1.25 µg/well (~ 12.5 µg/ml). Published CSF-1R-blocking antibodies are effective in the range of 0.1 – 1 µg/ml (Haegel et al., 2013). This indicates that, if mAb 3.1 or the other mAbs tested here do bind to the CSF-1R, the interaction is weak, which would probably affect the practical use of these antibodies.

Because of the difficulties in studying macrophage proliferation – such as the responsiveness of these cells to a wide range of stimuli, among which the antibody Fc region – future studies with these and other CSF-1R-blocking antibodies should include assays with cells that rely on recombinant CSF-1R expression for survival (Gow et al., 2012; L. Moffat et al., 2014). This allows the comparison against similar cells that are not expressing the receptor and removes the confounding factor of Fc receptor expression.

4.5 Conclusions

The monoclonal antibody 3.1 was able to reduce proliferation and survival of macrophages and canine mammary cancer cells. Based on the staining patterns of this antibody in tissues and cell lines, this effect appears to be mediated through CSF-1R. However, it is not possible to eliminate that non-specific binding to other proteins and Fc receptor interactions are responsible for some or all effects of the mAb, based on the results of the ELISA, staining of monocytes and the suppression of the Akt pathway in osteoclasts. For the practical use of this mAb, further specificity assays are needed. *In vitro* alterations of the CDRs of mAb 3.1 are an alternative to improve its binding characteristics, and this approach is explored in Chapter 6.

Chapter 5

Production of chimeric and caninised antibodies

Highlights

- Four anti-CSF-1R antibodies were subjected to chimerization by exchanging the Fc region of the murine mAbs for the canine equivalent.
- Three of the four chimerized antibodies maintained the capacity to affect macrophage proliferation following CSF-1R stimulation. When macrophages were conditioned with IL-4 (which is CSF-1R-independent), the antibodies lost their effect.
- mAb 3.1 was further speciated by caninising the framework regions of the variable fraction.

Abstract

Chimerization and humanization of therapeutic antibodies has become the norm in the industry. This process offers the benefit of reducing antibody antigenicity when administered *in vivo* as well as increasing effector functions through the Fc fraction. This Chapter aimed to implement the process of chimerization and speciation of antibodies against the CSF-1R, developing a caninised version of these mAbs. Speciation should provide additional information on the efficacy of these antibodies and also offer an insight into the viability of these techniques for further studies. Antibody candidates from the mouse hybridomas were selected on their ability to inhibit macrophage proliferation. These clones were chimerized into a canine version by altering the Fc region. Three of the four clones that underwent chimerization maintained the ability to reduce macrophage proliferation when under the influence of CSF-1, and showed partial inhibition of cells in the presence of IL-34, the CSF-1R ligands. The chimeric antibodies had no effect on IL-4-conditioned macrophages. mAb 3.1 was further speciated into a fully caninised antibody. This was achieved by altering the framework regions of the variable fraction. Speciation offers the possibility to investigate the

importance of the Fc region for the effect of the anti-CSF-1R mAbs. In a review of the techniques used here, some improvements will be needed to increase expression levels in future studies.

5.1 Introduction

The presence of CSF-1R$^+$ cells within tumours is related to poor clinical outcome (Chambers et al., 1997; Lin et al., 2001). These cells are usually infiltrates of myeloid-derived cells, which are then differentiated into tumour-associated macrophages (TAMs) by factors within the tumour microenvironment. TAMs can contribute to almost every stage of tumour progression, such as neovascularization, tissue invasion, intravasation and increased cancer cell proliferation, among other attributes (Król et al., 2013, 2011; Mitchem et al., 2013). However, the cancer cells themselves can express CSF-1R and also its ligand, CSF-1 (Ide et al., 2002; Solinas et al., 2010), creating a loop of self-activation and macrophage recruitment and differentiation which is then fed back by the TAMs, as indicated by the results in Chapter 3. These pathogenic effects of CSF-1R make this receptor a prospective target for cancer treatment (Hume and MacDonald, 2012).

The goal of this project was the production of monoclonal antibodies (mAbs) with the capacity to bind and block the CSF-1R in canine cancer patients. The formation of anti-antibody responses during the administration of mAbs is a common occurrence and often represents an obstacle for the clinical usefulness of these biological products (Hwang and Foote, 2005). For this reason, the monoclonal antibodies originating from mice hybridomas should be expressed in a format that is less likely to induce canine anti-murine responses. There are three main reasons why antibody "speciation" is relevant: the formation of anti-antibody responses; the importance of FcRn in antibody pharmacokinetics; and the importance of the Fc region for effector functions. (A/N: henceforth, "speciation", "caninisation" and their derivatives will be written without quotes for clarity).

Prevention of anti-antibody responses through speciation has for long been known to be important in the clinical setting; anti-antibody responses are deleterious to the efficacy and safety of the mAb. The first commercial monoclonals used for treatment of cancer were purified murine antibodies. These pioneering attempts ended with the withdrawal of the products due to efficacy concerns. Edrecolomab (Panorex), an anti-epithelial cell adhesion molecule (EpCAM) antibody, was the first anti-cancer mAb to be licensed for human use in the world, having been approved in Germany in 1996 for the treatment of colorectal tumours (Reichert, 2012). However, later tests proved that the antibody lacked efficacy. Human anti-

mouse antibody responses were a common occurrence in patients receiving edrecolomab, and these were indicated as possible reasons for the clinical failure of this mAb (Punt et al., 2002). The efficacy of mAbs is reduced in the presence of host responses because there is increased clearance from the circulation (Lobo et al., 2004).

The importance of speciation of murine mAbs was also observed in canine patients. An anti-lymphoma murine monoclonal antibody, mAb 231, has been used in dogs. This was the first ever licensed monoclonal antibody for cancer therapy, preceding the drugs for human use (Jeglum, 2009). Although clinical benefit was encountered in the initial assessments, canine anti-mouse reactions were commonly seen and these were progressively increased with subsequent applications of the drug – as expected in secondary immune responses – therefore limiting its utility (Jeglum, 2009, 1996). As illustrated by these initial attempts with anti-cancer mAbs and later confirmed by antibody speciation experiments, murine antibodies are much more likely to induce marked anti-antibody responses. This adverse event has an incidence of over 80 % in humans receiving murine mAbs, and this is halved after antibody chimerization (Hwang and Foote, 2005).

The ability of the antibody to bind to the neonatal Fc receptor (FcRn) is another reason why antibody speciation is relevant. This receptor is responsible for recovering IgG from degradation in the lysosomes, allowing for increased antibody serum half-life. However, binding to FcRn is dependent on species-specificity. The human receptor, for example, is strict in its binding partners, not being able to rescue the murine immunoglobulins from degradation (Ober et al., 2001). Therefore, murine antibodies have a half-life of only 2 – 3 days in humans, whereas natural human antibodies last in the circulation for about 23 days (Lobo et al., 2004).

Besides its importance in increasing circulating time for antibodies, the Fc antibody fraction also mediates effector functions, such as antibody-dependent cell-mediated cytotoxicity (ADCC) through binding to receptor FcγRIIIa, and complement-dependent cytotoxicity (CDC) through binding to the complement protein C1q (Kubota et al., 2009) (Figure 5.1). Once more, these effects are largely, although not entirely, Fc species-specific, which makes speciation relevant (Bergeron et al., 2014).

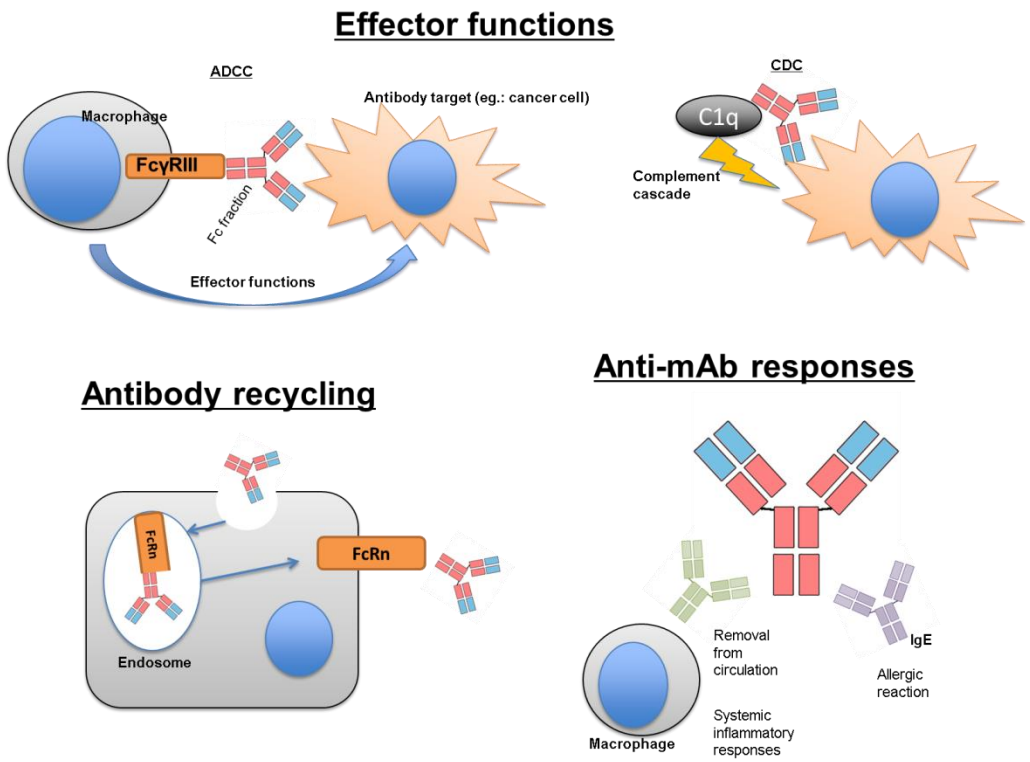

Figure 5.1 – Speciation improves antibody function and reduces side-effects. The antibody Fc region is important for: effector functions, such as antibody-dependent cellular cytotoxicity (ADCC), complement-dependent cytotoxicity (CDC); antibody "recycling" through the neonatal Fc receptor (FcRn), avoiding endosome degradation; reduction of anti-antibody responses, such as rapid clearance from the circulation and inflammatory reactions.

In many cases the effector functions are significant for the clinical usefulness of the mAbs, and therefore inhibiting anti-mAb responses would not be sufficient to implement these antibodies in the clinic (Kubota et al., 2009). Immune suppression of the patient has been studied as an alternative to antibody speciation for the reduction of anti-mAb responses. Cyclosporin and other immunosuppressant drugs are capable of reducing the formation of anti-mAb immune responses – although the suppression is not complete (Dhingra et al., 1995; Ledermann et al., 1988; Weiden et al., 1994). However, even if immunosuppression could fully inhibit anti-murine antibody responses, this strategy would still not enable the mAb effector functions, which depend on the Fc fraction.

Consequently, because of anti-mAb responses, FcRn and Fc effector functions, not only the antibody binding properties through the variable regions determine the success of monoclonal antibodies in therapy. The antibody constant fraction is crucial for the

distribution and cellular functions of this biological drug, therefore affecting the clinical utility of the mAbs.

The expression of the anti-CSF-1R antibodies in a canine framework was, therefore, an important step to achieve the goal of an anti-cancer drug. Several methods of antibody speciation exist, varying in the level of amino acid substitution from the murine sequence to that of the desired species. The levels of speciation are illustrated in Figure 5.2. Chimerization is the simplest form of species conversion of the antibody structure, in which the variable regions are originated from the mouse hybridomas and the constant regions are from the species of interest (dog, for instance). By genetic engineering, these fractions are then expressed as a chimeric protein. Full speciation of the antibody structure – such as humanization or caninisation – refers to the substitution of amino acids within the variable region, therefore further reducing the presence of murine sequences. Because full speciation alters amino acids near the antigen binding sites of the antibody, this process is more likely than chimerization to alter binding affinity. However, if full speciation is successful, it also leads to improved pharmacokinetics characteristics due to reduced formation of anti-mouse antibodies that may remove the mAb from circulation (Adams et al., 2006; Lobo et al., 2004). The production of 100 % canine sequences (the last possible step in the speciation process, Figure 5.2) would only be possible starting with display techniques using libraries of canine antibodies.

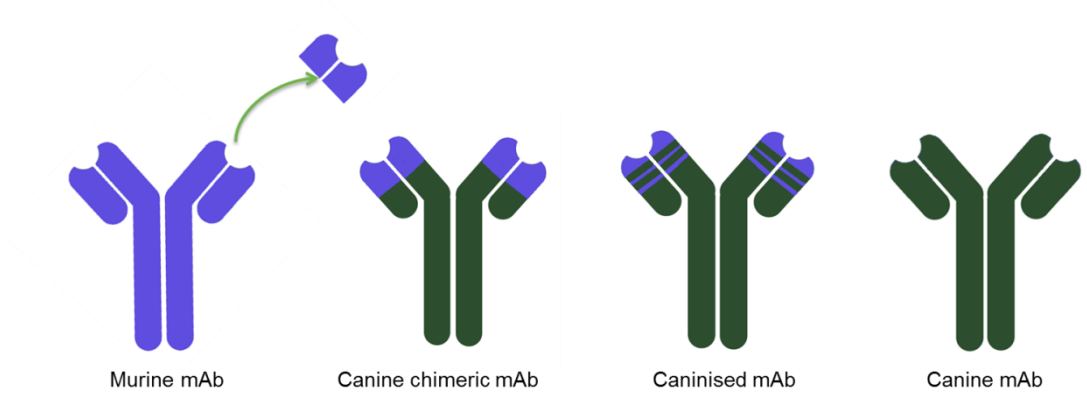

Figure 5.2 – Schematic representation of the different antibody formats with regard to their level of speciation. Green colour depicts canine sequences and blue represents murine.

This chapter describes the construction of chimeric and caninised anti-CSF-1R antibodies with the goal of studying the feasibility of the technique and the functionality of the derived antibodies. The first step for the construction of the chimeric antibody was the isolation of the variable region from the hybridoma clones. For this, mRNA was isolated

from the hybridoma cells and the variable regions were amplified by a specialized technique, RACE-PCR. This structure was then coupled to a canine constant region, generating a chimeric molecule. The chimeric mAbs were expressed in mammalian cells and seemed to maintain function when compared to the parental antibodies. For further reduction of dog anti-mouse reactions, mAb 3.1, described previously, was caninised by altering the variable framework regions (Figure 5.3). Although chimerization and full speciation could be achieved, the vectors and host systems for expression of these antibodies require optimization to allow for higher production scales.

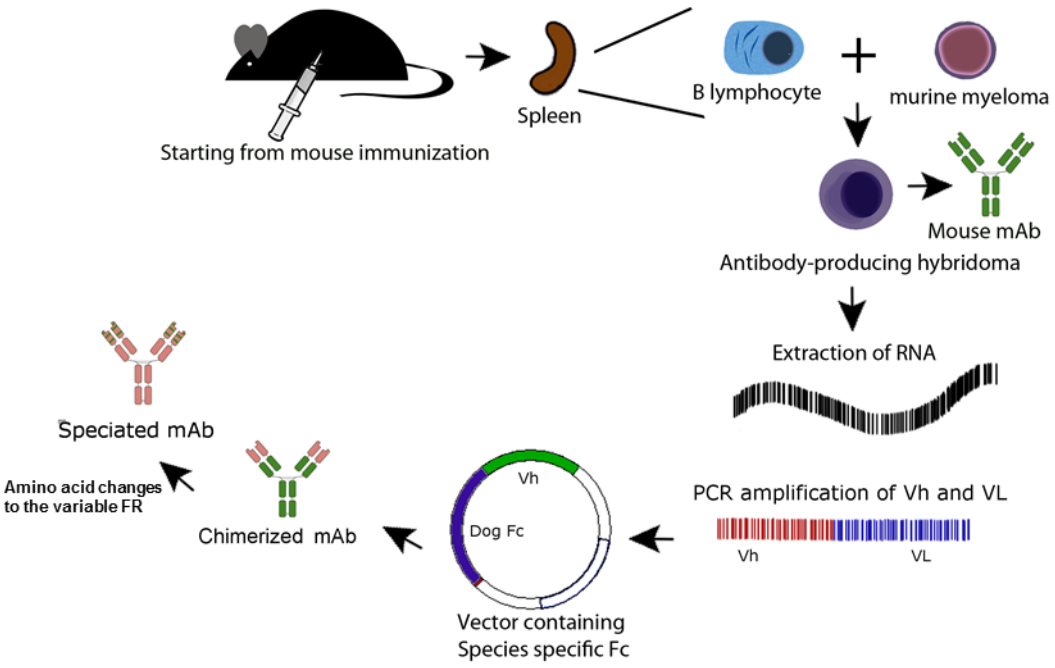

Figure 5.3 – Overview of the speciation process used in this chapter. mRNA was obtained from the candidate hybridoma cells. The variable regions were sequenced and chimerized by inserting into a plasmid containing the canine constant regions. Full speciation was performed by altering the framework regions (FR). Immunization and hybridoma production are described in Chapter 7.

5.2 Materials and Methods

Basic methodological descriptions and brands not stated here are presented in Chapter 2. HotStarTaq polymerase kits are supplied by Qiagen. Phusion polymerase kits and

restriction enzyme kits are supplied by Thermo Scientific. dNTPs are supplied by Promega.

5.2.1 Sequencing the antibody variable region

The cloning of the antibody variable region was conducted according to the protocol from Bradbury, 2010 (Bradbury, 2010) for RACE amplification of variable regions. All primers are shown on Table 5.1.

Table 5.1 – Primers for sequencing the antibody variable regions. Primers shown as 5` to 3`.

Heavy chain reverse transcription primers	
RACEMOG1 (mouse IgG_1)	TATGCAAGGCTTACAACCACA
RACEMOG2b (mouse IgG_{2b})	AGGACAGGGGTTGATTGTTGA
Mouse IgM	Reverse transcription from mAb 6C2, an IgM, was done using random nonamers (Sigma)
Light chain reverse transcription primers	
MOCKFOR (mouse κ)	CTCATTCCTGTTGAAGCTCTTGACAAT
CL1FOR (mouse λ 1)	ACACTCAGCACGGGACAAACTCTTCTC
CL2FOR (mouse λ 2)	ACACTCTGCAGGAGACAGACTCTTTTC
RACE PCR primers	
MOCG12FOR (mouse IgG_1, IgG_{2a} heavy)	CTCAATTTTCTTGTCCACCTTGGTGC
MOCG2bFOR (mouse IgG_{2b} heavy)	CTCAAGTTTTTTGTCCACCGTGGTGC
MOCMFOR (mouse IgM heavy)	TGGAATGGGCACATGCAGATCTCT
CKMOsp (mouse κ light)	CTCATTCCTGTTGAAGCTCTTGACAATGGG
CL1FOR (mouse λ1 light)	ACACTCAGCACGGGACAAACTCTTCTC
CL2FOR (mouse λ2 light)	ACACTCTGCAGGAGACAGACTCTTTTC
XSCTnTag (anneals to the poly-A tail)	GACTCGAGTCGACATCGATTTTTTTTTTTTTTTT

RNA was extracted (RNeasy Mini Kit, Qiagen) from the hybridoma monoclonal cell lines. cDNA was synthetized using MLV-V reverse transcriptase using one or two-steps approaches, for comparison (Table 5.2).

Table 5.2 – Strategies tested for reverse transcription of the antibody variable regions (all reagents by Promega).

One-step approach	Two-steps approach
mRNA (1 µg) was denatured at 65°C for 5 min and immediately transferred to ice	mRNA (2 µg) was annealed to 7.93 µl of the primer RACEMOG1 or MOCKFOR (10 µM) at 70° C for 5 min and immediately cooled on ice
The remaining reagents were added: 5 × M-MLV transcriptase buffer (5 µl) dNTP (to 0.25 mM) M-MLV reverse transcriptase (10 U) RNAse inhibitor (10 U) water (to 25 µl)	
Incubated at 42°C for 60 min	
52°C for 30 min	42°C for 30 min
95°C for 5 min	

After cDNA synthesis, excess primer was removed using a Centricon 100 spin filter (Millipore), diluting the reaction to 500 µl with 0.1 × buffer TE (TE: Tris (10 mM), EDTA (1 mM), pH 8.0) and centrifuging at 300 × *g* until nearly all the volume passed through the filter, as determined visually. The volume was again brought to 500 µl with 0.1 × buffer TE. The solution was centrifuged again until concentrated to 10 µl, determined by pipetting. A poly-A overhang was added to the 5`-end of the cDNA sequence of the mAbs with the following reaction: terminal deoxynucleotidyl transferase (Promega) (10 U), dATP (to 0.3 mM), tailing buffer (4 µl, supplied with enzyme). The reaction was incubated at 37°C for 5 min and then 65°C for 5 min. The volume of the reaction was adjusted to 500 µl with 0.1 × buffer TE, and this was used as a template in subsequent PCR reactions at 10 % of the final volume. The variable light cDNA was unstable after freeze/thaw cycles, so it was divided in aliquots after this process.

PCR was performed using primer XSCTnTag and a specific primer for the light or heavy chain (Table 5.1, above). Protocol for PCR was: 10 × HotStarTaq buffer (to 1 ×), dNTP (to 0.2 mM), forward and reverse primers (to 0.5 µM each), HotStarTaq polymerase (2.5 U), cDNA (10 µl), nuclease-free water (to 100 µl). Thermal cycling conditions were: 95°C for 15 min, 60°C for 5 min, 72°C for 40 min; 40 × [95°C for 1 min, 60°C for 1 min, 72°C for 3 min].

An illustration of the PCR strategy is depicted in Figure 5.4:

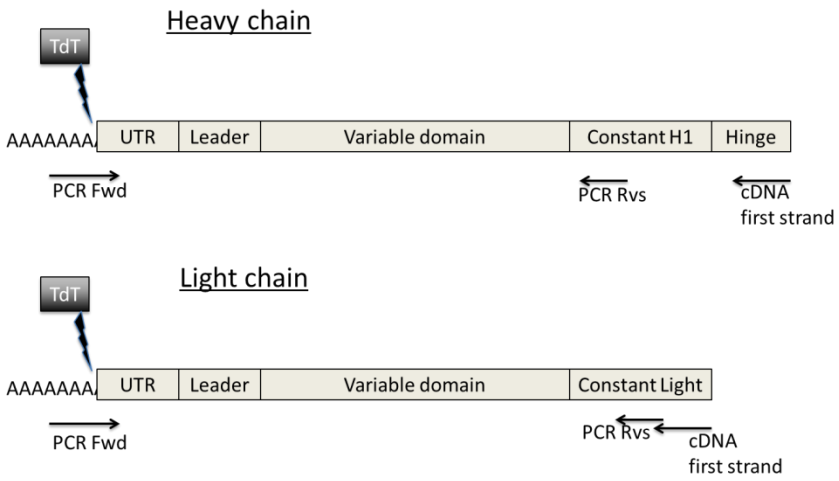

Figure 5.4 – Rapid amplification of cDNA ends (RACE) strategy for amplification of the hybridoma variable regions. Primers are indicated as arrows. UTR, unstranslated region. TdT, Terminal deoxynucleotidyl transferase. Fwd, forward primer. Rvs, reverse primer.

After PCR amplification of the antibody sequences, the products were run on 1 % agarose and were gel extracted using QIAquick Gel Extraction Kit (Qiagen). The product was quantified by Nanodrop spectrometry (Thermo Scientific) at 260 nm, and sequenced using the reverse PCR primer as initiator (Dundee DNA Sequencing and Services).

5.2.2 Construction of the chimeric antibodies

Having identified the antibody variable sequences with the PCR strategy above, primers were designed for each individual variable heavy and variable light clones (Table 5.3). The primer design strategy in relation to the antibody sequence is illustrated here for mAb 3.1 (Figure 5.5).

The primers contained specific restriction digestion sites to insert the amplicons into the plasmids pVH (BssHII and BamHI) and pVL (ApaLI and XhoI). The forward primers had to contain the necessary sequence to maintain the translation of the leader within the plasmids after the enzymatic digestion (Figure 5.5). The cloning sites of the pVH and pVL plasmids are shown in Figure 5.6.

Table 5.3 – Primers used for inserting the variable regions into the chimerization plasmids. EF-1α was the sequencing primer after chimerization. Primers shown as 5` to 3`.

Antibody chain	Primers
1C6 D6 VL	FWD – TATCCGTGCACTCCGACATTGTGCTGACCCAATC RVS – TTTGATCTCGAGCTTGGTG
1C6 D6 VH	FWD – TATCCGCGCGCACTCCCAGGTGCAACTGAAGGAG RVS – CGGGATCCTGAGGAGACTGTGAGAGTG
3.1 VL	FWD – TATCCGTGCACTCCAATATTGTGCTAACTCAGTCTCCAG RVS (same as 1C6 D6 VL) – TTTGATCTCGAGCTTGGTG
3.1 VH	FWD – TATCCGCGCGCACTCCGAAGTGAAGCTGGTGGAGTC RVS – CGGGATCCTGAGGAGACGGTGACTGAG
2H1 VL	FWD – TATCCGTGCACTCCGACATCCAGATGACTCAG RVS – TTTGATCTCGAGCTTGGTG
2H1 VH	FWD – TATCCGCGCGCACTCCCAGGTCCAACTGCAGCAG RVS – CGGGATCCTGAGGAGACTGTGAGAGTG
6C2 D6 VL	FWD – TATCCGTGCACTCCGACATCCCGATGACTCAG RVS – TTTGATCTCGAGCTTGGTG
6C2 D6 VH	FWD – TATCCGCGCGCACTCCGATGTGCAGCTTCAGGAGTC RVS – CGGGATCCTGAGGAGACGGTGACCGTGGTC
12.2 VL	FWD – TATCCGTGCACTCCGACATCCAGATGAACCAG RVS – TTTGATCTCGAGCTTGGTG
12.2 VH	FWD – TATCCGCGCGCACTCCGAGGTTCAGCTGCAGCAGTC RVS – CGGGATCCTGCAGAGACAGTGACCAG
EF-1α	TCAAGCCTCAGACAGTGGTTC

VH

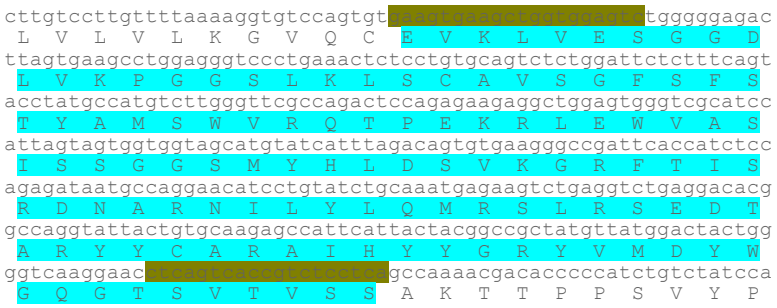

VL

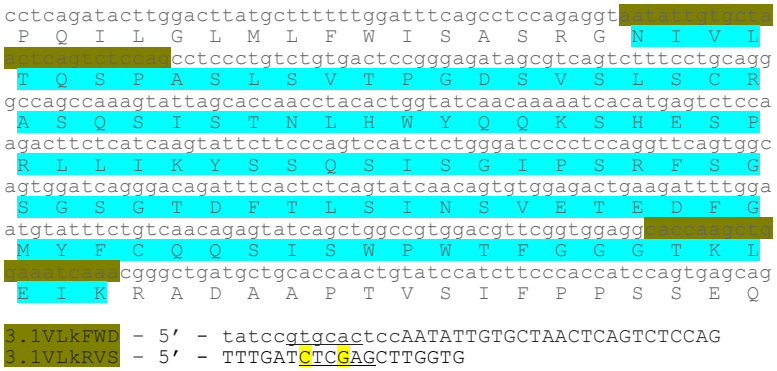

Figure 5.5 – Design of primers for insertion of the variable heavy/light regions from monoclonal antibody 3.1 into pVH/pVL plasmids. The antibody variable region amino acids are highlighted in blue. Priming regions are outlined in green. The 5` to 3` sequence of the primers is shown under the variable regions, already containing the restriction sites, in lowercase lettering. The two bases highlighted in yellow in the 3.1VLkRVS primer were altered from the original antibody sequence to produce an XhoI site, although the amino acids encoded were not changed. Sequence translation performed using ExPASy translate (http://web.expasy.org/translate/).

Using the antibody-specific primers, variable regions were amplified using Phusion high fidelity Taq polymerase. PCR reactions were as follows: Phusion HF buffer (to 1 ×), dNTP (to 0.2 mM), forward and reverse primers from Table 5.3 (to 0.5 µM), cDNA (2 µl), Phusion enzyme (0.008 U), nuclease-free water (to 20 µl). Samples were again ran on 1 % agarose and gel extracted for ligation with pVL and pVH.

The pVL and pVH plasmids were built from the backbone described in (Persic et al., 1997). The human constant regions were removed from the backbones and were substituted for canine constant regions, isotype B (Figure 5.6). The construction of these vectors was

performed by Jianguo Shi (Theodore Hupp Group, Edinburgh Cancer Research UK, University of Edinburgh).

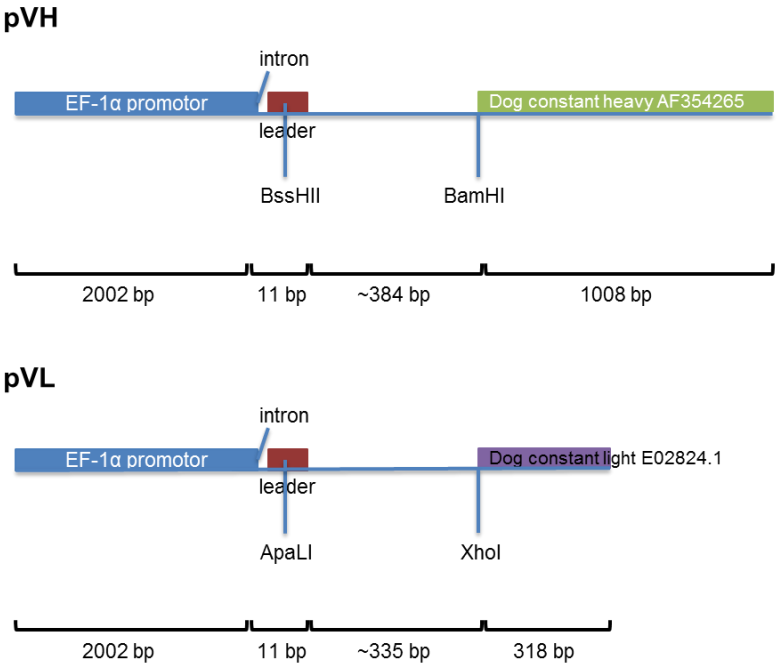

Figure 5.6 – Cloning sites of the pVH (upper) and pVL (lower) plasmids, adapted from (Persic et al., 1997). The Vh sequence of the antibody was inserted into pVH using the BssHII and BamHI restriction sites. The VL sequence of the antibody was inserted into pVL using the ApaLI and XhoI sites. The Genbank accession numbers of the canine constant sequences are shown in the boxes. The sizes of each region are indicated in base pairs (bp) (drawing not to scale). The size of the inserts was inconstant because the variable regions of different antibodies differ in length.

Plasmid digestion was as follows: pVH: plasmid (1 µg), Buffer Tango (to 2 ×), twofold excess BamHI (10 U), PauI (5 U), nuclease-free water (to 20 µl). pVL: plasmid (1 µg), Buffer R (to 1 ×), twofold excess Alw44I (10 U), XhoI (5 U), nuclease-free water (to 20 µl). The reactions were incubated for 4 h at 37°C. Enzymes were inactivated at 80°C for 20 min. Product digestion was as for the plasmids with the exception that digestion time was reduced to 1 h. Plasmids were run in 1 % agarose and were gel extracted to remove the digested product. A PCR clean-up kit (Wizard SV Gel and PCR Clean-Up System, Promega) was used for the ligands after restriction digest.

Ligation was as follows: pVH or pVL (50 ng), insert (25 ng), ligase buffer (to 1 ×), T4 DNA ligase (0.6 U), nuclease-free water (to 10 µl). This was incubated for 3 h at room

temperature and was transformed into chemocompetent Bronze Efficiency *E. coli* (Bioline). Three colonies from each construct (pVH/pVL) were purified by miniprep.

Once the antibody Vh and VL sequences had been ligated into pVH/pVL, respectively, their insertion was confirmed by sequencing the cloning site using the primer EF-1α (Table 5.3, above), which binds to the promoter upstream of that region.

5.2.3 Expression of chimeric antibodies

Chinese Hamster Ovary (CHO)-K1 cells were double-transfected by lipofection with the plasmids pVH and pVL containing the variable regions of mouse mAbs recognizing CSF-1R (Figure 5.7). The lipofection complexes were removed 4 h after transfection of the CHO-K1 cells and the medium was substituted for fresh complete DMEM. This had the aim of avoiding toxicity of Lipofectamine 2000 when the supernatant was subsequently used on the macrophages in the proliferation assays. Supernatant containing mAbs was collected 72 h after transfection.

For the production of antibodies for subsequent purification, CHO-K1 cells were grown and transfected with Ultra-Low IgG FBS-supplemented medium (Life Technologies). Alternatively, suspension CHO-K1-S cells in serum-free medium were transfected by lipofection. Suspension CHO cells (denominated as CHO-K1-S) were selected from adherent CHO-K1 cells by successive passages in CHO-S-SFM II medium (Invitrogen) in 125 ml spinner bottles (Sigma) at 125 rpm, reducing the percentage of FBS by 2 % every two passages. Once cells were completely adapted in suspension and serum-free conditions, they were transfected following previously published protocols (Rosser et al., 2005) using Lipofectamine 2000 (Invitrogen). Briefly, Lipofectamine 2000 (120 µl) and plasmids (20 µg each) were mixed in CHO-S-SFM II medium (2.5 ml) and incubated at room temperature for 20 min. Cells were counted and 2.5 x 10^7 cells were centrifuged at 100 × *g* for 10 min. Cells were resuspended in fresh medium (47.5 ml). The mixture of Lipofectamine and plasmids was added to the cells. Cells were incubated in the spinner flask for 3 d. Supernatant was collected and analysed for antibody production.

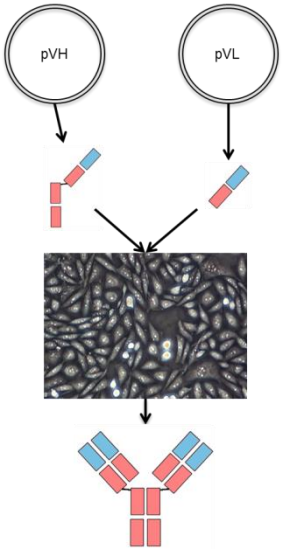

Figure 5.7 – Production strategy of recombinant chimeric canine mAbs. The mouse variable heavy and light chains were cloned into the pVH and pVL plasmids, which contained the canine constant regions. These plasmids were transfected into CHO cells for recombinant expression and assembly of the full antibody protein.

5.2.4 Selection of stable transfectants

After transfection of CHO-K1 cells, stable transfectants were selected using a combination of mycophenolic acid (20 µg/ml, Sigma) and G418 (400 µg/ml, Sigma) added to the DMEM medium. These were added every two days, when the medium was changed. Cells were kept in subconfluent densities to ensure antibiotic effectiveness. After two weeks in the selection medium, cells were subcloned by limiting dilution. Cells were trypsinized and diluted to 0.5 cells/100 µl in selection medium. Then, 100 µl were plated into each well of a 96-well plate. Cells were grown until colonies were observable. The supernatants were then collected and assessed by dot blot for antibody expression.

5.2.5 Antibody purification

To assess antibody production, the canine immunoglobulins were purified from the transfected medium using protein A and G affinity chromatography. Protein A sepharose 4B (Sigma) and Protein G sepharose 4 fast flow (GE Healthcare) were used to bind the

antibodies from serum free (CHO-S-SFM II medium) or low IgG FBS-containing media (Life Technologies). The protocol for purification is described in Chapter 7.

5.2.6 Western blot, dot blot and silver staining

Tissue culture supernatants containing the chimeric antibodies were loaded at 30 µl/well in a 10 % SDS-PAGE gel in non-reducing buffer, without heating samples. After resolving the proteins, they were transferred onto nitrocellulose membranes and probed with a 1:500 dilution of anti-dog H+L immunoglobulins (Alpha Biotechnology) in PBST + skimmed milk powder (5 %) for 2 h at room temperature. Secondary swine anti-rabbit, HRP-conjugated antibody was used in the same buffer as the primary antibody (1:1700, Dako).

The assessment of the purity of the chimeric antibodies after affinity chromatography was made by resolving the proteins using a 10 % SDS-PAGE gel with non-reducing sample buffer and staining the gel using a silver stain protocol.

5.2.7 Caninisation of the variable regions of mAb 3.1

mAb 3.1 was assessed for similarities to a group of canine sequences. Only the frameworks of the variable regions were considered (the complementarity-determining regions were not included in this analysis). Where the murine antibody sequences corresponded to the canine matrix, no changes were made to the murine antibody; where they differed, the most similar amino acid (by charge, size, polarity) found in the canine matrix was used, even if it only occurred in a single sequence of the matrix; if no similar amino acid was available, the most abundant canine residue was chosen (Gearing et al., 2013). Amino acid similarity was determined using the algorithm from Clustal Omega (www.ebi.ac.uk/Tools/msa/clustalo/).

The matrix of canine Vh cDNA sequences (112 sequences) is described in (Bao et al., 2010). The VL kappa sequences (41 sequences) were from NCBI (accession numbers EU295719.1 to EU295758 and EU305402.1). Variable light kappa chain was chosen in detriment of lambda – despite this being the most common in dogs (Arun et al., 1996) – because that corresponds to the original mouse monoclonal isotype chain, meaning that fewer amino acid substitutions were necessary to achieve caninisation.

The determination of what the framework regions consisted of was made by comparison with other murine antibodies (resource available from www.bioinf.org.uk). Comparison between canine and murine antibodies was done by aligning the sequences

using BioEdit 7.2.5 (Ibis Biosciences) and by analysing the amino acid "logo" of the canine matrix. The amino acid logos were built using the online application available at weblogo.berkley.edu. Sequence alignment between the caninised and murine sequences was done using Clustal Omega.

Three-dimensional analysis of the caninised structures was performed by modelling the antibody structures on The Rosetta Online Server That Includes Everyone (ROSIE) (http://rosie.rosettacommons.org/antibody) (Lyskov et al., 2013). The variable regions of the antibodies were submitted to the website and the relaxed structure models were used for comparisons. Comparisons between mutated and the original mAb 3.1 sequences and root-mean-square deviation of atomic positions (RMSD) measurements were made using UCSF Chimera 1.8.1 (University of California).

Gene synthesis of the caninised mAb 3.1 was performed by Eurofins Genomics.

5.2.8 Real time cell proliferation assay

The xCELLigence Real-Time Cell Analyzer (Roche) was standardized with 50 µl of DMEM medium before adding cells. Between 10^4 and 3×10^4 canine bone marrow macrophages were used. Bone marrow macrophages were grown in the presence of recombinant human CSF-1 (20 ng/ml, Invitrogen), rhIL-34 (R&D Systems, 70 ng/ml) or recombinant canine (rc) IL-4 (R&D Systems, 70 ng/ml) for at least 48 h after initial cell differentiation from bone marrow in rhCSF-1. Cells were placed in an xCelligence 16-well plate (Roche) in 100 µl of medium. The plate was scanned to measure the initial numbers of cells in each well, and then treatment was added. Forty microliters of CHO-K1 transiently transfected supernatants containing chimeric antibodies were used for each assay. Controls received similar amounts of either regular medium, of mock-transfected CHO cell medium or of hybridoma supernatant of murine mAb 3.1. Cells received CSF-1, IL-4 or IL-34 and antibody-containing supernatants *circa* every 48 h during the experiment. Cells were then maintained at the usual culture conditions for the duration of the experiment. The amount of cells attached to the bottom of each well was measured by the equipment through assessment of the interference with the electrical impedance of the sensor on the plate. Plate readings were made every 15 min.

The results of the proliferation assays were statistically evaluated by repeated-measures two-way analysis of variance (ANOVA) using the software package GraphPad Prism 5 (GraphPad Software). The graphs shown for these assays were made using the accompanying software for the xCelligence system (Acea Biosciences).

5.3 Results

5.3.1 Chimerization of the monoclonal antibodies

Anti-canine CSF-1R mAbs were selected based on their capacity to block macrophage and REM134 cancer cell proliferation (Chapter 4). Clones 3.1, 12.2, 2H1 (IgG) and 6C2 (IgM) were then selected for chimerization. The first antibody clone to be amplified by rapid amplification of cDNA ends (RACE) PCR was 1C6. This clone was therefore used to optimise the PCR technique for amplification of the antibody chains, testing two different reverse transcription protocols. The two-step protocol of reverse transcription yielded the best results and was then used for all antibodies subsequently. The variable light isotypes were not known beforehand, so when amplifying the variable light regions, primers for both the VL κ and λ chains were tested. All antibodies expressed the κ light chain. The variable heavy and light were amplified and sequenced. The products contained the full length variable region in association with the leader and constant domains (Figure 5.8).

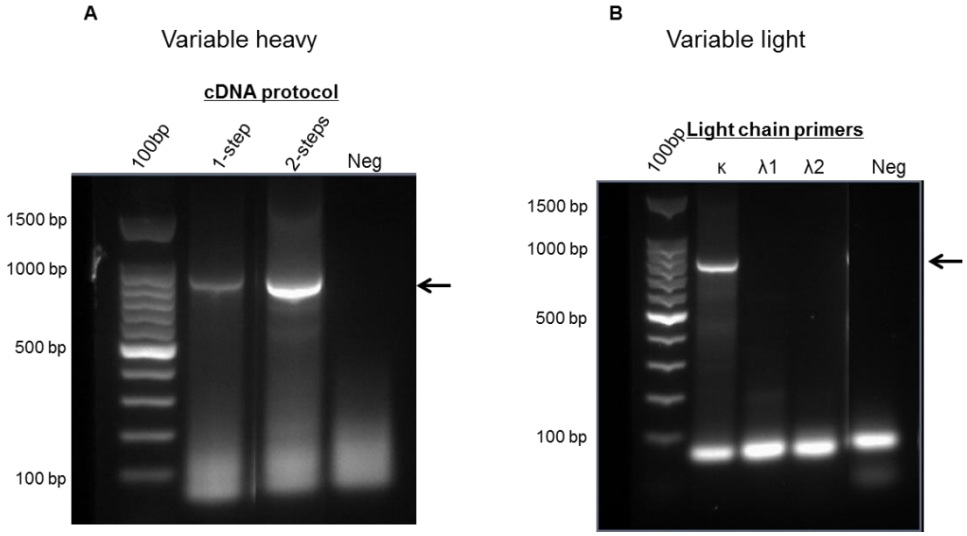

C

```
                Leader                                                  CDR 1
1c6       MAVLALLLCLVAFPGCTLSQVQL-KESGPGLVAPSQSLSITCTVSGFSLFSYD--ISWIR
1aag      -------------------EVML-VESGGGLVQPGGSLRLSCAASGFTFSRYA--MSWVR
1acy      -------------------QVKL-QESGPAVIKPSQSLSLTCIVSGFSITRTNYCWHWIR
1afv      -------------------QVQL-QQPGSVLVRPGASVKLSCKASGYTFTSSW--IHWAK
                             * **   *     *  *    *  **          *
                          CDR 2
1c6       QPPGKGLEWLGIIW---TGGGTNYNSAFMSRLIISKDNSKGQVFLKMNSLVTDDTAVYYC
1aag      QPPGKRLEWVATIS--SGGSHTFHPDSVKGRFIISRDNAKNTLYLQMNALRAEDTAIYYC
1acy      QAPGKGLEWMGRIC---YEGSIYYSPSIKSRSTISRDTSLNKFFIQLISVTNEDTAMYYC
1afv      QRPGQGLEWIGEIH--PNSGNTNYNEKFKGKATLTVDTSSSTAYVDLSSLTSEDSAVYYC
          * **  ***   * **                    *          * * ***
                   CDR 3                                Constant region
1c6       VREGLRRG--F-------------DFWGQGTTLTVSSAKTTPPSVYPLAPGSAAQTNSMV
1aag      ARPPLISLVADYAM----------DYWGAGTTVTVSS-----------------------
1acy      SRENHMYETYF-------------DVWGQGTTVTVSS-----------------------
1afv      ARWRYGSPYYF-------------DYWGQGTTLTVSS-----------------------
           *           *********** ** *** ****
```

Figure 5.8 – RACE PCR amplification and sequencing of the mAb variable regions. **(A)** Amplification of the variable heavy region. mAb 1C6 D6 shown as example. Two protocols for reverse-transcription were tested (labelled as "cDNA protocol" in the figure). From these, the variable heavy region of IgG_1 mAbs was amplified using primers MOCG12FOR and XSCTnTag. **(B)** Amplification of the variable light region. Since the subisotype was unknown, primers were used for the κ and λ regions (CKMOsp, CL1FOR or CL2FOR with XSCTnTag) after cDNA production using the two-steps approach, which was selected from the results in (A). In this case, the VL κ chain was amplified. The arrows indicate the correct product size. Neg, no template control. "100 bp" indicates the molecular weight marker (Promega). **(C)** Sequencing of the variable heavy region, after translation and alignment to three other murine antibody sequences for identification of the antibody regions, shown in different colours in the figure with the respective annotation (sequences available at www.bioinf.org.uk). Alignment performed using Clustal Omega. Asterisks indicate complete alignment at the respective positions.

For canine chimerization, the pVL and pVH plasmids were constructed and kindly gifted by Jianguo Shi (Edinburgh Cancer Research UK). The plasmids were constructed based on backbones obtained from Persic and colleagues (Persic et al., 1997). The human constant regions present on the plasmid were removed and substituted for canine constant regions. These were named pVL (containing the canine constant light lambda region) and pVH (containing the canine constant heavy region of isotype IgG B). Expression in mammalian cells was driven by a constitutive EF-1α promoter. To chimerize antibodies, the variable light and heavy domains (shown in Figure 5.8, above) were inserted into pVL and pVH, respectively (one plasmid for each of the heavy and the light chains) (Figure 5.6, above).

Both plasmids were transfected into CHO cells and the production of the full antibody structure was confirmed by western blotting, as seen by the molecular size (Figure 5.9 A). Both adherent CHO-K1 cells and suspension and serum-free adapted CHO cells (CHO-K1-S) were transfected. Production levels in CHO-K1-S after transient antibody expression and later purification by Protein G affinity were around 200 ng/10^6 cells/day. Because expression was low, only small antibody quantities could be purified using transient transfections (Figure 5.9 B). Stable transfectants of CHO-K1 were created by selection with antibiotics, but antibody production was not assessed in these.

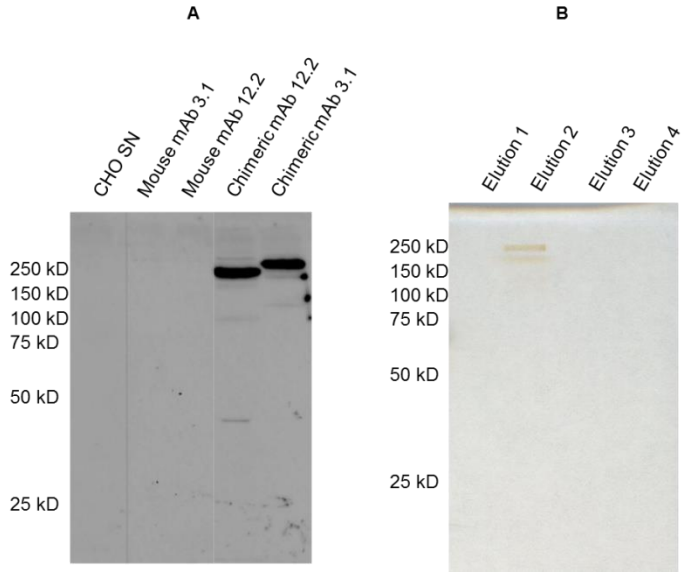

Figure 5.9 – The chimeric antibodies were correctly expressed and purified from cell culture. **(A)** Antibodies were transiently expressed by CHO-K1 cells. The presence of antibodies in supernatants of CHO-K1 cell culture (30 µl) transiently transfected with pVL/pVH containing the chimeric versions of anti-CSF-1R antibodies was confirmed by non-reducing SDS-PAGE resolution of the proteins and Western blot with anti-dog H+L Ig, HRP-conjugated (1:500, Alpha Biotechnology). The hybridoma culture supernatants containing the murine versions of the same mAbs were used as species negative controls. The mock-transfected CHO-K1 supernatant was used as an expression negative control. **(B)** Silver staining of SDS-PAGE-resolved, non-reduced samples of Protein G affinity-purified chimeric mAb, presenting the four elution steps used to remove the protein from the resin (30 µl). The proteins were detected by silver staining. Notice the low yield of antibodies.

5.3.2 Most antibodies conserved inhibitory function after chimerization

The canine chimeric antibodies were tested for their ability to block bone marrow-derived macrophage proliferation. The results demonstrate that the chimeric antibodies 3.1, 2H1 and 6C2 preserved the macrophage-blocking function from the parent mouse hybridomas (Figure 5.10).

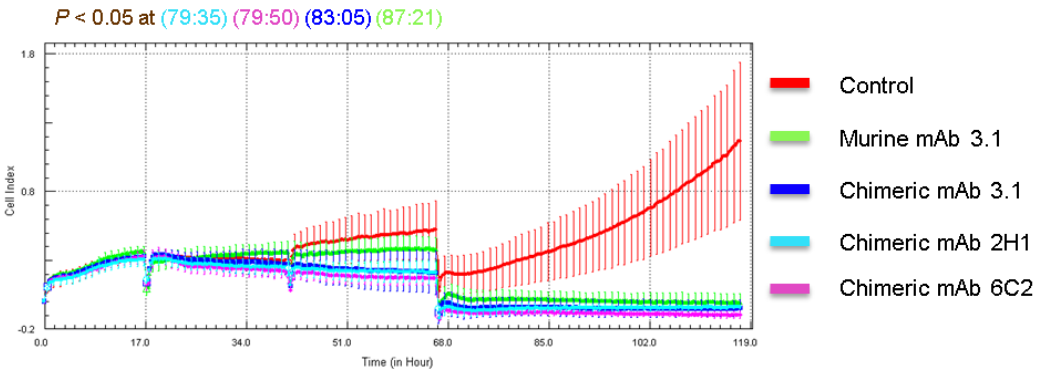

Figure 5.10 – Chimerization did not affect the efficacy of mAbs 3.1, 2H1 and 6C2 in inhibiting the proliferation of canine bone marrow-derived macrophages. Cells (in 100 µl medium) were grown with rhCSF-1 (20 ng/ml, Invitrogen) and treated with CHO-K1 transfected supernatant containing chimeric mAbs against CSF-1R or the hybridoma supernatant containing murine mAb 3.1, for comparison (40 µl). All antibodies shown reduced BMDM proliferation. Control received mock-transfected medium (40 µl). Data was collected every 15 min. Cell index (y-axis) is correlated to cell number. The abrupt drops in the graphs indicate when the plate was removed from the xCelligence equipment for change of medium/treatment. Results are shown as mean of 3 wells ± SD for each time point. Results analysed by repeated measures two-way ANOVA with a Bonferroni post-test comparing all groups to the control. The coloured values at the top of the figure indicate the time in hours when treatments were different from Control.

In contrast to the other chimeric antibodies tested, mAb 12.2 (originally a mouse IgG_{2b} isotype) lost its inhibitory activity against macrophages after chimerization. Two proliferation assays were conducted using this chimerized mAb. In both it showed no inhibition of macrophage proliferation. In the second trial, chimeric mAb 12.2 was compared to chimeric mAb 3.1 (which was shown to be effective in Figure 5.10, above), and while mAb 3.1 reduced macrophage proliferation, mAb 12.2 did not (Figure 5.11). As shown above in Figure 5.9, transfection of CHO-K1 cells with the plasmids for mAb 12.2 lead to the secretion of fully formed antibodies.

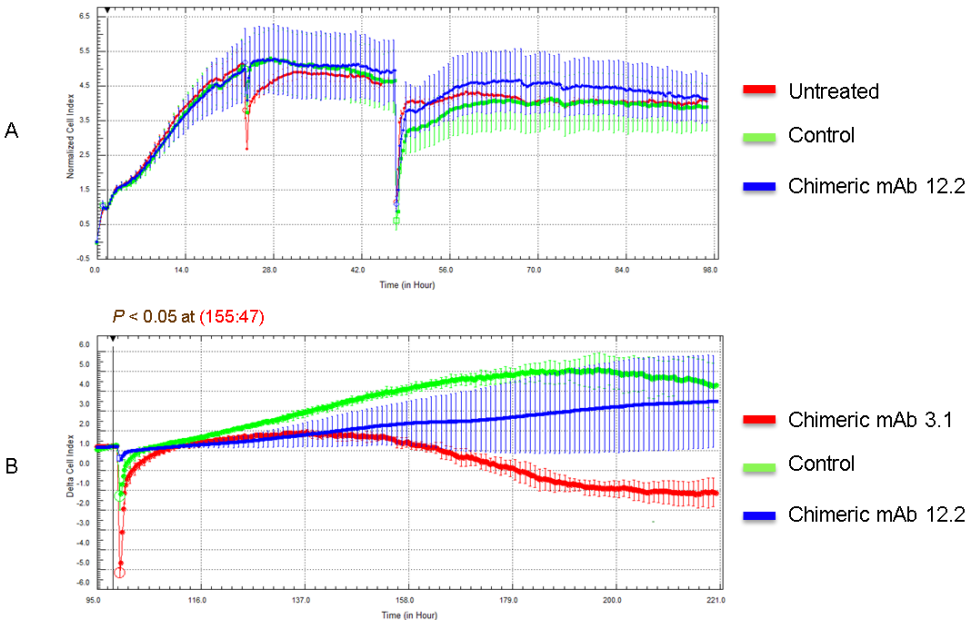

Figure 5.11 – Chimerization altered the efficacy of mAb 12.2 in inhibiting the proliferation of canine bone marrow-derived macrophages. **(A)** Cells (in 100 µl medium) were grown with rhCSF-1 (20 ng/ml, Invitrogen) and treated with CHO-K1 transfected supernatant containing chimeric mAb 12.2 against CSF-1R (40 µl). Control received mock-transfected medium (40 µl). Results are shown as mean of 3 wells ± SD for each time point. **(B)** Cells were grown with CSF-1 and treated with CHO-K1 transfected supernatant containing chimeric mAbs 12.2 or 3.1 against CSF-1R compared to the supernatant of mock-transfected cells. Results are shown as mean of 8 wells ± SD for each time point (4 wells for the mock control). Data was collected every 15 min. The vertical black line at the beginning of the graphs indicates the point where the antibodies were added. The data were also normalized at that point. Cell index (y-axis) is correlated to cell number. The abrupt drops in the graphs indicate when the plate was removed from the xCelligence equipment for change of medium/treatment. The coloured value at the top of the figure indicates the time in hours when treatment was different from control.

The capacity of the chimeric mAbs in blocking IL-34-induced proliferation was also tested. This cytokine is a ligand of CSF-1R (Chihara et al., 2010). The chimeric antibodies showed a trend of reducing the proliferation of the canine cells in the presence of IL-34 (Figure 5.12), although the differences were less pronounced than when CSF-1 was used (Figure 5.10, above). In the direct comparison of all groups against the control group, only mAb 2H1 showed statistically significant differences.

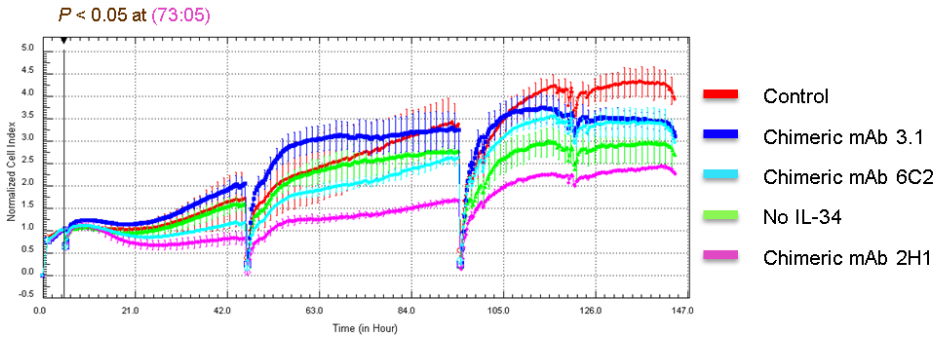

Figure 5.12 – Chimeric mAbs affected IL-34-conditioned macrophage proliferation. Cells (in 100 µl medium) were grown with rhIL-34 (70 ng/ml, R&D Systems) and treated with CHO-K1 transfected supernatant containing chimeric mAbs against CSF-1R (40 µl). One group did not receive IL-34. Although all mAbs showed a trend of reduction in proliferation, only mAb 2H1 had a significant effect. The control received an equivalent volume of mock-transfected medium. Data was collected every 15 min. The vertical black line around 3 h indicates the point where the antibodies were added. The curves were also normalized at that point. The y-axis indicates cell index (correlated to cell number). The abrupt drops in the graphs indicate when the plate was removed from the xCelligence equipment for change of medium/treatment. Results are shown as mean of 3 wells ± SD for each time point. Results analysed by repeated measures two-way ANOVA with a Bonferroni post-test comparing all groups to the control. The coloured value at the top of the figure indicates the time in hours when treatment was different from control.

To assess the effect of the antibodies on macrophages stimulated by a CSF-1R-independent growth factor (Jenkins et al., 2013), IL-4-conditioned macrophages were treated with the chimeric mAbs. BMDMs were differentiated from the bone marrow precursors in the presence of CSF-1, as had been done for the cells used in the previous proliferation assays. However, for the present analysis, BMDM were further conditioned with IL-4 and without CSF-1 for 48 h. No reduction of macrophage viability by the addition of mAbs was seen in the presence of IL-4. On the contrary, chimeric mAb 3.1 induced higher cell proliferation compared to control (Figure 5.13).

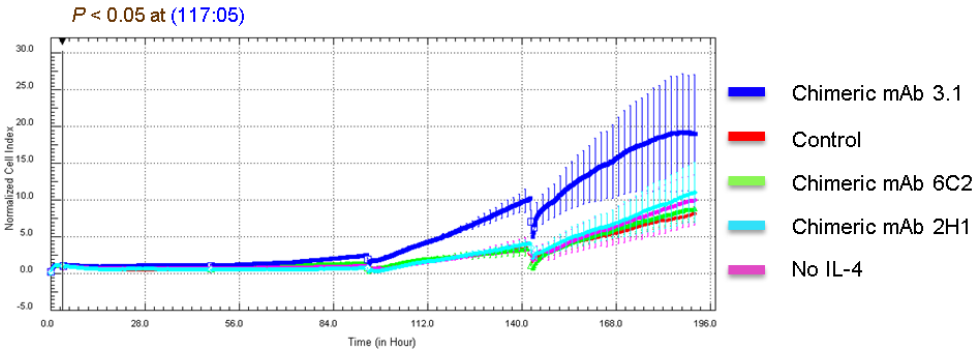

Figure 5.13 – The chimerized mAbs did not reduce IL-4-conditioned BMDM proliferation. Cells (in 100 µl medium) were treated with CHO-K1 transfected supernatant containing chimeric mAbs against CSF-1R (40 µl) in the presence or absence of recombinant canine IL-4 (70 ng/ml, R&D Systems). The control received mock-transfected medium (40 µl). Data was collected every 15 min. The vertical black line around 3 h indicates the point where the antibodies were added. The curves were also normalized at that point. The y-axis indicates cell index (correlated to cell number). The abrupt drops in the graphs indicate when the plate was removed from the xCelligence equipment for change of medium/treatment. Results are shown as mean of 3 wells ± SD for each time point. Results analysed by repeated measures two-way ANOVA with a Bonferroni post-test comparing all groups to the control. The coloured value at the top of the figure indicates the time in hours when treatment was different from control.

5.3.3 Caninisation of the variable regions of mAb 3.1

To achieve full speciation of the monoclonal antibody structure, amino acid residues from the variable framework regions were changed to allow for optimum similarity compared to canine antibodies, following a protocol described previously (Gearing et al., 2013). As a part of this protocol, a matrix of canine antibody cDNA was compiled and the most common amino acids were determined by drawing a "logo" of the primary structure of the framework regions of the antibodies (Figure 5.14). The complimentary determining regions (CDRs) were not included in this analysis and were not changed in an attempt to avoid losing antibody affinity.

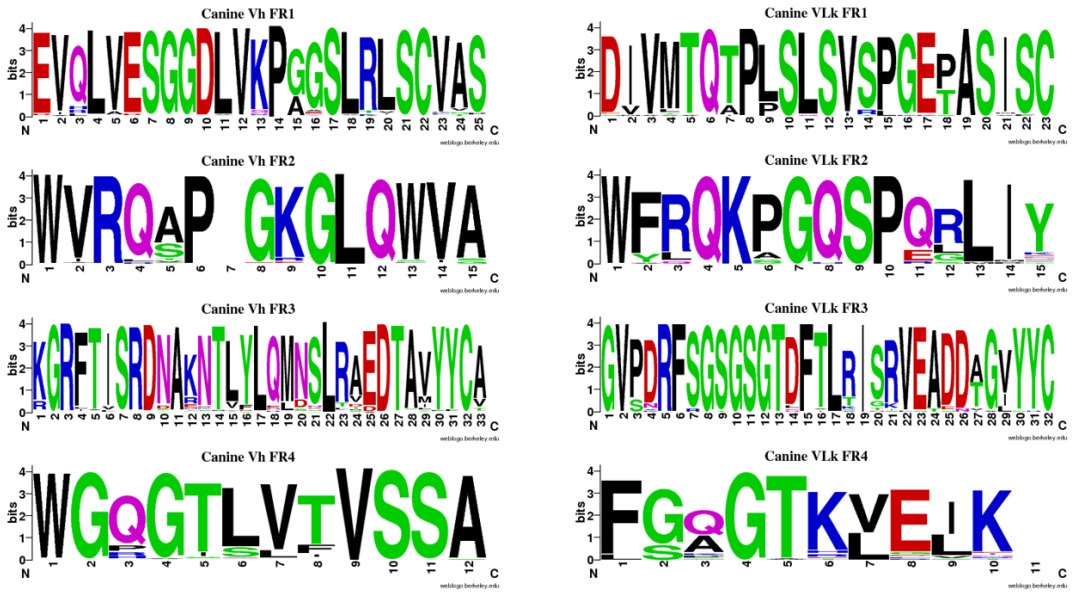

Figure 5.14 – Logo representation of the amino acids of a series of canine framework regions of Vh and VLκ antibody chains. For this, 112 Vh and 41 VLκ sequences were used to compose the logos (NCBI). Each framework region is represented separately, in a total of 8 regions (4 Vh and 4 VLκ). The most common amino acid in each position is shown as a letter of larger height, the size being proportional to the representativeness of that amino acid in that position. The maximum "bit" value for each position (y-axis) is 4.3. The x-axis indicates the residue number of each amino acid starting from 1 for each individual framework region (does not follow any antibody numbering scheme). The colours represent the physicochemical properties of the amino acids: polar amino acids (G,S,T,Y,C,Q,N) are green, basic (K,R,H) are blue, acidic (D,E) are red and hydrophobic (A,V,L,I,P,W,F,M) amino acids are black.

The murine and canine framework sequences were compared, and where the sequences did not match, amino acid substitutions were made in the murine sequence. In general, where changes had to be made, the amino acid residue in the canine matrix with most similar properties to the murine sequence was used. If no conserved substitutions could be made, the most frequent canine amino acid was used (based on Figure 5.14, above). For the Vh, 6 amino acid changes were made, of which 3 are conservative; for the VL, 14 amino acid changes were made, 8 of which are conservative. The caninised sequence that resulted from this process is shown in Figure 5.15.

```
Caninized3.1Vh      EVRLVESGGDLVKPGGSLKLSCAVSGFSFSTY
Natural3.1Vh        EVKLVESGGDLVKPGGSLKLSCAVSGFSFSTY
                    **:****************************

Caninized3.1Vh      AMSWVRQTPEKGLDWVASISSGGSMYHLDSVKGRFTISRDNARNALYLQMNSLRSEDTAV
Natural3.1Vh        AMSWVRQTPEKRLEWVASISSGGSMYHLDSVKGRFTISRDNARNILYLQMRSLRSEDTAR
                    *********** *:***************************** *****.********

Caninized3.1Vh      YYCARAIHYYGRYVMDYWGQGTSVTVSS
Natural3.1Vh        YYCARAIHYYGRYVMDYWGQGTSVTVSS
                    ****************************

Caninized3.1VLk      DIVLTQTPLSLSVTPGESASISCRASQSISTNLHWYQQKSGQSPRLLIKY
Natural3.1Vh         NIVLTQSPASLSVTPGDSVSLSCRASQSISTNLHWYQQKSHESPRLLIKY
                     :*****:* *******:*.*:******************** :********

Caninized3.1VLk      SSQSISGVPDRFSGSGSGTDFTLSINSVETEDAGVYYCQQSISWPWTFGQGTKLEIK
Natural3.1Vh         SSQSISGIPSRFSGSGSGTDFTLSINSVETEDFGMYFCQQSISWPWTFGGGTKLEIK
                     *******:*.********************** *:*:************ *******
```

Figure 5.15 – Caninised variable regions of mAb3.1 compared to the natural sequence. An asterisk below the alignment indicates a position where no amino acid changes were made. A ":" (colon) indicates amino acid substitutions between groups of strongly similar properties, as per the algorithm of Clustal Omega. A "."(period) indicates a conservative amino acid change with weak similar properties.

To assess the probability of the alterations made to the primary structure of mAb 3.1 changing antibody affinity, the 3-dimensional structures of the variable regions were analysed. A verification was made as to whether the amino acid substitutions affected the positioning of the complementarity-determining regions (CDRs); none of the changes affected CDR structure, as root-mean-square deviation of atomic positions (RMSD) was less than 1 for all six CDRs, when analysed pair-by-pair between the canine and murine structures. This is a measurement of atomic deviation between two structures, and is considered to be insignificant when lower than 1 (Zhang et al., 2013). A single amino acid change to the variable heavy framework region 2 led to a major conformation change (RMSD > 1) but because this structure is placed opposite to the binding sites, this did not affect the overall layout of the CDRs (Figure 5.16).

Since the caninisation process seemed not to affect the structure of the CDRs, the caninised antibody variable regions were synthesized and were inserted into pVL/pVH. This fully caninised version of the antibody 3.1 has yet to be tested in functional assays.

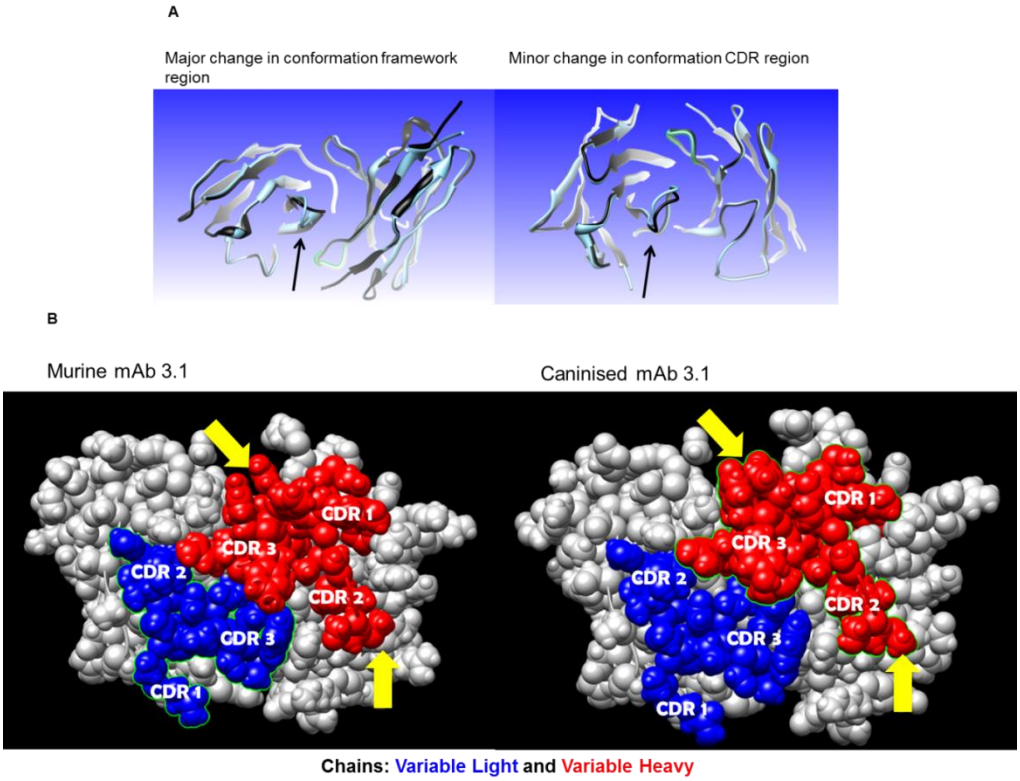

Figure 5.16 – Caninisation did not affect the CDR regions of mAb 3.1. Three-dimensional analysis of conformation changes after the caninisation process of the variable regions of mAb 3.1. **(A)** Homology model of the variable regions. Left: Conformation change to the framework regions, indicated by the arrow, caused by a single amino acid substitution. The antibody binding sites are shown in grey in the second plane of the image. Original antibody (mouse) is shown in blue; caninised is shown in black. Where the line traces differ there is change in conformation. Right: Variations of CDR loops of the variable heavy region (shown on the first plane of the image) after caninisation, as exemplified by the position indicated by the arrow. **(B)** Space-filling model of the variable regions. The CDRs are identified in the figure. Changes to the structural conformation are exemplified in the positions indicated by the arrows.

5.4 Discussion

Biological drugs have been described as the new frontier of drug development for a range of diseases including auto-immune syndromes, neurological conditions and cancer (Singh et al., 2011). Inside this class of drugs, monoclonal antibodies have become increasingly important in the clinical setting in recent years, with special relevance for cancer (Ecker et al., 2014). Although several antibodies exist for human clinical use, very few have been developed for use in dogs (Acharya et al., 2015; Jeglum, 2009; Scott et al.,

2012). Carry-over of drugs developed for humans to the veterinary practice, which has been common with other therapeutics, is not usually feasible for biologics; the efficacy of monoclonals is dependent not only on the specificity of the variable regions but also on the interaction of the immune system of the host with the antibody structure. The antibody framework is important for its antigenicity, pharmacokinetics and effector roles, and these effects are generally species-specific (Scott et al., 2012).

Improvements in the biodistribution and effector mechanisms of mAbs have been identified as crucial factors for achieving the full potential of monoclonal antibody therapies. Both factors are greatly dependent on the Fc regions of antibodies (Yan et al., 2009). Reducing the antigenicity of biological drugs is the single most relevant step to improve the pharmacokinetic properties and therefore the efficacy of these therapeutics (Lobo et al., 2004). For monoclonal antibodies, in many circumstances chimerization is sufficient to allow for clinical use of the mAb. Rituximab is an example of this. It is a human chimeric antibody; it was the first anti-cancer monoclonal licensed by the United States Food and Drug Administration (FDA) and one of the highest grossing anti-cancer drugs, which is still in the market after 17 years (Ziegelbauer and Light, 2008).

In this chapter it was demonstrated that the monoclonal antibodies of interest were successfully sequenced and cloned into a canine constant region, therefore generating canine chimeric monoclonals. The production of the chimeric antibodies was also performed effectively in adherent and suspension CHO-K1 cells, leading to the expression of fully formed molecules, composed of two heavy and two light chains joined by disulphide bridges, and probably containing other posttranslational modifications such as glycosylation, as shown by the apparent size on western blots (Braren et al., 2007). The absence of isolated heavy or light chains in non-reducing western blot indicates that all the antibody secreted by the cells are assembled into fully formed molecules (Dodev et al., 2014). However, expression of the heavy and light chains in separate plasmids and the consequent need for co-transfection with both plasmids may have been one of the factors limiting protein yield by the transiently transfected cells.

The level of antibody production after CHO-K1 cell transfection was low (200ng/10^6 cells/day), as assessed after affinity purification of the antibodies. This is in accordance with the original paper that described the plasmids pVH and pVL (Persic et al., 1997). Although this was assessed in the transient batch-transfected cells, instead of the stable transfectants, this laboratory scale of production still represents a hurdle for the progression of the antibodies to clinical trials. Improvements in the vector (promoter region, for instance), the use of a single vector containing both heavy and light chains, and improvements in the

process of production (cell type, media, suspension *vs.* attached cells) can significantly promote expression levels of antibodies (Jäger et al., 2013), and will be necessary as a next step in this project.

Canine IgG isotype B was used in the present work as the constant region into which the murine variable regions were inserted. Canine IgG isotypes are named from A to D following their relative quantities within the body (Tang et al., 2001). Isotype B is capable of strongly binding CD64 and of activating the complement cascade, therefore showing the greatest similarities to the human IgG_1 (Bergeron et al., 2014; Gearing et al., 2013). The circulation half-life of canine IgG B chimeric antibodies is of 14 days (Rue et al., 2015). The constant light chain used for chimerization was lambda. Contrarily to mouse and human antibodies, the lambda chain is the most common light constant chain in the dog (91 % of all antibodies in circulation) (Arun et al., 1996).

The activity of all antibodies was maintained after chimerization, with the exception of mAb 12.2, which lost the ability to decrease macrophage proliferation. Among the chimerized antibodies, this was the only one that originated from an IgG_{2b} mouse mAb.

Mouse antibodies are capable of inducing effector functions on canine macrophages through Fc receptors. The murine isotype subclasses IgG_{2a} and IgG_3 can promote antibody-dependent cell cytotoxicity (ADCC) having dog macrophages as effectors (Rosales et al., 1988). Murine IgG_{2b}, however, cannot bind to canine FcγRI or FcγRIII (Bergeron et al., 2014). When the antibodies were chimerized using the canine IgG B as the recipient constant region, all mAbs should have become able to bind to canine Fc receptors. Chimerization may have affected the binding of mAb 12.2 because of FcR affinity to canine IgG B (Bergeron et al., 2014). Just as Fc receptor affinity has been shown to increase CSF-1R binding for a previously published mAb (Haegel et al., 2013), it is possible that Fc binding of the chimeric 12.2 obstructed the coupling site of this mAb on the CSF-1R. Acting in a "cis" conformation may have impeded correct binding of this antibody (see Figure 4.31, Chapter 4). This could be further clarified by testing this chimeric antibody using cells transfected with CSF-1R, such as Ba/F3 cells. These cells can be induced to survive in the presence of CSF-1 after being transfected with the receptor (Gow et al., 2012). If Fc binding was the cause of the disruption of the activity of mAb 12.2 after chimerization, it should still be active against the Ba/F3 cells, which do not express Fc receptors.

It is also possible that the loss of activity of mAb 12.2 was due to the reduction in antibody concentration after chimerization. Its inhibitory function may have been dependent on high antibody concentrations; the chimerized antibodies were present in much lower concentrations in the supernatants than the murine mAbs. However, the murine mAb 12.2

was the most effective antibody at low concentrations in reducing BMDM proliferation (Figure 4.24, Chapter 4). Since the concentration of other chimeric mAbs was sufficient to inhibit BMDM proliferation, antibody concentration is unlikely to have been the most prominent factor affecting chimeric mAb 12.2.

Given that the CSF-1R is able to bind both CSF-1 and IL-34 (Chihara et al., 2010), it was expected that the antibodies would also be able to block CSF-1R signalling following IL-34 stimulation. One of the three chimeric antibodies tested with IL-34-macrophages was raised against the dimerization domain of the receptor (mAb 3.1), and should block CSF-1R dimerization irrespective of the ligand. Stable dimerization of two CSF-1R monomers after ligand binding is essential for signal transduction (Li and Stanley, 1991). All the tested mAbs seemed to reduce IL-34-conditioned macrophage proliferation, although the antibodies did not fully block cell survival as was seen with CSF-1-conditioned cells. Indeed, statistical significance against the control group only occurred for mAb 2H1. IL-34 and CSF-1 have mostly overlapping signals in macrophages, but IL-34 seems to induce a more mild cellular activation of some pathways when compared to CSF-1 (Barve et al., 2013). The results found here following IL-34 activation may be due to lower stimulation of the control group rather than reduced antibody effect. If the proliferative signal in the control group was driving slow cellular proliferation, it would take longer for treated and untreated cells to differ.

When CSF-1, IL-34 or CSF-1R is blocked *in vivo*, not all macrophage activity is hindered. Inflammatory responses are still seen after CSF-1R signalling blockade (MacDonald et al., 2010). Indeed, even in the CSF-1 knockout, the *op/op* mouse, some macrophages remain, such as in the lymphoid tissues or in the skin (Stanley et al., 1997). Local self-renewal of macrophages is at least in some cases dependent on IL-4. Because IL-4 acts on its own specific receptor (IL-4R) and its function is independent of CSF-1R (Sieweke and Allen, 2013), the anti-CSF1R mAbs being studied here were not expected to block IL-4-associated macrophage proliferation. This cytokine drives macrophages into what is described as an anti-inflammatory phenotype that is typical of the response against helminthic infection. In these situations, as the levels of IL-4 increase, this cytokine takes over from CSF-1 in maintaining macrophage proliferation. It not only drives tissue macrophage survival but may also have an effect on monocyte-derived macrophages. Although IL-4 has little capacity to induce macrophage proliferation *in vitro*, it is still able to affect the cellular phenotype (Jenkins et al., 2013; Sieweke and Allen, 2013; te Velde et al., 1992). IL-4 treatment reduces CSF-1R expression by macrophages, reducing the need for

CSF-1 by individual cells (Jenkins et al., 2013), and is known to block CSF-1 dependent proliferation (Arpa et al., 2009).

Therefore, the results of the present work confirmed that hypothesis, and the use of chimeric anti-CSF-1R had no impact on the survival of IL-4 conditioned macrophages. This also supports the demonstration of the specificity of the antibodies. It could be expected that if the effect of the antibodies on the macrophages were due to off-target binding, these effects would also be present when the mAbs were used against IL-4-conditioned macrophages. However, in human macrophages IL-4 decreases the expression of the FcγRI (te Velde et al., 1992). If the activity of the chimeric mAbs was mediated through these receptors, then it would be expected that the mAbs would have no effect on IL-4-conditioned macrophages. Therefore, it cannot be ruled out that IL-4 conditioning of macrophages reduced Fc receptor expression, and, with it, the effect of the mAbs through Fc receptors. Conversely, if all activity of the mAbs was mediated through FcγRI, chimeric mAb 12.2 also would have inhibited the proliferation of CSF-1-conditioned macrophages, which did not occur.

No literature could be found to provide explanation as to the apparent proliferative effect of mAb 3.1 on IL-4-conditioned macrophages. All antibodies tested possessed the same Fc fraction and IL-4 decreases FcγRI expression (te Velde et al., 1992), therefore the differences cannot have derived from FcR-binding. All antibodies were also expressed at approximately similar concentrations (as assessed by western blot), and therefore differences in effect related to varying chimeric antibody concentrations are unlikely. Whether mAb 3.1 non-specifically activated the IL-4 receptor or other receptors to drive proliferation was not tested.

The recent trend in the development of monoclonal antibodies is towards full speciation of these biologicals (Modjtahedi et al., 2012). The mouse monoclonal antibody 3.1 was selected for full caninisation based on its cellular staining and macrophage proliferation inhibition capacities (Chapter 4). However, it is known that speciation of the variable regions can alter antibody affinity since the loop conformation given by the framework regions, which are altered during the speciation process, are relevant towards the antibody binding characteristics (Kettleborough et al., 1991). The issue of loss of affinity is usually only circumvented by maintaining or returning to a structure which has to be similar to the original murine antibody, therefore not really reducing the overall immunogenicity of the protein (Clark, 2000). The caninisation technique used here has an advantage over other speciation techniques, such as CDR grafting, in that only some framework amino acids are altered from the original sequence, therefore reducing the likelihood of lowering the

antibody affinity (Gearing et al., 2013; Safdari et al., 2013). The process used in the present study is similar to that of "resurfacing", previously used for the humanization of antibodies. Both methods alter only some of the amino acids in the framework region to achieve speciation, but in the technique of resurfacing only those residues close to the surface of the molecule are considered for alterations. This is because it is believed that the amino acid residues turned toward the centre of the antibody cannot be reached by the immune system of the host and are therefore not immunogenic (Safdari et al., 2013). Since resurfacing is usually done using the germline antibody sequences as models for choosing which amino acids should be substituted, it tends to require more alterations than the process used here, where the cDNA of fully functional circulating antibodies are used as the frames of reference (Gearing et al., 2013).

The method used here for speciation had the drawback that it did not consider the Vernier zones in the process of changing the amino acids. The Vernier zones are areas within the variable framework regions of the antibodies which are relevant for antibody affinity, although these areas do not contact the antigen. The Vernier zones are important for the maintenance of the structural conformation of the variable region, supporting the CDRs in the optimal configuration for binding. Therefore, antibody speciation strategies that do not contemplate the Vernier zones risk reducing or losing the binding affinity not by altering the contact areas themselves, but by changes in the conformation of the entire variable region (Makabe et al., 2008; Safdari et al., 2013).

Speciation in itself does not guarantee low anti-antibody responses, and cautious and selective speciation procedures such as the one used in the present work are probably even less likely to fully prevent host immune reactions (Clark, 2000; Hwang and Foote, 2005). The main effect of full antibody speciation seems to be in reducing "marked" anti-antibody responses, while chimeric and fully humanized are similar in the amount of "tolerable" and "negligible" anti-antibody responses elicited (Hwang and Foote, 2005). It is also recognized that even fully speciated protein sequences may be immunogenic due to several factors, such as differences in the normal glycosylation pattern of the protein (Singh et al., 2012; van Meer et al., 2013).

The value of full speciation has also been disputed since the idiotype will, by definition, always be variable and therefore susceptible to the formation of anti-idiotype antibodies (Figure 5.17).

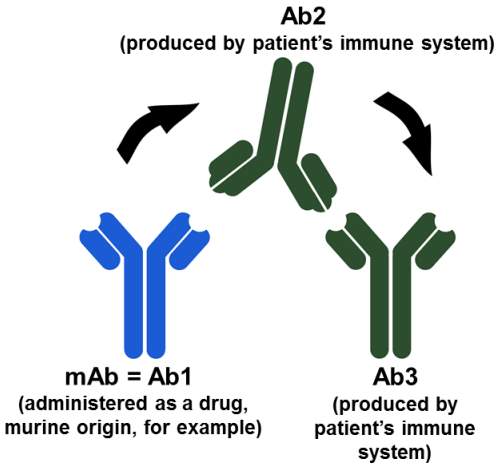

Figure 5.17 – The anti-idiotype cascade. The recognition of the mAb by the host immune system leads to the production of antibodies (Ab2) against the variable region of the mAb; the variable regions of Ab2 are the mirrored image of the mAb variable regions. Ab2 also serves as an antigen for the production of a third antibody (Ab3), whose variable region is the mirrored image of the variable region of Ab2. Therefore, the original mAb and Ab3 are equal with regard to their variable regions.

It is known, for instance, that some fully humanized antibodies can still elicit significant anti-mAb responses (Clark, 2000; Waldmann, 2014). It can be also argued that the humanization process may not necessarily produce antibodies that resemble those that are naturally in the circulation. Humanization is commonly done using human germline sequences as templates for the modification of the murine sequences. These may not correctly represent the most common amino acid composition found in circulating antibodies, since many modifications occur from the germline sequence, such as somatic hypermutation, which increase the variability of the antibodies. The use of germline sequences as template may create regions in the humanized antibody which have an amino acid repertoire bias that is different to that of circulating antibodies (Ackerman et al., 2011; Briney et al., 2012). Some researchers suggest, however, that immunogenicity in humanized mAbs arises only against the CDRs but not the framework regions, implicating that, whereas humanization is successful in reducing anti-antibody responses against the framework regions, the presence of anti-idiotypes cannot be fully avoided unless laborious alterations of the CDRs are performed (Harding et al., 2010).

However, even fully human antibodies (not only humanized but from human origin) can induce anti-antibody responses, illustrating the unavoidable possibility of anti-idiotype immune reactions. Adalimumab is such an example. It is a human antibody (thus containing

100 % of human sequences) against TNF-α that shows marked human-anti human antibody responses in 89 % of the patients (Berdougo et al., 2011).

To circumvent the problem of anti-idiotype immune responses, one alternative would be the induction of immune tolerance against the antibody. It has been argued that the clustering of several mAb molecules on their binding site is a strong inducer of anti-antibody responses. Monomeric forms of the mAbs are reportedly tolerogenic, and it has been proposed that a pre-treatment administration of a mAb with low binding affinity – therefore preventing the formation of immune complexes – should induce immune tolerance towards the high-affinity binding version of the same mAb, when it is administered later (Gilliland et al., 1999; Waldmann, 2014).

5.5 Conclusion

Three monoclonal antibodies were successfully chimerized and maintained the same activity as the parent hybridomas in inhibiting macrophage proliferation. Because of possible specificity issues with these antibodies, discussed in Chapter 4, further work is necessary before they can be used in the clinical setting.

However, the chimerization process assisted in understanding the mode of action of the monoclonal antibodies tested. The comparison of the results of the murine and the chimerized mAb 12.2 contributed in the comprehension of the role of Fc receptor binding in macrophage proliferation, for instance. It is possible that the activity of the chimeric mAb 12.2 was hindered by Fc receptor binding after chimerization. This is a relevant finding for the discussion of the activity of murine mAbs in Chapter 4.

Finally, the development and application of the technology of chimerization and caninisation may prove useful in future projects. Some of the difficulties within this protocol of chimeric antibody production, such as low expression levels, have been acknowledged and can be appropriately addressed when these biologicals are produced for clinical use in the future.

Chapter 6

Phage display screening of a semi-synthetic antibody library based on mAb 3.1

Highlights

- mAb 3.1, described in Chapter 4, contained only a few mutations from the germline sequence, indicating that the antibody did not undergo profound affinity maturation.
- Two complementarity-determining regions (CDRs) of mAb 3.1 were mutated by PCR using degenerate primers, in an attempt to alter the antibody binding characteristics.
- This library of mutated variations of mAb 3.1 was screened by phage display and clones with lower non-specific binding were selected.
- The technique of CDR mutation proved successful in the generation of antibody clones with different binding characteristics. Shuffling of the mutated VL and Vh chains will further increase variability, possibly increasing affinity.

Abstract

Although mAb 3.1 was shown to bind to macrophages by immunostaining and to inhibit CSF-1R-dependent proliferation, it demonstrated low binding to the native form of the CSF-1R. When compared to mouse immunoglobulin germline sequences, mAb 3.1 presented only a few mutations at the complementarity determining regions (CDRs), which indicate a low level of affinity maturation. Therefore, two CDRs within the sequence of mAb 3.1 were mutated with the intention of identifying new clones with improved binding characteristics when compared to the original antibody. Two semi-synthetic antibody libraries were created by PCR site-directed mutagenesis of the CDRs of mAb 3.1. Each library contained either a mutated version of the variable light chain or of the variable heavy chain of mAb 3.1. These libraries were then screened by phage display for binding to the extracellular region of canine CSF-1R. Several clones were identified which successfully bound to CSF-1R with reduced interaction to unrelated proteins, which represents an increment in relation to the

characteristics of mAb 3.1. Several clones were further expressed as soluble proteins in the absence of phage for assessment of their characteristics. In conclusion, by introducing small mutations within the CDRs, it was possible to create antibody variants with improved binding characteristics when compared to the parental mAb 3.1.

6.1 Introduction

Inhibition of tumour-associated macrophages (TAMs) is a potential therapeutic pathway against cancers (Król et al., 2011). Among the possible strategies to reduce the influence of TAMs within tumours is the inhibition of CSF-1R, a crucial receptor for macrophage survival and polarization into the TAM phenotype (Pyonteck et al., 2013). CSF-1R inhibitory antibodies have been described in the literature which exert anti-proliferative activity over macrophages at concentrations as low as 0.1 – 1 μg/ml (Haegel et al., 2013). In Chapter 4, antibodies were described which were also able to inhibit macrophage proliferation, although at concentrations tens of times higher than those referred in the literature. Of these antibodies, monoclonal antibody (mAb) 3.1 was identified as one of the most promising anti-canine CSF-1R clones, since it was able to bind to macrophages by immunostaining and to inhibit cellular proliferation. However, this mAb also showed cross-reactivity with other antigens by ELISA, and seemed unable to immunostain cells expressing low levels of CSF-1R.

Therefore, it was theorized that, by generating and screening mutant variations of mAb 3.1, it would be possible to identify clones with improved binding properties. The initial step in this process was the creation of variants of mAb 3.1.

6.1.1 The generation of antibody variability

The natural production of antibodies by the immune system is dependent on a range of events that lead to variations of the germline antibody sequences. In the bone marrow, the antibody variable (V), joining (J) and diversity (D) genes undergo rearrangements in an initial step to create variability. At the junctional points of rearrangements, nucleotide insertions and deletions also occur, adding diversification to the germline variable sequences. In the secondary immune organs, these genes are altered by somatic hypermutation followed by positive selection of the high affinity-binding antibody clones through the process of affinity maturation (Teng and Papavasiliou, 2007). Hypermutation occurs preferentially at specific positions of the antibody variable regions. These positions are appropriately named

hypervariable regions or complementarity-determining regions (CDRs). The parts of the variable region which are less mutated are named the framework regions (Figure 6.1). The alterations induced by hypermutation amount to 1 – 2 mutations per cellular generation, which is much higher than the average rate in other cells. High variability within the CDRs is important because these are the points of contact between the antibody and the epitopes on the antigens (Mirsky et al., 2015).

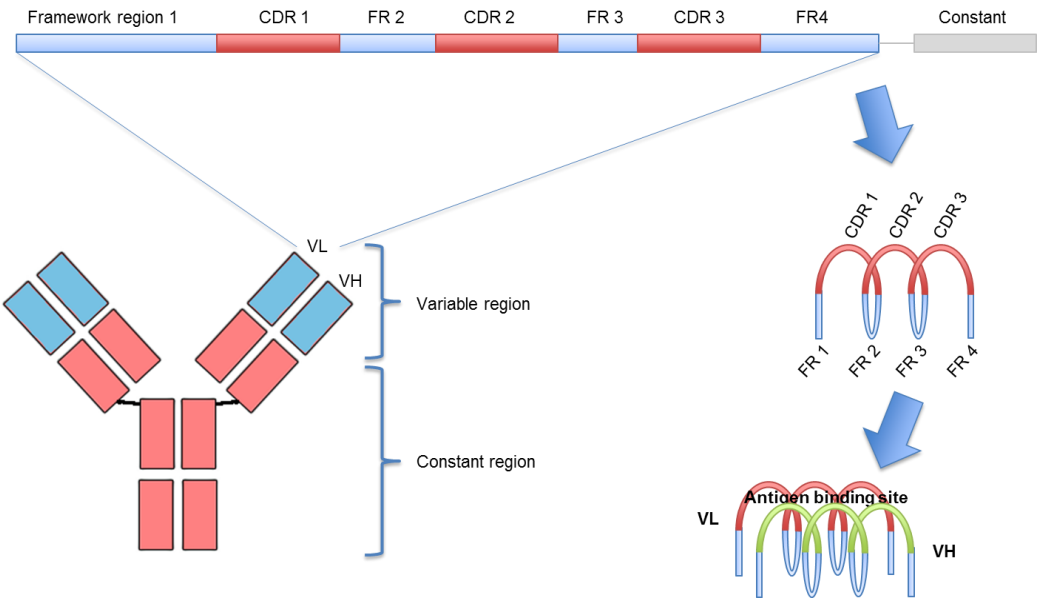

Figure 6.1 – The structure of the antibody variable regions. There are two variable regions in each antibody "arm", termed heavy (VH) and light (VL) variable regions. Within the mature variable region genes, diversity is created through hypermutation of the CDRs. When the protein is expressed and folded, the CDRs form the points of contact of the antibody with the epitope. The CDRs of the VL and VH chains must combine to form the antigen binding site. Therefore, each antibody arm will have 6 CDRs which will determine binding affinity and specificity.

6.1.2 Semi-synthetic libraries

Semi-synthetic antibody libraries are composed of mutational derivations from an original antibody clone. Since the original clone is usually resultant of mouse immunizations (a "natural" antibody) and the mutations are purposefully generated in the laboratory ("synthetic", therefore), these libraries are called semi-synthetic. By mutating the antibody variable regions, mimicking somatic hypermutation, it is possible to create new antibodies that have either improved or reduced binding properties in relation to the original clone. If

the mutations in the antibody variable regions are extensive enough, antibodies with affinity for entirely different antigens can be found, therefore circumventing the necessity for new mouse immunizations for production of antibodies against these targets (Chen and Sidhu, 2014).

As is also the case with the natural process of generating antibody variations, the site where mutations are inserted is extremely relevant to the creation of semi-synthetic libraries. Methods that create random alterations to the entire variable region will equally change the framework regions (FR) and the CDRs. These methods include error-prone PCR and mutator *E. coli* strains. However, changes to the FR are less likely to generate large improvements to the antibody affinity, therefore restricting their relevance in finding improved antibody clones (Gram et al., 1992). Random mutations spread throughout the variable regions require larger antibody libraries to be screened in order to find useful clones. Large library sizes represent a technical hurdle in the antibody display technologies, since they require improved transformation/transfection efficiencies of the host organism and more intensive selection processes to enrich the best clones (Ponsel et al., 2011).

Therefore, *in vitro* affinity alterations of antibodies have more commonly been directed to the CDRs (Bradbury et al., 2011). Since alterations of the CDRs are much more efficient in producing active antibody conformations than changes to the framework regions, reduced library sizes are adequate to find clones of interest. Few mutations in a single CDR are sufficient to completely alter the binding affinity of an antibody (Gilliland et al., 1999). Since each CDR is crucial to the binding characteristics of an antibody, semi-synthetic libraries have been generated by altering one or just a few CDRs. For example, by mutating exclusively the CDR3 of the variable heavy chain, it is possible to generate a library that is able to bind to a large number of unrelated antigens (Mahon et al., 2013).

6.1.3 Antibody display

After generating a semi-synthetic or another form of an antibody library, the challenge rests in finding which of the clones contained within the library are suitable for the desired purposes. The technology of antibody display has the purpose of selecting specific monoclonal antibodies within a combinatorial library. Although it is a time-consuming method, it poses some benefits in comparison to the hybridoma approach for antibody production. It permits selection from synthetic libraries without the need for animal immunization, easily allows negative selection of unwanted binders, does not require laborious tissue culture work and is easily accessible for molecular biology alterations of the

antibody structure, such as chimerization and affinity maturation (Frenzel et al., 2013; Hammers and Stanley, 2014; Thie et al., 2008). These advantages of the technique have been translated into increased contribution of the display methods for newly approved clinical antibodies. Phage display, for instance, has been used in the development of the best-selling monoclonal antibody adalimumab (Humira), used for autoimmune conditions (King, 2013; Thie et al., 2008).

Several antibody display platforms are available, such as mammalian cell and yeast display; of these, phage display is the most widespread. It consists of the expression of scFv antibody fractions on the surface of a bacteriophage virus, commonly on the pIII coat protein (Figure 6.2). This is accomplished by introducing into host bacteria a phagemid containing the scFv fraction coupled to the pIII-coding gene (gIII). When these bacteria are infected with a phage (called helper phage), the virus packages the phagemid-coded pIII protein containing the scFv, forming a virion containing the antibody fraction on its surface.

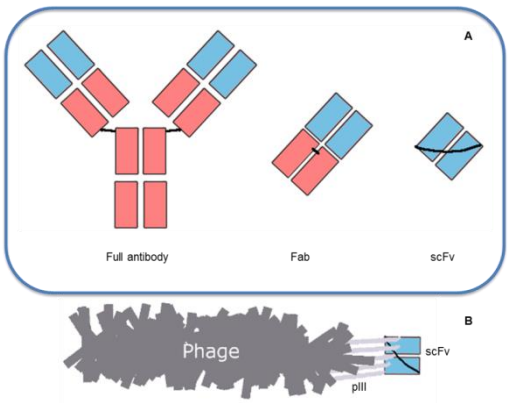

Figure 6.2 – Antibody fractions and the phage display system. **(A)** Three antibody fractions. The black lines represent linkers between the chains. **(B)** Schematic representation of the bacteriophage virus and the displayed scFv fraction on the pIII protein. Structures not to scale.

Since each bacteriophage will contain a scFv copy on its surface and the corresponding phagemid, the best scFv can then be selected and enriched from the original library, which can potentially contain billions of different clones. Selection is done by a process called biopanning, where specific phages are enriched from the original pool by selecting for binding affinity to an immobilized antigen. This is repeated for several rounds and the enriched pool is examined for its binding capacity (in an ELISA, for instance). If

positive, individual clones are picked, the phagemid are sequenced and the scFv is tested in a monoclonal ELISA and in further desired assays (Figure 6.3).

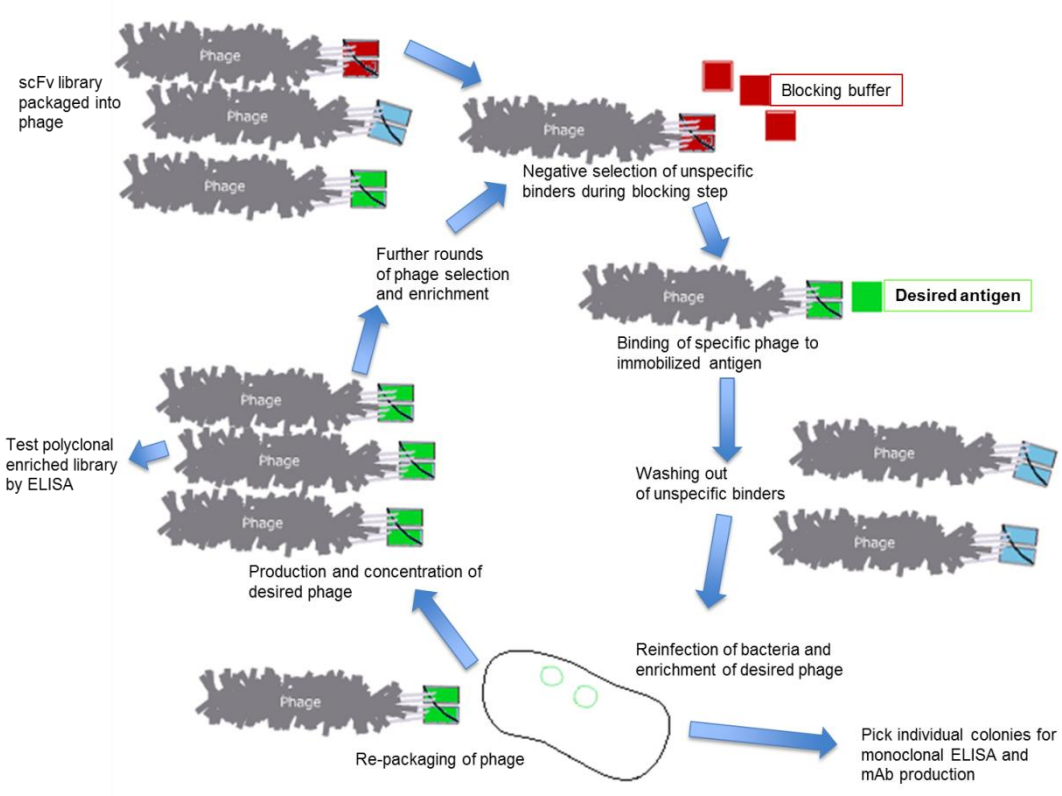

Figure 6.3 – Phage display biopanning for selection of scFv. The phagemid library is packaged by helper phages. The newly formed phage particles express the scFv with the pIII protein, and are selected and enriched based on binding affinity to a specific antigen.

The goal in this chapter was to generate and test a library of semi-synthetic antibodies based on mAb 3.1, a monoclonal antibody raised against the canine CSF-1R. As demonstrated in Chapter 4, despite initial promising results, mAb 3.1 showed specificity issues and weak affinity for the correctly folded CSF-1R. Since mAb 3.1 was raised using a misfolded bacterially produced antigen, it did not react against CSF-1R protein produced by mammalian cells, which displayed the correct conformation. To create novel antibodies starting from mAb 3.1 as a template, two CDRs from this antibody were altered, namely CDR2 from the heavy chain and CDR3 from the light chain. These mutated versions were tested in parallel in two separate libraries. Phage display was used to screen the two libraries for binders to the native form of CSF-1R. Antibodies with improved binding properties in

relation to mAb 3.1 could be isolated. These mutated variants bound to CSF-1R and had reduced cross-reactivity with unrelated proteins (Figure 6.4).

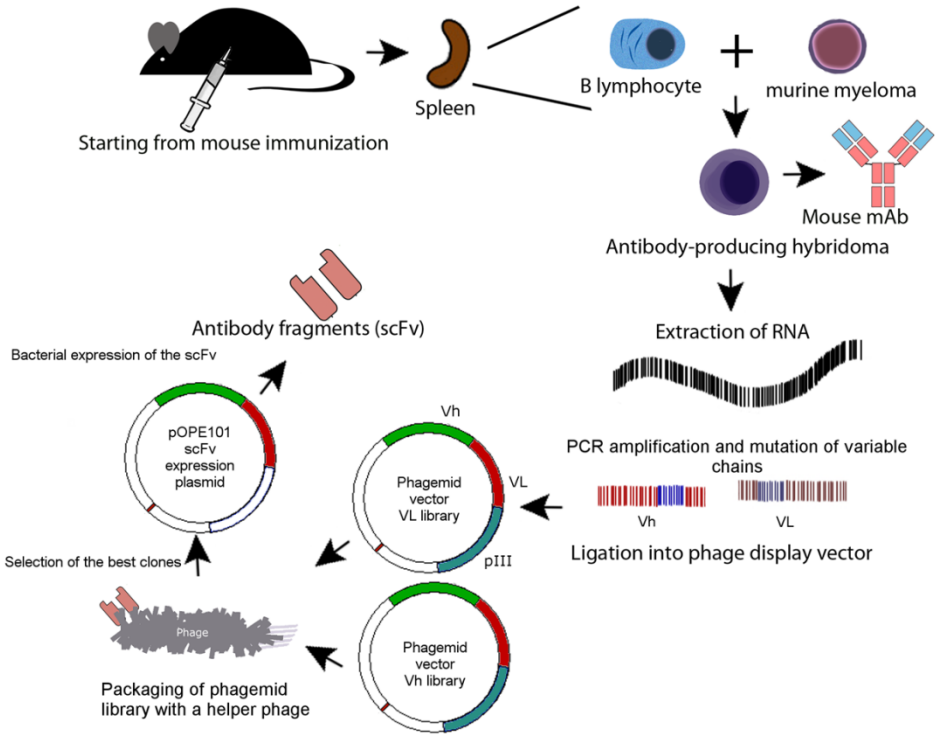

Figure 6.4 – Overview of the method used in the present chapter. mAb 3.1 was generated by hybridoma, as described in Chapter 7. The variable regions of mAb 3.1 were mutated and two libraries were constructed by insertion into phagemid vectors. The mutated libraries were then screened by phage display. The best candidates were expressed in the pOPE101 plasmid in *E. coli*, independently from the phage.

6.2 Materials and Methods

Basic methodological descriptions and brands not stated here are presented in Chapter 2. QIAprep Spin Miniprep Kit and QIAquick Gel Extraction Kit are supplied by Qiagen. Phusion polymerase kits and restriction digest kits are supplied by Thermo Scientific. dNTPs, DNA ligase kits and Wizard SV Gel and PCR Clean-Up System are

supplied by Promega. The protocol for the construction of the semi-synthetic antibodies and library construction was obtained from Martineau, 2010.

6.2.1 Comparison to germline

The level of antibody hypermutation was estimated by comparing the sequence of mAb 3.1 to murine germline genes. This was performed on IMGT/V-QUEST (http://www.imgt.org/IMGT_vquest/share/textes/) using the nucleotide sequence of mAb 3.1 (Giudicelli et al., 2004).

6.2.2 Site-directed CDR mutagenesis

CDR mutagenesis was performed by PCR using specific oligonucleotides. Two CDRs of mAb 3.1 were mutated, CDR3 of the variable light chain and CDR2 of the variable heavy chain. The sequence of mAb 3.1 was determined in Chapter 5. Mutagenesis primers were designed to bind to the regions around the aforementioned CDRs. Within the CDRs the mutagenesis primers contained areas of degenerate sequences that coded for all possible amino acids and one stop codon (amber codon, TAG). The primers contained restriction sites for insertion into the plasmid pSEX81 (Progen).

The PCR strategy for the production of the mutated regions of mAb 3.1 is outlined in Figure 6.5. The primers are shown in Table 6.1.

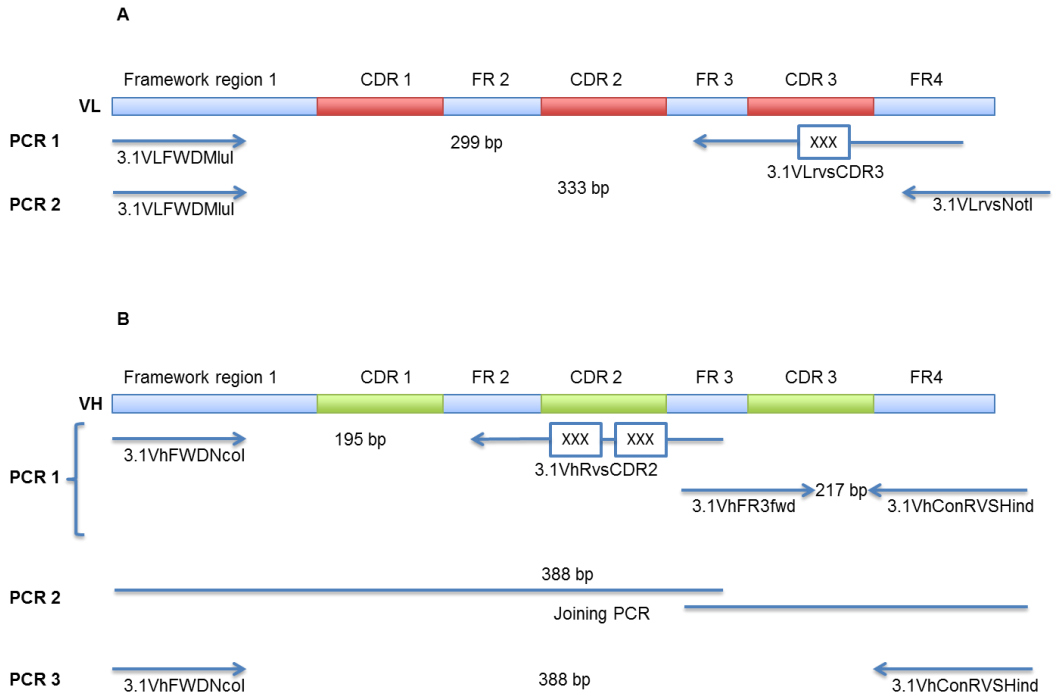

Figure 6.5 – PCR strategy for the mutagenesis of mAb 3.1. **(A)** Mutagenesis strategy for the variable light region. **(B)** Mutagenesis strategy for the variable heavy region. The arrows represent primers, as respectively named. The PCR product sizes are indicated in base pairs (bp). The figure is not to scale. The boxes within primers 3.1VLrvsCDR3 and 3.1VhRvsCDR2 show the points where mutations were inserted in each region. Several PCR steps were required for the full assembly of each of the variable regions, shown as PCR 1, PCR 2 and PCR 3. The lines in PCR 2 of the VH indicate the products from PCR 1.

Table 6.1 – Primers for site-directed mutagenesis of mAb 3.1. The degenerate sites for inserting mutations into the CDRs are highlighted. Primer 3.1VhFWDNcoI contained 2 bp after the NcoI site to maintain the Vh sequence in frame. Primers shown as 5` to 3`.

Vh primers	
3.1VhFWDNcoI	ATAACCATGGCAGAAGTGAAGCTGGTGGAGTC
3.1VhRvsCDR2	GCCCTTCACACTGTCTAAATGATAMNNMNNACCMNNMNNMNNAATGGATGCGACCCACTC
3.1VhConRVSHind	TATAAAGCTTCGTGGTGGAGGCGGATC
3.1VhFR3fwd	TATCATTTAGACAGTGTGAAGGGC
VL primers	
3.1VLFWDMluI	ATTAACGCGTAAATATTGTGCTAACTCAGTCTCCAGCCTC
3.1VLrvsNotI	ATATGCGGCCGCTTTTATCTCGAGCTTGGTGCCTCCACCGAACGTCCACGGC
3.1VLrvsCDR3	CCACCGAACGTCCACGGCCAMNNMNNMNNCTGTTGACAGAAATACATTCCAAAATCTTCAGTCTC

PCR was performed using the following protocols (Table 6.2). Schematic representations of the reactions are shown in Figure 6.5, above.

Table 6.2 – Protocol for the PCR-directed mutagenesis of CDRs. Primers are shown in Table 6.1 and in Figure 6.5.

Vh chain	VL chain
PCR 1	
Reaction: 5 × HF buffer (to 1 ×); dNTP mix (to 0.2 mM); forward and reverse primers (to 0.5 µM); template (0.2 µl of pVH containing mAb 3.1, Chapter 5); Phusion enzyme (0.4 U); nuclease-free water (to 20 µl). Thermal cycling protocol: VH chain: 98°C for 30 sec, 35 × [98°C for 10 sec, 72°C for 15 sec, 72°C for 10 sec], 72°C for 10 min.	Reaction: 5 × HF buffer (to 1 ×); dNTP mix (to 0.2 mM); forward and reverse primers (to 0.5 µM); template (0.2 µl of pVL plasmid containing mAb 3.1, Chapter 5); Phusion enzyme (0.4 U); nuclease-free water (to 20 µl). Thermal cycling protocol: 98°C for 30 sec, 35 × [98°C for 10 sec, 65°C for 15 sec, 72°C for 10 sec], 72°C for 10 min.
The products from PCR 1 were run on 1.5 % agarose and were gel extracted.	
PCR 2	
Reaction: Gel extracted 5`-fraction of Vh chain (200 ng); gel extracted 3`-fraction of Vh chain (200 ng); 5 × HF buffer (to 1 ×); dNTP (to 0.2 mM); Phusion enzyme (0.4 U), nuclease-free water (to 20 µl). Thermal cycling protocol: 98°C for 30 sec, 20 × [98°C for 10 sec, 65°C for 20 sec, 72°C for 15 sec], 72°C for 5 min.	Reaction: 5 × HF buffer (to 1 ×); dNTP mix (to 0.2 mM); forward and reverse primers (to 0.5 µM); template (0.1 µl of gel purified PCR 1 product); Phusion enzyme (0.8 U); nuclease-free water (to 40 µl). Thermal cycling protocol: 98°C for 30 sec, 35 × [98°C for 10 sec, 72°C for 25 sec], 72°C for 10 min.
The products from PCR 2 were run on 1 % agarose and were gel extracted.	
PCR 3 (Vh only). The assembled Vh region was further amplified with a third PCR.	
Reaction: HF buffer (to 1 ×); dNTP (to 0.2 mM); forward and reverse primers (to 0.5 µM); gel purified assembled Vh (1 µl); Phusion enzyme (0.8 U); nuclease-free water (to 40 µl). Thermal cycling protocol: 98°C for 30 sec, 35 × [98°C for 10 sec, 65°C for 15 sec, 72°C for 25 sec], 72°C for 10 min.	
The products from PCR 3 were run on 1 % agarose and were gel extracted.	

6.2.3 Amplification of non-mutated Vh and VL chains of mAb 3.1 with restriction sites for pSEX81

The non-mutated mAb 3.1 Vh and VL chains were also amplified using the primers above to append the restriction sites at the ends of the products, allowing the insertion of the non-mutated chains into pSEX81 (Progen).

PCR for non-mutated variable chains of mAb 3.1: 5 × HF buffer (to 1 ×); dNTP (to 0.2 mM); primers 3.1VHfwdNcoI/3.1VHConRvsHind for Vh region or 3.1VLfwdMluI/3.1VLrvsNotI for VL region (to 0.5 µM); template (3.1 pVH/pVL plasmids, 0.1 µl, Chapter 5); Phusion enzyme (0.8 U); nuclease-free water (to 40 µl).

Cycling temperature for non-mutated variable chain PCR: 98°C for 30 sec, 35 × [98°C for 10 sec, 65°C for 15 sec [Vh] or 72°C for 15 sec [VL], 72°C for 25 sec], 72°C for 7 min. The products from non-mutated mAb 3.1 regions were run on a 1.5 % agarose gel and were gel extracted using a commercial kit.

6.2.4 Restriction digests of pSEX81 and ligation products

VL (or pSEX81 to receive VL): DNA (1 µg); MluI (20 U); NotI (10 U); Buffer O (to 1 ×), nuclease-free water (to 20 µl).

Vh (or pSEX81 to receive Vh): DNA (1 µg); NcoI (20 U); HindIII (10 U); Buffer R (to 1 ×), nuclease-free water (to 20 µl).

pSEX81 was digested for 4 h at 37°C. The inserts Vh and VL were digested for 1 h at 37°C. Enzymes were inactivated at 80°C for 20 min. The digested fragments were removed from the insert using PCR clean-up kit. The fragments were removed from pSEX81 by running the digestion in a 0.8 % gel and gel-extracting the plasmid using a gel extraction kit.

6.2.5 Ligation of non-mutated VL/Vh mAb 3.1 and pSEX81

Reaction was as follows: pSEX81 vector (50 ng); digested VL/Vh inserts (10.75 ng); ligase buffer (to 1 ×); T4 ligase (1 U); nuclease-free water (to 10 µl). Reaction was incubated overnight at 4°C. Next day it was inactivated at 65°C for 15 min. In preparation for electroporation, the ligation had salts removed using a PCR clean-up kit. The reaction was eluted in 15 µl of nuclease-free water.

6.2.6 Transformation of XL-1blue *E. coli* with pSEX81 + non-mutated Vh/VL

pSEX81 containing non-mutated VL or Vh were added (5 µl) to 100 µl of electrocompetent XL-1blue. Bacteria were transformed with a 2500 V pulse (CellJect Basic Electroporator) using a 2 mm-gap cuvette (VWR). Cells were incubated with 900 µl of SOC

medium for 1 h at 37°C and plated on LB agar plates containing ampicillin. Plates were incubated overnight at 37°C.

6.2.7 Construction of the mutated libraries

pSEX81 containing the non-mutated Vh/VL sequences of mAb 3.1 were digested as above (increasing concentrations tenfold). The plasmids that contained non-mutated Vh were digested with MluI and NotI to receive the mutated VL. The digested plasmids were gel-purified in a 0.8 % agarose gel.

The mutated Vh/VL inserts were also digested as above (increasing concentrations fivefold). The digested fragments were removed from the inserts with a PCR clean-up kit.

Plasmids and inserts were ligated: Digested pSEX81 containing non-mutated Vh/VL (5 µg); digested insert (1 µg); ligase buffer (to 1 ×), ligase (50 U); nuclease-free water (to 500 µl). The ligation reaction was incubated overnight at 4°C and 2 h at room temperature. It was inactivated at 65°C for 10 min. Salts were removed using a PCR clean-up kit, eluting the products in 80 µl of nuclease-free water.

The ligation was then transformed into XL-1blue. Freshly made electrocompetent cells (300 µl) received the purified ligation products (20 µl) and were electroporated. This process was repeated until all ligation was used (4 times in total). The transformed bacteria were recovered with SOC medium. The bacteria were removed from the cuvette with 1 ml of SOC, and were placed into an Erlenmeyer flask containing 25 ml of SOC. This was incubated for 1 h at 37°C, shaking at 200 rpm. Dilutions of the library were plated for quantification (10^{-2} to 10^{-5}) on LB plates containing glucose (1 %) and carbenicillin. The four Erlenmeyer flasks for each library were pooled and centrifuged at 5000 × *g* for 10 min at 8°C. The supernatant was discarded and the pellet was resuspended in 4 ml SOC. This was then placed on 15 LB plates containing glucose (1 %) and carbenicillin. Plates were incubated overnight at 37°C.

The following day, the contents from each plate was scraped using scalpel blades and 2 ml of 2xTY/glycerol (7.5 ml of 2xTY + 2.5 ml of glycerol (40 %)). The contents of all plates were pooled. To calculate the bacterial density, a 1:200 dilution was measured at OD_{600nm} using a S2100 spectrophotometer (Biowave). An $OD_{600nm} = 1 = 5.10^8$ cell/ml. The size of the library was then calculated based on the results of the plated dilutions of the library.

6.2.8 Sequencing of library products

Colonies from each of the Vh/VL mutated libraries were picked from the plates using for titration of the library size and sent for sequencing. Primers were 3.1VHfwdNcoI (for pSEX81 + mutated VL) or 3.1VLrvsNotI (for pSEX81 + mutated Vh). The composition of each of the libraries is illustrated in Figure 6.6.

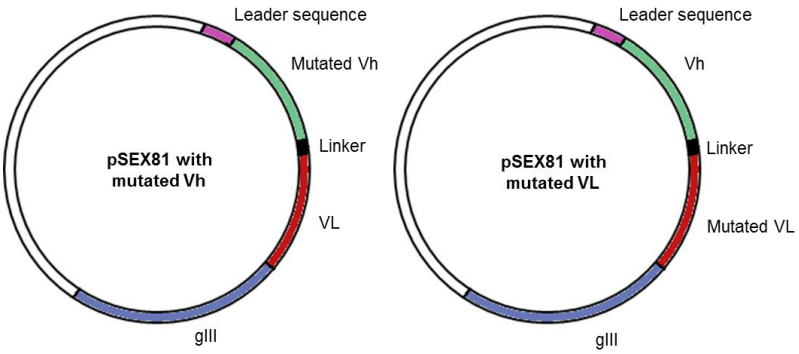

Figure 6.6 – Phagemid architecture of the two semi-synthetic libraries. Libraries were constructed using mAb 3.1 as a backbone, containing either a VL or Vh region with inserted mutations. The library was inserted into pSEX81, which expresses the scFv antibody with a leader sequence for periplasmic localization, a linker between the Vh and VL regions and the coupled phage gIII, which expresses a viral coat protein.

6.2.9 Phage display – preparation of helper phage

Protocols described below were obtained from Kontermann, 2010 and Clackson and Lowman, 2004. Top agar was melted and cooled down to 50^{o}C. Commercially available M13KO7 helper phage (New England Biolabs) was serially diluted in 2xTY medium (from 10^{-8} to 10^{-12}). The dilutions were mixed with 100 µl of log-phase XL-1blue (OD_{600nm} = 0.5) and incubated at 37^{o}C for 15 min. Bacteria and phage were mixed with 3 ml of top agar. The mixture was plated on 2xTY agar plates and incubated overnight at 37^{o}C. A single small plaque of bacteriophage was picked by touching with a pipette tip. The tip was placed inside a tube with XL-1blue at an OD_{600nm} = 0.5 in 3 ml of 2xTY. The tube was incubated at 37^{o}C for 3 h. The grown plaque was added to 500 ml of 2xTY. The flask was incubated for 1 h shaking at 37^{o}C, and then kanamycin was added. The flask was incubated overnight shaking at 200 rpm and at 37^{o}C. The culture was centrifuged at 4000 × *g* for 30 min at room

temperature. The supernatant, containing the helper phage, was filtered through a 0.45 µm filter (Nalgene) using a 50 ml syringe (Becton Dickinson). Phage was titrated using the same dilutions and protocol as was done with the commercial M13KO7. The helper phage solution was stored at 4°C.

6.2.10 Phage display – packaging the phage library

XL-1blue bacteria containing the pSEX81 + mutated antibodies were added to 2 l culture flasks containing 250 ml of 2xTY with ampicillin and glucose (2 %). For the mutated variable heavy library, 10^{10} bacteria were added to 500 ml.
The culture was grown at 37°C with shaking (250 rpm) to an OD_{600nm} = 0.5 (approximately 2 h). The helper phage was added to the bacteria in a ratio of 20:1, following the formula below.

$$Helper\ phage\ added\ (ml) = 20 \times \frac{0.5\ OD\ (2.5 \times 10^8\ bacteria) \times 250\ ml}{Helper\ phage\ titer\ (\frac{phage}{ml})}$$

The mutated VL library was packaged using the M13KO7 helper phage, expanded as explained in section 6.2.9, above. The Vh was packaged separately with two different helper phages, the M13KO7 (prepared as shown above) and Hyperphage, obtained commercially (Progen).

After adding the helper phage, the culture was incubated at 37°C for 30 min standing to allow the helper phage to infect the cells, followed by 30 min shaking (200 rpm). To assess the efficiency of helper phage infection, 1 µl was removed from each flask and diluted in 1 ml of 2xTY. One and 10 µl of the dilution were plated on 2xTY agar plates containing either ampicillin + glucose (1 %) or kanamycin + glucose. The proportion of kanamycin resistant clones should be at least 10 % of the number of ampicillin resistant clones.

The bacterial cultures were centrifuged at 1520 × g. The supernatant was removed; the pellet was resuspended in 500 ml of 2xTY with ampicillin and kanamycin. This was grown in two 2 l flasks overnight at 30°C, shaking. The following day the bacteria were centrifuged at 14000 × g for 30 min. The supernatant was added to a new flask. PEG solution (polyethyleneglycol 6000 (20 %), NaCl (2.5 M)) was added to the supernatant, which was incubated on ice for 1 h. The phage precipitates were removed from the solution by centrifuging at 3000 × g for 15 min at 4°C. The supernatant was discarded. The pellet was

dried by centrifuging again for 30 sec. The remaining liquid was pipetted out and the phage pellet was resuspended in 5 ml of PBS. The phage was stored at – 80^{o}C until used.

6.2.11 Phage display – phage library biopanning

For the identification of the most suitable clones from the phage libraries, these were screened against the extracellular region of the canine CSF-1R. Immunotubes (Greiner) were coated overnight at 4^{o}C with 0.5 ml of PBS containing 25 µg (rounds 1 and 2 of panning) or 12.5 µg (further rounds) of the CSF-1R protein. A fresh colony of XL-1blue was grown overnight in 5 ml of 2xTY with tetracycline. The following day, the immunotube was rinsed thrice with PBS and blocked with PBS + milk (2 %) for 2 h at room temperature. During this time, the packaged phage library or the outputs from previous rounds of selection were blocked for 30 min at room temperature with 1 ml of PBS + milk. After blocking, the immunotube was emptied and the pre-blocked phage was added. This was incubated for 2 h at room temperature with occasional shaking.

At this point, 12 ml of 2xTY with tetracycline were inoculated with 100 µl of overnight XL-1blue culture. The culture was grown to OD_{600nm} = 0.5 shaking (200 rpm) at 37^{o}C. In rounds 1 and 2 of panning, the immunotubes were rinsed 10 × with PBS + Tween 20 (0.1 %) followed by 10 × with PBS only. In the further rounds of panning, washings were increased to 20 × for each buffer. The tubes were blotted after each rinse to remove excess washing buffer.

The bound viruses were eluted either by trypsin elution or direct infection. Trypsin elution was done by adding 0.5 ml of trypsin (10 mg/ml diluted in PBS, Gibco) for 15 min at room temperature followed by 10 × pipetting up and down. Direct infection of the bacteria was done by adding 2 ml of the log-phase XL-1blue in the immunotube for 30 min at room temperature.

The eluted phage was then added to 10 ml of the log-phase XL-1blue. The flasks were incubated for 30 min at 37^{o}C standing and then 30 min shaking (200 rpm). Serial tenfold dilutions of the cultures were made in 2xTY and 100 µl of each was plated in 2xTY agar plates with ampicillin and glucose (1 %). Plates were incubated overnight at 37^{o}C. These were used to determine the number of eluted phage. This was the "phage output". The remaining culture was spun at 2000 × *g* for 10 min. The pellet was resuspended in 0.5 ml of 2xTY and was plated onto 6 × 2xTY plates with ampicillin and glucose. These plates were named "stock plates" and were incubated at 30^{o}C.

The following day 1 ml of 2xTY was added to each of the stock plates, and these were scraped with L-scrapers. The contents were transferred to a 15 ml tube. A glycerol stock was made from 1 ml of the bacteria. Approximately 2 – 3 ml of the bacteria was added to 50 ml of 2xTY with ampicillin and 2 % glucose to get a starting OD_{600nm} = 0.1. This was incubated at 37°C shaking (200 rpm) until OD_{600nm} = 0.5 (around 2 h). Tenfold excess of helper phage was added to the bacteria. The flask was incubated at 37°C for 30 min standing and then 30 min shaking.

The culture was centrifuged for 10 min at 2000 × *g* and 40 ml of the supernatant was transferred to a new 50 ml tube. PEG solution was added (8 ml) and mixed; the tube was incubated on ice for 1 h. The phage was removed by centrifugation at 3500 × *g* for 30 min. Supernatant was discarded. The pellet was resuspended in 1 ml of PBS. This was spun twice at 10000 × *g* to remove remaining bacteria. This was termed the "rescued phage".

To determine the phage titre, serial dilutions of the phage were made (up to 10^{-12}) and these were incubated with 1 ml of log-phase XL-1blue, as described previously. The bacteria (100 µl) was plated on 2xTY with ampicillin and glucose, grown overnight at 37°C. The colonies were counted to determine phage titre. Phage was then used for the following round of selection, using > 10^{12} particles.

6.2.12 Phage display – polyclonal phage ELISA

Plates were coated overnight at 4°C with 400 ng/well of the extracellular fraction of the canine CSF-1R in 50 µl of PBS. As a control protein for coating the ELISA plate, BSA was used at the same concentration. The plate was rinsed with PBS and wells were blocked with PBS + milk (2%) for 2 h at room temperature. Blocking buffer was removed. The rescued phage (10 – 20 µl) was added to PBS + milk (to 50 µl) into the wells, and was incubated for 1 h at room temperature. The plate was washed at least 6 times with PBS, blotting the plate against paper to completely remove the washing buffer each time. Mouse anti-M13 antibody (1:1000, GE Healthcare) was used to detect phage particles bound to the plate. A tertiary antibody was added, rabbit anti-mouse IgG, HRP-conjugated (1:2000, Dako). Secondary and tertiary antibodies were diluted in PBS + 2 % milk and were incubated for 1 h at room temperature. HRP activity was detected using 50 µl of TMB substrate (Millipore). The reaction was stopped with the same volume of H_2SO_4 (2 M). Positive control was serum from mice immunized with the CSF-1R protein for hybridoma production (1:4000 in blocking buffer). Negative control wells received only the secondary and tertiary antibodies.

6.2.13 Phage display – monoclonal phage ELISA

Bacterial colonies on plates were directly screened to detect individual phage clones with binding activity. The phage selection rounds with enriched binding were identified using the polyclonal phage ELISA (6.2.12, above). Bacterial colonies in the output titration plates were individually picked using pipette tips. As a positive control, several colonies were picked together, therefore generating again a polyclonal pool. The colonies were transferred to 100 µl of 2xTY + ampicillin + glucose (1 %) in deep-well 96-well plates (VWR). The plate was sealed and incubated at 37^{o}C for 5 h, shaking (200 rpm). M13KO7 helper phage was added into each well (10 µl of 10^{10} cfu/ml, from the commercial stock, New England Biolabs). The plate was incubated for 30 min standing and then 30 min shaking (200 rpm) at 37^{o}C. The plate was centrifuged for 10 min at 2000 × *g*. The supernatant was discarded and 150 µl of 2xTY + ampicillin + kanamycin (NO glucose) was added to the bacterial pellets. The plate was sealed again and incubated at 37^{o}C overnight. The plate was spun as previously. The supernatant was used for ELISA.

ELISA was performed as for the polyclonal phages in 6.2.12. The bacterial supernatant containing the phage (50 µl) was diluted into the same volume of PBS + milk (2 %). Serum from mice immunized with the CSF-1R protein for hybridoma production was also used as a positive control (1:4000 in PBS + milk (2 %)). Negative control wells received only the secondary and tertiary antibodies.

The positive clones were picked from the deep-well plates and grown overnight in 5 ml of 2xTY with ampicillin. The phagemids were purified by miniprep and sequenced using the pSEXfwdSignal primer (5` - TACCTATTGCCTACGGCAG).

6.2.14 Testing the phage scFv – western blot

The extracellular portion of the canine CSF-1R was expressed in HEK293T cells as detailed in Chapter 7. The supernatant of the transfected HEK293T culture (30 µl) was prepared in reducing sample buffer and was run in a 10 % SDS acrylamide gel and transferred to a nitrocellulose membrane. After blocking the membrane, PEG-concentrated phage expressing the scFv was overlaid on the membrane (between 1:4 to 1:1000). The membrane was washed and probed with the anti-M13 (1:1000, GE Healthcare) followed by the anti-mouse, HRP-conjugated (1:1000, Dako). All antibodies were diluted in PBST + milk (5 %).

6.2.15 Testing the phage scFv – immunofluorescence

HEK293T cells or BMDM were grown on tissue culture-treated glass slides (Nunc Lab-Tek II Chamber Slide System, Thermo Scientific). No CSF-1 was added to the BMDM culture. HEK293T cells were transfected using Lipofectamine 2000 (Invitrogen) with the full canine CSF-1R receptor. The following day, cells were fixed with ice cold acetone at – 20^{o}C for 20 min, washed with PBS and blocked for 60 min with PBS + normal goat serum (10 %) at room temperature. Staining was performed using murine immune serum against CSF-1R extracellular region (1:4000) as a positive control or purified phage expressing the scFv (between 1:2 and 1:1000 dilutions). Antibodies were incubated overnight at 4^{o}C. Bound phage was detected using the mouse anti-M13 antibody (1:1000) followed by a goat anti-mouse IgG, Alexa 488-conjugated (1:400, Invitrogen) for 1 h at room temperature. Slides were washed with PBS thrice for 5 min after the antibody incubation steps. Antibodies were diluted in blocking buffer. DAPI (4',6-diamidino-2-phenylindole) nuclear stain was included in the mounting medium (Vectashield Mounting Media with DAPI, Vector Labs). A coverslip was placed on top of the section with a drop of mounting medium. The section was isolated using nail polish.

6.2.16 Testing the phage scFv – BMDM proliferation assay

Canine bone marrow-derived macrophages (BMDM) were added to 96-well tissue culture plates. The cells were left to adhere to the plate for 3 h with rhCSF-1 (20 ng/ml, Invitrogen) and then received 10 µl of either: PBS (vehicle control for the purified phage); PEG-precipitated phage containing the scFv, monoclonal or polyclonal; M13KO7 helper phage, produced as detailed in section 6.2.9. The cells were then incubated for 60 h in tissue culture. Live cells were detected using CellTiter-Glo (Promega). The amount of phage present in the monoclonal, polyclonal and helper phage solutions were estimated by dot blot. The phage solutions were serially diluted 1:10 in PBS and 1 µl of each was dotted on a nitrocellulose membrane. Bound phage was detected using the anti-M13 antibody and anti-mouse HRP as for the western blot (section 6.2.14).

6.2.17 Expressing the scFv in a new system – ligation into pOPE101

The variable regions of the monoclonal antibodies identified from the mutated library were amplified by PCR to allow the ligation into pOPE101. The PCR for mAbs from

both the VL and Vh mutated libraries was as follows. 5 × HF buffer (to 1 ×); dNTP (to 0.2 mM); primers 3.1VHfwdNcoI/3.1VLrvsNotI (to 0.5 µM); pSEX81 miniprep of the desired clone (0.1 µl); Phusion enzyme (0.4 U); nuclease-free water (to 20 µl). Cycling temperatures: 98°C for 30 sec, 35 × [98°C for 10 sec, 72°C for 20 sec], 72°C for 10 min. The PCR products were run on 1.5 % agarose gel and were gel-purified using a gel extraction kit.

The pOPE101 vector and the PCR products were digested before ligation. Vector digestion was: vector (1.6 µg); NcoI (80 U); NotI (20 U); Buffer O (to 1 ×); nuclease-free water (to 100 µl). The reaction was kept for 4 h at 37°C and then run on a gel and the band was gel extracted. The antibody PCR products were digested with the same reaction but to a final volume of 50 µl. The digestion was performed for 1 h and the products were cleaned using a PCR clean-up kit.

Products and plasmid were ligated as follows: Digested pOPE101 vector (50 ng); insert (29 ng); ligase buffer (to 1 ×); T4 DNA ligase (1 U); nuclease-free water (to 10 µl). The reaction was kept for 1 h at room temperature and at 4°C overnight. Salts were removed from the ligation with a PCR clean-up kit and the reaction was eluted in 10 µl of water. Two microliters were used to electroporate XL-1blue *E. coli*. The resulting colonies were expanded in 10 ml of 2xTY media with ampicillin, the plasmids were purified using a miniprep kit. Confirmation of ligation was obtained by sequencing using the primers 3.1VhConRvsHind and pSEXfwdSignal.

6.2.18 Expressing the scFv in a new system – expression of the scFv

Expression of soluble scFv by XL-1blue was tested under several conditions. Glycerol stocks of the transformed bacteria were picked to grow in a starter culture overnight in 2xTY (10 ml) with ampicillin. The starter culture was then added to a larger volume of medium (1:50). The bacteria were grown at 37°C shaking at 200 rpm until the OD_{600nm} = 0.7 and were induced to express the scFv with IPTG (200 or 500 µM, Sigma). Induction was then carried out at either 25°C, 30°C or 37°C in the presence or absence of sucrose (0.4 M). The duration of induction was tested between 1 h, 4h and overnight.

6.2.19 Expressing the scFv in a new system – purification of the single-chain fraction variable (scFv)

Soluble scFv were purified from the periplasm of XL-1blue bacteria using a mild lysis buffer (Tris-HCl (200 mM); sucrose (20 %); EDTA (1 mM), pH 8.0). Lysozyme was

added just before using the buffer (0.1 mg/ml, Thermo Scientific). The bacterial culture was centrifuged at 5000 × *g* for 15 min. The supernatant was removed and the bacterial pellet was lysed with the buffer above (added at 5 % of the initial culture volume). The bacteria were incubated in the lysis buffer for 1 h on ice. Insoluble proteins were removed by centrifugation at 14000 × *g* for 40 min. The supernatant was then filtered using a 0.45 µm syringe filter (Nalgene). The solution was dialyzed against a dialysis buffer (Tris-HCl (200mM), NaCl (200mM), pH 8.0) using a 3000 molecular weight cut-off (MWCO) cellulose ester membrane (Spectrum Labs). The following day, the dialyzed scFv solution was affinity purified.

For the production of insoluble scFv, the bacterial culture was induced with 500 µM of IPTG (Sigma) at OD_{600nm} = 0.5 – 0.6, at 37^{o}C, shaking at 200 rpm overnight. The soluble protein fraction was removed by lysing the bacteria as above. The insoluble remaining pellet was then resuspended (in 5 % of the initial culture volume) in a denaturing buffer (Tris-HCl (50 mM), NaCl (50 mM), EDTA (1 mM), urea (8 M), pH 8.0; DTT (10 mM) was added immediately before using the buffer). The pellet was solubilized in this buffer overnight at 4^{o}C. The scFv were then refolded by dialysis with stepwise reduction in the concentration of urea in 1.5 l of the same buffer. Urea was reduced to 6 M, 4 M, 2 M, 1 M, 0.5 M and no urea. The dialysis steps were performed stirring overnight using a 10000 MWCO membrane (Spectrum Labs). After all urea had been removed, the soluble scFv was affinity purified.

6.2.20 Expressing the scFv in a new system – affinity purification of scFv

Ni-NTA resin (Qiagen) was used for affinity purification of scFv, as described in the section 2.6.1, Chapter 2, using 200 µl of resin. When stated, after affinity purification refolded scFv G3 was dialysed thrice against PBS (1 l) to remove impurities. Dialysis membrane had a 3000 MWCO (Spectrum Labs). Protein concentration was later measured with a Nanodrop spectrophotometer (Thermo Scientific) at 280 nm.

6.2.21 Expressing the scFv in a new system – testing the pure scFv

BMDM inhibition was performed as for the phage-bound scFv, above, section 6.2.16. Staining of the duodenal tissue was performed as in Chapter 4, using the scFv either neat or diluted 1:2, 1:5, 1:10 in blocking buffer. The secondary antibody was unlabelled mouse anti-c-Myc tag (1:3000, Cell Signalling) diluted in blocking buffer. The tertiary

antibody was goat anti-mouse Ig, Alexa 488-conjugated (1:300, Invitrogen). Coomassie staining and western blot were performed using a 12 % SDS acrylamide gel. Ten microliters of the eluates were resolved on the gel in reducing sample buffer. scFv was detected using an HRP-conjugated anti-c-Myc tag (1:10000, Bethyl Laboratories) diluted in blocking buffer.

Flow cytometry was performed with live or fixed cells, obtained from canine peripheral blood as described in Chapter 4. Cells were fixed with 1 % paraformaldehyde in PBS for 20 min at 4^{o}C. Cells were stained with 50 µl of pure scFv H8 for 40 min in ice. Secondary antibody was anti-His (1:700, Invitrogen). Tertiary antibody was goat anti-mouse, Alexa 488-conjugated (1:800, Invitrogen).

For ELISAs, the scFv were tested as for the phage monoclonal ELISAs, above, section 6.2.13. Soybean trypsin inhibitor (Sigma) was also used as a negative control for coating plates, in parallel to BSA. The secondary antibody was an HRP-conjugated anti-c-Myc tag (1:10000, Bethyl Laboratories), diluted in blocking buffer.

6.2.22 Statistical analyses

The BMDM proliferation assay using phage-coupled antibodies was analysed using Kruskal-Wallis test comparing all groups against the "Helper phage" group. The proliferation assay using purified scFv was analysed using one-way ANOVA ($P < 0.05$). The assumption tests were performed on Minitab 16 (Minitab Inc.). The statistical tests and graphs were made on GraphPad Prism 5 (GraphPad Inc.).

6.3 Results

6.3.1 mAb 3.1 showed few mutations compared to the germline

mAb 3.1 was shown to cross-react with other antigens apart from CSF-1R (Chapter 4), indicating that it may have undergone low affinity maturation. The level of hypermutation undergone by mAb 3.1 (an anti-canine CSF-1R) was estimated by comparing its sequence to germline murine antibody genes using the database available on IMGT/V-QUEST (Giudicelli et al., 2004). This database finds the closest murine germline sequence to the input mAb. A low level of amino acid changes was present between mAb 3.1 and the closest germline genes, especially for the variable light chain. For this chain, only 3 amino acid variations were identified within the three CDRs (Figure 6.7). The "diversity" (D) gene could not be identified, and therefore only the first two CDRs of the Vh are shown. For these

two Vh CDRs, also only three mutations were present compared to the germline. This indicates that mAb 3.1 suffered few mutations from the germline sequence.

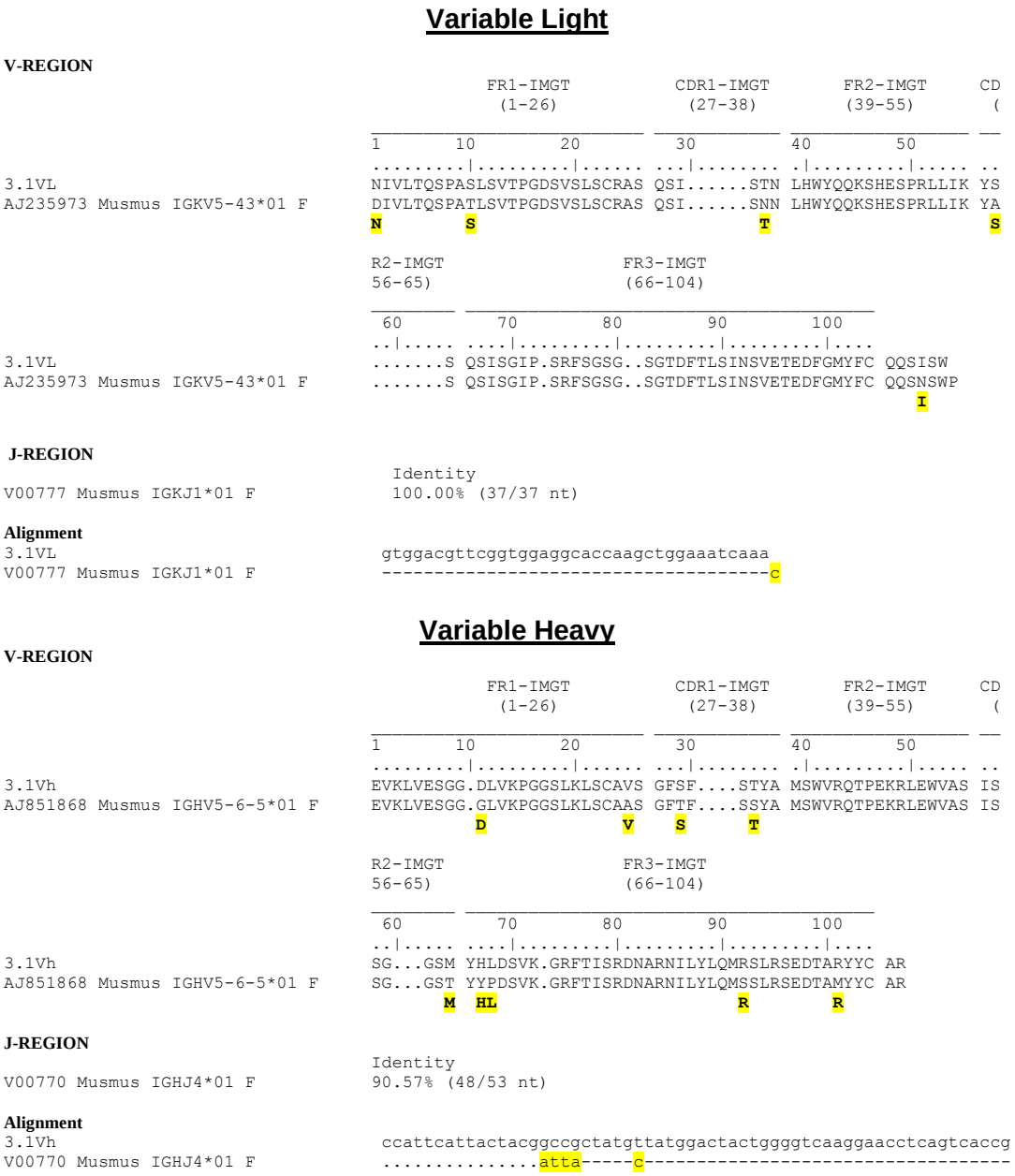

Figure 6.7 – A limited number of mutations differentiate mAb 3.1 from the closest murine germline sequence. The sequence of mAb 3.1 (Chapter 5) was inserted into IMGT/V-QUEST, which identified the closest murine germline antibody genes, named on the left column. The genes are displayed separately for the variable heavy and light chains, showing the V and J-regions for each. The framework regions (FR) and the complementarity-determining regions (CDR) are annotated. The differences between mAb 3.1 and the germline are highlighted. Notice the reduced number of mutations, especially in the light chain.

6.3.2 Construction of mutated mAb 3.1 libraries

Due to the low apparent level of maturation and affinity of mAb 3.1, this antibody was mutated with the intention of creating variant clones with different – perhaps improved – binding properties. To generate mutations in mAb 3.1 and create a semi-synthetic antibody library, the sequences for the variable regions of this antibody were amplified using primers containing degenerate sites within two of the CDRs (Figure 6.5, above). These mutated PCR products were then ligated into the pSEX81 phagemid, which codes the antibody variable regions in the format of a scFv antibody coupled to the pIII bacteriophage coat protein (Figure 6.6, above). After ligation and transformation of the libraries into XL-1blue *E. coli*, individual colonies were picked and their plasmid contents were purified by miniprep. These were then sequenced, showing that the library constructs were correct and contained mutations in the desired sites. The mutated VL library contained the non-mutated mAb 3.1 Vh chain and an array of mutations was present in the VL CDR 3. The mutated Vh library contained the non-mutated mAb 3.1 VL chain and an array of mutations was present in the Vh CDR 2 (Figure 6.8).

By counting the colonies in the plate dilutions after library electroporation, the size of the mutated Vh library was estimated to be of 6×10^8 clones and the size of the mutated VL library was estimated to be of 1.6×10^{10}. These library sizes were significantly higher than the quantity of necessary clones, since the number of possible mutations for Vh was of 3.2×10^6 (possible amino acids$^{\text{Number of mutated sites}} = 20^5 = 3.2 \times 10^6$) and for VL it was of only 8000 mutations ($= 20^3$).

The insertion of the mutated antibodies into the pSEX81 phagemid allowed for the selection of the best mutated candidates through phage display.

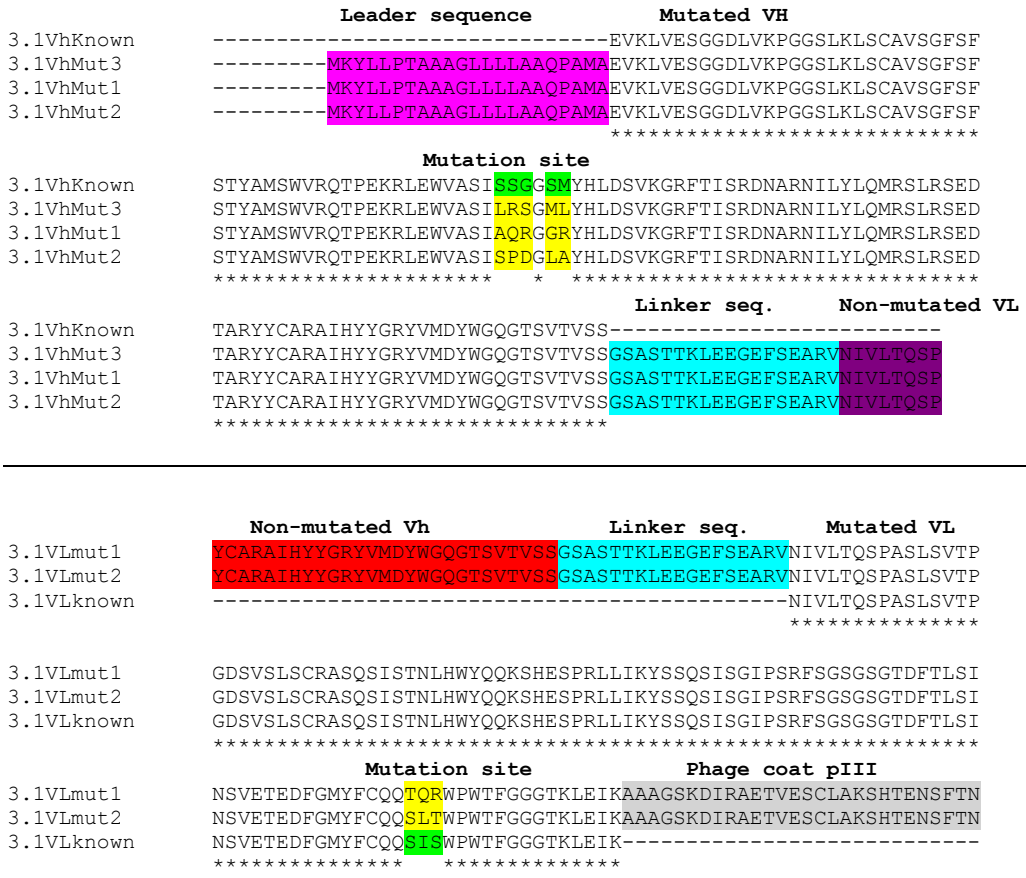

Figure 6.8 – The mutated scFv libraries displayed the expected modifications. Single colonies were picked after library electroporation into XL-1blue bacteria. The phagemids were purified and sent for sequencing. The mutated Vh and VL libraries are shown respectively, compared to the known mAb 3.1 parental sequences (named in the figure as "3.1V_Known"). The yellow highlights show the mutation sites, compared to the parental mAb 3.1, in green. Other plasmid hallmarks are highlighted and identified. "Linker seq.", linker sequence between Vh and VL. The asterisks under the sequence identify where the parental antibody and the mutated libraries coincide.

6.3.3 The mutated VL phage display

The mutated VL library was the first to be screened. Since the VL library was very small (8000 possible clones), only 3 rounds of biopanning were performed. The library was screened against CSF-1R extracellular region, immobilized in immunotubes. The original mAb 3.1 was raised against the dimerization region of CSF-1R, produced in bacteria, so it was desired to find clones with increased binding towards the CSF-1R produced in mammalian cells, which possessed correct folding and conformation.

Two protocols were compared side-by-side for the elution of the bacteriophage from the immunotubes. Adding the bacteria to the immunotube after washing (direct infection elution method) was not capable of eluting the bound phage, as shown by the output number of bacterial colonies after biopanning (Figure 6.9). Trypsin could successfully elute the phage and allowed the amplification of the library after three rounds of panning.

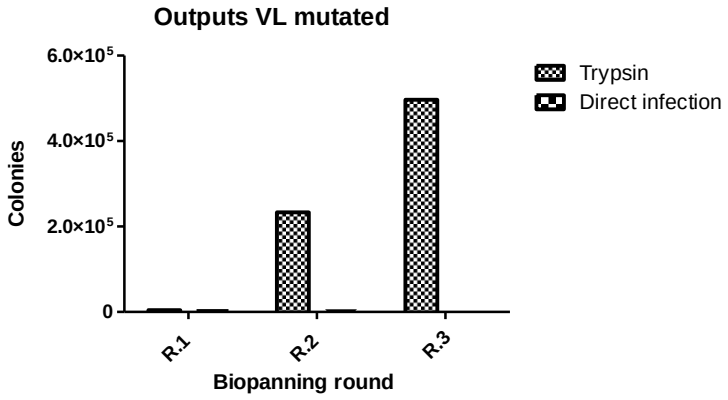

Figure 6.9 – Trypsin efficiently eluted phage and allowed for increasing bacterial outputs after selection. Two methods of phage elution were tested after panning the mutated VL library against CSF-1R extracellular region immobilized in an immunotube. After washing out non-specific binders from the immunotube, bacteriophage attached to the antigen were removed by adding either 0.5 ml trypsin for 15 min (10 mg/ml, Gibco) or by adding 2 ml of log-phase XL-1blue for 30 min. Both elution conditions were incubated at room temperature. After incubation, the contents (outputs) were removed from the immunotube and used to infect XL-1blue. Only trypsin effectively eluted the phage. The y-axis shows the total estimated resulting colony number by titration of the outputs after each round of biopanning.

The phage mixture selected in each round by biopanning was then used in a polyclonal ELISA to determine binding to CSF-1R. The ELISA test is termed polyclonal at this stage because several different phages with diverse mutated sequences are tested together. The most significant results by ELISA were seen after two rounds of biopanning the VL library using trypsin for phage elution. The activity of the phage was significantly increased from the first to the second round of selection, but it was again reduced in the third round. Phage eluted by direct infection showed no enrichment after the first round. Biopanning selected phage with specific binding affinity to CSF-1R, since there was no binding in ELISA to a control protein, BSA (Figure 6.10).

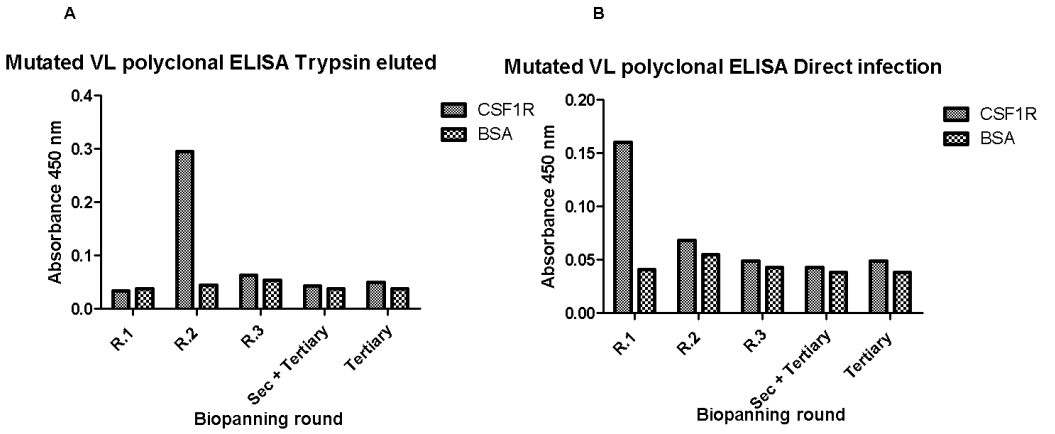

Figure 6.10 – Trypsin-eluted VL phage had enriched activity after two rounds of selection. Phage was eluted from immunotube either with trypsin **(A)** or by direct infection of the bacteria **(B)**. The eluted phages were then expanded in XL-1blue and precipitated by the addition of PEG. The precipitated polyclonal phages expressing scFv were then tested by ELISA for binding to canine CSF-1R. Plates were coated with either CSF-1R extracellular region (400 ng/well in 50 µl of PBS) or BSA (same concentration), as a control. R.1, R.2 and R.3 refer to the rounds of biopanning. Secondary antibody was mouse anti-M13 (1:1000, GE Healthcare). Tertiary antibody was rabbit anti-mouse Ig, HRP-conjugated (1:2000, Dako). Negative controls received only the tertiary or secondary + tertiary antibodies.

To test the activity of mutated antibodies separately, colonies were individually picked from the output titration plates from the VL library biopanning and were induced to express their monoclonal phage. These were then tested by ELISA, thus termed monoclonal. All three rounds of VL biopanning were tested in monoclonal ELISA, but more clones were screened from round 2 of trypsin-eluted phage and from round 1 of direct infection elution, since these yielded the best results in the polyclonal ELISA. As a control, several colonies were scraped together from round 2 of trypsin-eluted phage. This composed a polyclonal pool.

Only colonies originated from round 2 of the trypsin elution produced phages that bound to CSF-1R in the monoclonal ELISA. BSA was used as a control protein in ELISA, but no clones cross-reacted with BSA. A representative ELISA result, presenting trypsin eluted clones from round 2 is shown in Figure 6.11.

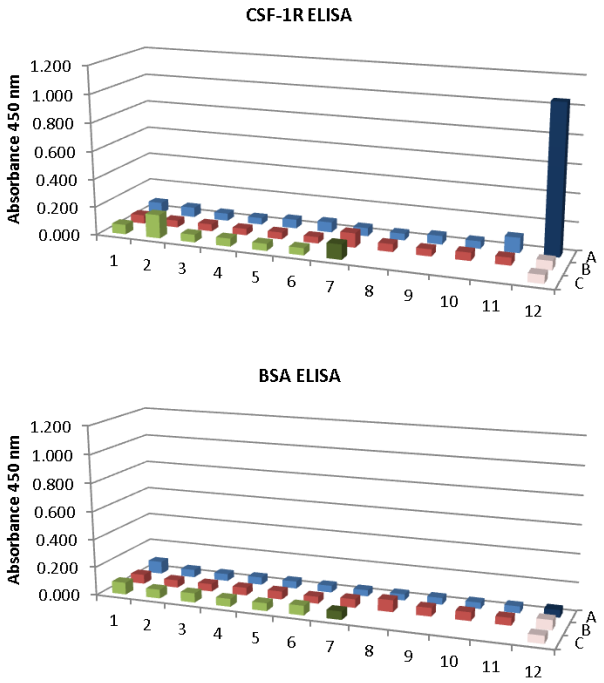

Figure 6.11 – Monoclonal phage from the VL-mutated library bound specifically to CSF-1R. Individual XL-1blue colonies containing bacteriophage were expanded separately in deep-well 96-well plates and expressed the phage containing scFv. The culture supernatant was then used for ELISA (50 µl + 50 µl of PBS/milk (2 %)). Plates were coated with either CSF-1R extracellular region (400 ng/well in 50 µl of PBS) or BSA (same concentration), as a control. Each bar represents a well with a single clone in a 96-well plate. An individual clone is shown in the same position in both graphs. The dark blue bar is the positive control, using serum from mice immunized with CSF-1R extracellular region (1:4000). The dark green bar is the phage positive control, where several bacterial colonies were scraped together, thus producing polyclonal antibodies. Secondary antibody was mouse anti-M13 (1:1000, GE Healthcare). Tertiary antibody was rabbit anti-mouse Ig, HRP-conjugated (1:2000, Dako). Negative controls (pink bars) received only the tertiary or secondary + tertiary antibodies.

Colonies A11 and C2 (respectively called scFv 11 and 24) from Figure 6.11 and also scFv E9 from another plate were picked and expanded overnight. Their phagemids were purified by miniprep and sequenced to identify the mutations each clone contained. Each of the three monoclonal scFv had unique mutations in the CDR 3 of VL (Figure 6.12 A). The sequencing chromatograms confirm the monoclonality of the newly identified mAbs, in contrast with the polyclonal positive control used in the ELISA in Figure 6.11, which was comprised of several colonies grown together (Figure 6.12 B).

A

```
Phage11          NIVLTQSPASLSVTPGDSVSLSCRASQSISTNLHWYQQKSHESPRLLIKYSSQSISGIPS
3.1pVL           NIVLTQSPASLSVTPGDSVSLSCRASQSISTNLHWYQQKSHESPRLLIKYSSQSISGIPS
                 ************************************************************

Phage11          RFSGSGSGTDFTLSINSVETEDFGMYFCQQSCQWPWTFGGGTKLEIK
3.1pVL           RFSGSGSGTDFTLSINSVETEDFGMYFCQQSISWPWTFGGGTKLEIK
                 ****************************** .**************

Phage24          NIVLTQSPASLSVTPGDSVSLSCRASQSISTNLHWYQQKSHESPRLLIKYSSQSISGIPS
3.1pVL           NIVLTQSPASLSVTPGDSVSLSCRASQSISTNLHWYQQKSHESPRLLIKYSSQSISGIPS
                 ************************************************************

Phage24          RFSGSGSGTDFTLSINSVETEDFGMYFCQQFLSWPWTFGGGTKLEIK
3.1pVL           RFSGSGSGTDFTLSINSVETEDFGMYFCQQSISWPWTFGGGTKLEIK
                 ****************************** :***************

PhageE9          NIVLTQSPASLSVTPGDSVSLSCRASQSISTNLHWYQQKSHESPRLLIKYSSQSISGIPS
3.1pVL           NIVLTQSPASLSVTPGDSVSLSCRASQSISTNLHWYQQKSHESPRLLIKYSSQSISGIPS
                 ************************************************************

PhageE9          RFSGSGSGTDFTLSINSVETEDFGMYFCQQPGIWPWTFGGGTKLEIK
3.1pVL           RFSGSGSGTDFTLSINSVETEDFGMYFCQQSISWPWTFGGGTKLEIK
                 ******************************   **************
```

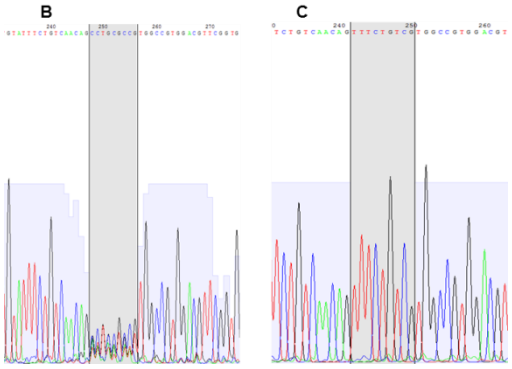

Figure 6.12 – Sequence of the monoclonal VL-mutated scFv 11, 24 and E9. The best clones found by monoclonal ELISA of the mutated VL library were sequenced. **(A)** Amino acid sequences of the mutated clones compared to the parental mAb 3.1 (shown as "3.1pVL"). The yellow highlights show the mutation sites, compared to the parental mAb 3.1, in green. The asterisks under the sequence identify where the parental antibody and the mutated libraries coincide. Alignment made using Clustal Omega. **(B)** Sequencing chromatogram of the VL CDR3 of the polyclonal positive control, comprised of several individual phage-containing XL-1blue colonies grown together. The mutation sites are inside the highlighted area, demonstrating the variability. Lower and mixed peaks demonstrate that more than one sequence was present in the sample sent for sequencing. **(C)** Sequencing chromatogram of the CDR3 of the monoclonal scFv 24. The mutation sites are inside the highlighted area. Higher discrete peaks indicate where the antibody sequence is unanimous within a sample. Chromatograms made using ApE 2.0.47 (M. Wayne Davis).

6.3.4 The mutated Vh phage display

The Vh-mutated library was considerably larger than the VL library, presented above. Therefore, four rounds of biopanning were performed to enrich the clones that bound to the extracellular CSF-1R region protein. Two packaging strategies were tested for the Vh library. Packaging is the capture of the phagemid vectors containing the scFv by the bacteriophages, which will then express the scFv on the viral surface. The phagemids were packaged either with the M13KO7 helper phage, which was also used for the VL library, or with Hyperphage. After the first round of biopanning, however, the phage eluates from both packaging formats were re-packaged using M13KO7 (see Figure 6.3 above for packaging and re-packaging of phage). The phages were eluted from the immunotube using trypsin, since the best results for the VL mutated library were obtained using this elution method.

The bacterial colony counts in the outputs of biopanning were enriched to a level 200 × higher in round 3 for the Hyperphage packaged Vh library compared to the M13KO7 Vh library. However, by round 4 the output for the Hyperphage Vh was zero, while it continued to grow for the M13KO7 Vh library (Figure 6.13).

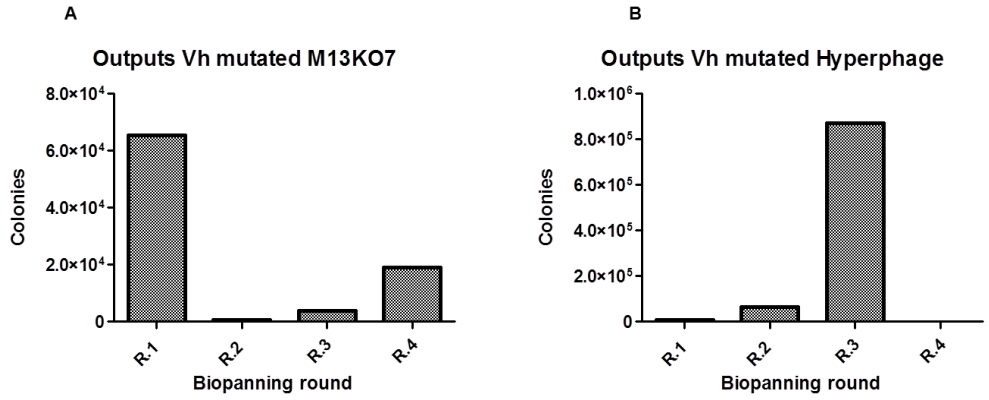

Figure 6.13 – Hyperphage packaging yielded higher bacterial outputs after selection until round 3. Two helper phages (M13KO7, New England Biolabs or Hyperphage, Progen) were tested for packaging the phagemids containing mutated Vh. After the first biopanning round, both phagemids were packaged using M13KO7. **(A)** Bacterial outputs of the M13KO7-packaged Vh mutated library after each round of biopanning. **(B)** Outputs of the Hyperphage-packaged Vh mutated library after each round of biopanning. The y-axis shows the total resulting colony number estimated by titration of the outputs.

However, the increased output of phage after the biopanning did not translate into enrichment of phage containing active scFv. In the polyclonal ELISA evaluating the eluted phage after each round, the M13KO7 packaged Vh library showed a significant enrichment after four rounds, while the Hyperphage Vh library demonstrated a modest result (Figure 6.14).

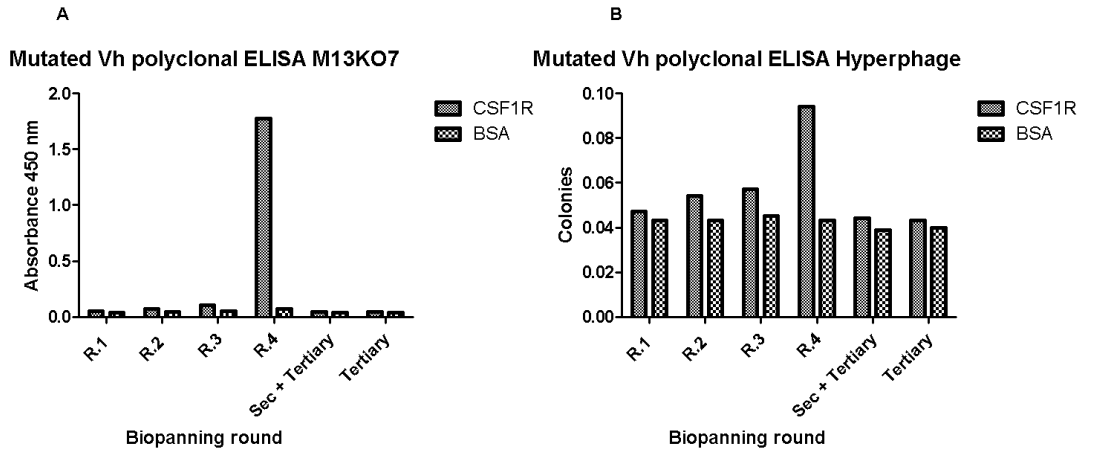

Figure 6.14 – The M13KO7-packaged mutated Vh library had enriched activity after four rounds of selection. The mutated Vh phagemid library was packaged either with **(A)** M13KO7 (New England Biolabs) or **(B)** Hyperphage (Progen). After each biopanning round, the eluted phages were then expanded in XL-1blue and precipitated by the addition of PEG. The precipitated polyclonal phages expressing scFv were then tested by ELISA for binding to canine CSF-1R. Plates were coated with either CSF-1R extracellular region (400 ng/well in 50 µl of PBS) or BSA (same concentration), as a control. R1, R2 and R3 refer to the rounds of biopanning. Binding was strongest at R.4 for the M13KO7-packaged library (A). Secondary antibody was mouse anti-M13 (1:1000, GE Healthcare). Tertiary antibody was rabbit anti-mouse Ig, HRP-conjugated (1:2000, Dako). Negative controls received only the tertiary or secondary + tertiary antibodies.

Individual colonies were picked from the M13KO7 packaged Vh mutated library. These were grown individually and induced to express the phage containing the monoclonal scFv. The bacterial supernatant was used in an ELISA.

Several clones displayed strong reactions in ELISA, which surpassed the mouse immune serum positive control. There was no cross-reactive binding with BSA in a second plate coated with this protein (Figure 6.15).

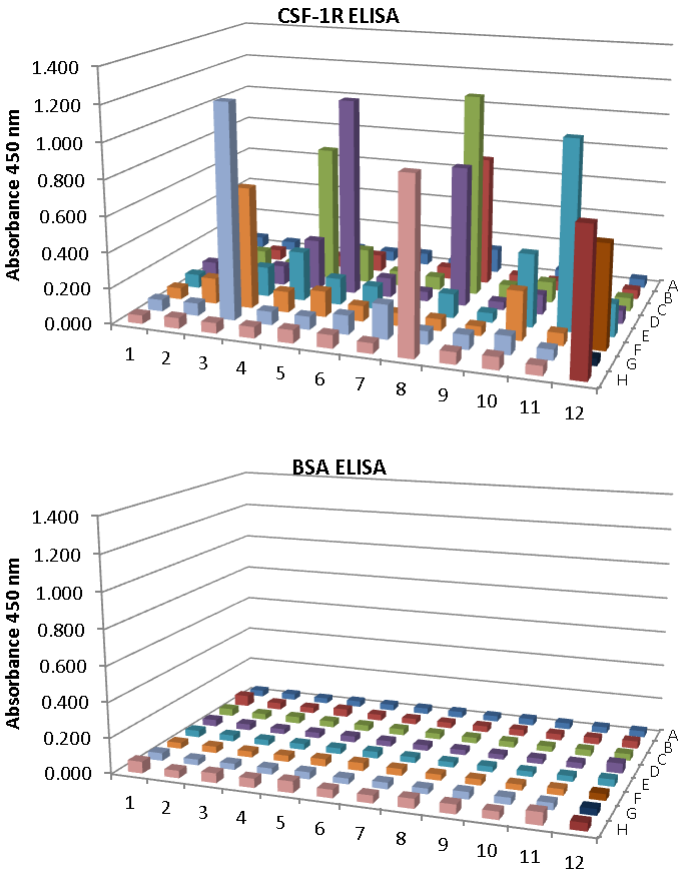

Figure 6.15 – Monoclonal phage from the Vh-mutated library bound specifically to CSF-1R. Individual XL-1blue colonies containing bacteriophage were expanded separately in deep-well 96-well plates. The colonies were allowed to express the phage containing scFv. The culture supernatant was then used for ELISA (50 µl + 50 µl of PBS + milk (2 %)). Plates were coated with either CSF-1R extracellular region (400 ng/well in 50 µl of PBS) or BSA (same concentration) as a control. Each bar represents a well with a single clone in a 96-well plate. An individual clone is shown in the same position in both graphs. The H12 position is the positive control, using serum from mice immunized with CSF-1R extracellular region (1:4000). The F12 bar shows the phage positive control, where several bacterial colonies were scraped together, thus producing polyclonal antibodies. Secondary antibody was mouse anti-M13 (1:1000, GE Healthcare). Tertiary antibody was rabbit anti-mouse Ig, HRP-conjugated (1:2000, Dako). Negative controls (G12) received only the secondary + tertiary antibodies.

Fifteen clones were selected based on the Vh monoclonal ELISA results (Figure 6.15). These were B8, C4, C8, D5, D8, E2, E4, E10, E11, F3, F10, F12, G3, G7 and H8. The bacteria harbouring these phagemids were grown and the vectors were extracted by miniprep. These were then sent for sequencing to identify the mutations present in each. Five

of these clones had the same sequence, containing the same mutations in the Vh CDR 2. Surprisingly, for these 5 clones the VL chain was not the expected non-mutated sequence originated from mAb 3.1, but was the insert present in the plasmid before restriction digest, indicating that digest had not been complete and some clones still retained the plasmid insert (Figure 6.16 A).

The other 9 clones contained the correct mAb 3.1 VL. Each of these 9 clones contained a different mutation in the CDR 2 (Figure 6.16 A). All of these clones had an amber stop codon in CDR 2 (Figure 6.16 B).

A

```
                                Vh sequence                Mutation site
D8        -----LVESGGDLVKPGGSLKLSCAVSGFSFSTYAMSWVRQTPEKRLEWVASIRRRGHAY
F10       MAEVKLVESGGDLVKPGGSLKLSCAVSGFSFSTYAMSWVRQTPEKRLEWVASIRRRGHAY
E11       MAEVKLVESGGDLVKPGGSLKLSCAVSGFSFSTYAMSWVRQTPEKRLEWVASIRRRGHAY
C8        --EVKLVESGGDLVKPGGSLKLSCAVSGFSFSTYAMSWVRQTPEKRLEWVASIRRRGHAY
E4        MAEVKLVESGGDLVKPGGSLKLSCAVSGFSFSTYAMSWVRQTPEKRLEWVASIRRRGHAY
               ********************************************************

D8        HLDSVKGRFTISRDNARNILYLQMRSLRSEDTARYYCARAIHYYGRYVMDYWGQGTSVTV
F10       HLDSVKGRFTISRDNARNILYLQMRSLRSEDTARYYCARAIHYYGRYVMDYWGQGTSVTV
E11       HLDSVKGRFTISRDNARNILYLQMRSLRSEDTARYYCARAIHYYGRYVMDYWGQGTSVTV
C8        HLDSVKGRFTISRDNARNILYLQMRSLRSEDTARYYCARAIHYYGRYVMDYWGQGTSVTV
E4        HLDSVKGRFTISRDNARNILYLQMRSLRSEDTARYYCARAIHYYGRYVMDYWGQGTSVTV
          ************************************************************
               Linker seq.        Plasmid VL
D8        SSGSASTTKLEEGEFSEARVQSVLTQPPSVSAAPGQKVTISCSGSSSNIGNNYVSWYVQL
F10       SSGSASTTKLEEGEFSEARVQSVLTQPPSVSAAPGQKVTISCSGSSSNIGNNYVSWYVQL
E11       SSGSASTTKLEEGEFSEARVQSVLTQPPSVSAAPGQKVTISCSGSSSNIGNNYVSWYVQL
C8        SSGSASTTKLEEGEFSEARVQSVLTQPPSVSAAPGQKVTISCSGSSSNIGNNYVSWYVQL
E4        SSGSASTTKLEEGEFSEARVQSVLTQPPSVSAAPGQKVTISCSGSSSNIGNNYVSWYVQL
          ************************************************************

D8        PGTAPKLLIYDNNKRFSGVPDRFSGSKSGTSATLGITGLQTGDEADYYCGAWDGSLREAV
F10       PGTAPKLLIYDNNKRFSGVPDRFSGSKSGTSATLGITGLQTGDEADYYCGAWDGSLREAV
E11       PGTAPKLLIYDNNKRFSGVPDRFSGSKSGTSATLGITGLQTGDEADYYCGAWDGSLREAV
C8        PGTAPKLLIYDNNKRFSGVPDRFSGSKSGTSATLGITGLQTGDEADYYCGA---------
E4        PGTAPKLLIYDNNKRFSGVPDRFSGSKSGTSATLGITGLQTGDEADYYCGAWDGSLREAV
          ************************************************
                               Phage pIII
D8        FGGGTKVTVLGAAAGSKDIRAETVESCLAKSHTENSFTNVWKDDKTLDRYANYEGCLWNA
F10       FGGGTKVTVLGAAAGSKDIRAETVESCLAKSHTENSFTNVWKDDKTLDRYANYEGCLWNA
E11       FGGGTKVTVLGAAAGSKDIRAETVESCLAKSHTENSFTNVWKDDKTLDRYANYEGCLWNA
C8        ------------------------------------------------------------
E4        FGGGTKVTVLGAAAGSKDIRAETVESCLAKSHTENSFTNVWKDDKTLDRYANYEGCLWNA
```

```
                                Vh sequence                Mutation site
B8        --EVKLVESGGDLVKPGGSLKLSCAVSGFSFSTYAMSWVRQTPEKRLEWVASIQ-PGAQY
D5        ---VKLVESGGDLVKPGGSLKLSCAVSGFSFSTYAMSWVRQTPEKRLEWVASIAL-GESY
G7        MAEVKLVESGGDLVKPGGSLKLSCAVSGFSFSTYAMSWVRQTPEKRLEWVASINCPG-RY
E10       MAEVKLVESGGDLVKPGGSLKLSCAVSGFSFSTYAMSWVRQTPEKRLEWVASI-TKGSTY
C4        ------VESGGDLVKPGGSLKLSCAVSGFSFSTYAMSWVRQTPEKRLEWVASI-PNGAQY
H8        MAEVKLVESGGDLVKPGGSLKLSCAVSGFSFSTYAMSWVRQTPEKRLEWVASIAP-GPGY
F3        ---VKLVESGGDLVKPGGSLKLSCAVSGFSFSTYAMSWVRQTPEKRLEWVASI-TRGPRY
E2        ---VKLVESGGDLVKPGGSLKLSCAVSGFSFSTYAMSWVRQTPEKRLEWVASIPH-GTCY
G3        MAEVKLVESGGDLVKPGGSLKLSCAVSGFSFSTYAMSWVRQTPEKRLEWVASIH-RGRVY
               ********************************************   *  *

B8        HLDSVKGRFTISRDNARNILYLQMRSLRSEDTARYYCARAIHYYGRYVMDYWGQGTSVTV
D5        HLDSVKGRFTISRDNARNILYLQMRSLRSEDTARYYCARAIHYYGRYVMDYWGQGTSVTV
G7        HLDSVKGRFTISRDNARNILYLQMRSLRSEDTARYYCARAIHYYGRYVMDYWGQGTSVTV
E10       HLDSVKGRFTISRDNARNILYLQMRSLRSEDTARYYCARAIHYYGRYVMDYWGQGTSVTV
C4        HLDSVKGRFTISRDNARNILYLQMRSLRSEDTARYYCARAIHYYGRYVMDYWGQGTSVTV
H8        HLDSVKGRFTISRDNARNILYLQMRSLRSEDTARYYCARAIHYYGRYVMDYWGQGTSVTV
F3        HLDSVKGRFTISRDNARNILYLQMRSLRSEDTARYYCARAIHYYGRYVMDYWGQGTSVTV
E2        QLDSVKGRFTISRDNARNILYLQMRSLRSEDTARYYCARAIHYYGRYVMDYWGQGTSVTV
G3        HLDSVKGRFTISRDNARNILYLQMRSLRSEDTARYYCARAIHYYGRYVMDYWGQGTSVTV
          :************************************************************
```

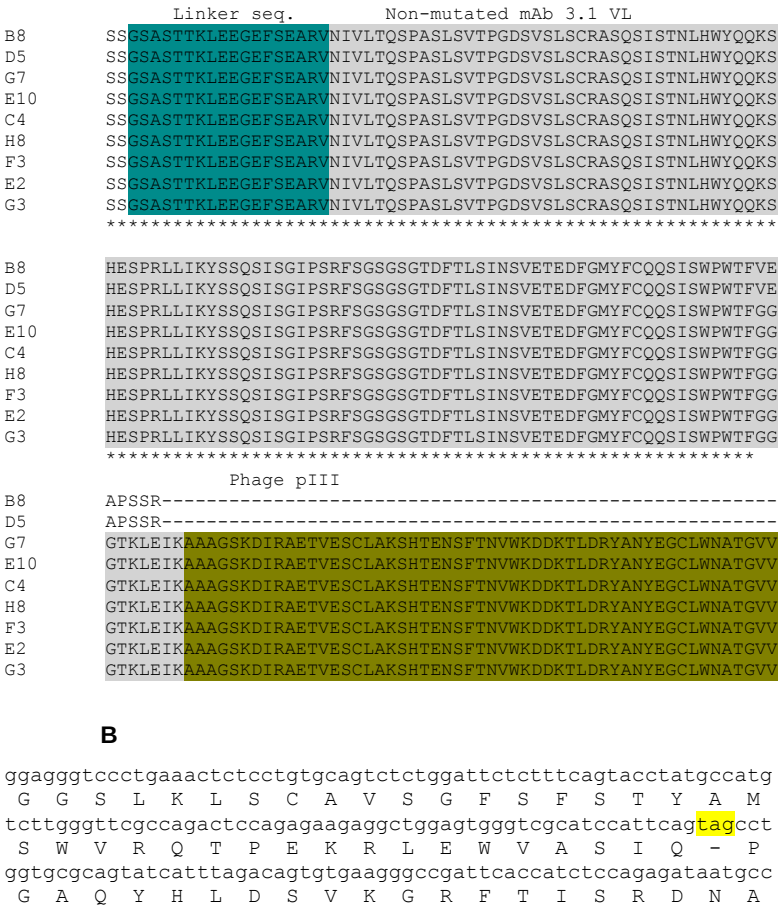

Figure 6.16 – Sequencing the monoclonal Vh-mutated scFv. The best 14 clones found by monoclonal ELISA of the mutated Vh library were sequenced. **(A)** Amino acid sequences of the mutated clones, grouped based on the correct expression of the non-mutated VL chain from mAb 3.1 (found in 9 scFv). Five clones showed the same sequence (top) but expressed the "wrong" VL, while other 9 selected scFv had unrelated mutations, but expressed the VL from mAb 3.1. The VL chains are highlighted in grey. "Plasmid VL" refers to a VL sequence that was already present in the pSEX81 vector before the library was inserted (found in 5 scFv). The red highlights show the expected mutation sites in CDR2. The asterisks under the sequence identify where the mutated antibodies coincide. The column on the left indicate the names of the individual clones. Alignment made using Clustal Omega. **(B)** Paired base pair/amino acid sequence of scFv B8, demonstrating the amber stop codon, highlighted in yellow. Protein translation made using ExPASy.

6.3.5 Testing the phage-conjugated scFv

The scFv, still coupled to the phage particle, were tested in other assays beyond ELISA to assess their functionality. No binding was seen when the phage scFv (all relevant

monoclonal and polyclonal outputs) were used to probe for the recombinant extracellular CSF-1R by western blot, regardless of the dilution of the phage, from 1:4 to 1:1000 (not shown).

The monoclonal phages and the M13KO7 Vh round 4 polyclonal phages were used to stain BMDM or cells transfected with the full CSF-1R. All monoclonal phages from the Vh library were tested in the staining of canine BMDM, and only scFv G3 (also from the Vh library) was tested in the staining of transfected HEK293T cells. No cellular staining was seen at lower concentrations (phage diluted 1:300), and phage precipitates formed at higher concentrations, which affected image quality (Figure 6.17).

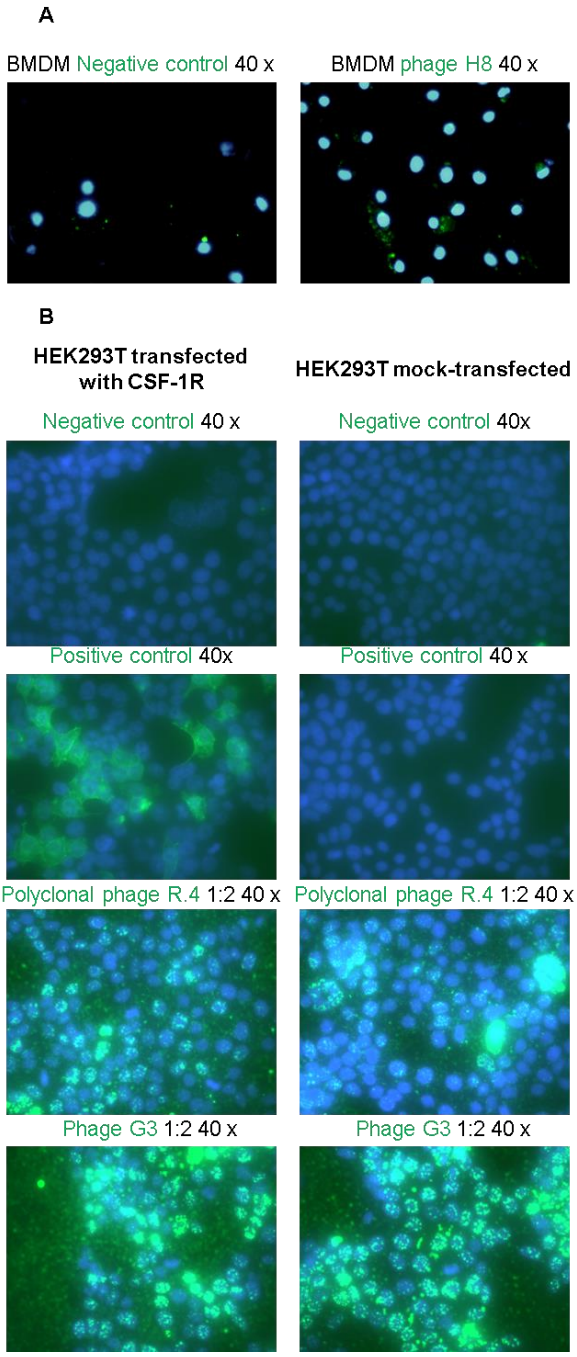

Figure 6.17 – Phage-conjugated scFv from the Vh library did not stain CSF-1R^{+} cells. **(A)** Canine BMDM was grown overnight without CSF-1 and was stained with undiluted monoclonal phage H8. **(B)** CSF-1R-transfected and mock-transfected HEK293T were stained with phage expressing scFv (polyclonal from round 4 of the Vh biopanning or phage G3) (both diluted at 1:2). Notice the intense background precipitates on phage-stained images. The positive control was serum from mice immunized with CSF-1R extracellular region (1:4000). Secondary antibody was mouse anti-M13 (1:1000, GE Healthcare). Tertiary antibody was goat anti-mouse, Alexa 488-conjugated (1:400, Invitrogen). Negative controls received only the secondary + tertiary antibodies. 40 × refers to the magnification used to acquire the images.

The phage-conjugated scFv were also tested for the capacity to affect the proliferation and survival of canine BMDM. The addition of the control helper phage was sufficient to reduce BMDM survival, but the phage expressing scFv had a more prominent effect. The polyclonal phage from the M13KO7 output from round 4 showed a trend of reducing BMDM survival, an effect which was diminished if the amount of phage added was also reduced. The monoclonal phage G3 had the most evident effect, completely killing all BMDM (Figure 6.18 A). The phage solutions were titrated to assess if their effects in the proliferation assay were merely dependent on the number of particles instead of relying on scFv binding. On the contrary, scFv G3 contained the lowest concentration of phage particles of the three samples used, although it showed the strongest effect on BMDM (6.18 B).

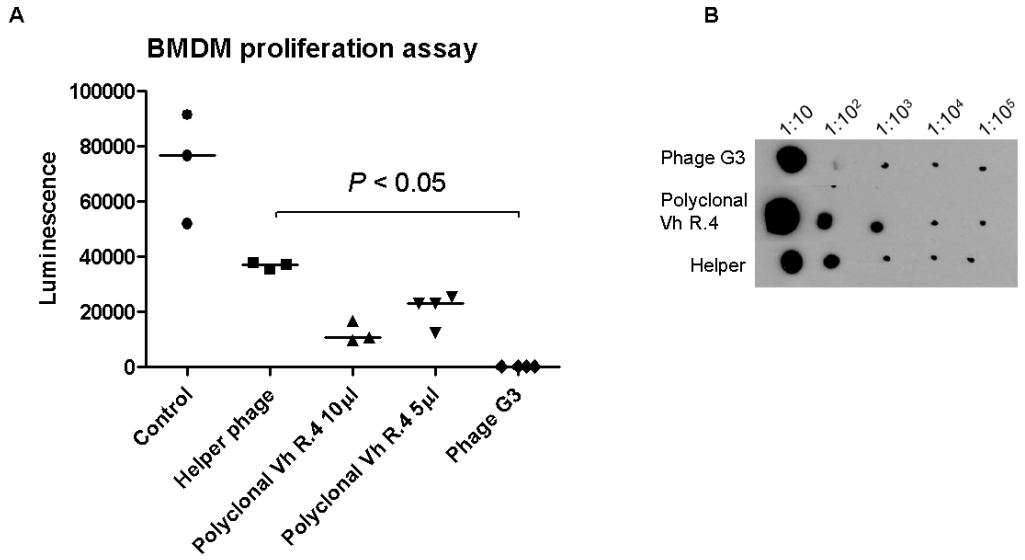

Figure 6.18 – The scFv-expressing phage reduced BMDM survival. **(A)** BMDMs were maintained with rhCSF-1 (20 ng/ml, Invitrogen) and were treated with 5 – 10 µl of the phage expressing scFv (polyclonal from round 4 of the Vh biopanning or phage G3, originated from the M13KO7 Vh library). The helper phage (M13KO7) was used as a control for the presence of the virus. PBS was the vehicle control for the scFv-expressing phage (shown in the figure as "Control"). Cells were incubated for 60 h with the treatments, and Phage G3 inhibited BMDM survival compared to its control. The horizontal bar within each group indicates the median. Statistical analysis (Kruskal-Wallis) comparing all groups against the "Helper phage" group. Proliferation results as measured by luciferase activity (CellTiter-Glo, Promega). **(B)** Titration of the phage contents from the solutions used in the assay. The three solutions were serially diluted and phage content was analysed by detecting the M13 antigen on the membrane. Based on this result, the effect seen in (A) cannot be attributed to different viral quantities. Detection antibody was mouse anti-M13 (1:1000, GE Healthcare). Secondary antibody was rabbit anti-mouse Ig, HRP-conjugated (1:2000, Dako).

6.3.6 Testing purified scFv

Testing the scFv still conjutated to the phage particle has several drawbacks, such as the low scFv expression levels, the confounding presence of the virus when used in tissue culture assays and the higher background staining in immunoassays. Therefore, it was necessary to express the scFv antibody fractions independently of the bacteriophage. To achieve this, the variable regions of the mutated antibodies of interest were ligated into a new vector, pOPE101, which allows the soluble expression of the scFv independently of the phage particle. The scFv D8, E9, H8 and G3 from the Vh library and the scFv 24 from the VL library were inserted into this vector.

Induction conditions for the production of soluble scFv in the bacterial periplasmic space were initially standardized using scFv G3. Shorter induction times were more adequate for the production of soluble protein. Bacteria induced overnight accumulated the protein as insoluble aggregates (Figure 6.19 A). Induction intensity was relevant to the yield of soluble protein. Lower concentrations of the inducing agent IPTG (and therefore slower inductions) produced more soluble proteins. Lower temperatures, which reduce bacterial metabolism, also increased protein solubility. Sucrose, which is reported to increase production of soluble recombinant protein (Kipriyanov et al., 1997), negatively affected solubility of the scFv (Figure 6.19 B).

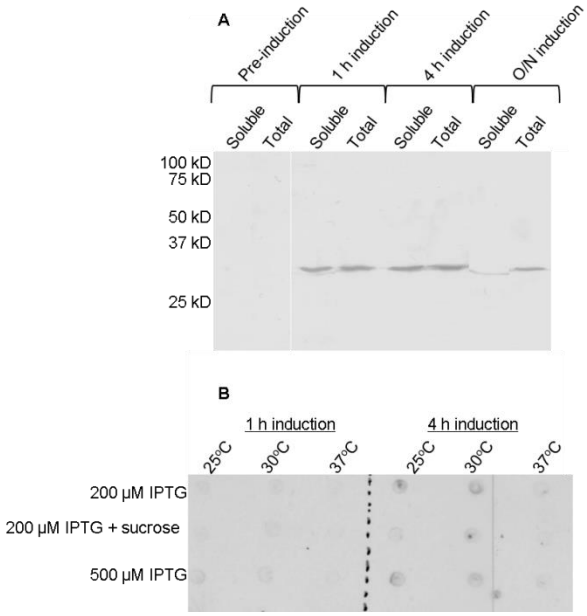

Figure 6.19 – Shorter and slower induction conditions increased scFv G3 solubility. XL-1blue were transfected with pOPE101 containing the scFv fractions selected by phage display. **(A)** Expression of soluble and total scFv protein before or after 1 h, 2 h or overnight (O/N) induction of expression (500 µM IPTG). Soluble protein was removed from the bacterial periplasmic space using a mild lysis buffer and was detected by western blot. Protein became insoluble after overnight induction. **(B)** Dot blot presenting the effect of different induction protocols for scFv expression. Soluble proteins were released from the bacterial periplasmic space and quantified by dotting the resulting solution on a nitrocellulose membrane. Higher solubility occurred at lower temperatures and with less IPTG. For both membranes, scFv were detected with an anti-c-Myc tag, HRP-conjugated (1:10000, Bethyl Laboratories).

The scFv antibodies were expressed using the optimized protocol established as shown in Figure 6.19 above, using 200 µM of IPTG, at 30^{o}C for 4 h induction. scFv 24 was more soluble than scFv G3 (not shown), and was expressed using a different protocol, using 500 µM of IPTG at 30^{o}C. After bacterial lysis and nickel affinity purification of the scFv, these were tested in an ELISA. However, the soluble scFv bound more avidly to a control protein than to CSF-1R in ELISA. The only exception was scFv 24, which showed increased binding for CSF-1R in one of the four elution fractions after Ni-NTA purification (Figure 6.20).

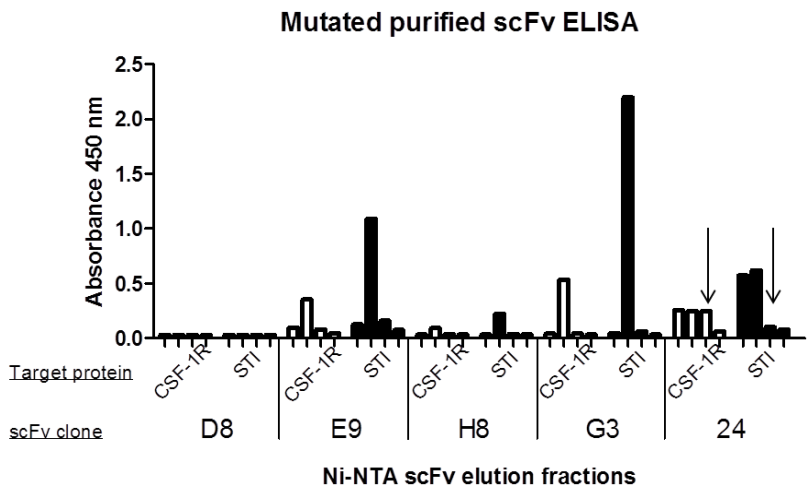

Figure 6.20 – The scFv expressed in the bacterial periplasm generally showed no specificity for CSF-1R. Soluble scFv expressed in XL-1blue was removed from the bacterial periplasm using a mild lysis buffer. Binding properties were tested against two antigens, a control protein (soybean trypsin inhibitor, STI, Sigma), represented by the black columns, or CSF-1R, coated onto ELISA plates (400 ng/well in 50 µl of PBS), represented by the white columns. Each column shows one of the elution fractions after Ni-NTA purification of each of the scFv clones (D8, E9, H8, G3, 24). Notice that binding to STI was generally higher than binding to CSF-1R. The arrows indicate the only elution fraction (n^{o} 3), of scFv 24, which showed specific binding for CSF-1R. scFv were detected with an anti-c-Myc tag, HRP-conjugated (1:10000, Bethyl Laboratories).

The scFv G3 was also expressed as an insoluble protein, as it has been previously reported that levels of expression are significantly higher when scFv are produced as insoluble aggregates and then refolded by dialysis (Sun et al., 2014). Therefore, production of scFv G3 was induced by adding a high concentration of IPTG (500 µM) at a high temperature (37^{o}C) for 4 h. This induction protocol lead to a strong production of insoluble protein, which was dissolved in a buffer with 8 M urea. The scFv was then refolded to the correct conformation by reducing the urea by stepwise dialysis. The antibody was then purified by affinity chromatography (Figure 6.21 A).

The majority of the refolded antibody was presented in the expected size of around 30 kD. However, some aggregation occurred probably during refolding, as larger bands of *circa* 75 kD could be seen by western blot after scFv affinity purification (Figure 6.21 B).

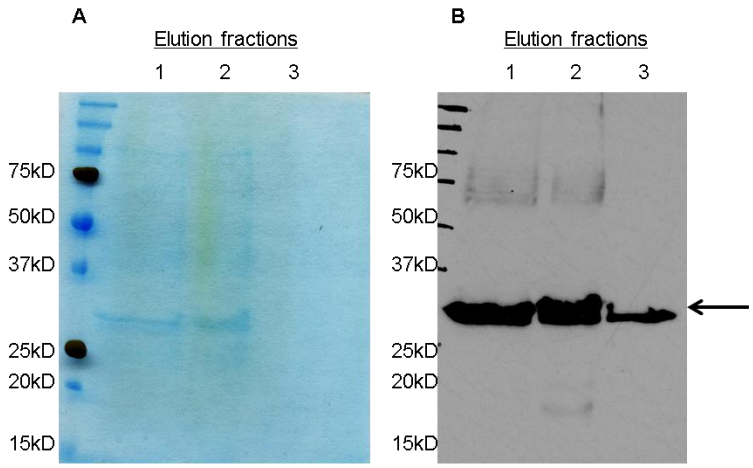

Figure 6.21 – Refolding of scFv G3 produced some scFv aggregation. scFv G3 was expressed by XL-1blue with high IPTG concentration (500 µM) and temperature (37^{o}C). The protein was extracted under denaturing conditions with urea and was refolded by dialysis removal of the urea. The protein was then purified by affinity chromatography. **(A)** Purity was assessed after affinity chromatography with Coomassie staining of the eluates from the purification after SDS-PAGE. **(B)** The aggregation of the eluates was assessed by western blot. The scFv expected size is shown by the arrow. scFv were detected with an anti-c-Myc tag, HRP-conjugated (1:10000, Bethyl Laboratories).

The refolded format of scFv G3 showed improved properties in ELISA, when compared to the originally soluble format shown in Figure 6.20, above. Whereas the soluble scFv G3 extracted from the periplasmic space showed strong cross-reactivity with the control protein in ELISA, the scFv G3 produced as an insoluble protein and then refolded by dialysis bound preferentially to CSF-1R. When compared to the original mAb 3.1, from which the mutated semi-synthetic antibody libraries were originated, scFv G3 demonstrated improved binding characteristics, with reduced binding to two control proteins, BSA and soybean trypsin inhibitor (Figure 6.22).

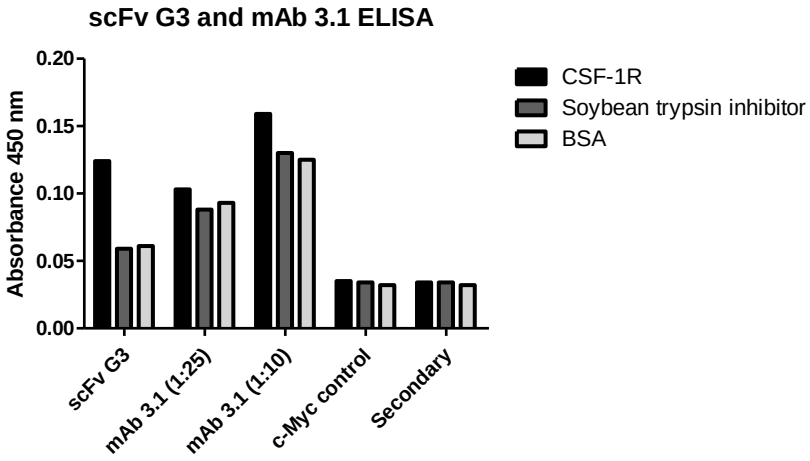

Figure 6.22 – The refolded scFv G3 displayed improved binding characteristics when compared to the parent mAb 3.1. The purified and refolded scFv G3 and the murine mAb 3.1 were tested by ELISA in wells coated either with the canine extracellular region of CSF-1R, BSA or soybean trypsin inhibitor (Sigma) (all at 400 ng/well in 50 µl of PBS). scFv G3 had reduced binding to the control proteins when compared to mAb 3.1. scFv G3 was detected with an anti-c-Myc tag, HRP-conjugated (1:10000, Bethyl Laboratories). mAb 3.1 was detected with an anti-mouse Ig HRP-conjugated antibody (1:2000, Dako). Negative controls received only the secondary anti-mouse or anti-cMyc antibodies. Result representative of three independent assays.

Refolding was then tested for other scFvs, as performed for scFv G3 (Figure 6.22, above). The clones scFv 24 (VL mutated), D8 and H8 (Vh mutated) were refolded in urea after insoluble expression. The activity of these scFv was then tested by ELISA. scFv H8 was the only one that showed binding after refolding (Figure 6.23).

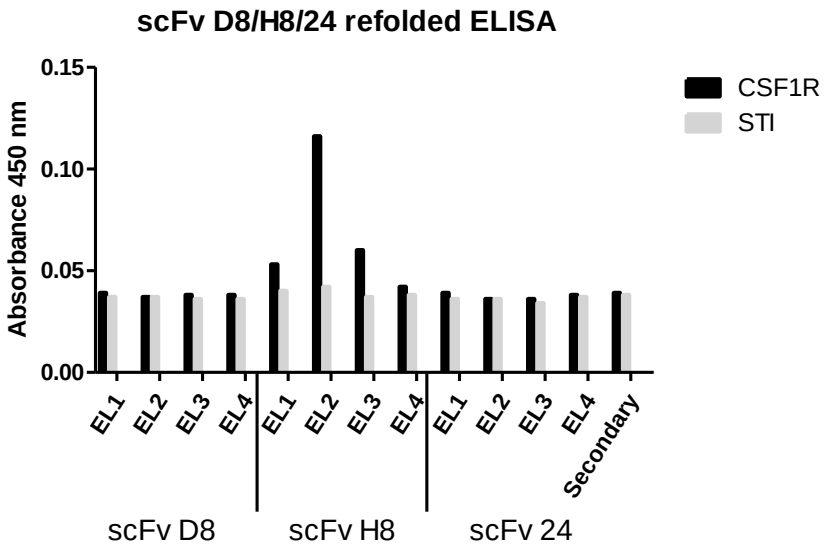

Figure 6.23 – The refolded scFv H8 showed activity by ELISA. Using the same method tried for scFv G3, other antibody fragments were expressed in bacteria as insoluble aggregates and were refolded by stepwise removal of urea. These scFv were tested by ELISA against the extracellular region of CSF-1R or against soybean trypsin inhibitor (STI), as a control. Bound scFv were detected with anti-myc tag, 1:10000 (Bethyl Laboratories). Reaction was developed with TMB substrate.

Storage stability of the refolded scFv was tested next. scFv activity was reduced but still detectable after storage at 4^{o}C for 1 week. The refolded scFv G3 was maintained in the elution solution from Ni-NTA purification (in imidazole, pH 7.75). The stored scFv was then compared in ELISA with a recently-purified counterpart. The binding signal was reduced after storage, but was still measurable (Figure 6.24).

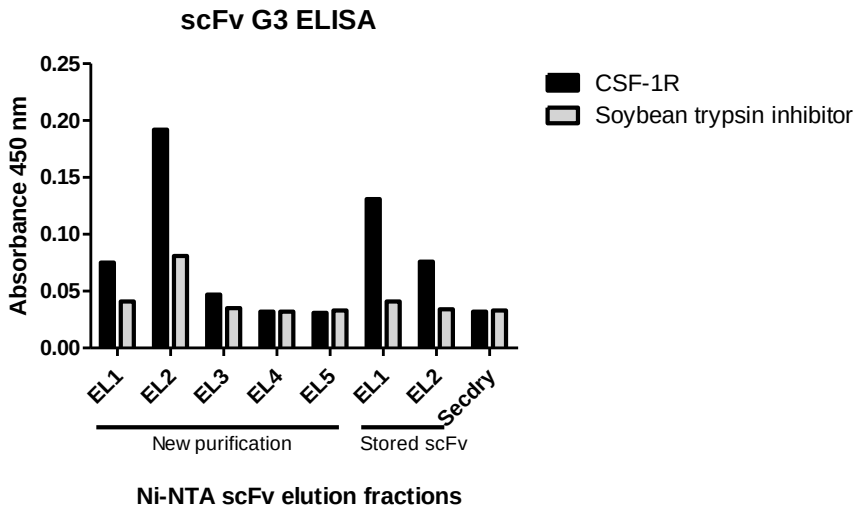

Figure 6.24 – The refolded scFv G3 could be stored at 4°C for 1 week. scFv G3 was extracted under denaturing conditions, refolded by dialysis, affinity purified and was stored at 4°C for 1 week. After the storage period, the scFv was compared to a recently-purified counterpart. Specific binding could still be seen after one week. "EL1-5" refers to different elution fractions from the affinity column. Binding to the extracellular portion of CSF-1R or to soybean trypsin inhibitor (STI, Sigma), as a control, was tested by ELISA. CSF-1R and STI were used at 400 ng/well in 50 µl of PBS to coat the plate. scFv G3 was detected with an anti-c-Myc tag, HRP-conjugated (1:10000, Bethyl Laboratories). Negative controls received only the secondary antibody.

The biological activity of scFv G3 and H8 against BMDM was tested in a proliferation assay. BMDMs were treated with either scFv G3/H8, the parental mAb 3.1 (at the same concentration) or PBS, as the vehicle control for the scFv. The murine fibroblast NIH/3T3 cell line was used as a control to assess if the effect of scFv was not indiscriminate or dependent on any bacterial contaminant remaining from the purification process. Whereas mAb 3.1 marginally reduced BMDM proliferation at the concentration used, the scFv G3 and scFv H8 reduced BMDM survival even when compared to mAb 3.1 (Figure 6.25 A). Also, scFv did not reduce NIH/3T3 survival, actually apparently increasing cellular proliferation (Figure 6.25 B). This indicates that the effect on BMDM was dependent on the specific activity of the antibody binding region.

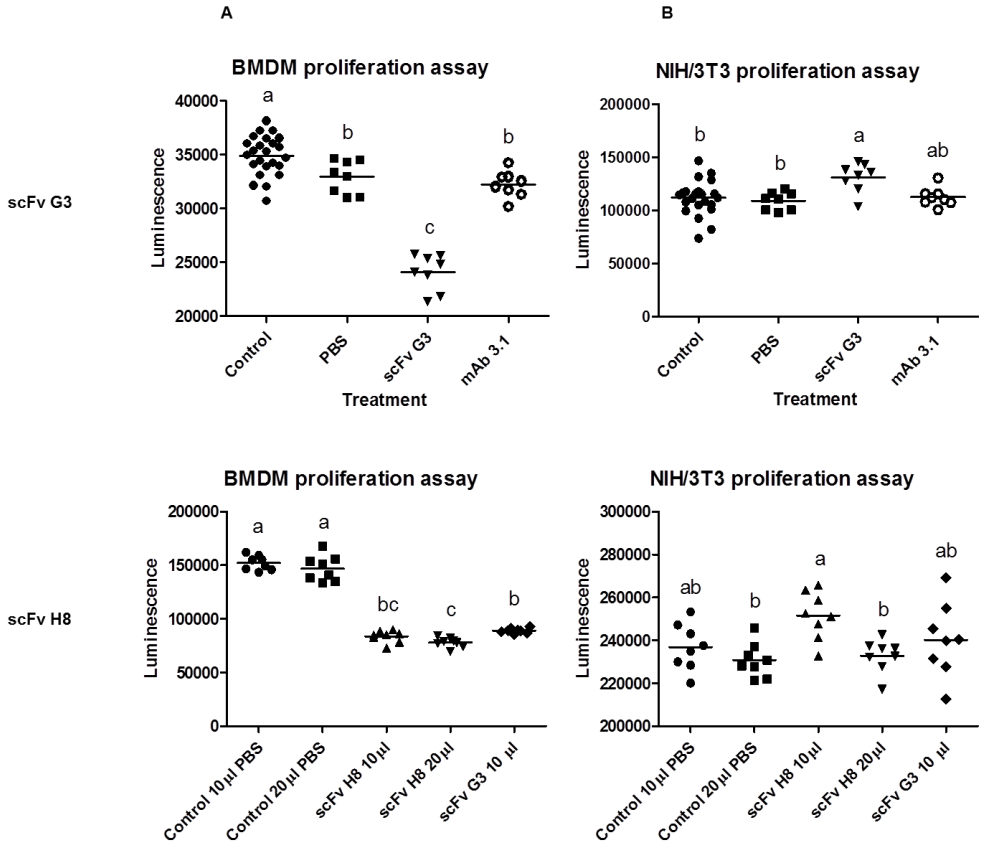

Figure 6.25 – The scFv G3 and H8 significantly reduced BMDM proliferation. **(A)** Canine BMDM were grown with rhCSF-1 (20 ng/ml, Invitrogen) and treated with 10 – 20 µl of scFv G3/H8 or of the parental mAb 3.1 (at 0.3 mg/ml). PBS was used as a vehicle control for the scFv. Notice the effect of scFv G3 compared to mAb 3.1. **(B)** The murine fibroblast NIH/3T3 cell line was used as a control to assess if bacterial products remaining from the purification had toxic effects. These cells received the same treatments as the BMDM (but no CSF-1). Cells were incubated with the treatments for 60 h. The treatment had no effect on these cells. Proliferation results as measured by luciferase activity (CellTiter-Glo, Promega). Results are the means of at least 8 wells. Data representative of three independent experiments. Data analysed by ANOVA. Statistically significant differences are indicated by differing letters above each group.

To further assess the specificity of the scFv G3, it was used to stain canine duodenal sections. The slides were probed with either the neat scFv solution (0.3 mg/ml) or with 1:2, 1:5 or 1:10 dilutions of the scFv in blocking buffer. Staining could only be detected up to the 1:5 dilution. The stained cells were isolated and were rare (1 cell/ 20 × field) (Figure 6.26).

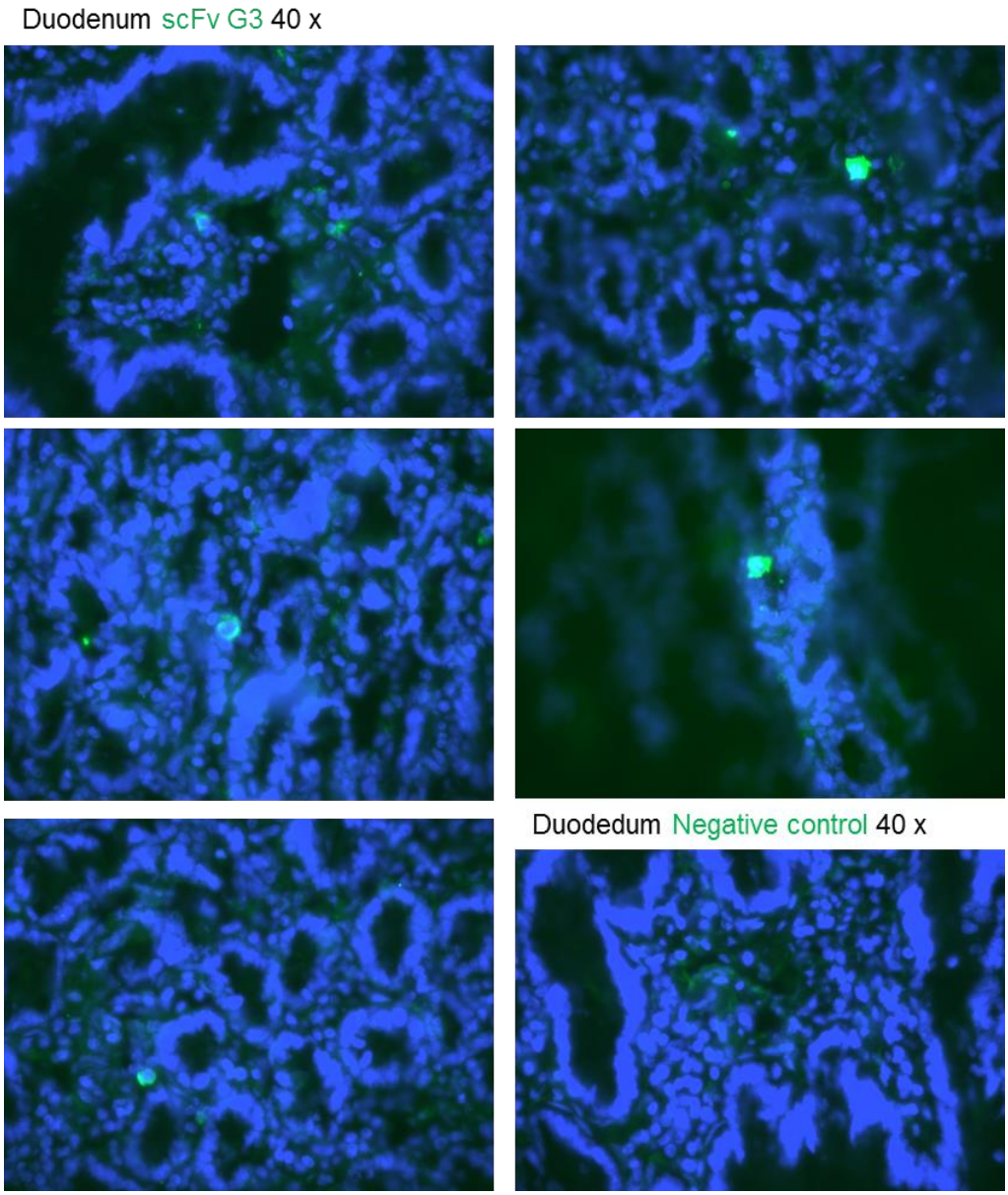

Figure 6.26 – The scFv G3 stained isolated cells in the canine duodenum. Tissue was fixed in paraformaldehyde and frozen in OCT (Fisher). Cryosections were permeabilized with PBS + Triton X-100 (0.2 %), blocked with PBS + goat serum (10 %) and probed with scFv G3 (pictures show 1:2 dilution of 0.3 mg/ml in blocking buffer). The secondary antibody was mouse anti-c-Myc tag (1:3000, Cell Signalling). The tertiary antibody was goat anti-mouse Ig, Alexa 488-conjugated (1:300, Invitrogen). The negative control was received the secondary and tertiary antibodies. "40 ×" refers to the magnification used to acquire the images.

The scFv H8 was tested by flow cytometry for binding to canine peripheral blood mononuclear cells (PBMC). This scFv bound exclusively to live canine monocytes. Staining was greatly reduced if the cells were previously fixed in paraformaldehyde (PFA) (Figure 6.27).

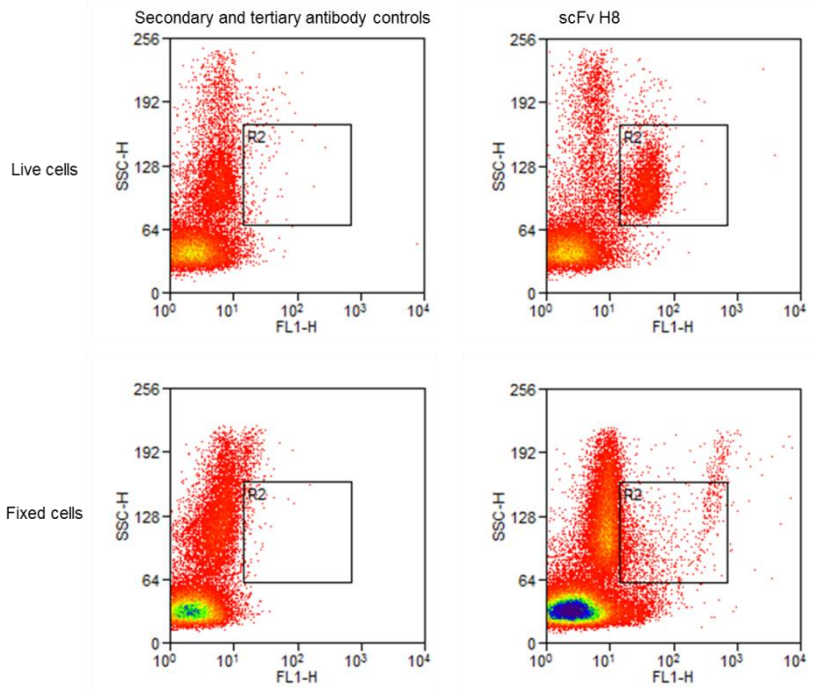

Figure 6.27 – Refolded scFv H8 bound to canine monocytes. Live or fixed (1 % PFA) canine peripheral blood mononuclear cells were stained with 50 µl of urea-refolded scFv H8 for 40 min on ice. After washing cells, bound scFv was detected using mouse anti-His tag (1:700, Invitrogen) and goat anti-mouse, Alexa 488-conjugated (1:800, Invitrogen). scFv bound selectively to live monocytes, but not to fixed monocytes.

It was tested whether combining the mutated Vh and VL chains improved antibody binding. The Vh-mutated scFv D8, G3 and H8 received the VL chain from scFv 24. These antibodies were then expressed as insoluble proteins, and were refolded in urea. These antibody fragments were tested by ELISA. Adding a mutated VL chain to the Vh chain from scFv G3 or H8 did not seem to improve the binding characteristics of these clones (see Figures 6.22 and 6.23, above). scFv D8, which did not show binding in Figure 6.23, above, displayed affinity for CSF-1R after being expressed with the VL from scFv 24 (Figure 6.28).

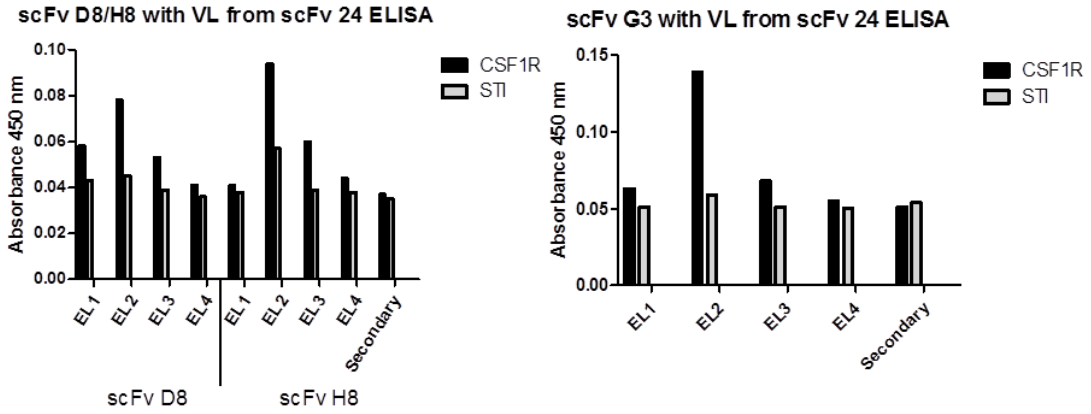

Figure 6.28 – Shuffling of mutated VL chains only affected binding of scFv D8. The mutated VL from scFv 24 was coupled to the mutated Vh from scFv D8, H8 and G3. The proteins were expressed and refolded as previously described, and were tested by ELISA (two separate experiments were made for scFv D8/H8 and scFv G3). scFv D8, which did not bind to CSF-1R in its original form, became active after receiving the VL chain from scFv 24. Bound scFv were detected with anti-myc tag, 1:10000 (Bethyl Laboratories). Reaction was developed with TMB substrate.

6.4 Discussion

In Chapter 4, it was shown that mAb 3.1 failed to bind to the recombinant extracellular CSF-1R. The reduced capacity to bind to the CSF-1R may be due to differences in conformation between the antigen used to create mAb 3.1 and the native CSF-1R protein. mAb 3.1 was produced using a small recombinant protein produced in bacteria, whereas the full extracellular CSF-1R possesses the correct folding and conformation, since it was generated by mammalian cells in culture. Immunization with a non-conformational peptide is known to reduce the formation of antibodies that recognize the conformational epitopes (Beil et al., 1973).

Analysing the number of mutations/CDR in mAb 3.1 compared to the germline genes, it could be verified that few residues were altered by hypermutation, especially in the VL chain. The number of mutations is linked at least partially to the maturity of an antibody (Willis et al., 2013). VL had a reduced number of mutations when compared to the Vh chain of mAb 3.1. It is known that there is a disparity in the onset of hypermutation between the chains, with the Vh being prioritized (Van Der Keyl et al., 2000). In an average naïve (non-immunized) antibody library, about 55 % of antibody sequences display more mutations in

VL than 3.1. Regarding the VH, around 35 % of naïve antibodies have more mutations than 3.1 (Tomlinson et al., 1996).

Therefore, two semi-synthetic libraries were produced by mutating the variable region of mAb 3.1. The CDR2 of the Vh chain was mutated, while the CDR3 of the VL chain was altered. Even small alterations of the CDRs are sufficient to alter the binding specificity and affinity of an antibody (Gilliland et al., 1999; Mahon et al., 2013). It was therefore expected that some of the mutants should present improved binding characteristics when compared to the parental antibody.

The mutated antibody libraries were created with small numbers of possible clones in order to verify the capacity of such reduced libraries in generating improving mutations. Also, it was intended that the mutations would be selected in parallel and then coupled in a single new scFv. This new scFv would contain mutated VL and Vh chains which had been selected for improved binding separately. Another group has successfully explored this possibility with an anti-GM-CSF library, altering the same CDRs changed in the present chapter (Steidl et al., 2008). Smaller, separate libraries also have technical advantages, such as not requiring extreme bacterial transformation efficiencies (Martineau, 2010).

These scFv libraries with reduced numbers of clones can be screened in few biopanning rounds. Enrichment by biopanning favours the growth of clones that bind to the antigen. Once full enrichment is reached, further rounds of selection allow the selection of phage that have a growth advantage over the binding phages. Phage clones that do not express the scFv coupled to the pIII protein have growth advantages, for instance, since this protein is necessary for infecting the *E. coli*. Given that the VL library is very small (8000 clones), two rounds of biopanning were sufficient to enrich the desired clones, and further rounds probably selected for non-specific phage which possessed growth advantage. Therefore, in the third selection round of the VL library, the majority of the bacteriophages present were likely to not express scFv, reducing the binding in the polyclonal ELISA assay.

The mutated variable heavy chain library was considerably larger than the VL counterpart (the Vh contained 3.2×10^6 clones). After four rounds of biopanning, there was significant enrichment in the ELISA binding of the polyclonal output phage, and several monoclonal scFv were identified with strong results by ELISA. Of the 14 clones sequenced from the VH mutated library, 5 contained an unexpected VL chain. This VL chain was already present in the plasmid before the library was constructed, and was not fully removed from all the phagemids by restriction digest.

It has been found that frequently antibodies of different specificities possess similar or equal VL chains, with variations between them being present only in the VH chains. The

contrary is not true, and rarely is antibody variability only confined to the VL domain (Kabat and Wu, 1991). This may justify why scFv which contained the "wrong" VL chain were so numerous after phage panning. The fact that 5 clones presented the same sequence indicates that there was selective enrichment of these scFv through strong binding to CSF-1R.

The remaining 9 monoclonal scFv sequenced from the Vh mutated library contained TAG stop codons within the mutation sites. However, XL-1blue is an amber suppressor strain and reads through the TAG codon as a glycine in around half of the translations (O'Brien and Aitken, 2004). Whether the reduced expression of scFv due to the stop codon conferred a growth advantage to these clones is not known, but irrespective of that these scFv bound to the CSF-1R specifically in ELISA. It could be speculated that a truncated version of the scFv was expressed, starting after the TAG codon, and this truncated protein could have affinity for the CSF-1R. However, the antibody fragment must have been expressed in its entirety, since the leader sequence coded by the plasmid at the N-terminus of the scFv is essential for the production of the phage particle, which is needed for the biopanning of the library.

Hyperphage is an altered helper phage which does not contain gIII, which translates the viral coat protein pIII. This protein is required for phage infectivity. The role of the helper phage is to package a phagemid library containing gIII coupled to a scFv. Therefore, when Hyperphage packages the phagemid library, all infective viruses will contain the scFv, frequently with more than one copy per virus. The more common M13KO7 helper phage contains wild viral gIII, and therefore the resultant bacteriophages do not need to express the scFv-coupled pIII in order to become infective. Also, the M13 phages that do express the scFv tend to only express a single copy per virus (Rondot et al., 2001). Therefore, the Hyperphage packaged Vh mutated library was expected to produce better results when compared to the M13KO7 library. Although the number of output colonies after biopanning was increased using the Hyperphage, this result did not translate into active scFv in the ELISA assay.

Because of the difficulties in testing scFv coupled to the bacteriophage, the scFv were expressed independently as soluble proteins. The presence of the phage introduces a confounding factor when interpreting the BMDM inhibition assay, since some of the effect over the BMDM could have originated by the presence of the phage particle, as could be seen with the use of the helper phage as a control. Also, phage scFv expression is low and production is time-consuming. Therefore, the scFv were transferred to a new vector, pOPE101, to allow the independent expression of the antibody fragments.

However, the soluble scFv, expressed and folded in the bacterial periplasm, showed strong cross-reactivity with a control protein in ELISA. Protein folding within the bacterial periplasm is dependent on a number of factors, such as the intensity of protein expression and the very identity of the protein (Baneyx and Mujacic, 2004). As an example, scFv 24 and G3, originated respectively from the VL and Vh mutant libraries, showed significant differences in solubility and activity after periplasm production, although these antibody fragments were only different by a few amino acids. To avoid issues with periplasm protein folding and to increase protein production, the scFv G3 was produced as an insoluble aggregate by increasing expression intensity (altering IPTG concentration, growth temperature, the starting point for induction and induction time). Refolding was then carried out in a controlled manner, by removing the denaturing reagent by dialysis.

This insoluble and "refolded" mAb G3 showed significant improvements in binding to the CSF-1R compared to the periplasm-produced soluble counterpart. The refolded scFv preferentially bound to CSF-1R and had reduced cross-reaction with a control protein also when compared to the parental mAb 3.1, whose sequence was the framework for the construction of the scFv libraries. This indicates that mutation of the CDR 2 of the Vh chain of mAb 3.1 was a step towards perfecting the binding properties of the parental mAb. The refolding was tested with other scFvs (D8, H8 and 24). Of these, scFv H8 also showed specific binding after refolding.

Phage display offers a significant advantage over hybridoma screening of antibody clones in the ease with which non-specific clones can be eliminated from the process. Before the phage library is incubated with the immobilized target antigen, it can be "blocked" to remove any undesired cross-binders (O'Brien and Aitken, 2004). In the present study, the libraries were blocked using bovine milk, which de-selected clones that bound to BSA and other proteins. The parental mAb 3.1 showed significant cross-reactivity with BSA, and mutant clones displaying this characteristic were easily removed from the screened pool by the blocking step. Further improvements of the mutant scFv could be accompanied by blocking the library with proteins of similar structure to CSF-1R, such as c-Kit and the platelet-derived growth factor receptor (PDGFR) (Qiu et al., 1988). In this manner, antibodies that undesirably recognized these related proteins would be removed.

The scFv D8 was one of the selected clones that expressed the VL chain that was present in the plasmid before library construction. After expression and refolding of this scFv, it did not bind to CSF-1R by ELISA. However, this was the only scFv that benefited from receiving the mutated VL chain from scFv 24. The intent of shuffling the VL chain was to improve the binding of the Vh-mutated clones. However, scFv G3 and H8 showed no

improvement by ELISA after receiving a mutated VL. Therefore, it is possible that scFv D8 would have equally benefited from receiving the scFv from mAb 3.1, non-mutated, that is.

The "refolded" scFv G3 still presented some aggregation after purification. Aggregation is a common occurrence in the production and purification of scFv (Borras et al., 2010). However, only a minor amount of scFv aggregated, and this seemed not to interfere with the binding properties of scFv G3. The refolded G3 could be stored for at least 1 week at 4^{o}C, albeit with some loss of activity. This is in accordance with the literature (Shepherd and Dean, 2000). These proteins are expected to be stable at up to 50^{o}C (Borras et al., 2010).

Addition of refolded scFv G3 or H8 affected BMDM proliferation to a greater extent than the parental mAb 3.1. Confounding factors include contaminant *E. coli* bacterial proteins after scFv purification, since affinity chromatography did not completely remove non-specific proteins, as shown by Coomassie staining. The scFv (or the impurities) had no effect over the proliferation of a murine fibroblast cell line (NIH/3T3) that was used as a control. Both macrophages and NIH/3T3 cells express at least some pathogen-associated molecular pattern receptors, such as Toll-like receptors, that could recognize residues of *E. coli* and negatively affect cellular proliferation. Since NIH/3T3 proliferation was unaffected by the scFv solution there is an indication that bacterial contaminants were not an issue. Nevertheless, macrophages are more sensitive to some bacterial products than the fibroblast cell line, and could have been more negatively affected by the presence of residues (Jung et al., 2005; Lin et al., 2000). Since the scFv antibody fragment does not possess an Fc fraction, Fc receptor binding can be excluded as a confounding factor in affecting cellular proliferation.

Staining of canine duodenum was not conclusive in establishing if scFv G3 could bind to canine tissue macrophages. Only few and isolated cells were stained using this scFv, which is significantly different from the staining patterns of the parental antibody 3.1 (Chapter 4). This could indicate a significant change in the binding properties between the original and the mutant antibody versions. However, protein stability of the scFv in the assay conditions needs to be considered when interpreting the results. scFv can have varying stability and have been subject to several engineering studies to improve constancy (Brockmann et al., 2005).

Confirming that the binding properties were greatly changed by mutation of CDR2, scFv H8 was shown to specifically bind to unfixed monocytes from canine peripheral blood. This is in contrast with the parental mAb 3.1, which could not stain cells from blood

(Chapter 4). This confirms the specificity of scFv H8 to CSF-1R, since other peripheral blood cells do not express this receptor (Moffat et al., 2014).

Future steps in this work would be to add further mutations to the already improved scFv. These should be screened for blocking ability against a cell line dependent on recombinant CSF-1R for survival. Mutation could also be inserted into mAb 12.2, which was later found to bind to a wider range of CSF-1R glycoforms than mAb 3.1, which was used to build the phage library described here (Chapter 4).

6.5 Conclusion

In this chapter, two semi-synthetic antibody fraction libraries were successfully constructed by mutating the CDRs of a murine anti-canine CSF-1R antibody, mAb 3.1. By panning these libraries using the phage display method, it was possible to identify scFv clones that bound to the extracellular region of the canine CSF-1R with improved characteristics when compared to the parent mAb 3.1. Production of functional scFv benefited from a process of insoluble expression followed by refolding of the protein by dialysis, as tested with the scFv G3 and H8. The refolded scFv bound to the CSF-1R by ELISA and seemed to specifically inhibit BMDM proliferation.

Overall, these results show that it is possible to change and improve antibody specificity and binding through the construction and selection of small libraries of mutant antibodies created with only selected CDR alterations. These findings enable further enhancements of the anti-CSF-1R antibodies through further mutations of the already improved antibodies.

Chapter 7

Production of monoclonal antibodies and recombinant proteins

Highlights

- With the purpose of producing anti-canine CSF-1R antibodies, two antigens were produced: the complete extracellular (EC) portion of the receptor, expressed in mammalian cells, and a smaller fraction of the EC, comprising only the region responsible for receptor dimerization, expressed in bacteria.
- The EC portion was structurally accurate, since it was capable of binding to CSF-1. The dimerization domain was expressed either with a His tag or with a GST tag. The former formed multimers, the latter was of difficult purification.
- Mice were immunized with both the extracellular and the dimerization domains and mAbs were generated. The extracellular region produced mainly IgM clones. The dimerization domain produced several IgG clones.

Abstract

Monoclonal antibodies are most commonly generated through the hybridoma technique. Hybridomas are created by the fusion of splenocytes from immunized mice with a myeloma cell line. This fusion immortalizes the antibody-producing cells of the spleen and allows continuous antibody production. In order to generate blocking antibodies against the canine CSF-1R, mice were immunized with two recombinant fractions of this protein. The complete extracellular portion of the CSF-1R was cloned and expressed in mammalian cells. The dimerization domain, which is a component of the extracellular portion of the receptor, was expressed in bacteria. The extracellular region of CSF-1R was a glycosylated protein and was probably folded similarly to the wild-type receptor, since it was capable of binding to one of its ligands, CSF-1. The dimerization domain formed aggregates, although at low concentrations. After immunization with these proteins, mouse sera were shown to be

strongly reactive against the antigens by dot blots or ELISA. In an initial test to identify blocking activity, the immunized sera could not affect the proliferation of bone marrow macrophages, cancer cells or of cells stably expressing recombinant CSF-1R. The subsequent procedures for hybridoma production from these mice are described. The extracellular region hybridomas generated a disproportional amount of IgM clones which could not be avoided with magnetic cell sorting depletion of IgM^+ lymphocytes before fusion. Several IgG clones were obtained following fusion from the dimerization domain-immunized animals.

7.1 Introduction

The CSF-1 receptor (CSF-1R) is composed of five extracellular immunoglobulin-like domains, with high glycosylation content (Yeung and Stanley, 2003). Domains 2 and 3 are responsible for ligand binding. Following contact with CSF-1/IL-34, the ligands of CSF-1R, the fourth domain responds for receptor dimerization (Chen et al., 2008), which leads to the formation of intracellular receptor complexes and protein phosphorylation. This process of receptor activation drives increased protein expression, cytoskeletal remodelling, cellular motility and chemotaxis (Stanley and Chitu, 2014). This signalling process through the CSF-1R is crucial for the survival and activation of many macrophage subsets and their development from the progenitor cells (Sasmono et al., 2003).

CSF-1R expression within tumours, both by the cancer cells themselves and by infiltrating macrophages, is associated with poor clinical prognosis (Król et al., 2013; Patsialou et al., 2009). Therefore, this receptor is believed to be a potential target for cancer therapies (Hume and MacDonald, 2012). Several studies have verified that blocking the CSF-1R reduces cancer cell growth and invasion, diminishes neovascularization and cancer intravasation, among other benefits (Haegel et al., 2013; MacDonald et al., 2010; Pyonteck et al., 2013).

7.1.1 Constructing antibodies against the CSF-1R

With the goal of producing blocking antibodies against the canine CSF-1R, two proteins were produced for immunization of mice. The entire extracellular (EC) region of the receptor was expressed in HEK293T cells, and the dimerization domain – which is a fraction of the extracellular region – was expressed in BL21 (DE3) bacteria.

Other groups have produced blocking antibodies against the CSF-1R. The antigen production strategies for immunizing mice varied between each of the publications, but while the expression format varied, animals were generally immunized with the extracellular region of CSF-1R or the full receptor. Sherr and colleagues raised mAb 2-4A5, which targets the human CSF-1R. For this, rats were immunized with normal rat kidney cells expressing the human CSF-1R (Sherr et al., 1989). M279, an antibody that targets the murine receptor, was obtained by immunizing rats with the mouse CSF-1R coupled to the human Fc region. The strategy for antibody production of mAb H27K15 was not stated, but this mAb binds to the first two (*N*-terminal) extracellular domains of CSF-1R (Grellier et al., 2014).

7.1.2 The hybridoma technology

The generation of monoclonal antibodies is commonly accomplished using the hybridoma technique. It consists of immortalizing the antibody-producing cells to allow the continuous generation of antibodies in culture. To achieve immortalization, the mortal splenocytes are "fused" with an immortal myeloma cell line, generating a hybrid organism, called a hybridoma (Köhler and Milstein, 1975). Each myeloma cell fuses with a different B-lymphocyte, and therefore after the fusion process the culture contains a mixture of hybridoma clones. Each hybridoma clone secretes a different antibody, as also would the B-lymphocytes from which they originated. These clones can be separated and grown individually, producing antibodies derived from a single B-lymphocyte. These are thus termed monoclonal antibodies (Figure 7.1).

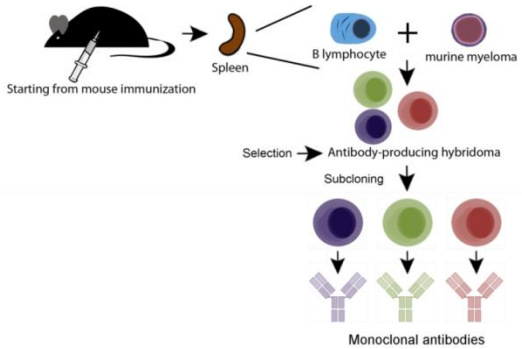

Figure 7.1 – Overview of the process of hybridoma production of antibodies. Mice were immunized until antibody responses could be detected in the murine serum. Spleens were collected and splenocytes were harvested. These cells were fused with a murine myeloma cell line, generating a hybridoma. Stable hybridomas were selected using a specific medium. Monoclonal antibodies were derived by growing hybridoma cells individually (subcloning). The mAbs were then characterized by ELISA.

Stable hybridomas are selected using medium containing aminopterin. Aminopterin blocks the *de novo* DNA synthesis pathway. An alternative salvage pathway of DNA synthesis exists, but the myeloma cells are mutated so as not to produce hypoxanthine-guanine phosphoribosyltransferase (HGPRT), which is necessary for the salvage route. Therefore, myeloma cells cannot survive in medium containing aminopterin. The B-lymphocytes have a functional salvage pathway. In the presence of aminopterin, the *de novo* DNA synthesis is also blocked for the B-lymphocytes, as for the myelomas. However, these cells can activate the salvage pathway because they express HGPRT. The selection medium, beyond providing negative selection through aminopterin, also provides two necessary intermediates for the salvage pathway, hypoxanthine and thymidine. Nevertheless, B-lymphocytes are mortal cells and cannot survive beyond a few days in culture (Figure 7.2).

The process of cell fusion generates a hybrid with the cell culture immortality of the myelomas and with the DNA salvage pathway from the B-lymphocytes, ensuring that cells survive in selection medium containing aminopterin (Köhler and Milstein, 1975).

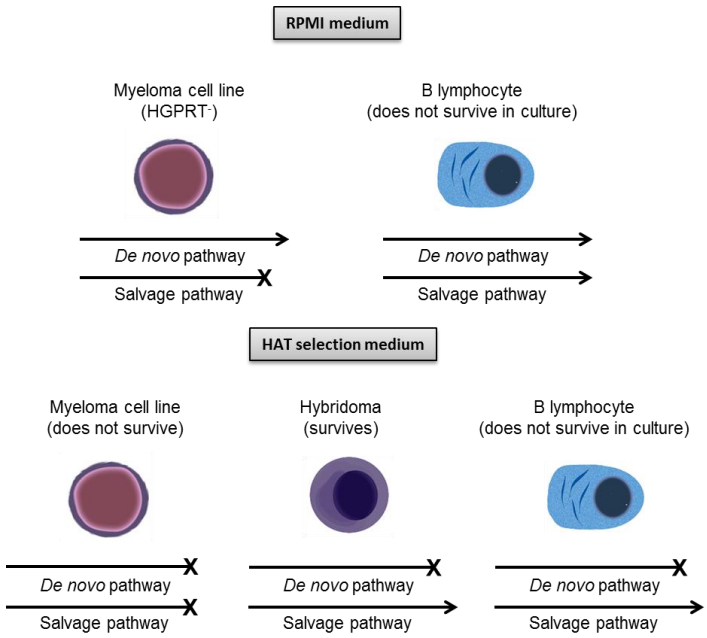

Figure 7.2 – Selection of stable hybridomas is made based on the ability to survive in an aminopterin-containing medium, called HAT. Splenic B-lymphocytes are mortal and do not survive for prolonged periods in culture. The myeloma cells are mutated and do not possess the salvage pathway for DNA synthesis (shown as the cross-ended arrow). Aminopterin in the selection medium blocks the *de novo* pathway. Therefore, the HAT medium, containing aminopterin, only allows the survival of hybrid fused cells.

7.1.3 Protein production

Proteins used for immunization are commonly produced as recombinant products, which can be derived from different expression systems. Each system offers benefits and disadvantages, which are relevant to the work presented in this chapter.

Bacteria are commonly used as hosts for protein expression because these organisms can be grown in large culture volumes and can stably produce substantial quantities of recombinant protein. However, it is common for proteins to be incorrectly folded by the bacteria and to become aggregated as inclusion bodies. Also, the most commonly used bacterial expression systems do not glycosylate proteins (Chen, 2012). Therefore, protein purification can be challenging and may require the use of strong denaturing conditions. In most cases, recombinant protein purification and refolding after bacterial expression is a complicated multi-step process (Sørensen and Mortensen, 2005; Terpe, 2006). Immunization with incorrectly folded antigens can generate responses against the primary protein structure that do not recognize conformational epitopes (Beil et al., 1973). Because of these characteristics, bacteria are usually chosen as expression hosts when the protein to be produced is relatively small and does not require post-translational modifications.

The most common bacterial host for protein expression is the *E. coli* BL21. It is non-pathogenic and is deficient in proteases, maintaining the integrity of the recombinant products (Sørensen and Mortensen, 2005).

The advantage of mammalian cells as expression hosts is the ability to carry out any necessary post-translational modifications. However, compared to bacteria, these cells have very slow growth rates and expansion of the culture volume is expensive. Also, mammalian cells do not maintain episomal plasmid DNA and stable transfection requires a long selection process. Therefore, the total yields of protein production are several folds lower than the bacterial system (Dietmair et al., 2012).

Human embryonic kidney 293T (HEK293T) and Chinese hamster ovary (CHO) cells are commonly used for protein production. These cells are easily transfectable and express relatively high amounts of protein even after transient transfection. The glycosylation patterns are similar between cells originated from different species, although there are some differences in the post-translational modifications when comparing human and hamster cells, for example, which can alter protein immunogenicity (Butler and Spearman, 2014).

This chapter describes the production of the antigens used for mouse immunization and the antibody production process that followed.

The extracellular region of CSF-1R, synthesized in mammalian cells, was correctly folded and was glycosylated. The dimerization domain, produced in bacteria, was highly expressed, but formed aggregates. Both were administered into mice, and the antibody response was monitored in the serum. In total, 4 hybridoma fusions were made for production of anti-CSF-1R monoclonals. Three of these were made having the full extracellular region of the receptor as the immunogen and one fusion was made after immunization with the dimerization domain. In the initial screens several clones were found with binding activity against the CSF-1R. The screening process is presented here. Immunization with the extracellular region led to the production of mostly IgM clones. Depleting IgM^+ B-cells through magnetic cell sorting could not prevent this. Among the few IgG generated by immunizations with the extracellular region are mAbs 1C6 and 2H1, described in Chapter 4. The dimerization domain hybridoma produced several IgG clones, among which are mAbs 3.1 and 12.2, described in Chapters 4 and 5.

7.2 Materials and methods

Basic methodological descriptions and brands not stated here are presented in Chapter 2. HotStarTaq polymerase kit and Omniscript RT kit are supplied by Qiagen. Phusion polymerase kits are supplied by Thermo Scientific. Pfu polymerase kit, dNTPs, RNAsin and GoTaq PCR Core System I Taq Polymerase are supplied by Promega.

7.2.1 Bioinformatics analyses

Sequence accession numbers were: canine CSF-1R, XM_546306; murine, AAH36343.1; human, AAH47521, NCBI; feline, ENSFCAG00000003633, Ensembl. Comparisons between the sequences were performed using Clustal Omega (http://www.ebi.ac.uk/Tools/msa/clustalo/).

Evaluation of the mRNA structure of the canine CSF-1R and HPRT (accession AY283372.1) was performed at http://rna.tbi.univie.ac.at.

7.2.2 Amplification of the canine CSF-1R

Primers for the canine CSF-1R were constructed based on the published canine genome (accession XM_546306, NCBI). The extracellular region and the dimerization domain of the CSF-1R were amplified and cloned for the purpose of expressing the proteins and performing mouse immunizations. The positioning of the primers is displayed in Figure 7.3 and in Table 7.1.

The entire CSF-1R receptor was used for expression on the cell surface and testing of antibodies by flow cytometry. Three nucleotides were added before the "ATG" in the forward primer to create a Kozak sequence (CSF1R full sequence forward, Table 7.1). The stop codon was not in the reverse primer (CSF1R full sequence reverse, Table 7.1) to allow the translation of the tags encoded by the pEF6-V5-His plasmid (Invitrogen), into which the sequence was cloned.

Canine samples were collected from animals from the Edinburgh Dog and Cat home euthanized for humane reasons. CSF-1R mRNA was obtained from canine liver. RNA extraction was conducted using RNeasy Mini Kit (Qiagen). Quality was assessed by the presence and integrity of ribosomal 28S/18S bands after electrophoresis of the sample in a 1 % agarose gel.

The initial attempt at reverse transcription of CSF-1R mRNA using oligodT priming used the Omniscript enzyme. The optimized protocol for the PCR amplification of the CSF-1R fractions is shown in Table 7.2.

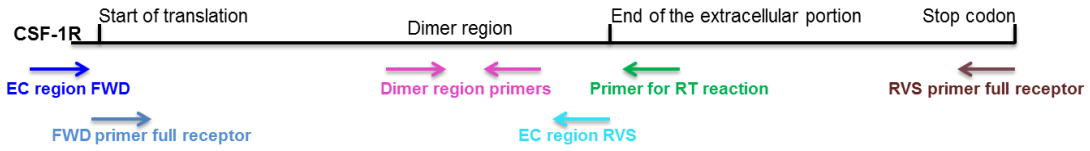

Figure 7.3 – Position of primers for the reverse transcription and amplification of the canine CSF-1R. Primers are indicated by the arrows (drawing is not to scale). The black horizontal line indicates the CSF-1R sequence with the annotated points of reference.

Table 7.1 – Primers used in this chapter. Primers shown as 5` to 3`.

Primer	Sequence	Position on the canine CSF-1R nucleotide sequence starting from ATG (where relevant)
Dimerization domain forward for pTriex1.1 ligation	AAGATAGAATTCTGACCAGCAGGCCAAACTCAAG	1028
Dimerization domain reverse for pTriex 1.1 ligation	CTTATACTCGAGTTGGGCCTCATCACATCTATCTG	1306
Dimerization domain forward for pFN2a ligation	ATTAGCGATCGCCGACCAGCAGGCCAAACTCAAGTTTGTCATCA	1028
Dimerization domain reverse for pFN2a ligation	ACGCGTTTAAACTTGGGCCTCATCACATCTATCTGTGTGG	1302
Extracellular region forward	TGTCTATCCCTCAGCCCC	-48
Extracellular region reverse	CGGCTCGTCAGGAGGCTG	1513
RT reaction primer	GATGATCTTCCAGCGCACCT	1631
CSF1R full sequence forward	ACCATGGGCCTAGGGGCTCCACTG	1
CSF1R full sequence reverse	GCAGAACTGGTAGTTGTTGGGCTGCAGCAG	2901
pTriex sequencing primer UP	GGTTATTGTGCTGTCTCATCA	/
pTriex sequencing primer DOWN	TCGATCTCAGTGGTATTTGTG	/
HPRT forward	AGCTTGCTGGTGAAAAGGAC	/
HPRT reverse	TTATAGTCAAGGGCATATCC	/
T3	GCAATTAACCCTCACTAAAGG	/
T7	TAATACGACTCACTATAGGG	/

Table 7.2 – Protocol for amplification and cloning of the CSF-1R fractions. Primers shown in Table 7.1. Wizard SV Gel and PCR Clean-Up System, pFN2a, JM109, Flexi and restriction digestion reagents (Promega). QIAquick Gel Extraction Kit, QIAprep Spin Miniprep Kit (Qiagen). pTriex 1.1 (Millipore). pEF6-V5-His TOPO plasmid and Top 10 bacteria (Invitrogen). Random nonamers (Sigma).

Full CSF-1R	Extracellular region CSF-1R	Dimerization domain (GST-tagged)	Dimerization domain (His-tagged)
Reverse transcription			
As shown to the right, exchanging the specific primer for random nonamers (10 µM).	Step 1: Mixed the RT reaction primer (20 pmol), RNA (500 ng), DMSO (to 10 %), nuclease-free water (to 5 µl). Incubated for 95°C for 5 min, then 42°C. The reaction was put on hold. Added to the same tube: 10 × RT buffer (to 1 ×), dNTPs (to 0.625 mM), RNAsin enzyme (4 U), reverse transcription Omniscript RT enzyme (4 U), DMSO (to 10 %), nuclease-free water (to 15 µl). Kept at 42°C for 1 h, then 72°C for 15 min.		
PCR			
Reaction: 5 × HF buffer (to 1 ×), dNTP (to 0.2 mM), primers "CSF1R full seq FWD/RVS" (to 0.5 µM), cDNA (1µl), Phusion polymerase (0.4 U), nuclease-free water (to 20 µl). Thermal cycling protocol: 98°C for 2 min, 35 × [98°C for 10 sec, 72°C for 2 min 35 sec], 72°C for 10 min.	Reaction: 10 × Pfu buffer (to 1 ×), dNTP (to 0.5 mM), primers "Extracellular region FWD/RVS" (to 0.25 µM), $MgCl_2$ solution (to 2 mM), cDNA (1 µl), Pfu polymerase (3 U), nuclease-free water (to 50 µl). Thermal cycling protocol: 95°C for 1.5 min, 35 × [95°C for 30 sec, 59.5°C for 30 sec, 72°C for 3.5 min], 72°C for 5 min.	Reaction: 10 × Pfu buffer (to 1 ×), dNTP (to 0.3 mM), primers "Dimerization domain forward/reverse for pFN2a ligation" (to 0.25 µM), cDNA (1µl), Pfu polymerase (3 U), nuclease-free water (to 50 µl). Thermal cycling protocol: 95°C for 1.5 min, 35 × [95°C for 30 sec, 65°C for 30 sec, 72°C for 45 sec], 72°C for 5 min.	As for the GST-tagged, but: primers "Dimerization domain forward/reverse for pTriex ligation" annealing changed to 58°C
Specific bands were extracted from gel.	Specific bands were extracted from gel.	The PCR product was purified using a PCR clean-up kit.	
Addition of adenosine overhangs		Restriction digest	Restriction digest
After gel purification, dNTP (to 0.25 µM) and 1.25 U of GoTaq polymerase were added to the PCR product. Incubated at 72°C for 15 min.		PCR digest: 5 × Flexi Digest Buffer (to 1 ×), purified PCR product (500ng), Flexi Enzyme Blend (SgfI & PmeI) (4 µl) Plasmid digest: Nuclease-free Water 12 µl, 5 × Flexi Digest Buffer 4 µl, pFN2a (200ng) 2 µl, Flexi Enzyme Blend (SgfI & PmeI) 2 µl	PCR digest: PCR product (1 µg), Buffer H (to 1 ×), acetylated BSA (0.2 µl), EcoRI (6 U), Xho I (6 U), nuclease-free water to 20 µl Plasmid digest: pTriex1.1 (500 ng), other reagents as above
PCR product was subjected to PCR clean-up, and plasmid was gel purified (except for pEF6 TOPO).			
Ligation: PCR product (4 µl), salt solution (1 µl), pEF6 TOPO vector (1 µl). Incubated at room temperature for 30 min. Transformation: Top10 chemocompetent cells.		Ligation: 2 × Flexi Ligase Buffer (to 1 ×), pFN2a, digested (50ng), PCR product (100ng), T4 Flexi DNA Ligase (HC) (20 U). Incubated at room temperature for 1 h. Transformation: JM109 chemocompetent cells.	Ligation: T4 ligase buffer (to 1 ×), pTriex1.1 (100 ng), insert (17 ng), T4 DNA ligase (0.6 U), nuclease-free water (to 20 µl). Transformation: JM109 chemocompetent cells.
The plasmids were extracted from transformed bacteria by miniprep.			

After overnight growth in LB plates with ampicillin at 37°C, colony-PCR of pEF6 + extracellular region was conducted using GoTaq DNA polymerase. Reaction protocol: $MgCl_2$ (to 1.5 mM), 5 × GoTaq buffer (to 1 ×), dNTP (to 0.2 µM), primers (same as for product amplification) (to 0.25 mM), GoTaq polymerase (0.625 U), template (colony

dilution in LB (1 µl)), nuclease-free water (to 25 µl). Thermal cycling conditions were: 95°C for 2 min, 35 × [95°C for 30 sec, 59.5°C for 30 sec, 72°C for 2 min], 72°C for 10 min.

Three positive colonies were sent for sequencing at the Sequencing Services at the University of Dundee. Primers used for sequencing the His-tagged dimerization domain were "pTriex sequencing primer UP/DOWN". The extracellular region was sequenced with primers T3 and T7 (Table 7.1, above). The GST-tagged dimerization domain was sequenced with primer T7.

7.2.3 Expression and initial purification of rCSF-1R peptides

The pEF6 vector containing the extracellular region of canine CSF-1R (EC region) was transfected into HEK293T cells using Lipofectamine 2000 (Invitrogen). Lipofectamine was titrated down from the volume indicated by the manufacturer by transfecting cells with different concentrations of the reagent (from 100 % to 25 % of the volumes indicated by the manufacturer). After standardization, 75 % of the recommended volumes of Lipofectamine were used. Cells were allowed to express the protein for 48 h before the medium was harvested and cells were lysed using RIPA buffer (NaCl (150 mM), NP-40 (1 %), DOC (0.5 %), SDS (0.1 %), Tris (50 mM), pH 8.0).

The full CSF-1R was transfected into CHO-K1-S cells using the protocol in Chapter 5.

The pFN2A and pTriex 1.1 vectors containing the dimerization domain were transformed into chemocompetent BL21 (DE3) *E. coli*. Bacteria were grown in LB medium at 37°C shaking (200 rpm) until OD_{600nm} = 0.6 and expression was induced by addition of IPTG (to 1 mM, Sigma). The bacteria were allowed to express the protein for 3 h at 37°C, and were then centrifuged (3200 × *g* for 20 min at 4°C).

For clearing the GST-tagged dimerization domain (in pFN2a), bacteria were lysed by addition of lysis buffer (Tris (20 mM), NaCl (150 mM), EDTA (1 mM), NP-40 (0.5 %), PMSF (2 mM), lysozyme (1 mg/ml, Thermo Scientific), pH 8.0) at 1:50 of the bacterial culture volume, left on ice for 30 min. This was followed by four cycles of sonication of 30 sec each with 10 sec breaks on ice and centrifugation at 9000 × *g*. The supernatant contained the desired protein.

For clearing of the His-tagged dimerization domain (in pTriex1.1), denaturing conditions were used. Buffer B (NaH_2PO_4 (100 mM), Tris-Cl (10 mM), urea (8 M), pH 8.0) was added at 1:50 of the bacterial culture volume. The bacteria were subjected to 8

sonication steps of 30 sec, done on ice, with 10 sec breaks between sonications. This was followed by centrifugation at 10000 × *g* for 30 min. The supernatant was collected.

For the test bleeds with the extracellular region, which was produced in pEF6, the tags contained in this vector were expressed alone, that is, with no insert attached. To produce the pEF6 vector tags alone, the vector was "closed" with a start codon (TOPO vectors are linearized). Two oligos were synthesized to create an insert. These were perfectly reverse and complementary with the exception of two adenosine overhangs on both ends. In conjunction, the two oligos formed a double-strand with a start codon (5` - GCTATGGTAA and 5` - ACGATACCAT). These oligos were ligated with pEF6. It was then transformed into bacteria as for the extracellular region. This plasmid was transfected into HEK293T cells by lipofection and the tags were expressed. The tags were then affinity purified from the culture supernatant as for the extracellular region.

7.2.4 Western blotting and gel stains

The expression of both protein fragments (extracellular region and dimerization domain) was verified by western blotting against the respective tags. Samples were loaded at the concentrations indicated in each figure. The pEF6 vector (containing the extracellular fraction) and pTriex 1.1 (containing the dimerization domain) expressed a His tag, and western blot probing was done under denaturing conditions using a primary mouse anti-His (1:500, Invitrogen) for 2 h at room temperature. Secondary antibody was rabbit anti-mouse, HRP-conjugated (1:1000, Dako), left for 1 h at room temperature. The pFN2A plasmid (also containing the dimerization domain) expressed the GST tag, and western blot was done using a mouse anti-GST (1:3000, Sigma) and rabbit anti-mouse, HRP-conjugated (1:3000). For determination of protein aggregation of the His-tagged dimerization domain, the proteins were mixed with non-reducing sample buffer and were not heated before loading the gel.

The extracellular region and the GST-tagged dimerization domain were resolved with 10 % acrylamide gels. The His-tagged dimerization domain was resolved with 4 – 12 % gradient NuPAGE Bis-Tris gels (Invitrogen). Where stated, gels were silver or Coomassie stained.

7.2.5 Purification of recombinant CSF-1R peptides

Transfected HEK293T cells were allowed to express the extracellular region of CSF-1R protein for 48 h before the medium was harvested and protein was purified using a native

protocol with a Ni-NTA resin (Qiagen). The purified fractions were buffer-exchanged into PBS by centrifuging and concentrating the samples in a concentrator tube containing a semi-permeable membrane (10000 MWCO, Vivascience). After adding the samples to the Centricon tube, it was centrifuged for 30 min at 3000 × *g*. The concentrated protein fraction was diluted to the original volume using PBS. The procedure was repeated 3 times to completely exchange the buffer.

The GST-tagged dimerization domain was purified using a glutathione column. The glutathione beads (1 ml, Amersham) were placed on 12 ml Poly-Prep columns (Bio-Rad). The beads were washed with GST purification buffer (Tris (20 mM), NaCl (250 mM), EDTA (1 mM), NP-40 (0.5 %), pH 8.0) to remove the storage solution and prepare for protein binding. The bacterial cell lysate was added to the column beads and incubated in a tube at 4^{o}C with agitation for 2 h. The contents were allowed to flow through the column (the "unbound" fraction). The resin was washed by the addition of 20 column volumes of GST purification buffer. The bound protein was eluted from the resin by the addition of one column volume of elution buffer thrice (Tris (100 mM), reduced glutathione (20 mM), NaCl (120 mM), pH 8.0).

The pTriex1.1 vector containing the dimerization domain was affinity purified after bacterial lysis. The supernatant was incubated with Ni-NTA resin pre-washed with Buffer B (see section 7.2.3). The resin was then washed with 20 column volumes of Buffer B at pH 6.3 to remove non-specific binders. Elution was performed with Buffer B at pH 5.9 (four elution fractions of 1 column volume) and then pH 4.5 (another four elution fractions of 1 column volume). The eluates were dialyzed against PBS four times after purification to remove the urea in 1 litre of PBS. Urea was reduced to 4 M, 2 M, 1 M and no urea. Dialysis was performed using a 3000 MWCO cellulose ester membrane (Spectrum Labs).

Protein concentration of the purified fractions was performed using the Bradford method and by spectrophotometry using a Nanodrop (Thermo Scientific) with reading at 280 nm. For spectrophotometry, the extinction coefficient of the proteins was calculated using ExPASy (web.expasy.org/protparam/). The purified proteins were aliquoted and stored at –20^{o}C until used.

7.2.6 De-glycosylation of the extracellular region

N-linked oligosaccharides were removed from the extracellular region of CSF-1R using PNGase F (Promega). The purified EC region (50 µg in 12 µl of 0.5 M sodium phosphate buffer, pH 7.5) was mixed with 1 µl SDS (5 %) and 1 µl DTT (1 M). The sample

was denatured at 95^{o}C for 5 min and was cooled at room temperature for 5 min. Sodium phosphate buffer, NP-40 (10 %) and PNGase F (2 µl each) were added to the mixture. This was incubated at 37^{o}C for 2 h. Samples were resolved in a 10 % SDS-PAGE gel and were analysed by Ponceau S staining of the proteins transferred to a nitrocellulose membrane.

7.2.7 CSF-1 binding activity

To test the capacity of the recombinant extracellular region of CSF-1R of binding to one of its ligands, CSF-1, a transparent ELISA plate (Thermo Scientific) was coated with the recombinant receptor (300 ng/well in 50 µl of PBS) overnight at 4^{o}C. The plate was also coated with BSA at the same concentration, as a control. The following day, the plate was blocked with PBS + BSA (2 %) for 1 h at 37^{o}C. rhCSF-1 (Biolegend) was added to the wells at the stated concentrations in blocking buffer and was incubated for 2 h at 37^{o}C. The plate was washed 6 × 2 min with PBST. Bound CSF-1 was detected with a biotinylated rabbit anti-human CSF-1 (1:1000, Peprotech) incubated for 2 h at 37^{o}C. After washing the plate, Streptavidin-HRP (1:10000, Thermo Scientific) was added for 30 min at room temperature. The plate was washed and the reaction was developed with 50 µl of TMB Ultra (Pierce) and was stopped with the same volume of H_2SO_4 (2 M). The developed colour was read at 450 nm using the Victor3 plate reader (Perkin Elmer).

7.2.8 Mass spectrometry

The purified His-tagged dimerization domain of CSF-1R was evaluated by mass spectrometry to assess purity and conformation status. This was performed by the Proteomics service at the Roslin Institute using amaZon ETD (Brucker). The sample was run in 8 M urea.

7.2.9 Immunization of mice and test bleeds

Mice were immunized every 21 days (extracellular fragment of CSF-1R at 15 µg/dose) or every 28 days (dimerization domain, His-tagged, at 50 µg/dose) using Freund's adjuvant (50 µl). The dimerization domain was conjugated to BSA to increase immunogenicity (performed by the Regional Centre for Applied Molecular Oncology, Masaryk Memorial Cancer Institute, Brno). Four doses were used for both antigens. Initial

doses were administered via intraperitoneal route, with adjuvant, and the last dose for each immunization was administered intravenously, without adjuvant.

The immunization using the dimerization domain was performed at the Regional Centre for Applied Molecular Oncology, Masaryk Memorial Cancer Institute, Brno, Czech Republic and the immunizations using the extracellular region were performed at the Scottish National Blood Transfusion Service, Pentlands Science Park, Penicuik, UK. The immunizations and sera collection were performed under the license of the Scottish National Blood Transfusion Service.

Serum was collected from the animals before and after the third dose of immunization. The mice sera were tested by dot blots and ELISA to assess antibody production. For testing the immune response against the extracellular region, dot blots were carried out by dotting 1 µl of the target protein on a nitrocellulose membrane (GE Healthcare Life Sciences) (protein concentration of at least 0.2 mg/ml). The membrane was then blocked in PBST + milk (5 %). The membrane was cut to separate the dots. Each of these was then incubated with a dilution of the mouse serum, from 1:400 to 1:204800 in a 1:2 progression. Secondary rabbit anti-mouse, HRP-conjugated (1:1000, Dako) was incubated for 1 h at room temperature in blocking buffer. The membranes were washed thrice with PBST after the primary and secondary antibody incubations. The substrate used for dot blot was ECL reagent (GE Healthcare), added to the membrane for 1 min.

ELISA was performed by coating the 96-well plate with 200 ng/well of the extracellular fraction of CSF-1R in 50 µl of PBS overnight at 4^{o}C. The plate was blocked with PBS + BSA (1 %) for 1 h at 37^{o}C. Serum was diluted from 1:50 to 1:800 in in PBS + BSA (0.1 %). Wells were washed 5 times with PBST (2 min each). Secondary rabbit anti-mouse, HRP-conjugated (1:1000, Dako) was used and incubated for 1 h at 37^{o}C (for the ELISA). The substrate used for ELISA was TMB Ultra (Pierce).

The dot blot for the dimerization domain was performed by the laboratory responsible for the immunizations in the Czech Republic. The technique used, therefore, differed from the one used for the immunization using the extracellular region. Dot blot was performed as follows. The membrane was wetted in PBS and afterwards covered with the protein in solution in PBS (20 µg/ml) for 1 h at 37^{o}C. The protein solution was removed and the membrane was blocked for 1 h at room temperature in DMEM complete medium (Gibco). Blocking medium was removed, the membrane was dried with blotting paper and the mouse serum was added to the membrane in 2 µl dots per sample. The membrane was incubated at room temperature in a humid environment for 1 h. Membrane was washed 3 times in PBS (5 min washes). Secondary antibody (HRP conjugated) was added and also

incubated for 1 h, at room temperature. Membrane was washed again 3 times in PBS to remove unbound secondary. Chloronaphtol (Sigma) was used as substrate, which precipitates on the membrane generating a visible blue dot on the positive samples.

7.2.10 Effect of immune serum on cellular proliferation

Either BMDM (7×10^3 cells/well), REM134 cells (5×10^3 cells/well) or Ba/F3 cells (2×10^4 cells/well) were plated in 100 µl of media in black opaque 96-well plates. Ba/F3 cells expressed either the ovine or the swine CSF-1R and were dependent on signalling through this receptor for survival. Produced by Lindsey Waddell and Anna Raper (The Roslin Institute) (L. Moffat et al., 2014). Cells were treated with pre-immune/immune serum from mice immunized against the extracellular regions of CSF-1R. BMDM and Ba/F3 cells were treated with serum at 1:2000 in DMEM medium. REM134 cells were treated with serum at different concentrations. BMDM received rhCSF-1 (Invitrogen) at 20 ng/ml. Where indicated, CSF-1 was added to the other cells at 100 ng/ml. All Ba/F3 cells also received IL-3 (5 % of conditioned medium from X63 cells expressing IL-3, provided by Lindsey Waddell). All cells were grown for 48 h in the presence of the serum and cell viability was assessed using CellTiter-Glo (Promega).

7.2.11 Hybridoma fusions

Sp2/0 mouse myeloma cells were selected in 8-azaguanine (Sigma) for one week before fusions to ensure that the HGPRT pathway was defective. Sensitivity to HAT supplement (Invitrogen) was tested after selection by adding HAT containing medium and evaluating cellular survival over two days. Absence of mycoplasma in the Sp2/0 was tested using MycoAlert (Lonza).

The fusion using the animals immunized with the dimerization domain of CSF-1R was performed by the Regional Centre for Applied Molecular Oncology, Brno. The fusions using the animals immunized with the EC region of CSF-1R were made using a protocol adapted from several sources (Clonacell; Harlow and Lane, 1988), and is shown in Annex 1. Three fusions were performed from mice immunized with the extracellular region of CSF-1R. The hybridoma fusions 1 and 2 used semi-solid medium (medium D) containing HAT selection supplement for colony growth after fusion. All cells were diluted in 10 × 96-well plates after fusion number 3, containing 200 µl of DMEM with HAT. Magnetic cell exclusion of IgM cells was used for the second fusion with the extracellular region of CSF-

1R, as published elsewhere (Apiratmateekul et al., 2009) and as detailed in the Annex. Fusions were performed two days after the last dose of antigen.

7.2.12 Screening the hybridoma fusions

Screening of the resulting clones from fusion number 1 for the EC region and for the dimerization domain was done by dot blot following the protocol described above for screening the immune serum for the dimerization domain (section 7.2.9), with the difference that the colour substrate used was DAB-HCl (Sigma) (DAB (0.05 %), H_2O_2 (0.015 %) in PBS). Isotyping was performed by dotting the hybridoma supernatant on a membrane coated with an anti-mouse immunoglobulin [no HRP] (1:1000, Dako) and detecting the bound hybridoma antibody with anti-mouse IgG or IgM, HRP-conjugated (1:1500, Southern Biotech). The mouse immune serum (1:4000) was used as a positive control.

Screening of hybridomas 2 and 3 for the EC region was done by ELISA. Plates were coated with the EC CSF-1R and tested similarly to the mouse serum, above (section 7.2.9). The mouse immune serum (1:4000) was used as a positive control. The secondary antibody was used as the negative control.

For the hybridoma 3 for the EC region, positive clones in the initial ELISA were tested for cross-reactivity to BSA by coating wells with the same concentration of BSA and testing the same hybridoma antibody in both CSF-1R/BSA coated wells. IgG or IgM production was tested by coating the plate with an anti-mouse immunoglobulin [no HRP] (1:1000, Dako). The hybridoma supernatants were incubated in the wells and the bound isotype was detected by adding anti-mouse IgG or IgM, HRP-conjugated (1:1500, Southern Biotech). The IgG positive control (and also IgM negative control) was a murine IgG_1 isotype control (1:1000, Abcam). The IgM positive control (and also IgG negative control) was a murine IgM isotype control (1:1000, eBioscience).

For flow cytometry, CHO-K1-S cells were transfected with the full canine CSF-1R receptor using Lipofectamine, as described in Chapter 5. Transfected and non-transfected cells (10^6/test) were incubated with the hybridoma supernatants on ice for 30 min. Cells were washed 3 × on ice cold PBS and incubated for 30 min on ice with an anti-mouse, Alexa 488-conjugated secondary antibody (1:800, Invitrogen). The positive control was the serum of mice immunized with the extracellular CSF-1R, diluted 1:4000 in PBS. The cells were analysed on a FACScalibur flow cytometer (Becton Dickinson). The results were analysed using Summit 4.1 software (Dako).

7.2.13 Subcloning

Subcloning was carried out by laying 200 cells of each desired clone into a well of a 96-well plate. The cells were sequentially diluted 1:2 in medium for 12 wells. Individual clones after 10 days were and re-screened by dot blot, as above, and by functional assays (Chapter 4).

Isotyping of the subclones was carried out by resolving the hybridoma supernatants by SDS-PAGE and detecting the isotype using rabbit anti-mouse IgG or IgM, HRP-conjugated (1:1500, SouthernBiotech). Isotyping of the most relevant clones was confirmed using IsoQuick IgG strips (Sigma).

7.2.14 Antibody purification by protein G chromatography

The antibodies from the hybridomas were purified using Protein G Sepharose 4 Fast Flow (GE Healthcare). The resin (500 µl) was placed in a 12 ml Poly-Prep Chromatography Column (BioRad). Twenty volumes of sodium phosphate equilibration buffer (Na_3PO_4 (20 mM), pH 7.0) were run through the column to remove the storage buffer. The hybridoma was grown in low-IgG FBS (Gibco) for 3 days and the culture supernatant was collected, centrifuged at 400 × *g* and was incubated with the resin for 30 min. The supernatant was allowed to flow through the column with the unbound fraction. Non-specific binders were removed by washing the resin with 40 column volumes of the sodium phosphate buffer. One column volume of glycine elution buffer (0.1 M, pH 2.7) was added in each of four steps to remove the IgG from the resin. Tris-HCl (1 M, pH 9.0), was added to the eluates at 130 µl/ml to neutralize the acidity.

After purification, protein concentration was assessed using Nanodrop 2000 (Thermo Scientific) at 280 nm using the extinction coefficient for IgG set in the software of the equipment. The blank point for measurement was set using the neutralized elution buffer.

7.2.15 Statistical analyses

The effect of immunized murine serum on REM134 proliferation was analysed by two-way ANOVA with a Bonferroni post-test. Its effect on BMDM was analysed by Mann-Whitney. Its effect on Ba/F3 proliferation was analysed by Student's t-test. For all tests, $P < 0.05$. The assumption tests were performed on Minitab 16 (Minitab Inc.). The statistical tests and graphs were made on GraphPad Prism 5 (GraphPad Inc.).

7.3 Results

7.3.1 The extracellular region of the canine CSF-1R differs from that of mice and humans

This project intended to identify an antibody against the extracellular region of canine CSF-1R. Therefore it was relevant to identify if existing antibodies generated for other species were likely to already target the canine receptor. Dog (*Canis familiaris*), mouse (*Mus musculus*), human (*Homo sapiens*) and cat (*Felis catus*) possess similar CSF-1R, comprised of 967 – 982 amino acids, with the biggest differences between the primary structures occurring up to the 540th amino acid of the mouse sequence. These amino acids correspond mainly to the five immunoglobulin domains which constitute the extracellular portion of the protein (NCBI/Dog Genome Project) (Table 7.3). As expected, the feline and canine sequences are the most similar among these species, while the mouse is the most diverse from the dog (Figure 7.4).

Table 7.3 – CSF-1R inter-species variation is derived from differences in the extracellular region. Identity matrix between the CSF-1R sequences of different species (NCBI and Ensembl), comparing either the entire receptor or the intra/extracellular regions. Values indicate the percentage identity between the amino acid sequences. Obtained with Clustal Omega.

CSF-1R				
	Mouse	Human	Dog	Cat
Mouse	100.00	75.03	76.40	75.82
Human	75.03	100.00	84.47	84.31
Dog	76.40	84.47	100.00	89.04
Cat	75.82	84.31	89.04	100.00
Intracellular region of the CSF-1R				
	Mouse	Human	Dog	Cat
Mouse	100.00	91.70	91.45	89.91
Human	91.70	100.00	94.96	94.12
Dog	91.45	94.96	100.00	96.72
Cat	89.91	94.12	96.72	100.00
Extracellular region of the CSF-1R				
	Mouse	Human	Dog	Cat
Mouse	100.00	60.39	62.94	62.94
Human	60.39	100.00	75.44	75.83
Dog	62.94	75.44	100.00	82.16
Cat	62.94	75.83	82.16	100.00

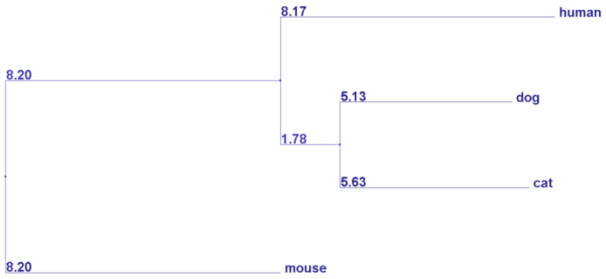

Figure 7.4 – Neighbour joining tree of CSF-1R. Branches are calculated based on the percent distance between two species in relation to the amino acid sequence of CSF-1R. Constructed using Clustal Omega. Sequences from NCBI and Ensembl.

7.3.2 Cloning and expression of the canine CSF-1R extracellular region

Messenger RNA (mRNA) was obtained from canine liver. As seen in Figure 7.5 A, the canine CSF-1R RNA has several folds and sub-folds of high affinity binding. This can cause early termination or "slippage" of the reverse transcription, where large folds of RNA are skipped by the cDNA synthesis machinery (Zhang et al., 2001). When comparing to HPRT, as a control, it can be seen that the entropy in the CSF-1R mRNA is considerably higher (Figure 7.5 B). While amplification of HPRT was possible using oligodT priming, the same approach yielded no results for amplification of CSF-1R by PCR (Figure 7.6). Thus, a primer was used to perform specific cDNA synthesis with a starting point close to the extracellular region. The RNA strand was denatured at a higher temperature to break the folds.

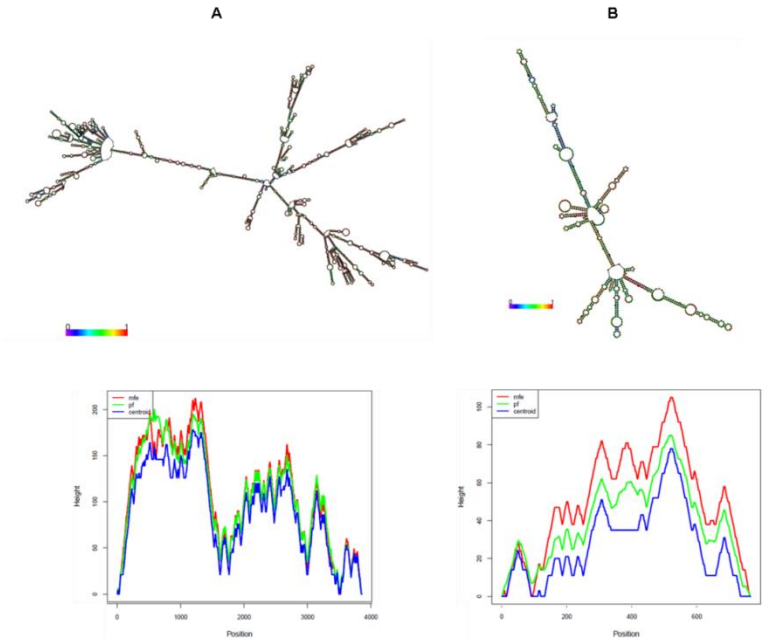

Figure 7.5 – The canine CSF-1R mRNA showed high folding and entropy. **(A)** Canine CSF-1R mRNA structure (above) and the mountain plot of the entropy (below) (NCBI accession number XM_546306). **(B)** Canine HPRT mRNA (accession AY283372.1), showed for comparison. CSF-1R showed greater number of folds, with higher entropy. The colours on the linear sequence of mRNA indicate higher (red dots) or lower (purple dots) affinity clamps. On the mountain plot, the y-axis indicates entropy. The x-axis shows the nucleotide numbering of the respective sequences. The three colours on the mountain plots indicate three possible models for entropy calculation (Gruber et al., 2008). Constructed with http://rna.tbi.univie.ac.at.

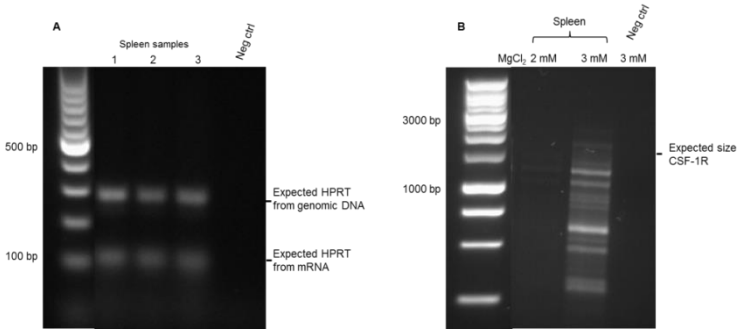

Figure 7.6 – The extracellular region of CSF-1R could not be amplified using oligo-dT priming. Total mRNA was extracted from canine spleen and cDNA was created using OligodT (Promega) and Omniscript RT Kit (Qiagen). **(A)** Amplification of HPRT from three spleen samples (primers "HPRT forward/reverse". **(B)** CSF-1R amplification (primers "Extracellular region forward/reverse") using cDNA template from spleen sample 1. Rows in (B) show different magnesium concentration in the PCR reaction. "Neg ctrl" is the no-template control. The expected size of each PCR product is indicated.

When cDNA was synthesized using a specific primer for the canine CSF-1R, the fraction of cDNA correspondent to the extracellular region of this receptor could be amplified by PCR. In an attempt to facilitate the PCR, various concentrations of dimethyl sulfoxide (DMSO) were tested. However, it was found that the reaction was better developed in the absence of this substance (Figure 7.7).

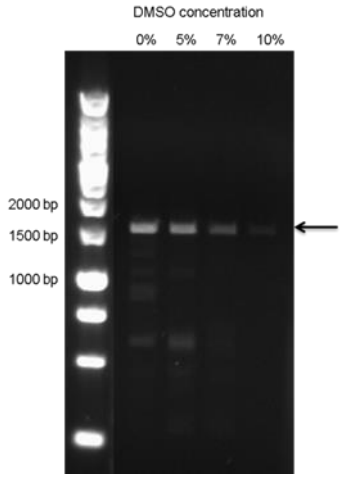

Figure 7.7 – The extracellular portion of CSF-1R was amplified after the primer-specific RT reaction. Total mRNA was extracted from canine spleen and cDNA was created using "RT reaction primer" and Omniscript RT Kit (Qiagen). PCR reaction for CSF-1R (primers "EC region FWD" and "EC region RVS") was tested using different concentrations of DMSO (0-10%). The arrow indicates the product that corresponded to the CSF-1R.

The extracellular region of CSF-1R was ligated into the pEF6-V5-His TOPO vector, creating a construct of the CSF-1R extracellular region attached to a V5-His tag. The correct placement of the insert in the vector was confirmed by sequencing the samples. The results showed that between the obtained CSF-1R sequence and the expected sequence (NCBI) there were only a few changes in isolated bases, which lead to a change in a single amino acid (Figure 7.8).

```
Predicted   MGLGAPLVLLVATAWHVRGVPVIEPRGPELVVEPGTAVTLRCVGNGSVEWEGPISPHWNL 60
Sequenced   MGLGAPLVLLVATAWHVRGVPVIEPRGPELVVEPGTAVTLRCVGNGSVEWEGPISPHWNL 60

Predicted   DPDSPSSILSTNNATFLNTGTYRCTEPGSPLGGSATIHIYVKDPVRPWKVLTQEVTVLEG 120
Sequenced   DPDSPSSILSTNNATFLNTGTYRCTEPGSPLGGSATIHIYVKDPVRPWKVLTQEVTVLEG 120

Predicted   QDALLPCLLTDPALEAGVSLMRVRGRPVLRQTNYSFSPWYGFTIHKAQFTETQGYQCSAR 180
Sequenced   QDALLPCLLTDPALEAGVSLMRVRGRPVLRQTNYSFSPWYGFTIHKAQFTETQGYQCSAR 180

Predicted   VGGRTVTSMGIWLKVQKVIPGPPTLTLKPAELVRIQGEAANIECSASNVDVNFDVFLQHE 240
Sequenced   VGGRTVTSMGIWLKVQKVIPGPPTLTLKPAELVRIQGEAANIECSASNVDVNFDVFLQHE 240

Predicted   DTKLTIPQQSDFQGNQYQKVLTLELDHVGFQDAGNYTCVATNVRGISSTSMIFRVVESAY 300
Sequenced   DTKLTIPQQSDFQGNQYQKVLTLELDHVGFQDAGNYTCVATNVRGISSTSMIFRVVESAY 300

Predicted   LNLTSEQSLLQEVTVGEKVDLQVKVEAYPSLEGYNWTYLGPFSDQQAKLKFVITKDTYRY 360
Sequenced   LNLTSEQSLLQEVTVGEKVDLQVKVEAYPSLEGYNWTYLGPFSDQQAKLKFVITKDTYRY 360

Predicted   TSTLSLPRLKPSEAGRYSFLARNTRGGDSLTFELTLLYPPEVRITWTTVNGSDALLCEAS 420
Sequenced   TSTLSLPRLKPSEAGRYSFLARNTRGGDSLTFELTLLYPPEVRITWTTVNGSDALLCEAS 420

Predicted   GYPQPNVTWLQCRGHTDRCDEAQALVLEDSYSEVLSQEPFHKVIVHSLLAMGTMEHNMTY 480
Sequenced   GYPQPNVTWLQCRGHTDRCDEAQALVLEDSYSEVLSQEPFHKVIVHSLLAMGTMEHNMTY 480

Predicted   ECRALNSVGNSSQAFRPIPIGAHI 504
Sequenced   ECRALNSVGNSSQAFRPISIGAHI 504
```

Figure 7.8 – The canine extracellular CSF-1R differed by one amino acid from the predicted sequence (NCBI, accession number XM_546306). The figure shows the amino acid sequence of the extracellular region of CSF-1R after cloning with the pEF6 vector (shown as "Sequenced" in the figure). The highlight indicates where the obtained sequence varied from the predicted sequence. Alignment made with Clustal Omega.

Expression of the extracellular fraction of CSF-1R was conducted in HEK293T cells. A titration of Lipofectamine 2000 was made to assess the amount of the reagent required to successfully transfect the cells. The volume of Lipofectamine used for transient protein expression could be reduced to 75 % of the recommended amount. The extracellular region of CSF-1R was successfully expressed; a large proportion of the protein was secreted by the cells into the culture medium, since the recombinant extracellular fraction did not include a transmembrane region (Figure 7.9).

The predicted size of the extracellular region of CSF-1R, based on its amino acid composition, was of 61 kD. However, the bands observed on western blot were between 76 kD and 102 kD. The difference in size and the diffuse form of the bands indicate that the recombinant protein was glycosylated (Figure 7.9).

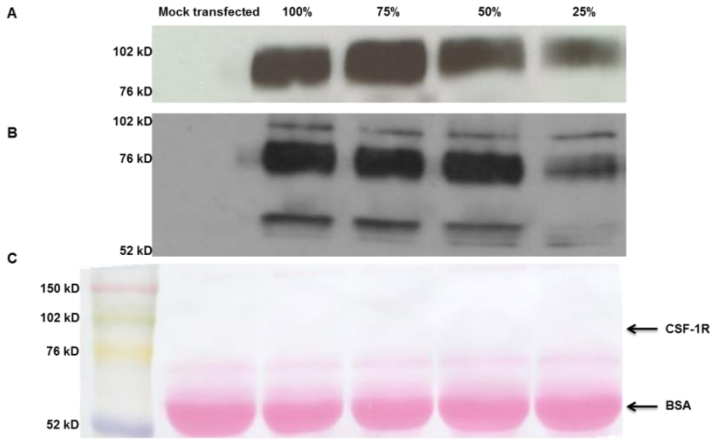

Figure 7.9 – Expression of CSF-1R extracellular region by transient transfection of HEK293T cells. The amount of Lipofectamine 2000 (Invitrogen) for transfecting HEK293T cells was reduced from the recommendation of the manufacturer (from 100 % to 25 % of the recommended volume). Cells were lysed with RIPA buffer. Cell protein (20 µg) and culture supernatant (30 µl) were loaded under denaturing conditions in a 10 % SDS gel. **(A)** Western blot detection of the His tag on the culture supernatant **(B)** Detection of the His tag in the transfected cells. Western blot was performed with mouse anti-His tag (1:500, Invitrogen) and a secondary rabbit anti-mouse Ig, HRP-conjugated (1:1000, Dako). **(C)** Ponceau red staining of the nitrocellulose membrane loaded with the culture supernatant, shown as a loading control for the supernatant. The expected size of BSA and the size of extracellular region of CSF-1R (as seen on western blot) are indicated by the arrows.

The extracellular region of CSF-1R was purified by affinity chromatography using a resin containing nickel-agarose, which binds to the His tag present in the vector pEF6. A single affinity chromatography step was sufficient to extract the CSF-1R extracellular region from the culture supernatant with the purity required for immunization (Figure 7.10). Purification of the recombinant protein from the transfected cells yielded reduced amounts when compared to the culture supernatant, and affinity chromatography was insufficient to remove contaminants. Therefore, CSF-1R extracellular region was routinely purified from the culture medium supernatant.

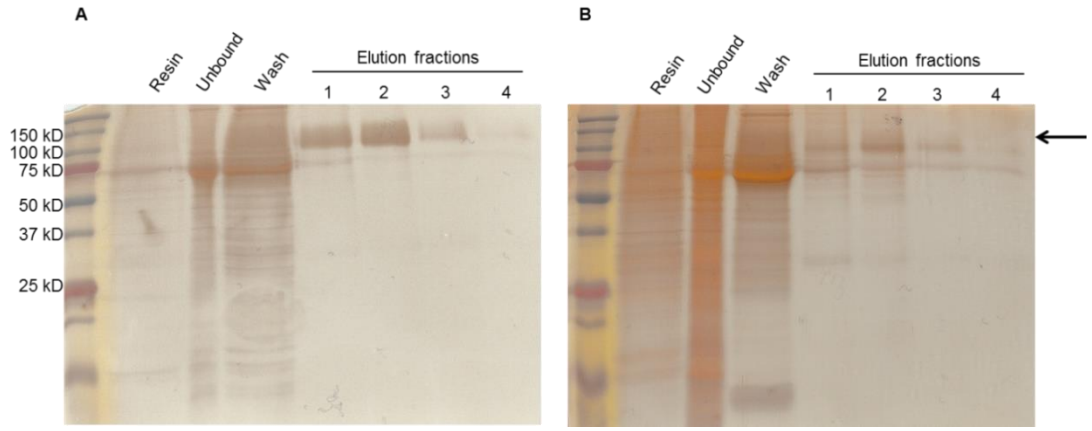

Figure 7.10 – Purification of recombinant CSF-1R extracellular region. **(A)** Silver stain of SDS-PAGE resolved fractions from the purification of the extracellular region of CSF-1R from the tissue culture supernatant of transfected HEK293T. Proteins were resolved under denaturing conditions with 10 % gel. Notice purified bands in the elution fractions. **(B)** Purification steps from the transfected cells. The lanes show proteins still bound to the resin after elution (labelled as "Resin"), the flow-through contents from the resin with unbound proteins ("Unbound"), the fraction of proteins removed by washing ("Wash") and the purified CSF-1R in the elution fractions ("Elution fractions"). Lanes were loaded with 30 µl/well of each sample. The arrow indicates the size of the CSF-1R protein, as determined by western blot.

The glycosylation status of the purified extracellular region of CSF-1R was confirmed by removing *N*-linked oligosaccharides from purified CSF-1R extracellular region with the enzyme *N*-Glycosidase F. The difference in size between glycosylated and deglycosylated CSF-1R was evaluated by resolving the digested and the control undigested CSF-1R by SDS-PAGE, transferring to a nitrocellulose membrane and staining the proteins using Ponceau red. After deglycosylation, the size of CSF-1R extracellular region corresponded to the expected from the amino acid sequence, 61 kD (Figure 7.11).

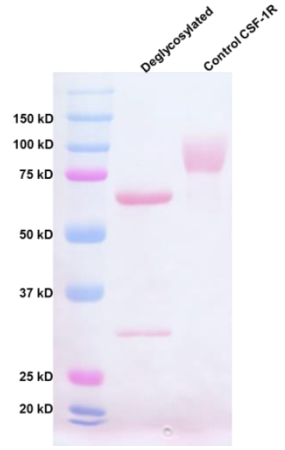

Figure 7.11 – The recombinant extracellular region of CSF-1R was glycosylated. The recombinant protein was digested with PNGase F and the resulting difference in molecular size was evaluated by SDS-PAGE separation of the deglycosylated and control CSF-1R. The band around 30 kD is expected to be the PNGase F enzyme.

The correct folding of the recombinant extracellular region of CSF-1R was tested by assessing its capacity to bind to CSF-1. The receptor bound sensitively to increasing concentrations of the ligand, whereas no CSF-1 was bound to BSA, as a control (Figure 7.12).

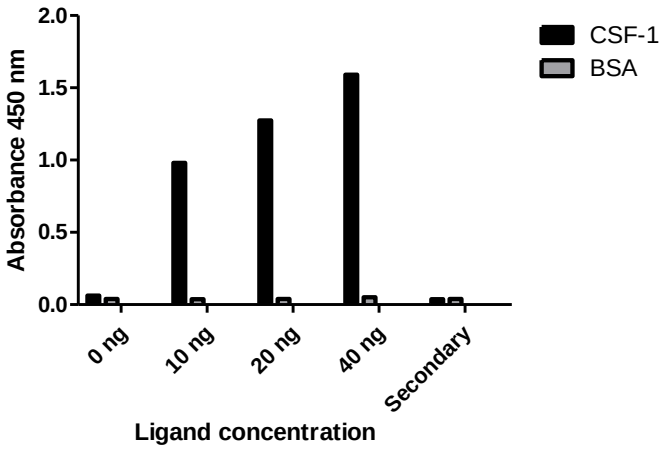

Figure 7.12 – The recombinant extracellular region of CSF-1R was folded to a functional state. Either the recombinant CSF-1R extracellular region or BSA (control) (300 ng/well in 50 µl PBS) was used to coat an ELISA plate. rhCSF-1 (Biolegend) was added at three concentrations and unbound ligand was washed away. Bound ligand was detected using a rabbit anti-CSF-1, biotinylated (1:1000, Peprotech). CSF-1R bound to CSF-1 in a dose-dependent manner. Streptavidin-HRP (1:10000, Thermo Scientific) was used to detect the reaction. "Secondary" indicates the secondary streptavidin-HRP control.

7.3.3 Cloning and expression of the canine CSF-1R dimerization domain

The dimerization domain of CSF-1R was amplified using cDNA produced as described for the extracellular region. The dimerization domain was PCR-amplified using two pairs of primers, either for insertion into pFN2a, a vector containing a GST tag, or into pTriex1.1, which contains a His tag (Figure 7.13). The insertion into the vectors was confirmed by sequencing.

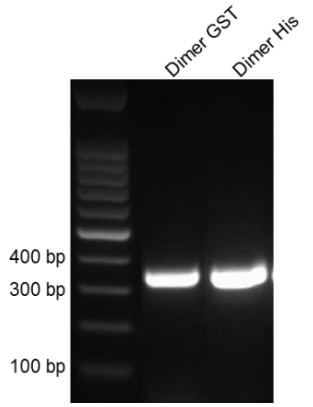

Figure 7.13 – Amplification of the dimerization domain of CSF-1R. The dimerization domain was amplified with primers for insertion into pFN2a, which couples the peptide to a GST tag (primers "Dimerization domain forward/reverse for pFN2a ligation") or pTriex1.1, which couples the peptide to a His tag (primers "Dimerization domain forward/reverse for pFN2a ligation").

The His-tagged dimerization domain protein was expressed in BL21 (DE3) *E. coli* and was affinity purified by nickel chromatography. After solubilisation of the protein from the bacteria under denaturing conditions (8 M urea), purification was carried out also in the presence of urea. Protein elution from the nickel resin was done by acidifying the resin. Affinity purification was able to enrich for the desired protein, although some contaminants were still present after a single round of chromatography (Figure 7.14).

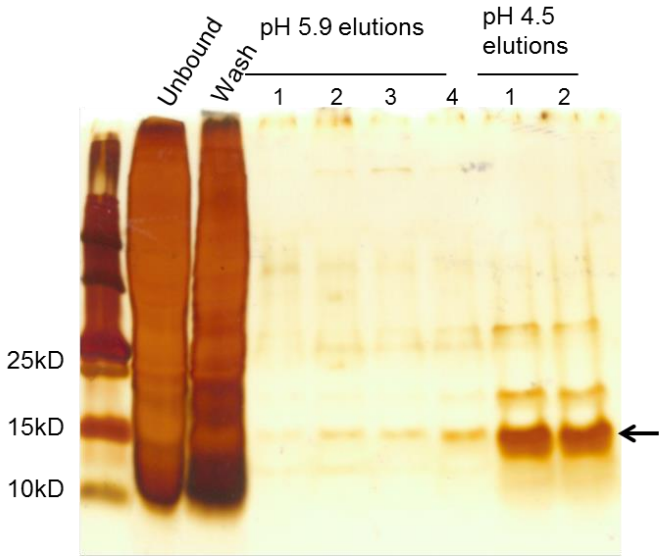

Figure 7.14 - Purification of the His-tagged dimerization domain of CSF-1R. Protein was purified from BL21 (DE3) bacteria under denaturing conditions. The protein was affinity-purified in urea (8 M) and eluted by acidifying the resin. pH 5.9 and 4.5 were tested for protein elution, as shown in the figure. Proteins (30 µl/sample) were resolved in denaturing conditions in a 4 – 12 % Bis-tris-PAGE gel and were detected by silver staining. The expected size for the His-tagged dimerization domain is indicated by the arrow. Non-specific proteins which did not adhere to the resin are shown as "Unbound". Proteins washed away from the resin are shown in "Wash".

However, the recombinant His-tagged dimerization domain formed aggregates even in the presence of 8 M urea. Resolving the protein with or without reducing conditions demonstrated the presence of several bands higher than the original 15 kD dimer domain in non-reducing conditions (Figure 7.15 A). In order to allow the purified protein to be used for immunization, urea was removed by sequential dialysis in solutions with lower concentrations of urea. The level of protein aggregation was maintained also after urea removal, although at low levels, since these multimers could not be detected by silver stain (Figure 7.15 B).

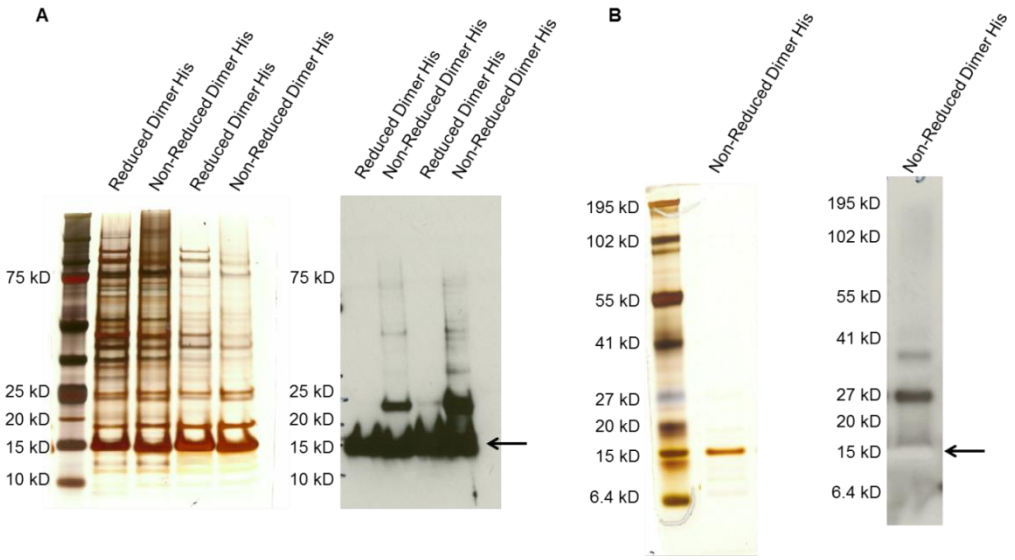

Figure 7.15 - The His-tagged dimerization domain formed multimers. **(A)** Samples in the presence of 8 M urea, after affinity purification. Samples in reducing and non-reducing conditions (20 µl of each sample) were resolved with 4 – 12 % Bis-Tris PAGE and were detected using silver stain and western blot. The His tag was detected in western blot using mouse anti-His (1:500, Invitrogen). Secondary antibody was rabbit anti-mouse, HRP-conjugated (1:1000, Dako). **(B)** Purified fractions of dimer-His were dialyzed to remove the urea from the buffer. The resulting protein band is shown in silver staining and western blot detecting the His tag. Notice that the 15 kD band had depleted the luminescent signal in the western blot ("ghost band") and there are multimers at 27 kD and ~ 35 kD that cannot be seen on the silver stain. The expected size for the His-tagged dimerization domain is shown by the arrows.

The protein aggregation was confirmed by mass spectrometry of the samples in 8 M urea (samples shown in Figure 7.15 A, above). However, no discrete peak could be identified. A large plateau was distinguishable, with a left shift that indicated the presence of a His tag in all the peptides present (Figure 7.16). Therefore, mice that were immunized with the dimerization domain received not only the pure monomer form of the peptide, but also associated multimers, as even purified fractions contained aggregates.

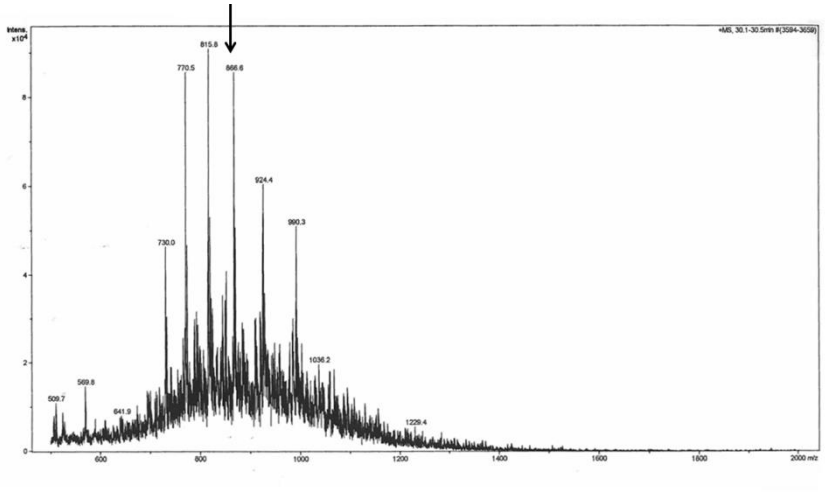

Figure 7.16 – The His-tagged dimerization domain showed multiple aggregates by mass spectrometry. The sample from Figure 7.15 A was analysed by mass spectrometry under denaturing conditions. The peak indicated by the arrow has the molecular weight of 13.8 kD, similar to the expected size of the His-tagged dimerization domain. Notice the contaminant proteins surrounding that peak, probably of aggregates of the dimerization region.

For the screening of the hybridoma from mice immunized with the His-tagged dimerization domain, this fraction of the CSF-1R was also expressed with the vector pFN2a (Promega), containing the GST tag. The vector was transformed into BL21 (DE3) bacteria. The protein was expressed and purified by affinity chromatography in a column containing glutathione resin, which binds to the GST tag present in the pFN2A vector (Figure 7.17). The complete solubilisation of the protein after bacterial production required sonication steps that denatured the GST tag, reducing binding of the protein to the resin. Significant amounts of the recombinant protein were lost during the binding and washing steps. Complete removal of contaminant proteins could not be accomplished after a single affinity purification round.

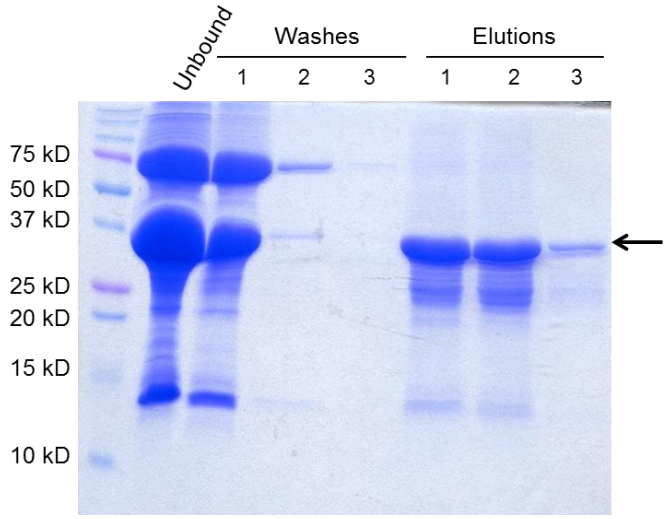

Figure 7.17 - Purification of the GST-tagged dimerization domain of CSF-1R. BL21 (DE3) bacteria expressed the GST-tagged dimerization domain. The protein was extracted from bacteria by sonication and was affinity purified. The purification steps (30 µl of each sample) were resolved by SDS-PAGE (10 % gel) and proteins were detected by Coomassie stain. Non-specific proteins that did not adhere to the resin are shown as "Unbound" in the figure. Proteins washed away from the resin are shown in the rows marked "Washes". Elution was carried out in several steps by the addition of free reduced glutathione, shown in the rows marked "Elutions". The expected size of GST-tagged dimerization domain is indicated by the arrow. The contaminants of lower molecular weight could not be removed by washing or repeated GST purification.

7.3.4 Test bleed

Sera from the four mice immunized with the recombinant extracellular portion of the CSF-1R protein were tested for the production of antibodies by dot blots (Figure 7.18) and ELISA (Figure 7.19). Post-immunization sera were compared to the pre-immunization sera. There was a strong immune response following immunization, and reactive titres against the CSF-1R recombinant protein could be detected until the last serum dilution tested, at 1:204800.

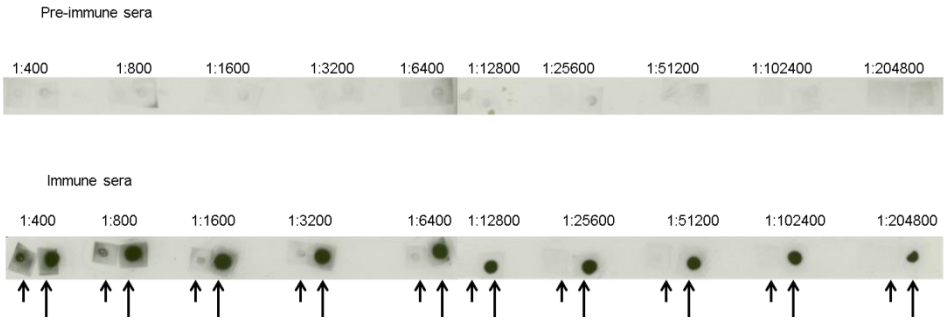

Figure 7.18 – Immunization against the extracellular region of CSF-1R induced antibody production as assessed by dot blot. Serological response was tested against the target protein (extracellular region of CSF-1R) [long arrow at each dilution] or against the V5-histidine tag only [short arrow at each dilution] before and after the immunizations. The target protein and tag were dotted on the membrane (1 µl) and probed using the immunized/pre-immune mouse sera in the dilutions shown. Notice the strong reaction of immunized sera against the CSF-1R. Secondary antibody was rabbit anti-mouse, HRP-conjugated (1:1000, Dako). This is a representative result of one of the four mice tested.

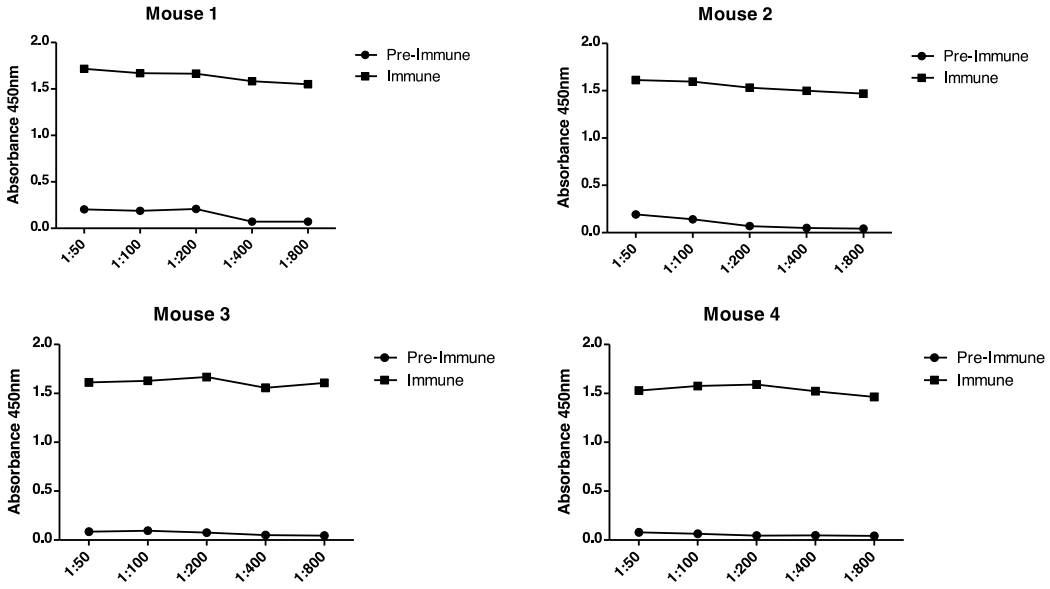

Figure 7.19 – Immunization against the extracellular region of CSF-1R induced antibody production as assessed by ELISA. CSF-1R extracellular region was coated onto ELISA plates (200 ng/well in PBS). Sera from mice were serially diluted and were tested against CSF-1R, with positive results from all animals. The bound complex was detected using rabbit anti-mouse Ig, HRP-conjugated (1:2000, Dako).

The sera of mice immunized against the extracellular region (EC) of CSF-1R were also tested for the capacity to inhibit the proliferation of CSF-1R^{+} cells. When added to REM134 cells, the immune sera induced reduction in the cell viability at some concentrations. The difference was statistically significant in an overall analysis of the dilutions for the sera of two mice (2 and 3). In the individual analysis of each dilution, the difference was significant in two points (mice 1 and 3). However, the results were not consistent with serum concentration, as some effects were only seen at low serum doses. The immune serum of mouse 4 (at 1:2000) had no effect on BMDM cellular viability and increased proliferation of Ba/F3 cells expressing the swine CSF-1R (Figure 7.20).

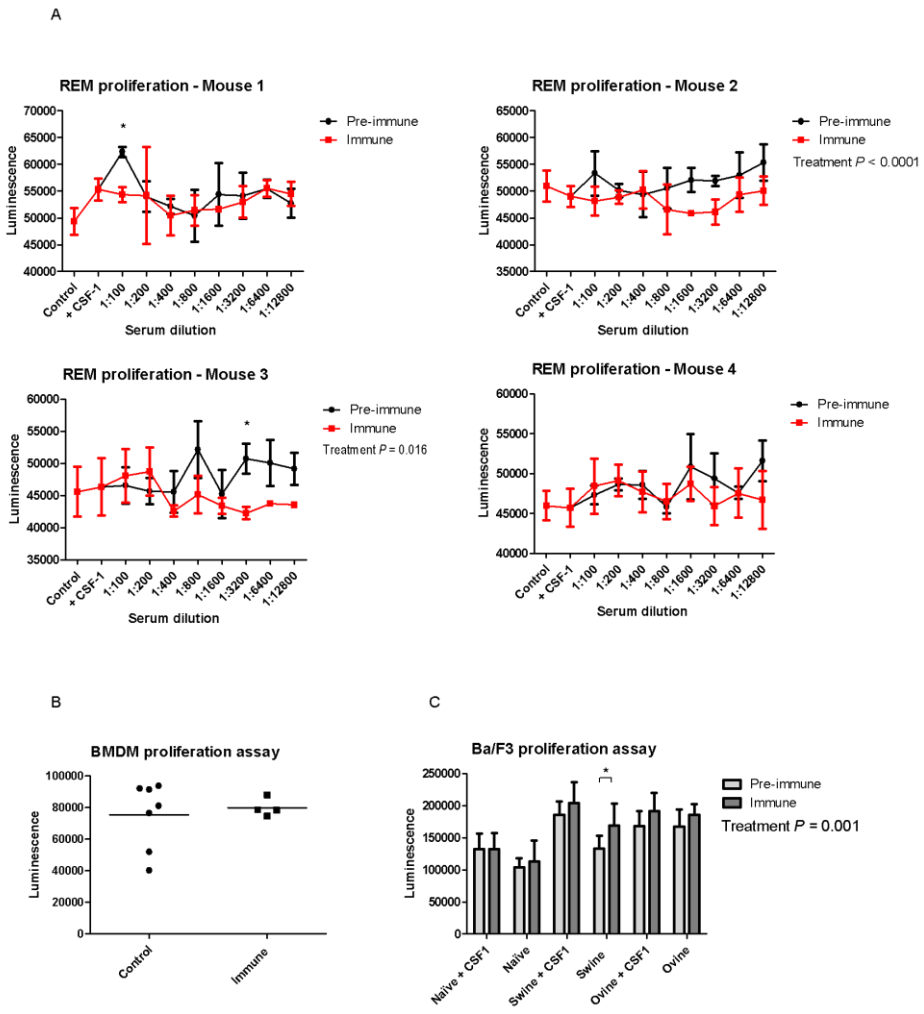

Figure 7.20 – Effect of sera of mice immunized against the extracellular CSF-1R on cells expressing the receptor. **(A)** REM134 cells were treated with different concentrations of the (pre-)immune sera of 4 mice, diluted from 1:100 to 1:12800. Control wells received rhCSF-1 (100 ng/ml, Invitrogen). Statistical differences in an individual dilution are shown by an asterisk. The overall effect of the treatment is shown next to the figure legends, when present, as analysed by two-way ANOVA with a Bonferroni post-test. The effects of the immune sera were inconsistent. **(B)** BMDM cells were grown with rhCSF-1 (20 ng/ml) and were treated with the immune serum of mouse 4 at 1:2000. Analysed by Mann-Whitney. **(C)** Ba/F3 cells expressing the swine, ovine or no (naïve) CSF-1R were treated with the (pre-)immune serum of mouse 4 at 1:2000. Where indicated, cells received CSF-1 (100 ng/ml). All Ba/F3 cells received IL-3. Immune sera induced Ba/F3 proliferation. Statistical difference between treatments by two-way ANOVA with a Bonferroni post-test is indicated by an asterisk. The statistic relevance of the overall effect of the treatment is indicated next to the figure legend. All cells were incubated for 48 h with the treatments. Proliferation results as measured by luciferase activity (CellTiter-Glo, Promega).

The sera of the two mice immunized with the His-tagged dimerization domain of the canine CSF-1R were tested by dot blot and the reaction was developed with a colorimetric method (Figure 7.21). Serological responses were apparent after immunizations, although the antibody titres were lower than those seen after the inoculations with the extracellular region of CSF-1R.

Figure 7.21 – Dot blot test of the immune mouse sera against the dimerization domain. The His-tagged dimerization region was used to coat a nitrocellulose membrane (20 µg/ml). The murine sera were serially diluted and dotted onto the membrane. Bound antibody was detected using an anti-mouse Ig, HRP-conjugated secondary. The dot blot reaction was developed with chloronaphtol [blue colour] (Sigma).

7.3.5 Hybridoma screening

As presented above, mice were immunized with one of two antigens from the canine CSF-1R: either the full extracellular region or the dimerization domain of CSF-1R. After the fusion of the spleen of the mice with the myeloma cell line (fusions were performed at different time points for each mouse and antigen), the hybridoma culture supernatants were screened for the presence of antibodies that reacted against the target protein (either the dimerization domain or the extracellular region of CSF-1R).

The first hybridoma fusion for the extracellular region of CSF-1R and the only fusion for the dimerization domain were screened by dot blot; for this, membranes were coated with the recombinant GST-tagged dimerization domain or extracellular region, respectively.

The overall antibody production (regardless of specificity) was also tested to assist in the choice of the clones to be selected. The antibodies that bound to the antigens were then analysed to detect the isotype (IgM or IgG) (Figure 7.22).

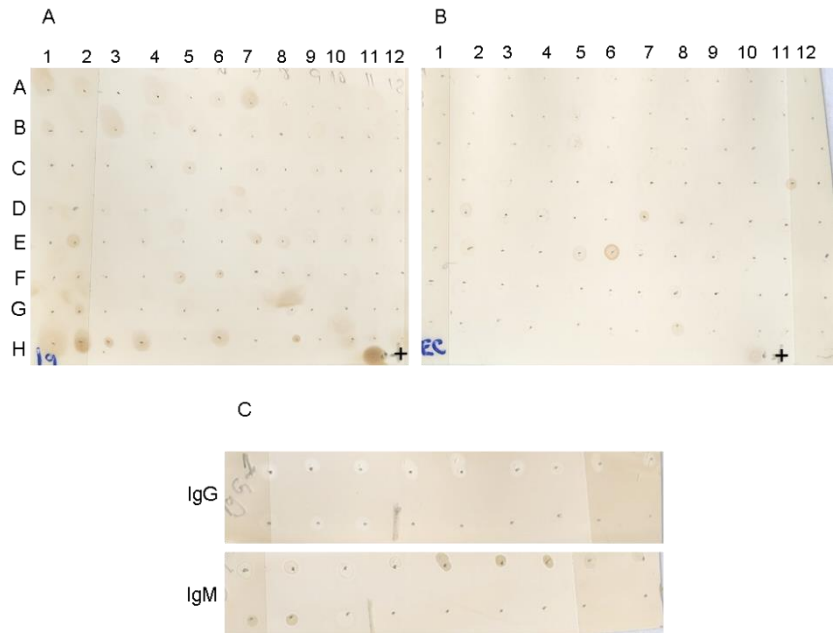

Figure 7.22 – Representative dot blots of the first hybridoma screening procedures. **(A)** The supernatant of each isolated hybridoma colony was dotted on a nitrocellulose membrane coated with rabbit anti-mouse immunoglobulin (no HRP, 1:1000, Dako) for detection of antibody production. Each dot represents a single colony. The dark spots represent positive colonies. **(B)** Supernatants were also tested for reactivity against CSF-1R (20 µg/ml, dimerization or extracellular region, depending on which hybridoma was being tested). "+" indicates the mouse immune serum, used as a positive control (1:4000). The bound antibodies were detected with rabbit anti-mouse Ig, HRP-conjugated (1:1000, Dako). **(C)** The best results from (A) and (B) were then tested for antibody isotype. The supernatants were again dotted on membranes coated with anti-mouse Ig. The bound antibodies were detected with anti-mouse IgG or anti-mouse IgM (1:1500, Southern Biotech). In the example, all colonies tested were IgM^+. The reactions were developed using DAB HCl (Sigma).

The second and third hybridoma fusions for the extracellular region of CSF-1R were screened by ELISA. The plates were coated with the antigen and colonies were evaluated for binding (Figure 7.23 A). In the third fusion, positive colonies were further screened on a plate comparing CSF-1R to BSA binding, as well as IgM to IgG production (7.23 B). The final selection step for the third fusion was by flow cytometry. CHO-K1-S cells were transfected to express the canine CSF-1R on the cell surface, and the positive clones from ELISA were screened to identify antibodies that bound specifically to transfected cells (Figure 7.23 C).

In all three hybridoma fusions from mice immunized with the EC region, more IgM than IgG -producing clones were generated. To avoid this, in the second fusion IgM^+ cells

were excluded using magnetic-activated cell sorting (MACS). However, this did not affect the proportion of IgM/IgG clones. Only one CSF-1R-binding IgG clone was identified for each of the first and second hybridoma fusions using the extracellular region, respectively mAbs 1C6 and 2H1. Only two mAbs from the third hybridoma bound to the CSF-1R on CHO cells as assessed by flow cytometry, clones 6D9 and 6F4 (Figure 7.23 C). 6D9 and 6F4 did not affect BMDM proliferation (not shown), and were therefore not investigated further.

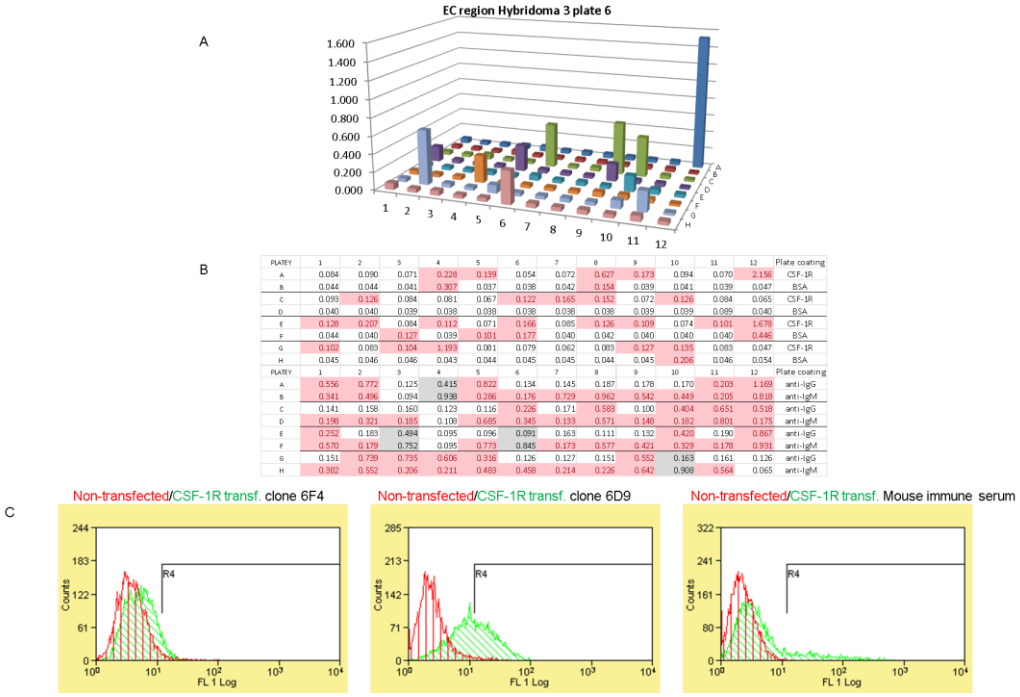

Figure 7.23 – Screening procedures for the third extracellular region hybridoma. **(A)** Clones were initially assessed by ELISA for binding to CSF-1R-coated plates (200 ng/ml). Each bar shows the result of a clone. Well A12 is the mouse immune serum positive control (1:4000). The bound complex was detected using rabbit anti-mouse Ig, HRP-conjugated (1:2000, Dako). Well B12 shows the secondary antibody negative control. **(B)** mAbs were then tested for cross-reactivity with BSA and for IgG/IgM production by ELISA. Plates were coated with either CSF-1R or BSA (as above); for detection of antibody production, plates were coated with anti-mouse Ig (no HRP, Dako). For instance, wells A1 and B1 in both plates contain one mAb clone. Red highlights indicate positive results. Grey highlights show poor results. A12 and B12 show the positive controls: mouse immune serum (1:4000) (CSF-1R/BSA plate) or isotype antibodies (IgG_1 or IgM, 1:1000, Abcam) (IgG/IgM plate). Binding to the CSF-1R/BSA plate was detected using anti-mouse Ig, HRP-conjugated (1:1000, Dako). Binding to the isotype plate was detected with anti-mouse IgM or anti-mouse IgG (1:1500, Southern Biotech). G12 and H12 show the negative controls. **(C)** As a last selection round, hybridoma supernatants containing mAbs were tested for binding to CSF-1R-transfected CHO-K1-S cells *versus* binding to non-transfected cells. The murine immune serum was used as the positive control (1:4000). Secondary antibody was goat anti-mouse, Alexa 488-conjugated (1:800, Invitrogen).

The best antibody clones identified in the screening assays were then subcloned by limiting dilution to guarantee antibody monoclonality. The screening assays shown in Figures 7.22 and 7.23 above were then repeated for the subcloned monoclonal antibodies.

Antibodies that were subcloned based on the above assays include: all the antibodies shown in other chapters against the dimerization domain (including mAbs 3.1 and 12.2); the anti-CSF-1R extracellular region mAbs 1C6, 2H1, 7G3 (IgM) and 6C2, the only IgM clone to be chimerized. These antibodies were characterized by immunostaining assays and the capacity to inhibit cellular proliferation. This is detailed in Chapter 4.

7.3.6 IgG purification from mouse hybridomas

The IgG hybridoma colonies that were selected based on dot blots/ELISA as well as on immunostaining and cellular inhibition properties (Chapter 4) were cultured in 175 cm^2 flasks with low IgG-FBS and supernatant was collected to purify the immunoglobulins. Protein G chromatography was successful in removing most tissue culture contaminant proteins, yielding relatively pure antibodies with a single purification step (Figure 7.24).

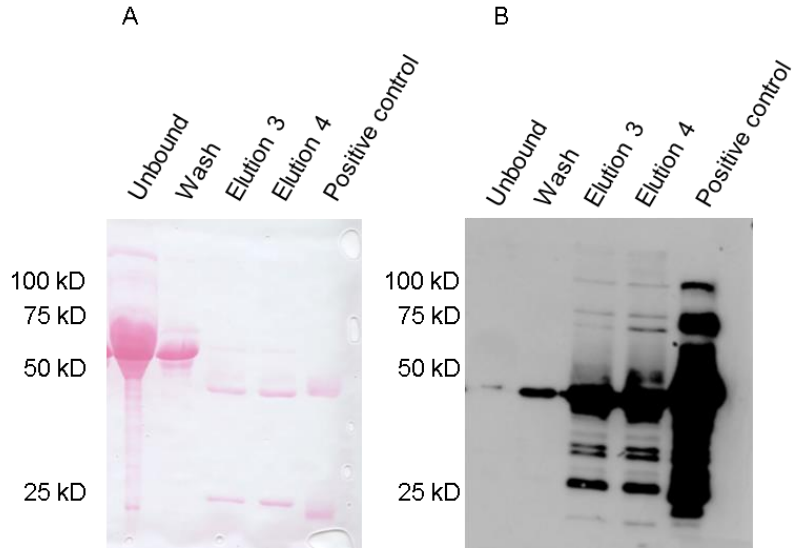

Figure 7.24 – Purification of IgG from hybridoma supernatants. Antibodies were grown in low IgG-medium and were affinity purified with protein G. **(A)** Ponceau red staining of the membrane containing the purification steps. **(B)** Western blot using the membrane in (A) probed using rabbit anti-mouse Ig, HRP-conjugated (1:1000, Dako). Non-specific proteins which did not adhere to the resin are shown as "Unbound" in the figure. Proteins washed away from the resin are shown in "Wash". The purified IgG collected from the resin is shown in the "Elution" fractions. Notice the purified Ig heavy (50 kD) and light (25 kD) chains in the elution fractions. Mouse serum IgG (Sigma) is the positive control.

7.4 Discussion

With the purpose of blocking CSF-1R in canine cancer patients, antibodies were generated against this receptor by immunization of mice. Two different antigens were used for mouse immunization and the generation of hybridomas in this study: the extracellular portion of the canine CSF-1R and the dimerization domain of the receptor (Figure 7.25). Given that the antibodies should be able to inhibit signal transduction through the receptor *in vivo*, it was necessary that the antigen was positioned in the extracellular compartment, allowing targeting by the antibody. The extracellular portion of the receptor is responsible for binding the CSF-1R ligands, CSF-1 and IL-34, as well as for the dimerization of two receptor monomers following ligand contact (Yeung and Stanley, 2003).

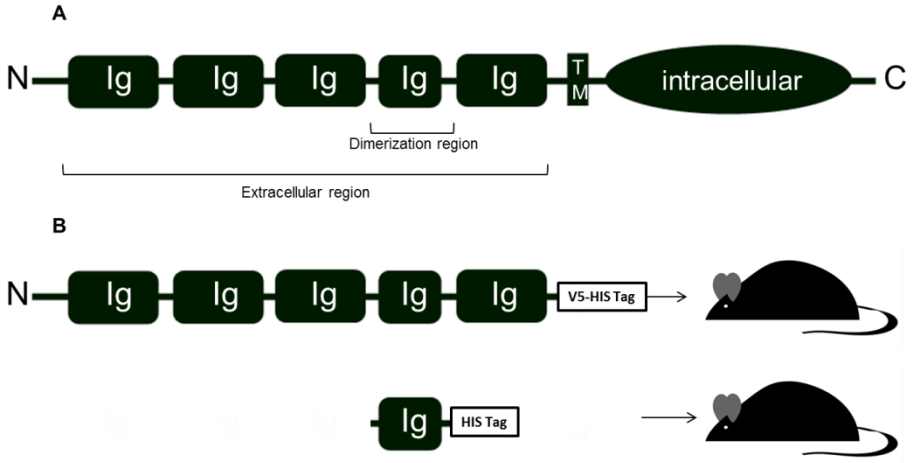

Figure 7.25 – Immunization strategy for the production of antibodies against the canine CSF-1R. **(A)** Representation of the full CSF-1R molecule. The rectangles marked "Ig" depict the five extracellular regions of the receptor. "TM" depicts the transmembrane region. **(B)** The antigens used for mouse immunization. Animals were administered either the complete extracellular portion of the canine CSF-1R or the dimerization domain, coupled to protein tags.

When injected into mice, the recombinant extracellular portion of CSF-1R should elicit the formation of antibodies against several epitopes in that region. Antibodies that targeted the ligand binding site or the dimerization domain would potentially block receptor function (Bradbury et al., 2011).

However, the CSF-1R has two ligands which bind to different positions on the CSF-1R (Ma et al., 2012). Because of this characteristic, it is possible for an antibody to block the binding of one ligand but not the other (Chihara et al., 2010). Also, immunizing mice with the whole extracellular portion of CSF-1R also leads to the production of antibodies against regions of the receptor which do not directly affect receptor function. Consequently, the dimerization domain was also used as an antigen, to increase the probability that the mice would produce blocking antibodies against the CSF-1R.

The two immunization strategies used in this chapter were devised to take advantage of different protein expression systems. The extracellular portion of the canine CSF-1R was produced in mammalian cells in culture and the dimerization domain was produced in *E. coli*.

The mammalian cell culture system was chosen to express the extracellular region recombinant protein because the extracellular portion of the receptor is highly glycosylated (Sherr, 1990), and this post-translational modification cannot usually be performed in a bacterial system in the same proportion or containing the same carbohydrates as those seen in mammalian cells (Abu-Qarn et al., 2008). As was expected, the recombinant extracellular CSF-1R protein was glycosylated after production in HEK cells. The glycosylation patterns can change when using cells derived from different species (Butler and Spearman, 2014). This is relevant because it raises the possibility that antibodies produced against a protein derived from HEK cells, a human cell line, could not recognize the canine version of the same protein. However, the immune mouse serum, produced with the peptide from HEK, was also able to recognize the recombinant protein when expressed by CHO cells, a hamster cell line.

The recombinant extracellular region was also able to bind to CSF-1, indicating that folding of the protein was correct. The transfected HEK cells secreted the largest part of the expressed extracellular region to the cell culture medium, facilitating purification of the protein. This protein was highly purified after a single round of affinity chromatography using a nickel resin, and this antigen was used for mouse immunization.

As a drawback of the use of mammalian cells for expression, mice immunized with this antigen received reduced quantities of the protein (15 µg) when compared to the indicated protocols in the literature, which recommend from 50 to 100 µg (Harlow and Lane, 1988), since the production yield of the system is low. The small antigen dose of the extracellular region may have contributed for the large number of IgM clones identified after all three hybridoma fusions from this antigen. Immune activation following immunization is necessary for the affinity maturation and isotype switch of the antibodies (Teng and

Papavasiliou, 2007), and this is affected by antigenic load (Harlow and Lane, 1988). For the second fusion from the extracellular region immunizations, IgM^+ cells were depleted using magnetic cell sorting, as it had been published that this would greatly increase the proportion of IgG mAbs generated (Apiratmateekul et al., 2009). This had no effect on the proportion of IgM/IgG colonies produced, and IgM still largely surpassed the number of IgG monoclonals created. Despite the apparent lack of immune activation driving IgG formation after immunizations with the extracellular region, the primed sera were able to avidly bind to the antigen in dot blots and ELISA even to very low dilutions. Another possibility for the low production of IgG could be that the Sp2/0 myeloma fusion partner expresses CSF-1R. If this is the case, productive fusions with inhibitory IgG would have killed the myeloma cells, reducing the yield of IgG-producing clones.

The sera from mice immunized with the extracellular CSF-1R were also able to reduce viability of the canine mammary cancer cell line, REM134. This cell line expresses the CSF-1R and is capable of replicating in response to receptor activation (Chapter 3). However, the effect was not correlated to the concentration of the serum, indicating that it was not a result of antibody function. This is corroborated by the lack of effect of the immune serum against canine BMDM, which require CSF-1R signalling for maturation and survival (Garcia-Morales et al., 2014; Temeles et al., 1993). Another possibility is that the immune serum also provided agonist antibodies, which would have counteracted the effect of antagonistic clones (Bradbury et al., 2011).

Ba/F3 cells can be induced to replicate in the presence of foreign kinase receptors. This cell line usually depends on IL-3 for survival, but this signal can be substituted for CSF-1 after transfection with CSF-1R (Gow et al., 2012; Liu et al., 1999). Ba/F3 cells were present in greater number after incubation with immune serum when compared to pre-immune serum. The immune serum had an overall effect of increasing Ba/F3 cell proliferation, independently of the expression of CSF-1R by these cells, as assessed by two-way ANOVA. After immunization of mice, IL-3 levels are increased in the serum (Valensi et al., 1994), and this may be justify the general induction of proliferation of Ba/F3 cells in the presence of immune serum.

The His-tagged dimerization domain, used for immunization, avidly formed multimers of several different sizes. Since the aggregates of dimerization-His tagged protein could not be seen in silver staining, it was evaluated that their presence would not impede the use of the recombinant protein for immunization. Also, the presence of contaminant proteins after purification of the GST-tagged dimerization domain precluded its use for inoculations.

However, as later identified when studying mAb 3.1, originated from this immunization strategy, the presence of aggregates may have affected the quality of the derived antibodies. mAb 3.1 showed cross-reactivity with at least two control proteins in ELISA, and its variable regions seem not to have undergone extensive hypermutation (Chapters 4 and 5). These results indicate that immunization was not successful in maturing the antibodies. Lymphocyte activation following immunization with the dimerization domain may not have been directed towards a single immunogen, and could have been dispersed between the several aggregation formats. Consequently, although immunization with the dimerization domain led to the production of several IgG clones, antibody maturation may have been dispersed between several different antigens, instead of being directed against a single protein format. Also, the multimer format does not occur with the soluble receptor expressed by cells. If the mAbs were generated against the multimer, it is likely that they would not recognize the native antigen.

The sera of the animals immunized with the dimerization domain were not made available by the institute that performed the injections in the Czech Republic. It would be interesting to evaluate the capacity of those sera against soluble antigens, expressed by cells.

7.5 Conclusion

The CSF-1R extracellular region was successfully expressed as a recombinant protein. Mouse inoculations using this protein led to the production of highly reactive sera, which could identify the recombinant receptor in dot blots, ELISA and flow cytometry. Three hybridoma fusions were performed from this immunization strategy. However, several IgM antibodies resulted from these fusions. The His-tagged dimerization domain of CSF-1R generated several IgG clones, among which mAb 3.1, which is extensively described in Chapters 4 and 5.

7.6 Annex

7.6.1 Hybridoma Fusion

Materials:

- □ 3 ml syringe
- □ 50 ml falcon tubes and cell strainer (100 μm)
- □ H_2O deionized, sterile
- □ Erythrocyte lysis buffer (150 mM NH_4Cl, 10 mM $NaHCO_3$, 0.1 mM EDTA, pH 7.2)
- □ PEG 1500 at 50 % (Roche)
- □ 100 mm tissue culture-treated plates
- □ Ice
- □ 250 ml of Cell Mab Medium, Quantum Yield (BD) with pen/strep/fungizone + Glutamax + 10 % FBS + 10 % BM Condimed H1 Hybridoma Cloning Supplement (Roche). This medium can be substituted for RPMI (add IL-6 (Sigma)).
- □ 200 ml of Advanced RPMI with pen/strep/fungizone + 20 % FBS + glutamax
- □ 300 ml of Advanced RPMI with pen/strep/fungizone + glutamax NO SERUM
- □ Clonal cell medium D with HAT, if using this for growth of clones after fusion (Stemcell). This can be substituted for RPMI + 10 % FBS + 10 % BM Condimed H1 Hybridoma Cloning Supplement (Roche) + pen/strep/fungizone + glutamax + IL-6 supplement (36 μl, Sigma) + HAT supplement
- □ Sp2/0 myeloma cells, previously selected with 8-azaguanine; 10^7 to 10^8 cells are needed.
- □ If carrying out magnetic sorting: LD column, MidiMACS separator, anti-mouse IgM microbeads (all from Miltenyi Biotech) and PBS + 2 mM EDTA + 0.5 % BSA.
- □ If desired, feeder cells can be used: 10 ml of RPMI is injected into the peritoneum of a recently euthanized mouse. The abdominal contents are shaken for 2 min and the volume is then withdrawn. This is diluted to 100 ml and plated on 10 × 96-well plates. This is done 2 days before the fusion.

The recommendations in italics were obtained from the manual of Medium D (Stemcell).

A total of 1 × 10^7 Sp2/0 cells (i.e., 1:10 ratio to immune spleen cells) are used for fusion. Cell viability at the time of collection should be greater than 95 %. To ensure that cells are collected in log phase of growth, adjust the cell density to 2 × 10^5 cells/ml

the day before the fusion by adding fresh medium. Determine cell viability using the trypan blue.

Fusion:

1. Warm up the media and the PEG at 37^{o}C (except medium D)
2. Remove all possible fat from the murine spleen
3. Transfer the spleen to a cell strainer placed on top of a 50 ml conical centrifuge tube, perforate the spleen several times with a needle and perfuse it with RPMI NO SERUM. After this is done several times, use the plunger of a 3 ml syringe to grind the remaining cells out of the spleen. Rinse the screen with RPMI (5 to 10 ml) to assist the cells through the screen. Only the spleen capsule should remain on the screen. Gently pipette the cells up and down to disrupt clumps, but try not to cause the solution to foam
4. Centrifuge the tube at 400 × *g* for 10 min.
5. Resuspend the pellet in the residual medium (drops of medium left after inverting the tube to discard SN) – important step, as the cells must be very loose for the next step
6. Lyse erythrocytes using 5 ml of lysis buffer for 5 min on ICE, without agitating
7. Add 25 ml of RPMI NO SERUM
8. Centrifuge at 400 × *g* for 10 min and discard supernatant
9. If the pellet is clear, carry on to step 10. If it is still red, repeat the steps 5, 6, 7 and 8.
10. If carrying out magnetic sorting of cells, go to step 11. If not, go to step 12.
11. Resuspend pellet in 80 µl of PBS + BSA + EDTA per 10^7 cells. Incubate 1 × 10^7 spleen cells with 20 µl of anti-mouse IgM microbeads for 30 min on ice (scale up as necessary, never down). Cells are then washed twice with PBS containing 2 mM EDTA and 0.5 % BSA and centrifuged. Prepare LD Column by rinsing with buffer: apply 2 ml of degassed buffer on top of the column and let the buffer run through. LD Columns are "flow stop" and do not run dry. Discard effluent and change collection tube. The LD Column is now ready for magnetic separation.

    The cell pellet is resuspended in 500 µl of PBS + EDTA + BSA and is then applied onto the pre-prepared LD column and separated by MidiMACS separator. For cell numbers above 1.25 × 10^8, scale up the volume. Collect unlabelled cells which pass through. Wash LD Column with 2 × 1 ml degassed buffer, adding buffer each time once the column reservoir is empty. Collect total effluent. This is the unlabelled (depleted) cell fraction. ** **The negative fraction (the flow through) is collected and used for fusion.**
12. Centrifuge the negative fraction at 400 × *g* for 12 min and discard supernatant.
13. Wash the pellet with 25 mL of RPMI NO SERUM

14. Centrifuge at 400 × *g* for 12 min and discard supernatant.
15. During the centrifugation, take myeloma cells from bottles. Spin down myelomas and wash with 30 ml RPMI NO SERUM. Centrifuge at 400 × *g* for 12 min. Perform viable cell count with trypan blue exclusion, and wash cells with 30 ml of RPMI NO SERUM. Spin down as above, resuspend in 20 ml RPMI NO SERUM and disperse. Leave at 37°C until spleens are retrieved.
16. Resuspend splenocytes in 20 ml of RPMI NO SERUM and count cells
17. Mix myeloma and splenocytes in the ratio of 1:5 (myeloma:splenocyte) [if fusing IgM depleted cells, fuse at 1:3].
18. Complete the volume to 50 ml with RPMI NO SERUM.
19. Centrifuge at 400 × *g* for 12 min and discard supernatant with vacuum line or with pipette (all media must be removed not to dilute the PEG)
20. Break up pellet by gently tapping on the flow hood surface. Add 1 ml PEG1500 (prewarmed to 37°C) dropwise with a 1 ml needle over 1 minute. Swirl and tap the conical gently while adding the PEG to resuspend the cells.
21. Continue to mix for 1 min 30 seconds (IMPORTANT STEP)
22. Add 1 ml of RPMI NO SERUM to the PEG cells gently over 1 min while swirling (to dilute the PEG).
23. Add 8 ml RPMI NO SERUM over 2 min to slowly dilute out the PEG.
24. Incubate the cells in the 37°C water bath for 10 min (do not disturb the cells!!).
25. If using ClonaCell-HY Hybridoma Selection Medium (Medium D), go to step 26. If not, Centrifuge the tube at 400 × *g* for 5 min. Resuspend the cells in 100 ml of RPMI containing cloning supplement, IL-6 and HAT. Plate the hybridomas on the plates containing the feeder cells. Culture for 7 days. Change medium to HT supplementation. Screen colonies within 3 – 4 days.
26. Slowly add 30 ml of RPMI WITH SERUM and centrifuge the cells at 250 × *g* for 15 min. Discard the supernatant and wash cells with 40 ml of RPMI WITH SERUM without resuspending the cells to ensure that all PEG is removed.
27. Slowly resuspend the cell pellet in 10 ml of CellMab Medium with BM condimed supplement.

    Transfer the cell suspension to a T-75 cm^2 tissue culture flask containing 20 ml of the same medium (total culture volume = 30 ml). Incubate for 16 – 24 hours at 37°C in 5 % CO_2 atmosphere.
28. On the day of the fusion, place ClonaCell-HY Hybridoma Selection Medium (Medium D) at 2 – 8°C and thaw overnight. On the day after the fusion, shake vigorously to mix

contents well and let warm to **room temperature (do NOT use a water bath)**.

29. Transfer fused cell suspension into a 50 ml conical tube and centrifuge for 10 min at 400 x *g* at RT or 37°C. Remove the supernatant. Resuspend the cells in CellMab Medium with BM condimed supplement to a total of 10 ml (that is: 1 ml of CellMab Medium + 9 ml of Condimed).

It is critical not to exceed the 10 ml final volume. If you wish to add any additional cytokines or growth factors to Medium D, include this volume in the total 10 ml volume that the cells are being resuspended in.

To achieve optimal colony density for colony picking, plating at several cell densities is recommended as fusion efficiency may vary.

30. Transfer the 10 ml cell suspension into the 90 ml of Medium D. Mix thoroughly by gently inverting the bottle several times. Let sit for 15 min at RT or 37°C to allow the bubbles to rise to the top.
31. Using a 12 ml syringe and 16 gauge blunt-end needle, aseptically plate out 9.5 ml of cell suspension medium into each of ten 100 mm petri plates. Tilt each plate to evenly distribute the medium to cover the bottom of the plate. Avoid the introduction of bubbles during plating. Incubate plates at 37°C in 5 % CO2 atmosphere. Do not disturb plates for 10 – 14 days.

It is advisable to put the plates in a separate plastic container together with a 100 mm petri dish containing 10 mL sterile distilled water (no lid!) to maintain moisture content methylcellulose cultures. It is important not to disturb the plates for the first 10 days; doing so will result in runny or hazy colonies.

7.6.2 Hybridoma Maintenance when using Medium D

1. 10 – 14 days after cells are plated in Medium D, examine the plates for the presence of colonies visible to the naked eye. A typical fusion will produce 1000 or more colonies over the ten plates. Remove isolated colonies (usually 500 – 1000 colonies are harvested) from the plates using a pipette set to 10 µl and sterile pipette tips. Pipette each clone into an individual well of a 96-well tissue culture plate containing 200 µl of BD Clonacell WITH SERUM and HT. With the pipette set at 150 µl, pipette the entire contents of the well up and down several times to resuspend the colony. The colony does not need to be resuspended into a perfect single-cell suspension but should be dispersed sufficiently to get good growth.

   The resuspension of the colonies may be performed using a multi-channel pipette after all selected colonies have been transferred to 96-wells. Ensure a new sterile tip is used for each clone to maintain monoclonality of the colony. Incubate the plates at 37°C in 5 % CO_2 for 1 - 4 days without feeding.

   By the fourth day, each well should have a high cell density and medium that is turning yellow. As the colonies have different growth rates, some wells may have media that turns yellow sooner than 4 days. It is a good idea to pick clones of different sizes as slower growing clones (i.e. smaller colonies) are often very good antibody producers.

2. Transfer 150 µl of supernatant from each hybridoma to a separate well on a new 96-well plate and analyse by using an assay system appropriate for the antigen involved (e.g. ELISA, flow cytometry, western Blotting, etc.).
3. Add 150 µl of fresh BD Clonacell WITH SERUM and HT to every well of the original hybridoma containing plates.
4. Gently resuspend the hybridomas that showed a positive response in Step 2. Transfer 100 µl of cells to each of 2 wells of a 24-well plate, containing 1 ml of BD Clonacell WITH SERUM and HT.
5. When cells have grown to a suitable density (approximately 4×10^5 cells/ml), freeze the cells from one well and expand the remaining positive clones in a T-25 cm^2 tissue culture flask containing 5 ml of BD Clonacell WITH SERUM and 5 mL of BD Clonacell WITH SERUM and HT. This step adapts the cells to growth in BD Clonacell WITH SERUM. In addition, keep a sample of cells in BD Clonacell WITH SERUM and HT, in case the cells don't adapt well to the 1:1 mixture.
6. When cells have grown to a suitable density (approximately 4×10^5 cells/ml), transfer 5 - 10

ml of cell culture by pipette into 20 ml of BD Clonacell WITH SERUM in a T-75. Adjust the volume of cells to ensure the final cell concentration is between $1 \times 10^4 – 5 \times 10^4$ cells/ml. Maintain expanded hybridomas in 100 % BD Clonacell WITH SERUM at a concentration of $5 \times 10^4 – 5 \times 10^5$ cells/ml. More aliquots of cells can be frozen at this point in order to secure the supply of the hybridoma. This is also the time to gradually wean cells off the BM Condimed H1 Hybridoma Cloning Supplement (Roche).

Chapter 8

Conclusions and future perspectives

The negative role of tumour-associated macrophages (TAMs) in cancer is currently receiving great attention. In a variety of studies, TAMs correlate to malignant progression of cancer by contributing towards several mechanisms of aggressiveness, such as invasiveness and immunosuppression (Noy and Pollard, 2015). CSF-1R is an important receptor for mononuclear phagocytes, including TAMs. CSF-1R mediates cell survival, recruitment and regulates the activation phenotype. Overexpression of CSF-1R and its ligands by cancer cells has also been shown to provide a transforming signal that sustains tumour growth (Hume and MacDonald, 2012). Therefore, in many cancers, CSF-1 or CSF-1R expression levels have been associated with poor prognosis (Chambers et al., 1997; Lin et al., 2001).

In this thesis, the interaction between macrophages and canine mammary cancer cells was confirmed. Mammary carcinoma cells reduced macrophage inflammatory activation, while macrophages stimulated mammary cancer cell proliferation and metabolic activity. In the cross-talk between these two cells, CSF-1R signalling was likely to have a pivotal role. Both canine mammary carcinoma cells and macrophages proliferated in response to exogenous CSF-1. Two canine cancer cell lines were repressed by a CSF-1R-selective small molecule kinase inhibitor. Cancer cells also proliferated and expressed more CSF-1R in response to macrophage-conditioned medium. When CSF-1 was competitively inhibited, the effects of cancer cells over macrophages were annulled. Finally, while CSF-1 alone could lead to expression of macrophage inflammatory markers, it reduced Toll-like receptor-induced activation of macrophages.

Further study is needed to fully clarify the role of CSF-1R in macrophage inflammatory activation. The response of CSF-1-conditioned macrophages to LPS stimulation is varied in different studies. CSF-1 has been shown to induce and suppress the production of inflammatory factors in response to LPS (Saccani et al., 2006; Sierra-Filardi et al., 2011; Sweet and Hume, 2003). Also, some of the inflammatory cytokines CSF-1-conditioned macrophages are reported to express following LPS stimulation (*e.g.* IL-6) have been shown to promote anti-inflammatory characteristics under conditions found in tumours (Lewis and Pollard, 2006; Yasukawa et al., 2003). Therefore, it is necessary to fully dissect the biological relevance of CSF-1R activation in monocytes and macrophages from different

origins (blood, tissue, different tumours and various tumour sites) and the consequences of an inflammatory stimulus such as LPS. Isolated cultures of macrophages extracted from these various origins could be stimulated with CSF-1/IL-34 or their "opposite" factor, GM-CSF. The effect of LPS stimulation of these cells then needs to be analysed holistically, with special relevance to functional assays, since it is hard to predict the biological effects of cytokine production based on their label of "pro-inflammatory" or "anti-inflammatory", as was shown in the case of IL-6. Furthermore, although LPS is used as a model of inflammation, it is unlikely to be relevant in the context of cancer. Other inflammatory agonists, such as bacterial DNA, have very different effects from LPS on macrophage activation, showing that LPS is not an universal inflammatory model (Sweet et al., 2002). It can also be argued that the complexities of the tumour microenvironment are unlikely to be reproduced by addition of one or two factors in 2-dimensional cultures. Analysis of the cancer cell/macrophage secretome in more complex 3-dimensional cultures and the transcriptome from cancer samples will assist in piecing together the many factors involved in TAM/cancer interactions (Makridakis and Vlahou, 2010; Tang et al., 2011; Thoma et al., 2014).

While CSF-1R is not expressed by most epithelial cells during maturity, it would be important to understand how and when its expression is upregulated in carcinomas (Ide et al., 2002). Although this study was originally aimed at reducing the effects of TAMs in cancer, it is likely that blocking CSF-1R expressed by epithelial cancer cells will also be of benefit. The isolated effect of blocking CSF-1R in the carcinoma cells (isolated from the effect of blocking CSF-1R in TAMs) has received little attention, but will be important for understanding how anti-CSF-1R therapies will work.

In order to block the cancer-promoting effects of tumour-associated macrophages and of CSF-1R signalling, monoclonal antibodies were raised against this receptor. Mice were immunized using either the extracellular region or the dimerization domain of canine CSF-1R as antigens.

Immunization with the extracellular region of CSF-1R induced strong antibody responses, as measured by the serum reactivity. Nevertheless, this approach consistently produced more IgM than IgG clones after three hybridoma fusions, perhaps as a result of the low doses of antigen used. It is also possible that the myeloma fusion partner expresses CSF-1R and production of IgG inhibited the survival of the hybridomas. Serum reactivity after immunization with the dimerization domain seemed weaker, but many IgG clones were isolated from this approach.

Hybridoma fusions were screened by dot blots or ELISA, followed by immunostaining and inhibition of carcinoma cell/bone marrow macrophage proliferation. The best antibodies from these assays were carried on to replicate assays and further studies, such as chimerization. The canine mammary carcinoma cell line used for the first proliferation assays was shown to express the CSF-1R and to proliferate in response to CSF-1. However, responsiveness to CSF-1 and CSF-1R expression proved to be very sensitive to culture cell contact inhibition, and this may have affected the initial proliferation screenings. All clones that did not affect proliferation were no longer studied. Carcinoma cells were used due to the limited availability of canine primary macrophages at the time.

Although the macrophages responded sensitively to antibody inhibition, these cells introduced confounding factors: the expression of Fc receptors (Luo et al., 2010) and pathogen-associated molecular pattern (PAMP) receptors (Jung et al., 2005). Fc receptors may have affected the results seen with some of the antibody clones studied here, such as mAb 12.2 after chimerization. Fc receptors can alter the binding affinity of some antibodies (Haegel et al., 2013). PAMP receptors may have interfered in the analysis of the proliferation effects of bacterially produced scFv. Residual bacterial contamination from the expression host could have affected the proliferation of canine macrophages when studying the effect of scFv. Future attempts in finding blocking antibodies against the CSF-1R should concentrate in using cell lines stably transfected with the CSF-1R and that rely on it for survival (Gow et al., 2012; Roussel and Sherr, 1989). This has the advantage of removing the confounding factors cited above and of permitting direct comparison against a non-transfected counterpart, against which the antibodies should have no effect. Also, intermediary assays such as ELISAs and immunostaining could be avoided. The first screening of the hybridoma clones should be a proliferation assay using the cell line expressing CSF-1R compared to non-transfected cells. Antibodies with specific proliferation inhibition could then be further analysed in other assays such as flow cytometry or western blots to confirm their identity.

Using immunostaining and inhibition of cell proliferation as the selection criteria, mAb 3.1 was selected as a promising antibody. This clone could stain cells in known macrophage tissue niches and could inhibit macrophage and REM134 cell proliferation. Although other antibodies such as mAb 12.2 showed better cell inhibition properties, these clones could not stain cells, making their characterization difficult. The immunoprecipitation assay shown in Chapter 4, which confirms the specificity of mAb 12.2, was performed after the first submission of this work. Chimerization did not affect the binding properties of mAb 3.1, and the chimerized mAb inhibited CSF-1-induced macrophage proliferation, but did not affect IL-4-conditioned macrophages. IL-4 induces macrophage survival independently of

CSF-1R, and it was expected that IL-4-macrophages were not affected by the anti-CSF-1R mAbs (Arpa et al., 2009; Jenkins et al., 2013).

However, this antibody did not bind to circulating monocytes and showed cross-reactivity against other proteins in ELISA. This is likely to be a result from the conformation of the antigen used for mouse immunization, which was produced in bacteria and formed stable aggregates. Immunoprecipitation confirmed that mAb 3.1 bound to few CSF-1R glycoforms. In this way, mAb 3.1 may bind to fixed antigens in tissue sections but not to the native CSF-1R expressed by monocytes. Another CSF-1R blocking antibody has been shown not to bind to the surface antigen by flow cytometry possibly due to epitope accessibility (Haegel et al., 2013). The bacterial peptides produced for immunization in this study proved complex to express and purify in the correct conformation, and future efforts to generate antibodies active against native canine molecules should concentrate on the mammalian expression system.

Another explanation for the results with mAb 3.1 is the possible low antibody affinity. The cells stained by mAb 3.1 in the lymph node and spleen have been reported to express high levels of CSF-1R (MacDonald et al., 2010; Sasmono et al., 2003). Since ELISA showed that affinity of this antibody is likely to be low, mAb 3.1 may only recognize cells expressing high levels of CSF-1R, and blood monocytes have lower levels than tissue macrophages (Byrne et al., 1981).

Therefore, to find antibodies with higher affinity and specificity towards the soluble conformation of CSF-1R, antibody libraries were constructed and screened by phage display. One complementarity-determining region of each of the variable chains (heavy and light) of mAb 3.1 was mutated by PCR. These were inserted into phagemids to construct two phage display libraries. Although library sizes were small, both libraries produced clones with lower cross-reactivity against control proteins than mAb 3.1, as assessed by ELISA. Some of the clones found by phage display, scFv G3, D8 and H8, were also successfully produced in bacteria isolated from the bacteriophage. scFv H8 was shown to bind to the native CSF-1R by flow cytometry of peripheral blood mononuclear cells. Expression of the scFv had to be performed by purifying in the presence of urea and refolding the protein by stepwise dialysis. This was an initial attempt at modifying mAb 3.1. The literature also often describes the use of sequential steps of mutation of the variable regions to accumulate positive alterations. Therefore, after the identification of these positive clones by phage display, further mutations can be added to them, generating new libraries that will possibly contain clones with even superior characteristics (Martineau, 2010). Mutation of mAb 12.2 could also yield better results than for mAb 3.1. This antibody inhibited macrophage proliferation more

intensely than mAb 3.1. Immunoprecipitation proved the specificity of mAb 12.2, and it seemed to bind to a wider range of CSF-1R glycoforms than mAb 3.1. However, immunoprecipitation was only performed after the production of phage display libraries with mAb 3.1.

These mutated versions of mAb 3.1 can also be tested in the chimerization vectors pVH and pVL, tested here using several antibodies. These vectors allow the expression of the antibodies containing all post-translational modifications and in their full conformation. For future pre-clinical trials using chimeric antibodies, an improved expression system will need to be used, since expression levels using pVH/pVL is low. This may be due to the need of using two plasmids and the fact that only transient transfections were tested in the present work. However, even in fully optimized culture conditions antibody production costs are high. The monoclonal antibodies that are reaching the veterinary market at the time of writing are unlikely to be used by a wide audience due to the price of the products (Pollack, 2014). Future advancements in antibody expression will be necessary for increasing production efficiency and reducing costs. The creation of transgenic animals and plants expressing recombinant antibodies has a high implantation cost but low maintenance. These may represent viable alternatives for the cost-efficient production of biologicals in the future (Frenzel et al., 2013; Schillberg et al., 2005).

In future experiments, some of the techniques tested in the present work can be further explored. The CAM assay can be used with co-cultures of canine macrophages and cancer cells while testing the efficacy of therapeutic antibodies. The CAM assay shown here only tested the direct effect of mAb 3.1 over mammary carcinoma cells. However, there is great importance in repeating this assay including macrophages.

The full antibody caninisation procedure (altering the variable regions) should be compared to chimerization with regards to binding properties and generation of anti-antibody responses. Although this could not be tested in the present work due to time constraints, if caninisation is successful it can increase the value of the resulting therapeutic mAb by reducing antigenicity (Hwang and Foote, 2005).

8.1 Conclusion

CSF-1R signalling can have tumour-promoting abilities by stimulating direct cancer cell growth and by influencing the phenotype of tumour-associated macrophages. In order to block this receptor in canine cancer patients, antibodies were raised in this study by mouse immunizations. mAb 3.1, one of such antibodies, was able to inhibit the proliferation of bone

marrow-derived macrophages and of canine mammary carcinoma cells bearing CSF-1R. This antibody also stained putative macrophages in tissues, but showed specificity and affinity deficiencies. Some of the binding characteristics of mAb 3.1 were then improved by mutations to its complementarity-determining regions. Additional work is required to confirm the initial findings with these mutated clones and to further improve their properties. When satisfactory antibodies are identified, these can be altered by chimerization or caninisation and be used for clinical tests. However, these results indicate that interesting antibodies for blocking canine CSF-1R have been identified.

References

Abu-Qarn, M., Eichler, J., Sharon, N., 2008. Not just for Eukarya anymore: protein glycosylation in Bacteria and Archaea. Curr. Opin. Struct. Biol. 18, 544–550. doi:http://dx.doi.org/10.1016/j.sbi.2008.06.010

Acharya, N., Gohel, D., Kuberkar, V., Natesan, S., 2015. Recent advances in immunotherapy for the treatment of cancer. Adv. Anim. Vet. Sci 3, 23–29.

Ackerman, M.E., Lai, J.I., Pastan, I., Wittrup, K.D., 2011. Exploiting bias in a non-immune human antibody library to predict antigenicity. Protein Eng. Des. Sel. . doi:10.1093/protein/gzr046

Adams, C.W., Allison, D.E., Flagella, K., Presta, L., Clarke, J., Dybdal, N., McKeever, K., Sliwkowski, M.X., 2006. Humanization of a recombinant monoclonal antibody to produce a therapeutic HER dimerization inhibitor, pertuzumab. Cancer Immunol. Immunother. 55, 717–727.

Adams, G.P., Weiner, L.M., 2005. Monoclonal antibody therapy of cancer. Nat. Biotechnol. 23, 1147–57. doi:10.1038/nbt1137

Aguiar, P.H.P., Borges dos Santos, R.R., Larangeira, D.F., Almeida dos Santos, M., Barrouin-Melo, S.M., Silva, T.M.C., Mengel, J.O., Conrado dos Santos, W.L., Pontes-De-Carvalho, L., 2004. A novel monoclonal antibody against canine monocytes/macrophages. Hybrid. Hybridomics 23, 250–257.

Aguirre, S.A., Heyen, J.R., Collette, W., Bobrowski, W., Blasi, E.R., 2010. Cardiovascular effects in rats following exposure to a receptor tyrosine kinase inhibitor. Toxicol. Pathol. 38, 416–428. doi:10.1177/0192623310364027

Aharinejad, S., Paulus, P., Sioud, M., Hofmann, M., Zins, K., Schäfer, R., Stanley, E.R., Abraham, D., 2004. Colony-stimulating factor-1 blockade by antisense oligonucleotides and small interfering RNAs suppresses growth of human mammary tumor xenografts in mice. Cancer Res. 64, 5378–5384. doi:10.1158/0008-5472.CAN-04-0961

Aikawa, Y., Katsumoto, T., Zhang, P., Shima, H., Shino, M., Terui, K., Ito, E., Ohno, H., Stanley, E.R., Singh, H., 2010. PU. 1-mediated upregulation of CSF1R is crucial for leukemia stem cell potential induced by MOZ-TIF2. Nat. Med. 16, 580–585.

Akcora, D., Huynh, D., Lightowler, S., Germann, M., Robine, S., Jan, R., Pollard, J.W., Stanley, E.R., Malaterre, J., Ramsay, R.G., 2013. The CSF-1 receptor fashions the intestinal stem cell niche. Stem Cell Res. 10, 203–212.

Albagha, O.M.E., Visconti, M.R., Alonso, N., Langston, A.L., Cundy, T., Dargie, R., Dunlop, M.G., Fraser, W.D., Hooper, M.J., Isaia, G., 2010. Genome-wide association study identifies variants at CSF1, OPTN and TNFRSF11A as genetic risk factors for Paget's disease of bone. Nat. Genet. 42, 520–524.

Alenza, M.D.P., Tabanera, E., Peña, L., 2001. Inflammatory mammary carcinoma in dogs: 33 cases (1995-1999). J. Am. Vet. Med. Assoc. 219, 1110–1114.

Allavena, P., Sica, A., Garlanda, C., Mantovani, A., 2008. The Yin-Yang of tumor-associated macrophages in neoplastic progression and immune surveillance. Immunol. Rev. 222, 155–161.

Álvaro, T., Lejeune, M., Camacho, F.I., Salvadó, M.T., Sánchez, L., Garc'\ia, J.F., Lopez, C., Jaén, J., Bosch, R., Pons, L.E., others, 2006. The presence of STAT1-positive tumor-associated macrophages and their relation to outcome in patients with follicular lymphoma. Haematologica 91, 1605.

Ancuta, P., Liu, K.-Y., Misra, V., Wacleche, V.S., Gosselin, A., Zhou, X., Gabuzda, D., 2009. Transcriptional profiling reveals developmental relationship and distinct biological functions of CD16+ and CD16-monocyte subsets. BMC Genomics 10, 403.

Apiratmateekul, N., Phunpae, P., Kasinrerk, W., 2009. A modified hybridoma technique for production of monoclonal antibodies having desired isotypes. Cytotechnology 60, 45–51.

Araki, H., Katayama, N., Yamashita, Y., Mano, H., Fujieda, A., Usui, E., Mitani, H., Ohishi, K., Nishii, K., Masuya, M., 2004. Reprogramming of human postmitotic neutrophils into macrophages by growth factors. Blood 103, 2973–2980.

Arpa, L., Valledor, A.F., Lloberas, J., Celada, A., 2009. IL-4 blocks M-CSF-dependent macrophage proliferation by inducing p21Waf1 in a STAT6-dependent way. Eur. J. Immunol. 39, 514–526.

Arun, S.S., Breuer, W., Hermanns, W., 1996. Immunohistochemical Examination of Light-chain Expression (Λ/k Ratio) in Canine, Feline, Equine, Bovine and Porcine Plasma Cells. J. Vet. Med. Ser. A 43, 573–576.

Azzam, G., Wang, X., Bell, D., Murphy, M.E., 2013. CSF1 is a novel p53 target gene whose protein product functions in a feed-forward manner to suppress apoptosis and enhance p53-mediated growth arrest. PLoS One 8, e74297.

Bailey, K.L., Poole, J.A., Mathisen, T.L., Wyatt, T.A., Von Essen, S.G., Romberger, D.J., 2008. Toll-like receptor 2 is upregulated by hog confinement dust in an IL-6-dependent manner in the airway epithelium. Am. J. Physiol. Cell. Mol. Physiol. 294, L1049–L1054.

Bain, C.C., Scott, C.L., Uronen-Hansson, H., Gudjonsson, S., Jansson, O., Grip, O., Guilliams, M., Malissen, B., Agace, W.W., Mowat, A.M., 2013. Resident and pro-inflammatory macrophages in the colon represent alternative context-dependent fates of the same Ly6Chi monocyte precursors. Mucosal Immunol. 6, 498–510.

Bak, S.P., Alonso, A., Turk, M.J., Berwin, B., 2008. Murine ovarian cancer vascular leukocytes require arginase-1 activity for T cell suppression. Mol. Immunol. 46, 258–268.

Baldwin, G.C., Chung, G.Y., Kaslander, C., Esmail, T., Reisfeld, R.A., Golde, D.W., 1993. Colony-stimulating factor enhancement of myeloid effector cell cytotoxicity towards neuroectodermal tumour cells. Br. J. Haematol. 83, 545–53.

Bamias, A., Dimopoulos, M.A., 2003. Angiogenesis in human cancer: implications in cancer therapy. Eur. J. Intern. Med. 14, 459–469. doi:10.1016/j.ejim.2003.10.003

Banaei-Bouchareb, L., Gouon-Evans, V., Samara-Boustani, D., Castellotti, M.C., Czernichow, P., Pollard, J.W., Polak, M., 2004. Insulin cell mass is altered in Csf1op/Csf1op macrophage-deficient mice. J. Leukoc. Biol. 76, 359–367.

Baneyx, F., Mujacic, M., 2004. Recombinant protein folding and misfolding in Escherichia coli. Nat Biotech 22, 1399–1408.

Bao, Y., Guo, Y., Xiao, S., Zhao, Z., 2010. Molecular characterization of the VH repertoire in< i> Canis familiaris</i>. Vet. Immunol. Immunopathol. 137, 64–75.

Barbetti, V., Morandi, A., Tusa, I., Digiacomo, G., Riverso, M., Marzi, I., Cipolleschi, M.G., Bessi, S., Giannini, A., Di Leo, A., 2014. Chromatin-associated CSF-1R binds to the promoter of proliferation-related genes in breast cancer cells. Oncogene 33, 4359–4364.

Bartocci, a, Mastrogiannis, D.S., Migliorati, G., Stockert, R.J., Wolkoff, a W., Stanley, E.R., 1987. Macrophages specifically regulate the concentration of their own growth factor in the circulation. Proc. Natl. Acad. Sci. U. S. A. 84, 6179–83.

Barve, R. a, Zack, M.D., Weiss, D., Song, R.-H., Beidler, D., Head, R.D., 2013. Transcriptional profiling and pathway analysis of CSF-1 and IL-34 effects on human monocyte differentiation. Cytokine 63, 10–7. doi:10.1016/j.cyto.2013.04.019

Bauknecht, T., Kiechle-Schwarz, M., Du Bois, A., Wölfle, J., Kacinski, B., 1993. Expression of transcripts for CSF-1 and for the“ macrophage” and“ epithelial” isoforms of the CSF-1R transcripts in human ovarian carcinomas. Cancer Detect. Prev. 18, 231–239.

Beil, W., Timpl, R., Furthmayr, H., 1973. Conformation dependence of antigenic determinants on the collagen molecule. Immunology 24, 13–24.

Bell, D., Chomarat, P., Broyles, D., Netto, G., Harb, G.M., Lebecque, S., Valladeau, J., Davoust, J., Palucka, K.A., Banchereau, J., 1999. In Breast Carcinoma Tissue, Immature Dendritic Cells Reside within the Tumor, Whereas Mature Dendritic Cells Are Located in Peritumoral Areas. J. Exp. Med. 190, 1417–1426.

Bellone, G., Turletti, A., Artusio, E., Mareschi, K., Carbone, A., Tibaudi, D., Robecchi, A., Emanuelli, G., Rodeck, U., 1999. Tumor-Associated Transforming Growth Factor-β and Interleukin-10 Contribute to a Systemic Th2 Immune Phenotype in Pancreatic Carcinoma Patients. Am. J. Pathol. 155, 537–547.

Berdougo, E., Couto, J.R., Doranz, B.J., 2011. Maximal Humanization of Monoclonal Abs. Genet. Eng. Biotechnol. News 31, 42. doi:doi:10.1089/gen.31.14.18.

Bergeron, L.M., McCandless, E.E., Dunham, S., Dunkle, B., Zhu, Y., Shelly, J., Lightle, S., Gonzales, A., Bainbridge, G., 2014. Comparative functional characterization of canine IgG subclasses. Vet. Immunol. Immunopathol. 157, 31–41. doi:http://dx.doi.org/10.1016/j.vetimm.2013.10.018

Bernabe, L.F., Portela, R., Nguyen, S., Kisseberth, W.C., Pennell, M., Yancey, M.F., London, C.A., 2013. Evaluation of the adverse event profile and pharmacodynamics of toceranib phosphate administered to dogs with solid tumors at doses below the maximum tolerated dose. BMC Vet. Res. 9, 190.

Biswas, S.K., Allavena, P., Mantovani, A., 2013. Tumor-associated macrophages: functional diversity, clinical significance, and open questions, in: Seminars in Immunopathology. Springer, pp. 585–600.

Biswas, S.K., Gangi, L., Paul, S., Schioppa, T., Saccani, A., Sironi, M., Bottazzi, B., Doni, A., Vincenzo, B., Pasqualini, F., Vago, L., Nebuloni, M., Mantovani, A., Sica, A., 2006. A distinct and unique transcriptional program expressed by tumor-associated macrophages (defective NF-kappaB and enhanced IRF-3/STAT1 activation). Blood 107, 2112–22. doi:10.1182/blood-2005-01-0428

Biswas, S.K., Mantovani, A., 2010. Macrophage plasticity and interaction with lymphocyte subsets: cancer as a paradigm. Nat. Immunol. 11, 889–896.

Bonde, A.-K., Tischler, V., Kumar, S., Soltermann, A., Schwendener, R. a, 2012. Intratumoral macrophages contribute to epithelial-mesenchymal transition in solid tumors. BMC Cancer 12, 35. doi:10.1186/1471-2407-12-35

Borras, L., Gunde, T., Tietz, J., Bauer, U., Hulmann-Cottier, V., Grimshaw, J.P.A., Urech, D.M., 2010. Generic Approach for the Generation of Stable Humanized Single-chain Fv Fragments from Rabbit Monoclonal Antibodies. J. Biol. Chem. 285 , 9054–9066. doi:10.1074/jbc.M109.072876

Bos, R., van der Hoeven, J.J.M., van der Wall, E., van der Groep, P., van Diest, P.J., Comans, E.F.I., Joshi, U., Semenza, G.L., Hoekstra, O.S., Lammertsma, A.A., 2002. Biologic correlates of 18fluorodeoxyglucose uptake in human breast cancer measured by positron emission tomography. J. Clin. Oncol. 20, 379–387.

Bosse, P., Bernex, F., De Sepulveda, P., SalauÈn, P., Panthier, J.-J., 1997. Multiple neuroendocrine tumours in transgenic mice induced by c-kit-SV40 T antigen fusion genes. Oncogene 14, 2661–2670.

Bouhlel, M.A., Derudas, B., Rigamonti, E., Dièvart, R., Brozek, J., Haulon, S., Zawadzki, C., Jude, B., Torpier, G., Marx, N., 2007. PPARγ activation primes human monocytes into alternative M2 macrophages with anti-inflammatory properties. Cell Metab. 6, 137–143.

Bradbury, A., 2010. Cloning hybridoma cDNA by RACE, in: Kontermann, R., Dubel, S. (Eds.), Antibody Engineering. Springer-Verlag, Berlin, pp. 15–20.

Bradbury, A.R.M., Sidhu, S., Dübel, S., McCafferty, J., 2011. Beyond natural antibodies: the power of in vitro display technologies. Nat. Biotechnol. 29, 245–254.

Braren, I., Blank, S., Seismann, H., Deckers, S., Ollert, M., Grunwald, T., Spillner, E., 2007. Generation of Human Monoclonal Allergen-Specific IgE and IgG Antibodies from Synthetic Antibody Libraries. Clin. Chem. 53 , 837–844. doi:10.1373/clinchem.2006.078360

Briney, B.S., Willis, J.R., McKinney, B.A., Crowe, J.E., 2012. High-throughput antibody sequencing reveals genetic evidence of global regulation of the naive and memory repertoires that extends across individuals. Genes Immun 13, 469–473.

Brockmann, E.-C., Cooper, M., Strömsten, N., Vehniäinen, M., Saviranta, P., 2005. Selecting for antibody scFv fragments with improved stability using phage display with denaturation under reducing conditions. J. Immunol. Methods 296, 159–170.

Bronte, V., Serafini, P., Apolloni, E., Zanovello, P., 2001. Tumor-Induced Immune Dysfunctions Caused by Myeloid Suppressor Cells HOSTS : A SHORT HISTORY OF 24, 431–446.

Brown, R.S., Leung, J.Y., Kison, P. V, Zasadny, K.R., Flint, A., Wahl, R.L., 1999. Glucose transporters and FDG uptake in untreated primary human non-small cell lung cancer. J. Nucl. Med. 40, 556–565.

Bruchard, M., Mignot, G., Derangère, V., Chalmin, F., Chevriaux, A., Végran, F., Boireau, W., Simon, B., Ryffel, B., Connat, J.L., 2013. Chemotherapy-triggered cathepsin B release in myeloid-derived suppressor cells activates the Nlrp3 inflammasome and promotes tumor growth. Nat. Med. 19, 57–64.

Buchwalow, I., Samoilova, V., Boecker, W., Tiemann, M., 2011. Non-specific binding of antibodies in immunohistochemistry: fallacies and facts. Sci. Rep. 1.

Butler, M., Spearman, M., 2014. The choice of mammalian cell host and possibilities for glycosylation engineering. Curr. Opin. Biotechnol. 30, 107–112. doi:http://dx.doi.org/10.1016/j.copbio.2014.06.010

Byrne, P. V, Guilbert, L.J., Stanley, E.R., 1981. Distribution of cells bearing receptors for a colony-stimulating factor (CSF-1) in murine tissues. J. Cell Biol. 91, 848–853.

Caescu, C.I., Guo, X., Tesfa, L., Bhagat, T.D., Verma, A., Zheng, D., Stanley, E.R., 2015. Colony stimulating factor-1 receptor signaling networks inhibit mouse macrophage inflammatory responses by induction of microRNA-21. Blood 125, e1–e13. doi:10.1182/blood-2014-10-608000

Carlsten, K.S., London, C.A., Haney, S., Burnett, R., Avery, A.C., Thamm, D.H., 2012. Multicenter prospective trial of hypofractionated radiation treatment, toceranib, and prednisone for measurable canine mast cell tumors. J. Vet. Intern. Med. 26, 135–141.

Cassier, P.A., Gomez-Roca, C.A., Italiano, A., Cannarile, M., Ries, C., Brillouet, A., Mueller, C., Meneses-Lorente, G., Baehner, M., Ratnayake, J., 2014. Phase 1 study of RG7155, a novel anti-CSF1R antibody, in patients with locally advanced pigmented villonodular synovitis (PVNS)., in: ASCO Annual Meeting Proceedings. p. 10504.

Caux, C., Dezutter-Dambuyant, C., Schmitt, D., Banchereau, J., 1992. GM-CSF and TNF-cooperate in the generation of dendritic Langerhans cells. Nature 258.

Cavnar, M.J., Zeng, S., Kim, T.S., Sorenson, E.C., Ocuin, L.M., Balachandran, V.P., Seifert, A.M., Greer, J.B., Popow, R., Crawley, M.H., Cohen, N.A., Green, B.L., Rossi, F., Besmer, P., Antonescu, C.R., DeMatteo, R.P., 2013. KIT oncogene inhibition drives intratumoral macrophage M2 polarization. J. Exp. Med. 210 , 2873–2886. doi:10.1084/jem.20130875

Chambers, S.K., 2009. Role of CSF-1 in progression of epithelial ovarian cancer. Futur. Oncol. 5, 1429–1440.

Chambers, S.K., Kacinski, B.M., 1994. Messenger RNA Decay of Macrophage Colony-Stimulating Factor in Hum an Ovarian Carcinomas in Vitro. J. Soc. Gynecol. Investig. 1, 310–316.

Chambers, S.K., Kacinski, B.M., Ivins, C.M., Carcangiu, M.L., 1997. Overexpression of epithelial macrophage colony-stimulating factor (CSF-1) and CSF-1 receptor: a poor prognostic factor in epithelial ovarian cancer, contrasted with a protective effect of stromal CSF-1. Clin. cancer Res. 3, 999–1007.

Chang, Y.-N., Guo, H., Li, J., Song, Y., Zhang, M., Jin, J., Xing, G., Zhao, Y., 2013. Adjusting the balance between effective loading and vector migration of macrophage vehicles to deliver nanoparticles. PLoS One 8.

Chen, G., Sidhu, S., 2014. Design and Generation of Synthetic Antibody Libraries for Phage Display, in: Ossipow, V., Fischer, N. (Eds.), Monoclonal Antibodies SE - 8, Methods in Molecular Biology. Humana Press, pp. 113–131. doi:10.1007/978-1-62703-992-5_8

Chen, R., 2012. Bacterial expression systems for recombinant protein production: E. coli and beyond. Biotechnol. Adv. 30, 1102–1107. doi:http://dx.doi.org/10.1016/j.biotechadv.2011.09.013

Chen, X., Liu, H., Focia, P.J., Shim, A.H.-R., He, X., 2008. Structure of macrophage colony stimulating factor bound to FMS: Diverse signaling assemblies of class III receptor tyrosine kinases. Proc. Natl. Acad. Sci. U. S. A. 105, 18267–18272.

Chihara, T., Suzu, S., Hassan, R., Chutiwitoonchai, N., Hiyoshi, M., Motoyoshi, K., Kimura, F., Okada, S., 2010. IL-34 and M-CSF share the receptor Fms but are not identical in biological activity and signal activation. Cell Death Differ. 17, 1917–27. doi:10.1038/cdd.2010.60

Chitu, V., Stanley, E.R., 2006. Colony-stimulating factor-1 in immunity and inflammation. Curr. Opin. Immunol. 18, 39–48. doi:10.1016/j.coi.2005.11.006

Chon, E., McCartan, L., Kubicek, L.N., Vail, D.M., 2011. Safety evaluation of combination toceranib phosphate (Palladia®) and piroxicam in tumour-bearing dogs (excluding mast cell tumours): a phase I dose-finding study*. Vet. Comp. Oncol. no–no. doi:10.1111/j.1476-5829.2011.00265.x

Chon, E., McCartan, L., Kubicek, L.N., Vail, D.M., 2012. Safety evaluation of combination toceranib phosphate (Palladia®) and piroxicam in tumour-bearing dogs (excluding mast cell tumours): a phase I dose-finding study. Vet. Comp. Oncol. 10, 184–193. doi:10.1111/j.1476-5829.2011.00265.x

Cianga, P., Medesan, C., Richardson, J.A., Ghetie, V., Ward, E.S., 1999. Identification and function of neonatal Fc receptor in mammary gland of lactating mice. Eur. J. Immunol. 29, 2515–2523. doi:10.1002/(SICI)1521-4141(199908)29:08<2515::AID-IMMU2515>3.0.CO;2-D

Ciccia, F., Alessandro, R., Rodolico, V., Guggino, G., Raimondo, S., Guarnotta, C., Giardina, A., Sireci, G., Campisi, G., De Leo, G., 2013. IL-34 is overexpressed in the inflamed salivary glands of patients with Sjögren's syndrome and is associated with the local expansion of pro-inflammatory CD14brightCD16+ monocytes. Rheumatology kes435.

Clackson, T., Lowman, H.B., 2004. Phage Display : A Practical Approach, Practical approach series. OUP Oxford.

Clark, M., 2000. Antibody humanization: a case of the "Emperor"s new clothes'? Immunol. Today 21, 397–402. doi:http://dx.doi.org/10.1016/S0167-5699(00)01680-7

Conway, J.G., McDonald, B., Parham, J., Keith, B., Rusnak, D.W., Shaw, E., Jansen, M., Lin, P., Payne, A., Crosby, R.M., Johnson, J.H., Frick, L., Lin, M.-H.J., Depee, S., Tadepalli, S., Votta, B., James, I., Fuller, K., Chambers, T.J., Kull, F.C., Chamberlain, S.D., Hutchins, J.T., 2005. Inhibition of colony-stimulating-factor-1 signaling in vivo with the orally bioavailable cFMS kinase inhibitor GW2580. Proc. Natl. Acad. Sci. United States Am. 102 , 16078–16083. doi:10.1073/pnas.0502000102

Conway, J.G., Pink, H., Bergquist, M.L., Han, B., Depee, S., Tadepalli, S., Lin, P., Crumrine, R.C., Binz, J., Clark, R.L., Selph, J.L., Stimpson, S.A., Hutchins, J.T., Chamberlain, S.D., Brodie, T.A., Hill, C., C, N.C.R.L., 2008. Effects of the cFMS Kinase Inhibitor 5- (3-Methoxy-4- ((4- in Normal and Arthritic Rats □. doi:10.1124/jpet.107.129429.

Coussens, L., Van Beveren, C., Smith, D., Chen, E., Mitchell, R.L., Isacke, C.M., Verma, I.M., Ullrich, A., 1986. Structural alteration of viral homologue of receptor proto-oncogene fms at carboxyl terminus.

Coxon, F.P., Thompson, K., Rogers, M.J., 2006. Recent advances in understanding the mechanism of action of bisphosphonates. Curr. Opin. Pharmacol. 6, 307–312.

Cupp, J.S., Miller, M.A., Montgomery, K.D., Nielsen, T.O., O'Connell, J.X., Huntsman, D., van de Rijn, M., Gilks, C.B., West, R.B., 2007. Translocation and expression of CSF1 in pigmented villonodular synovitis, tenosynovial giant cell tumor, rheumatoid arthritis and other reactive synovitides. Am. J. Surg. Pathol. 31, 970–976.

Dai, X.-M., 2002. Targeted disruption of the mouse colony-stimulating factor 1 receptor gene results in osteopetrosis, mononuclear phagocyte deficiency, increased primitive progenitor cell frequencies, and reproductive defects. Blood 99, 111–120. doi:10.1182/blood.V99.1.111

Dai, X.-M., Zong, X.-H., Sylvestre, V., Stanley, E.R., 2004. Incomplete restoration of colony-stimulating factor 1 (CSF-1) function in CSF-1-deficient Csf1op/Csf1op mice by transgenic expression of cell surface CSF-1. Blood 103, 1114–23. doi:10.1182/blood-2003-08-2739

Daly, M., Sheppard, S., Cohen, N., Nabity, M., Moussy, A., Hermine, O., Wilson, H., 2011. Safety of masitinib mesylate in healthy cats. J. Vet. Intern. Med. 25, 297–302. doi:10.1111/j.1939-1676.2011.0687.x

Daurkin, I., Eruslanov, E., Stoffs, T., Perrin, G.Q., Algood, C., Gilbert, S.M., Rosser, C.J., Su, L.-M., Vieweg, J., Kusmartsev, S., 2011. Tumor-associated macrophages mediate immunosuppression in the renal cancer microenvironment by activating the 15-lipoxygenase-2 pathway. Cancer Res. 71, 6400–6409.

Davies, L.C., Jenkins, S.J., Allen, J.E., Taylor, P.R., 2013. Tissue-resident macrophages. Nat. Immunol. 14, 986–995.

De Villiers, W.J., Fraser, I.P., Hughes, D.A., Doyle, A.G., Gordon, S., 1994. Macrophage-colony-stimulating factor selectively enhances macrophage scavenger receptor expression and function. J. Exp. Med. 180, 705–709.

DeNardo, D.G., Brennan, D.J., Rexhepaj, E., Ruffell, B., Shiao, S.L., Madden, S.F., Gallagher, W.M., Wadhwani, N., Keil, S.D., Junaid, S.A., 2011. Leukocyte complexity predicts breast cancer survival and functionally regulates response to chemotherapy. Cancer Discov. 1, 54–67.

Dewar, A.L., Cambareri, A.C., Zannettino, A.C.W., Miller, B.L., Doherty, K. V, Hughes, T.P., Lyons, A.B., 2005. Macrophage colony-stimulating factor receptor c-fms is a novel target of imatinib. Blood 105 , 3127–3132. doi:10.1182/blood-2004-10-3967

Dhingra, K., Fritsche, H., Murray, J.L., LoBuglio, A.F., Khazaeli, M.B., Kelley, S., Tepper, M.A., Grasela, D., Buzdar, A., Valero, V., Booser, D., Whealin, H., Collins, T.J., Pursley, J.M., Hortobagyi, G., 1995. Phase I Clinical and Pharmacological Study of Suppression of Human Antimouse Antibody Response to Monoclonal Antibody L6 by Deoxyspergualin. Cancer Res. 55 , 3060–3067.

Diel, I.J., Solomayer, E.-F., Costa, S.D., Gollan, C., Goerner, R., Wallwiener, D., Kaufmann, M., Bastert, G., 1998. Reduction in New Metastases in Breast Cancer with Adjuvant Clodronate Treatment. N. Engl. J. Med. 339, 357–363. doi:10.1056/NEJM199808063390601

Dietmair, S., Nielsen, L.K., Timmins, N.E., 2012. Mammalian cells as biopharmaceutical production hosts in the age of omics. Biotechnol. J. 7, 75–89. doi:10.1002/biot.201100369

Dodev, T.S., Karagiannis, P., Gilbert, A.E., Josephs, D.H., Bowen, H., James, L.K., Bax, H.J., Beavil, R., Pang, M.O., Gould, H.J., Karagiannis, S.N., Beavil, A.J., 2014. A tool kit for rapid cloning and expression of recombinant antibodies. Sci. Rep. 4.

Doedens, A.L., Stockmann, C., Rubinstein, M.P., Liao, D., Zhang, N., DeNardo, D.G., Coussens, L.M., Karin, M., Goldrath, A.W., Johnson, R.S., 2010. Macrophage

expression of hypoxia-inducible factor-1α suppresses T-cell function and promotes tumor progression. Cancer Res. 70, 7465–7475.

Dougherty, G.J., Selvendran, Y., Murdoch, S., Palmer, D.G., Hogg, N., 1987. The human mononuclear phagocyte high-affinity Fc receptor, FcRI, defined by a monoclonal antibody, 10.1. Eur. J. Immunol. 17, 1453–1459. doi:10.1002/eji.1830171011

Douglass, T.G., Driggers, L., Zhang, J.G., Hoa, N., Delgado, C., Williams, C.C., Dan, Q., Sanchez, R., Jeffes, E.W.B., Wepsic, H.T., Myers, M.P., Koths, K., Jadus, M.R., 2008. Macrophage colony stimulating factor: not just for macrophages anymore! A gateway into complex biologies. Int. Immunopharmacol. 8, 1354–1376. doi:10.1016/j.intimp.2008.04.016

Droin, N., Solary, E., 2010. Editorial: CSF1R, CSF-1, and IL-34, a "menage a trois" conserved across vertebrates. J. Leukoc. Biol. 87, 745–747.

Duluc, D., Corvaisier, M., Blanchard, S., Catala, L., Descamps, P., Gamelin, E., Ponsoda, S., Delneste, Y., Hebbar, M., Jeannin, P., 2009. Interferon-γ reverses the immunosuppressive and protumoral properties and prevents the generation of human tumor-associated macrophages. Int. J. Cancer 125, 367–373.

Ecker, D.M., Jones, S.D., Levine, H.L., 2014. The therapeutic monoclonal antibody market. MAbs 7, 9–14. doi:10.4161/19420862.2015.989042

Eda, H., Shimada, H., Beidler, D.R., Monahan, J.B., 2011. Proinflammatory cytokines, IL-1β and TNF-α, induce expression of interleukin-34 mRNA via JNK-and p44/42 MAPK-NF-κB pathway but not p38 pathway in osteoblasts. Rheumatol. Int. 31, 1525–1530.

El-Gamal, M.I., Jung, M.-H., Oh, C.-H., 2010. Discovery of a new potent bisamide FMS kinase inhibitor. Bioorg. Med. Chem. Lett. 20, 3216–3218. doi:10.1016/j.bmcl.2010.04.088

Else, R.W., Norval, M., Neill, W.A., 1982. The characteristics of a canine mammary carcinoma cell line, REM 134. Br. J. Cancer 46, 675.

Erblich, B., Zhu, L., Etgen, A.M., Dobrenis, K., Pollard, J.W., 2011. Absence of colony stimulation factor-1 receptor results in loss of microglia, disrupted brain development and olfactory deficits. PLoS One 6, e26317.

Erreni, M., Mantovani, A., Allavena, P., 2011. Tumor-associated macrophages (TAM) and inflammation in colorectal cancer. Cancer Microenviron. 4, 141–154.

Escamilla, J., Schokrpur, S., Liu, C., Priceman, S.J., Moughon, D., Jiang, Z., Pouliot, F., Magyar, C., Sung, J.L., Xu, J., 2015. CSF1 Receptor Targeting in Prostate Cancer Reverses Macrophage-Mediated Resistance to Androgen Blockade Therapy. Cancer Res. 75, 950–962.

Eubank, T.D., Roda, J.M., Liu, H., O'Neil, T., Marsh, C.B., 2011. Opposing roles for HIF-1α and HIF-2α in the regulation of angiogenesis by mononuclear phagocytes. Blood 117, 323–332.

Fend, L., Accart, N., Kintz, J., Cochin, S., Reymann, C., Le Pogam, F., Marchand, J.-B., Menguy, T., Slos, P., Rooke, R., 2013. Therapeutic effects of anti-CD115 monoclonal antibody in mouse cancer models through dual inhibition of tumor-associated macrophages and osteoclasts. PLoS One 8, e73310.

Fogg, D.K., Sibon, C., Miled, C., Jung, S., Aucouturier, P., Littman, D.R., Cumano, A., Geissmann, F., 2006. A clonogenic bone marrow progenitor specific for macrophages and dendritic cells. Science (80-.). 311, 83–87.

Fogle, J., 2015. A translational study of monocyte receptor expression and chemotaxis between dogs and humans with and without osteosarcoma (TUM6P. 975). J. Immunol. 194, 123–141.

Foucher, E.D., Blanchard, S., Preisser, L., Garo, E., Ifrah, N., Guardiola, P., Delneste, Y., Jeannin, P., 2013. IL-34 induces the differentiation of human monocytes into immunosuppressive macrophages. antagonistic effects of GM-CSF and IFNγ. PLoS One 8, e56045.

Frenzel, A., Hust, M., Schirrmann, T., 2013. Expression of Recombinant Antibodies. Front. Immunol. 4, 217. doi:10.3389/fimmu.2013.00217

Fridman, W.H., 1991. Fc receptors and immunoglobulin binding factors. FASEB J. 5 , 2684–2690.

Gallagher, S.R., 2001. One-Dimensional SDS Gel Electrophoresis of Proteins, in: Current Protocols in Molecular Biology. John Wiley & Sons, Inc. doi:10.1002/0471142727.mb1002as75

Garceau, V., Smith, J., Paton, I.R., Davey, M., Fares, M.A., Sester, D.P., Burt, D.W., Hume, D.A., 2010. Pivotal Advance: Avian colony-stimulating factor 1 (CSF-1), interleukin-34 (IL-34), and CSF-1 receptor genes and gene products. J. Leukoc. Biol. 87, 753–764.

Garcia-Morales, C., Rothwell, L., Moffat, L., Garceau, V., Balic, A., Sang, H.M., Kaiser, P., Hume, D.A., 2014. Production and characterisation of a monoclonal antibody that recognises the chicken CSF1 receptor and confirms that expression is restricted to macrophage-lineage cells. Dev. Comp. Immunol. 42, 278–285. doi:http://dx.doi.org/10.1016/j.dci.2013.09.011

Gauci, C.L., Alexander, P., 1975. The macrophage content of some human tumours. Cancer Lett. 1, 29–32.

Gearing, D.P., Virtue, E.R., Gearing, R.P., Drew, A.C., 2013. A fully caninised anti-NGF monoclonal antibody for pain relief in dogs. BMC Vet. Res. 9, 226.

Geissmann, F., Manz, M.G., Jung, S., Sieweke, M.H., Merad, M., Ley, K., 2010. Development of monocytes, macrophages, and dendritic cells. Science 327, 656–61. doi:10.1126/science.1178331

Gerber, J.S., Mosser, D.M., 2001. Stimulatory and inhibitory signals originatingfrom the macrophage Fcγ receptors. Microbes Infect. 3, 131–139. doi:http://dx.doi.org/10.1016/S1286-4579(00)01360-5

Gerngross, L., Fischer, T., 2014. Evidence for cFMS signaling in HIV production by brain macrophages and microglia. J. Neurovirol. 21, 249–256.

Gerngross, L., Lehmicke, G., Belkadi, A., Fischer, T., 2015. Role for cFMS in maintaining alternative macrophage polarization in SIV infection: implications for HIV neuropathogenesis. J. Neuroinflammation 12, 58.

Gilliland, L.K., Walsh, L.A., Frewin, M.R., Wise, M.P., Tone, M., Hale, G., Kioussis, D., Waldmann, H., 1999. Elimination of the Immunogenicity of Therapeutic Antibodies. J. Immunol. 162 , 3663–3671.

Giudicelli, V., Chaume, D., Lefranc, M.-P., 2004. IMGT/V-QUEST, an integrated software program for immunoglobulin and T cell receptor V–J and V–D–J rearrangement analysis. Nucleic Acids Res. 32 , W435–W440. doi:10.1093/nar/gkh412

Gliniak, B.C., Rohrschneider, L.R., 1990. Expression of the M-CSF receptor is controlled posttranscriptionally by the dominant actions of GM-CSF or multi-CSF. Cell 63, 1073–1083. doi:10.1016/0092-8674(90)90510-L

Gocheva, V., Wang, H.-W., Gadea, B.B., Shree, T., Hunter, K.E., Garfall, A.L., Berman, T., Joyce, J.A., 2010. IL-4 induces cathepsin protease activity in tumor-associated macrophages to promote cancer growth and invasion. Genes Dev. 24, 241–255.

Gordon, I., Paoloni, M., Mazcko, C., Khanna, C., 2009. The Comparative Oncology Trials Consortium: using spontaneously occurring cancers in dogs to inform the cancer drug development pathway. PLoS Med. 6, e1000161.

Gordon, S., 2007. The macrophage: past, present and future. Eur. J. Immunol. 37, S9–S17.

Gordon, S., Taylor, P.R., 2005. Monocyte and macrophage heterogeneity. Nat. Rev. Immunol. 5, 953–64. doi:10.1038/nri1733

Goswami, S., Sahai, E., Wyckoff, J.B., Cammer, M., Cox, D., Pixley, F.J., Stanley, E.R., Segall, J.E., Condeelis, J.S., 2005. Macrophages promote the invasion of breast carcinoma cells via a colony-stimulating factor-1/epidermal growth factor paracrine loop. Cancer Res. 65, 5278–5283.

Gow, D.J., Garceau, V., Kapetanovic, R., Sester, D.P., Fici, G.J., Shelly, J.A., Wilson, T.L., Hume, D.A., 2012. Cloning and expression of porcine Colony Stimulating Factor-1 (CSF-1) and Colony Stimulating Factor-1 Receptor (CSF-1R) and analysis of the species specificity of stimulation by CSF-1 and Interleukin 34. Cytokine 60, 793–805.

Gow, D.J., Sester, D.P., Hume, D. a, 2010. CSF-1, IGF-1, and the control of postnatal growth and development. J. Leukoc. Biol. 88, 475–81. doi:10.1189/jlb.0310158

Gram, H., Marconi, L.A., Barbas, C.F., Collet, T.A., Lerner, R.A., Kang, A.S., 1992. In vitro selection and affinity maturation of antibodies from a naive combinatorial immunoglobulin library. Proc. Natl. Acad. Sci. 89 , 3576–3580. doi:10.1073/pnas.89.8.3576

Green, C.E., Liu, T., Montel, V., Hsiao, G., Lester, R.D., Subramaniam, S., Gonias, S.L., Klemke, R.L., 2009. Chemoattractant signaling between tumor cells and macrophages regulates cancer cell migration, metastasis and neovascularization.

Gregory, S., Wing, E., Tweardy, D., 1992. Primary listerial infections are exacerbated in mice administered neutralizing antibody to macrophage colony-stimulating factor. J. 188–193.

Grellier, B., Grellier, B., Le Pogam, F., Le Pogam, F., Vitorino, M., Vitorino, M., Starck, J.-P., Starck, J.-P., Geist, M., Geist, M., 2014. 3D modeling and characterization of the human CD115 monoclonal antibody H27K15 epitope and design of a chimeric CD115 target, in: mAbs. Taylor & Francis, pp. 533–546.

Gruber, A.R., Lorenz, R., Bernhart, S.H., Neuböck, R., Hofacker, I.L., 2008. The Vienna RNA Websuite. Nucleic Acids Res. 36 , W70–W74. doi:10.1093/nar/gkn188

Grugan, K.D., McCabe, F.L., Kinder, M., Greenplate, A.R., Harman, B.C., Ekert, J.E., van Rooijen, N., Anderson, G.M., Nemeth, J. a, Strohl, W.R., Jordan, R.E., Brezski, R.J., 2012. Tumor-associated macrophages promote invasion while retaining Fc-dependent anti-tumor function. J. Immunol. 189, 5457–66. doi:10.4049/jimmunol.1201889

Gu, T., Mercher, T., Tyner, J.W., Goss, V.L., Walters, D.K., Cornejo, M.G., Reeves, C., Popova, L., Lee, K., Heinrich, M.C., 2007. A novel fusion of RBM6 to CSF1R in acute megakaryoblastic leukemia. Blood 110, 323–333.

Guilliams, M., Ginhoux, F., Jakubzick, C., Naik, S.H., Onai, N., Schraml, B.U., Segura, E., Tussiwand, R., Yona, S., 2014. Dendritic cells, monocytes and macrophages: a unified nomenclature based on ontogeny. Nat. Rev. Immunol. 14, 571–578.

Guth, A.M., Hafeman, S.D., Elmslie, R.E., Dow, S.W., 2013. Liposomal clodronate treatment for tumour macrophage depletion in dogs with soft-tissue sarcoma. Vet. Comp. Oncol. 11, 296–305. doi:10.1111/j.1476-5829.2012.00319.x

Haegel, H., Thioudellet, C., Hallet, R., Geist, M., Menguy, T., Le Pogam, F., Marchand, J.-B., Toh, M.-L., Duong, V., Calcei, A., 2013. A unique anti-CD115 monoclonal antibody which inhibits osteolysis and skews human monocyte differentiation from M2-polarized macrophages toward dendritic cells, in: MAbs. Taylor & Francis, pp. 736–747.

Hagar, J.A., Powell, D.A., Aachoui, Y., Ernst, R.K., Miao, E.A., 2013. Cytoplasmic LPS activates caspase-11: implications in TLR4-independent endotoxic shock. Science (80-.). 341, 1250–1253.

Hagemann, T., Biswas, S.K., Lawrence, T., Sica, A., Lewis, C.E., 2009. Regulation of macrophage function in tumors: the multifaceted role of NF-kappaB. Blood 113, 3139–3146. doi:10.1182/blood-2008-12-172825

Hammers, C.M., Stanley, J.R., 2014. Antibody Phage Display: Technique and Applications. J Invest Dermatol 134, e17.

Hammes, L.S., Tekmal, R.R., Naud, P., Edelweiss, M.I., Kirma, N., Valente, P.T., Syrjänen, K.J., Cunha-Filho, J.S., 2008. Up-regulation of VEGF, c-fms and COX-2 expression correlates with severity of cervical cancer precursor (CIN) lesions and invasive disease. Gynecol. Oncol. 110, 445–451. doi:10.1016/j.ygyno.2008.04.038

Harding, F.A., Stickler, M.M., Razo, J., DuBridge, R.B., 2010. The immunogenicity of humanized and fully human antibodies: Residual immunogenicity resides in the CDR regions. MAbs 2, 256–265.

Harlow, E., Lane, D., 1988. Antibodies a laboratory manual, 1st ed. Cold Spring Harbor Laboratory, New York.

Heisterkamp, N., Groffen, J., Stephenson, J.R., 1983. Isolation of v-fms and its human cellular homolog. Virology 126, 248–58.

Hirota, K., Oishi, Y., Taniguchi, H., Sawachi, K., Inagawa, H., Kohchi, C., Soma, G.-I., Terada, H., 2010. Antitumor effect of inhalatory lipopolysaccharide and synergetic effect in combination with cyclophosphamide. Anticancer Res. 30, 3129–3134.

Hirschfeld, M., Ma, Y., Weis, J.H., Vogel, S.N., Weis, J.J., 2000. Cutting edge: repurification of lipopolysaccharide eliminates signaling through both human and murine toll-like receptor 2. J. Immunol. 165, 618–22.

Holash, J., Davis, S., Papadopoulos, N., Croll, S.D., Ho, L., Russell, M., Boland, P., Leidich, R., Hylton, D., Burova, E., Ioffe, E., Huang, T., Radziejewski, C., Bailey, K., Fandl, J.P., Daly, T., Wiegand, S.J., Yancopoulos, G.D., Rudge, J.S., 2002. VEGF-Trap: a VEGF blocker with potent antitumor effects. Proc. Natl. Acad. Sci. U. S. A. 99, 11393–8. doi:10.1073/pnas.172398299

Holla, S., Sharma, M., Vani, J., Kaveri, S. V, Balaji, K.N., Bayry, J., 2014. GM-CSF along with IL-4 but not alone is indispensable for the differentiation of human dendritic cells from monocytes. J. Allergy Clin. Immunol. 133, 1500–1502.e1. doi:http://dx.doi.org/10.1016/j.jaci.2014.02.021

Hume, D., 2008. Differentiation and heterogeneity in the mononuclear phagocyte system. Mucosal Immunol. 1, 432–441. doi:10.1038/mi2008.36

Hume, D. a, MacDonald, K.P. a, 2012. Therapeutic applications of macrophage colony-stimulating factor-1 (CSF-1) and antagonists of CSF-1 receptor (CSF-1R) signaling. Blood 119, 1810–20. doi:10.1182/blood-2011-09-379214

Hume, D.A., 2006. The mononuclear phagocyte system. Curr. Opin. Immunol. 18, 49–53. doi:10.1016/j.coi.2005.11.008

Hume, D.A., 2008. Macrophages as APC and the dendritic cell myth. J. Immunol. 181, 5829–5835.

Hume, D.A., Donahue, R.E., Fidler, I.J., 1989. The therapeutic effect of human recombinant macrophage colony stimulating factor (CSF-1) in experimental murine metastatic melanoma. Lymphokine Res. 8, 69–77.

Hume, D.A., Ross, I.L., Himes, S.R., Sasmono, R.T., Wells, C.A., Ravasi, T., 2002. The mononuclear phagocyte system revisited. J. Leukoc. Biol. 72, 621–627.

Huynh, D., Dai, X., Nandi, S., Lightowler, S., Trivett, M., Chan, C., Bertoncello, I., Ramsay, R.G., Stanley, E.R., 2009. Colony stimulating factor-1 dependence of paneth cell development in the mouse small intestine. Gastroenterology 137, 136–144.

Hwang, W.Y.K., Foote, J., 2005. Immunogenicity of engineered antibodies. Methods 36, 3–10. doi:http://dx.doi.org/10.1016/j.ymeth.2005.01.001

Iannello, A., Ahmad, A., 2005. Role of antibody-dependent cell-mediated cytotoxicity in the efficacy of therapeutic anti-cancer monoclonal antibodies. Cancer Metastasis Rev. 24, 487–99. doi:10.1007/s10555-005-6192-2

Ide, H., Seligson, D.B., Memarzadeh, S., Xin, L., Horvath, S., Dubey, P., Flick, M.B., Kacinski, B.M., Palotie, A., Witte, O.N., 2002. Expression of colony-stimulating factor 1 receptor during prostate development and prostate cancer progression. Proc. Natl. Acad. Sci. U. S. A. 99, 14404–14409. doi:10.1073/pnas.222537099

Islam, S., 2013. Thyroid gland general histology [WWW Document]. PathologyOutlines. URL http://pathologyoutlines.com/topic/thyroidhistology.html (accessed 5.2.15).

Ito, W.D., Khmelevski, E., 2003. Tissue macrophages:“ satellite cells” for growing collateral vessels? A hypothesis. Endothelium 10, 233–235.

Jabs, A., Moncada, G.A., Nichols, C.E., Waller, E.K., Wilcox, J.N., 2005. Peripheral blood mononuclear cells acquire myofibroblast characteristics in granulation tissue. J. Vasc. Res. 42, 174–180.

Jadus, M.R., Irwin, M.R.C., Horansky, R.D., Sekhon, S., Pepper, K.A., Kohn, D.B., Wepsic, H.T., 1996. Macrophages can recognize and kill tumor cells bearing the membrane isoform of macrophage colony-stimulating factor. Blood 87, 5232–5241.

Jäger, V., Büssow, K., Wagner, A., Weber, S., Hust, M., Frenzel, A., Schirrmann, T., 2013. High level transient production of recombinant antibodies and antibody fusion proteins in HEK293 cells. BMC Biotechnol. 13, 52.

Jämsä, J., Huotari, V., Savolainen, E., Syrjälä, H., Ala-kokko, T., 2015. Kinetics of leukocyte CD11b and CD64 expression in severe sepsis and non-infectious critical care patients. Acta Anaesthesiol. Scand.

Jay, T.R., Miller, C.M., Cheng, P.J., Graham, L.C., Bemiller, S., Broihier, M.L., Xu, G., Margevicius, D., Karlo, J.C., Sousa, G.L., 2015. TREM2 deficiency eliminates TREM2+ inflammatory macrophages and ameliorates pathology in Alzheimer’s disease mouse models. J. Exp. Med. 212, 287–295.

Jeglum, K.A., 1996. Chemoimmunotherapy of canine lymphoma with adjuvant canine monoclonal antibody 231. Vet. Clin. North Am. Small Anim. Pract. 26, 73–85.

Jeglum, K.A., 2009. The history and future of canine lymphoma monoclonal antibody 231 Review Article. Cancer Ther. 7, 59–61.

Jenkins, S.J., Ruckerl, D., Cook, P.C., Jones, L.H., Finkelman, F.D., van Rooijen, N., MacDonald, A.S., Allen, J.E., 2011. Local macrophage proliferation, rather than recruitment from the blood, is a signature of Th2 inflammation. Science 332, 1284–1288. doi:10.1126/science.1204351

Jenkins, S.J., Ruckerl, D., Thomas, G.D., Hewitson, J.P., Duncan, S., Brombacher, F., Maizels, R.M., Hume, D.A., Allen, J.E., 2013. IL-4 directly signals tissue-resident macrophages to proliferate beyond homeostatic levels controlled by CSF-1. J. Exp. Med. 210 , 2477–2491. doi:10.1084/jem.20121999

Jinushi, M., Chiba, S., Yoshiyama, H., Masutomi, K., Kinoshita, I., Dosaka-Akita, H., Yagita, H., Takaoka, A., Tahara, H., 2011. Tumor-associated macrophages regulate tumorigenicity and anticancer drug responses of cancer stem/initiating cells. Proc. Natl. Acad. Sci. 108, 12425–12430.

Jögi, A., 2015. Tumour Hypoxia and the Hypoxia-Inducible Transcription Factors: Key Players in Cancer Progression and Metastasis, in: Mazurek, S., Shoshan, M. (Eds.), Tumor Cell Metabolism SE - 4. Springer Vienna, pp. 65–98. doi:10.1007/978-3-7091-1824-5_4

Joimel, U., Gest, C., Soria, J., Pritchard, L.-L., Alexandre, J., Laurent, M., Blot, E., Cazin, L., Vannier, J.-P., Varin, R., Li, H., Soria, C., 2010. Stimulation of angiogenesis resulting from cooperation between macrophages and MDA-MB-231 breast cancer cells: proposed molecular mechanism and effect of tetrathiomolybdate. BMC Cancer 10, 375. doi:10.1186/1471-2407-10-375

Jung, D.Y., Lee, H., Jung, B.-Y., Ock, J., Lee, M.-S., Lee, W.-H., Suk, K., 2005. TLR4, but not TLR2, signals autoregulatory apoptosis of cultured microglia: a critical role of IFN-β as a decision maker. J. Immunol. 174, 6467–6476.

Kabat, E.A., Wu, T.T., 1991. Identical V region amino acid sequences and segments of sequences in antibodies of different specificities. Relative contributions of VH and VL genes, minigenes, and complementarity-determining regions to binding of antibody-combining sites. J. Immunol. 147 , 1709–1719.

Kacinski, B.M., 1997. CSF-1 and its receptor in breast carcinomas and neoplasms of the female reproductive tract. Mol. Reprod. Dev. 46, 71–74.

Kataki, A., Scheid, P., Piet, M., Marie, B., Martinet, N., Martinet, Y., Vignaud, J.-M., 2002. Tumor infiltrating lymphocytes and macrophages have a potential dual role in lung cancer by supporting both host-defense and tumor progression. J. Lab. Clin. Med. 140, 320–328.

Katsuno, Y., Lamouille, S., Derynck, R., 2013. TGF-β signaling and epithelial–mesenchymal transition in cancer progression. Curr. Opin. Oncol. 25, 76–84.

Kawai, T., Akira, S., 2007. Signaling to NF-κB by Toll-like receptors. Trends Mol. Med. 13, 460–469.

Kayagaki, N., Wong, M.T., Stowe, I.B., Ramani, S.R., Gonzalez, L.C., Akashi-Takamura, S., Miyake, K., Zhang, J., Lee, W.P., Muszyński, A., 2013. Noncanonical

inflammasome activation by intracellular LPS independent of TLR4. Science (80-.). 341, 1246–1249.

Kelley, T.W., Graham, M.M., Doseff, A.I., Pomerantz, R.W., Lau, S.M., Ostrowski, M.C., Franke, T.F., Marsh, C.B., 1999. Macrophage colony-stimulating factor promotes cell survival through Akt/protein kinase B. J. Biol. Chem. 274, 26393–26398.

Kerbel, R.S., Dennis, J.W., 1980. Are there Fc receptors on non-lymphoreticular tumor cells? Immunol. Today 1, 69–72. doi:10.1016/0167-5699(80)90024-9

Kettleborough, C.A., Saldanha, J., Heath, V.J., Morrison, C.J., Bendig, M.M., 1991. Humanization of a mouse monoclonal antibody by CDR–grafting: the importance of framework residues on loop conformation. Protein Eng. 4, 773–783.

Khatami, M., 2007. Standardizing cancer biomarkers criteria: data elements as a foundation for a database. Inflammatory mediator/M-CSF as model marker. Cell Biochem. Biophys. 47, 187–198.

Killick, D.R., Stell, A.J., Catchpole, B., 2015. Immunotherapy for canine cancer – Is it time to go back to the future? J. Small Anim. Pract. 56, 229–241. doi:10.1111/jsap.12336

Kimura, F., Takemura, Y., Ohtsuki, T., Mizukami, H., Takagi, S., Yamamoto, K., Nagata, N., Motoyoshi, K., 1992. Serial changes of the serum macrophage colony-stimulating factor level after cytoreductive chemotherapy. Int. J. Hematol. 55, 147–155.

Kimura, H., Kimura, M., Westra, W.H., Rose, N.R., Caturegli, P., 2005. Increased thyroidal fat and goitrous hypothyroidism induced by interferon-γ. Int. J. Exp. Pathol. 86, 97–106.

King, S., 2013. The Best Selling Drugs of All Time; Humira Joins The Elite. Forbes.

Kipriyanov, S.M., Moldenhauer, G., Little, M., 1997. High level production of soluble single chain antibodies in small-scale Escherichia coli cultures. J. Immunol. Methods 200, 69–77. doi:http://dx.doi.org/10.1016/S0022-1759(96)00188-3

Kirma, N., Luthra, R., Jones, J., Liu, Y.-G., Nair, H.B., Mandava, U., Tekmal, R.R., 2004. Overexpression of the colony-stimulating factor (CSF-1) and/or its receptor c-fms in mammary glands of transgenic mice results in hyperplasia and tumor formation. Cancer Res. 64, 4162–4170.

Kirshenbaum, A.S., Goff, J.P., Semere, T., Foster, B., Scott, L.M., Metcalfe, D.D., 1999. Demonstration That Human Mast Cells Arise From a Progenitor Cell Population That Is CD34+, c-kit+, and Expresses Aminopeptidase N (CD13). Blood 94, 2333–2342.

Kitagawa, D., Gouda, M., Kirii, Y., Sugiyama, N., Ishihama, Y., Fujii, I., Narumi, Y., Akita, K., Yokota, K., 2012. Characterization of kinase inhibitors using different phosphorylation states of colony stimulating factor-1 receptor tyrosine kinase . J. Biochem. 151 , 47–55. doi:10.1093/jb/mvr112

Kluger, H.M., 2004. Macrophage Colony-Stimulating Factor-1 Receptor Expression Is Associated with Poor Outcome in Breast Cancer by Large Cohort Tissue Microarray Analysis. Clin. Cancer Res. 10, 173–177. doi:10.1158/1078-0432.CCR-0699-3

Kluger, H.M., Kluger, Y., Gilmore-Hebert, M., DiVito, K., Chang, J.T., Rodov, S., Mironenko, O., Kacinski, B.M., Perkins, A.S., Sapi, E., 2004. cDNA microarray analysis of invasive and tumorigenic phenotypes in a breast cancer model. Lab. Investig. 84, 320–331.

Koh, Y.W., Kang, H.J., Park, C., Yoon, D.H., Kim, S., Suh, C., Go, H., Kim, J.E., Kim, C.-W., Huh, J., 2012. The ratio of the absolute lymphocyte count to the absolute monocyte count is associated with prognosis in Hodgkin's lymphoma: correlation with tumor-associated macrophages. Oncologist 17, 871–880.

Köhler, G., Milstein, C., 1975. Continuous cultures of fused cells secreting antibody of predefined specificity. Nature 256, 495–497.

Komano, Y., Nanki, T., Hayashida, K., Taniguchi, K., Miyasaka, N., 2006. Identification of a human peripheral blood monocyte subset that differentiates into osteoclasts. Arthritis Res. Ther. 8, R152.

Komohara, Y., Hirahara, J., Horikawa, T., Kawamura, K., Kiyota, E., Sakashita, N., Araki, N., Takeya, M., 2006. AM-3K, an anti-macrophage antibody, recognizes CD163, a molecule associated with an anti-inflammatory macrophage phenotype. J. Histochem. Cytochem. 54, 763–771.

Kondo, Y., Lemere, C.A., Seabrook, T.J., 2007. Osteopetrotic (op/op) mice have reduced microglia, no Abeta deposition, and no changes in dopaminergic neurons. J. Neuroinflammation 4, 31. doi:10.1186/1742-2094-4-31

Kontermann, R., 2010. Immunotube Selections, in: Kontermann, R., Dübel, S. (Eds.), Antibody Engineering SE - 9. Springer Berlin Heidelberg, pp. 127–137. doi:10.1007/978-3-642-01144-3_9

Król, M., Majchrzak, K., Mucha, J., Homa, A., Bulkowska, M., Jakubowska, A., Karwicka, M., Pawłowski, K.M., Motyl, T., 2013. CSF-1R as an inhibitor of apoptosis and promoter of proliferation, migration and invasion of canine mammary cancer cells. BMC Vet. Res. 9, 65.

Król, M., Pawlowski, K.M., Majchrzak, K., Dolka, I., Abramowicz, A., Szyszko, K., Motyl, T., 2011. Density of tumor-associated macrophages (TAMs) and expression of their growth factor receptor MCSF-R and CD14 in canine mammary adenocarcinomas of various grade of malignancy and metastasis. Pol. J. Vet. Sci. 14, 3–10.

Król, M., Pawłowski, K.M., Majchrzak, K., Gajewska, M., Majewska, A., Motyl, T., 2012. Global gene expression profiles of canine macrophages and canine mammary cancer cells grown as a co-culture in vitro. BMC Vet. Res. 8, 16. doi:10.1186/1746-6148-8-16

Kubota, T., Niwa, R., Satoh, M., Akinaga, S., Shitara, K., Hanai, N., 2009. Engineered therapeutic antibodies with improved effector functions. Cancer Sci. 100, 1566–1572.

Kusmartsev, S., Gabrilovich, D.I., 2005. STAT1 Signaling Regulates Tumor-Associated Macrophage-Mediated T Cell Deletion. J. Immunol. 174 , 4880–4891. doi:10.4049/jimmunol.174.8.4880

Lacey, D.L., Tan, H.L., Lu, J., Kaufman, S., Van, G., Qiu, W., Rattan, A., Scully, S., Fletcher, F., Juan, T., Kelley, M., Burgess, T.L., Boyle, W.J., Polverino, A.J., 2000. Osteoprotegerin Ligand Modulates Murine Osteoclast Survival in Vitro and in Vivo. Am. J. Pathol. 157, 435–448. doi:http://dx.doi.org/10.1016/S0002-9440(10)64556-7

Lamprecht, B., Walter, K., Kreher, S., Kumar, R., Hummel, M., Lenze, D., Köchert, K., Bouhlel, M.A., Richter, J., Soler, E., 2010. Derepression of an endogenous long terminal repeat activates the CSF1R proto-oncogene in human lymphoma. Nat. Med. 16, 571–579.

Laoui, D., Van Overmeire, E., De Baetselier, P., Van Ginderachter, J.A., Raes, G., 2014. Functional relationship between tumor-associated macrophages and macrophage colony-stimulating factor as contributors to cancer progression. Front. Immunol. 5.

Lauder, I., Aherne, W., Stewart, J., Sainsbury, R., 1977. Macrophage infiltration of breast tumours: a prospective study. J. Clin. Pathol. 30, 563–568.

Lauener, R.P., Goyert, S.M., Geha, R.S., Vercelli, D., 1990. Interleukin 4 down-regulates the expression of CD14 in normal human monocytes. Eur. J. Immunol. 20, 2375–2381.

Lawrence, T., Natoli, G., 2011. Transcriptional regulation of macrophage polarization: enabling diversity with identity. Nat. Rev. Immunol. 11, 750–761.

Lay, G., Poquet, Y., Salek-Peyron, P., Puissegur, M., Botanch, C., Bon, H., Levillain, F., Duteyrat, J., Emile, J., Altare, F., 2007. Langhans giant cells from M. tuberculosis induced human granulomas cannot mediate mycobacterial uptake. J. Pathol. 211, 76–85.

Ledermann, J.A., Begent, R.H., Bagshawe, K.D., Riggs, S.J., Searle, F., Glaser, M.G., Green, A.J., Dale, R.G., 1988. Repeated antitumour antibody therapy in man with suppression of the host response by cyclosporin A. Br. J. Cancer 58, 654–657.

Lee, a W., Nambirajan, S., Moffat, J.G., 1999. CSF-1 activates MAPK-dependent and p53-independent pathways to induce growth arrest of hormone-dependent human breast cancer cells. Oncogene 18, 7477–94. doi:10.1038/sj.onc.1203123

Lee, a W.-M., States, D.J., 2006. Colony-stimulating factor-1 requires PI3-kinase-mediated metabolism for proliferation and survival in myeloid cells. Cell Death Differ. 13, 1900–14. doi:10.1038/sj.cdd.4401884

Lerebours, F., Vacher, S., Andrieu, C., Espie, M., Marty, M., Lidereau, R., Bieche, I., 2008. NF-kappa B genes have a major role in inflammatory breast cancer. BMC Cancer 8, 41.

Levine, J. a, Jensen, M.D., Eberhardt, N.L., O'Brien, T., 1998. Adipocyte macrophage colony-stimulating factor is a mediator of adipose tissue growth. J. Clin. Invest. 101, 1557–1564. doi:10.1172/JCI2293

Lewis, C., Murdoch, C., 2005. Macrophage Responses to Hypoxia: Implications for Tumor Progression and Anti-Cancer Therapies. Am. J. Pathol. 167, 627–635. doi:http://dx.doi.org/10.1016/S0002-9440(10)62038-X

Lewis, C.E., Pollard, J.W., 2006. Distinct role of macrophages in different tumor microenvironments. Cancer Res. 66, 605–612. doi:10.1158/0008-5472.CAN-05-4005

Li, W., Stanley, E.R., 1991. Role of dimerization and modification of the CSF-1 receptor in its activation and internalization during the CSF-1 response. EMBO J. 10, 277.

Liao, A.T., Chien, M.B., Shenoy, N., Mendel, D.B., McMahon, G., Cherrington, J.M., London, C.A., 2002. Inhibition of constitutively active forms of mutant kit by multitargeted indolinone tyrosine kinase inhibitors. Blood 100, 585–593.

Lin, E.Y., Li, J.-F., Gnatovskiy, L., Deng, Y., Zhu, L., Grzesik, D.A., Qian, H., Xue, X., Pollard, J.W., 2006. Macrophages regulate the angiogenic switch in a mouse model of breast cancer. Cancer Res. 66, 11238–11246. doi:10.1158/0008-5472.CAN-06-1278

Lin, E.Y., Nguyen, a V, Russell, R.G., Pollard, J.W., 2001. Colony-stimulating factor 1 promotes progression of mammary tumors to malignancy. J. Exp. Med. 193, 727–40.

Lin, H., Lee, E., Hestir, K., Leo, C., Huang, M., Bosch, E., Halenbeck, R., Wu, G., Zhou, A., Behrens, D., 2008. Discovery of a cytokine and its receptor by functional screening of the extracellular proteome. Science (80-.). 320, 807–811.

Lin, K.-Y., Guarnieri, F.G., Staveley-O'Carroll, K.F., Levitsky, H.I., August, J.T., Pardoll, D.M., Wu, T.-C., 1996. Treatment of established tumors with a novel vaccine that enhances major histocompatibility class II presentation of tumor antigen. Cancer Res. 56, 21–26.

Lin, Y., Lee, H., Berg, A.H., Lisanti, M.P., Shapiro, L., Scherer, P.E., 2000. The lipopolysaccharide-activated toll-like receptor (TLR)-4 induces synthesis of the closely related receptor TLR-2 in adipocytes. J. Biol. Chem. 275, 24255–24263.

Liu, C.-B., Itoh, T., Arai, K., Watanabe, S., 1999. Constitutive activation of JAK2 confers murine interleukin-3-independent survival and proliferation of BA/F3 cells. J. Biol. Chem. 274, 6342–6349.

Liu, H., Leo, C., Chen, X., Wong, B.R., Williams, L.T., Lin, H., He, X., 2012. The mechanism of shared but distinct CSF-1R signaling by the non-homologous cytokines IL-34 and CSF-1. Biochim. Biophys. Acta - Proteins Proteomics 1824, 938–945. doi:http://dx.doi.org/10.1016/j.bbapap.2012.04.012

Liu, Y., Wang, Y., Yamakuchi, M., Isowaki, S., Nagata, E., Kanmura, Y., Kitajima, I., Maruyama, I., 2001. Upregulation of Toll-like receptor 2 gene expression in macrophage response to peptidoglycan and high concentration of lipopolysaccharide is involved in NF-κB activation. Infect. Immun. 69, 2788–2796.

Lobo, E.D., Hansen, R.J., Balthasar, J.P., 2004. Antibody pharmacokinetics and pharmacodynamics. J. Pharm. Sci. 93, 2645–68. doi:10.1002/jps.20178

London, C., Mathie, T., Stingle, N., Clifford, C., Haney, S., Klein, M.K., Beaver, L., Vickery, K., Vail, D.M., Hershey, B., 2012. Preliminary evidence for biologic activity of toceranib phosphate (Palladia®) in solid tumours. Vet. Comp. Oncol. 10, 194–205.

London, C.A., Hannah, A.L., Zadovoskaya, R., Malignancies, S., Chien, M.B., Kollias-baker, C., Rosenberg, M., Downing, S., Post, G., Boucher, J., Shenoy, N., Mendel, D.B., Mcmahon, G., Cherrington, J.M., 2003. Phase I Dose-Escalating Study of SU11654 , a Small Molecule Receptor Tyrosine Kinase Inhibitor , in Dogs with Spontaneous Malignancies , Phase I Dose-Escalating Study of SU11654 , a Small Molecule Receptor Tyrosine Kinase Inhibitor , in Dogs with 2755–2768.

London, C.A., Malpas, P.B., Wood-Follis, S.L., Boucher, J.F., Rusk, A.W., Rosenberg, M.P., Henry, C.J., Mitchener, K.L., Klein, M.K., Hintermeister, J.G., Bergman, P.J., Couto, G.C., Mauldin, G.N., Michels, G.M., 2009. Multi-center, placebo-controlled, double-blind, randomized study of oral toceranib phosphate (SU11654), a receptor tyrosine kinase inhibitor, for the treatment of dogs with recurrent (either local or distant) mast cell tumor following surgical excision. Clin. Cancer Res. 15, 3856–3865. doi:10.1158/1078-0432.CCR-08-1860

Louis, C., Cook, A.D., Lacey, D., Fleetwood, A.J., Vlahos, R., Anderson, G.P., Hamilton, J.A., 2015. Specific Contributions of CSF-1 and GM-CSF to the Dynamics of the Mononuclear Phagocyte System. J. Immunol. 1500369.

Lu, C., Shimaoka, M., Salas, A., Springer, T.A., 2004. The binding sites for competitive antagonistic, allosteric antagonistic, and agonistic antibodies to the I domain of integrin LFA-1. J. Immunol. 173, 3972–3978.

Luo, J., Elwood, F., Britschgi, M., Villeda, S., Zhang, H., Ding, Z., Zhu, L., Alabsi, H., Getachew, R., Narasimhan, R., 2013. Colony-stimulating factor 1 receptor (CSF1R) signaling in injured neurons facilitates protection and survival. J. Exp. Med. 210, 157–172.

Luo, Y., Pollard, J.W., Casadevall, A., 2010. Fcγ receptor cross-linking stimulates cell proliferation of macrophages via the ERK pathway. J. Biol. Chem. 285, 4232–4242.

Lyskov, S., Chou, F.-C., Conchúir, S.Ó., Der, B.S., Drew, K., Kuroda, D., Xu, J., Weitzner, B.D., Renfrew, P.D., Sripakdeevong, P., 2013. Serverification of molecular modeling applications: the Rosetta Online Server that Includes Everyone (ROSIE). PLoS One 8, e63906.

Ma, G., Pan, P., Eisenstein, S., 2011. Paired Immunoglobin Like Receptor-B regulates the suppressive function and fate of myeloid derived suppressor cells. Immunity 34, 385–395. doi:10.1016/j.immuni.2011.02.004.Paired

Ma, X., Lin, W.Y., Chen, Y., Stawicki, S., Mukhyala, K., Wu, Y., Martin, F., Bazan, J.F., Starovasnik, M.A., 2012. Structural Basis for the Dual Recognition of Helical Cytokines IL-34 and CSF-1 by CSF-1R. Structure 20, 676–687. doi:http://dx.doi.org/10.1016/j.str.2012.02.010

MacDonald, K.P. a, Rowe, V., Bofinger, H.M., Thomas, R., Sasmono, T., Hume, D.A., Hill, G.R., 2005. The Colony-Stimulating Factor 1 Receptor Is Expressed on Dendritic Cells during Differentiation and Regulates Their Expansion. J. Immunol. 175, 1399–1405.

MacDonald, K.P.A., Palmer, J.S., Cronau, S., Seppanen, E., Olver, S., Raffelt, N.C., Kuns, R., Pettit, A.R., Clouston, A., Wainwright, B., Branstetter, D., Smith, J., Paxton, R.J., Cerretti, D.P., Bonham, L., Hill, G.R., Hume, D.A., 2010. An antibody against the colony-stimulating factor 1 receptor depletes the resident subset of monocytes and tissue- and tumor-associated macrophages but does not inhibit inflammation . Blood 116 , 3955–3963.

MacEwen, E.G., Kurzman, I.D., 1996. Canine osteosarcoma: amputation and chemoimmunotherapy. Vet. Clin. North Am. Small Anim. Pract. 26, 123–133.

Mahon, C.M., Lambert, M.A., Glanville, J., Wade, J.M., Fennell, B.J., Krebs, M.R., Armellino, D., Yang, S., Liu, X., O'Sullivan, C.M., Autin, B., Oficjalska, K., Bloom, L., Paulsen, J., Gill, D., Damelin, M., Cunningham, O., Finlay, W.J.J., 2013. Comprehensive Interrogation of a Minimalist Synthetic CDR-H3 Library and Its Ability to Generate Antibodies with Therapeutic Potential. J. Mol. Biol. 425, 1712–1730. doi:http://dx.doi.org/10.1016/j.jmb.2013.02.015

Mahon, K.L., Lin, H.M., Castillo, L., Lee, B.Y., Lee-Ng, M., Chatfield, M.D., Chiam, K., Breit, S.N., Brown, D.A., Molloy, M.P., 2015. Cytokine profiling of docetaxel-resistant castration-resistant prostate cancer. Br. J. Cancer 112, 1340–1348.

Makabe, K., Nakanishi, T., Tsumoto, K., Tanaka, Y., Kondo, H., Umetsu, M., Sone, Y., Asano, R., Kumagai, I., 2008. Thermodynamic Consequences of Mutations in Vernier Zone Residues of a Humanized Anti-human Epidermal Growth Factor Receptor Murine Antibody, 528. J. Biol. Chem. 283 , 1156–1166. doi:10.1074/jbc.M706190200

Makridakis, M., Vlahou, A., 2010. Secretome proteomics for discovery of cancer biomarkers. J. Proteomics 73, 2291–2305. doi:http://dx.doi.org/10.1016/j.jprot.2010.07.001

Mantovani, A., Allavena, P., 2015. The interaction of anticancer therapies with tumor-associated macrophages. J. Exp. Med. . doi:10.1084/jem.20150295

Mantovani, A., Allavena, P., Sica, A., Balkwill, F., 2008. Cancer-related inflammation. Nature 454, 436–44. doi:10.1038/nature07205

Mantovani, A., Sica, A., 2010. Macrophages, innate immunity and cancer: balance, tolerance, and diversity. Curr. Opin. Immunol. 22, 231–237.

Mantovani, A., Sozzani, S., Locati, M., Allavena, P., Sica, A., 2002. Macrophage polarization: tumor-associated macrophages as a paradigm for polarized M2 mononuclear phagocytes. Trends Immunol. 23, 549–555.

Marabelle, A., Kohrt, H., Caux, C., Levy, R., 2014. Intratumoral Immunization: A New Paradigm for Cancer Therapy. Clin. Cancer Res. 20 , 1747–1756. doi:10.1158/1078-0432.CCR-13-2116

Marech, I., Patruno, R., Zizzo, N., Gadaleta, C., Introna, M., Zito, A.F., Gadaleta, C.D., Ranieri, G., 2014. Masitinib (AB1010), from canine tumor model to human clinical development: where we are? Crit. Rev. Oncol. Hematol. 91, 98–111.

Marks, S.C., Lane, P.W., 1976. Osteopetrosis, a new recessive skeletal mutation on chromosome 12 of the mouse. J. Hered. 67, 11–18.

Martineau, P., 2010. Synthetic Antibody Libraries, in: Kontermann, R., Dübel, S. (Eds.), Antibody Engineering SE - 6. Springer Berlin Heidelberg, pp. 85–97. doi:10.1007/978-3-642-01144-3_6

Martinez, F.O., Gordon, S., 2014. The M1 and M2 paradigm of macrophage activation: time for reassessment. F1000Prime Rep. 6, 13. doi:10.12703/P6-13

Maruyama, K., Ii, M., Cursiefen, C., Jackson, D.G., Keino, H., Tomita, M., Rooijen, N. Van, Takenaka, H., Amore, P.A.D., Stein-streilein, J., Losordo, D.W., Streilein, J.W., 2005. Inflammation-induced lymphangiogenesis in the cornea arises from CD11b-positive macrophages 115, 2363–2372. doi:10.1172/JCI23874.lymphatic

Mashkani, B., Griffith, R., Ashman, L.K., 2010. Colony stimulating factor-1 receptor as a target for small molecule inhibitors. Bioorg. Med. Chem. 18, 1789–1797. doi:10.1016/j.bmc.2010.01.056

Matsumura, T., Ito, A., Takii, T., Hayashi, H., Onozaki, K., 2000. Endotoxin and cytokine regulation of toll-like receptor (TLR) 2 and TLR4 gene expression in murine liver and hepatocytes. J. Interf. Cytokine Res. 20, 915–921.

Mcdonough, S.K., Larsen, S., Brodey, R.S., Stock, N.D., Hardy, W.D., 1971. A Transmissible Feline Fibrosarcoma of Viral Origin A Transmissible Feline Fibrosarcoma of Viral Origin ' 953–956.

McLaren, J., Prentice, A., Charnock-Jones, D.S., Millican, S.A., Müller, K.H., Sharkey, A.M., Smith, S.K., 1996. Vascular endothelial growth factor is produced by peritoneal fluid macrophages in endometriosis and is regulated by ovarian steroids. J. Clin. Invest. 98, 482–489. doi:10.1172/JCI118815

Michel, J.B., Quertermous, T., 1989. Modulation of mRNA levels for urinary- and tissue-type plasminogen activator and plasminogen activator inhibitors 1 and 2 in human fibroblasts by interleukin 1. J. Immunol. 143, 890–895.

Michelsen, K.S., Aicher, A., Mohaupt, M., Hartung, T., Dimmeler, S., Kirschning, C.J., Schumann, R.R., 2001. The role of toll-like receptors (TLRs) in bacteria-induced maturation of murine dendritic cells (DCS) Peptidoglycan and lipoteichoic acid are inducers of DC maturation and require TLR2. J. Biol. Chem. 276, 25680–25686.

Milas, L., Wike, J., Hunter, N., Volpe, J., Basic, I., 1987. Macrophage content of murine sarcomas and carcinomas: associations with tumor growth parameters and tumor radiocurability. Cancer Res. 47, 1069–1075.

Mirsky, A., Kazandjian, L., Anisimova, M., 2015. Antibody-Specific Model of Amino Acid Substitution for Immunological Inferences from Alignments of Antibody Sequences. Mol. Biol. Evol. 32 , 806–819. doi:10.1093/molbev/msu340

Mitchem, J.B., Brennan, D.J., Knolhoff, B.L., Belt, B. a, Zhu, Y., Sanford, D.E., Belaygorod, L., Carpenter, D., Collins, L., Piwnica-Worms, D., Hewitt, S., Udupi,

G.M., Gallagher, W.M., Wegner, C., West, B.L., Wang-Gillam, A., Goedegebuure, P., Linehan, D.C., DeNardo, D.G., 2013. Targeting tumor-infiltrating macrophages decreases tumor-initiating cells, relieves immunosuppression, and improves chemotherapeutic responses. Cancer Res. 73, 1128–41. doi:10.1158/0008-5472.CAN-12-2731

Modjtahedi, H., Ali, S., Essapen, S., 2012. Therapeutic application of monoclonal antibodies in cancer: advances and challenges. Br. Med. Bull. 104, 41–59.

Moffat, J.G., Rudolph, J., Bailey, D., 2014. Phenotypic screening in cancer drug discovery [mdash] past, present and future. Nat Rev Drug Discov 13, 588–602.

Moffat, L., Rothwell, L., Garcia-Morales, C., Sauter, K.A., Kapetanovic, R., Gow, D.J., Hume, D.A., 2014. Development and characterisation of monoclonal antibodies reactive with porcine CSF1R (CD115). Dev. Comp. Immunol. 47, 123–128. doi:http://dx.doi.org/10.1016/j.dci.2014.07.001

Morandi, A., Barbetti, V., Riverso, M., Sbarba, P. Dello, Rovida, E., 2011. The colony-stimulating factor-1 (CSF-1) receptor sustains ERK1/2 activation and proliferation in breast cancer cell lines. PLoS One 6, e27450.

Morantz, R.A., Wood, G.W., Foster, M., Clark, M., Gollahon, K., 1979. Macrophages in experimental and human brain tumors: Part 2: Studies of the macrophage content of human brain tumors. J. Neurosurg. 50, 305–311.

Murayama, T., Yokode, M., Kataoka, H., Imabayashi, T., Yoshida, H., Sano, H., Nishikawa, S., Kita, T., 1999. Intraperitoneal administration of anti-c-fms monoclonal antibody prevents initial events of atherogenesis but does not reduce the size of advanced lesions in apolipoprotein E-deficient mice. Circulation 99, 1740–6.

Murdoch, C., Giannoudis, A., Lewis, C.E., 2004. Mechanisms regulating the recruitment of macrophages into hypoxic areas of tumors and other ischemic tissues. Blood 104, 2224–2234.

Muzio, M., Bosisio, D., Polentarutti, N., D'amico, G., Stoppacciaro, A., Mancinelli, R., van't Veer, C., Penton-Rol, G., Ruco, L.P., Allavena, P., 2000. Differential expression and regulation of toll-like receptors (TLR) in human leukocytes: selective expression of TLR3 in dendritic cells. J. Immunol. 164, 5998–6004.

Nandi, S., Akhter, M.P., Seifert, M.F., Dai, X.-M., Stanley, E.R., 2006. Developmental and functional significance of the CSF-1 proteoglycan chondroitin sulfate chain. Blood 107, 786–795. doi:10.1182/blood-2005-05-1822

Nandi, S., Cioce, M., Yeung, Y.-G., Nieves, E., Tesfa, L., Lin, H., Hsu, A.W., Halenbeck, R., Cheng, H.-Y., Gokhan, S., 2013. Receptor-type protein-tyrosine phosphatase ζ is a functional receptor for interleukin-34. J. Biol. Chem. 288, 21972–21986.

Nasir, L., Devlin, P., Mckevitt, T., Rutteman, G., Argyle, D.J., 2001. Telomere lengths and telomerase activity in dog tissues: a potential model system to study human telomere and telomerase biology. Neoplasia 3, 351–9. doi:10.1038/sj/neo/7900173

Natanson, L., 2011. New report shows monoclonal antibody development times are lengthening. Biotechnol. Ind. Organ. 1.

Nicolin, V., Bortul, R., Bareggi, R., Baldini, G., Martinelli, B., Narducci, P., 2008. Breast adenocarcinoma MCF-7 cell line induces spontaneous osteoclastogenesis via a RANK-ligand-dependent pathway. Acta Histochem. 110, 388–96. doi:10.1016/j.acthis.2007.12.002

Novak, U., Harpur, A.G., Paradiso, L., Kanagasundaram, V., Jaworowski, A., Wilks, A.F., Hamilton, J.A., 1995. Colony-stimulating factor 1-induced STAT1 and STAT3 activation is. Blood 86, 2948–2956.

Nowicki, A., Szenajch, J., Ostrowska, G., Wojtowicz, A., Wojtowicz, K., Kruszewski, A.A., Maruszynski, M., Aukerman, S.L., Wiktor-Jedrzejczak, W., 1996. Impaired tumor growth in colony-stimulating factor 1 (CSF-1)-deficient, macrophage-deficient op/op mouse: Evidence for a role of CSF-1-dependent macrophages in formation of tumor stroma. Int. J. Cancer 65, 112–119.

Noy, R., Pollard, J.W., 2015. Tumor-Associated Macrophages: From Mechanisms to Therapy. Immunity 41, 49–61. doi:10.1016/j.immuni.2014.06.010

O'Brien, P.M., Aitken, R., 2004. Antibody Phage Display: Methods and Protocols, Biomed Protocols. Humana Press.

Ober, R.J., Radu, C.G., Ghetie, V., Ward, E.S., 2001. Differences in promiscuity for antibody–FcRn interactions across species: implications for therapeutic antibodies. Int. Immunol. 13 , 1551–1559. doi:10.1093/intimm/13.12.1551

Ohno, S., Inagawa, H., Dhar, D.K., Fujii, T., Ueda, S., Tachibana, M., Ohno, Y., Suzuki, N., Inoue, M., SOMA, G.-I., 2005. Role of tumor-associated macrophages (TAM) in advanced gastric carcinoma: the impact on FasL-mediated counterattack. Anticancer Res. 25, 463–470.

Ohno, S., Inagawa, H., Dhar, D.K., Fujii, T., Ueda, S., Tachibana, M., Suzuki, N., Inoue, M., Soma, G., Nagasue, N., 2002. The degree of macrophage infiltration into the cancer cell nest is a significant predictor of survival in gastric cancer patients. Anticancer Res. 23, 5015–5022.

Ohno, S., Ohno, Y., Suzuki, N., Kamei, T., Koike, K., Inagawa, H., Kohchi, C., Soma, G.-I., Inoue, M., 2004. Correlation of histological localization of tumor-associated macrophages with clinicopathological features in endometrial cancer. Anticancer Res. 24, 3335–3342.

Ojalvo, L.S., Whittaker, C.A., Condeelis, J.S., Pollard, J.W., 2010. Gene Expression Analysis of Macrophages That Facilitate Tumor Invasion Supports a Role for Wnt-Signaling in Mediating Their Activity in Primary Mammary Tumors. J. Immunol. 184 , 702–712.

Okazaki, T., Ebihara, S., Takahashi, H., Asada, M., Kanda, A., Sasaki, H., 2005. Macrophage colony-stimulating factor induces vascular endothelial growth factor

production in skeletal muscle and promotes tumor angiogenesis. J. Immunol. 174, 7531–7538.

Ono, M., 2008. Molecular links between tumor angiogenesis and inflammation: inflammatory stimuli of macrophages and cancer cells as targets for therapeutic strategy. Cancer Sci. 99, 1501–1506. doi:10.1111/j.1349-7006.2008.00853.x

Palucka, K.A., Taquet, N., Sanchez-Chapuis, F., Gluckman, J.C., 1998. Dendritic Cells as the Terminal Stage of Monocyte Differentiation. J. Immunol. 160, 4587–4595.

Paoloni, M., Khanna, C., 2008. Translation of new cancer treatments from pet dogs to humans. Nat. Rev. Cancer 8, 147–156. doi:10.1038/nrc2273

Paoloni, M.C., Khanna, C., 2007. Comparative oncology today. Vet. Clin. North Am. Small Anim. Pract. 37, 1023–1032.

Park, J.E., Barbul, A., 2004. Understanding the role of immune regulation in wound healing. Am. J. Surg. 187, S11–S16.

Park, S.-J., Nakagawa, T., Kitamura, H., Atsumi, T., Kamon, H., Sawa, S., Kamimura, D., Ueda, N., Iwakura, Y., Ishihara, K., 2004. IL-6 regulates in vivo dendritic cell differentiation through STAT3 activation. J. Immunol. 173, 3844–3854.

Paterson, A.H., Powles, T.J., Kanis, J.A., McCloskey, E., Hanson, J., Ashley, S., 1993. Double-blind controlled trial of oral clodronate in patients with bone metastases from breast cancer. J. Clin. Oncol. 11, 59–65.

Patsialou, A., Wang, Y., Pignatelli, J., Chen, X., Entenberg, D., Oktay, M., Condeelis, J.S., 2015. Autocrine CSF1R signaling mediates switching between invasion and proliferation downstream of TGFβ in claudin-low breast tumor cells. Oncogene 34, 2721–2731.

Patsialou, A., Wyckoff, J., Wang, Y., Goswami, S., Stanley, E.R., Condeelis, J.S., 2009. Invasion of human breast cancer cells in vivo requires both paracrine and autocrine loops involving the colony-stimulating factor-1 receptor. Cancer Res. 69, 9498–9506. doi:10.1158/0008-5472.CAN-09-1868

Paulus, P., Stanley, E.R., Schäfer, R., Abraham, D., Aharinejad, S., 2006. Colony-stimulating factor-1 antibody reverses chemoresistance in human MCF-7 breast cancer xenografts. Cancer Res. 66, 4349–56. doi:10.1158/0008-5472.CAN-05-3523

Pei, X.H., Nakanishi, Y., Takayama, K., Bai, F., Hara, N., 1999. Granulocyte, granulocyte-macrophage, and macrophage colony-stimulating factors can stimulate the invasive capacity of human lung cancer cells. Br. J. Cancer 79, 40–46. doi:10.1038/sj.bjc.6690009

Peña, L., Perez-Alenza, M.D., Rodriguez-Bertos, A., Nieto, A., 2003. Canine inflammatory mammary carcinoma: histopathology, immunohistochemistry and clinical implications of 21 cases. Breast Cancer Res. Treat. 78, 141–148.

Persic, L., Roberts, a, Wilton, J., Cattaneo, a, Bradbury, a, Hoogenboom, H.R., 1997. An integrated vector system for the eukaryotic expression of antibodies or their fragments after selection from phage display libraries. Gene 187, 9–18.

Pixley, F.J., Stanley, E.R., 2004. CSF-1 regulation of the wandering macrophage: complexity in action. Trends Cell Biol. 14, 628–638. doi:10.1016/j.tcb.2004.09.016

Pollack, A., 2014. Start-Ups Work on Biotech Drugs for Pets. New York Times.

Pollard, J.W., 2004. Tumour-educated macrophages promote tumour progression and metastasis. Nat. Rev. Cancer 4, 71–8. doi:10.1038/nrc1256

Polverini, P.J., Leibovich, S.J., 1984. Induction of neovascularization in vivo and endothelial proliferation in vitro by tumor-associated macrophages. Lab. Invest. 51, 635–42.

Ponsel, D., Neugebauer, J., Ladetzki-Baehs, K., Tissot, K., 2011. High affinity, developability and functional size: the holy grail of combinatorial antibody library generation. Molecules 16, 3675–3700.

Porta, C., Rimoldi, M., Raes, G., Brys, L., Ghezzi, P., Di Liberto, D., Dieli, F., Ghisletti, S., Natoli, G., De Baetselier, P., 2009. Tolerance and M2 (alternative) macrophage polarization are related processes orchestrated by p50 nuclear factor κB. Proc. Natl. Acad. Sci. 106, 14978–14983.

Priceman, S.J., Sung, J.L., Shaposhnik, Z., Burton, J.B., Torres-collado, A.X., Moughon, D.L., Johnson, M., Lusis, A.J., Cohen, D.A., Iruela-arispe, M.L., Wu, L., 2010. Targeting distinct tumor-infiltrating myeloid cells by inhibiting CSF-1 receptor: combating tumor evasion of antiangiogenic therapy. Blood 115, 7–9. doi:10.1182/blood-2009-08-237412.

Pujol, B.F., Lucibello, F.C., Gehling, U.M., Lindemann, K., Weidner, N., Zuzarte, M., Adamkiewicz, J., Elsässer, H., Müller, R., Havemann, K., 2000. Endothelial-like cells derived from human CD14 positive monocytes. Differentiation 65, 287–300.

Pukrop, T., Klemm, F., Hagemann, T., Gradl, D., Schulz, M., Siemes, S., Trümper, L., Binder, C., 2006. Wnt 5a signaling is critical for macrophage-induced invasion of breast cancer cell lines. Proc. Natl. Acad. Sci. 103, 5454–5459.

Punt, C.J.A., Nagy, A., Douillard, J.-Y., Figer, A., Skovsgaard, T., Monson, J., Barone, C., Fountzilas, G., Riess, H., Moylan, E., 2002. Edrecolomab alone or in combination with fluorouracil and folinic acid in the adjuvant treatment of stage III colon cancer: a randomised study. Lancet 360, 671–677.

Pyonteck, S.M., Akkari, L., Schuhmacher, A.J., Bowman, R.L., Sevenich, L., Quail, D.F., Olson, O.C., Quick, M.L., Huse, J.T., Teijeiro, V., Setty, M., Leslie, C.S., Oei, Y., Pedraza, A., Zhang, J., Brennan, C.W., Sutton, J.C., Holland, E.C., Daniel, D., Joyce, J.A., 2013. CSF-1R inhibition alters macrophage polarization and blocks glioma progression. Nat. Med. 19, 10.1038/nm.3337. doi:10.1038/nm.3337

Qiu, F.H., Ray, P., Brown, K., Barker, P.E., Jhanwar, S., Ruddle, F.H., Besmer, P., 1988. Primary structure of c-kit: relationship with the CSF-1/PDGF receptor kinase family--

oncogenic activation of v-kit involves deletion of extracellular domain and C terminus. EMBO J. 7, 1003–11.

Quatromoni, J.G., Eruslanov, E., 2012. Tumor-associated macrophages: function, phenotype, and link to prognosis in human lung cancer. Am. J. Transl. Res. 4, 376.

Ramakrishnan, S., Xu, F.J., Brandt, S.J., Niedel, J.E., Bast, R.C., Brown, E.L., 1989. Constitutive production of macrophage colony-stimulating factor by human ovarian and breast cancer cell lines. J. Clin. Invest. 83, 921–6. doi:10.1172/JCI113977

Ramana, C. V, Chatterjee-Kishore, M., Nguyen, H., Stark, G.R., 2000. Complex roles of Stat1 in regulating gene expression. Oncogene 19, 2619–2627.

Ramanathan, M., Pinhal-Enfield, G., Hao, I., Leibovich, S.J., 2007. Synergistic up-regulation of vascular endothelial growth factor (VEGF) expression in macrophages by adenosine A2A receptor agonists and endotoxin involves transcriptional regulation via the hypoxia response element in the VEGF promoter. Mol. Biol. Cell 18, 14–23.

Ranieri, G., Pantaleo, M., Piccinno, M., Roncetti, M., Mutinati, M., Marech, I., Patruno, R., Rizzo, A., Sciorsci, R.L., 2013. Tyrosine kinase inhibitors (TKIs) in human and pet tumours with special reference to breast cancer: A comparative review. Crit. Rev. Oncol. Hematol. 88, 293–308. doi:http://dx.doi.org/10.1016/j.critrevonc.2013.05.009

Raposo, T., Gregório, H., Pires, I., Prada, J., Queiroga, F.L., 2012. Prognostic value of tumour-associated macrophages in canine mammary tumours. Vet. Comp. Oncol. 1–10. doi:10.1111/j.1476-5829.2012.00326.x

RCUK, 2015. Updated RCUK guidance for funding applications involving animal research. United Kingdom.

Reichert, J., 2012. Marketed therapeutic antibodies compendium. MAbs 3, 413–415.

Reichert, J.M., Dhimolea, E., 2012. The future of antibodies as cancer drugs. Drug Discov. Today 17, 954–963. doi:http://dx.doi.org/10.1016/j.drudis.2012.04.006

Reis, A.B., Teixeira-Carvalho, A., Giunchetti, R.C., Guerra, L.L., Carvalho, M.G., Mayrink, W., Genaro, O., Corrêa-Oliveira, R., Martins-Filho, O.A., 2006. Phenotypic features of circulating leucocytes as immunological markers for clinical status and bone marrow parasite density in dogs naturally infected by Leishmania chagasi. Clin. Exp. Immunol. 146, 303–311.

Rettenmier, C.W., Roussel, M.F., Ashmun, R.A., Ralph, P., Price, K., Sherr, C.J., 1987. Synthesis of membrane-bound colony-stimulating factor 1 (CSF-1) and downmodulation of CSF-1 receptors in NIH 3T3 cells transformed by cotransfection of the human CSF-1 and c-fms (CSF-1 receptor) genes. Mol. Cell. Biol. 7, 2378–2387.

Rey-Giraud, F., Hafner, M., Ries, C.H., 2012. In vitro generation of monocyte-derived macrophages under serum-free conditions improves their tumor promoting functions. PLoS One 7, e42656.

Ribatti, D., Nico, B., Vacca, A., Presta, M., 2006. The gelatin sponge–chorioallantoic membrane assay. Nat. Protoc. Ed. 1, 85.

Riccardo, F., Aurisicchio, L., Impellizeri, J.A., Cavallo, F., 2014. The importance of comparative oncology in translational medicine. Cancer Immunol. Immunother. 1–12.

Richardsen, E., Uglehus, R.D., Johnsen, S.H., Busund, L.-T., 2015. Macrophage-Colony Stimulating Factor (CSF1) Predicts Breast Cancer Progression and Mortality. Anticancer Res. 35, 865–874.

Ries, C.H., Cannarile, M.A., Hoves, S., Benz, J., Wartha, K., Runza, V., Rey-Giraud, F., Pradel, L.P., Feuerhake, F., Klaman, I., 2014. Targeting tumor-associated macrophages with anti-CSF-1R antibody reveals a strategy for cancer therapy. Cancer Cell 25, 846–859.

Rizk, S.S., Paduch, M., Heithaus, J.H., Duguid, E.M., Sandstrom, A., Kossiakoff, A.A., 2011. Allosteric control of ligand-binding affinity using engineered conformation-specific effector proteins. Nat Struct Mol Biol 18, 437–442.

Robinson, B.D., Sica, G.L., Liu, Y.-F., Rohan, T.E., Gertler, F.B., Condeelis, J.S., Jones, J.G., 2009. Tumor microenvironment of metastasis in human breast carcinoma: a potential prognostic marker linked to hematogenous dissemination. Clin. Cancer Res. 15, 2433–41. doi:10.1158/1078-0432.CCR-08-2179

Rondot, S., Koch, J., Breitling, F., Dübel, S., 2001. A helper phage to improve single-chain antibody presentation in phage display. Nat. Biotechnol. 19, 75–78.

Rosa, G.T., Gillet, L., Smith, C.M., De Lima, B.D., Stevenson, P.G., 2007. IgG Fc receptors provide an alternative infection route for murine gamma-herpesvirus-68. PLoS One 2, e560.

Rosas, M., Gordon, S., Taylor, P.R., 2007. Characterisation of the expression and function of the GM-CSF receptor α-chain in mice. Eur. J. Immunol. 37, 2518–2528.

Rosner, M., Schipany, K., Hengstschläger, M., 2013. Merging high-quality biochemical fractionation with a refined flow cytometry approach to monitor nucleocytoplasmic protein expression throughout the unperturbed mammalian cell cycle. Nat. Protoc. 8, 602–626.

Ross, R.J., Zhou, M., Shen, D., Fariss, R.N., Ding, X., Bojanowski, C.M., Tuo, J., Chan, C.-C., 2008. Immunological protein expression profile in Ccl2/Cx3cr1 deficient mice with lesions similar to age-related macular degeneration. Exp. Eye Res. 86, 675–683.

Rosser, M.P., Xia, W., Hartsell, S., McCaman, M., Zhu, Y., Wang, S., Harvey, S., Bringmann, P., Cobb, R.R., 2005. Transient transfection of CHO-K1-S using serum-free medium in suspension: a rapid mammalian protein expression system. Protein Expr. Purif. 40, 237–43. doi:10.1016/j.pep.2004.07.015

Roussel, M.F., Dull, T.J., Rettenmier, C.W., Ralph, P., Ullrich, A., Sherr, C.J., 1987. Transforming potential of the c-fms proto-oncogene (CSF-1 receptor).

Roussel, M.F., Sherr, C.J., 1989. Mouse NIH 3T3 cells expressing human colony-stimulating factor 1 (CSF-1) receptors overgrow in serum-free medium containing human CSF-1 as their only growth factor. Proc. Natl. Acad. Sci. 86, 7924–7927.

Rowell, J.L., McCarthy, D.O., Alvarez, C.E., 2011. Dog models of naturally occurring cancer. Trends Mol. Med. 17, 380–388.

Rue, S.M., Eckelman, B.P., Efe, J.A., Bloink, K., Deveraux, Q.L., Lowery, D., Nasoff, M., 2015. Identification of a candidate therapeutic antibody for treatment of canine B-cell lymphoma. Vet. Immunol. Immunopathol. 164, 148–159. doi:http://dx.doi.org/10.1016/j.vetimm.2015.02.004

Ruffell, B., Coussens, L.M., 2015. Macrophages and Therapeutic Resistance in Cancer. Cancer Cell 27, 462–472.

Rutledge, H.R., Jiang, W., Yang, J., Warg, L. a, Schwartz, D. a, Pisetsky, D.S., Yang, I. V, 2012. Gene expression profiles of RAW264.7 macrophages stimulated with preparations of LPS differing in isolation and purity. Innate Immun. 18, 80–8. doi:10.1177/1753425910393540

Saarto, T., Blomqvist, C., Virkkunen, P., Elomaa, I., 2001. Adjuvant Clodronate Treatment Does Not Reduce the Frequency of Skeletal Metastases in Node-Positive Breast Cancer Patients: 5-Year Results of a Randomized Controlled Trial. J. Clin. Oncol. 19 , 10–17.

Saba, T.M., 1970. Physiology and physiopathology of the reticuloendothelial system. Arch. Intern. Med. 126, 1031–1052.

Saccani, A., Schioppa, T., Porta, C., Biswas, S.K., Nebuloni, M., Vago, L., Bottazzi, B., Colombo, M.P., Mantovani, A., Sica, A., 2006. p50 nuclear factor-κB overexpression in tumor-associated macrophages inhibits M1 inflammatory responses and antitumor resistance. Cancer Res. 66, 11432–11440.

Safdari, Y., Farajnia, S., Asgharzadeh, M., Khalili, M., 2013. Antibody humanization methods – a review and update. Biotechnol. Genet. Eng. Rev. 29, 175–186. doi:10.1080/02648725.2013.801235

Saio, M., Radoja, S., Marino, M., Frey, A.B., 2001. Tumor-infiltrating macrophages induce apoptosis in activated CD8+ T cells by a mechanism requiring cell contact and mediated by both the cell-associated form of TNF and nitric oxide. J. Immunol. 167, 5583–5593.

Sakurai, T., Yamada, M., Simamura, S., Motoyoshi, K., 1996. Recombinant human macrophage-colony stimulating factor suppresses the mouse mixed lymphocyte reaction. Cell. Immunol. 171, 87–94. doi:10.1006/cimm.1996.0177

Sapi, E., 2004. The role of CSF-1 in normal physiology of mammary gland and breast cancer: an update. Exp. Biol. Med. (Maywood). 229, 1–11.

Sasmono, R.T., Ehrnsperger, A., Cronau, S.L., Ravasi, T., Kandane, R., Hickey, M.J., Cook, A.D., Himes, S.R., Hamilton, J.A., Hume, D.A., 2007. Mouse neutrophilic granulocytes express mRNA encoding the macrophage colony-stimulating factor

receptor (CSF-1R) as well as many other macrophage-specific transcripts and can transdifferentiate into macrophages in vitro in response to CSF-1. J. Leukoc. Biol. 82, 111–123.

Sasmono, R.T., Oceandy, D., Pollard, J.W., Tong, W., Pavli, P., Wainwright, B.J., Ostrowski, M.C., Himes, S.R., Hume, D. a, 2003. A macrophage colony-stimulating factor receptor-green fluorescent protein transgene is expressed throughout the mononuclear phagocyte system of the mouse. Blood 101, 1155–63. doi:10.1182/blood-2002-02-0569

Sauter, K.A., Pridans, C., Sehgal, A., Tsai, Y.T., Bradford, B.M., Raza, S., Moffat, L., Gow, D.J., Beard, P.M., Mabbott, N.A., 2014. Pleiotropic effects of extended blockade of CSF1R signaling in adult mice. J. Leukoc. Biol. 96, 265–274.

Savina, A., Amigorena, S., 2007. Phagocytosis and antigen presentation in dendritic cells. Immunol. Rev. 219, 143–156.

Sawachi, K., Shimada, Y., Taniguchi, H., Hirota, K., Inagawa, H., Kohchi, C., Soma, G.-I., Makino, K., Terada, H., 2010. Cytotoxic effects of activated alveolar macrophages on lung carcinoma cells via cell-to-cell contact and nitric oxide. Anticancer Res. 30, 3135–3141.

Saxena, R.K., Vallyathan, V., Lewis, D.M., 2003. Evidence for lipopolysaccharide-induced differentiation of RAW264.7 murine macrophage cell line into dendritic like cells. J. Biosci. 28, 129–34.

Schillberg, S., Twyman, R.M., Fischer, R., 2005. Opportunities for recombinant antigen and antibody expression in transgenic plants—technology assessment. Vaccine 23, 1764–1769.

Schmeisser, A., Garlichs, C.D., Zhang, H., Eskafi, S., Graffy, C., Ludwig, J., Strasser, R.H., Daniel, W.G., 2001. Monocytes coexpress endothelial and macrophagocytic lineage markers and form cord-like structures in Matrigel® under angiogenic conditions. Cardiovasc. Res. 49, 671–680.

Scott, A.M., Allison, J.P., Wolchok, J.D., 2012. Monoclonal antibodies in cancer therapy. Cancer Immun. 12, 14.

Scott, D. a, Balliet, C.L., Cook, D.J., Davies, A.M., Gero, T.W., Omer, C. a, Poondru, S., Theoclitou, M.-E., Tyurin, B., Zinda, M.J., 2009. Identification of 3-amido-4-anilinoquinolines as potent and selective inhibitors of CSF-1R kinase. Bioorg. Med. Chem. Lett. 19, 697–700. doi:10.1016/j.bmcl.2008.12.046

Scott, D.A., Dakin, L.A., Del Valle, D.J., Diebold, R.B., Drew, L., Gero, T.W., Ogoe, C. a, Omer, C. a, Repik, G., Thakur, K., Ye, Q., Zheng, X., 2011. 3-amido-4-anilinocinnolines as a novel class of CSF-1R inhibitor. Bioorg. Med. Chem. Lett. 21, 1382–4. doi:10.1016/j.bmcl.2011.01.033

Segawa, M., Fukada, S., Yamamoto, Y., Yahagi, H., Kanematsu, M., Sato, M., Ito, T., Uezumi, A., Hayashi, S., Miyagoe-Suzuki, Y., 2008. Suppression of macrophage

functions impairs skeletal muscle regeneration with severe fibrosis. Exp. Cell Res. 314, 3232–3244.

Seljelid, R., Eskeland, T., 1993. The biology of macrophages: I General principles and properties. Eur. J. Haematol. 51, 267–275.

Serbina, N. V, Jia, T., Hohl, T.M., Pamer, E.G., 2008. Monocyte-mediated defense against microbial pathogens. Annu. Rev. Immunol. 26, 421.

Sester, D.P., Beasley, S.J., Sweet, M.J., Fowles, L.F., Cronau, S.L., Stacey, K.J., Hume, D.A., 1999. Bacterial/CpG DNA Down-Modulates Colony Stimulating Factor-1 Receptor Surface Expression on Murine Bone Marrow-Derived Macrophages with Concomitant Growth Arrest and Factor-Independent Survival. J. Immunol. 163, 6541–6550.

Shepherd, P., Dean, C.J., 2000. Monoclonal Antibodies: A Practical Approach, Monoclonal Antibodies: A Practical Approach. Oxford University Press.

Sherr, C.J., 1990. Colony-stimulating factor-1 receptor. Blood 75 , 1–12.

Sherr, C.J., Ashmun, R.A., Downing, J.R., Ohtsuka, M., Quan, S.G., Golde, D.W., Roussel, M.F., 1989. Inhibition of colony-stimulating factor-1 activity by monoclonal antibodies to the human CSF-1 receptor. Blood 73, 1786–1793.

Sherr, C.J., Rettenmier, C.W., Sacca, R., Roussel, M.F., Look, a T., Stanley, E.R., 1985. The c-fms proto-oncogene product is related to the receptor for the mononuclear phagocyte growth factor, CSF-1. Cell 41, 665–76.

Shibata, Y., Berclaz, P.-Y., Chroneos, Z.C., Yoshida, M., Whitsett, J.A., Trapnell, B.C., 2001a. GM-CSF regulates alveolar macrophage differentiation and innate immunity in the lung through PU. 1. Immunity 15, 557–567.

Shibata, Y., Zsengeller, Z., Otake, K., Palaniyar, N., Trapnell, B.C., 2001b. Alveolar macrophage deficiency in osteopetrotic mice deficient in macrophage colony-stimulating factor is spontaneously corrected with age and associated with matrix metalloproteinase expression and emphysema. Blood 98, 2845–2852.

Shree, T., Olson, O.C., Elie, B.T., Kester, J.C., Garfall, A.L., Simpson, K., Bell-McGuinn, K.M., Zabor, E.C., Brogi, E., Joyce, J.A., 2011. Macrophages and cathepsin proteases blunt chemotherapeutic response in breast cancer. Genes Dev. 25, 2465–2479.

Sica, A., Porta, C., Morlacchi, S., Banfi, S., Strauss, L., Rimoldi, M., Totaro, M.G., Riboldi, E., 2012. Origin and functions of tumor-associated myeloid cells (TAMCs). Cancer Microenviron. 5, 133–149.

Sica, A., Saccani, A., Bottazzi, B., Polentarutti, N., Vecchi, A., Van Damme, J., Mantovani, A., 2000. Autocrine production of IL-10 mediates defective IL-12 production and NF-κB activation in tumor-associated macrophages. J. Immunol. 164, 762–767.

Sica, A., Schioppa, T., Mantovani, A., Allavena, P., 2006. Tumour-associated macrophages are a distinct M2 polarised population promoting tumour progression: potential targets of anti-cancer therapy. Eur. J. Cancer 42, 717–727. doi:10.1016/j.ejca.2006.01.003

Sierra-Filardi, E., Nieto, C., Domínguez-Soto, Á., Barroso, R., Sánchez-Mateos, P., Puig-Kroger, A., López-Bravo, M., Joven, J., Ardavín, C., Rodríguez-Fernández, J.L., Sánchez-Torres, C., Mellado, M., Corbí, Á.L., 2014. CCL2 Shapes Macrophage Polarization by GM-CSF and M-CSF: Identification of CCL2/CCR2-Dependent Gene Expression Profile. J. Immunol. 192 , 3858–3867. doi:10.4049/jimmunol.1302821

Sierra-Filardi, E., Puig-Kröger, A., Blanco, F.J., Nieto, C., Bragado, R., Palomero, M.I., Bernabéu, C., Vega, M.A., Corbí, A.L., 2011. Activin A skews macrophage polarization by promoting a proinflammatory phenotype and inhibiting the acquisition of anti-inflammatory macrophage markers. Blood 117, 5092–5101.

Sieweke, M.H., Allen, J.E., 2013. Beyond stem cells: self-renewal of differentiated macrophages. Science (80-.). 342, 1242974. doi:10.1126/science.1242974

Singh, J.A., Wells, G.A., Christensen, R., Tanjong Ghogomu, E., Maxwell, L., MacDonald, J.K., Filippini, G., Skoetz, N., Francis, D.K., Lopes, L.C., 2011. Adverse effects of biologics: a network meta-analysis and Cochrane overview. Cochrane Libr.

Singh, S.K., Cousens, L.P., Alvarez, D., Mahajan, P.B., 2012. Determinants of immunogenic response to protein therapeutics. Biologicals 40, 364–368. doi:http://dx.doi.org/10.1016/j.biologicals.2012.06.001

Smith, M.P., Sanchez-Laorden, B., O'Brien, K., Brunton, H., Ferguson, J., Young, H., Dhomen, N., Flaherty, K.T., Frederick, D.T., Cooper, Z.A., 2014. The Immune Microenvironment Confers Resistance to MAPK Pathway Inhibitors through Macrophage-Derived TNFα. Cancer Discov. 4, 1214–1229.

Smyth, M.J., Dunn, G.P., Schreiber, R.D., 2006. Cancer immunosurveillance and immunoediting: the roles of immunity in suppressing tumor development and shaping tumor immunogenicity. Adv. Immunol. 90, 1–50.

Soares, M.J.F. da S., 2007. Relevância biológica e clínica das alterações do número de cópias e da expressão do gene CSFIR nos carcinomas renais. Instituto de Ciências Biomédicas Abel Salazar ICBAS.

Solinas, G., Schiarea, S., Liguori, M., Fabbri, M., Pesce, S., Zammataro, L., Pasqualini, F., Nebuloni, M., Chiabrando, C., Mantovani, A., Allavena, P., 2010. Tumor-conditioned macrophages secrete migration-stimulating factor: a new marker for M2-polarization, influencing tumor cell motility. J. Immunol. 185, 642–652. doi:10.4049/jimmunol.1000413

Sørensen, H.P., Mortensen, K.K., 2005. Advanced genetic strategies for recombinant protein expression in Escherichia coli. J. Biotechnol. 115, 113–128. doi:http://dx.doi.org/10.1016/j.jbiotec.2004.08.004

Soria, G., Ben-Baruch, A., 2008. The inflammatory chemokines CCL2 and CCL5 in breast cancer. Cancer Lett. 267, 271–285. doi:http://dx.doi.org/10.1016/j.canlet.2008.03.018

Sorrentino, A., Liu, C.-G., Addario, A., Peschle, C., Scambia, G., Ferlini, C., 2008. Role of microRNAs in drug-resistant ovarian cancer cells. Gynecol. Oncol. 111, 478–486.

Sozzani, S., Introna, M., Bernasconi, S., Polentarutti, N., Cinque, P., Poli, G., Sica, A., Mantovani, A., 1997. MCP-1 and CCR2 in HIV infection: regulation of agonist and receptor expression. J. Leukoc. Biol. 62, 30–33.

Stanley, E.R., 2000. CSF-1, in: Oppenheim, J.J., Feldmann, M., Durum, S.K. (Eds.), Cytokine Reference: A Compendium of Cytokines and Other Mediators of Host Defense. Ligands, Volume 1. Academic Press, p. 1436. doi:10.1006/rwcy.2000.09005.SUMMARY

Stanley, E.R., Berg, K.L., Einstein, D.B., Lee, P.S.W., Pixley, F.J., Wang, Y., Yeung, Y.-G., 1997. Biology and action of colony-stimulating factor-1. Mol. Reprod. Dev. 46, 4–10. doi:10.1002/(SICI)1098-2795(199701)46:1<4::AID-MRD2>3.0.CO;2-V

Stanley, E.R., Chitu, V., 2014. CSF-1 Receptor Signaling in Myeloid Cells. Cold Spring Harb. Perspect. Biol. 6 . doi:10.1101/cshperspect.a021857

Steidl, S., Ratsch, O., Brocks, B., Dürr, M., Thomassen-Wolf, E., 2008. In vitro affinity maturation of human GM-CSF antibodies by targeted CDR-diversification. Mol. Immunol. 46, 135–144. doi:http://dx.doi.org/10.1016/j.molimm.2008.07.013

Sternberg, R., Pondenis, H., Segre, M., Wypij, L.G., Fan, T., 2011. Characterizing the innate immune and potential anticancer effects of TLR7 agonism in normal balb/c mice, in: Oncology, V. and C. (Ed.), Abstracts Presented at the 30th Annual VCS Conference; San Diego; CA; USA; 29 October–1 November 2010. Blackwell Publishing, San Diego.

Strauss-Ayali, D., Conrad, S.M., Mosser, D.M., 2007. Monocyte subpopulations and their differentiation patterns during infection. J. Leukoc. Biol. 82, 244–252.

Sudo, T., Nishikawa, S., Ogawa, M., Kataoka, H., Ohno, N., Izawa, A., Hayashi, S., Nishikawa, S., 1995. Functional hierarchy of c-kit and c-fms in intramarrow production of CFU-M. Oncogene 11, 2469–2476.

Sun, H., Ding, Y., Yang, S., Yin, Z., Yue, Y., 2014. Expression, production and renaturation of a functional single-chain variable antibody fragment (scFv) against human intercellular adhesion molecule-1 (ICAM-1). African J. Biotechnol. 13, 1588.

Sunderkötter, C., Nikolic, T., Dillon, M.J., Van Rooijen, N., Stehling, M., Drevets, D. a, Leenen, P.J.M., 2004. Subpopulations of mouse blood monocytes differ in maturation stage and inflammatory response. J. Immunol. 172, 4410–7.

Suriano, F., Santini, D., Perrone, G., Amato, M., Vincenzi, B., Tonini, G., Muda, A., Boggia, S., Buscarini, M., Pantano, F., 2013. Tumor associated macrophages polarization dictates the efficacy of BCG instillation in non-muscle invasive urothelial bladder cancer. J Exp Clin Cancer Res 32, 10.

Sweet, M.J., Campbell, C.C., Sester, D.P., Xu, D., McDonald, R.C., Stacey, K.J., Hume, D. a, Liew, F.Y., 2002. Colony-stimulating factor-1 suppresses responses to CpG DNA

and expression of toll-like receptor 9 but enhances responses to lipopolysaccharide in murine macrophages. J. Immunol. 168, 392–399.

Sweet, M.J., Hume, D. a, 2003. CSF-1 as a regulator of macrophage activation and immune responses. Arch. Immunol. Ther. Exp. (Warsz). 51, 169–177.

Tang, C.-H., Tsai, C.-C., 2012. CCL2 increases MMP-9 expression and cell motility in human chondrosarcoma cells via the Ras/Raf/MEK/ERK/NF-κB signaling pathway. Biochem. Pharmacol. 83, 335–344.

Tang, F., Lao, K., Surani, M.A., 2011. Development and applications of single-cell transcriptome analysis. Nat. Methods 8.

Tang, L., Sampson, C., Dreitz, M.J., McCall, C., 2001. Cloning and characterization of cDNAs encoding four different canine immunoglobulin γ chains. Vet. Immunol. Immunopathol. 80, 259–270. doi:http://dx.doi.org/10.1016/S0165-2427(01)00318-X

Taskinen, M., Karjalainen-Lindsberg, M.-L., Nyman, H., Eerola, L.-M., Leppä, S., 2007. A high tumor-associated macrophage content predicts favorable outcome in follicular lymphoma patients treated with rituximab and cyclophosphamide-doxorubicin-vincristine-prednisone. Clin. cancer Res. 13, 5784–5789.

Te Velde, A.A., de Waal Malefijt, R., Huijbens, R.J., de Vries, J.E., Figdor, C.G., 1992. IL-10 stimulates monocyte Fc gamma R surface expression and cytotoxic activity. Distinct regulation of antibody-dependent cellular cytotoxicity by IFN-gamma, IL-4, and IL-10. J. Immunol. 149 , 4048–4052.

Teicher, B.A., Chari, R.V.J., 2011. Antibody Conjugate Therapeutics: Challenges and Potential. Clin. Cancer Res. 17 , 6389–6397. doi:10.1158/1078-0432.CCR-11-1417

Temeles, D.S., McGrath, H.E., Kittler, E.L., Shadduck, R.K., Kister, V.K., Crittenden, R.B., Turner, B.L., Quesenberry, P.J., 1993. Cytokine expression from bone marrow derived macrophages. Exp. Hematol. 21, 388–393.

Teng, G., Papavasiliou, F.N., 2007. Immunoglobulin Somatic Hypermutation. Annu. Rev. Genet. 41, 107–120. doi:10.1146/annurev.genet.41.110306.130340

Terpe, K., 2006. Overview of bacterial expression systems for heterologous protein production: from molecular and biochemical fundamentals to commercial systems. Appl. Microbiol. Biotechnol. 72, 211–222.

Thie, H., Meyer, T., Schirrmann, T., Hust, M., Dubel, S., 2008. Phage display derived therapeutic antibodies. Curr. Pharm. Biotechnol. 9, 439–446.

Thoma, C.R., Zimmermann, M., Agarkova, I., Kelm, J.M., Krek, W., 2014. 3D cell culture systems modeling tumor growth determinants in cancer target discovery. Adv. Drug Deliv. Rev. 69–70, 29–41. doi:http://dx.doi.org/10.1016/j.addr.2014.03.001

Thomas, G., Tacke, R., Hedrick, C.C., Hanna, R.N., 2015. Nonclassical Patrolling Monocyte Function in the Vasculature. Arterioscler. Thromb. Vasc. Biol. 35, 1306–1316.

Tomlinson, I.M., Walter, G., Jones, P.T., Dear, P.H., Sonnhammer, E.L.L., Winter, G., 1996. The Imprint of Somatic Hypermutation on the Repertoire of Human Germline V Genes. J. Mol. Biol. 256, 813–817. doi:http://dx.doi.org/10.1006/jmbi.1996.0127

Toy, E.P., Azodi, M., Folk, N.L., Zito, C.M., Zeiss, C.J., Chambers, S.K., 2009. Enhanced ovarian cancer tumorigenesis and metastasis by the macrophage colony-stimulating factor. Neoplasia 11, 136–144.

Toy, E.P., Chambers, J.T., Kacinski, B.M., Flick, M.B., Chambers, S.K., 2001. The activated macrophage colony-stimulating factor (CSF-1) receptor as a predictor of poor outcome in advanced epithelial ovarian carcinoma. Gynecol. Oncol. 80, 194–200.

Tridandapani, S., Siefker, K., Teillaud, J.-L., Carter, J.E., Wewers, M.D., Anderson, C.L., 2002. Regulated Expression and Inhibitory Function of FcγRIIb in Human Monocytic Cells. J. Biol. Chem. 277 , 5082–5089. doi:10.1074/jbc.M110277200

Udagawa, N., Takahashi, N., Akatsu, T., Tanaka, H., Sasaki, T., Nishihara, T., Koga, T., Martin, T.J., Suda, T., 1990. Origin of osteoclasts: mature monocytes and macrophages are capable of differentiating into osteoclasts under a suitable microenvironment prepared by bone marrow-derived stromal cells. Proc. Natl. Acad. Sci. U. S. A. 87, 7260–4.

Valensi, J.P., Carlson, J.R., Van Nest, G.A., 1994. Systemic cytokine profiles in BALB/c mice immunized with trivalent influenza vaccine containing MF59 oil emulsion and other advanced adjuvants. J. Immunol. 153, 4029–4039.

Van de Laar, L., Coffer, P.J., Woltman, A.M., 2012. Regulation of dendritic cell development by GM-CSF: molecular control and implications for immune homeostasis and therapy. Blood 119, 3383–3393.

Van Der Keyl, H., Gellad, Z.F., Owen, J.A., 2000. Disparity in the kinetics of onset of hypermutation in immunoglobulin heavy and light chains. Immunol Cell Biol 78, 224–237.

Van der Poel, C.E., Spaapen, R.M., van de Winkel, J.G.J., Leusen, J.H.W., 2011. Functional Characteristics of the High Affinity IgG Receptor, FcγRI. J. Immunol. 186 , 2699–2704. doi:10.4049/jimmunol.1003526

Van Ginderachter, J.O.A., Movahedi, K., Ghassabeh, G.H., Meerschaut, S., Beschin, A., Raes, G., De Baetselier, P., 2006. Classical and alternative activation of mononuclear phagocytes: picking the best of both worlds for tumor promotion. Immunobiology 211, 487–501.

Van Meer, P.J.K., Kooijman, M., Brinks, V., Gispen-de Wied, C.C., Silva-Lima, B., Moors, E.H.M., Schellekens, H., 2013. Immunogenicity of mAbs in non-human primates during nonclinical safety assessment. MAbs 5, 810–816. doi:10.4161/mabs.25234

Vellenga, E., Rambaldi, A., Ernst, T.J., Ostapovicz, D., Griffin, J.D., 1988. Independent regulation of M-CSF and G-CSF gene expression in human monocytes. Blood 71, 1529–1532.

Voloshin, T., Voest, E.E., Shaked, Y., 2013. The host immunological response to cancer therapy: An emerging concept in tumor biology. Exp. Cell Res. 319, 1687–1695. doi:http://dx.doi.org/10.1016/j.yexcr.2013.03.007

Vu, T.H., Shipley, J.M., Bergers, G., Berger, J.E., Helms, J.A., Hanahan, D., Shapiro, S.D., Senior, R.M., Werb, Z., 1998. MMP-9/Gelatinase B Is a Key Regulator of Growth Plate Angiogenesis and Apoptosis of Hypertrophic Chondrocytes. Cell 93, 411–422. doi:http://dx.doi.org/10.1016/S0092-8674(00)81169-1

Waldmann, H., 2014. Human monoclonal antibodies: the residual challenge of antibody immunogenicity, in: Human Monoclonal Antibodies. Springer, pp. 1–8.

Wall, M.J., Chen, J., Meegalla, S., Ballentine, S.K., Wilson, K.J., DesJarlais, R.L., Schubert, C., Chaikin, M. a, Crysler, C., Petrounia, I.P., Donatelli, R.R., Yurkow, E.J., Boczon, L., Mazzulla, M., Player, M.R., Patch, R.J., Manthey, C.L., Molloy, C., Tomczuk, B., Illig, C.R., 2008. Synthesis and evaluation of novel 3,4,6-substituted 2-quinolones as FMS kinase inhibitors. Bioorg. Med. Chem. Lett. 18, 2097–102. doi:10.1016/j.bmcl.2008.01.088

Wang, S.-C., Hong, J.-H., Hsueh, C., Chiang, C.-S., 2012. Tumor-secreted SDF-1 promotes glioma invasiveness and TAM tropism toward hypoxia in a murine astrocytoma model. Lab. Investig. 92, 151–162.

Wang, Y., Szretter, K.J., Vermi, W., Gilfillan, S., Rossini, C., Cella, M., Barrow, A.D., Diamond, M.S., Colonna, M., 2012. IL-34 is a tissue-restricted ligand of CSF1R required for the development of Langerhans cells and microglia. Nat. Immunol. 13, 753–760.

Wang, Z., Bapat, A.S., Rayanade, R.J., Dagtas, A.S., Departments, M.K.H., 2001. Interleukin-10 induces macrophage apoptosis and expression of CD16 (FcgRIII) whose engagement blocks the cell death programme and facilitates differentiation. Immunology 16, 331–337.

Warmerdam, P.A.M., van den Herik-Oudijk, I.E., Parren, P.W.H.I., Westerdaal, N.A.C., Capel, P.J.A., 1993. Interaction of a human FcγRIIb1 (CD32) isoform with murine and human IgG subclasses. Int. Immunol. 5 , 239–247. doi:10.1093/intimm/5.3.239

Wasserman, J., Diese, L., VanGundy, Z., London, C., Carson, W.E., Papenfuss, T.L., 2012. Suppression of canine myeloid cells by soluble factors from cultured canine tumor cells. Vet. Immunol. Immunopathol. 145, 420–430. doi:http://dx.doi.org/10.1016/j.vetimm.2011.12.018

Wei, S., Dai, X.-M., Stanley, E.R., 2006. Transgenic expression of CSF-1 in CSF-1 receptor-expressing cells leads to macrophage activation, osteoporosis, and early death. J. Leukoc. Biol. 80, 1445–1453.

Wei, S., Lightwood, D., Ladyman, H., Cross, S., Neale, H., Griffiths, M., Adams, R., Marshall, D., Lawson, A., McKnight, A.J., Stanley, E.R., 2005. Modulation of CSF-1-regulated post-natal development with anti-CSF-1 antibody. Immunobiology 210, 109–119. doi:10.1016/j.imbio.2005.05.005

Wei, S., Nandi, S., Chitu, V., Yeung, Y.-G., Yu, W., Huang, M., Williams, L.T., Lin, H., Stanley, E.R., 2010. Functional overlap but differential expression of CSF-1 and IL-34 in their CSF-1 receptor-mediated regulation of myeloid cells. J. Leukoc. Biol. 88 , 495–505. doi:10.1189/jlb.1209822

Weiden, P.L., Wolf, S.B., Breitz, H.B., Appelbaum, J.W., Seiler, C.A., Mallett, R., Bjorn, M.J., Su, F.M., Fer, M.F., Salk, D., 1994. Human anti-mouse antibody suppression with cyclosporin A. Cancer 73, 1093–1097.

Weisberg, S.P., Mccann, D., Desai, M., Rosenbaum, M., Leibel, R.L., Ferrante, A.W., 2003. Obesity is associated with macrophage accumulation 112. doi:10.1172/JCI200319246.Introduction

Welsch, C.W., Nagasawa, H., 1977. Prolactin and murine mammary tumorigenesis: a review. Cancer Res. 37, 951–963.

West, R.B., Rubin, B.P., Miller, M.A., Subramanian, S., Kaygusuz, G., Montgomery, K., Zhu, S., Marinelli, R.J., De Luca, A., Downs-Kelly, E., 2006. A landscape effect in tenosynovial giant-cell tumor from activation of CSF1 expression by a translocation in a minority of tumor cells. Proc. Natl. Acad. Sci. U. S. A. 103, 690–695.

Wheeler, E.F., Rettenmier, C.W., Look, A.T., Sherr, C.J., 1986. The v-fms oncogene induces factor independence and tumorigenicity in CSF-1 dependent macrophage cell line.

Wiemer, A.J., Hegde, S., Gumperz, J.E., Huttenlocher, A., 2011. A Live Imaging Cell Motility Screen Identifies Prostaglandin E2 as a T Cell Stop Signal Antagonist. J. Immunol. 187 , 3663–3670. doi:10.4049/jimmunol.1100103

Wiktor-Jedrzejczak, W., Ahmed, A., Szczylik, C., Skelly, R.R., 1982. Hematological characterization of congenital osteopetrosis in op/op mouse. Possible mechanism for abnormal macrophage differentiation. J. Exp. Med. 156, 1516.

Wiktor-Jedrzejczak, W., Urbanowska, E., Szperl, M., 1994. Granulocyte-macrophage colony-stimulating factor corrects macrophage deficiencies, but not osteopetrosis, in the colony-stimulating factor-1-deficient op/op mouse. Endocrinology 134, 1932–1935.

Willis, J.R., Briney, B.S., DeLuca, S.L., Crowe, J.E., Meiler, J., 2013. Human Germline Antibody Gene Segments Encode Polyspecific Antibodies. PLoS Comput. Biol. 9, e1003045. doi:10.1371/journal.pcbi.1003045

Willman, C.L., Stewart, C.C., Miller, V., Yi, T.L., Tomasi, T.B., 1989. Regulation of MHC class II gene expression in macrophages by hematopoietic colony-stimulating factors (CSF). Induction by granulocyte/macrophage CSF and inhibition by CSF-1. J. Exp. Med. 170, 1559–1567.

Wilson, H.M., 2014. SOCS proteins in macrophage polarization and function. Front. Immunol. 5.

Witmer-Pack, M.D., Hughes, D. a, Schuler, G., Lawson, L., McWilliam, a, Inaba, K., Steinman, R.M., Gordon, S., 1993. Identification of macrophages and dendritic cells in the osteopetrotic (op/op) mouse. J. Cell Sci. 104 (Pt 4), 1021–9.

Witsell, A.L., 1991. Macrophage Heterogeneity Occurs Through a Developmental Mechanism. Proc. Natl. Acad. Sci. 88, 1963–1967. doi:10.1073/pnas.88.5.1963

Wong, H.L., Welch, G.R., Brandes, M.E., Wahl, S.M., 1991. IL-4 antagonizes induction of Fc gamma RIII (CD16) expression by transforming growth factor-beta on human monocytes. J. Immunol. 147 , 1843–1848.

Wong, K.L., Tai, J.J.-Y., Wong, W.-C., Han, H., Sem, X., Yeap, W.-H., Kourilsky, P., Wong, S.-C., 2011. Gene expression profiling reveals the defining features of the classical, intermediate, and nonclassical human monocyte subsets. Blood 118, e16–e31.

Woo, H.H., Zhou, Y., Yi, X., David, C.L., Zheng, W., Gilmore-Hebert, M., Kluger, H.M., Ulukus, E.C., Baker, T., Stoffer, J.B., 2009. Regulation of non-AU-rich element containing c-fms proto-oncogene expression by HuR in breast cancer. Oncogene 28, 1176–1186.

Wyckoff, J., Wang, W., Lin, E.Y., Wang, Y., Pixley, F., Stanley, E.R., Graf, T., Pollard, J.W., Segall, J., Condeelis, J., 2004. A Paracrine Loop between Tumor Cells and Macrophages Is Required for Tumor Cell Migration in Mammary Tumors. Cancer Res. 64 , 7022–7029. doi:10.1158/0008-5472.CAN-04-1449

Wyckoff, J.B., Wang, Y., Lin, E.Y., Li, J., Goswami, S., Stanley, E.R., Segall, J.E., Pollard, J.W., Condeelis, J., 2007. Direct visualization of macrophage-assisted tumor cell intravasation in mammary tumors. Cancer Res. 67, 2649–2656. doi:10.1158/0008-5472.CAN-06-1823

Xie, H., Ye, M., Feng, R., Graf, T., 2004. Stepwise reprogramming of B cells into macrophages. Cell 117, 663–676.

Xu, J., Escamilla, J., Mok, S., David, J., Priceman, S., West, B., Bollag, G., McBride, W., Wu, L., 2013. CSF1R signaling blockade stanches tumor-infiltrating myeloid cells and improves the efficacy of radiotherapy in prostate cancer. Cancer Res. 73, 2782–2794.

Xu, R., Sun, H.-F., Williams, D.W., Jones, A. V, Al-Hussaini, A., Song, B., Wei, X.-Q., 2015. IL-34 Suppresses Candida albicans Induced TNFα Production in M1 Macrophages by Downregulating Expression of Dectin-1 and TLR2. J. Immunol. Res. 2015.

Yamamoto, T., Kaizu, C., Kawasaki, T., Hasegawa, G., Umezu, H., Ohashi, R., Sakurada, J., Jiang, S., Shultz, L., Naito, M., 2008. Macrophage colony-stimulating factor is indispensable for repopulation and differentiation of Kupffer cells but not for splenic red pulp macrophages in osteopetrotic (op/op) mice after macrophage depletion. Cell Tissue Res. 332, 245–256.

Yamate, J., Yoshida, H., Tsukamoto, Y., Ide, M., Kuwamura, M., Ohashi, F., Miyamoto, T., Kotani, T., Sakuma, S., Takeya, M., 2000. Distribution of cells immunopositive for AM-3K, a novel monoclonal antibody recognizing human macrophages, in normal and diseased tissues of dogs, cats, horses, cattle, pigs, and rabbits. Vet. Pathol. Online 37, 168–176.

Yan, L., Ehrlich, P.J., Gibson, R., Pickett, C., Beckman, R.A., 2009. How can we improve antibody-based cancer therapy? MAbs 1, 67–70.

Yancey, M.F., Merritt, D.A., Lesman, S.P., Boucher, J.F., Michels, G.M., 2010. Pharmacokinetic properties of toceranib phosphate (Palladia, SU11654), a novel tyrosine kinase inhibitor, in laboratory dogs and dogs with mast cell tumors. J. Vet. Pharmacol. Ther. 33, 162–171. doi:10.1111/j.1365-2885.2009.01133.x

Yasukawa, H., Ohishi, M., Mori, H., Murakami, M., Chinen, T., Aki, D., Hanada, T., Takeda, K., Akira, S., Hoshijima, M., 2003. IL-6 induces an anti-inflammatory response in the absence of SOCS3 in macrophages. Nat. Immunol. 4, 551–556.

Ye, X., Xu, S., Xin, Y., Yu, S., Ping, Y., Chen, L., Xiao, H., Wang, B., Yi, L., Wang, Q., 2012. Tumor-associated microglia/macrophages enhance the invasion of glioma stem-like cells via TGF-β1 signaling pathway. J. Immunol. 189, 444–453.

Yeung, Y.-G., Stanley, E.R., 2003. Proteomic approaches to the analysis of early events in colony-stimulating factor-1 signal transduction. Mol. Cell. Proteomics 2, 1143–1155. doi:10.1074/mcp.R300009-MCP200

Yoshino, M., Yamazaki, H., Yoshida, H., Niida, S., 2003. Inhibition of Mouse Tooth Eruption. J. Bone Miner. Res. 18, 108–116.

Zeisberger, S.M., Odermatt, B., Marty, C., Zehnder-Fjällman, a H.M., Ballmer-Hofer, K., Schwendener, R. a, 2006. Clodronate-liposome-mediated depletion of tumour-associated macrophages: a new and highly effective antiangiogenic therapy approach. Br. J. Cancer 95, 272–81. doi:10.1038/sj.bjc.6603240

Zhang, D., Chen, C.-F., Zhao, B.-B., Gong, L.-L., Jin, W.-J., Liu, J.-J., Wang, J.-F., Wang, T.-T., Yuan, X.-H., He, Y.-W., 2013. A Novel Antibody Humanization Method Based on Epitopes Scanning and Molecular Dynamics Simulation. PLoS One 8, e80636.

Zhang, J., Yang, P.L., Gray, N.S., 2009. Targeting cancer with small molecule kinase inhibitors. Nat. Rev. Cancer 9, 28–39. doi:10.1038/nrc2559

Zhang, Y.J., Pan, H.Y., Gao, S.J., 2001. Reverse transcription slippage over the mRNA secondary structure of the LIP1 gene. Biotechniques 31, 1286–1288.

Zhao, H., Zhang, J., Puligedda, R., Swider, C., Simon, P., Heimbach, B., Adekar, S., Murphy, M., Borghaei, H., Dessain, S., 2014. Abstract 3625: Tumor-specific human monoclonal antibodies isolated from cancer patients. Cancer Res. 74 , 3625. doi:10.1158/1538-7445.AM2014-3625

Zhu, Y., Knolhoff, B.L., Meyer, M.A., Nywening, T.M., West, B.L., Luo, J., Wang-Gillam, A., Goedegebuure, S.P., Linehan, D.C., DeNardo, D.G., 2014. CSF1/CSF1R blockade reprograms tumor-infiltrating macrophages and improves response to T-cell checkpoint immunotherapy in pancreatic cancer models. Cancer Res. 74, 5057–5069.

Ziegelbauer, K., Light, D.R., 2008. Monoclonal antibody therapeutics: Leading companies to maximise sales and market share. J. Commer. Biotechnol. 14, 65–72.